VOL. 549 NOS. 1 + 2 JULY 19, 1991

COMPLETE IN ONE ISSUE

NAL OF HROMATOGRAPHY

UDING ELECTROPHORESIS AND OTHER SEPARATION METHOD

ELSEVIER

Scope. The *Journal of Chromatography* publishes papers on all aspects of chromatography, electrophoresis and related methods. Contributions consist mainly of research papers dealing with chromatographic theory, instrumental development and their applications. The section *Biomedical Applications*, which is under separate editorship, deals with the following aspects: developments in and applications of chromatographic and electrophoretic techniques related to clinical diagnosis or alterations during medical treatment; screening and profiling of body fluids or tissues with special reference to metabolic disorders; results from basic medical research with direct consequences in clinical practice; drug level monitoring and pharmacokinetic studies; clinical toxicology; analytical studies in occupational medicine.

Submission of Papers. Manuscripts (in English; *four* copies are required) should be submitted to: Editorial Office of *Journal of Chromatography*, P.O. Box 681, 1000 AR Amsterdam, The Netherlands, Telefax (+31-20) 5862 304, or to: The Editor of *Journal of Chromatography, Biomedical Applications*, P.O. Box 681, 1000 AR Amsterdam, The Netherlands. Review articles are invited or proposed by letter to the Editors. An outline of the proposed review should first be forwarded to the Editors for preliminary discussion prior to preparation. Submission of an article is understood to imply that the article is original and unpublished and is not being considered for publication elsewhere. For copyright regulations, see below.

Publication. The *Journal of Chromatography* (incl. *Biomedical Applications*) has 38 volumes in 1991. The subscription prices for 1991 are:

J. Chromatogr. (incl. *Cum. Indexes, Vols. 501–550*) + *Biomed. Appl.* (Vols. 535–572):
Dfl. 7220.00 plus Dfl. 1140.00 (p.p.h.) (total *ca.* US$ 4519.00)

J. Chromatogr. (incl. *Cum. Indexes, Vols. 501–550*) only (Vols. 535–561):
Dfl. 5859.00 plus Dfl. 810.00 (p.p.h.) (total *ca.* US$ 3604.75)

Biomed. Appl. only (Vols. 562–572):
Dfl. 2387.00 plus Dfl. 330.00 (p.p.h.) (total *ca.* US$ 1468.75).

Subscription Orders. The Dutch guilder price is definitive. The US$ price is subject to exchange-rate fluctuations and is given as a guide. Subscriptions are accepted on a prepaid basis only, unless different terms have been previously agreed upon. Subscriptions orders can be entered only by calender year (Jan.–Dec.) and should be sent to Elsevier Science Publishers, Journal Department, P.O. Box 211, 1000 AE Amsterdam, The Netherlands, Tel. (+31-20) 5803 642, Telefax (+31-20) 5803 598, or to your usual subscription agent. Postage and handling charges include surface delivery except to th following countries where air delivery via SAL (Surface Air Lift) mail is ensured: Argentina, Australia, Brazil, Canada, Hong Kong, India, Israel, Japan*, Malaysia, Mexico, New Zealand, Pakistan, PR CHina, Singapore, South Africa, South Korea, Taiwan, Thailand, USA. * For Japan air delivery (SAL) requires 50% additional charge of the normal postage and handling charge. For all other countries airmail rates are available upon request. Claims for missing issues must be made within three months of our publication (mailing) date, otherwise such claims cannot be honoured free of charge. Back volumes of the *Journal of Chromatography* (Vols. 1–534) are available at Dfl. 208.00 (plus postage). Customers in the USA and Canada wishing information on this and other Elsevier journals, please contact Journal Information Center, Elsevier Science Publishing Co. Inc., 655 Avenue of the Americas, New York, NY 10010, USA, Tel. (+1-212) 633 3750, Telefax (+1-212) 633 3990.

Abstracts/Contents Lists published in Analytical Abstracts, Biochemical Abstracts, Biological Abstracts, Chemical Abstracts, Chemical Titles, Chromatography Abstracts, Clinical Chemistry Lookout, Current Contents/Life Sciences, Current Contents/Physical, Chemical & Earth Sciences, Deep-Sea Research/Part B: Oceanographic Literature Review, Excerpta Medica, Index Medicus, Mass Spectrometry Bulletin, PASCAL-CNRS, Pharmaceutical Abstracts, Referativnyi Zhurnal, Research Alert, Science Citation Index and Trends in Biotechnology.

See inside back cover for Publication Schedule, Information for Authors and information on Advertisements.

0021-9673/91/$03.50

This issue is printed on acid-free paper.

Printed in The Netherlands

VOL. 549, NOS. 1 + 2 JOURNAL OF CHROMATOGRAPHY JULY 19, 1991

CONTENTS

(*Abstracts/Contents Lists published in Analytical Abstracts, Biochemical Abstracts, Biological Abstracts, Chemical Abstracts, Chemical Titles, Chromatography Abstracts, Current Contents/Life Sciences, Current Contents/Physical, Chemical & Earth Sciences, Deep-Sea Research/Part B: Oceanographic Literature Review, Excerpta Medica, Index Medicus, Mass Spectrometry Bulletin, PASCAL-CNRS, Referativnyi Zhurnal, Research Alert and Science Citation Index*)

REGULAR PAPERS

Liquid Chromatography

Silica: backbone material of liquid chromatographic column packings (Review)
by A. Berthod (Villeurbanne, France) (Received February 21st, 1991) 1

Selectivity of carbon packing materials in comparison with octadecylsilyl- and pyrenylethylsilylsilica gels in reversed-phase liquid chromatography
by N. Tanaka, T. Tanigawa, K. Kimata, K. Hosoya and T. Araki (Kyoto, Japan) (Received March 19th, 1991) 29

Study of the fluoride adsorption characteristics of porous microparticulate zirconium oxide
by J. A. Blackwell (St. Paul, MN, USA) and P. W. Carr (Minneapolis, MN, USA) (Received April 9th, 1991) 43

Fluoride-modified zirconium oxide as a biocompatible stationary phase for high-performance liquid chromatography
by J. A. Blackwell (St. Paul, MN, USA) and P. W. Carr (Minneapolis, MN, USA) (Received April 9th, 1991) 59

Comparison of the selectivity of di(methacryloyloxymethyl)-naphthalene–divinylbenzene copolymers in reversed-phase high-performance liquid chromatography
by B. Gawdzik (Lublin, Poland) (Received March 19th, 1991) 77

Metal affinity displacement chromatography of proteins
by Y. J. Kim and S. M. Cramer (Troy, NY, USA) (Received March 22nd, 1991) 89

Two-dimensional viscous flow analysis in a micro flow-cell of an ultraviolet absorption detector for high-performance liquid chromatography
by M. Kamahori, Y. Watanabe and H. Miyagi (Tokyo, Japan) and H. Ohki and R. Miyake (Ibaraki, Japan) (Received October 30th, 1990) 101

High-performance liquid chromatography of reaction mixtures from the oxidation and degradation of lactose
by L. A. Th. Verhaar, H. E. J. Hendriks, W. P. Th. Groenland and B. F. M. Kuster (Eindhoven, Netherlands) (Received February 28th, 1991) 113

Column liquid chromatographic determination of saccharides with a single calibration graph using post-column enzyme reactors and coulometric detection
by N. Kiba, K. Shitara, H. Fuse and M. Furusawa (Kofu, Japan) and Y. Takata (Katsuta, Japan) (Received March 14th, 1991) 127

Improved separation of lysoglycolipids from solvolysates by reversed-phase high-performance liquid chromatography
by N. Kato, S. Gasa, A. Makita and H. Oguchi (Sapporo, Japan) (Received February 27th, 1991) 133

Ovine luteinizing hormone. V. Significance of flow-through peaks observed during chromatofocusing as revealed by various methods of sample preparation and application
by H. E. Grotjan and B. D. Schanbacher (Lincoln, NE, USA) and B. A. Keel (Wichita, KS, USA) (Received March 11th, 1991) 141

Ovine luteinizing hormone. VI. Analysis of the misclassification errors in the separation of intrapituitary isohormones by chromatofocusing
by H. E. Grotjan and D. D. Zalesky (Lincoln, NE, USA) (Received March 11th, 1991) . 153

(Continued overleaf)

Experimental design for the optimization of the separation of aliphatic amines by ion chromatography
by J. Vialle, P. Navarro and T. T. Nguyet (Vernaison, France) and P. Lanteri and R. Longeray (Villeurbanne, France) (Received March 26th, 1991) 159

Large-scale purification of the synthetic peptide fragment 163–171 of human interleukin-β by multidimensional displacement chromatography
by G. C. Viscomi, C. Cardinali, M. G. Longobardi and A. S. Verdini (Siena, Italy) (Received April 3rd, 1991) 175

Bioanalysis of the neuropeptide des-enkephalin-γ-endorphin by high-performance liquid chromatography with on-line sample pretreatment using gel permeation and solid-phase isolation
by D. S. Stegehuis, U. R. Tjaden, C. M. B. van den Beld and J. van der Greef (Leiden, Netherlands) (Received March 12th, 1991) 185

Mobile phase effects in the high-performance affinity purification of thermolysin
by M. Zamai (Padova, Italy) and G. Fassina (Milan, Italy) (Received February 13th, 1991) 195

High-performance liquid chromatography of synthetic oligonucleotides. A new affinity protecting group
by R. K. Gaur (Delhi, India) (Received February 1st, 1991) 207

Separation and simultaneous high-performance liquid chromatographic determination of benzocaine and benzyl benzoate in a pharmaceutical preparation
by B. Gigante, A. M. V. Barros, A. Teixeira and M. J. Marcelo-Curto (Queluz, Portugal) (Received March 8th, 1991) 217

Stability-indicating high-performance liquid chromatographic assay for α-methyldopa in sustained-release capsules
by M. E.-S. Metwally (El-Mansoura, Egypt) (Received March 19th, 1991) 221

High-performance liquid chromatographic determination of atrazine, deisopropylatrazine and deethylatrazine in soils from corn fields
by G. Karlaganis and R. von Arx (Berne, Switzerland), H. U. Ammon (Zurich, Switzerland) and R. Camenzind (Belp, Switzerland) (Received March 20th, 1991) 229

Carrier effect in the analysis of phenylurea herbicides using high-performance liquid chromatography–particle beam-mass spectrometry
by M. J. Incorvia Mattina (New Haven, CT, USA) (Received March 5th, 1991) 237

Separation and identification of sulfurized alkylphenols in oil by high-performance liquid chromatography with evaporative light scattering and mass spectrometric detection
by E. N. Chen, Jr. and V. P. Nero (Beacon, NY, USA) (Received April 16th, 1991) . . . 247

Simultaneous analysis of anions and cations by single-column ion chromatography
by R. Saari-Nordhaus and J. M. Anderson, Jr. (Deerfield, IL, USA) (Received March 26th, 1991) 257

Ion chromatography of inorganic iodine species using C_{18} reversed-phase columns coated with cetyltrimethylammonium
by K. Ito, E. Shoto and H. Sunahara (Higashi-Hiroshima, Japan) (Received March 5th, 1991) 265

Gas Chromatography

Gas chromatographic properties of organoammonium exchanged montmorillonites. I. Tetraalkylammonioum cations
by G. A. Eiceman and A. S. Lara (Las Cruces, NM, USA) (Received January 28th, 1991) 273

Gas chromatographic retention properties of organoammonium exchanged montmorillonites. II. $CH_3N^+H_3$, $(CH_3)_4N^+$, $(CH_3)_3N^+CH_2C_6H_5$ and 1,4-diazabicyclo[2.2.2]octane · $2H^+$
by A. S. Lara and G. A. Eiceman (Las Cruces, NM, USA) (Received January 28th, 1991) 283

Evaluation of gas chromatography–Fourier transform infrared spectroscopy–mass spectrometry for analysis of phenolic compounds
by D. T. Williams (Ottawa, Canada), Q. Tran and P. Fellin (Toronto, Canada) and K. A. Brice (Downsview, Canada) (Received October 18th, 1991) 297

Gas chromatographic determination of nitrophenols in atmospheric liquid water and airborne particulates
by R. Herterich (Bayreuth, Germany) (Received March 20th, 1991) 313

Improved method for prediction of gas chromatographic retention indices of C_9–C_{12} alkylbenzenes
by N. Dimov (Sofia, Bulgaria) and E. Matisová (Bratislava, Czechoslovakia) (Received March 26th, 1991) 325

Continuous automatic monitoring of volatile organic compounds in aqueous streams by a modified purge-and-trap system
by J. G. Schnable, M. B. Capangpangan and I. H. Suffet (Philadelphia, MA, USA) (Received April 8th, 1991) 335

Electrophoresis

Quantitative analysis in capillary zone electrophoresis with conductivity and indirect UV detection
by M. T. Ackermans, F. M. Everaerts and J. L. Beckers (Eindhoven, Netherlands) (Received March 19th, 1991) 345

Quantitation of insulin injection by high-performance liquid chromatography and high-performance capillary electrophoresis
by M. Lookabaugh (Winchester, MA, USA), M. Biswas (Burlington, MA, USA) and I. S. Krull (Boston, MA, USA) (Received April 8th, 1991) 357

Application of micellar electrokinetic capillary chromatography to the determination of flavonoid drugs
by P. G. Pietta and P. L. Mauri (Milan, Italy), A. Rava (Pavia, Italy) and G. Sabbatini (Milan, Italy) (Received March 25th, 1991) 367

Separation of seven tricyclic antidepressants using capillary electrophoresis
by K. Salomon, D. S. Burgi and J. C. Helmer (Palo Alto, CA, USA) (Received January 9th, 1991) 375

Planar Chromatography

Rapid and sensitive method for the quantitation of non-polar lipids by high-performance thin-layer chromatography and fluorodensitometry
by M. J. Kurantz, R. J. Maxwell, R. Kwoczak and F. Taylor (Philadelphia, PA, USA) (Received April 3rd, 1991) 387

SHORT COMMUNICATIONS

Liquid Chromatography

Detection of octopamine in an insect ganglion by high-performance liquid chromatography–native fluorescence
by F. Miyagawa, Y. Tsuchida and T. Shimizu (Tokyo, Japan) (Received February 14th, 1991) 400

The effect of ^2H_2O and an ion-pairing agent on the liquid chromatographic separation of dansylated amino acids
by G. N. Okafo and P. Camilleri (Welwyn, UK) (Received February 12th, 1991) 404

High-performance liquid chromatographic method for the determination of cloxacillin in commercial preparations and for stability studies
by M.-C. Hsu and M.-C. Cheng (Taipei, Taiwan) (Received March 26th, 1991) 410

(Continued overleaf)

Gas Chromatography

Hydrogen–deuterium exchange in fused-silica capillary columns
by M. E. Mahmoud, A. M. Moussa, D. A. Forsyth and P. Vouros (Boston, MA, USA) (Received March 13th, 1991) 416

Application of substituted liquid crystals as stationary phases in gas–liquid chromatography for the separation of mono- and dimethyl naphthalenes
by B. B. Ghatge and N. V. Bhalerao (Pune, India) (Received April 5th, 1991) 423

Cyclic aryleneazachalcogenenes. IV. Gas chromatographic properties of polyfluorinated 2,1,3-benzoselenadiazoles
by V. L. Salenko, M. L. Troshkov and A. V. Zibarev (Novosibirsk, USSR) (April 3rd, 1991) 429

Application of a metal capillary column in gas chromatographic determination of catechol-O-methyltransferase activity
by S. Koh, K. Urayama and S. Kawai (Gifu, Japan) and Y. Takayama (Toyohashi, Japan) (Received March 22nd, 1991) 434

Gas chromatography of some polymethoxylated flavones and their determination in orange peel oils
by E. M. Gaydou, T. Berahia, J.-C. Wallet and J.-P. Bianchini (Marseille, France) (Received March 13th, 1991) 440

Electrophoresis

Capillary zone electrophoresis with a linear, non-cross-linked polyacrylamide gel: separation of proteins according to molecular mass
by A. Widhalm, C. Schwer, D. Blaas and E. Kenndler (Vienna, Austria) (Received April 4th, 1991) 446

Author Index 453

Erratum 456

In articles with more than one author, the name of the author to whom correspondence should be addressed is indicated in the article heading by a 6-pointed asterisk (*)

JOURNAL OF CHROMATOGRAPHY

VOL. 549 (1991)

JOURNAL of CHROMATOGRAPHY

INCLUDING ELECTROPHORESIS AND OTHER SEPARATION METHODS

ELSEVIER

AMSTERDAM — OXFORD — NEW YORK — TOKYO

J. Chromatogr., Vol. 549 (1991)

0021-9673/91/$03.50

Printed in The Netherlands

Journal of Chromatography, 549 (1991) 1–28
Elsevier Science Publishers B.V., Amsterdam

CHROM. 23 261

Review

Silica: backbone material of liquid chromatographic column packings

ALAIN BERTHOD

Laboratoire des Sciences Analytiques, Université de Lyon 1, UA CNRS 0435 (J. M. Mermet), 69622 Villeurbanne (France)

(First received April 4th, 1990; revised manuscript received February 21st, 1991)

ABSTRACT

More than 90% of column packings used in normal- and reversed-phase liquid chromatography (LC) are based on silica. This paper reviews the general properties of silica (SiO_2), the backbone material for LC column packings. First, the properties of the chemical SiO_2 are reported. A description of the crystallography and surface state of silica and the natural and artificial origin of silica is given. Next, the chemical properties of silica are surveyed. Acid–base properties, surface hydroxyl or silanol properties, silica derivatization reactions and the effect of hydrofluoric acid are detailed. The physico-chemical properties, particle shape and size, specific suface area and porosity with pore size and pore volume are given. The chromatographic requirements are outlined: pH and mechanical resistance, surface area, pore size and pore volume related to solute retention and selectivity, particle size related to efficiency and column permeability and carbon content and bonding density for reversed-phase LC packings. The properties of silica are tabulated listing the characteristics of several commercially available packings used for analytical normal- and reversed-phase LC.

CONTENTS

1. Introduction 2
2. The chemical SiO_2 3
2.1. Crystallography and surface state 3
2.1.1. Crystalline phases 3
2.1.2. Surface silanols 3
2.1.3. Silanol assessment 4
2.2. Origin of amorphous silica 6
2.2.1. Natural silica: diatomites 7
2.2.2. Liquid-phase synthesis of silica: silicate hydrolysis 7
2.2.3. The gas-phase route for synthesis of amorphous silica: pyrogenic silica 9
2.3. Chemical properties of synthetic silica 10
2.3.1. Water adsorption and desorption 10
2.3.2. Water solubility 11
2.3.3. Acid–base properties 11
2.3.4. Chemical reactions involving surface silanols 12

0021-9673/91/$03.50

3. Physico-chemical properties of silica 14
3.1. Particle size 14
3.1.1. Definition 14
3.1.2. Particle size determination 15
3.2. Surface area and porosity 15
3.2.1. Surface area 15
3.2.2. Porosity 16
3.2.3. Relationship between surface area and porosity 17
4. Applications to LC column packings 18
4.1. Particle size, pressure and efficiency 18
4.2. Polarity, surface, porosity and surface modification 19
4.2.1. Surface silanols and polarity 19
4.2.2. Silica surface and porosity 23
4.2.3. Carbon content and bonding density 24
4.3. Chemical and physical chromatographic requirements 24
4.4. Examples 26
5. Conclusions 26
6. Symbols 26
References 27

1. INTRODUCTION

Today, more than 90% of column packings used in normal- and reversed-phase liquid chromatography (LC) are based on silica. Silica exists in various forms with the stoichiometric composition SiO_2. Silicon, atomic number 14, atomic weight 28.08, makes up 25.7% (w/w) of the Earth's crust, and it is the second most abundant element, being exceeded only by oxygen, which constitutes 49.2%. Silicon is not found free in nature, but occurs chiefly as the oxide and as silicates. Interestingly, carbon, the first element of Group IVA of the Periodic Table, is the most important element in the living world. Silicon, the second element of Group IVA, with the same external electron layers (s^2p^2 with sp^3 hybridization) is the most important element in the lithosphere. More than 55% (w/w) of the Earth's crust is made up of silicon oxide and silicates. Granite, sand, asbestos, feldspar, clay, mica and flint are a few of the common silicate minerals. Quartz, rock crystal, amethyst, agate, jasper and opal are less common or rare silicon-containing stones used in jewelry [1].

In contrast of the widespread use of silica as LC column packings, its physico-chemical structure and chemical properties are often neglected by chromatographers. The books by Unger [2] and Snyder [3] can still be regarded as basic references in this field. The chemistry of silica is extensively described in the book by Iler [4].

The silica used for LC column packings is essentially porous and non-crystalline with the general formula $SiO_2 \cdot xH_2O$. Water is chemically bound in a non-stoichiometric amount, forming the Si–OH silanol groups most important for LC packing use [2,3]. Silanols are responsible for the polar character of silica packings used in normal-phase LC. They are used to graft organic moieties. This treatment changes the silica surface and allows to obtain the bonded phases used in reversed-phase and other modes of LC.

This paper reviews the physico-chemical attributes of silica, focusing on its use as an LC column packing. The chemical SiO_2 is the topic of Section 2. The crystallography and surface state of silica are briefly described; the origin of amorphous silica is

given and the chemical properties of SiO_2 are surveyed. Section 3 deals with the physico-chemical properties and structure of silica: particle size, surface area, and porosity. Part 4 considers the relevance of such properties in LC applications.

2. THE CHEMICAL SiO_2

2.1. Crystallography and surface state

As already stated, the silica used for LC column packings is mostly non-crystalline. Crystalline silica has a well defined network of Si and O atoms. The surface of the crystal is partially hydrated and bears some silanol groups.

2.1.1. Crystalline phase

Temperature changes induce crystallographic changes of silica. This can be simplified as follows: the crystalline quartz form is stable from room temperature to 870°C, the quartz form evolves into tridymite between 870 and 1470°C and from 1470°C up to the melting point (*ca.* 1700°C) the crystalline form is cristobalite. Fused silica can be moulded and cooled into silica glass, an amorphous form. Silica glass has good mechanical and optical properties, with a low coefficient of thermal expansion and high transparency in the ultraviolet, visible and near-infrared regions of the electromagnetic spectrum. Quartz is the most common crystalline form. There are more than 35 crystalline silica polymorphs known, with nine different crystalline forms of tridymite and at least three forms of cristobalite [5,6].

Such a variety of crystalline forms of silica exists because silicon and oxygen atoms can be arranged in octahedra (Fig. 1A) or in tetrahedra (Fig. 1B). The most stable forms, quartz and cristobalite, contain the tetrahedral structure with an Si–O bond length of 0.162 nm and an O–O distance of 0.264 nm.

It is possible to obtain hydrated pseudo-crystalline forms of silica by acid hydrolysis of crystalline silicates. The acid makes soluble the metallic ions of the silicate which are washed out. After rinsing with water and drying with acetone, a hydrated silica retaining the original silicate structure is obtained. For example, asbestos or chrysotile is a fibrous crystalline magnesium silicate. A fibrous "crystalline' hydrated silica is obtained by acid hydrolysis of asbestos [7].

Silicas used in chromatography do not produce any X-ray spectrum as they are amorphous.

2.1.2. Surface silanols

The surface of most silica forms is covered by hydroxylated silanol (Si–OH) groups. Fig. 2 shows the possible types of surface silanols. Two hydroxyl groups on two vicinal silicon atoms are vicinal silanols (Fig. 2, region 1). When they are borne by the same silicon atom, the two groups are termed geminal silanols (Fig. 2, region 2). Fig. 2, region 3, shows an isolated or free silanol group [2].

The surface of a crystalline form of silica is covered mainly by isolated silanol groups. Amorphous silica, with a porous structure and highly disordered surface, bears the three kinds of silanol arrangements as shown in Fig. 2.

Silanol groups can form hydrogen bonding with water molecules. The more elevated the surface silanol concentration, the greater is the hydrophilic character of

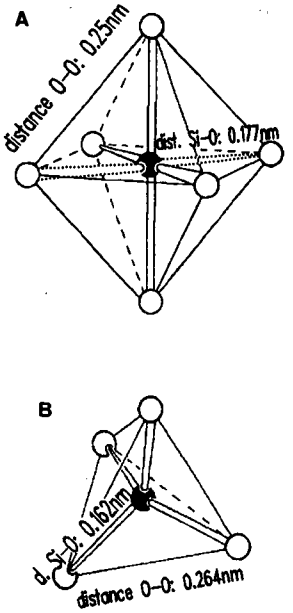

Fig. 1. Silica crystallography. (A) Octahedral organization; (B) tetrahedral organization.

the surface. As fully indicated elsewhere [62], the role of silanols in LC selectivity is essential. This is why it is very important to know the concentration of surface silanols for a given silica-based LC stationary phase.

2.1.3. Silanol assessment

There are several methods for the determination of surface hydroxyl groups, such as chemical, isotopic exchange and spectroscopic methods.

Chemical methods. All chemical methods use the acidic character of the hydrogen of the silanol hydroxyl group. The water hydrogens are more acidic than the silanol hydrogens, so all physisorbed water must be removed by heating the silica

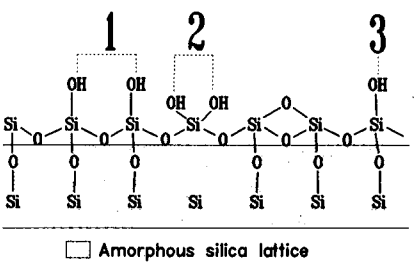

Fig. 2. Three different types of hydroxyl groups on the amorphous silica surface: (1) vicinal silanols; (2) geminal silanols; (3) isolated silanol.

sample at 150°C, under vacuum, for several hours. After the drying treatment under vacuum, the sample must not be exposed to the open air because water molecules of the atmosphere can be physisorbed again and rehydrate the sample. All chemicals must be added under a dry nitrogen atmosphere.

The most reliable estimate of surface silanol concentration is obtained by reaction of the hydroxyl groups with methyllithium [2,8]. Methyllithium is dissolved in a solvent [diisopentyl or diethyl ether, 5% (w/v)]. Provided that the sample was carefully dried, the solution reacts with hydroxyl groups as follows:

$$\equiv Si\text{–}O\text{–}H + LiCH_3 \rightleftharpoons \equiv Si\text{–}O^- Li^+ + CH_4$$

The amount of methane evolved is a direct measure of the silanol group surface content. If water molecules are present, methyllithium reacts with them first, producing lithium oxide (Li_2O) and methane; then it reacts with silanols. In such a situation, the measurement of methane is pointless. The methane is determined by gas chromatography [9,10]. The gas chromatograph is calibrated by injecting a known volume, C, of methane, which allows the determination of the volume, V, obtained when a mass, m, of dry silica with a specific surface area, S, is titrated by methyllithium. The surface silanol concentration, σ_{SiOH}, is then calculated with the equation

$$\sigma_{SiOH} = (V/22\,400) \cdot (P/101.5) \cdot (273/T) \cdot (10^6/mS) \quad (1)$$

where P and T are the measurement pressure (kPa) and temperature (K), respectively; V, m, S and σ_{SiOH} are measured in ml, g, m^2/g and $\mu mol/m^2$, respectively. The reaction is sterically hindered with silicas of an average pore diameter of $p_d < 6$ nm, owing to the formation of an etherate complex [11].

Diborane has also been used for silanol determination [12]. The reaction is

$$\equiv Si\text{–}O\text{–}H + B_2H_6 \rightleftharpoons \equiv Si\text{–}O\text{–}B_2H_5 + H_2$$

the hydrogen evolved being titrated. However, the result is very dependent on the stoichiometry of the reaction, which makes the method highly unreliable [8]. Trimethylchlorosilane has also been used:

$$\equiv Si\text{–}O\text{–}H + (CH_3)_3Si\text{–}Cl \rightleftharpoons \equiv Si\text{–}O\text{–}Si(CH_3)_3 + HCl$$

Owing to the difference in the molecular cross-sectional area of a trimethylsilyl group relative to a hydroxyl group (factor of two), only half of the total concentration of the surface hydroxyl group content is measured on a fully hydroxylated surface.

Isotopic exchange methods. Heavy water was used to determine the surface silanol concentration by isotopic exchange [2]:

$$\equiv Si\text{–}O\text{–}H + {}^2H_2O \rightleftharpoons \equiv Si\text{–}O\text{–}{}^2H + H^2HO$$

σ_{SiOH} is determined by weighing the dry sample before and after the exchange and/or by using spectroscopic methods [13].

Titrium-labelled water, H^3HO, is preferably employed instead of heavy water,

because radioactive counting of the exchanged sample is easy [11,14]. The exchange reaction is

$$\equiv Si\text{–}O\text{–}H + H^3HO \rightleftharpoons \equiv SiO\text{–}^3H + H_2O$$

A detailed procedure is given in ref. 11.

A dynamic isotopic exchange method was recently developed [15]. An LC column is packed with the silica under investigation and dehydrated with a dry solvent that cannot exchange protons (*e.g.*, dichloromethane or benzene). Next, the eluent is switched to the same one but containing a 1% (v/v) concentration of methanol or another miscible proton-exchange solvent. The breakthrough volume is measured. The solvent delivery system is then switched to an isocomposition eluent, but the methanol is isotopically tagged with tritium. The breakthrough volume of the tagged eluent is measured. The difference between the two measured volumes give the amount of silanols in the column [15].

Spectroscopic methods. Infrared (IR) spectroscopy has been used to assess surface silanol concentration [16]. The dried silica sample is formed in pellets under high pressure in a steel die. The IR spectrometer must be able to work under vacuum or a dry nitrogen atmosphere [17]. Three bands, located at 3747, 3680 and 3535 cm^{-1}, correspond to isolated hydroxyl groups, internal hydroxyl groups and vicinal hydrogen-bonded hydroxyl groups, respectively. On heating at 600°C, the 3680 and 3535 cm^{-1} bands disappear, showing the sensitivity of surface silanols to annealing treatment. IR spectroscopy can distinguish isolated silanol groups from vicinal groups. However, this technique cannot discriminate geminal silanol groups (Fig. 2, region 2) [16].

Nuclear magnetic resonance (NMR) of ^{29}Si with cross-polarization and magic angle spinning (MAS) can assess free and geminal silanol groups and also silicon atoms with no silanol [17–20]. NMR bands are observed at 91, 100 and 109 ppm, corresponding to geminal silanol groups, isolated silanol groups and siloxane without hydroxyl, respectively. Proton MAS-NMR can also be used. Broad bands are observed at 1 and 2.2 ppm for isolated and geminal hydroxyl groups. The sharpness and intensity of the band can be greatly enhanced on isotopic exchange with fully deuterated methanol [20]. The combination of MAS with multiple-pulse line narrowing (^1H combined rotation and multiple-pulse spectroscopy, ^1H CRAMPS) is a powerful method for detecting hydrogen-bonded hydroxyl groups and physisorbed water [19].

Other methods, such as thermogravimetric analysis, diffuse reflectance Fourier transform infrared spectroscopy or pH measurements, can be used for silanol determination. Several methods were compared by Köhler *et al.* [20].

2.2. Origin of amorphous silica

Crystalline forms of silica are found in nature. The unique natural amorphous silica source has a biological origin: it is diatomaceous earth. All other amorphous silicas used in industry are made by synthetic means. There are two methods to obtain pure silica: the liquid-phase route and the gas-phase route.

2.2.1. Natural silica: diatomites

Diatoms are microscopic aquatic, single-cel algae, disk-like or elongated in shape. They consist of single cells surrounded by two half-cell walls or valves of transparent silica about 0.1 μm thick and made up of patterns of chambers and lace-like partitions of extreme beauty and complexity [4]. Fig. 3 shows an intact shell of a diatom. Most natural deposits of diatom skeletons are millions of years old and partially crystalline.

Diatomaceous earth or diatomite contains mainly silica. However, the exact composition of a given sample differs depending on the extraction point. The silica content is often around 90% with minor elements such as aluminium, calcium, iron, magnesium and sodium [21]. Diatomite is occasionally used as an LC packing but most often in gas chromatography (*e.g.*, Chromosorb stationary phases).

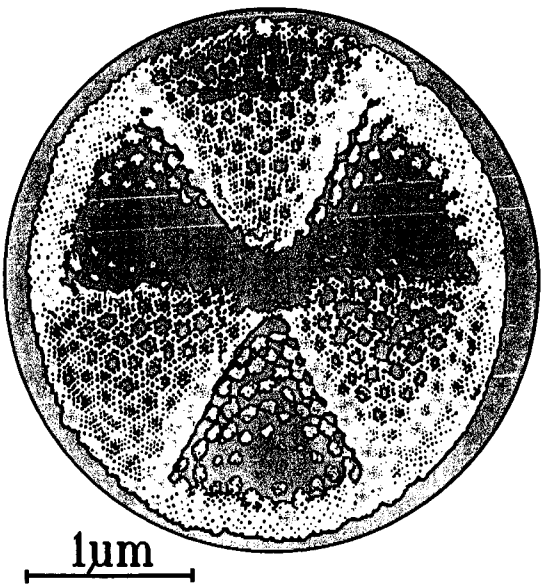

Fig. 3. An intact diatom.

2.2.2. Liquid-phase synsthesis of silica: silicate hydrolysis

Most porous silicas used in LC packings originate from the liquid-phase synthesis route. Fig. 4 is a simplified diagram of the industrial scheme used to produce 99% pure silica gel or silica powder. Sand or a silica-containing ore is heated with sodium carbonate to form a vitreous sodium silicate, which is dissolved in water. The basic solution is filtered and then acidification with sulphuric acid induces silicic and polysilicic acid formation. The polysilicic acids are the nuclei for the formation of colloidal silica particles. Next these microparticles can form a three-dimensional aggregate of pure and porous silica gel, or a precipitate. The silica gel is washed and dried. The drying process produces a hard silica gel or xerogel. On drying the washed precipitate produces a polydisperse porous silica powder.

Drying the bulk wet silica gel produces shrinkage. The wet silica gel consists of

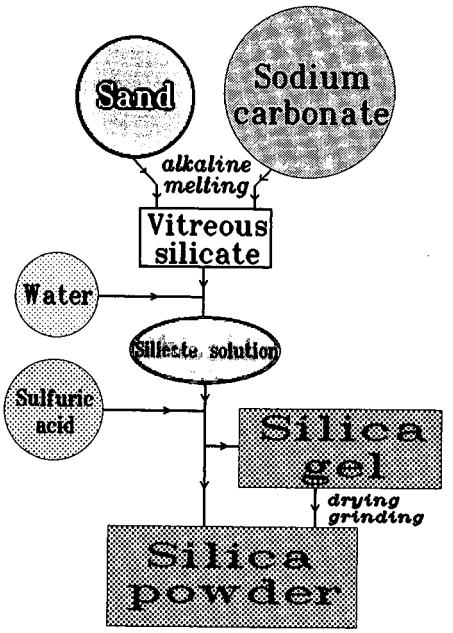

Fig. 4. Preparation of synthetic silica.

very fine grains separated by water capillary tubes, and arranged in a three-dimensional network. As the gel dries, shrinkage occurs owing to the surface tension of water in the tubes that become pores. A certain number of particle-to-particle bonds are created during the process, which makes it irreversible [4]. The solid pieces of hard silica gel are ground and sieved to give porous silica powders with angular particules.

If the neutralized silicic acid solution is allowed to age with gentle stirring, Ostwald ripening occurs, *i.e.*, the larger silica particles grow at the expense of the smaller particles. Ageing and ripening increase the size of silica particles, decreasing the specific surface area and increasing the pore volume.

To obtain spherical porous silica powder, it is necessary to dry it without shrinkage. The aqueous phase can be replaced with an organic phase, *e.g.*, an alcohol. Heating above the critical temperature so that there is no meniscus between the liquid and gas phases and venting off the vapours allows drying withough shrinkage [4]. Perfectly spherical silica particles for LC packing are often prepared by subdividing the neutralized silicate solution (the colloidal silica sol) into fine droplets before gelling. Next, the droplets are suspended in air and dried. It is also possible to disperse the colloidal silica sol in an immiscible liquid (oil) to form emulsions in which the sol droplets solidify in a spherical form [22]. Also, coacervation of the colloidal silica sol can be induced by an organic agent to form droplets which are subsequently solidified. A heat treatment burns out the organic material and induces some sintering that strengthens the silica framework and produces spherical porous silica particles [4,22].

As shown, the drying process can dramatically change the characteristics of the porous silica obtained. The problem is that many parameters influence the final prop-

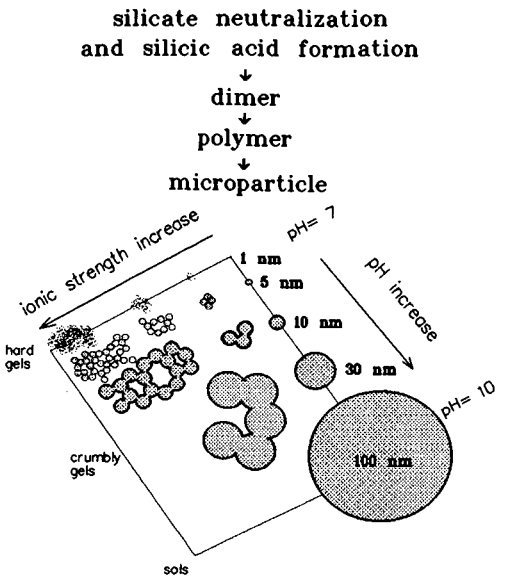

Fig. 5. Effect of ionic strength and pH gradient on the structure of the silica obtained.

erties of porous silica, namely the temperature, the concentration of the silicate solution and the neutralizing acid solution, the pH gradient, the ionic strength, the final pH, the delay time for gel ageing, the effect of additives (*e.g.*, ammonia acts as a coagulant) and the stirring energy or other external pressure or forces applied to the reactor.

Fig. 5 illustrates the effect of two parameters, ionic strength and pH gradient. The pH value of sodium silicate is *ca.* 12. On addition of an acid, the pH can be rapidly lowered to 7 or slowly lowered to 10. A rapid decrease in pH induces very small microparticles, with diameters in the nanometre range. A gentle decrease in pH produces 100 times larger initial particles. A low ionic strength does not favour the three-dimensional organization and produces precipitates. A high ionic strength favours gel formation (Fig. 5) [4]. The crucial effect of these two parameters on the final porous silica obtained shows the importance of know-how in silica-based LC packing preparation. Each manufacturer has developed their own skills to prepare porous silica with the required particle size, specific surface area, pore volume, pore size and pore size distribution.

Trace amounts of sodium may be present in silicas obtained by silicate hydrolysis. Highly pure silicas, without sodium, withstand alkaline solutions: they are stable in aqueous solutions of pH 9. Such silicas are synthesized by hydrolysis of purified tetraethoxysilane [$Si(OC_2H_5)_4$].

2.2.3. The gas-phase route for amorphous silica synthesis: pyrogenic silica

Pyrogenic silica are non-porous micro-powders with particle diameters in the few nanometres range. The industrial process uses the oxidation of silicon tetrachloride vapour. Silicon tetrachloride ($SiCl_4$) is easily prepared from lump silicon

which burns in chlorine gas. $SiCl_4$ is purified by distillation (boiling point 57.6°C). The oxidation reactions [23]

$$SiCl_4 + 2H_2 + O_2 \rightleftharpoons SiO_2 + 4HCl$$

or

$$SiCl_4 + CH_4 + 2O_2 \rightleftharpoons SiO_2 + 4HCl + CO_2$$

occur in a flame. Changing the combustion speed and the gas composition will affect the particle diameter and hydrophobicity. An excess of hydrogen or methane produces silanol-containing particles. An excess of oxygen gives hydrophobic particles without silanols. However, the gas-phase route is not well suited for the preparation of silica LC packings because poreless silica microspheres with too small diameters are obtained.

2.3. Chemical properties of synthetic silica

Most chemical properties of silica are due to surface silanols. Interactions of silica with water are silanol dependent. The hydroxyl acidity is responsible for the acid–base properties of silica. Silanols are used to graft various organic moieties on the silica surface and to obtain the wide variety of bonded silica essential for LC packings.

2.3.1. Water adsorption and desorption

As stated before, silica hydroxyl groups are associated with water molecules by hydrogen bonding. This adsorbed water is tightly bound to the silica surface, and is removed by heating at 150°C under vacuum for several hours. Overheating a silica sample produces dehydroxylation. Geminal silanols are reversibly dehydroxylated giving siloxane bridges:

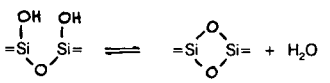

Between 200 and 800°C, the temperature treatment under vacuum of a silica sample induces a monotonous decrease in the hydroxyl group concentration with siloxane bridge formation. If the calcination temperature does not exceed 600°C, the reactive siloxane group completely rehydroxylates when exposed to water [24].

Complete dehydroxylation and sintering occur on heating above 1200°C. At this elevated temperature, the amorphous character of the silica can be slowly lost. The sample crystallizes in the stable cristobalite form. The hydrophilic surface is converted into a hydrophobic surface [24,25]. The conversion of amorphous silica into the crystalline form is very dependent on the purity of the silica, particularly on its sodium content. A highly pure silica remains amorphous even on exposure to a temperature of 1400°C for several weeks.

At room temperature, synthetic porous silica can adsorb water reversibly. Silica

powder is used to dry gases and is added to powders to reduce agglomeration due to humidity.

2.3.2. Water solubility

Water solubility is very dependent on the crystalline or amorphous form of the sample, and also on physico-chemical characteristics such as porosity, surface area and particle size. The water temperature, pressure and pH change the solubility of silica. The solubilization equation is

$$SiO_2 + 2H_2O \rightleftharpoons Si(OH)_4$$

The solubility of crystalline and glass forms of silica is in the parts per million range (ppm = mg/l) [4]. The concentration of dissolved silica in rivers varies from 5 to 20 ppm. In sea water, the range is from 0.01 ppm in the Pacific Ocean to 10 ppm in the Mediterranean Sea. The dissolved silica concentration is very sensitive to the presence and concentration of other salts. All living cell fluids contain a few ppm of dissolved silica [4]. The solubility of silicic acid [$Si(OH)_4$] is greatly dependent on the pH of the solution.

2.3.3. Acid–base properties

Silicic acid is a weak acid. The ionization constant of the reaction

$$Si(OH)_4 \rightleftharpoons Si(OH)_3O^- + H^+$$

is $1.6 \cdot 10^{-10}$ at 20°C, which corresponds to a pK_a value of 9.8. The pK_a value of the second ionization:

$$Si(OH)_3O^- \rightleftharpoons Si(OH)_2O_2^{2-} + H^+$$

is 11.7. At a pH of 11.7, all silanol groups ionize simultaneously. Most glasses contain silica and they can be attacked by a strongly alkaline solution.

The hydroxyl groups on the porous silica surface have also an acidic character. The pK_a value of the reaction

$$\equiv Si\text{–}O\text{–}H \rightleftharpoons \equiv Si\text{–}O^- + H^+$$

is about 6.8 ($\pm$ 0.5), which is 3 pH units lower than the free silicic acid first ionization [26]. There are several explanations for the higher mobility of the silanol proton compared with the silicic acid. The tendency for splitting off a proton from a particular silanol group is markedly promoted by its environment. For example, hydrogen bonding between adjacent surface silanols can facilitate the reaction with hydroxide ions [2,26].

The acidic character of surface silanols confers some ion-exchange properties on porous silica. In buffer or electrolyte solutions, the hydronium ions (protons) of the silanol groups are exchangeable by cations of the solution. The ion-exchange properties of silica are highly dependent on the pH of the solution, the surface area and the silanol concentration. At pH 7, silica bears negative charges in solution. The

isoelectric point of silica is close to pH 2.5 [2,4], but is at higher pH for some silica samples [27]. Owing to its low capacity, between 0.1 and a maximum of 2 mequiv./g, porous silica is not a suitable sorbent for ion-exchange chromatography. However, its mechanical and chemical properties make silica useful as an ion exchanger for the removal of cations in radioactive waste materials [28,29]. This ability to exchange ions must be known when porous silica is used as an LC column packing.

The other result of the mobility of proton silanols is well known by chromatographers namely the rapid dissolution of silica at mobile phase pH values higher than 10 and/or at temperatures higher than 40°C. A slow and insidious solubilization occurs from pH 8. This can produce small voids in the column packing, inducing changes in solute retention and especially efficiency losses. This is known as column ageing. It can be reduced by the use of a guard column or a precolumn installed between the pump and the injection valve to saturate the mobile phase in soluble silica. Important work has been done to improve the pH stability. As the solubility is a function of the purity of silica, it is economically worthwhile to make highly pure silica from alkoxysilanes (*e.g.*, Kromasil, Table 2). Such silicas are stable for months in aqueous solutions at pH 9.2 (ammonia buffer) [30]. Another way to reduce the dissolution problem is the "doping" of silica with metal oxides such as alumina or zirconia. Zirconia-treated silica were found to be stable at pH 9.5 for a long period [31].

The acid–base properties of porous synthetic silica are due to surface hydroxyl groups. There are several other chemical reactions involving surface silanols.

2.3.4. Chemical reactions involving surface silanols

As far as LC packing are concerned, the most important chemical reactions involving surface silanols are the surface changes of silica by organic bonding reactions. Such reactions are used to produce the wide assortment of bonded phases for LC use [24]. The goal of such reactions is to create Si–C bonds on the silica surface. The Si–C bond was found to be the most suitable for chromatographic use of the derivatized silica. The Si–C bond withstands hydrolysis when the derivatized silica is used as packing in reversed-phase LC with aqueous–organic mobile phases; Si–O–C, Si–N–C and Si–O–C=O bonds do not.

Bonding reactions. The full description of the wide variety of bonding reactions used to produce LC packings is beyond the scope of this section; such a description can be found elsewhere [62]. Only the mechanism of silica bonding reactions is given here. It is possible to create Si–C bonds directly by reaction of a Grignard organometallic compound with the chlorinated silica [32]:

$$\equiv Si\text{–}Cl + RMgBr \rightleftharpoons \equiv Si\text{–}R + MgBrCl$$

where R is an alkyl group. This route is less frequently used to prepare bonded silica. Most often, the Si–C bond pre-exists in the bonding reagent. Alkylchlorosilanes and alkylaminosilanes are used. They react directly with silanols after desorption of adsorbed water by heating the silica sample at 200°C under vacuum for about 12 h. With an alkylmonochlorosilane, the reaction in dry toluene is

$$\equiv Si\text{–}O\text{–}H + Cl\text{–}SiR_3 \rightleftharpoons \equiv Si\text{–}O\text{–}SiR_3 + HCl$$

Usually the three R alkyl groups are not identical for steric hindrance reasons. For example, two of them may be methyl groups and the third a long-chain alkyl (butyl, octyl, decyl or octadecyl). Bonding with an alkyl monochlorosilane produces a monomeric or monofunctional "brush-type" bonded silica. Polymeric or polyfunctional bonded layers can be obtained using an alkyldi- or -trichlorosilane bonding reagent. With a trichlorosilane, the reaction is

$$\equiv Si\text{–}O\text{–}H + R\text{–}SiCl_3 \rightleftharpoons \equiv Si\text{–}O\text{–}SiRCl_2 + HCl$$

Trace amounts of water may hydrolyse some Si–Cl bonds:

$$\equiv Si\text{–}O\text{–}SiRCl_2 + 2H_2O \rightleftharpoons \equiv Si\text{–}O\text{–}Si(OH)_2R + 2HCl$$

and another trichlorosilane molecule can react with newly created silanols:

$$\equiv Si\text{–}O\text{–}Si(OH)_2R + R\text{–}SiCl_3 \rightleftharpoons \equiv Si\text{–}O\text{–}Si(OH)R\text{–}O\text{–}SiCl_2R + HCl$$

and so on. A polymer layer is generated. The structure of the bonded organosilane layer was elucidated by ^{13}C and ^{29}Si cross-polarization MAS-NMR spectroscopy [33].

Alkyldimethylaminosilanes can react with more silanol groups than chlorosilanes. The produce the highest bonding density [34]. Alkyldimethylaminosilanes are synthesized from the corresponding alkylmonochlorosilane:

$$R_3Si\text{–}Cl + 2HN(CH_3)_2 \rightleftharpoons R_3Si\text{–}N(CH_3)_2 + (CH_3)_2H_2N^+ Cl^-$$

The alkylammonium chloride precipitates. The bonding reaction in dry toluene or dichloromethane is

$$\equiv Si\text{–}OH + R_3Si\text{–}N(CH_3)_2 \rightleftharpoons \equiv Si\text{–}O\text{–}SiR_3 + HN(CH_3)_2$$

Because there is one additional step, the aminosilane route is seldom used to produce derivatized silica in industry.

Reaction with HF. Silica is acid resistant, but hydrofluoric acid (HF) can convert it rapidly to fluorosilicic acid at room temperature:

$$SiO_2 + 6HF \rightleftharpoons 2H^+ + SiF_6^{2-} + 2H_2O$$

Although HF, at any concentration, is a dangerous reagent, this reaction can be useful for silica characterization. HF destroys and dissolves the silica backbone of bonded silica used as LC packings without disrupting the Si–C bonds. The bonded moieties are released as volatile organo mono-, di- or trifluorosilanes, R_3–Si–F, R_2–SiF_2 or R–SiF_3, respectively. The determination, by gas chromatography, of the volatile organosilanes released allows the characterization of the structure of the bonded layer of the silica attacked by HF [35–37].

3. PHYSICO-CHEMICAL PROPERTIES OF SILICA

The three most important physico-chemical parameters for silica are the particle size, the surface area and the porosity. Other important parameters are the particle shape, the carbon percentage, the ligand density and bonding structure and the surface silanol concentration.

3.1. Particle size

3.1.1. Definition

Silica packings are always obtained with a particle distribution, *i.e.*, a stated 5-μm particle diameter is an average diameter. The average particle diameter can be defined as the average diameter in number, d_n, the average particle diameter in surface, d_s, or the average diameter in mass, d_m, as follows:

$$d_n = \Sigma n_i d_i / N = \Sigma n_i d_i / \Sigma n_i \tag{2}$$

$$d_s = (1/S)\Sigma n_i d_i^3 \, \pi/4 = \Sigma n_i d_i^3 / \Sigma n_i d_i^2 \tag{3}$$

$$d_m = (4\pi\rho/3M)(\Sigma n_i d_i^4) = \Sigma n_i d_i^4 / \Sigma n_i d_i^3 \tag{4}$$

where n_i is the number of particles with diameter d_i, N is the total number of particles in the studied sample, S is the surface area of the sample, M is the sample mass and ρ is the density of the particles.

Fig. 6 illustrates the case of an imaginary sample which contain 10% of 1-μm, 20% of 2-μm, 40% of 3-μm, 20% of 4-μm and 10% of 5-μm particles. The average diameters are 3, 3.71 and 3.95 μm in number, surface and mass, respectively. The values d_{90} and d_{10} are the diameters of which 90% and 10% of the particles are smaller than or equal to, respectively; they are 4 and 2 μm, respectively, for the sample in Fig. 6. The ratio d_{90}/d_{10} gives information on the width of the particle size distrubtion.

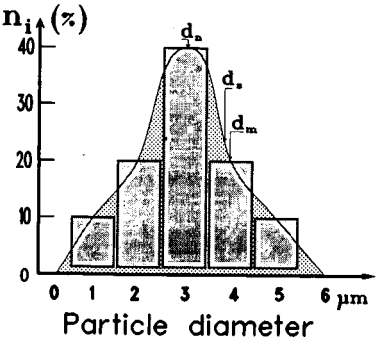

Fig. 6. Histogram of the hypothetical silica sample described in the text. d_n = Mean particle diameter in number; d_s = mean particle diameter in surface; d_m = mean particle diameter in mass.

For spherical packings, most manufacturers give the average particle diameter in number, seldom with the d_{90}/d_{10} ratio. For irregularly shaped particles, the average particle diameter given is often expressed as an equivalent mass diameter of a sphere.

3.1.2. Particle size determination

Silica-based LC packings have a particle size ranging from 1 to 100 μm. Microscopy is the simplest method to determine particle sizes. Electronic counting scanners can give a particle size distribution, with little or no assumptions on the particle shape. Sedimentation is another widely used method for particle size analysis. The particle sample is suspended in a liquid at a concentration below 1% (v/v). The suspension is homogenized in an ultrasonic bath and poured into the cell of the apparatus. Some types of apparatus use a centrifugal field with optical detection to analyse the particle size distribution. Others use a laser beam whose diffused light is analysed and deconvoluted to produce the results. Most often a particle size histogram is printed together with the average diameter in number and in mass. Brinkman, Coulter, Duke, Malvern and Perkin-Elmer are some companies making reliable particle size analysers [38]. However, these analysers, being based on different principles, yield different diameter values (number, surface or mass) for the same material. Monodisperse latex beads are used for calibration.

3.2. Surface area and porosity

3.2.1. Surface area

The specific surface area of a porous solid is equal to the sum of its internal and external surface areas [2,4]. The external surface area corresponds to the geometric surface of particles per gram of sample. For spherical particles of equal size, d_p, the external surface area is given by

$$A_s = 6/d_p\rho \tag{5}$$

where ρ is the particle density, defined as the ratio of particle mass to particle volume. For non-porous particles, ρ is the solid silica density, 2.2 g/cm^3. The external surface area is inversely proportional to the particle diameter. A monodisperse non-porous silica, with a particle size of 3 μm, has a surface area of 0.91 m^2/g. Polydisperse non-porous silica with an average particle diameter of 3 μm (Fig. 6) has a surface area of 0.74 m^2/g, which corresponds to a monodisperse silica with a particle diameter of 3.71 μm, by definition.

Surface area is routinely measured using the BET method [39]. Gas adsorption isotherms are determined at different partial pressure and at a temperature at which the gas is in the liquid state (77 K for nitrogen). The surface area is directly proportional to X_m (mol/m^2), the amount of gas corresponding to a monolayer of adsorbed molecules:

$$A_s = X_m a_m N \tag{6}$$

where a_m is the area of one gas molecule (0.162 nm^2 per nitrogen molecule) and N is Avogadro's number ($6.02 \cdot 10^{23}$ molecules/mol). The BET equation is [40]

$$[P/X(P - P_o)] = (1/X_mC) + [(C - 1)/X_mC)(P/P_o)] \quad (7)$$

where P is the gas partial pressure, P_o is the saturation vapour pressure, X is the amount of gas adsorbed, X_m is the amount of gas adsorbed when the monolayer is complete and C is a constant related to the energy of interaction between the adsorbate (gas) and the adsorbent (silica).

Using a mixture of 3% (v/v) nitrogen in helium, it is possible to determine the adsorbed amount, X, by gas chromatography [41]. Increasing stepwise the pressure of the gas mixture on the sample at 77 K increases the partial pressure, P, of nitrogen, giving several X values that allow one to extrapolate and to calculate X_m and C [41,42].

The complete theory of gas adsorption and specific surface area determination can be found in the book by Gregg and Sing [40]. The surface area of a silica sample is greatly dependent on the porosity which produces the internal surface area. The specific surface area of silicas used in high-performance liquid chromatography ranges from 10 to about 500 m^2/g, depending on the average pore diameter.

3.2.2. Porosity

A pore can be defined as a hole, a cavity or a channel communicating with the surface of the solid. The spaces or interstices between particles are voids rather than pores. A cavity that does not communicate with the surface is called a closed pore or an internal void and will not contribute to the porosity or specific surface area [40].

Pore systems and their characteristics are the topic of numerous works [43]. The pore shape may have a wide variety. The pore size covers a range of several orders of magnitude. A feature of special interest is the width, p_d, of the pores which is the diameter of an equivalent cylindrical pore. The classification of Dubinin [44], adopted by IUPAC [45], is micropores with $p_d < 2$ nm, mesopores with $2 < p_d < 50$ nm and macropores with $p_d > 50$ nm.

The porosity of a sample, ε_p, is defined as the total pore volume, V_p, divided by the volume of the sample, V_T:

$$V_T = V_p + V_s \quad (8)$$

where V_s is the volume of solid silica, assuming there are no closed pores. The pore volume and pore size distribution are estimated by gas adsorption–desorption isotherms or by mercury intrusion techniques [2,40].

The adsorption–desorption isotherms of gas onto solids can be arranged in six different types [40,43,45]. Type I, IV and V isotherms show hysteresis, *i.e.*, the desorption branch of the curve does not coincide with the adsorption branch. Both branches are used in pore shape and volume determination. Types I, IV and V correspond to microporous, mesoporous and polydisperse porosity, respectively. Types II and III correspond to non-porous samples with strong interaction and non- or macroporous samples with weak interaction, respectively. Type VI, the step-like isotherm, corresponds to non-porous material [45]. A mathematical treatment with as-

sumptions allows one to estimate the mean pore diameter with some information on the pore size distribution. Nitrogen, at the nitrogen boiling point (77 K), is the most commonly used gas for sorption studies. Experimentally, before any measurement, the sample must be carefully degassed under vacuum and heated at about 200°C.

The mercury intrusion method is used in automated apparatus to produce the pore size distribution and the mean pore diameter. Mercury does not wet a solid surface. At atmospheric pressure it does not penetrate pores whose diameters are smaller than 15 μm. To force mercury to penetrate a pore with diameter p_d, a pressure ΔP must be applied:

$$\Delta P = 4\gamma_{Hg} \cos \theta / p_d \tag{9}$$

where γ_{Hg} is the surface tension of mercury (0.48 N/m at 25°C) and θ the mercury contact angle (140° at 25°C). It can be calculated that a pressure of 100 MPa (1000 bar or 14 300 p.s.i.) is necessary to push mercury into a 15-nm pore [40]. The volume taken up by the porous sample, V_{Hg}, is measured as the applied ΔP pressure is gradually increased. At any ΔP value, V_{Hg} corresponds to the cumulative volume of all pores having a radius greater than or equal to the corresponding p_d (eqn. 9). The pore size distribution curve is the derivative of the V_{Hg} *versus* ΔP curve.

For a sample with a wide pore size range, the gas sorption and mercury intrusion methods must be used. The gas sorption method produces accurate results in the pore size range between 0.5 and 50 nm (micro- and small mesopores), whereas mercury porosimetry measures pores larger dan 5 nm up to 15 μm (large macropores). The minimum pore size measurable is determined by the maximum pressure of mercury; 5 nm corresponds to 300 MPa (3000 bar or 43 000 p.s.i.). The two methods are complementary [40].

3.2.3. Relationship between surface area and porosity

Pore size, pore volume and specific surface area are related. Assuming there are no closed pores, the specific pore volume, V_p, in cm^3/g, is related to ρ_a, the apparent density of the particle defined as the ratio of the mass of the porous particle to its total volume (g/cm^3):

$$\rho_a = \rho/(1 + V_p\rho) = 2.2/(1 + 2.2V_p) \tag{10}$$

The density of solid silica is 2.2 g/cm^3. Assuming a monodisperse distribution of perfectly cylindrical pores with diameter p_d, the internal surface area due to the pores is expressed by

$$A_p = 4V_p/p_d \tag{11}$$

The specific surface area is the sum of the external surface area (eqn. 5) with the corrected density (eqn. 10) and the internal surface area (eqn. 11):

$$A_s = 6(1 + V_p\rho)/d_p\rho + 4V_p/p_d \tag{12}$$

Table 1 shows the great importance of the pore diameter on the surface area and the

relative weight of the internal and external surface areas. The ranges of value for particle diameters, pore volumes and pore diameters are typical for silica used in LC packings. For most samples, more than 97% of the specific surface area is internal surface area due to pores. Hence, the particle diameter has little importance with regard to the surface area, which depends mainly on the pore size and volume. A silica sample with pore volume 0.5 cm^3/g and mean pore size 10 nm has a specific surface area of 200 m^2/g, whatever the particle size is (Table 1).

4. APPLICATIONS TO LC COLUMN PACKINGS

Most of the examples given to illustrate the chemical or physico-chemical properties of silica were taken from silica samples typically used for LC packings. The chromatographic technique constrains the range of the particle size, the pore size and volume for reasons considered below.

4.1. Particle size, pressure and efficiency

Particle size is one of the most important parameters acting on chromatographic efficiency. The smaller the LC packing particle size, the higher is the efficiency [46]. The plate height, H, of a well packed column can be as low as twice the mean particle diameter (100 000 plates/m, $H = 10$ μm with $d_p = 5$ μm).

TABLE 1

EFFECT OF PORE VOLUME AND PORE SIZE ON SPECIFIC SURFACE AREA

Particle diameter (μm)	Pore volume (cm^3/g)	Pore diameter (nm)	Surface area[a]	
			Total (m^2/g)	Internal (% of total surface)
100	1.0	50	80.1	99.9
		10	400.1	99.9
		5	800.1	100
	0.5	50	40.1	99.8
		10	200.1	99.9
		5	400.1	100
	0.1	50	8.0	99.6
		10	40.0	99.9
		5	80.0	99.9
3	1.0	50	82.9	96.5
		10	402.9	99.3
		5	802.9	99.6
	0.5	50	41.9	95.4
		10	201.9	99.1
		5	401.9	99.5
	0.1	50	9.1	87.8
		10	41.1	97.3
		5	81.1	98.6

[a] Surface area calculated with eqn. 12. Internal % due to pores in the ratio A_p (eqn. 11) to total surface area.

Unfortunately the particle size affects the column permeability, $\bar{P}$ (cm^2), in the following way:

$$\bar{P} = (d_p^2/Y)[\varepsilon_o^2/(1 - \varepsilon_o)^2] \quad (13)$$

where Y is a dimensionless shape factor ($Y = 180$ for spherical particles) and ε_o is the interstitial volume or external porosity (cm^3). The permeability is a parameter of the column pressure drop, ΔP

$$\Delta P = u\eta L/\bar{P} \quad (14)$$

where u is the linear mobile phase velocity (cm/s), η the mobile phase viscosity (g/cm · s) and L the column length (cm). If the particle diameter is divided by a factor of two, the column driving pressure should be four times higher in order to obtain the same flow-rate.

The optimum particle size with regard to analysis time, plate number and pressure drop is *ca.* 2–4 μm [47,48]. Packings with average particle diameter 5 μm are the most commonly used for 10–25-cm analytical columns with I.D. 4–4.6 mm. Packings of 3 μm are used to obtain high efficiency with short columns; 10-μm, 20-μm or larger particle size packings are used when pressure is an important factor, such as in preparative chromatography.

Pyrogenic silicas cannot be used directly for LC packings as their mean diameter, in the few nanometres range, is too small. The column permeability (eqn. 13) would be very low and a tremendous driving pressure (eqn. 14) would be necessary to push any mobile phase, which is mechanically impossible. Pyrogenic non-porous silicas have been used to coat 30-μm glass beads to obtain a 1-μm superficially porous layer. Such packings were popular in the 1970s and commercialized under trade names such as Corasil, Pellosil, Perisorb, Vydac 101 and Zypax [2].

4.2. Polarity, surface, porosity and surface modification

4.2.1. Surface silanols and polarity

Silanol groups are responsible for the polarity of the silica surface. A silica completely dehydroxylated by prolonged heating at 1300°C is hydrophobic. The silanol concentration of a fully hydroxylated silica is about 9 $\mu mol/m^2$. The pretreatment temperature under vacuum can decrease the silanol concentration and adjust the hydrophilic character of a sample [49]. Fig. 7 shows the evolution of silanol concentration *versus* temperature for a precipitated silica. Above 200°C, the hydroxyl surface concentration decreases rapidly. At 500°C, only one quarter of the initial silanols remain (concentration between 2 and 3 $\mu mol/m^2$). However, as long as the temperature does not exceed 1200°C, the dehydroxylation is partially reversible.

It has been shown that the selectivity with a thermally treated silica used in normal-phase LC is greatly dependent on the apolar mobile phase water content [3,50]. Reproducible results with activated silicas and apolar solvents such as *n*-hexane are only obtained when the water content of the silica and the mobile phase is adjusted and controlled [51]. Water molecules, always present in trace amounts in an apolar solvent, adsorb on the most polar silanol sites, decreasing the retention of

TABLE 2

SOME SILICA-BASED LC STATIONARY PHASES

Name	Manufacturer[a]	Particle size (μm)	Particle shape[b]	Surface area (m^2/g)	Pore diameter (nm)	Pore volume (cm^3/g)	Bonding		
							Type[c]	C (%)	Density ($\mu mol/m^2$)
Accusphere	J&W	3, 5, 7	O	210	12	0.63	C_1	2.6	3.6
							C_8	7.0	3.1
							C_{18}	10.5	2.4
Adsorbosphere	Alt	3, 5, 7, 10	O	200	8	0.40	C_{18} m ec	12	3.0
Adsorbosphere HS	Alt	3, 5, 7, 10	O	350	6	0.53	C_{18} m ec	20	3.2
Apex	JoC	8, 15, 20	O	190	13	0.80	C_8	7	3.4
							C_{18}	11	2.8
Bakerbond	JTB	3, 5, 10	K	200	15	0.75	Bare	–	–
							C_8 ec	–	–
							C_{18} ec	15	3.9
Bakerbond Wp	JTB	3, 15, 40	K	100	30	0.75	C_4	–	–
							C_8	–	–
							C_{18}	–	–
Econosil	Alt	5, 10	K	450	6	0.68	C_8 m	10	2.2
							C_{18} m	15	1.7
Econosphere	Alt	3, 5, 10	O	200	8	0.80	C_8 m	5	2.2
							C_{18} m	10	2.4
Hypersil	Shd	3, 5, 10	O	170	12	0.60	C_1 m ec	2.6	4.5
							C_8 m ec	7	3.8
							C_{18} m ec	10	2.8
Inertsil	Int	5	K	320	15	1.20	Bare	–	–
							C_8 m ec	10.5	3.2
							C_{18} m ec	18.5	3.2
Intersphere	Int	5, 7	O	500	8	1.0	Bare	–	–
							C_{18} m ec	18	2.0
							C_{18} p ec	22	–
Kromasil	Eka	5–20	O	340	10	0.90	Bare	–	–
							C_8 m	12	3.5
							C_{18} m	19	3.1
LiChrosorb Si 100	Mer	5, 10	K	300	10	0.75	C_8	8	2.5
							C_{18}	13	2.2

LiChrosorb Si 60	Mer	5, 10	K	500	6	0.75	C_8	9	1.7
							C_{18}	16	1.7
LiChrosphere 100	Mer	5, 10	O	340	10	1.0	C_{18} p	21	–
							C_{18} p ec	21.5	–
Nucleosil	Nag	3, 5, 7, 10	O	500	5	0.80	Bare	–	–
				350	10	1.0	Bare	–	–
				350	10	1.0	C_8 m	8	2.1
				350	10	1.0	C_{18} m	14	2.0
				200	12	0.7	Bare	–	–
				100	30	0.75	Bare	–	–
				35	50	0.9	Bare	–	–
				25	100	0.75	Bare	–	–
				10	400	0.7	Bare	–	–
Partisil	Wht	5, 10	K	350	8.5	0.74	C_8 m ec	9	2.5
							C_{18} p	5	–
							C_{18} p	15	–
							C_{18} p ec	10.5	–
Partisphere	Wht	5, 10	O	160	12	0.48	C_8 m ec	6	3.4
							C_{18} m ec	11	3.3
Rexchrom	Reg	3, 5	O	200	10	0.5	C_1 ec	–	–
							C_8 ec	–	–
							C_{18} ec	–	–
R-Sil	Mer	5, 10	K	400	8	0.8	C_8 m ec	9	2.2
							C_{18} m ec	16	2.1
RoSil	Alt	5, 10	O	250	9	0.56	C_{18} m	18	3.9
Spheri S	Bro	5, 10	O	–	8	–	C_8 ec m	–	–
							C_8 p	–	–
							C_{18} m ec	–	–
							C_{18} p	–	–
Spherisorb	PhS	3, 5, 10	O	220	8	0.44	C_1 m	2	2.6
							C_8 m ec	6	2.5
							C_{18} m	6	1.2
							C_{18} m ec	12	2.7
Spherisorb WP	PhS	5, 10	O	190	30	1.43	C_1	2	3.0
							C_3	3	2.8
							C_6	5	3.0
							C_{18}	12	3.1

(*Continued on p. 22*)

TABLE 2 (*continued*)

Name	Manufacturer[a]	Particle size (μm)	Particle shape[b]	Surface area (m^2/g)	Pore diameter (nm)	Pore volume (cm^3/g)	Bonding		
							Type[c]	C (%)	Density ($\mu mol/m^2$)
Supelcosil	Sup	3, 5	O	170	10	0.43	C_8 m	–	–
							C_{18} m	–	–
Ultrabase	SFC	5, 10	O	340	10	0.90	C_8 m	12	3.4
							C_{18} m	19	3.1
Ultracarb	Phe	5, 7	O	550	6	0.83	C_{18}	31	3.9
		5, 10	O	370	9	0.82	C_{18}	22	3.5
Ultrapore	Bec	5	O	–	30	–	C_3 m ec	–	–
							C_8 m ec	–	–
Ultrasil	Bec	10	K	–	8	–	C_8 m ec	–	–
							C_{18} m ec	–	–
Ultrasphere	Bec	5	O	–	8	–	C_8 m ec	–	–
							C_{18} m ec	–	–
Versapack	Alt	10	K	200	8	0.4	C_{18} m ec	10	2.4
Vydac HS	TSG	5, 10, 20	O	400	8	0.65	C_{18} m	13	1.6
Vydac TP	TSG	5, 10, 20	K	100	30	0.7	C_4 m	2.8	4.1
							C_{18} m	9	4.2
Zorbax	DPN	5, 7, 10	O	300	8	0.6	Bare	–	–

[a] Manufacturers' abbreviations and addresses, see Table 3.
[b] Shape: O = spherical; K = irregular.
[c] Type: m = monomer bonding; p = polymer bonding; ec = end-capping treatment. When the bonding type was not given, a monomer bonding was assumed in order to calculate the bonding density.

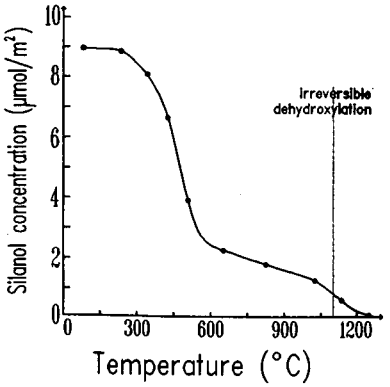

Fig. 7. Evolution of silanol concentration *versus* temperature. Dotted area: the dehydroxylation becomes irreversible. Data from ref. 2.

polar solutes and modifying the solute–stationary phase exchanges [52]. Peak shape and efficiency are also affected by the adsorption of water on silica. Methanol and other polar solvents can be added to the apolar mobile phase to adjust the selectivity [3].

As already described, surface silanols are used as anchor points to graft organic moieties. For steric reasons, it is not possible to fix an organic derivative on every hydroxyl group. Of the 9 μmol/m^2 initial silanol concentration, only 50% can be derivatized. The maximum bonding density is about 4.5 μmol/m^2 [53].

Acid silanols have a great affinity for basic groups. The low efficiencies and peak tailings obtained with the amino-containing solutes are well documented. They are due to $\equiv$Si–OH $\cdots$ NH– acid–base interactions. To reduce the residual silanol concentration of bonded silica, the end-capping treatment was used. The small trimethylchlorosilane molecule was used to react with silanols that were not accessible to the large octadecyl-containing reagent. An end-capped silica still bears unreacted silanols. The modern trend in manufacturing base-deactivated silica packings is to increase the ligand density (see section 4.2.3 and ref. 62).

4.2.2. Silica surface and porosity

The specific surface area of silica has an important impact on solute retention and selectivity. Obviously, the higher the specific surface area of a silica, the higher is the solute–stationary phase exchange area [3,54]. Solute retention is roughly proportional to the specific surface area, all other parameters being constant (same kind of stationary phase, same column length, same mobile phase, same flow-rate, etc.). For LC, Snyder [3] recommends the use of stationary phases possessing a specific surface area of at least 50 m^2/g. Silicas with A_s values higher than 500 m^2/g have been used (Table 2).

Surface area and porosity are related (Table 1 and section 3.2.3). Eqn. 10 shows that the apparent particle density depends on the pore volume. With V_p = 0.4 ml/g, the apparent particle density is 1.2 g/cm^3. The density drops to 0.5 g/cm^3 when the pore volume is 1.4 ml/g. By actually measuring the volume of 1 g of packing, it is

possible to define the actual packing density of a bonded phase. A 1-g amount of packing occupies between 1.2 and 5 cm^3. The packing density varies between 0.2 and 0.8 g/cm^3. It affects the specific surface area in $m^2/(cm^3$ of packing) in the column. A 10-cm column filled with a 150 m^2/g packing of density 0.6 g/cm^3 has twice the surface area of a 10-cm column filled with the same 150 m^2/g packing but with density only 0.3 g/cm^3.

4.2.3. Carbon content and bonding density

The bonding reactions described in paragraph 2.3.4 lead to partial coverage of the silica surface. The maximum concentration of 4.5 $\mu mol/m^2$ is difficult to achieve. It is important to characterize the chemically treated silica. The two important parameters for the characterization of bonded silica are the carbon content, in grams of C per 100 g of packing, and the surface concentration or bonding density, in micromoles of bonding moiety per square metre of initial silica surface area. The assessment of these two parameters is treated in depth in ref. 62.

Although the bonding density is almost never given by manufacturers (see section 4.4), it is one of the most important parameters for a bonded silica-based stationary phase. A high bonding density means a low residual silanol concentration; such a phase has a better resistance to elevated pH mobile phases and a better ability to separate amino-containing compounds. A pragmatic test procedure for comparison and evaluation of reversed-phase silica-based LC packings was proposed recently [55].

4.3. Chemical and physical chromatographic requirements

Owing to dissolution of silica, basic and hydrofluoric acid aqueous solutions must not be used as mobile phases in LC with silica-based stationary phases. The safe working pH range for the mobile phase is 2–9. Below pH 2, Si–C bonds of derivatized LC packings can be split; above pH 9, silica is slowly solubilized into silicate. The working pH range increases when the bonding density and/or the silica purity is high. A small addition of sodium silicate to the mobile phase greatly reduces the dissolution of silica at elevated pH (pH 12) [56]. Zirconia-cladded silicas were introduced to enhance the resistance of silica to alkaline solutions [31].

The stationary phase must have some mechanical strength to withstand the column back-pressure, usually in the range 1–20 MPa (10–200 bar or 140–2900 p.s.i.). With a typical pore volume in the cm^3/g range, the maximum pore size available for LC packings is 100 nm; in rare cases 400-nm pore size silicas can be used. Wide-pore silica particles have a low mechanical resistance and can break during the slurry packing procedure which operates at high pressures of 50 MPa or more (500 bar or 7200 p.s.i.). Particle breakage during the column packing procedure produces interstitial clogging; the column permeability becomes zero and the column and the packing are useless.

The silica pore size may be a critical parameter in the case of bulky solute analysis. For example, large-pore silicas are required for biopolymer separations, peptides or proteins [57]. In such analyses, 30- and 50-nm pore size packings are commonly used to enhance external silica–solute interactions and to avoid internal interactions such as restricted and slow diffusion of biopolymers [19]. The large mole-

TABLE 3

LIST OF SUPPLIERS

Name	Abbreviation	Address[a]
Alltech	Alt	Alltech Associates Inc., Applied Science Labs., 2051 Waukegan Road, Deerfield, IL 60015, USA
Asahi	Asa	Asahi Chemical Industry, Ltd., 1-3-2 Yakoo, Kawasaki-Ku, Kawasaki-Shi, 210, Japan
Beckman	Bec	Beckman Instruments Inc., 160 Hopper Avenue, Waldwick, NJ 07463, USA; Beckman Instruments International SA, 22 rue Juste-Oliver, CH-1260 Nyon, Switzerland
Brownlee	Bro	Brownlee Applied Biosystems, 850 Lincoln Center Dr., Foster City, CA 94404, USA
DuPont	DPN	E. I. DuPont de Nemours, 1007 Market St., Wilmington, DE 19898, USA
Eka Nobel	Eka	Eka Nobel AB, S-445 01 Surte, Sweden
Interchim	Int	Interchim, 213 avenue J. F. Kennedy, B.P. 15, 03103 Montlucon, France
J&W Scientific	J&W	J&W Scientific, Inc., 91 Blue Ravine Rd., Folsom, CA 95630, USA
Jones Chromatography	JoC	Jones Chromatography, Ltd., New Road, Hengoed, Mid-Glamorgan CF8 8AU, UK
J. T. Baker	JTB	J. T. Baker, Inc., 222 Red School Lane, Phillipsburg, NJ 08865, USA
Macherey, Nagel & Co.	Nag	Macherey, Nagel GmbH & Co. KG, Neumann-Neander Str., P.O. Box 101 352, W-5160 Düren, Germany
Merck	Mer	E. Merck, Frankfurter Strasse 250, Postfach 4119, W-6100 Darmstadt, Germany
Phase Separations	PhS	Phase Separations Ltd., Deeside Industrial Park, Queensferry, Clwyd CH5 2NU, UK
Phenomenex	Phe	Phenomenex, 6100 Palos Verdes Drive S., Rancho Palos Verdes, CA 90274, USA
Regis	Reg	Regis Chemical Co., 8210 N Austin Avenue, Morton Grove, IL 60053, USA
Shandon	Shd	Shandon Southern Products Ltd., Chadwich Road, Astmoor, Runcorn, Cheshire WA7 1PR, UK
Separations Group	TSG	The Separations Group, Vydac, P.O. Box 867, 17 434 Mojave Street, Hesperia, CA 92345, USA
SFCC	SFC	Société Française Chromato Colonne, Z. I. des Renoullères, 9 rue Marcel Dassault, 93360 Neuilly-Plaisance, France
Supelco	Sup	Supelco, Inc., Supelco Park, Bellefonte, PA 16823-0048, USA
Whatman	Wht	Whatman Ltd., Springfield Mill, Maidstone, Kent ME14 2LE, UK

[a] From *International Laboratory*, 1989 Buyer's Guide Edition, and Labguide, *Analytical Chemistry*, 61 (1989) 1G–294G.

cules can be trapped inside medium-size pores, inducing peak tails [24,58]. This is why a large pore size with a narrow pore size distribution should be used [59]. A narrow pore size distribution is also required in size-exclusion chromatography to obtain sufficient efficiency [60].

4.4. Examples

A non-exchaustive list of some commercially available silica-based LC packings is given in Table 2. Owing to the multiplicity of different bondings, only the linear alkyl bondings were considered together with the bare silica. Commercial catalogues give the characteristics of the products available in a form such as particle diameter, 100%; pore size, 94%, bonding moiety, 91%; particle shape, 90%; surface area, 53%; pore volume, 37%; bonding reaction (monomeric, polymeric and/or end-capping), 23%; carbon content, 21%; and bonding density, 4%. In Table 2, the pore volume and the bonding density were calculated when they were not given by the manufacturer. The bonding densities listed are only indicative because it is not possible to consider exactly the effect of the end-capping treatment on the carbon content and bonding density, and when the bonding reagent was not indicated a monomeric layer was assumed for the calculation. The abbreviations in the "Manufacturer" column refer to the company names and addresses listed in Table 3.

5. CONCLUSIONS

The qualities of silica, *i.e.*, high surface area and porosity, facile and versatile preparation, adjustable polarity and good mechanical strength, explain its widespread use in LC stationary phases. Its weak point is its low resistance to alkaline solutions. pH-resistant substitutes are commercially available today; they are mainly organic polymer-based materials. Styrene–divinylbenzene copolymer can be processed into spherical and macroporous particles with surface area 400 m^2/g (Benson Polymeric, EM Science, Brownlee Applied Biosystems, Hamilton, Polymer Labs.). Vinyl alcohol copolymer is also used to mimic silica. The hydroxyl groups (alcohol groups) of this polymer can be chemically modified to form a bonded polymer that can withstand strongly alkaline solutions because it contains only C–C bonds (Asahi Chemical). Such packings and uses are discussed in ref. 62. Eventually, these polymers or others may supplant silica-based packings. Composite materials, such as polymer-coated silicas, are another promising route to design of LC packings of tomorrow [61]. Meanwhile, silica is likely to be used satisfactorily for many more years.

6. SYMBOLS

a_m	area of a gas molecule in the BET method (0.162 nm^2 per N_2 molecule)
A_s	surface area (m^2/g)
A_p	internal surface area due to pores (m^2/g)
C	BET constant
d_p	particle diameter (μm)
d_m	average particle diameter in mass (μm)
d_n	average particle diameter in number (μm)
d_s	average particle diameter in surface (μm)
L	column length (cm)
n_i	number of particles with a diameter d_i
N	Avogadro's number ($6.02 \cdot 10^{23}$ molecules/mol)

P gas partial pressure in BET measurements (Pa)
$\bar{P}$ column permeability (cm^2)
ΔP back pressure (pascal, bar or p.s.i.)
P_o gas saturation vapour pressure in BET measurements (Pa)
p_d pore diameter (nm)
S surface area of a sample (m^2/g)
u linear mobile phase velocity (cm/s)
V_{Hg} mercury volume pushed into pores at a pressure ΔP (cm^3)
V_p pore volume (cm^3/g)
X amount of adsorbed gas (mol/m^2)
X_m amount of adsorbed gas corresponding to a monolayer (mol/m^2)
Y dimensionless shape factor in column permeability equation

Greek letters

ε_o external porosity or interstitial volume (cm^3)
ε_p particle porosity (ratio of particle pore volume to total particle volume)
γ_{Hg} surface tension of mercury (0.48 N/m at 25°C)
ρ density of solid silica (2.2 g/cm^3)
ρ_a apparent particle density in the case of a porous silica particle (g/cm^3)
η mobile phase viscosity (g/cm · s)
σ_{SiOH} surface silanol concentration ($\mu mol/m^2$)
θ mercury contact angle (140° at 25°C)

REFERENCES

1 C. R. Hammond, in R. C. Weast (Editor), *Handbook of Chemistry and Physics*, CRC Press, Boca Raton, FL, 67th ed., 1987, p. B34.
2 K. K. Unger, *Porous Silica (Journal of Chromatography, Library*, Vol. 16), Elsevier, Amsterdam, 1979.
3 L. R. Snyder, *Principles of Adsorption Chromatography*, Marcel Dekker, New York, 1968.
4 R. K. Iler, *The Chemistry of Silica*, Wiley, New York, 1979.
5 R. B. Sosman, *Phases of Silica; Am. Ceram. Soc. Bull.*, 43 (1964) 213.
6 F. Liebau, *Structural Chemistry of Silicates, Structure, Bonding and Classification*, Springer, Berlin, 1985.
7 S. E. Frazier, J. A. Bedford, J. Hower and M. E. Kennedy, *Inorg. Chem.*, 6 (1967) 1693.
8 M. V. Tongelen, J. Uytterhoeven and J. J. Fripiat, *Bull. Soc. Chim. Fr.*, 31 (1965) 2318.
9 L. Nondek and V. Vyskocil, *J. Chromatogr.*, 206 (1981) 581.
10 S. C. Antakli and J. C. Serpinet, *Chromatographia*, 23 (1987) 767.
11 K. K. Unger and E. Gallei, *Kolloid Z. Z. Polym.*, 237 (1970) 358.
12 J. Shapiro and H. G. Weiss, *J. Phys. Chem.*, 57 (1953) 219.
13 L. T. Zhuralev, *Langmuir*, 3 (1987) 316.
14 P. Roumeliotis and K. K. Unger, *J. Chromatogr.*, 149 (1978) 211.
15 J. Goworek, F. Nooitgedacht, M. Rikhof and H. Poppe, *J. Chromatogr.*, 352 (1986) 399.
16 B. Camara, H. Dunken and P. Fink, *Z. Chem.*, 8 (1968) 155.
17 G. E. Maciel and D. W. Sindorf, *J. Am. Chem. Soc.*, 102 (1980) 7606.
18 B. A. Morrow and I. D. Gay, *J. Phys. Chem.*, 92 (1988) 5569.
19 C. E. Bronnimann, R. C. Zeigler and G. E. Maciel, *J. Am. Chem. Soc.*, 110 (1988) 2023.
20 J. J. Köhler, D. B. Chase, R. D. Farlee, A. J. Vega and J. J. Kirkland, *J. Chromatogr.*, 352 (1986) 275.
21 G. K. Barashkov, *Bot. Zh.*, 45 (1960) 1350.
22 K. K. Unger, *Angew. Chem., Int. Ed. Engl.*, 11 (1972) 267.
23 H. Kloepfner (Degussa), *Ger. Pat.*, 762 723 and 830 786 (1942).

24 K. K. Unger, R. Janzen, G. Jilge, K. D. Lork and B. Anspach, in Cs. Horvath (Editor), *High Performance Liquid Chromatography: Advances and Perspectives*, Vol. 5, Academic Press, London, 1988, pp. 1–93.
25 A. V. Kiselev and V. J. Lygin, *Infrared Spectra of Surface Compounds*, Wiley-Interscience, New York, 1975.
26 M. L. Hair, in E. R. Corey, J. Y. Corey and P. P. Gaspar (Editors), *Silicon Chemistry*, Ellis Horwood, Chichester, 1988, Ch. 44, pp. 481–489.
27 R. Demoyel, F. Rouquerol and J. Rouquerol, in A. Liapis (Editor), *Fundamentals of Adsorption, Proceedings of the Engineering Foundation Conference*, Engineering Foundation, New York, 1987, pp. 199–210.
28 I. L. Cunha and L. G. Audrade e Silva, *J. Radioanal. Nucl. Chem.*, 104 (1986) 293.
29 M. Montjoie, J. R. Costes and F. Josso, *Proc. Inst. Mech. Eng.*, 1988, 127.
30 B. Law and P. F. Chan, *J. Chromatogr.*, 467 (1989) 267.
31 R. W. Stout, S. I. Sivaroff, R. D. Ricker, H. C. Palmer, M. A. Jackson and T. J. Odiorne, *J. Chromatogr.*, 352 (1986) 381.
32 J. J. Pesek and J. A. Graham, *Anal. Chem.*, 49 (1977) 133.
33 E. Bayer, K. Albert, J. Reiners, M. Nieder and D. Muller, *J. Chromatogr.*, 264 (1983) 197.
34 K. D. Lork, K. K. Unger and J. N. Kinkel, *J. Chromatogr.*, 352 (1986) 199.
35 J. F. Erard and E. sz. Kováts, *Anal. Chem.*, 54 (1982) 193.
36 S. D. Fazio, S. A. Tomellini, H. S. Hsien, J. B. Crowther, T. V. Raglione and T. R. Hartwick, *Anal. Chem.*, 57 (1985) 1559.
37 C. Gaget, D. Morel, M. Traore and J. Serpinet, *Analusis*, 12 (1984) 386.
38 Labguide 90, *Anal. Chem.*, 61 (1989) 150G.
39 S. Brunauer, P. H. Emmett and E. Teller, *J. Am. Chem. Soc.*, 60 (1938) 309.
40 S. J. Gregg and K. S. W. Sing, *Adsorption, Surface Area and Porosity*, Academic Press, New York, 2nd ed., 1982.
41 B. Pommier, F. Juillet and S. J. Teichner, *Bull. Soc. Chim. Fr.*, 38 (1972) 1268.
42 J. Serpinet, G. Untz, C. Gachet, L. Demourgues and M. Perrin, *J. Chim. Phys.*, 71 (1974) 949.
43 D. H. Everett, in K. K. Unger, J. Rouquerol, K. S. W. Sing and H. Kral (Editors), *Characterization of Porous Solids*, Elsevier, Amsterdam, 1988, pp. 1–21.
44 M. M. Dubinin, *Zh. Fiz. Khim.*, 34 (1960) 959.
45 K. S. W. Sing, *Pure Appl. Chem.*, 54 (1982) 2201.
46 J. C. Giddings, *Dynamics of Chromatography*, Marcel Dekker, New York, 1965.
47 J. N. Done and J. H. Knox, *J. Chromatogr. Sci.*, 13 (1972) 606.
48 P. A. Bristow and J. H. Knox, *Chromatographia*, 10 (1976) 279.
49 R. P. W. Scott and P. Kucera, *J. Chromatogr. Sci.*, 13 (1975) 837.
50 Z. El Rassi, C. Gonnet and J. L. Rocca, *J. Chromatogr.*, 125 (1976) 179.
51 H. Engelhardt and H. Elgass, in Cs. Horvath (Editor), *High Performance Liquid Chromatography —Advances and Perspectives*, Vol. 2, Academic Press, London, 1980, pp. 57–108.
52 R. P. W. Scott, *Faraday Symp. Chem. Soc.*, 15 (1980) 49.
53 F. Gobet and E. sz. Kováts, *Adsorpt. Sci. Technol.*, 9 (1984) 77.
54 H. Engelhardt, *High Performance Liquid Chromatography*, Springer, Berlin, 1979.
55 H. Engelhardt and M. Jungheim, *Chromatographia*, 29 (1990) 59.
56 N. T. Miller and J. M. Di Bussolo, *J. Chromatogr.*, 499 (1990) 317.
57 M. A. Stadalius, H. S. Gold and L. R. Snyder, *J. Chromatogr.*, 327 (1985) 27 and 93.
58 K. K. Unger and R. Jansen, *J. Chromatogr.*, 373 (1986) 227.
59 H. J. Richtie, P. Ross and D. R. Woodward, *Chromatogr. Anal.*, 13 (1990) 9.
60 F. E. Regnier, *Anal. Chem.*, 55 (1983) 1298A.
61 H. Figge, A. Deege, J. Köhler and G. Schomburg, *J. Chromatogr.*, 351 (1986) 393.
62 K. K. Unger, F. E. Regnier and R. E. Majors (Editors), *Liquid Chromatography Packings*; *J. Chromatogr.*, 544 (1991).

Journal of Chromatography, 549 (1991) 29–41
Elsevier Science Publishers B.V., Amsterdam

CHROM. 23 343

Selectivity of carbon packing materials in comparison with octadecylsilyl- and pyrenylethylsilylsilica gels in reversed-phase liquid chromatography[a]

NOBUO TANAKA*, TETSUYA TANIGAWA, KAZUHIRO KIMATA, KEN HOSOYA and TAKEO ARAKI

Kyoto Institute of Technology, Department of Polymer Science and Engineering, Matsugasaki, Sakyo-ku, Kyoto 606 (Japan)

(First received February 5th, 1991; revised manuscript received March 19th, 1991)

ABSTRACT

The retention selectivity of graphitic carbon packing materials was compared with those of octadecylsilyl- and pyrenylethylsilylsilica packing materials in reversed-phase liquid chromatography. A carbon stationary phase showed the highest hydrophobicity and selective retention of planar, unsaturated compounds. The presence of hydrophilic groups did not cause as great a retention decrease on carbon as on silica-based materials. A much greater influence of structural planarity of solutes on selectivity was observed with carbon than with silica-based phases, presumably because the solute planarity emphasizes the interaction with the graphite surface based on charge transfer and dispersion forces. Pyrenylethyl-bonded silica gel was found to be intermediate between alkylsilica and graphitized carbon packing materials with respect to the selectivity based on the electronic and steric interactions with the fused-ring aromatic systems on the stationary phase.

INTRODUCTION

In addition to a variety of silica C_{18} phases [1,2] and polymer-based packing materials [3,4], several stationary phases capable of charge-transfer-type interactions are currently used for the separation of compounds with structural similarity in reversed-phase liquid chromatography (RPLC) [5–19].

The differences in steric selectivity between polymeric- and monomeric-type silica C_{18} packing materials have been well documented [20,21]. The selective retention of rigid, compact solutes by polymer-based packing materials has been explained by the contribution of biporous structures of polymer gels [3,4,22], macroporous gels composed of microporous materials. To add positive interactions to the retention process with hydrophobic stationary phases in RPLC, pyrenylethylsilylated (PYE) silica gel was prepared to have charge-transfer, dipole–pi and steric interactions. The

[a] Presented at the *14th International Symposium on Column Liquid Chromatography, Boston, MA, May 1990*. The majority of the papers presented at this symposium have been published in *J. Chromatogr.*, Vol. 535 (1990) and 536 (1991).

0021-9673/91/$03.50

PYE phase provided isomer separations of tetrachlorodibenzo-*p*-dioxins and disubstituted cyclohexanes that were not possible with silica C_{18} phases [5–10].

Graphitized carbon packing material is one of the extremes of stationary phases for RPLC, possessing rigid, planar surfaces in addition to functions capable of strong charge-transfer interactions [11–19]. These stationary phases have been reported to be useful for the separation of solutes with closely related structures including stereoisomers. Recently, applications of this packing material to isomer separations and mechanistic studies have been reported. In these reports, interactions including steric interaction, charge-transfer and dispersion forces were shown to be responsible for the discrimination of solutes, as studied with unsaturated compounds. The effects of organic solvents and additives have also been studied.

The pyrenyl groups on the PYE phase possesses fused aromatic systems with sixteen π-electrons which may be regarded as a small part of a graphite surface. The PYE phase provided a much greater effect of a planar aromatic structure on retention selectivity than a phenylethylsilylated silica phase [5,8].

A comparison of carbon packing materials with PYE and C_{18} silica was thought to be of value for providing information on the retention mechanisms with packing materials having large differences in structure. We report here a study of the retention characteristics of graphitized carbon packing materials from two manufacturers in comparison with C_{18} and pyrene-bonded silica gels. The study indicates that some of the characteristic selectivity of a carbon phase, very different from those of silica C_{18} phases, occurs with a PYE phase having some structural similarity.

EXPERIMENTAL

The HPLC system consisted of a Model 880-PU pump, a Model 875-UV detector, a Model 830-RI refractive index detector (all from JASCO, Tokyo, Japan) and a C-R4A data processor (Shimadzu, Kyoto, Japan). Chromatographic measurements were carried out at 30°C.

Silica-based packing materials were prepared from Develosil (particle size 5 μm, pore size 11 nm) (Nomura Chemical, Seto, Japan), as reported previously [5,23], and packed into stainless-steel columns [100 mm × 4.6 mm I.D. for C_{18} and nitrophenylethyl (NPE) and 150 mm × 4.6 mm I.D. for pyrenylethyl (PYE)]. Packed carbon columns of Hypercarb, designated carbon I in this paper (Shandon, Runcorn, Cheshire, UK) (100 mm × 4.7 mm I.D.), Carbonex, designated carbon II (Tonen, Tokyo, Japan) (100 mm × 4.6 mm I.D.) and a polymer gel column of Shodex DE-613 (Showa Denko, Tokyo, Japan) were loaned by Senshu Kagaku (Tokyo, Japan), Tonen and Showa Denko, respectively. Mobile phases were made up by volume from HPLC-grade solvents.

Electron microscopy was carried out at Nitto Technical Information Centre (Osaka, Japan), as described previously [24], by employing ultra-thin sections of the porous particles embedded in epoxy resin.

RESULTS AND DISCUSSION

Hydrophobic properties

The hydrophobic properties of the packing materials were studied by mea-

suring the retention increase caused by the addition of one methylene group to the solute structure. Table I summarizes the $\alpha(CH_2)$ values calculated from a values in the equation

$$\log k' = a\,C_n + b \tag{1}$$

or the slope of the plots of $\log k'$ (capacity factor) against carbon number (C_n) of alkyl groups in alkyl alcohols and alkylbenzenes in aqueous methanol.

Smaller a values were found with PYE than with C_{18} phase, indicating a less hydrophobic character of the PYE phase. The major driving force of hydrophobic interaction is the release of water molecules from the solvation shell around the so-called hydrophobic molecules, by transferring the solute from the aqueous phase to the organic phase in liquid–liquid two-phase systems. From the same mobile phase, the transfer of a methylene group to a C_{18} phase is more favourable than that to a PYE phase, presumably because some solvent-like behaviour can be expected with the aggregated alkyl chains on the C_{18} phase.

However, it has been reported that the a value on a C_{18} phase, or the increase in k' values is slightly smaller than those in partition coefficients in water–organic liquid–liquid two-phase systems [25]. This is due to the restriction of alkyl chains bonded to the silica surface, having a lower density and less mobility than liquid alkanes [1]. The a values with C_1 and C_8 phases, where a solvent-like interaction with the solute is unfavourable owing to the small size of the alkyl groups, are much smaller than those on C_{18} phases [5].

Table I indicates that the a value, or the hydrophobic property of the stationary phase, on the carbon phase is always greater than those on alkyl- or aryl-bonded silica phases. The free-energy change associated with the transfer of one methylene group from water to the stationary phase was about -900 cal/mol with the carbon phase compared with -810 cal/mol on the C_{18} phase. The latter was slightly larger than that previously obtained with a C_{18} phase with a lower surface coverage [25]. The difference between the C_{18} and carbon phases was even greater at a higher methanol concentration. The free energy change associated with the transfer of one methylene

TABLE I

HYDROPHOBIC PROPERTIES OF PACKING MATERIALS

The $\alpha(CH_2)$ values (retention increment with one additional methylene group in solute structure) calculated from a in eqn. 1 at methanol concentrations from 0 to 80% in the mobile phase. $\alpha(CH_2) = 10^a$.

Stationary phase	$\alpha(CH_2)^a$				
	0%	10%	30%	50%	80%
C_{18}	3.84	3.62	2.94	2.25	1.54
PYE	3.27	3.15	2.81	2.13	1.45
Carbon I	4.50	4.09	3.67	2.83	2.10
Carbon II	4.53	4.49	3.74	2.87	2.11

[a] Calculated from the retention times of alkyl alcohols ($C_nH_{2n+1}OH$, $n = 2$–5), except in 80% methanol, where alkylbenzenes (ethylbenzene to amylbenzene) were used.

group from water to the organic phase was −820 to −850 cal/mol for polar solutes and −884 cal/mol for alkane–water partition [26].

The present results are striking if it is assumed that the solutes are partitioned onto the rigid planar graphite surface. Some solvent-like flexibility of a C_{18} stationary phase is expected to give such an interaction to reduce the contact between the C–H surface of a solute and water as in aqueous–organic liquid–liquid partition systems that lowers the free energy of the system. On the other hand, the rigid carbon surface would not be able to completely surround the alkyl chain of the solute.

The results suggest the presence of some positive interactions between the stationary phase and the solute, namely dispersion forces, as suggested by previous workers [21,27]. Karger *et al.* [28] suggested the contribution of dispersion forces on the graphite surface which arises from the high polarizability of the graphite surface, coupled with a high dispersive solubility parameter for a methylene group. Close proximity of the molecular surface of the solute and the stationary phase allowed by mutual steric compatibility should be a critical factor for this to occur.

Polar group selectivity

In order to show the nature of the interaction between polar functional groups and the stationary phase, the log k' values of monosubstituted alkanes (RX) on carbon and C_{18} phases were plotted against the carbon number of solutes, as shown in Fig. 1. Straight lines of good linearity were obtained for each homologous series of compounds. The plots were fitted to eqn. 1, and the resulting slopes (a values) and intercepts (b values) are listed in Table II.

The slopes (a values) obtained on one stationary phase were close to each other regardless of the functional groups of the solutes. The a values indicate how hydrophobic the stationary phase is, whereas the intercept (b values) gives information on how favourable the specific interaction is between the functional group and the stationary phase. Any difference in behaviour should be related to the stationary phase effect, because the interaction with mobile phase solvents is cancelled by employing the same mobile phase for all the columns.

On silica C_{18}, hydrophilic groups such as OH or CHO caused a large decrease

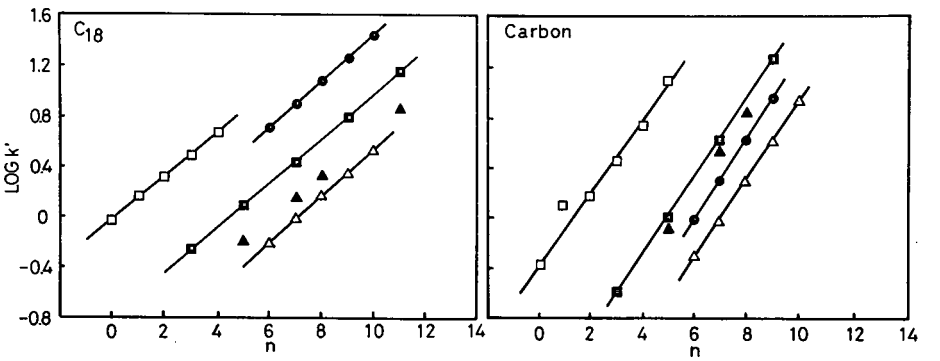

Fig. 1. Plots of log k' values against the carbon number of alkyl groups of monosubstituted alkanes on (right) carbon and (left) C_{18}, phases with methanol–water (80:20). □ = $C_6H_5C_nH_{2n+1}$; ◘ = $C_nH_{2n+1}COOCH_3$; ● = C_nH_{2n+2}; △ = $C_nH_{2n+1}OH$; ▲ = $C_nH_{2n+1}CHO$.

TABLE II

EFFECT OF TERMINAL GROUPS ON RETENTION

Stationary phase	*b* value (*a* value)[a]						
	C_6H_5	H	$COOCH_3$	CHO	OH	COOH	NH_2
C_{18}[b]	−0.03	−0.39	−0.80	−1.09	−1.33		
	(0.17)	(0.18)	(0.18)	(0.18)	(0.19)		
PYE[b]	−0.36	−0.84	−0.71	−1.19	−1.45		
	(0.15)	(0.14)	(0.13)	(0.15)	(0.16)		
Carbon I[b]	−0.38	−1.96	−1.52	−1.62	−2.28		
	(0.29)	(0.32)	(0.31)	(0.31)	(0.32)		
Carbon I					−2.12	−1.52	−3.46
(pH 2.5)[c]					(0.45)	(0.43)	(0.44)
Carbon I					−2.11	−2.11	−1.95
(pH 12)[d]					(0.45)	(0.41)	(0.44)

[a] Calculated according to the equation $\log k' = a C_n + b$, where C_n is the number of carbon atoms in the alkyl group in each homologous series of compounds.
[b] 80% methanol.
[c] 50% methanol, 0.02 *M* H_3PO_4–NaH_2PO_4.
[c] 50% methanol, 0.02 *M* NaOH–Na_2HPO_4.

in *b* values, and a large increase in *b* was seen with the phenyl group, taking the alkanes (X = H) as standard. Although the PYE showed a similar tendency, the decrease in *b* values was noticeably smaller for CHO or $COOCH_3$ groups. This can be explained in terms of the dipole–pi interactions with the stationary phase.

The tendency on the carbon phase was different. Hydrophilic groups, especially those containing a carbonyl group, were actually more favoured than H. The retention decrease due to the presence of an OH group was found to be very small in spite of the greater hydrophobic selectivity of this stationary phase. The increased interaction of a hydroxyl group with the mobile phase seems to be counteracted by an increased interaction with the stationary phase.

The results can be explained on the basis of proton donor–pi or electron donor–acceptor interactions. Complexation of proton donors with phenyl rings has been reported using NMR and UV spectroscopy [29,30]. Bassler *et al.* [15] showed the correlation between the pK_a values of aromatic compounds and the retention on a carbon phase working as an electron acceptor in the normal-phase mode.

The carbon phase gave high *a* values, generally resulting in a greater difference in retention than the other phases based on the increase in molecular weight. Logically, the carbon phase generally gave much greater separation factors than silica-based materials in the same mobile phase for a homologous series of compounds.

Stronger eluents should be used with a carbon phase to avoid prolonged retention times. Fig. 2 illustrates the characteristics shown above in the chromatogram of alkylamines in an aqueous mobile phase at high pH, where silica-based columns and polymer-based columns are either useless or accompanied by tailing. The excellent chemical stability of carbon phases under extreme pH values is an obvious advantage.

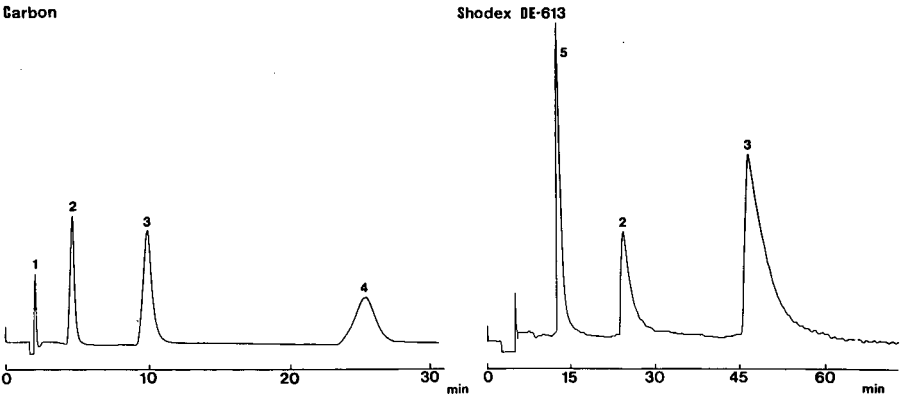

Fig. 2. Separation of alkylamines on carbon- and polymer-based packing materials. Mobile phase: Shodex DE-613 (polymer-based): 20% acetonitrile in 0.013 *M* phosphate buffer (pH 11.7). Carbon: 30% acetonitrile in 0.02 *M* phosphate buffer (pH 12.1). Solutes: 1 = butylamine; 2 = hexylamine; 3 = heptylamine; 4 = octylamine; 5 = cyclohexylamine.

Charge-transfer interaction

In Fig. 3, log *k'* values of monosubstituted benzenes on carbon I and silica-based phases are plotted against log *P* values [31] obtained from 1-octanol–water partition. A straight line was drawn through the plots for benzene, toluene and ethylbenzene. The contribution of hydrophobic interaciton is clearly seen on every phase from the contribution of alkyl groups to the retention.

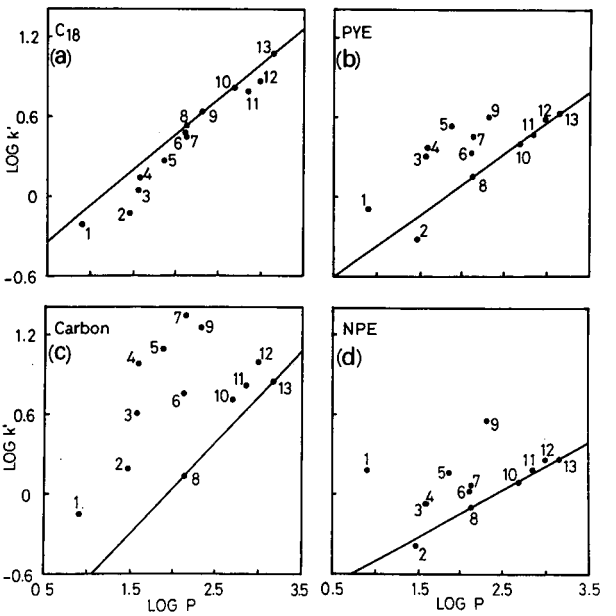

Fig. 3. Plots of log *k'* values against log *P* values of monosubstituted benzenes in 60% methanol. (a) C_{18}; (b) PYE; (c) carbon; (d) NPE. Substituents: 1 = NH_2; 2 = OH; 3 = CN; 4 = $COCH_3$; 5 = NO_2; 6 = OCH_3 7 = $COOCH_3$; 8 = H; 9 = $N(CH_3)_2$; 10 = CH_3; 11 = Cl; 12 = Br; 13 = C_2H_5.

Fairly good linearity was observed with silica C_{18} phase, as reported previously [32], indicating that the hydrophobic interaction plays a major role in determining the retention on this stationary phase, while additional factors provided by the stationary phase resulted in scattered plots on PYE, NPE and carbon phases.

All the points in Fig. 3c were above the straight line connecting the plots for benzene and ethylbenzene. The results indicate that any substituents, electron-withdrawing or electron-donating, with increase in molecular weight can contribute to the increase in k' on the carbon phase relative to aqueous–organic liquid–liquid partition or the chromatographic system with the C_{18} phase.

The results on the carbon phase, indicating the preferential retention of compounds with higher molecular weight, particularly for those with electron-withdrawing substituents (Nos. 4, 5 and 7 in Fig. 3), agree with a retention mechanism including the contributions of the dispersion forces and the charge-transfer interactions in addition to the hydrophobic interaction. The correlation between the magnitude of dispersion forces and molecular volume has been documented [33]. The results clearly show the utility of the carbon phase for the separation of compounds with similar hydrophobicities which were difficult to separate with the C_{18} phase (*e.g.* Nos. 6, 7 and 8 in Fig. 3).

In contrast to the carbon phase, the NPE phase showed a clear preference for compounds with electron-donating substituents, as expected on the basis of charge-transfer interactions between the solutes and the stationary phase. The results in Fig. 3 suggest that the PYE phase possesses some similarity to the carbon phase with respect to the selectivity for solutes with polar functional groups.

Steric selectivity

Chemically bonded silica stationary phases prepared from silanes of different functionality [20,21,34] or different alkyl chain length [35] showed the different selectivities for the aromatic compounds of different planarity. The rigid planar structure of the PYE phase was shown to be responsible for the better separation of disubstituted cyclohexanes than on C_{18} [8]. The use of cycloalkanes is appropriate for investigating the steric selectivity of various types of stationary phases, because only dispersion forces are expected to play a role in the interaction with the stationary phase.

As shown in Table III, the separation factor, $\alpha = k'_{(\text{decalin})}/k'_{(\text{adamantane})}$, was very large on the carbon phase compared with silica-based materials. The PYE phase showed a slightly greater steric selectivity than C_{18}. Note here that the results also include the difference in the hydrophobic properties between the two phases. The more hydrophobic C_{18} should have given a much larger α value than PYE if the recognition is achieved only on the basis of the hydrophobic effect. The slightly greater separation factor between decalin and adamantane on PYE is an indication of the selective retention of decalin, the more planar of the two. A clear difference in steric selectivity was seen between C_{18} and PYE when aromatic compounds, triphenylene and *o*-terphenyl, were used as probes [5,34].

The carbon phase resulted in much larger α values for alkanes with different bulkiness, indicating the retention of bulky, non-planar compounds to be unfavourable on this phase. It is interesting that a larger $k'_{(\text{hexane})}/k'_{(\text{cyclohexane})}$ ratio was found on carbon than C_{18}. This is in contrast to the polymer-based phases [4,22], which

TABLE III

STERIC SELECTIVITY FOR CYCLOALKANES

Mobile phase: methanol–water (80:20).

Stationary phase	k'		α^a	k'		α^b
	Hexane	Cyclohexane		Adamantane	*trans*-Decalin	
C_{18}	5.24	3.73	1.40	10.3	15.9	1.54
PYE	0.99	0.82	1.21	2.24	3.47	1.55
Carbon I	0.97	0.32	3.0	0.79	3.55	4.49
Carbon II	0.52	0.17	3.0	0.45	2.20	4.86
NPE	–	–	–	0.83	0.98	1.19

[a] Separation factor, $k'_{\text{hexane}}/k'_{\text{cyclohexane}}$.
[b] Separation factor, $k'_{\textit{trans}\text{-decalin}}/k'_{\text{adamantane}}$.

showed selective retention of the more rigid, compact solutes, with the order of preference planar aromatic compounds, bulky aromatic compounds, cycloaliphatic compounds, followed by the straight-chain alkyl compounds. The three-dimensional network structures of polymer gels seemed to be responsible for the selectivity [3,4,22].

The steric selectivity of the carbon phase is different from those of either polymer- or silica-based materials, showing preference in the order planar aromatic, bulky aromatic, *n*-alkyl and cycloaliphatic compounds, with adamantane showing a very small retention. The results indicate the contribution of dispersion forces to retention, because the greatest dispersion interaction is expected with planar solutes. Cyclohexane cannot assume a planar structure with the carbon chain like hexane. A cyclohex-

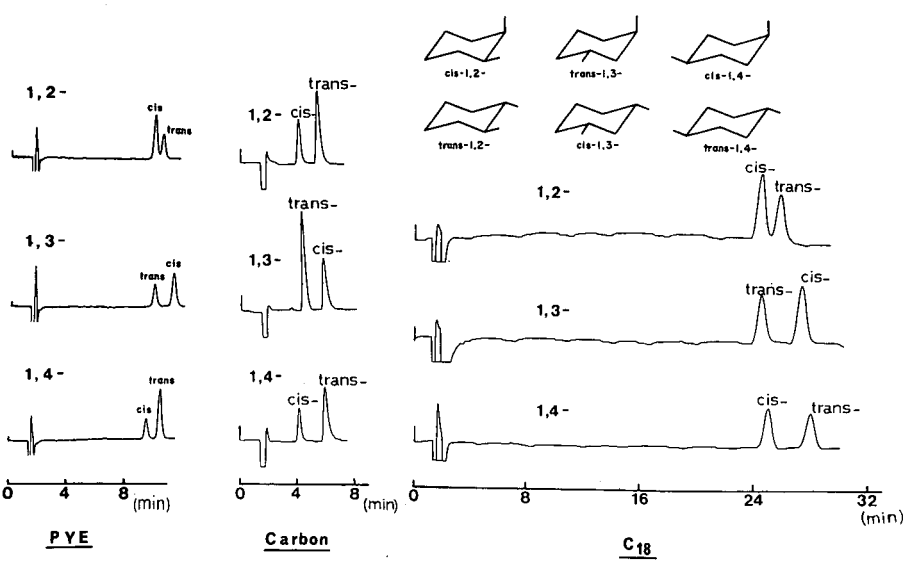

Fig. 4. Separation of dimethylcyclohexanes on C_{18}, PYE and carbon packing materials. Mobile phase: 70% methanol.

TABLE IV

SELECTIVITY FOR DISUBSTITUTED CYCLOHEXANES

Mobile phase: methanol–water (70:30).

Disubstituted cyclohexane solute[a]	Separation factor, α, between *cis*- and *trans*-isomers (k')[b]			
	C_{18}	PYE	Carbon I	Carbon II
1,2-$(CH_3)_2$	1.05(*c*;23.7)	1.07(*c*;4.39)	1.51(*c*;2.11)	1.45(*c*;1.49)
1,3-$(CH_3)_2$	1.12(*t*;23.8)	1.16(*t*;4.38)	1.49(*t*;2.44)	1.58(*t*;1.67)
1,4-$(CH_3)_2$	1.13(*c*;23.7)	1.13(*c*;4.21)	1.67(*c*;2.22)	1.58(*c*;1.57)
Menthol/isomenthol	1.10(4.63)	1.20(2.01)	1.71(3.11)	1.79(1.79)
1,2-$(COOEt)_2$	1.01(*t*;2.79)	1.19(*t*;3.41)	1.11(*c*;3.43)	1.03(*c*;2.08)
1,2-$(COOPr\text{-}n)_2$	1.01(*t*;6.98)	1.19(*t*;6.81)	1.32(*c*;10.3)	1.1(*c*;6.7)[c]
1,2-$(COOBu\text{-}n)_2$	1.01(*c*;17.7)	1.18(*t*;15.6)	1.16(*c*;4.33)[d]	–
1,2-$(COOBu\text{-}t)_2$	1.08(*t*;13.3)	1.20(*t*;8.27)	1.56(*c*;0.56)[d]	–
1,4-$(COOEt)_2$	1.10(*c*;2.40)	1.06(*c*;3.82)	4.88(*c*;1.81)	4.83(*c*;1.12)
1,4-$(COOBu\text{-}n)_2$	1.28(*c*;15.5)	1.14(*c*;18.0)	5.87(*c*;2.49)[d]	–
1,4-$(COOBu\text{-}t)_2$	1.25(*c*;11.5)	1.16(*c*;8.92)	2.84(*c*;0.83)[c]	–
1,2-$(OH)_2$[e]	1.07(*t*;6.62)	1.09(*t*;4.20)	1.10(*t*;2.37)	–
1,3-$(OH)_2$[e]	1.03(*c*;2.32)	1.14(*t*;1.67)	1.25(*t*;1.76)	–
1,4-$(OH)_2$[e]	5.42(*t*;0.46)	3.39(*t*;0.61)	1.05(*t*;1.70)	–

[a] ET = ethyl; Pr-*n* = *n*-propyl; Bu-*n* = *n*-butyl; Bu-*t* = *tert.*-butyl.
[b] k' of the first peak indicated by *t* or *c*, representing *trans*- or *cis*-isomer, respectively, in parentheses.
[c] Tailed peaks.
[d] Mobile phase: methanol–water (90:10).
[e] Mobile phase: methanol–water (5:95).

ane-bonded silica phase actually disfavoured planar aromatic compounds [5]. Previous workers have discussed the retention tendency of xylenes based on the points of contact [11,14] with the carbon surface. The present results with cycloalkanes, which are electronically most inert, support their conclusion.

Selectivity for disubstituted cyclohexanes

In the separation of dimethylcyclohexanes, those with two equatorial methyl groups, *trans*-1,2-, *cis*-1,3- and *trans*-1,4-isomers, were preferentially retained by all the stationary phases. As shown in Fig. 4 and Table IV, the PYE phase resulted in a similar resolution in a much shorter time than C_{18}. This tendency was further emphasized on the carbon phase, which showed a much greater preference toward the more planar isomers, resulting in an easy separation between the *trans* and *cis* forms of dimethylcyclohexanes.

In the case of cyclohexanediols, those with two equatorial hydroxyl groups, *trans*-1,2- and *trans*-1,4-diols, generally resulted in a shorter retention owing to the easier solvation in the mobile phase than those possessing an axial hydroxyl group. The C_{18} phase gave an easy separation of 1,4-diols, but could not separate 1,3-diols owing to the contribution of internal hydrogen bonding in the *cis* isomer [8]. The PYE phase provided a better separation for isomers of 1,2- and 1,3-diols than the C_{18} phase. The carbon phase resulted in a much easier separation of 1,3-diol isomers, but gave a very small separation factor for 1,4-diol isomers. This is due to the preference toward the more planar compounds shown by the carbon phase.

TABLE V

COMPARISON OF SELECTIVITIES TOWARD SIMPLE ALKENES

Mobile phase: methanol–water (70:30).

Solute	$\alpha(k')^a$		
	C_{18}	PYE	Carbon I
1-Heptene	– (13.9)	– (2.98)	– (2.87)
2-Heptene	1.09 (*Z*;13.0)	1.08 (*Z*;2.69)	1.27 (*Z*;2.25)
3-Heptene	1.07 (*Z*;12.8)	1.04 (*Z*;2.62)	1.23 (*Z*;1.88)
1-Octene	– (23.7)	– (4.64)	– (6.55)
2-Octene	1.11 (*Z*;22.1)	1.07 (*Z*;4.17)	1.41 (*Z*;4.95)

[a] Separation factor, α, between *E* and *Z* forms, and the configuration and k' of the first peak in parentheses.

The C_{18} phase gave little separation of isomers of 1,2-cyclohexanedicarboxylic acid dialkyl esters, whereas the PYE phase provided a much better separation based on the favourable dipole–pi interaction with *cis*-1,2-diesters having the two substituents in axial–equatorial positions [8]. The carbon phase also provided an easy separation. Preference, however, was shown toward the isomers with two equatorial ester groups. Here the dipole–pi interaction seemed to be overwhelmed by the preference for planar solutes.

Overall, the results with cyclohexane derivatives indicate the strong contribution of the steric effect on the carbon phase in addition to the hydrophobic interactions. One can obtain much better separations in a much shorter time by employing

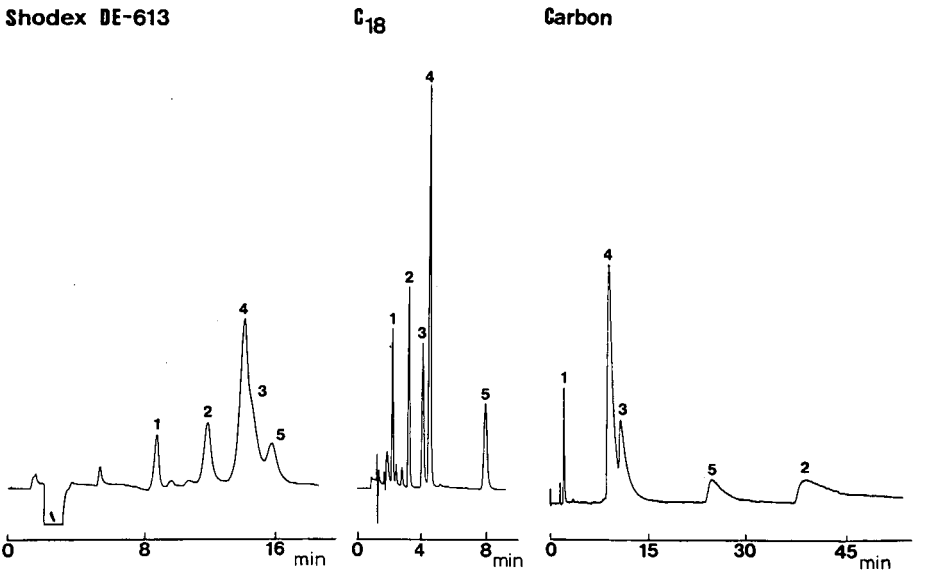

Fig. 5. Difference in selectivity toward aromatic hydrocarbons. (a) Polymer-based (in 50% tetrahydrofuran); (b) C_{18} (in 80% methanol); (c) carbon (in 80% methanol). Solute: (1) benzene; 2 = naphthalene; (3) triptycene; (4) diphenylmethane; (5) triphenylmethane.

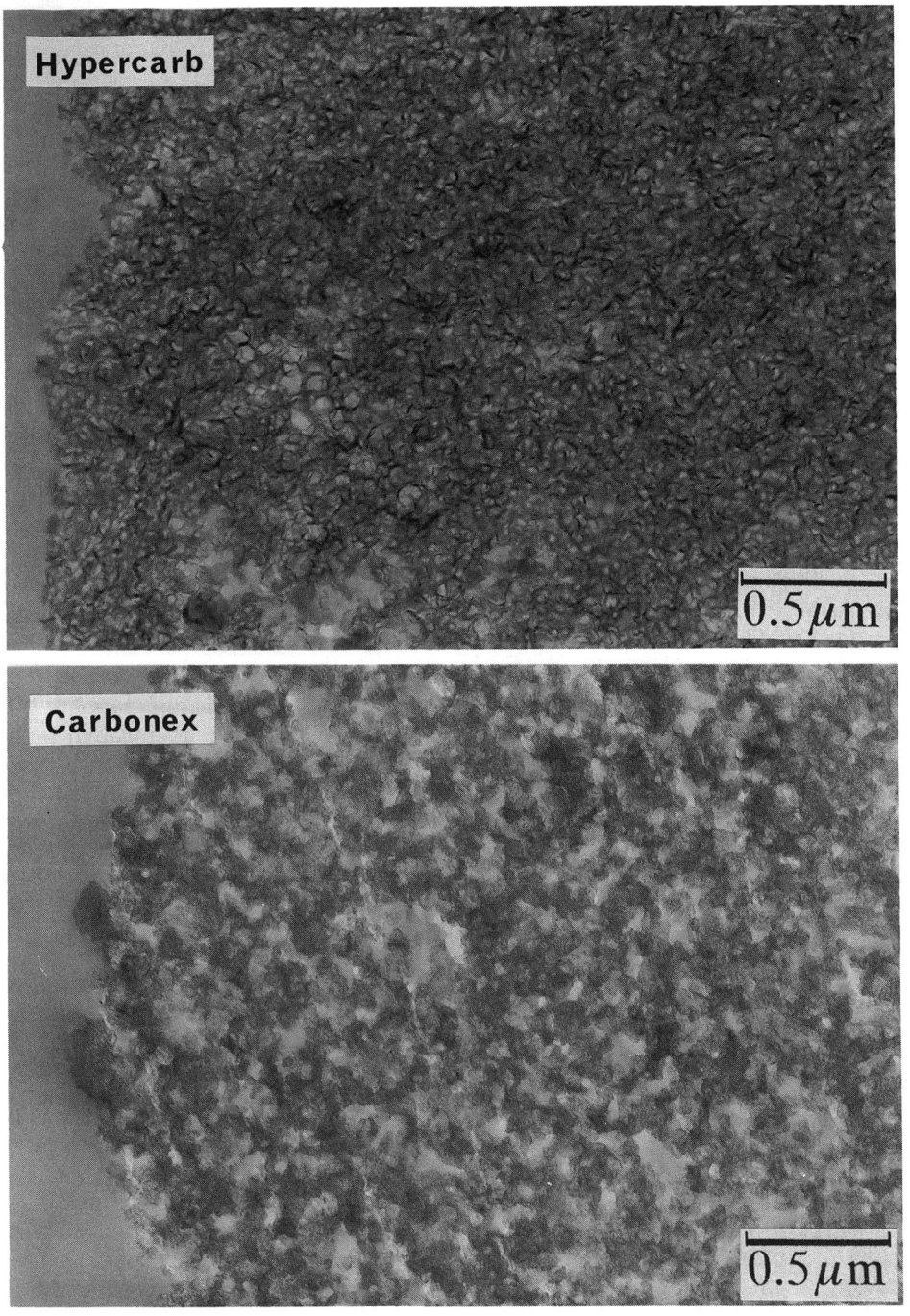

Fig. 6. Transmission electron micrographs of carbon packing material. (top) Hypercarb (carbon I); (bottom) Carbonex (carbon II).

an appropriate column. Although little tailing was seen with the carbon phase, the PYE phase showed a good performance with a selectivity similar to that of carbon in many instances.

Olefins

A comparison of selectivity toward simple alkenes is shown in Table V, which indicates the utility of the carbon phase in the separation of olefin isomers. The carbon phase gave much greater separation factors for the isomers, with preference toward terminal olefins over internal olefins and *E* isomers over *Z* isomers. The former observation can be explained by the greater exposure of π-electrons of the terminal olefins as in argentation chromatography [36], and the latter by structural planarity.

Fig. 5 shows an example of the different steric selectivities of a carbon phase from those of silica C_{18} and polymer-based packing materials for aromatic compounds. The number of π-electrons aligned on a plane has a critical influence on the selectivity on the carbon phase.

Comparison between the two carbon packing materials

Transmission electron micrographs of carbon packing materials I and II are shown in Fig. 6. The sizes of the primary structures of the latter are relatively uniform, within 50–80 nm, whereas the former possesses primary structures within the range 30–40 nm with some very large pores and skeletons. The chromatographic properties of these materials were very similar to each other with respect to selectivity for hydrocarbons, as shown in Tables I, III and IV, in spite of the difference in the internal structures and in the method of preparation. Carbon I was prepared from phenol–formaldehyde polymers via a template method [11], whereas carbon II was prepared from petroleum pitch without using a template.

CONCLUSIONS

Graphitic carbon packing materials showed retention characteristics based on the steric, charge-transfer and dispersion interactions of the solutes with the graphite surface, regardless of the method of preparation of the particles. These interactions on a carbon phase are much greater than those on any silica-based packing materials, resulting in the preferential retention of planar compounds. The silica-based PYE phase showed properties intermediate between those of the carbon and alkyl-type silica-based stationary phases.

ACKNOWLEDGEMENT

The authors are grateful to Tonen, Senshu Kagaku and Showa Denko for the loan of the carbon and polymer gel columns.

REFERENCES

1 L. C. Sander and S. A. Wise, *CRC Crit. Rev. Anal. Chem.*, 18 (1987) 299.
2 K. Kimata, K. Iwaguchi, S. Onishi, K. Jinno, R. Eksteen, K. Hosoya, M. Araki and N. Tanaka, *J. Chromatogr. Sci.*, 27 (1989) 721.

3 N. Tanaka and M. Araki, *Adv. Chromatogr.*, 30 (1989) 81.
4 N. Tanaka, T. Ebata, K. Hashizume, K. Hosoya and M. Araki, *J. Chromatogr.*, 475 (1989) 195.
5 N. Tanaka, Y. Tokuda, K. Iwaguchi and M. Araki, *J. Chromatogr.*, 239 (1982) 761.
6 N. Tanaka, Y. Tachibana and M. Araki, *Nippon Kagaku Kaishi*, (1986) 993.
7 E.R. Barnhart, D. G. Patterson, Jr., N. Tanaka and M. Araki, *J. Chromatogr.*, 445 (1988) 145.
8 N. Tanaka, K. Hosoya, Y. Tachibana, M. Araki, K. Tanaka and A. Kaji, *J. Chromatogr. Sci.*, 27 (1989) 735.
9 P. Haglund, L. Asplund, U. Jarnberg and B. Jansson, *J. Chromatogr.*, 507 (1990) 389.
10 K. Kimata, K. Hosoya, N. Tanaka, T. Araki, E. R. Barnhart, D. G. Patterson, Jr. and S. Terabe, *J. High Resolut. Chromatogr.*, 13 (1990)137.
11 J. H. Knox, B. Kaur and G. R. Millward, *J. Chromatogr.*, 352 (1986) 3.
12 J. H. Knox and B. Kaur, *Eur. Chromatogr. News*, 1, (1987) 12.
13 O. Chiantore, I. Novak and D. Berek, *Anal. Chem.*, 60 (1988) 638.
14 B. J. Bassler and R. A. Hartwick, *J. Chromatogr. Sci.*, 27 (1989) 162.
15 B. J. Bassler, R. Kaliszan and R. A. Hartwick, *J. Chromatogr.*, 461 (1989) 139.
16 M. F. Emery and C. K. Lim, *J. Chromatogr.*, 479 (1989) 212.
17 N. A. Eltekova, *J. Chromatogr.*, 506 (1990) 335.
18 F. Belliardo, O. Chiantore, D. Berek, I. Novak and C. Lucarelli, *J. Chromatogr.*, 506 (1990) 371.
19 G. Gu and C. K. Lim, *J. Chromatogr.*, 515 (1990) 183.
20 L. C. Sander and S. A. Wise, *Adv. Chromatogr.*, 25 (1986) 139.
21 K. Jinno, T. Ibuki, N. Tanaka, M. Okamoto, J. C. Fetzer, W. R. Biggs, P. R. Griffiths and J. M. Olinger, *J. Chromatogr.*, 461 (1989) 209.
22 N. Tanaka, K. Hashizume and M. Araki, *J. Chromatogr.*, 400 (1987) 33.
23 K. Jinno, S. Shimura, N. Tanaka, K. Kimata, J. C. Fetzer and W. R. Biggs, *Chromatographia*, 27 (1989) 285.
24 N. Tanaka, K. Hashizume, M. Araki, H. Tsuchiya, A. Okuno, K. Iwaguchi, S. Onishi and N. Takai, *J. Chromatogr.*, 448 (1988) 95.
25 N. Tanaka and E. R. Thornton, *J. Am. Chem. Soc.*, 99 (1977) 7300.
26 C. Tanford, *The Hydrophobic Effect: Formation of Micelles and Biological Membranes*, Wiley-Interscience, New York, 1980, Ch. 1 and 2.
27 E. Skutchanova, L. Feltl, E. Smolkova-Keulemansova and J. Skutchan, *J. Chromatogr.*, 292 (1984) 233.
28 B. L. Karger, L. R. Snyder and C. Eon, *Anal. Chem.*, 50 (1978) 2126.
29 A. A. Bothner-By and R. E. Glick, *J. Chem. Phys.*, 26 (1957) 1651.
30 M. Kilpatrick and H. H. Hyman, *J. Am. Chem. Soc.*, 80 (1958) 77.
31 R. F. Rekker, *Hydrophobic Fragmental Constant*, Elsevier, Amsterdam, 1977, Ch. 2.
32 T. L. Hafkenscheid and E. Tomlinson, *Adv. Chromatogr.*, 25 (1986) 1.
33 L. P. Hammett, *Physical Organic Chemistry*, McGraw-Hill, New York, 2nd ed., 1970, p. 245.
34 K. Jinno, T. Nagoshi, N. Tanaka, M. Okamoto, J. C. Fetzer and W. R. Biggs, *J. Chromatogr.*, 392 (1987) 75.
35 N. Tanaka, K. Sakagami and M. Araki, *J. Chromatogr.*, 199 (1980) 327.
36 B. Vonach and G. Schomburg, *J. Chromatogr.*, 149 (1978) 417.

Journal of Chromatography, 549 (1991) 43–57
Elsevier Science Publishers B.V., Amsterdam

CHROM. 23 365

Study of the fluoride adsorption characteristics of porous microparticulate zirconium oxide

J. A. BLACKWELL*

Minnesota Mining and Manufacturing Company (3M), Specialty Adhesives and Chemicals Division, Group Analytical Laboratory, 236-2B-11 3M Center, St. Paul, MN 55144 (USA)

and

P. W. CARR

Department of Chemistry and Institute for Advanced Studies in Bioprocess Technology, University of Minnesota, 207 Pleasant St. S.E., Minneapolis, MN 55455 (USA)

(First received October 23rd, 1990; revised manuscript received April 9th, 1991)

ABSTRACT

Lewis acid sites are present on the surface of metal oxide chromatographic supports and are responsible for the very strong adsorption of Lewis bases. Such sites must be masked or modified to elute solutes which contain Lewis base groups. Fluoride ion coordinates strongly with these sites on zirconium oxide and forms a surface whose composition is pH and ionic strength dependent. Coverages range from 13.7 μmol/m^2 fluoride at pH 4.8 to 0 μmol/m^2 fluoride at pH 13. Washing the particles with 0.1 *M* sodium hydroxide quantitatively desorbs all bound fluoride without harming the underlying zirconium oxide particle. Readsorption of the fluoride can be accomplished by equilibrating the particles in a buffer of suitable fluoride concentration. Such fluoride modification has been found to occur on a time scale suitable for displacement chromatography on the Lewis acid sites.

INTRODUCTION

Recently, there has been a resurgence of interest in the use of transition metal oxide particles as stationary phases for high-performance liquid chromatography (HPLC). Among the many possible oxide materials, zirconium oxide and titanium oxide show the greatest potential for successful use [1–5]. These materials have many characteristics of an ideal support including: mechanical strength, chemical stability, high surface area and a high percentage of mesopores. However, they lack the chemical homogeneity desired in an ideal phase.

The surfaces of these metal oxides, like other metal oxides, are very complex. A number of distinct classes of sites exist which can significantly contribute to the retention of a given solute. These sites include Brönsted acid sites, Brönsted base sites and Lewis acid sites [6–12]. These species are shown schematically in Fig. 1. Brönsted acid sites arise from the acidity of surface bound hydroxyls and tightly bound water molecules. The relative acidity is dependent on the metal ion, the mode of bonding and to a lesser extent the local environment.

0021-9673/91/$03.50

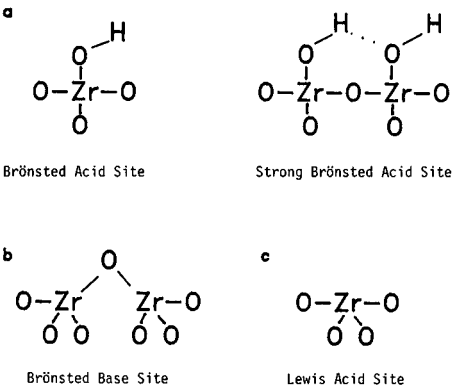

Fig. 1. Schematic of surface sites on zirconium oxide. (a) Brönsted acid sites; (b) Brönsted base sites; (c) Lewis acid sites.

Brönsted base sites arise from species such as bridging oxygen atoms shown in Fig. 1b. On the surface, such species can accept protons to form a cationic complex and have been observed spectroscopically [8,9,13]. Mono-, bi- and tridentate oxygen species have been identified on zirconium oxide surfaces [9,14,15] and it is expected that each will differ in Brönsted basicity.

The Lewis acid sites arise in a different manner. In the interior of metal oxides, such as zirconium oxide, the bonding of metal ions and oxygen atoms is governed by the coordination geometry of the metal ion. The metal ions bond to more oxygen atoms than charge stoichiometry would ordinarily allow, but the strength of each bond is less than in a stoichiometric bond. The result is an extensive network of bonding which gives metal oxides their high mechanical strength. When this bonding continuity is interrupted, at a surface for example, the coordination of the metal ions by oxygen atoms is not possible. As a result, a number of coordination sites are exposed at the surface. These sites are very electropositive and readily accept electron pairs, analogous to the coordination chemistry of soluble metal ions. To satisfy the coordination sphere of the metal ion, electron pair donors are coordinated to the available coordination sites. In aqueous solutions, these donors would include such species as water molecules, hydroxide ions and other available Lewis bases.

Within a given type of site, a great deal of heterogeneity can exist because of the varied geometries, surface defects and bonding types involved with a particular site. These complex surfaces can give rise to such interactions as ligand exchange on the exposed surface metal ions, hydrogen bonding to hydroxyl groups and ion exchange. The ion-exchange sites may be either cation or anion exchange or both due to the amphoteric nature of these metal oxides.

Undoubtedly, the most chromatographically troublesome sites on a zirconium oxide surface are the Lewis acid sites. These sites can form coordination complexes with a number of Lewis bases and are responsible for the irreversible adsorption of proteins and other solutes in systems where they are not blocked. For example, carboxylic acids could only be eluted from zirconium oxide when there was a high concentration of acetate ion (competing ion) in the eluent [2]. Phosphate is also observed to effectively block these sites [1].

However, these sites can be blocked by species other than oxyanions. The effectiveness of the blocking of the Lewis acid sites should be related to the strength of the interaction between the Lewis base used and the zirconium ion coordination site. Zirconium ion forms some of its strongest coordination compounds with fluoride ion [16]. We therefore tested fluoride as a mobile phase additive to control the Lewis acid properties of the material. This interaction is the subject of this investigation.

EXPERIMENTAL

Chemicals

Tris[hydroxymethyl]aminomethane (TRIS), cyclohexylaminopropane sulfonic acid (CAPS), 2-[N-morpholino]ethane sulfonic acid (MES), iminodiacetic acid (IDA) and N-tris[hydroxymethyl]methyl-3-aminopropane sulfonic acid (TAPS) were obtained from Sigma (St. Louis, MO, USA). Hydrochloric and acetic acids and sodium sulfate were obtained from EM Science (Gibbstown, NJ, USA). Sodium hydroxide was obtained as a 50% solution from Curtin Matheson Scientific (Houston,TX, USA). Sodium fluoride and sodium carbonate were obtained from J. T. Baker (Phillipsburg, NJ, USA) and sodium nitrate from MCB (East Rutherford, NJ, USA). Sodium thiocyanate, lithium chloride, sodium chloride, potassium chloride and ammonium chloride were obtained from Mallinckrodt (Paris, KY, USA). Sodium bromide, sodium perchlorate, sodium acetate, boric acid, oxalic acid and disodium phosphate were obtained from Fisher Scientific (Fairlawn, NJ, USA). Tetramethylammonium chloride and tetraethylammonium chloride were obtained from Aldrich (Milwaukee, WI, USA). All chemicals were reagent grade or better.

Water was prepared by passing house deionized water through a Barnstead Nanopure deionizing system with an organic free cartridge and a 0.2-μm final filter. The water was then boiled and cooled to remove any disolved carbon dioxide.

The porous zirconium oxide spherules were provided by the Ceramic Technology Center of the 3M Company. The spherules were prepared by a proprietary process and have been described previously [1–4]. Two types of particles were used in this investigation. The first type had a nominal diameter of 12.8 $\pm$ 1.2 μm, an average pore diameter of 308 Å by mercury porosimetry and an average BET surface area of 50.5 m^2/g. The second type had a nominal diameter of 37 $\pm$ 3 μm, an average pore diameter of 308 Å by mercury porosimetry and an average BET surface area of 33 m^2/g.

Apparatus

Solution fluoride measurements were made using an Orion Research (Boston, MA, USA) Model 96-09 combination fluoride electrode and a Model 501 Digital Ionalyzer. Polyethylene bottles were obtained from Nalge (Rochester, NY, USA).

Diffuse reflectance infrared spectroscopy was performed on a Bio-Rad (Cambridge, MA, USA) Digilab FTS-40 spectrometer with a Barnes Analytical/Spectra Tech (Stamford, CT, USA) Diffuse Reflectance Accessory. Spectral correction was performed with an internal Kubelka-Munk algorithm and a beam blocker was used during spectral acquisition.

Particle pretreatment

In order to remove as many of the manufacturing impurities as possible, the zirconium oxide particles were pretreated. This treatment consisted of three washes with 1 l of 0.5 *M* hydrochloric acid followed by three rinsings with 500 ml of treated water. The particles were then washed three times with 1 l of 0.5 *M* sodium hydroxide and then rinsed five times with 500 ml of treated water.

Fluoride adsorption rate studies

Three time domains were evaluated for the uptake of fluoride ion by zirconium oxide: minutes, hours and days. For the short term uptake studies, 1 g of particles was added to 49 ml TAPS buffer at pH 8.4 or MES buffer at pH 5.5. The solution was then stirred using a Teflon stir bar. An aliquot of 1 ml of a sodium fluoride solution was added using an Eppendorf pipette (Brinkman, Westbury, NJ, USA). The electrode response was monitored over the course of thirty minutes at 22°C.

The study of fluoride adsorption on the hour and day time scale was accomplished by placing 1 g of zirconium oxide particles in 50 ml of 0.1 *M* acetate buffer at pH 4.8 or 0.1 *M* TAPS buffer at pH 8.4. The slurry was ultrasonicated under vacuum and put into a waterbath at 35°C for an appropriate interval of time. Fluoride content was measured by adding 1 ml of the supernatant to 50 ml of 4 *M* acetate buffer at pH 4.8. The resulting solution was measured with the fluoride electrode and compared to similarly prepared standards.

Fluoride adsorption versus pH

Samples (1 g) of zirconium oxide were equilibrated with 50 ml of the appropriate buffer at 22°C. After 16 days, the supernatant solutions were analyzed for fluoride content in the same manner as for the timed adsorption assay.

Fluoride adsorption isotherm

Samples (1 g) of zirconium oxide were placed in 60 ml polyethylene bottles containing 50 ml of either 0.1 *M* acetate buffer at pH 4.75, 0.1 *M* TAPS buffer at pH 8.40 or 0.1 *M* MES buffer at pH 6.10. Various amounts of sodium fluoride were added to each bottle and the pH was readjusted by adding either concentrated hydrochloric acid or 50% sodium hydroxide solution. The bottles were placed in a shaker bath at 35°C for two days. The supernatant solutions were then analyzed for fluoride content in the same manner as for the timed assay. The supernatant solution was also submitted for inductively coupled plasma (ICP) analysis for zirconium.

The particles were then washed twice with 25 ml of treated water and 50 ml of 0.1 *M* sodium hydroxide was added to desorb the adsorbed fluoride. The samples were then placed in a shaker bath at 35°C for two days. The supernatant solution was analyzed for fluoride in the same manner as above.

A separate isotherm study was performed by placing 1-g samples of treated zirconium oxide particles into bottles and adding 50 ml of 20 m*M* sodium fluoride buffered to pH 8.4 with 0.1 *M* TAPS. Various amounts of sodium chloride were added to alter the total ionic strength of each sample. Following the addition of salt, the pH was readjusted to the desired pH. The bottles were placed in a shaker bath at 35°C for one day. The supernatant solutions were assayed for fluoride in the same manner as above. The base desorption procedure was the same as for the other isotherm studies with the incubation period shortened to one day.

Adsorption and desorption cycling

Polyethylene bottles containing 1 g of zirconium oxide particles were filled with 50 ml of either 0.1 *M* acetate buffer at pH 4.8, 0.1 *M* MES buffer at pH 6.1 or 0.1 *M* TAPS buffer at pH 8.4. Each solution was 20 m*M* in sodium fluoride. The bottles were then placed in a shaker bath at 35°C for 24 h. The supernatant solution was then assayed for fluoride in the same manner as for the timed assay. The remaining supernatant solution was removed and the particles were washed twice with 25 ml aliquots of treated water. The particles were then treated with 50 ml of 0.1 *M* sodium hydroxide solution at 35°C for 24 h. The supernatant solution was then assayed for fluoride. This procedure was repeated four times for each sample.

A fifth repetition of the cycle was performed on each sample, but after removing the excess supernatant buffer, the particles were washed twice with 50 ml aliquots of 1 *M* sodium chloride solution. This was followed by a washing with 50 ml treated water then base treatment in the usual manner. Each of the washing aliquots were assayed for fluoride.

Fluoride adsorption versus other salts

Solutions of the salts (1 *M*, except oxalate, lithium chloride and IDA which were 0.1 *M*) in 0.1 *M* TAPS buffer were made up with 20 m*M* sodium fluoride and the pH adjusted to 8.4. Zirconium oxide (1 g) was placed in a polyethylene bottle with 50 ml of a salt buffer. The bottles were transferred to a shaker bath at 35°C for two days. The fluoride content of the supernatant was measured in the same manner as in the timed adsorption assay.

Diffuse reflectance infrared (DRIFT) spectroscopy

Three samples of zirconium oxide particles were analyzed by DRIFT spectroscopy. The first sample consisted of the acid/base pretreated particles. The second sample consisted of particles which had been equilibrated for 16 days at 35°C with 0.1 *M* acetate buffer at pH 4.0 containing 0.5 *M* sodium fluoride. The last sample consisted of particles which had been equilibrated for 16 days at 35°C with 0.1 *M* sodium hydroxide containing 0.5 *M* sodium fluoride. The DRIFT cell was filled with sample and a beam blocker was put into place to decrease the amount of specular reflectance signal entering the detector. The samples were pulsed 256 times in the region of 400 to 4000 wavenumbers. Absorbances were corrected using a Kubelka–Munk algorithm.

RESULTS AND DISCUSSION

Because fluoride forms one of the strongest known zirconium complexes [16], it should be a very powerful displacing agent towards any Lewis base on a zirconium oxide surface. Previous studies have shown that metal oxides in general have a high affinity for fluoride ion [17–21]. However, its use as a modifier for controlling the retention of solutes on metal oxide surfaces has not yet been explored.

Zirconium ion is stable as a tetravalent cation. It has an especially high charge to radius ratio characteristic of hard metal ions and as such forms very strong coordination complexes with oxygen containing ligands [22,23]. It also displays a high affinity for other strong hard Lewis bases such as fluoride ion. Although these coordination properties are normally considered when dealing with solution species, we

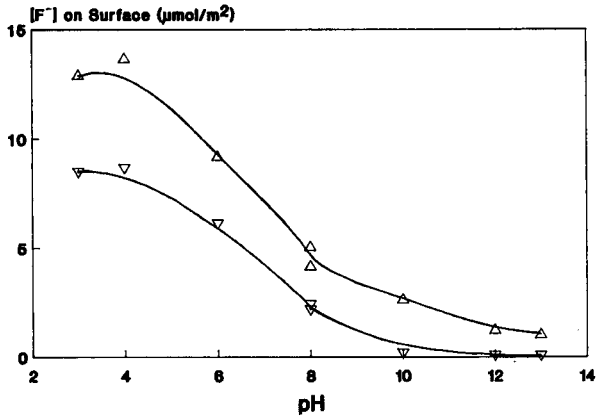

Fig. 2. Fluoride adsorption as a function of pH at 25°C. △ = Fluoride adsorption; ▽ = fluoride desorption at pH 13. Buffers are all 0.1 *M* and contain 20 m*M* sodium fluoride except where noted: pH 3, 0.001 *M* HCl; pH 4, acetate; pH 6, MES; pH 8, TAPS (top) and TRIS (bottom); pH 10, CAPS; pH 12, 0.01 *M* NaOH; pH 13, 0.1 *M* NaOH.

believe that they are also relevant to the chemical properties of the "vacant" coordination sites (Fig. 1c) on the surface of zirconium oxide.

In neutral solutions, these "vacant" sites are occupied by either water molecules, hydroxyl ions, or other Lewis bases. When the vacant sites are occupied by weakly held ligands, solutes containing stronger Lewis base groups will be retained until displaced by a yet stronger base. The strength of this interaction can be quite high. Fluoride's first formation constant [K_1] with zirconium ion [24] is $10^{8.8}$ which gives a Gibbs free energy of formation of 12.4 kcal/mol at 35°C. Thus a base such as fluoride can serve two functions: it can block Lewis acid sites occupied by weaker bases or it can displace coordinated solutes.

Since hydroxide ion is a Lewis base and also forms a strong complex with zirconium ion [25] ($K_1 = 10^{14.3}$), the adsorption of fluoride ion on zirconium oxide should have a very strong dependence on pH as shown by the data in Fig. 2. In very basic solutions, fluoride cannot effectively compete with the high concentration of hydroxide ions in solution. Above pH 13, fluoride does not adsorb at all on the zirconium oxide surface.

At low pH, the fluoride was more easily adsorbed onto the surface due to less effective competition from hydroxide ion. A maximum was reached at about pH 4 where 13.7 μmol/m^2 of fluoride was adsorbed on the large diameter particles. Adsorption of fluoride then decreases as the pH is lowered due to the protonation of fluoride.

At pH 8, less fluoride adsorbed in a TRIS buffer than in a TAPS buffer under the same conditions. TRIS is known to specifically solubilize zirconium phosphate by complexation of zirconium (IV) ion [1]. When TRIS molecules block some of the Lewis acid sites, decreased fluoride adsorption is expected.

A major consequence of the strong pH dependence is that it implies that fluoride adsorption can be reversed. Fluoride adsorbed at lower pH should be readily

TABLE I

REPETITIVE ADSORPTION AND DESORPTION OF FLUORIDE (μmol/m^2 ± S.D.)[a]

Cycle	Stage	pH 4.8	pH 6.1	pH 8.4
1	Adsorption[b]	11.3 ± 0.4	7.9 ± 0.3	3.4 ± 0.1
	Desorption[c]	8.4 ± 0.3	6.1 ± 0.2	1.8 ± 0.1
2	Adsorption	10.7 ± 0.3	8.3 ± 0.3	3.4 ± 0.1
	Desorption	8.1 ± 0.3	6.1 ± 0.2	2.1 ± 0.1
3	Adsorption	10.4 ± 0.3	7.9 ± 0.3	3.4 ± 0.1
	Desorption	8.1 ± 0.3	6.1 ± 0.2	2.0 ± 0.1
4	Adsorption	10.4 ± 0.3	7.9 ± 0.3	3.4 ± 0.1
	Desorption	8.1 ± 0.3	6.3 ± 0.2	2.0 ± 0.1
5	Adsorption	10.1 ± 0.3	7.9 ± 0.3	3.4 ± 0.1
	1st NaCl wash	0.5 ± 0.0	0.6 ± 0.0	0.7 ± 0.0
	2nd NaCl wash	0.3 ± 0.0	0.4 ± 0.0	0.4 ± 0.0
	Water wash	1.2 ± 0.0	0.9 ± 0.0	0.5 ± 0.0
	Desorption	8.4 ± 0.3	6.3 ± 0.2	2.0 ± 0.1
	Total desorbed	10.4 ± 0.3	8.2 ± 0.2	3.6 ± 0.1

[a] See Experimental for details.

[b] This amount is computed by measuring the decrease in fluoride concentration in solution upon contact with the zirconia particles.

[c] This amount is computed by measuring the concentration of fluoride in the base solution used to desorb fluoride. Note the particles are first washed with water to remove interstitial fluoride.

displaced by washing the particles with 0.1 *M* sodium hydroxide solution. It has previously been shown [2] that zirconium oxide is chemically and physically stable from pH 1 to 14. Equilibration with the appropriate fluoride containing buffer should restore the column to its original condition. This is shown quantitatively in Table I. Cyclic adsorption and desorption of fluoride showed that, at all three pH values tested, base treatment quantitatively removed the fluoride. Recovery of fluoride appears to be incomplete because the particles were washed with water to remove interstitial fluoride then adsorbed fluoride was released by washing with base. However, in each cycle, the base washing step restored the original capacity of the particles for adsorption of fluoride.

The desorption of fluoride in the water washes was monitored closely in cycle five. If fluoride were held by a simple ion-exchange rather than by a ligand-exchange mechanism, washing with 1 *M* sodium chloride should quantitatively displace fluoride. This is because on all ion exchangers, fluoride is more weakly held than is chloride due to the lower charge to radius ratio of the hydrated fluoride anion *versus* chloride ion. During the salt wash, a small amount of fluoride ion was removed. This can be attributed to the small fraction of fluoride held by ion-exchange forces and to the presence of fluoride ion in solution in the pores of the particles. However, when a water wash followed the salt washes, an increased amount of fluoride ion was recovered. We believe that this resulted from desorption of coordinated fluoride due to the lower ionic strength. The favorable thermodynamic driving force for coordination of

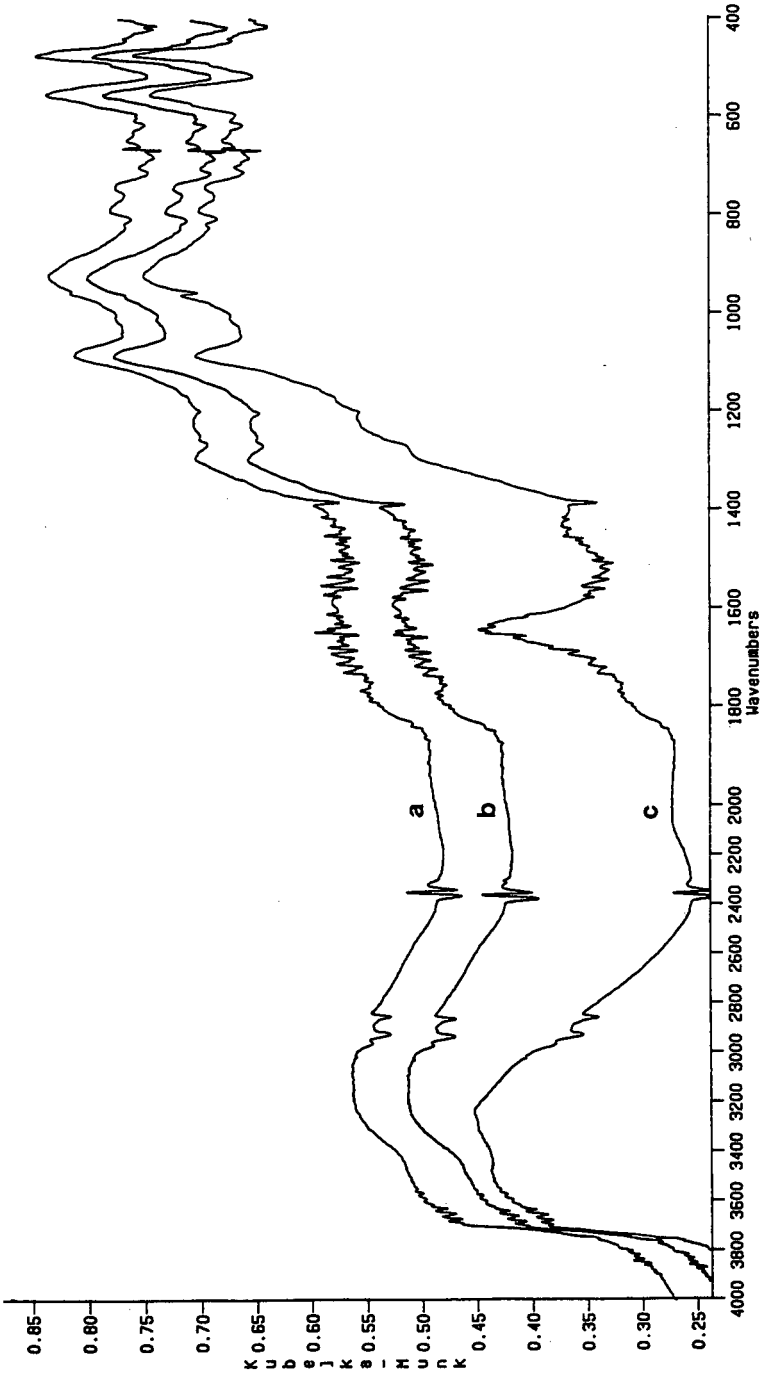

Fig. 3. DRIFT spectrum of (a) pretreated zirconium oxide particles, (b) particles treated with 0.5 *M* sodium fluoride at pH 13, (c) particles treated with 0.5 *M* sodium fluoride at pH 4.8.

fluoride is somewhat offset by the ionic repulsion between fluoride ions when two or more fluoride ions attempt to occupy the small Lewis acid site. In solutions of high ionic strength (as in 1 *M* sodium chloride), this ionic repulsion is screened (in a Debye sense) and a larger amount of fluoride can adsorb onto the surface. When the ionic strength is decreased, coulombic repulsion causes some surface fluoride ions to desorb.

The reversibility of fluoride adsorption is demonstrated spectroscopically by the results shown in Fig. 3. Spectrum 3a is for the acid and base pretreated zirconium oxide particles before exposure to fluoride. After equilibrating the particles in 0.5 *M* sodium fluoride solution, a noticeable difference in the spectrum was observed as shown in spectrum 3c. Spectrum 3b is for the same particles after treatment with 0.1 *M* sodium hydroxide in the presence of 0.5 *M* sodium fluoride. The spectrum is identical to that of the untreated particles indicating no modification to the particles under these conditions.

Close examination of the DRIFT spectra revealed some subtle but important aspects of the surface modification. Table II lists the infrared absorptions relevant to this material [8,9,14,15,26–31]. The most striking feature is the lack of modification to the non-Lewis acid sites on the surface. The high frequency (3800–3200 cm^{-1}) absorbance region is due to freely vibrating surface hydroxyl groups [9,31] and was found to be identical in all three spectra. However, the lower frequency (3200–2600 cm^{-1}) region, due to coordinated water molecules [9,30,31], showed a decrease in absorbance for the fluoride treated sample. This is consistent with fluoride induced displacement of coordinated water molecules from the Lewis acid sites. Comparison of the low frequency (1200–400 cm^{-1}) region again showed that the surface hydroxyl

TABLE II

INFRARED ABSORBANCES FOR ZIRCONIUM OXIDES AND FLUORIDES [8,9,14,15,26–31]

Functionality	Frequency (cm^{-1})
Zr–O non-bridging	420
Zr–O bridging	450
Zr–O stretch	550
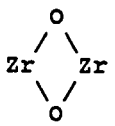 stretch	475
	610
asymmetric stretch	740
Zr–OH bend	700–1050
Zr–H	1371
	1562
O–H	2800–3800
H–O–H bend	1620
Coordinated H–O–H	2600–3500
Zr–OH stretch	3770
$(Zr)_n$–OH	3670
ZrF_6^{-2}	581
ZF_4	668

groups were intact. As a result, the surface retained its ionizable hydroxyl groups and thus its potential for cation exchange despite the presence of adsorbed fluoride ions.

A noticeable increase in absorbance at 1620 cm^{-1} was observed for the fluoride treated sample. This corresponds to the water bending frequency and reflects a difference in the water molecules bound to the surface of the particles. In the fluoride treated sample, the fluoride ions have displaced some of the coordinated water molecules and a decrease in the coordinated water absorptions was observed. Fluoride is normally hydrated to a great extent and when a fluoride ion is coordinated to the surface, the accessible surface of the fluoride ion is expected to be hydrated. This gives rise to an increased absorbance at 1620 cm^{-1} due to the bending frequency of these adsorbed water molecules. The untreated samples have their surface hydrated with water molecules coordinated to the Lewis acid sites whereas the fluoride treated surface has water bound due to fluoride hydration.

Zirconium forms a number of different types of compounds with fluoride and the final product is usually a mixture of complex hydroxyoxofluoro compounds [32]. As a result, there is a great diversity of binding types and strengths between zirconium and fluoride ions. From Fig. 3 it can be seen that the absorbance bands characteristic of the zirconium fluoride compounds showed no difference between the treated and untreated particles. In ZrF_4, fluoride is present entirely as bridging ions and this type of binding is not expected in adsorbed fluoride. A lack of definitive infrared absorbance data on the many types of zirconium fluoride compounds precludes any positive assignment of the bonding type from infrared spectroscopy.

Fluoride adsorption rate

Earlier studies on the adsorption of fluoride ion from solution by zirconium oxide indicated a relatively slow process [18]. However, under the conditions stated above, the adsorption rate for the zirconium oxide particles was faster than the response time of the fluoride electrode (less than two seconds). The discrepancy between our results and the previous findings are no doubt due to the differences in

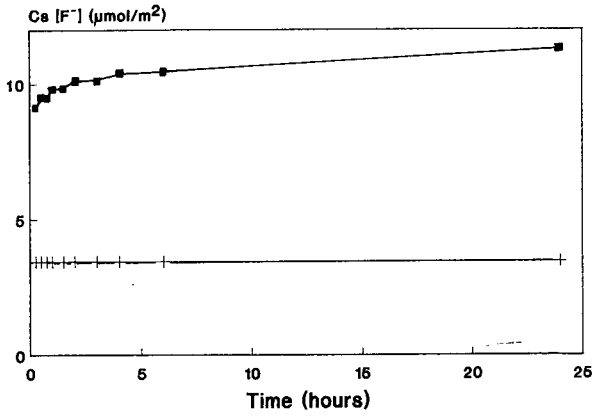

Fig. 4. Fluoride adsorption as a function of time. ■ = Fluoride adsorption in 0.1 *M* acetate buffer with 20 m*M* sodium fluoride at pH 4.75; + = fluoride adsorption in 0.1 *M* TAPS buffer with 20 m*M* sodium fluoride at pH 8.4 at 35°C. C_s = Surface fluoride concentration.

diffusion rates between the large, relatively non-porous particles used in prior studies and the small, highly porous particles used here.

When the adsorption rate was studied over much longer periods of time, a very slow increase in the amount of fluoride adsorbed was observed at low pH. Fig. 4 shows that at pH 8.4 there was no increase in fluoride adsorption while at pH 4.75, a slow increase was observed. We account for this by the slow dissolution of zirconium oxide by the hydrogen fluoride formed at this pH and the subsequent formation of fluorozirconates [32]. Such soluble fluoride species cannot be detected by the fluoride electrode and lead to high apparent adsorption of fluoride. It should be noted that this dissolution is a relatively slow process and rapid acid washing to remove base resistent species from the stationary phase may be tolerable. A very small increase in fluoride adsorption was observed over the period from one to sixteen days at pH 4.75, whereas no increase at all was observed at pH 8.4.

Adsorption isotherm

Fluoride adsorption isotherms showed that the surface was saturated with fluoride at fairly low fluoride concentrations. Fig. 5 shows the isotherm at pH 4.75. The desorption measurements show a maximum adsorption capacity of approximately 8 μmol/m^2 which was reached in 10 mM fluoride solutions and was maintained to 100 mM solutions. This high surface coverage is not entirely surprising. Lewis acid site density has been found to be approximately 6 μmol/m^2 by titration of such sites with sulfur trioxide [33]. Since the sites have a +2 charge [6,8,12], electronic neutrality can be reached with 2 fluoride ions per Lewis acid site, giving 12 μmol/m^2.

At fluoride concentrations greater than 100 mM, the zirconium oxide particle were attacked with formation of fluorozirconates. Fluorozirconates are slightly soluble in aqueous solutions and their solubility in higher fluoride concentration solutions is suppressed. This is obviously detrimental to the integrity of the particles, but is not surprising since at pH 4.75 a fair amount of fluoride ion is present as hydrofluoric acid, which is known to attack zirconium oxide.

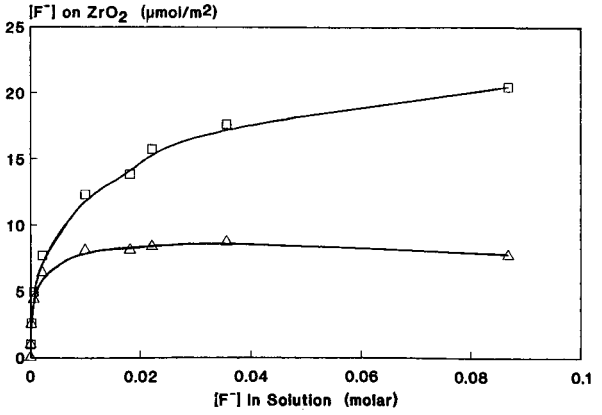

Fig. 5. Fluoride adsorption isotherm at pH 4.75. □ = Apparent adsorption isotherm; △ = base desorption isotherm. Buffer was 0.1 M acetate containing various amounts of sodium fluoride at 35°C for 48 h.

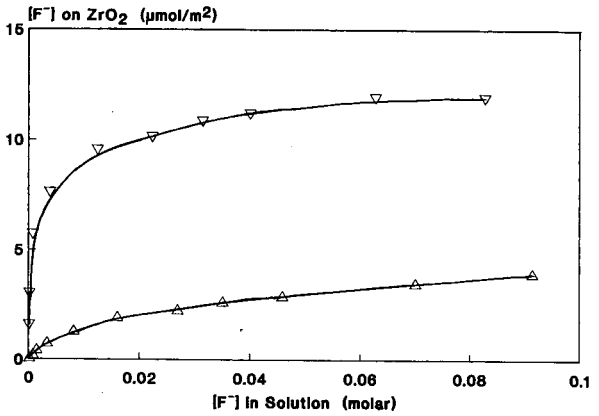

Fig. 6. Fluoride adsorption isotherm. ▽ = pH 6.1 0.1 *M* MES buffer; △ = pH 8.4 TAPS buffer; both 35°C for 48 h. Measurements made by desorbing fluoride ion in 0.1 *M* sodium hydroxide.

At higher pH, the problems associated with hydrogen fluoride generation were alleviated. Fig. 6 shows the adsorption isotherm for fluoride under more hospitable conditions. The maximum adsorption of fluoride ion was lower than that found at lower pH due to increased competition from hydroxide ion. The adsorption of fluoride leveled off when the surface concentration reached approximately 4 μmol/m^2 at pH 8.4 and 12 μmol/m^2 at pH 6.1 at 35°C. In contrast to what was observed at lower pH, the zirconium oxide particle was not rapidly attacked. The solution concentrations of zirconium never exceeded 0.6 nmol/ml. In comparison, silica dissolves in neutral solutions to approximately 1.67 μmol/ml [34] and at pH 8.4 to a much greater extent.

When the amount of fluoride adsorbed onto the zirconium oxide was measured in the original solution, a much higher apparent capacity was observed. Fig. 5 shows

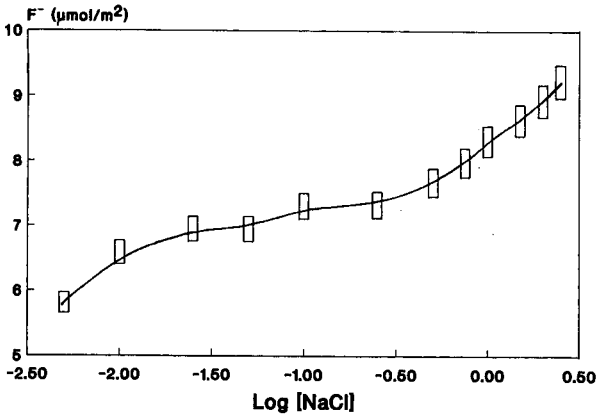

Fig. 7. Fluoride adsorption as a function of ionic strength. Buffer is 20 m*M* sodium fluoride in 0.1 *M* TAPS buffer at pH 8.4 and 35°C with added sodium chloride.

that the apparent capacity reached approximately 20 μmol/m^2 in 100 mM sodium fluoride solution. This higher apparent capacity is believed to be a result of the ionic strength masking of the electronic repulsion between adsorbed fluoride ions on the surface. As the ionic strength was increased, a greater number of fluoride ions could adsorb onto the surface. When the ionic strength was lowered to zero, as in the water washes, the ionic repulsion displaced excess fluoride until equilibrium was established. For comparison purposes, it was this equilibrium fluoride content which was measured in the isotherm studies at different pH values.

This ionic strength effect is shown in Fig. 7. An adsorption isotherm study was undertaken with a constant amount of fluoride in solution. The total ionic strength was increased by the addition of sodium chloride. Chloride ion has a formation constant of $10^{0.3}$ with zirconium ion [24] and therefore is not expected to form coordination compounds at pH 8.4. The surface concentration of fluoride rose from 5.8 μmol/m^2 at low ionic strength to 9.25 μmol/m^2 at high ionic strength. This 60% increase in capacity is believed to be due to the masking of the ionic repulsion of crowded surface fluoride ions thus allowing a greater mean coordination number of fluoride ions on each Lewis acid site.

Salt effects on fluoride adsorption

The effects on fluoride adsorption by a variety of salts is shown in Table III. A number of salts showed no effect other than to reduce the ionic repulsion between coordinated fluorides to increase the total adsorption capacity. Small differences exist

TABLE III

SALT EFFECTS ON FLUORIDE ADSORPTION[a]

Salt	Fluoride capacity (μmol/m^2) ± S.D. (n = 3)
Tetraethylammonium chloride	8.8 ± 0.3
Sodium perchlorate	8.7 ± 0.3
Sodium nitrate	8.0 ± 0.3
Sodium bromide	8.0 ± 0.3
Sodium acetate	8.0 ± 0.3
Sodium thiocyanate	7.4 ± 0.3
Sodium chloride	7.4 ± 0.3
Sodium sulfate	6.7 ± 0.2
Potassium chloride	6.2 ± 0.2
Ammonium chloride	6.2 ± 0.2
Tetramethylammonium chloride	6.2 ± 0.2
Iminodiacetic acid (0.1 M)	4.5 ± 0.2
None	4.5 ± 0.2
Lithium chloride (0.1 M)	4.3 ± 0.2
Oxalic acid (0.1 M)	3.8 ± 0.1
Sodium carbonate	3.8 ± 0.1
Sodium phosphate	3.0 ± 0.1
Boric acid	0.6 ± 0.1

[a] See Experimental for details.

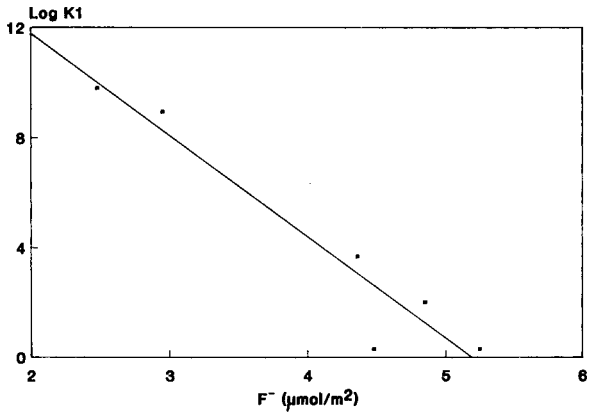

Fig. 8. Fluoride adsorption as a function of solution complex formation constant. Adsorption was in 0.1 *M* TAPS buffer with 20 m*M* sodium fluoride at pH 8.4 and 35°C.

between these salts and can be mainly ascribed to differences in the chaotropic nature of the salts. A second group of salts was effective in blocking a certain fraction of the available Lewis acid sites on the zirconium oxide surface. This was expected since these salts have stronger interactions with zirconium ion than does fluoride [35]. Using data for the formation constants of zirconium (IV) ion and the appropriate anion [25,26,35,36], Fig. 8 shows the relationship between fluoride adsorption and the strength of the coordination interaction.

Borate is an interesting case in itself since it is not a good Lewis base. Borate is known to form esters with polyhydroxy compounds [37] and may be preventing fluoride ion adsorption by sterically blocking the Lewis acid sites. The composition of such phases are known to vary strongly with the pH of the solution [38]. The resulting surface might be useful as a cation-exchange material and could also find use in the separation of sugars. This, however, is the subject of another investigation.

CONCLUSIONS

It has been demonstrated that the interactions of various ligands on the Lewis acid sites are similar to those of the soluble species. Since the composition of Lewis bases coordinated to the Lewis acid sites will be determined by the concentration and coordination thermodynamics of the bases in solution, the strength of these adsorptions can be modified to change the overall properties of the surface. In doing so, the zirconium oxide support can be modified to provide a more compatible and controllable surface for separation of solutes without losses due to irreversible adsorption on these strong sites.

It was also found that such interactions take place on a time scale suitable for their use in chromatography. In addition, the surface modification was found to be readily reversible by flushing the material with 0.1 *M* sodium hydroxide solution followed by re-equilibration with the appropriate buffer. However, care should be exercised when working with acidic solutions to prevent dissolution of the material when fluoride is present.

ACKNOWLEDGEMENTS

The authors would like to thank Eric Funkenbusch, Douglas Hanggi, Don Hagen, Tom Weber and Wes Schafer for their helpful discussions. We would also like to thank Shiela Kromer for her instruction in DRIFT spectroscopy and Wanda Bahmet for her prompt service with ICP results. J.A.B. acknowledges financial support from Specialty Adhesives and Chemicals Division and the Leading Edge Academic Program at 3M.

REFERENCES

1 W. A. Schafer, *MS Thesis*, University of Minnesota, 1990.
2 M. P. Rigney, *Ph.D. Thesis*, University of Minnesota, Minneapolis, MN, 1988.
3 W. A. Schafer, E. F. Funkenbusch, K. A. Parson and P. W. Carr, *J. Chromatogr.*, in press.
4 W. A. Schafer and P. W. Carr, *J. Chromatogr.*, in press.
5 M. Kawahara, H. Nakamura and T. Nakajima, *Anal. Sci.*, 5 (1989) 485–486.
6 A. A. Tsyganenko, D. V. Pozdnyakov and V. N. Filimonov, *J. Mol. Struct.*, 29 (1975) 299–318.
7 V. Vesely and V. Pekarek, *Talanta*, 19 (1972) 219–262.
8 W. Hertl, *Langmuir*, 5 (1989) 96–100.
9 P. A. Agron, E. L. Fuller and H. F. Holmes, *J. Coll. Int. Sci.*, 52 (1975) 553–561.
10 T. Yamaguchi, Y. Nakano and K. Tanabe, *Bull. Chem. Soc. Jpn.*, 51 (1978) 2482–2487.
11 N. E. Tret'yakov, D. V. Pozdnyakov, O. M. Oraskaya and V. N. Filimonov, *Zh. Fiz. Khim.*, 44 (1970) 596–600.
12 E. V. Lunina, A. K. Selivanovskii, V. B. Golubev, T. Y. Samgina and G. I. Markaryan, *Zh. Fiz. Khim.*, 56 (1982) 415–418.
13 J. D. McCullough and K. N. Trueblood, *Acta Cryst.*, 12 (1959) 507–511.
14 T. Yamaguchi, Y. Nakano and K. Tanabe, *Bull. Chem. Soc. Japan*, 51 (1978) 2482–2487.
15 A. A. Tsyganenko and V. N. Filimonov, *Spec. Lett.*, 5 (1972) 477–487.
16 S. Ahrland, D. Karipides and B. Noren, *Acta Chem. Scand.*, 17 (1963) 411–424.
17 H. Imai, J. Nomura, Y. Ishibashi and T. Konishi, *Chem. Soc. Japan*, 5 (1987) 807–813.
18 T. M. Suzuki, C. Chida, M. Kanesato and T. Yokoyama, *Chem. Lett.*, (1989) 1155–1158.
19 H. Hirai, T. Ishibashi, Y. Fujiwara and K. Tanaka, *J. P. Pat.*, 115 058 (1976).
20 Miyoshi Oil and Fat Co., *J. P. Pat.*, 107 287 (1982).
21 M. Kanesato, T. Yokoyama and T. M. Suzuki, *Chem. Lett.*, (1988) 207–210.
22 R. G. Pearson, *J. Chem. Ed.*, 45 (1968) 581–587.
23 R. G. Pearson, *J. Chem. Ed.*, 45 (1968) 643–648.
24 L. G. Sillen and A. E. Martell, *Stability Constants of Metal Ion Complexes*, The Chemical Society, London, 1964.
25 A. J. Zielen and R. E. Connick, *J. Am. Chem. Soc.*, 78 (1956) 5785–5792.
26 Y. Y. Kharitonov and L. M. Zaitsev, *Russ. J. Inorg. Chem.*, 13 (1968) 476–477.
27 K. A. Burkov, G. V. Kozhevnikova, L. S. Lilich and L. A. Myund, *Russ. J. Inorg. Chem.*, 27 (1982) 804–807.
28 D. A. Powers and H. B. Gray, *Inorg. Chem.*, 12 (1973) 2721–2726.
29 J. R. Ferraro, *Low-Frequency Vibrations of Inorganic and Coordination Compounds*, Plenum Press, New York, 1971, pp. 75, 118 and 127.
30 N. E. Tret'yakov, D. V. Pozdnyakov, O. M. Oranskaya and V. N. Filimonov, *Russ. J. Phys. Chem.*, 44 (1970) 596–600.
31 J. Erkelens, H. T. Rijnten and S. H. Eggink-DuBurck, *Receuil*, 91 (1972) 1426–1432.
32 W. B. Blumenthal, *The Chemical Behavior of Zirconium*, Van Nostrand & Co., Princeton, NJ, 1958.
33 R. G. Silver, C. J. Hou and J. G. Ekerdt, *J. Catal.*, 118 (1989) 400–416.
34 F. Guyon, L. Chardonnet, M. Caude and R. Rosset, *Chromatographia*, 20 (1985) 30–34.
35 A. M. Golub and V. N. Sergun'kin, *Zh. Neorg. Khim.*, 11 (1966) 770–774.
36 R. E. Connick and W. H. McVey, *J. Am. Chem. Soc.*, 71 (1949) 3182–3191.
37 A. Bergold and W. H. Scouten, *Chem. Anal.*, 66 (1983) 149–187.
38 H. T. S. Britton, *J. Chem. Soc.*, (1926) 125–147.

Journal of Chromatography, 549 (1991) 59–75
Elsevier Science Publishers B.V., Amsterdam

CHROM. 23 366

Fluoride-modified zirconium oxide as a biocompatible stationary phase for high-performance liquid chromatography

J. A. BLACKWELL*

Minnesota Mining and Manufacturing Company (3M), Specialty Adhesives and Chemicals Division, Group Analytical Laboratory, 236-2B-11 3M Center, St. Paul, MN 55144 (USA)

and

P. W. CARR

Department of Chemistry and Institute for Advanced Studies in Bioprocess Technology, University of Minnesota, 207 Pleasant St. S.E., Minneapolis, MN 55455 (USA)

(First received October 23rd, 1990; revised manuscript received April 9th, 1991)

ABSTRACT

Previously we found that porous microparticulate zirconium oxide strongly adsorbs fluoride from aqueous solutions. The adsorption is due in large part to a Lewis acid–base interaction between coordination sites on the zirconium oxide surface and fluoride. The resulting complex is very stable relative to many other species and therefore fluoride is hard to displace. The chromatographic properties of small molecules and proteins on zirconium oxide particles when fluoride is present in the mobile phase is investigated in this work. In the presence of fluoride, zirconium oxide is a very biocompatible adsorbent, the selectivities of which are analogous to those of calcium hydroxyapatite. The effect of fluoride is very reproducible even after the adsorbed fluoride is stripped by strong base and regenerated in fluoride buffer.

INTRODUCTION

Properly fabricated porous metal oxides have a number of physical characteristics which make them nearly ideal supports for high-performance liquid chromatography (HPLC). They are mechanically stable and can be processed into highly porous microparticulates which have a high proportion of mesopores. In addition, these particles display great resistance to chemical attack. Zirconium oxide, for example, is stable over the pH range 1 to 14 [1]. Such chemical resistance is advantageous when corrosive eluents are used or when the column must be sterilized.

However, a major drawback to the use of these materials as stationary phases is their chemical heterogeneity. The surface of metal oxides are covered with many different types of functional sites [2,3]. Among these are Brönsted acid sites, Brönsted base sites, Lewis acid sites and Lewis base sites. The surface of zirconium oxide has all but the Lewis base sites [3–5] as shown schematically in Fig. 1. These sites will interact differently with different solutes and can lead to badly broadened peaks or irreversible adsorption of strongly interacting solutes.

0021-9673/91/$03.50

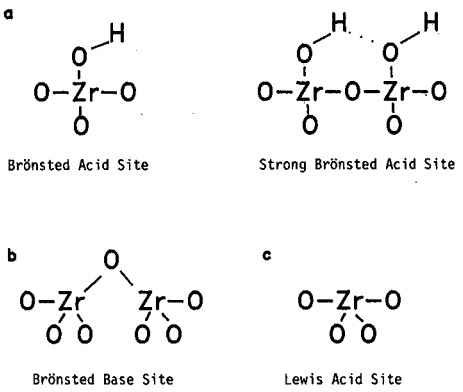

Fig. 1. Surface sites on zirconium oxide. (a) Brönsted acid sites; (b) Brönsted base sites; (c) Lewis acid sites.

The Lewis acid sites are the most troublesome of the various moieties present on the surface of zirconia. These sites arise from the surface discontinuity in bonding between metal and oxygen atoms. In bulk monoclinic zirconium oxide, the zirconium atoms are heptacoordinate. Therefore surrounding each zirconium (4+) ion are seven oxygen atoms with bond lengths of approximately 2.1 Å. The bonding valence is shared nearly equally among these bonds and the result is a very mechanically robust structure. The surface metal ions have satisfied their bonding valence to structural oxygen atoms but their coordinative bonding to other oxygen atoms is interrupted. This results in the existence of a number of accessible coordination sites on the particle surface.

Depending on the pH and other conditions, such sites are ordinarily occupied by hydroxide ions, water molecules or whichever Lewis bases may be present in solution. When a stronger Lewis base is introduced, it displaces the weaker Lewis bases and forms a stronger coordination complex at the surface. Chromatographically, this could lead to irreversible binding of a strong Lewis base unless an even stronger Lewis base is present in solution and acts to displace the bound solute [2]. This chemistry can be used to impart high selectivity to separations based on this elution strategy.

Fluoride interacts strongly with these hard surface Lewis acid sites since it is a very hard Lewis base [6–8]. The physical aspects of adsorption of fluoride onto these sites was investigated earlier [9]. Fluoride appears to be a reasonable candidate for modulating the strength of the Lewis acid site interactions. The effect of fluoride on the chromatographic properties of zirconium oxide, particularly towards protein separations, is the subject of this investigation.

EXPERIMENTAL

Cyclohexylaminopropanesulfonic acid (CAPS), N-tris[hydroxymethyl]methyl-3-aminopropanesulfonic acid (TAPS), 2-[N-morpholino]ethanesulfonic acid (MES), 3-[N-morpholino]propane sulfonic acid (MOPS), uracil and all proteins were obtained from Sigma (St. Louis, MO, USA). Phenylacetic acid, guanidine hydrochlo-

ride, benzamide and benzenesulfonic acid were obtained from Kodak (Rochester, NY, USA). Imidazole, benzylamine, lithium chloride, sodium thiocyanate, sodium acetate and benzyl mercaptan were from Aldrich (Milwaukee, WI, USA). Phenol, hydrochloric acid, acetic acid and sodium fluoride were from Mallinckrodt (St. Louis, MO, USA), 9-benzenephosphonic acid was from Pfaltz and Bauer (Waterbury, CT, USA) and benzyl alcohol was from J.T. Baker (Phillipsburg, NJ, USA). Sodium sulfate, potassium chloride, ammonium chloride and sodium chloride were obtained from EM Science (Gibbstown, NJ, USA) and 50% sodium hydroxide solution was obtained from CMS Scientific (Houston, TX, USA). Particle pretreatment and solution fluoride measurements were as described in detail earlier [9]. All chemicals were reagent grade or better.

The porous zirconium oxide spherules were provided by the Ceramic Technology Center of the 3M Company and were described earlier [1,9–14]. Particles used in this investigation had a nominal diameter of 5.3 μm $\pm$ 1.3 μm, an average pore diameter of 308 Å by mercury porosimetry and an average BET surface area of 30.5 m^2/g. Particles were suspended in isopropanol and packed at 4500 p.s.i. into 50 $\times$ 4.6 mm I.D. columns by the upward slurry method [15]. Titanium screens (2 μm) were used, instead of frits, to minimize protein losses in the inlet [16] and to minimize contamination of the column by solubilized metal ions. Whenever the buffer was changed, the column was regenerated by flushing with approximately 50 ml of 0.1 *M* sodium hydroxide solution followed by 50 ml of freshly boiled deionized water. This treatment is essential since it removes all "irreversibly" bound solutes from the zirconia and reproducibly prepares the surface for equilibration in the next buffer.

Chromatographic studies were carried out on two systems. The first system consisted of a Hewlett-Packard (Avondale, PA, USA) Model 1090M liquid chromatograph with a DR5 ternary solvent delivery system and a diode array detector. The optional expanded pH range kit as well as ultrahigh molecular weight polyethylene piston seals (UPC-10) obtained from Bal Seal Engineering (Santa Ana, CA, USA) were installed. Data were processed using a Hewlett-Packard 9000/series 300 computer outfitted with ChemStation software.

The second system consisted of an Altex 110A isocratic pump (Fullerton, CA, USA) with a Rheodyne (Cotati, CA, USA) 7120 injector valve. The detector was a Perkin-Elmer (Norwalk, CT, USA) LC-15 fixed wavelength detector with a 254-nm filter. For high pH eluents, the piston seals were replaced with unfilled PTFE piston seals. Both systems were outfitted with a 50 $\times$ 4.6 mm I.D. column filled with 10–20-μm zirconia particles. This guard column was placed before the injection valve to scavenge any contaminants in the buffer.

Protein recovery assays

Lysozyme and myoglobin solutions (*ca.* 10 mg/ml) were made up in 100 m*M* sodium chloride–20 m*M* MES pH 5.5 buffer. Injections of 10 μl were made onto a 50 $\times$ 4.6 mm I.D. column packed with 5-μm particles. A linear gradient of 0 to 0.75 *M* Na_2SO_4 in 100 m*M* sodium fluoride–20 m*M* MES pH 5.5 was run in 30 min at 35°C. The column effluent was collected and stored at 4°C for protein analysis later the same day. Each protein was run five times and the effluents saved for analysis. The column was then removed and the analysis repeated five times per protein as a control for protein recovery. Two separate bicinchoninic acid (BCA) protein assay protocols

[17,18] were used to quantitate the protein recovery in each case. The enhanced assay and the microreagent assay were performed using the effluent from a water blank injection as the diluent blank.

RESULTS AND DISCUSSION

Ion exchange is the most common mode of separating proteins and large biomolecules. Retention is reasonably predictable and a great deal of work on the process and its control by such factors as ionic strength, salt composition, pH and organic modifier [19–21] has been done. Recent developments in polymer science have produced polymeric ion-exchange resins with predictable and reproducible properties [22] and advances have been made in producing more mechanically stable materials for use in large scale separations. However, these materials suffer from "selectivity monotony". In anion-exchange chromatography, for example, differences in selectivity between ion-exchange materials are minimal and are mainly due to small secondary effects such as differences in the accessibility of the protein to the exchanger's pore structure and interactions with the exchanger's structural material.

This "selectivity monotony" has, in part, led to a renaissance in the use of materials such as calcium hydroxyapatite. Hydroxyapatite has long been used as a protein adsorbent but its use in preparative-scale HPLC has been limited [23,24]. The underlying mechanism of separation is multimodal [25–28]. Cation exchange takes place at the ionized hydroxyl groups of the phosphate groups on the surface of the particle. Both anion exchange and ligand exchange occur at the calcium (and magnesium) ions sites on the particle. This combination of separation mechanisms confers on hydroxyapatite a selectivity which is unique among all ion-exchange protein separation media. Unfortunately, this unique support is both physically and chemically unstable.

Although zirconium oxide is chemically very different from calcium hydroxyapatite, they share a number of chromatographic similarities. On hydroxyapatite, cation exchange takes place at the ionized hydroxyl groups of chemisorbed phosphate; the number of these sites is pH dependent. Similarly, ionized hydroxyl groups bound to the surface of the zirconium oxide particles serve as sites for cation exchange [2]. The isoelectric point of zirconium oxide is approximately 6.7 [2,29,30] but a wide range of individual pK_a values exist for the various types of Brönsted acid and base sites. This gives zirconium oxide a pH dependent cation-exchange capacity analogous to hydroxyapatite.

More importantly, both phases have Lewis acid sites which are responsible for both ligand and anion exchange. On hydroxyapatite, calcium ions form very labile coordination complexes with oxygen containing moieties and other hard Lewis bases. The calcium ions are also the sites for anion exchange for non-coordinating anionic species. Zirconium oxide also has Lewis acid sites [4,31,32] in the form of the surface zirconium ions. This Lewis acid site has a net 2+ charge [4] and one expects it to show anion-exchange properties for non-coordinating anions.

Ligand-exchange chemistry is slightly different for zirconium as compared to calcium, however, since zirconium (4+) ion has an especially high charge to radius ratio and therefore forms very strong coordination complexes with hard Lewis bases [8,33–35]. It coordinates with the same types of oxygen containing ligands and strong

Lewis bases as does calcium but the lability of such complexes is lower. The result is slower adsorption and desorption kinetics. Earlier investigations [9] have shown that the adsorption kinetics are still relatively fast. However, as long as the adsorption and desorption kinetics are fast on the chromatographic time scale, kinetics will not significantly broaden the elution profiles. Some broadening may be observed due to the heterogeneity of surface binding sites, but this is a relatively minor problem when the overall properties of this material are considered.

In order to determine which functional groups are responsible for the strong retention of proteins by either the ion-exchange or coordination mechanisms, a number of small solutes were studied. Table I summarizes the results of this study. The behavior of guanidine is typical for a cationic solute which has no other interaction with the surface other than electrostatic interactions. At low pH, guanidine is retained in both fluoride and chloride-containing buffers. This indicates that there are cation-exchange sites on the zirconia surface independent of the Lewis acid sites. Since fluoride coordinates at the Lewis acid sites and effectively competes with hydroxide at

TABLE I

SMALL SOLUTE CAPACITY FACTORS (k') *VS.* pH

All eluents contained 20 m*M* eluting salt and 20 m*M* buffer (MES, pH 6.1; TAPS, pH 8.4; or CAPS, pH 10.4). Flow-rate was 0.50 ml/min at 35°C. Diode array detection at 230 and 254 nm was used. Typically 5 μg solute were injected. Values in parentheses are reduced plate heights.

Solute	k' (h)					
	pH 6.1		pH 8.4		pH 10.4	
	NaF	NaCl	NaF	NaCl	NaF	NaCl
Guanidine	1.15	0.65	1.29	0.65	0.47	0.60
	(6.6)	(36.7)	(11.3)	(35.3)	(61.1)	(86.7)
Imidazole	0.41	−0.01	0.04	0.03	0.02	0.01
	(9.4)	(33.3)	(14.5)	(12.0)	(31.1)	(37.9)
Benzylamine	0.58	−0.01	0.79	0.39	0.20	0.18
	(7.3)	(7.5)	(6.1)	(7.6)	(19.2)	(17.8)
Uracil	0.01	0.50	0.06	0.52	0.01	0.06
	(7.2)	(26.7)	(5.0)	(44.5)	(23.2)	(29.7)
Benzamide	−0.02	0.00	−0.02	−0.01	−0.02	−0.04
	(7.6)	(7.1)	(7.8)	(7.0)	(17.0)	(16.3)
Benzyl alcohol	−0.03	−0.02	−0.03	−0.02	−0.03	−0.04
	(7.6)	(7.4)	(8.4)	(7.5)	(17.4)	(18.8)
Benzyl mercaptan	−0.01	0.03	−0.01	0.01	0.03	0.09
	(13.0)	(12.4)	(12.4)	(14.1)	(35.6)	(158)
Phenol	−0.02	0.11	0.00	0.13	−0.03	−0.02
	(7.5)	(8.1)	(8.3)	(11.0)	(14.0)	(14.6)
Phenylacetate	−0.05	0.65	−0.06	0.34	−0.11	−0.11
	(8.1)	(39.6)	(7.3)	(29.2)	(19.3)	(27.2)
Phenylsulfonate	−0.08	0.89	−0.10	−0.05	−0.12	−0.13
	(10.6)	(8.3)	(11.2)	(11.3)	(16.9)	(25.1)
Phenylphosphonate	−[a]	−	−	−	3.26	6.78
					(287)	(154)

[a] Elution not observed.

these low pH values, the cation-exchange capacity is increased. The chloride does not coordinate to those sites so it does not change the cation-exchange capacity. At higher pH, fluoride cannot effectively compete with hydroxide for the Lewis acid sites so the cation-exchange capacity does not increase when fluoride is in the eluent. The remaining cation-exchange capacity at pH 10.4 likely results from the ionized surface hydroxyl groups. The buffer salt has little effect on the number of these sites.

Imidazole acts like guanidine except that in buffers above its pK_a, it is not retained since it is uncharged. Benzylamine also displays this behavior except there is some slight retention at pH 10.4 which we attribute to hydrogen-bonding interactions. This interaction is also observed to a small extent in chloride buffer at pH 8.4 since retention is anomolously high compared to retention in chloride buffer at pH 6.1. Uracil shows retention patterns unlike the other cationic solutes, however. With fluoride in the buffer, little to no retention is observed at any pH. However, if the Lewis acid sites are available (occupied by coordinated water molecules) as in the chloride buffers of low pH, uracil is retained. This indicates that the oxygen atoms of uracil, although individually weak Lewis bases, work cooperatively with the proper geometry to form a complex with the Lewis acid site. This interaction is strong enough to enhance retention in solutions where no stronger Lewis base is present. At high pH, uracil cannot compete with hydroxide and is no longer retained in the chloride buffer.

The neutral solutes show little retention under any of the conditions used here. However, benzyl mercaptan is slightly retained in chloride buffers at pH 10.4 possibly due to hydrogen bonding interactions as seen with the benzylamine at high pH.

In the presence of fluoride, anionic solutes are not retained and are excluded from the pores to some extent. However, in the presence of chloride buffers at low pH, the anionic solutes are free to interact with the Lewis acid sites which bear a 2+ charge. Phenol is weakly retained in the chloride buffers up to pH 10.4. At this pH, the phenolic hydroxyl is ionized and the retention is diminished. This loss of retention may also be caused by the unfavorable competition between the phenoxy anion and hydroxide present in solution. Phenylacetic acid is retained quite strongly at low pH but is decreasingly retained as pH is increased. This indicates a direct competition between the carboxyl group of phenylacetate and solution hydroxide species.

In previous work in this laboratory, Rigney *et al.* [1,14] showed that species such as carboxylic and sulfonic acids will not elute from zirconia based columns except in the presence of acetate or phosphate in the mobile phase. The fact that both phenylacetate and phenylsulfonate elute in the absence of fluoride indicates that the elution buffer species (MES, TAPS and CAPS) are interacting with the surface to an observable extent. At high pH, phenylacetate is excluded to the same extent in chloride buffer as in fluoride buffer.

Phenylsulfonate proves to be a stronger Lewis base than phenylacetate at low pH but is more readily displaced by hydroxide ion. At pH 8.4, phenylsulfonate is less retained than phenylacetate indicating a reversal of strength. This may be due to a hydrogen-bonding contribution to the phenylacetate retention, however. Phenylphosphonate is not displaced by either chloride or fluoride at low pH. At higher pH, hydroxide ion has some difficulty in displacing the phosphonate indicating a very strong complexation constant between zirconium cation and phosphonate. A fair difference in retention is observed at high pH in the presence of fluoride compared to

that of chloride. Fluoride decreases the capacity factor of phenylphosphonate by a factor of two indicating that fluoride does have some displacing power relative to that of the phosphonate anion. Phosphonates and phosphates can be readily displaced by buffers containing higher concentrations of fluoride, which is in agreement with the thermodynamic coordination equilibria involved.

Taken together, the results indicate a surface the dominant features of which are Lewis acid sites and ionizable hydroxyl groups. Other groups such as the Brönsted base groups may be present in small numbers with relatively little effect on the overall retention mechanism for anionic solutes. These Brönsted base sites may be responsible for the hydrogen bond accepting properties observed for strong hydrogen bond donor solutes at high pH. At low pH, they may contribute to the anion-exchange capacity provided by the Lewis acid sites. The properties of the ionizable hydroxyl groups are determined by the solution pH and have a relatively predictable effect on solute retention.

The Lewis acid sites are much more complex, however. An equilibrium exists between all the Lewis bases present in the buffer and the Lewis acid sites. The displacing strength of each Lewis base is consistent with its thermodynamic formation constant; the higher the constant, the stronger the displacing effect. Due to the extensive hydrolysis of zirconium ion in aqueous solution, it is usually studied in extremely acidic solution (1–4 *M* $HC10_4$) to prevent hydrolysis and the formation of binuclear complexes thus little thermodynamic data exist at pH values relevant to this work. Therefore, the relative strengths of interaction must be experimentally determined for each Lewis base of interest.

In the presence of fluoride, cations are retained most strongly. They are held at the anionic ionized hydroxyl groups and/or coordinated fluoride ions. Such species are readily eluted isocratically with very good reduced plate heights (h = 6–10). Solutes containing weak Lewis base groups are either very weakly or not retained and also show very good reduced plate heights.

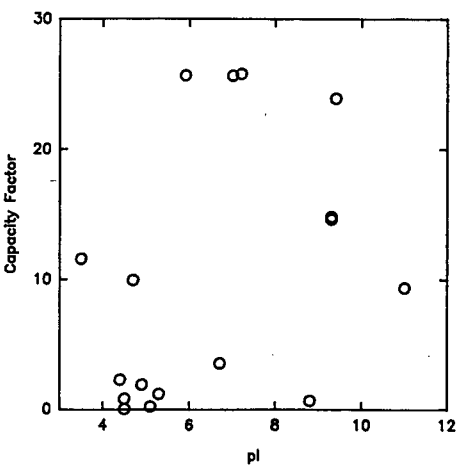

Fig. 2. Correlation of capacity factor with pI. Gradient elution from 0 to 0.5 *M* Na_2SO_4 in 30 min was used. Both buffers contained 20 m*M* sodium fluoride and 20 m*M* MES at pH 6.2 at 35°C. Flow-rate was 0.5 ml/min and detection was at 280 nm.

In the absence of fluoride, Lewis base containing ligands are increasingly retained since the Lewis acid sites are no longer blocked by fluoride. The reduced plate heights of these solutes are much higher (h = 15–70) due to the strong interactions with Lewis acid sites. The kinetics of ligand association and dissociation are slower than for ion-exchange interactions so the peaks become correspondingly wider. The cationic solutes do not show an increase in reduced plate height as do Lewis bases when fluoride is not present. While each of these simple interactions is small, a biopolymer containing many such groups can be very strongly retained due to the sum of a large number of such contributions.

For complex biopolymers, zirconium oxide particles display mixed mode retention analogous to calcium hydroxyapatite. Fig. 2 shows the absence of any correlation between isoelectric point of the protein and capacity factor at pH 6.2. It should

TABLE II

PROTEIN RETENTION AS A FUNCTION OF ELUENT pH[a]

Separations performed on a 50 × 4.6 mm I.D. column at 35°C with a flow-rate of 0.5 ml/min. Detection was at 280 nm with approximately 100 μg protein injected.

Protein	pI	Capacity factor at pH:		
		4.8[a]	6.2[b]	8.4[c]
Albumin, human	5.2, 4.6–5.3	25.46	–	–
Alkaline phosphatase	4.4	0.23	2.30	3.95
Cellulase	4.5, 4.2, 3.9	0.05	0.06	3.67
Cholinesterase, acetyl	4.5	–[d]	–	0.00
α-Chymotrypsin	8.8	0.28	0.68	9.92
Creatine phosphokinase	6.6, 6.7, 6.9	–	3.57	–
Cytochrome c	9.4, 9.0	20.23	23.89	25.87
Ferritin	4.1–4.6	–	–	0.00
Fetuin	3.2–3.8	6.34	11.60	0.02
β-Glucuronidase	5.1, 5.9	0.02	0.22	0.08
Hemoglobin	6.9–7.4	21.18	25.77	–
Hexokinase	4.9, 5.3	0.22	1.91	2.80
β-Lactoglobulin	5.3, 5.1	0.19	1.19	0.61
Lysozyme	11.0	8.73	9.35	11.20
Malate dehydrogenase	5.1	0.07	–	–
Myoglobin, equine	6.8, 7.3	25.61	25.63	–
Ovalbumin	4.7	9.27	9.92	–
Peroxidase, horseradish	4.0–8.4	1.66	2.35	0.02
Ribonuclease A	9.3	13.28	14.60	–
Ribonuclease B	9.3	8.71	14.78	–
Transferrin	5.9	23.80	25.65	–
Trypsin inhibitor	4.5	0.47	0.84	0.14

[a] Mobile phase was a 30 min linear gradient from 0 to 0.5 M Na_2SO_4 in 20 mM acetate buffer containing 20 mM sodium fluoride.

[b] Mobile phase was a 30 min linear gradient from 0 to 0.5 M Na_2SO_4 in 20 mM MES buffer containing 20 mM sodium fluoride.

[c] Mobile phase was a 30 min linear gradient from 0 to 0.5 M Na_2SO_4 in 20 mM TAPS buffer containing 20 mM sodium fluoride.

[d] Elution not observed.

be noted that without fluoride in the eluent, the proteins did not elute. When fluoride was present at pH 8.4, most proteins with low p*I* values are weakly retained while proteins with high p*I* values are well retained. This is similar to results found for cation-exchange supports, however, contributions from the Lewis acid sites and the protonated Brönsted base sites produce a more pronounced mixed retention behavior.

Since the pK_a values of the surface hydroxyls of zirconium oxide are approximately 8.1 a larger proportion of these hydroxyl groups are ionized at pH 8.4 than at pH 6.2. Cationic proteins will be more strongly retained under these conditions and anionic proteins will be excluded from the surface to a greater degree. At pH 4.8, a minute fraction of the surface hydroxyl groups are ionized and the surface charge will be determined primarily by coordinated fluoride ions and protonated Brönsted base sites. A summary of the results is given in Table II. A wide variety of patterns are observed. Some proteins show increased retention, others go through a minimum in retention, etc. Clearly several factors are responsible for retention. Most importantly, a very wide variety of proteins are retained.

To explore which factors are responsible for retention, the role of the cation and the anion in the eluent were explored. Four proteins with distinctly different isoelectric points and molecular weights were evaluated to assess the effect of changes in ionic strength and chemical parameters have on retention. Fig. 3 shows the effect of varying the cation and the ionic strength. Lipase (Fig. 3D) was not sensitive to either

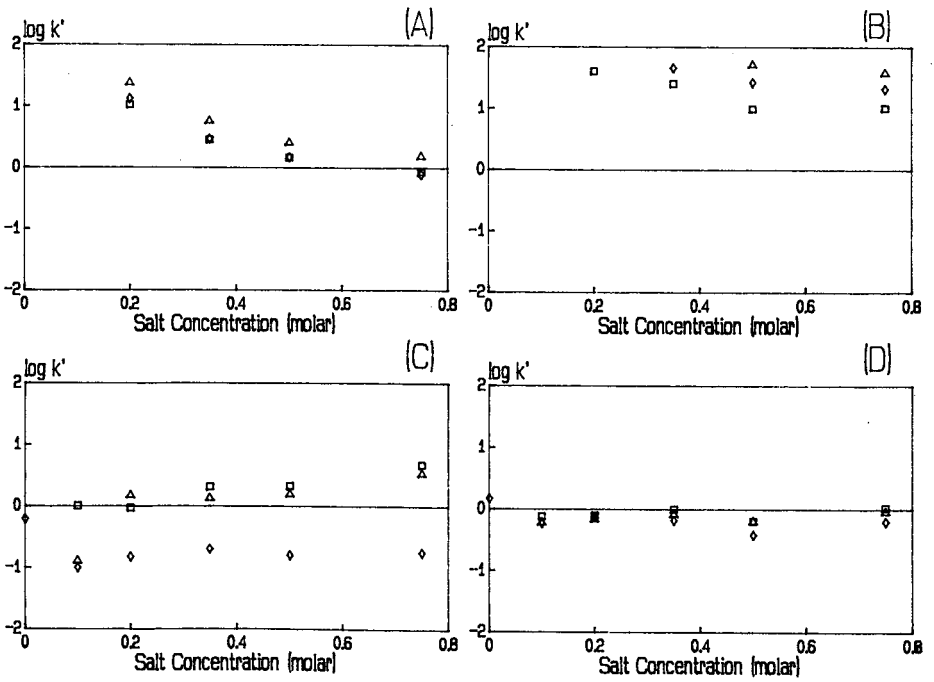

Fig. 3. Protein retention *versus* cation concentration. (A) lysozyme; (B) myoglobin; (C) trypsin inhibitor; (D) lipase. ◇ = NaCl; △ = NH_4Cl; □ = KCl. Isocratic elution at 35°C and 0.5 ml/min flow-rate were used. All buffers contained 20 m*M* NaF and 20 m*M* TAPS at pH 8.4.

the ionic strength or the cation used. Trypsin inhibitor (Fig. 3C) behaved similarly except that sodium salts promoted elution. Lysozyme (Fig. 3A) behaved as expected, based on a retention mechanism dominated by ion exchange, since retention increased at low ionic strength and was independent of the cation used. The ammonium cation appears to be a weaker eluent but since the study was performed at pH 8.4, a fair amount of the ammonium ion is unprotonated, thereby lowering the total ionic strength of the eluent. Myoglobin (Fig. 3B) is difficult to elute under these conditions and a trend is difficult to observe. Again it is important to reiterate the fact that without a small amount of fluoride in the eluent (20 m*M*), none of these or any other proteins are eluted from the zirconia particles at this pH.

Under these conditions, the surface of the particles should have a net negative charge. Coordinated fluoride and ionized hydroxyl groups contribute to this charge. A consequence of this high charge density is the formation of an ionic double layer. If this layer were partly responsible for the mixed mode ion-exchange behavior, there should be a large cation dependence on protein retention. This was not observed and may be ruled out as a contributing retention process.

Fig. 4 shows the effect of variations in the type of anion and its concentration on protein capacity factors. Again, lipase (Fig. 4D) and trypsin inhibitor (Fig. 4C) show little effect for any anion except for fluoride. Fluoride is an extremely potent eluent and therefore leads us to believe that these proteins are primarily retained by

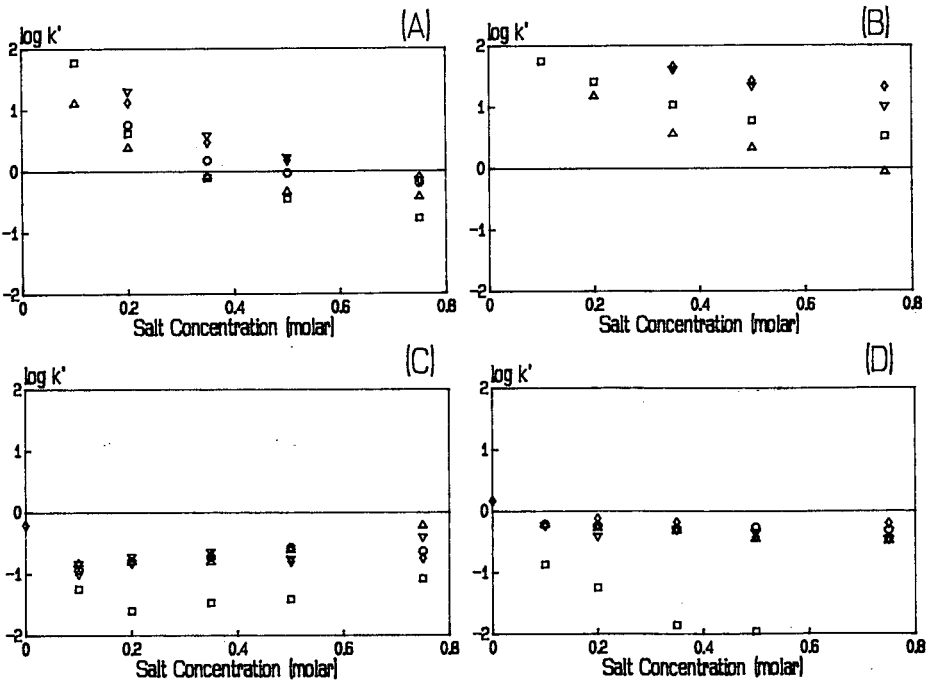

Fig. 4. Protein retention *versus* anion concentration. (A) lysozyme; (B) myoglobin; (C) trypsin inhibitor; (D) lipase. □ = NaF; ◇ = NaCl; △ = Na_2SO_4; ○ = NaSCN; ▽ = sodium acetate. Isocratic elution at 35°C and 0.5 ml/min flow-rate were used. All buffers contained 20 m*M* NaF and 20 m*M* TAPS at pH 8.4.

ligand exchange. None of the other salts are strong enough Lewis bases to displace the functional groups of the protein which are coordinated to the Lewis acid sites on the surface.

Lysozyme (Fig. 4A) shows the same dependence of retention on ionic strength as in the preceeding cation effect study (Fig. 3). Fluoride is an anomolously strong eluent indicating that at least some of the retention of lysozyme is due to ligand exchange. At lower salt concentrations, sulfate proves stronger than fluoride due possibly in part to the higher ionic strength of sulfate over fluoride at the same molarity. Myoglobin (Fig. 4B) is eluted more easily with sulfate or fluoride than with chloride. For all salt concentrations, sulfate proves the stronger eluent. However, at low salt concentration, only fluoride can elute myoglobin. For all proteins, anions other than fluoride or sulfate show little or no difference in eluotropic strength.

A brief study of the displacement mechanism parameters was undertaken for these test proteins. The logarithm of the capacity factors for each protein was plotted against the logarithm of the reciprocal displacing salt concentration for each of the salts tested above. The slope of such a plot is considered by some to be a measure of the displacement stoichiometry for each protein and is named the Z value [36,37]. For each protein, the Z values did not change significantly between eluting salt species. Lysozyme, for example, had Z values from 1.67 to 2.92 and myoglobin had values from 0.76 to 2.12. Lower displacement stoichiometry was observed for trypsin inhibitor and lipase with Z ranging from -1.4 to -0.17 and -0.15 to 0.32, respectively. There was no consistent trend in values for any of the proteins with relation to the eluting salt although the correlation coefficients for the regressions to calculate Z were fairly good in most cases. The relatively low stoichiometric values may be due in part to the inflexibility of the inorganic ion-exchange material. In organic resins and derivatized silicas, the ionic groups of the support have some degree of mobility associated with them because of the flexibility of the support or from the spacer arm between the point charge and the support backbone. Such flexibility allows greater access of the charged groups to the ionic sites on the globular protein. In the case of a rigid inorganic ion exchanger with the ionic sites firmly planted on the surface, such flexibility is not possible and less coulombic interactions are expected on a steric basis. In the case of denatured proteins, both types of ion exchangers should show similar Z values since the steric restraints on the solute are greatly diminished.

The great ability of fluoride to displace Lewis bases from the Lewis acid sites on the surface is a consequence of the strength of the coordination complex formed between fluoride and zirconium. Fluoride has a very large formation constant with tetravalent zirconium ($K_1 = 10^{8.94}$) [38]. Few Lewis bases form stronger complexes with zirconium ion therefore fluoride can displace almost any other Lewis base. Thus fluoride elutes bound proteins by displacing the coordinating groups on the accessible surface of the protein. Sulfate also forms a moderately strong complex with zirconium ion ($K_1 = 10^{3.67}$) [38] and we expect it to displace some Lewis bases. This may help to explain why sulfate elutes myoglobin more strongly than does fluoride.

The use of only fluoride as an eluent allows both displacement of Lewis bases and acts simultaneously as a displacer for ion-exchange mediated retention. Sulfate can displace weak Lewis bases but can also act as a more effective displacing salt than fluoride for ion exchange. This is an important difference which allows the optimization of the selectivity between proteins with similar total retention but different

amounts of ligand-exchange contributions to retention. When a protein has two proximal Lewis bases which both bind to a single Lewis acid site, it will form a less labile complex than the simple addition of their individual effects. An example of this is the comparison between oxalate and acetate ions. Acetate forms a very weak complex with zirconium ion ($K_1 = 10^{0.3}$) but oxalate forms an exceptionally strong complex ($K_1 = 10^{9.80}$) [38]. Sulfate readily displaces acetate ion but is not able to displace oxalate. Fluoride is able to displace both if it is present in sufficient concentration.

The anomolous behavior of sulfate *versus* fluoride for the elution of myoglobin may arise from such an effect. If no proximal Lewis bases are on the protein's surface, then a relatively weak Lewis base should be able to displace the individual bases from the Lewis acid sites. This would leave a relatively large contribution from the ion-exchange interactions. Sulfate will overcome these remaining ionic interactions more efficiently than fluoride. Lipase and trypsin inhibitor are both held by strong ligand-exchange contributions to retention but do not show this effect. This may be due to the presence or proximal Lewis bases on their surface combined with a relatively weak contribution from ion exchange. The ionic strength of the fluoride necessary to overcome the ligand-exchange retention is in excess of that required for the ionic retention. Clearly, the effect of formation constant on eluotropic selectivity requires further study.

Greater insight into the retention mechanism is obtained by plotting the logarithm of the capacity factor versus the logarithm of the fluoride concentration as shown in Fig. 5. A straight line indicates a single retention mechanism predominantly based on displacement by fluoride ion while curvature in such a plot may signify mixed retention mechanism. We hypothesize that the degree of curvature is a rough indication of the degree of contribution from other retention processes. Myoglobin displays a nearly linear relationship and the displacement mechanism is consistent with results based on cation and anion effect studies. As expected, lysozyme, lipase

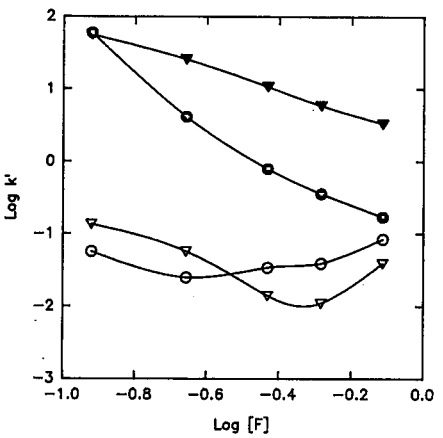

Fig. 5. Retention as a function of Lewis base concentration. △ = lysozyme; ○ = myoglobin; □ = trypsin inhibitor; ▽ = lipase. Isocratic elution at 35°C and 0.5 ml/min flow-rate were used. All buffers contained 20 m*M* TAPS at pH 8.4.

TABLE III

EFFECT OF ANION TYPE ON GRADIENT ELUTION CAPACITY FACTORS OF VARIOUS PROTEINS

Separations performed with a 30-min linear gradient from 0 to 0.5 *M* Na_2SO_4 or 0 to 1.5 *M* sodium chloride in 20 m*M* MES buffer at pH 5.5 containing 0.5 *M* sodium fluoride. Flow-rate was 1 ml/min at 35°C. Protein loadings were typically 10 μg and detection was at 280 nm.

Protein	Capacity factors	
	Sulfate	Chloride
Myoglobin	3.54	3.44
α-Chymotrypsin	2.34	1.39
Bovine albumin	14.18	–[a]
Lysozyme	0.23	0.09
Cytochrome *c*	5.09	3.91
Apotransferrin	16.60	32.00
Hemoglobin	3.89	3.04
Human albumin	17.00	–
Ribonuclease A	3.25	2.95
Ribonuclease B	3.56	0.22
Ovalbumin	10.55	0.40

[a] Elution not observed.

and trypsin inhibitor all exhibit multiple retention mechanisms. Lipase shows a fairly linear relationship between log k' and log $[F^-]$ at low fluoride concentrations. However, at high fluoride concentrations, a sharp change is observed and some other form of retention mechanism may take over. This would be the case if the concentration of fluoride necessary to displace the ligated Lewis bases on the protein was in excess of that required to overcome the electrostatic retention contributions.

When the retention mechanisms of various proteins are different, one can easily adjust the chromatographic selectivity. By changing the eluting salt during an ionic strength gradient, one can drastically change the order of elution. Table III shows the difference in retention between a gradient of sodium sulfate and a gradient at the same ionic strength using sodium chloride. Such a change has a dramatic effect on the retention of transferrin and ovalbumin while proteins like myoglobin and ribonuclease A are hardly affected.

Ligand exchange between the zirconium sites and the Lewis base groups on the proteins is expected to be relatively slower than simple ion exchange. Experimentally, this is observed in the effect of flow-rate on the reduced plate height at different pH values. For slow kinetic processes, the efficiency decreases as the flow-rate is increased. At low pH, the zirconium oxide surface will be saturated with fluoride ions [9]. This will make the support act as a high capacity cation-exchange material with some additional anion-exchange character due to the protonated Brönsted base sites. This surface should be very efficient and have a relatively small "*C* term" in a Van Deemter plot. However, at higher pH, there will be less fluoride masking the Lewis acid sites and the slower ligand-exchange mechanism will dominate the "*C* term" in the Van Deemter equation. Fig. 6 shows this effect for two proteins.

As stated earlier, we hypothesize that lysozyme is retained mainly by an ion-

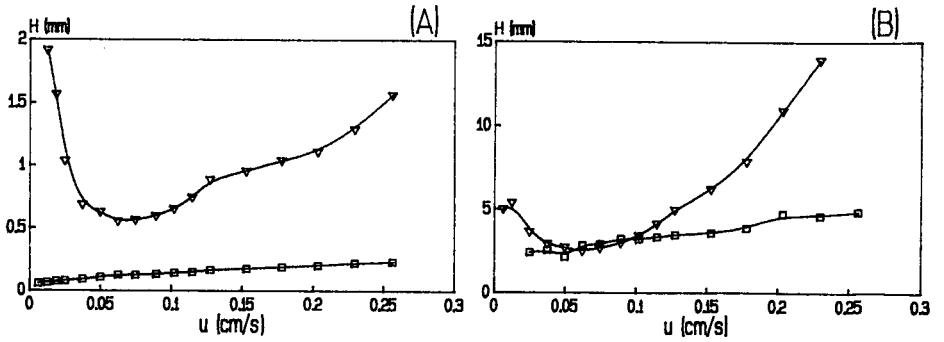

Fig. 6. Van Deemter plots. (A) lysozyme; (B) myoglobin. ▽ = 20 m*M* CAPS, pH 10.4; □ = 20 m*M* MES, pH 6.1. Isocratic elution at 35°C and 1.00 ml/min flow-rate were used. All buffers contained 20 m*M* NaF and 200 m*M* Na_2SO_4. *H* = plate height, *u* = linear velocity.

exchange interaction. At low pH, the plate height is quite satisfactory. At higher pH, the weak contribution of ligand exchange to retention becomes overwhelming due to its sluggishness. The efficiency therefore becomes highly flow dependent. We also believe that myoglobin is retained mainly by a ligand-exchange mechanism. At high pH, the efficiency is relatively poor due to the slowness of ligand-exchange kinetics on the relatively scarce Lewis acid sites. When the flow-rate is increased to 1.0 ml/min, the myoglobin separation becomes so inefficient at pH 10.4 that it is almost useless.

In addition to being essential for elution of proteins from zirconium oxide particles, fluoride serves another important purpose. Unless buffers are scrupulously pure, a number of Lewis base impurities will be present. Carbonate is ubiquitous.

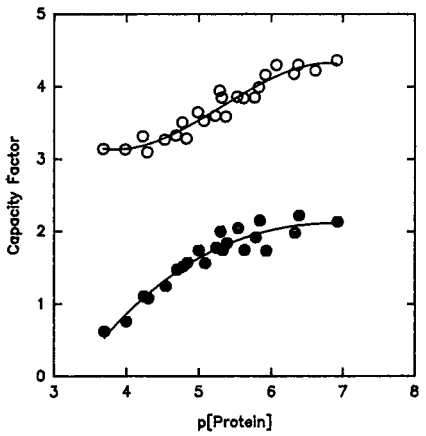

Fig. 7. Loading study on fluoride modified zirconium oxide. ○ = Lysozyme; ● = lipase. Isocratic elution at 35°C and 0.5 ml/min flow-rate were used. Eluent was 0.35 *M* potassium chloride with 20 m*M* NaF and 20 m*M* TAPS at pH 8.4.

TABLE IV

PROTEIN RECOVERY ± S.D. (n = 5)[a]

Protein	Enhanced assay	Micro assay
Lysozyme	103.9 ± 2.5%	101.2 ± 2.2%
Myoglobin	107.7 ± 6.1%	95.7 ± 4.1%

[a] See experimental for details.

When fluoride is not present in the mobile phase to block the Lewis acid sites, over time, carbonate builds up on the particle surface and changes the overall character of the surface. Since carbonate is not monodentate, it has a slow desorption rate and prevents other Lewis bases from reaching the Lewis acid sites. This masks the ligand-exchange mechanism and results in an inorganic cation-exchange material with less selectivity than the original material. Phosphate would act similarly and should be avoided if long term reproducibility between base flushings is desired. Therefore, for reproducible and consistent retention properties, it is essential to control interactions at the Lewis acid sites.

An important characteristic of separation materials, especially multimodal supports, is the effect of solute load on peak shape. Mixed mode materials are often readily overloaded if one type of site is less populous than the other retention site. The result is a complex relationship between capacity factor and solute load. This could lead to serious problems if a preparative separation is desired. Fig. 7 shows that the capacity factors do not change significantly even though the amount of protein injected was varied by over three orders of magnitude although some decrease in capacity factor is expected as sample size is increased [39]. This is consistent with earlier

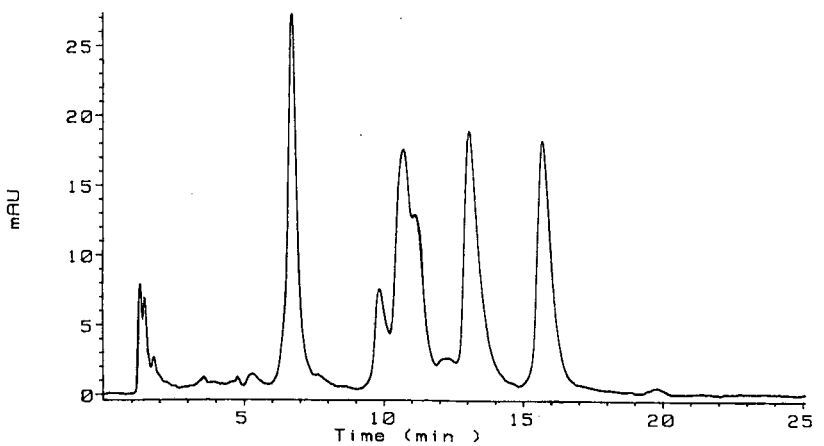

Fig. 8. Protein separation on fluoride modified zirconium oxide. A linear gradient of 0–0.75 M Na_2SO_4 in 100 mM NaF and 20 mM MES at pH 5.5 was used. Flow-rate was 0.5 ml/min at 35°C. Protein loadings were 4.4 μg lysozyme, 15.4 μg α-chymotrypsin, 13.6 μg myoglobin and 15.4 μg cytochrome c.

findings that the Lewis acid site density is quite high relative to the hydroxyl group density [9]. The variation in capacity factors for similar mass loadings for a given protein is an effect due to variations in injection volume. In the loading study, injection volumes varied from 20 to 0.1 μl and for isocratic elution would be expected to have a small effect on the retention volume of proteins.

For preparative separations, protein recovery is an important characteristic. Lysozyme and myoglobin were used as test proteins since their retention mechanisms are quite different. The results of mass recovery studies are summarized in Table IV. Quantitative recovery was accomplished by using two protein assay protocols. This demonstrates that both the ion-exchange mechanism and ligand-exchange mechanisms are free from irreversible binding of proteins under these conditions.

CONCLUSIONS

When zirconium oxide supports are used in fluoride-containing media, a very biocompatible surface is established. The unique overall retention properties of this material are operationally analogous to those of calcium hydroxyapatite. However, the system does not have the chemical and physical weaknesses that limit the use of hydroxyapatite. Fig. 8 shows that very efficient separations can be implemented in any of a number of elution schemes. There are few limitations to what may be present in the eluent compared to hydroxyapatite. However, strongly acidic solutions should be avoided since fluoride forms hydrofluoric acid at low pH. This substance is detrimental to the integrity of the packing material as well as the chromatographic system components.

The substantial base stability allows sterilization of the packing material and stripping of "irreversibly" bound proteins with 0.1 *M* sodium hydroxide solutions. Such treatments strip all solutes including fluoride. Equilibration of the stripped particles with a fluoride solution of the desired ionic strength and pH restores the selectivity and efficiency of the column to its original condition. The sorption/stripping cycle has been repeated at least fifty times on one column with no loss of efficiency or selectivity. This phase is a useful candidate for analytical and preparative separations of biomolecules.

ACKNOWLEDGEMENTS

The authors would like to thank Eric Funkenbusch, Douglas Hanggi and Tom Weber for their helpful discussions and Don Hagen for his encouragement. J.A.B. acknowledges financial support from Specialty Adhesives and Chemicals Division and the Leading Edge Academic Program at 3M. This work was supported in part by grants from the 3M Company and the Institute for Advanced Studies in Bioprocess Technology.

REFERENCES

1 M. P. Rigney, *Ph.D. Thesis,* University of Minnesota, Minneapolis, MN, 1988.
2 K. K. Unger and U.Trudinger, *Chem. Anal.*, 98 (1989) 145–188.
3 A. A. Tsyganenko and V. N. Filimonov, *Spec. Lett.*, 5 (1972) 477–487.

4 W. Hertl, *Langmuir*, 5 (1989) 96–100.
5 P. A. Agron, E. L. Fuller and H. F. Holmes, *J. Coll. Int. Sci.*, 52 (1975) 553–561.
6 R. G. Pearson, *J. Chem. Ed.*, 45 (1968) 581–587.
7 R. G. Pearson, *J. Chem. Ed.*, 45 (1968) 643–648.
8 S. Ahrland, D. Karipides and B. Noren, *Acta Chem. Scand.*, 17 (1963) 411–424.
9 J. A. Blackwell and P. W. Carr, *J. Chromatogr.*, 549 (1991) 43.
10 W. A. Schafer, *MS Thesis*, University of Minnesota, Minneapolis, MN, 1990.
11 W. A. Schafer, E. F. Funkenbusch, K. A. Parson and P. W. Carr, *J. Chromatogr.*, in press.
12 W. A. Schafer and P. W. Carr, *J. Chromatogr.*, in press.
13 M. P. Rigney, T. P. Weber and P. W. Carr, *J. Chromatogr.*, 484 (1989) 273–291.
14 M. P. Rigney, E. F. Funkenbusch and P. W. Carr, *J. Chromatogr.*, 499 (1990) 291–304.
15 P. A. Bristow, P. N. Brittain, C. M. Riley and B. F. Williamson, *J. Chromatogr.*, 131 (1977) 57–64.
16 P. C. Sadek, P. W. Carr, L. D. Bowers and L. C. Haddad, *Anal. Biochem.*, 144 (1985) 128–131.
17 *Instruction Pamphlets 23225 and 23230*, Pierce Chemical Company, Rockford, IL, 1988.
18 P. K. Smith, R. I. Krohn, G. T. Hermanson, A. K. Mallia, F. H. Gartner, M. D. Provenzano, E. K. Fujimoto, N. M. Goeke, B. J. Olson and D. C. Klenk, *Anal. Biochem.*, 150 (1985) 76–85.
19 A. N. Hodder, M. I. Aguilar and M. T. W. Hearn, *J. Chromatogr.*, 476 (1989) 391–411.
20 M. L. Heinitz, L. Kennedy, W. Kopaciewicz and F. E. Regnier, *J. Chromatogr.*, 443 (1988) 173–182.
21 M. T. W. Hearn, A. N. Hodder and M. I. Aguilar, *J. Chromatogr.*, 443 (1988) 97–118.
22 K. A. Tweeten and T. N. Tweeten, *J. Chromatogr.*, 359 (1986) 111–119.
23 M. J. Gorbunoff, *Methods Enzymol.*, 117 (1985) 370–379.
24 G. Bernardi, *Methods Enzymol.*, 27 (1973) 471–479.
25 T. Kawasaki, S. Takahashi and K. Ikeda, *Eur. J. Biochem.*, 152 (1985) 361–371.
26 M. J. Gorbunoff, *Anal. Biochem.*, 136 (1984) 425–432.
27 M. J. Gorbunoff, *Anal. Biochem.*, 136 (1984) 433–439.
28 M. J. Gorbunoff, *Anal. Biochem.*, 136 (1984) 440–445.
29 G. A. Parks, *Chem. Rev.*, 65 (1965) 177–198.
30 G. A. Parks, *Advan. Chem. Soc.*, 67 (1967) 121–160.
31 R. G. Silver, C. J. Hou and J. G. Ekerdt, *J. Catal.*, 118 (1989) 400–416.
32 N. E. Tret'yakov, D. V. Pozdnyakov, O. M. Oranskaya and V. N. Filimonov, *Russ. J. Phys. Chem.*, 44 (1970) 596–600.
33 A. J. Zielen and R. E. Connick, *J. Am. Chem. Soc.*, 78 (1956) 5785–5792.
34 R. E. Connick and W. H. McVey, *J. Am. Chem. Soc.*, 71 (1949) 3182–3191.
35 W. B. Blumenthal, *The Chemical Behavior of Zirconium*, Van Nostrand, Princeton, NJ, 1958.
36 W. Kopaciewicz, M. A. Rounds, J. Fausnaugh and F. E. Regnier, *J. Chromatogr.*, 266 (1983) 3–21.
37 M. A. Rounds and F. E. Regnier, *J. Chromatogr.*, 283 (1984) 37–45.
38 L. G. Sillen and A. E. Martell, *Stability Constants of Metal Ion Complexes*, Chemical Society, London, 1964.
39 H. Engelhardt, M. Czok, R. Schultz and E. Schweinhein, *J. Chromatogr.*, 458 (1988) 79–92.

Journal of Chromatography, 549 (1991) 77–88
Elsevier Science Publishers B.V., Amsterdam

CHROM. 23 316

Comparison of the selectivity of di(methacryloyloxymethyl)-naphthalene–divinylbenzene copolymers in reversed-phase high-performance liquid chromatography

BARBARA GAWDZIK
Faculty of Chemistry, M.C.S. University, pl. M. C. Sklodowskiej 3, PL-20031 Lublin (Poland)
(First received November 14th, 1990; revised manuscript received March 19th, 1991)

ABSTRACT

The influence of chemical composition of porous copolymers on chromatographic properties of high-performance liquid chromatography columns was studied. Columns were packed with three di(methacryloyloxymethyl)naphthalene–divinylbenzene copolymers of different molar ratio of monomers. The retention behaviour of five homologous series (alkylbenzenes, N-alkylanilines, alkyl aryl ethers, alkyl benzoates and alkyl aryl ketones) was investigated using different eluents. Using the alkyl aryl ketone scale, the retention indices of the homologues and column test compounds were calculated. Their values were used to compare the selectivities of the studied stationary phases.

INTRODUCTION

The retention of a substance in chromatography depends on its interactions with mobile and stationary phases. In reversed-phase high-performance liquid chromatography (HPLC) the major contribution to retention comes from hydrophobic interactions of the sample with the mobile phase, and the stationary phase plays a largely passive role [1]. An accurate definition of the quality of stationary phase used was stressed by Karch *et al.* [2] and Jandera *et al.* [3]. Smith [4] also reported that even non-polar alkyl-bonded silica gels indicate specific chemical effects on the stationary phase due to the presence of the unprotected silanol groups. According to Antle *et al.* [5] column strength and selectivity depend on the polarity of the bonded phase.

Among the techniques used to compare different stationary phases, the retention indices of standards based on an alkyl aryl ketone scale introduced by Smith [4] are the most effective. In order to determine the selectivity of the HPLC column, Smith and co-workers [6–10] selected a set of column test compounds (toluene, nitrobenzene, *p*-cresol, 2-phenylethanol and N-methylaniline) reflecting effects of specific interactions with different stationary phases. Column test compounds are chosen as the aromatic equivalents of the standards used by Rohrschneider [11] and McReynolds [12] in gas chromatography and represent solutes of different polarity.

As polarity is not a single-valued parameter, but rather the sum of contribu-

0021-9673/91/$03.50

tions due to dipole interaction, hydrogen donation, hydrogen acceptance and dispersion interaction, no solute is a probe for only one kind of interaction.

Except for toluene and nitrobenzene, each of the compounds tested belongs to different interaction groups as defined by Snyder [13,14].

Retention indices of column test compounds can be used in a similar manner as Rohrschneider or McReynolds constants for quantitative description of selectivity properties. Their values permit a direct comparison of different columns using the same eluent.

Using the alkyl aryl ketone index scale, Smith and Garside [15,16] studied the behaviour of four series of homologues and column test compounds on two commercially available polystyrene–divinylbenzene (PS–DVB) stationary phases. They showed that the selectivities of the two sorbents were similar but both had very different properties to an octadecyl silane (ODS)-silica column. The linearity of the retentions of the standard alkyl aryl ketones on PS–DVB was much poorer than on an ODS-silica column. The retention indices for test compounds were calculated basing on a linear relationship for the alkyl aryl ketones propiophenone to heptanophenone, because acetophenone is eluted much earlier than expected [16]. Similar deviations were noted for other homologous series studied on PS–DVB stationary phases.

In previous work [17], chromatographic properties of a porous copolymer of di(methacryloyloxymethyl)naphthalene (DMN) and DVB were studied under conditions identical to those used by Smith and Garside [16]. The behaviour of DMN–DVB copolymer in all studied mobile phases [methanol–buffer (90:10), acetonitrile–buffer (70:30) and tetrahydrofuran–buffer (40:60)] was similar to that of PS–DVB stationary phases, *e.g.* the first members of the homologous series indicated some deviations from linear relationship between the logarithm of the capacity factor and the carbon number. On the other hand, the selectivity of the DMN–DVB copolymer was quite different to that of PS–DVB.

In the present work, the influence of the chemical composition of DMN–DVB copolymers on their selectivities is studied. In order to examine the role of the chemical nature of the stationary phase in the reversed-phase HPLC retention mechanism, three DMN–DVB porous copolymers containing different mole fractions of polar monomer (DMN) were used: 0.2, 0.5 and 0.8.

EXPERIMENTAL

Chemicals and eluents

Methanol. acetonitrile and tetrahydrofuran were HPLC grade obtained from Merck (Darmstadt, Germany). The alkyl aryl ketones retention index standards, homologous alkylbenzenes, N-alkylanilines, alkyl aryl ethers, alkyl benzoates and other test compounds (nitrobenzene, *p*-cresol and 2-phenylethanol) were laboratory-reagent grade from a range of sources.

Preparation of the phosphate buffer solution (pH 7) has been described previously [17]. The buffer was prepared from 0.0029 *M* disodium hydrogenorthophosphate (0.5 g) and 0.0022 *M* potassium dihydrogenphosphate (0.301 g).

All eluents were filtered through suitable filters and degassed by agitation in an ultrasonic bath and kept under a weak stream of helium.

TABLE I

PROPERTIES OF THE DMN–DVB COPOLYMERS

Mole fraction of the DMN–DVB monomers	Weight of the copolymer in the column (g)	Specific surface area (BET), S (m^2/g)	Surface area of the copolymer in the column, S_c (m^2)
0.2:0.8	0.336	235	79.0
0.5:0.5	0.321	85.5	27.4
0.8:0.2	0317	84	26.6

HPLC equiment

Separations were carried out using an HPLC system comprising a Techma–Robot 302 syringe pump (Warsaw, Poland) fitted with a Rheodyne 7125 injection valve equipped with a 10-μl sampling loop, and a 100 mm × 4 mm I.D. column packed with the DMN–DVB copolymers. The column was encased in a water jacket through which water at 30°C was passed.

Peaks were detected using a Laboratorni Pristroje UV–visible LCD 2563 detector set at 254 nm and 0.04 a.u.f.s., and were recorded on a Laboratorni Pristroje 4001 recorder (Praque, Czechoslovakia). The measuring cell of the detector was also water-thermostated at 30°C. The flow-rate of the mobile phase was 0.5 ml/min.

Chromatographic measurements

The column void volume was determined by injecting 10 μl of an aqueous solution of sodium nitrate (24.3 g per 100 ml) [16]. The analyte concentrations in the mobile phases were adjusted to give on-scale peaks from a 10-μl injection. The recorded retention distances were the mean of three determinations.

Capacity factors (k') and retention indices (I) derived from the alkyl aryl ketones butyrophenone to heptanophenone were calculated as described previously [16,17].

Preparation of DMN–DVB copolymers

Porous copolymers of DMN and DVB were synthesized by the procedure published previously [17].

Using the mole fractions of DMN–DVB monomers of 0.2:0.8, 0.5:0.5 and 0.8:0.2 sorbents of different chemical nature were obtained [18].

In Table I the properties of the three copolymers used in this work are summarized.

The sieve fraction of the particles of the DMN–DVB copolymers was 5–15 μm. The HPLC columns were packed according to the procedure described previously [17,19].

RESULTS AND DISCUSSION

Following the work of Smith and Garside [16], the retention indices of five sets of homologous compounds and the selectivity test compounds were measured using methanol–buffer (90:10), acetonitrile–buffer (70:30) and tetrahydrofuran–buffer

(40:60) as the mobile phases. Independent of the mobile phase used, peak shapes were symmetrical, but theoretical plate numbers varying from 1500 to 2000 were rather low. Inlet pressure of the columns with increasing content of the DMN monomer (20, 50 and 80%) was 10, 8.2 and 14.2 MPa with methanol–buffer, 8, 7.8 and 10.7 MPa with acetonitrile–buffer and 12.5 and 18 MPa with tetrahydrofuran–buffer eluent, respectively.

In the case of 0.2 DMN–0.8 DVB copolymer, the measurements with tetrahydrofuran–buffer eluent were not possible because of a variable mobile phase flow-rate. With this mobile phase the inlet pressure of the column was increasing continuously.

In order to use the alkyl aryl ketone index scale in selectivity studies, a linear relationship between the logarithm of the capacity factor and the carbon number must be demonstrated. As expected from the previous work [17], the first members of the alkyl aryl ketone homologous series show some deviations from the expected linearity for all copolymers studied. Thus, the retention indices of the homologous and test compounds were calculated using the linear relationship for the alkyl aryl ketones from butyrophenone to heptanophenone.

In Tables II–IV the values of capacity factors (k') for alkyl aryl ketones, alkylbenzenes and column test compounds are presented. Using the retention times and the column void volumes measured with an aqueous sodium nitrate solution, the capacity factors on three columns were calculated. We observe that, in all eluents

TABLE II

CAPACITY FACTOR (k') AND SPECIFIC CAPACITY FACTORS ($k'_s = k'/S_c$) FOR ALKYL ARYL KETONES, ALKYLBENZENES AND TEST COMPOUNDS WITH METHANOL–BUFFER (90:10) ELUENT

Compound	0.2 DMN–0.8 DVB		0.5 DMN–0.5 DVB		0.8 DMN–0.2 DVB	
	k'	$k'_s \cdot 10^3$	k'	$k'_s \cdot 10^3$	k'	$k'_s \cdot 10^3$
Alkyl aryl ketone series						
Acetophenone	0.76	9.62	1.07	39.05	1.34	50.38
Propiophenone	1.11	14.05	1.59	58.03	1.90	71.43
Butyrophenone	1.34	16.96	1.94	70.80	2.29	86.09
Valerophenone	1.87	23.67	2.65	96.72	3.12	117.29
Hexanophenone	2.63	33.29	3.68	134.30	4.32	162.24
Heptanophenone	3.64	46.08	5.02	183.21	5.95	233.68
Alkylbenzene series						
Benzene	0.77	9.75	1.09	39.78	1.21	45.49
Toluene	1.14	14.43	1.52	55.47	1.77	66.54
Ethylbenzene	1.33	16.84	1.79	65.33	1.92	72.18
n-Propylbenzene	1.71	21.65	2.20	80.29	2.32	87.22
n-Butylbenzene	2.27	28.73	2.96	108.03	2.95	109.02
Test compounds						
Nitrobenzene	1.34	16.96	2.15	78.47	2.60	97.74
p-Cresol	0.41	5.19	0.54	19.70	0.67	25.19
2-Phenylethanol	0.23	2.91	0.37	13.50	0.45	16.92
N-Methylaniline	0.78	9.87	1.32	48.18	1.14	42.85

TABLE III

CAPACITY FACTOR (k') AND SPECIFIC CAPACITY FACTORS ($k'_s = k'/S_c$) FOR ALKYL ARYL KETONES, ALKYLBENZENES AND TEST COMPOUNDS WITH ACETONITRILE–BUFFER (70:30) ELUENT

Compound	0.2 DMN–0.8 DVB		0.5 DMN–0.5 DVB		0.8 DMN–0.2 DVB	
	k'	$k'_s \cdot 10^3$	k'	$k'_s \cdot 10^3$	k'	$k'_s \cdot 10^3$
Alkyl aryl ketone series						
Acetophenone	0.43	5.44	0.59	21.53	0.76	28.57
Propiophenone	0.66	8.35	0.89	32.48	1.11	41.73
Butyrophenone	0.86	10.89	1.15	41.97	1.45	54.51
Valerophenone	1.20	15.19	1.57	57.29	1.97	74.06
Hexanophenone	1.66	21.01	2.15	78.47	2.68	100.75
Heptanophenone	2.30	29.11	2.94	107.30	3.62	136.09
Alkylbenzene series						
Benzene	0.76	9.62	0.93	33.94	1.08	40.60
Toluene	1.07	13.54	1.23	44.89	1.52	57.14
Ethylbenzene	1.35	17.09	1.51	55.11	1.86	69.92
n-Propylbenzene	1.78	22.53	1.96	71.53	2.40	90.22
n-Butylbenzene	2.39	30.25	2.62	95.62	3.15	118.42
Test compounds						
Nitrobenzene	0.68	8.61	0.95	34.67	1.47	55.26
p-Cresol	0.31	3.92	0.39	14.23	0.49	18.42
2-Phenylethanol	0.22	2.78	0.26	9.49	0.32	12.03
N-Methylaniline	0.63	7.97	0.74	27.00	1.12	42.10

TABLE IV

CAPACITY FACTOR (k') AND SPECIFIC CAPACITY FACTORS ($k'_s = k'/S_c$) FOR ALKYL ARYL KETONES, ALKYLBENZENES AND TEST COMPOUNDS WITH TETRAHYDROFURAN–BUFFER (40:60) ELUENT

Compound	0.2 DMN–0.8 DVB		0.5 DMN–0.5 DVB		0.8 DMN–0.2 DVB	
	k'	$k'_s \cdot 10^3$	k'	$k'_s \cdot 10^3$	k'	$k'_s \cdot 10^3$
Alkyl aryl ketone series						
Acetophenone	–	–	1.21	44.16	1.69	63.53
Propiophenone	–	–	2.01	73.36	2.79	104.88
Butyrophenone	–	–	2.70	98.54	3.78	142.11
Valerophenone	–	–	3.85	140.51	5.42	203.76
Hexanophenone	–	–	5.47	199.63	7.68	288.72
Heptanophenone	–	–	7.52	274.45	10.51	395.11
Alkylbenzene series						
Benzene	–	–	2.64	96.35	3.88	145.86
Toluene	–	–	3.97	144.89	5.15	193.61
Ethylbenzene	–	–	5.13	187.23	6.58	247.37
n-Propylbenzene	–	–	6.52	237.96	8.29	311.65
n-Butylbenzene	–	–	8.53	311.31	10.85	407.89
Test compounds						
Nitrobenzene	–	–	2.58	94.16	3.66	137.59
p-Cresol	–	–	1.07	39.05	1.63	61.28
2-Phenylethanol	–	–	0.35	12.77	0.71	26.69
N-Methylaniline	–	–	2.17	79.20	3.23	121.43

TABLE V

RETENTION INDICES OF THE STUDIED COMPOUNDS WITH METHANOL–BUFFER (90:10) ELUENT

Compound	0.2 DMN–0.8 DVB	0.5 DMN–0.5 DVB	0.8 DMN–0.2 DVB
Alkyl aryl ketone series			
Benzaldehyde	838	835	854
Acetophenone	832	814	834
Propiophenone	943	938	944
Butyrophenone	999	1001	1001
Valerophenone	1100	1098	1098
Hexanophenone	1202	1202	1200
Heptanophenone	1299	1299	1300
Alkylbenzene series			
Benzene	836	819	803
Toluene	952	923	920
Ethylbenzene	998	975	946
n-Propylbenzene	1071	1040	1006
n-Butylbenzene	1158	1133	1081
N-Alkylaniline series			
Aniline	593	655	681
N-Methylaniline	838	877	784
N-Ethylaniline	876	952	894
N-Propylaniline	976	1040	989
N-Butylaniline	1077	1135	1092
Alkyl aryl ether series			
Methyl phenyl ether	934	959	941
Ethyl phenyl ether	980	979	965
n-Propyl phenyl ether	1076	1066	1038
n-Butyl phenyl ether	1172	1163	1131
Alkyl benzoate series			
Methyl benzoate	910	934	884
Ethyl benzoate	939	958	936
n-Propyl benzoate	1040	1045	1026
n-Butyl benzoate	1142	1142	1123
n-Pentyl benzoate	1241	1234	1216
Test compounds			
p-Cresol	650	595	617
Nitrobenzene	999	1032	1041
2-Phenylethanol	479	478	490
Void volume for sodium nitrate (ml)	1.01	0.96	0.93
Correlation coefficients for alkyl aryl ketone series			
Acetophenone–heptanophenone	0.9975	0.9978	0.9974
Butyrophenone–heptanophenone	0.9999	0.9999	0.9999

used, the values of k' increase with the increase of the polar monomer (DMN) content in the copolymers. For example, heptanophenone eluted with methanol–buffer has the capacity factors of 3.64, 5.02 and 5.95 on the studied columns. The corresponding values for *n*-butylbenzene are 2.27, 2.96 and 2.95. In order to make a direct compari-

TABLE VI

RETENTION INDICES OF THE STUDIED COMPOUNDS WITH ACETONITRILE–BUFFER (70:30) ELUENT

Compound	0.2 DMN–0.8 DVB	0.5 DMN–0.5 DVB	0.8 DMN–0.2 DVB
Alkyl aryl ketone series			
Benzaldehyde	809	785	828
Acetophenone	787	785	787
Propiophenone	916	917	913
Butyrophenone	1000	1001	999
Valerophenone	1101	1099	1100
Hexanophenone	1199	1200	1201
Heptanophenone	1300	1300	1299
Alkylbenzene series			
Benzene	960	931	904
Toluene	1066	1021	1017
Ethylbenzene	1137	1087	1082
n-Propylbenzene	1220	1170	1165
n-Butylbenzene	1311	1263	1254
N-Alkylaniline series			
Aniline	706	689	715
N-Methylaniline	902	857	916
N-Ethylaniline	951	931	984
N-Propylaniline	1055	1062	1067
N-Butylaniline	1160	1168	1175
Alkyl aryl ether series			
Methyl phenyl ether	918	968	924
Ethyl phenyl ether	1050	1031	1006
n-Propyl phenyl ether	1147	1125	1096
n-Butyl phenyl ether	1242	1222	1197
Alkyl benzoate series			
Methyl benzoate	882	874	841
Ethyl benzoate	937	937	916
n-Propyl benzoate	1054	1035	1035
n-Butyl benzoate	1160	1142	1137
n-Pentyl benzoate	1262	1235	1236
Test compounds			
p-Cresol	687	653	642
Nitrobenzene	927	938	1004
2-Phenylethanol	580	531	502
Void volume for sodium nitrate (ml)	0.97	0.94	0.89
Correlation coefficients for alkyl aryl ketone series			
Acetophenone–heptanophenone	0.9989	0.9985	0.9991
Butyrophenone–heptanophenone	0.9999	1.0000	0.9999

son of the columns, the values of capacity factors in reference to surface area of the copolymer in the column (k'_s) were calculated. Taking into account values of specific surface areas and the weights of the copolymers in the columns (Table I), the increase of the k' values means that the strength of sample–sorbent interactions also increases.

TABLE VII

RETENTION INDICES OF THE STUDIED COMPOUNDS WITH TETRAHYDROFURAN–BUFFER (40:60) ELUENT

Compound	0.2 DMN–0.8 DVB	0.5 DMN–0.5 DVB	0.8 DMN–0.2 DVB
Alkyl aryl ketone series			
Benzaldehyde	–	773	797
Acetophenone	–	764	762
Propiophenone	–	911	908
Butyrophenone	–	998	997
Valerophenone	–	1101	1102
Hexanophenone	–	1204	1204
Heptanophenone	–	1297	1296
Alkylbenzene series			
Benzene	–	991	1004
Toluene	–	1110	1087
Ethylbenzene	–	1185	1159
n-Propylbenzene	–	1255	1227
n-Butylbenzene	–	1334	1306
N-Alkylaniline series			
Aniline	–	646	733
N-Methylaniline	–	934	951
N-Ethylaniline	–	1019	1046
N-Propylaniline	–	1124	1143
N-Butylaniline	–	1229	1246
Alkyl aryl ether series			
Methyl phenyl ether	–	1000	983
Ethyl phenyl ether	–	1067	1051
n-Propyl phenyl ether	–	1160	1144
n-Butyl phenyl ether	–	1256	1240
Alkyl benzoate series			
Methyl benzoate	–	896	880
Ethyl benzoate	–	950	935
n-Propyl benzoate	–	1039	1029
n-Butyl benzoate	–	1141	1133
n-Pentyl benzoate	–	1238	1233
Test compounds			
p-Cresol	–	728	751
Nitrobenzene	–	985	988
2-Phenylethanol	–	399	506
Void volume for sodium nitrate (ml)	–	0.94	0.86
Correlation coefficients for alkyl aryl ketone series			
Acetophenone–heptanophenone	–	0.9972	0.9974
Butyrophenone–heptanophenone	–	0.9997	0.9995

However, in the methanol–buffer eluent, interactions between alkylbenzenes and copolymers containing 0.5 and 0.8 mole fractions of polar monomer are very similar.

In Tables V–VII, the retention indices of the studied substances are summarized. In all eluents, the retention indices of alkylbenzenes decrease with an increase of

TABLE VIII

RETENTION INDICES OF TEST COMPOUNDS ON DMN–DVB COLUMNS

Copolymer	Retention index				
	Toluene	Nitrobenzene	*p*-Cresol	2-Phenylethanol	N-Methylaniline
Methanol–buffer (90:10)					
0.2 DMN–0.8 DVB	952	999	650	479	838
0.5 DMN–0.5 DVB	923	1032	595	478	877
0.8 DMN–0.2 DVB	920	1041	617	490	784
Acetonitrile–buffer (70:30)					
0.2 DMN–0.8 DVB	1066	927	687	580	902
0.5 DMN–0.5 DVB	1021	938	653	531	857
0.8 DMN–0.2 DVB	1017	1004	642	502	916
Tetrahydrofuran–buffer (40:60)					
0.2 DMN–0.8 DVB	–	–	–	–	–
0.5 DMN–0.5 DVB	1110	985	728	399	934
0.8 DMN–0.2 DVB	1087	988	751	506	951

the DMN content in the copolymer. It is not clearly noticeable for the first members of the series, but is easily visible for the last members (Fig. 1). This means that interactions between alkylbenzenes and copolymers with an increasing content of DMN monomer are weaker in comparison with those for alkyl aryl ketones.

A similar phenomenon is observed for alkyl aryl ethers, but in this case the decrease in the retention index values is smaller than for alkylbenzenes. As expected, the smallest differences in retention index values are observed for alkyl benzoates, the compounds having the same functional groups as standards and the studied copolymers.

In the case of N-alkylanilines, irregular changes in retention indices occur. Generally, an increase in the polar monomer mole fraction in copolymers causes an increase in the retention indices for N-alkylanilines. However, in the methanol–buffer mobile phase, the greatest values of indices are on the copolymer 0.5 DMN–0.5 DVB (Fig. 2a). Additionally, N-alkylanilines do not exhibit deviations from a linear relationship between the retention index and the carbon number on the copolymer 0.8 DMN–0.2 DVB. With acetonitrile–buffer, the retention indices on all the studied copolymers are very similar, but the slopes of the relationships are different (Fig. 2b). With tetrahydrofuran–buffer, the differences between N-alkylaniline retention index values on both studied copolymers are rather constant (Fig. 2c).

In Table VIII, the retention indices of the column test compounds are presented. Because the results were calculated using the set of alkyl aryl ketones butyrophenone to heptanophenone, for all test compounds, considerable extrapolation is required. Despite this, a comparison of different columns is possible, assuming that each mobile phase is studied separately to remove the effects of sample–solvent interactions [4].

For all studied copolymers, toluene and nitrobenzene are retained most compared with other compounds. With an increase of the DMN mole fraction in

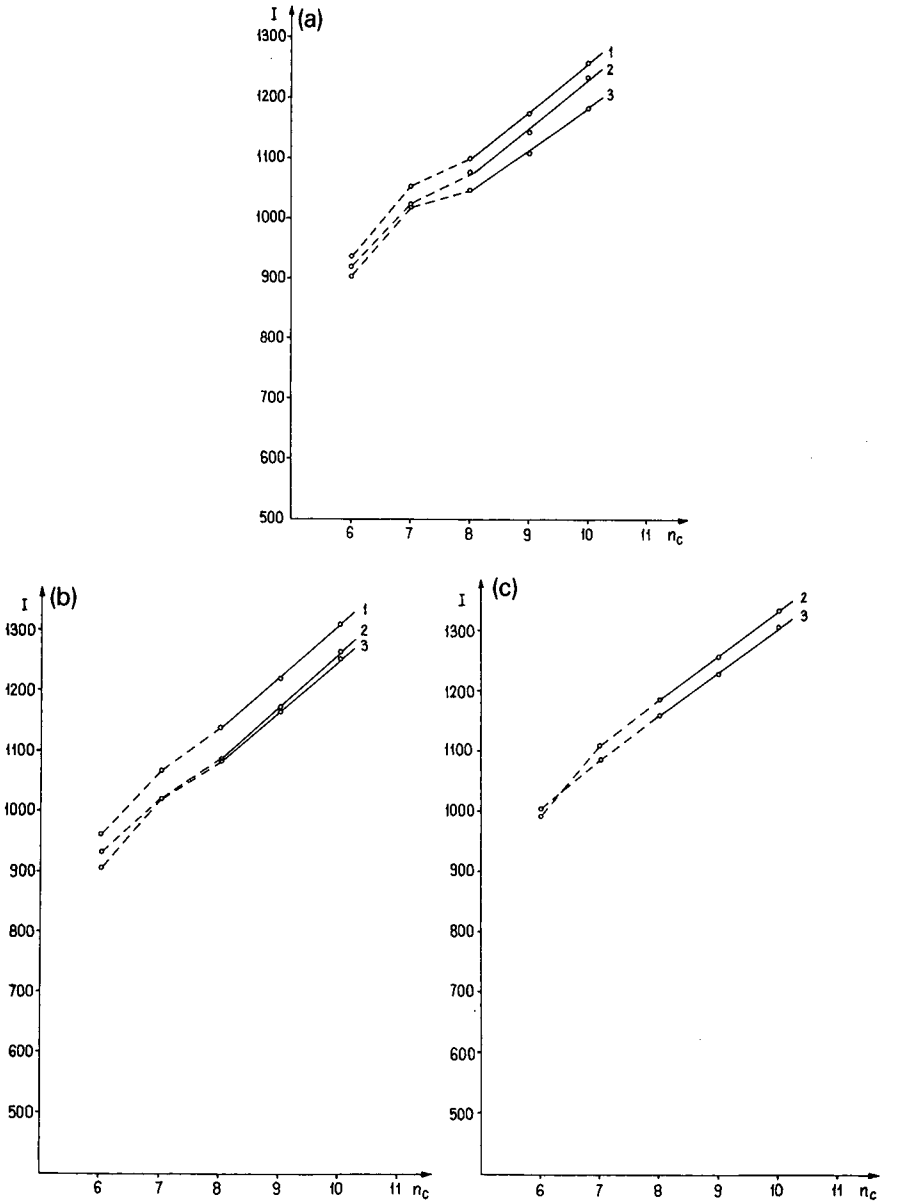

Fig. 1. Relationship between retention indices (I) and the carbon number (n_c) for homologous alkylbenzenes on the copolymers: 1 = 0.2 DMN–0.8 DVB; 2 = 0.5 DMN–0.5 DVB; 3 = 0.8 DMN–0.2 DVB. (a) Methanol–buffer (90:10); (b) acetonitrile–buffer (70:30); (c) tetrahydrofuran–buffer (40:60).

copolymers, the retention indices of toluene decrease and those of nitrobenzene increase.

The least retained compounds are the most polar: *p*-cresol and 2-phenylethanol. In the methanol–buffer mobile phase, changes in the chemical structure of DMN–

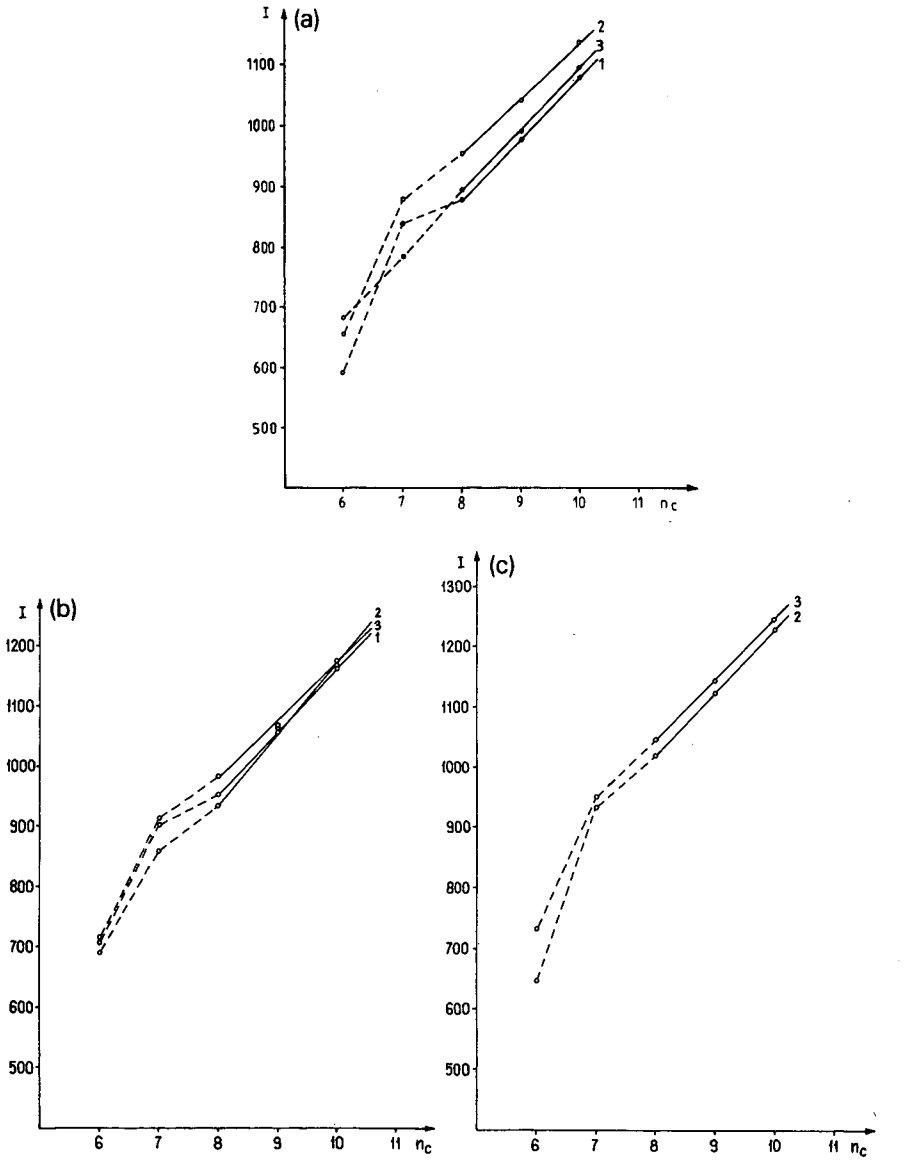

Fig. 2. Relationship between retention index (I) and the carbon number (n_c) for homologous N-alkylanilines on the copolymers: 1 = 0.2 DMN–0.8 DVB; 2 = 0.5 DMN–0.5 DVB; 3 = 0.8 DMN–0.2 DVB. (a) Methanol–buffer (90:10); (b) acetonitrile–buffer (70:30); (c) tetrahydrofuran–buffer (40:60).

DVB copolymers do not influence the relative retention of 2-phenylethanol. In the two other mobile phases its retention index values are significantly different. In particular, with the tetrahydrofuran–buffer eluent, the retention indices of 2-phenylethanol differ by over 100 units for 0.5 DMN–0.5 DVB and 0.8 DMN–0.2 DVB columns.

p-Cresol is relatively more retained, especially in the tetrahydrofuran–buffer eluent, and its retention indices have similar values.

Particularly noticeable is the variation in the retention index values of N-methylaniline, which range from $I = 877$ on the copolymer 0.5 DMN–0.5 DVB to $I = 784$ on the copolymer 0.8 DMN–0.2 DVB with methanol–buffer. In contrast, in acetonitrile–buffer and tetrahydrofuran–buffer, N-methylaniline is most highly retained on the copolymer 0.8 DMN–0.2 DVB. The behaviour of the copolymer 0.8 DMN–0.2 DVB in methanol–buffer is caused either by inaccessibility of the micropores presented in this copolymer for N-methylaniline [20,21], or by a difference in the nature of the interaction between N-methylaniline and the sorbent with the highest number of ester groups. Probably, these two effects overlap.

The results for column test compounds indicate that the DMN–DVB copolymers have a specifically much weaker retention for analytes containing hydroxyl groups (*p*-cresol and 2-phenylethanol). An increase in the DMN monomer content of the copolymers increases the retention of nitrobenzene and N-methylaniline. This means that the dipolar interactions and proton donation effects of the copolymers become stronger.

The behaviour of the studied compounds suggests that, in the case of polymeric stationary phases formed from monomers of different polarity, the molar ratio is responsible for the character of specific interactions. By changing the molar ratio of the monomers, copolymers of different selectivity can be obtained.

REFERENCES

1 P. J. Schoenmakers, H. A. H. Billiet, R. Tijssen and L. de Galan, *J. Chromatogr.*, 149 (1978) 519.
2 K. Karch, I. Sebestian and I. Halász, *J. Chromatogr.*, 122 (1976) 3.
3 P. Jandera, H. Colin and G. Guiochon, *Anal. Chem.*, 54 (1982) 435.
4 R. M. Smith, *Anal. Chem.*, 56 (1984) 256.
5 P. E. Antle, A. P. Goldberg and L. R. Snyder, *J. Chromatogr.*, 321 (1985) 1.
6 R. M. Smith, *J. Chromatogr.*, 236 (1982) 313.
7 R. M. Smith, *J. Chromatogr.*, 237 (1982) 144.
8 R. M. Smith, T. G. Hurdley, R. Gill and A. C. Moffat, *Chromatographia*, 19 (1984) 407.
9 R. M. Smith, G. A. Murilla and Ch. M. Burr, *J. Chromatogr.*, 338 (1987) 37.
10 R. M. Smith and S. L. Miller, *J. Chromatogr.*, 464 (1989) 297.
11 L. Rohrschneider, *J. Chromatogr.*, 17 (1965) 1.
12 W. O. McReynolds, *J. Chromatogr. Sci.*, 8 (1984) 685.
13 L. R. Snyder, *J. Chromatogr.*, 92 (1974) 223.
14 L. R. Snyder, *J. Chromatogr. Sci.*, 16 (1978) 223.
15 R. M. Smith, *J. Chromatogr.*, 291 (1984) 372.
16 R. M. Smith and D. R. Garside, *J. Chromatogr.*, 407 (1987) 19.
17 B. Gawdzik, J. Gawdzik and U. Czerwińska-Bil, *Chromatographia*, 26 (1988) 399.
18 A. Patrykiejew and B. Gawdzik, *J. Chromatogr.*, 365 (1986) 251.
19 S. Coppi, G. Blo and A. Betti, *J. Chromatogr.*, 388 (1987) 135.
20 F. Nevejans and M. Verzele, *J. Chromatogr.*, 406 (1987) 325.
21 B. Gawdzik, *Chromatographia*, 31 (1991) 21.

Journal of Chromatography, 549 (1991) 89–99
Elsevier Science Publishers B.V., Amsterdam

CHROM. 23 328

Metal affinity displacement chromatography of proteins

YOUNG J. KIM and STEVEN M. CRAMER*

Bioseparations Research Center, Howard P. Isermann Department of Chemical Engineering, Rensselaer Polytechnic Institute, Troy, NY 12180-3590 (USA)

(First received February 26th, 1991; revised manuscript received March 22nd, 1991)

ABSTRACT

Immobilized metal ion affinity chromatographic (IMAC) systems were employed in the displacement mode for the simultaneous concentration and purification of proteins. This work demonstrates that proteins can be employed as efficient displacers of other proteins under appropriate conditions in IMAC systems and that the displacement behavior is due to the specific interactions of the proteins with the immobilized Cu^{2+} support. The adsorption isotherms of a variety of proteins were measured and the effect of crossing adsorption isotherms on the displacement chromatographic process was investigated. Tailing observed with certain proteins in metal affinity displacement chromatography was significantly improved by the appropriate use of imidazole as a mobile phase modifier. This hybrid bioseparation technique combines the unique selectivity of IMAC with the high throughput and purity obtained in displacement chromatography.

INTRODUCTION

There is presently considerable interest in the use of group specific affinity adsorbents for the concentration and purification of biomolecules [1]. These relatively inexpensive adsorbent materials are capable of selectively interacting with classes of complementary biopolymers and have significant economic advantages over biospecific affinity systems.

While immobilized metal adsorbents have been used for the separation of small molecules since 1961 [2], it was not until the mid seventies that Porath *et al.* [3] extended the technique to the separation of proteins and nucleic acids. This powerful bioseparation tool employs the specific interaction of heavy metal ions with the amino acids histidine, cysteine, and tryptophan to effect a variety of bioseparations. Several workers have attempted to elucidate the mechanism of adsorption in immobilized metal ion affinity chromatographic (IMAC) systems [4–8]. However, the physicochemical properties of protein retention in IMAC are not well understood at present. While good correlations between surface histidine content and protein retention in IMAC have been established [9–12], differences in molecular size, amino acid composition, and net charge between various proteins can also affect retention in IMAC [13]. Porath's work has generated considerable work in the purification of biomolecules using IMAC systems in the elution and gradient mode [10,13–21].

0021-9673/91/$03.50

Displacement chromatography is rapidly emerging as a powerful bioseparation method due to the high throughput and product purity associated with the process [22–24]. This technique offers distinct advantages in preparative chromatography as compared to the conventional elution mode. The displacement process takes advantages of the non-linearity of the isotherms such that a larger feed can be separated on a given column with the purified components recovered at significantly higher concentrations. Furthermore, the tailing observed in elution chromatography is greatly reduced in displacement chromatography due to self-sharpening boundaries formed in the process. Whereas in elution chromatography the feed components are diluted during the separation, the feed components are often concentrated during displacement chromatography. These advantages are particularly significant for the isolation of biopolymers from dilute solutions such as those encountered in biotechnology processes. Although traditional stationary phase materials such as reversed phase and ion exchange have been successfully employed in the displacement mode [22–27], research on displacement chromatography with novel adsorbent materials is scarce at present [28,29].

The use of IMAC for preparative chromatographic separations requires appropriate modes of operation to enable high throughput and purity in these systems. In this report, we present experimental results on the metal affinity displacement chromatography (MADC) of proteins. This hybrid bioseparation technique combines the unique selectivity of IMAC with the high throughput and purity obtained in displacement chromatography.

EXPERIMENTAL

Materials

Bulk chelating Superose (10 μm) containing covalently bound iminodiacetic acid (IDA) and 50 × 5 mm I.D. glass columns were donated by Pharmacia LKB Biotechnology (Piscataway, NJ, USA). Bulk Bioseries strong cation exchanger (SCX) material was a gift from Rockland Technologies (Newport, DE, USA). The IDA and SCX materials were slurry packed into 50 × 5 mm and 100 × 4.6 mm I.D. columns, respectively. Tris–HCl and sodium monophosphate were purchased from Fisher Scientific (Rochester, NY, USA). Sodium chloride, ammonium sulfate, cupric sulfate, cytochrome *c* from horse heart, lysozyme, α-chymotrypsinogen A, ribonuclease A, lactoferrin (bovine), α-chymotrypsin, and imidazole were obtained from Sigma (St. Louis, MO, USA).

Apparatus

A fast protein liquid chromatography apparatus (FPLC) (Pharmacia LKB) was employed for the protein displacement experiments. This system consisted of 2 Model P-500 pumps connected to the chromatographic column via a Model MV-7 valve. The column effluent was monitored by a Model UV-M detector and a Pharmacia strip-chart recorder. Fractions of the column effluent were collected with a Model Frac-100 fraction collector. The system was controlled using a LCC-500-Plus controller.

Procedures

Immobilization of Cu^{2+}. The IDA columns were loaded with Cu^{2+} by sequential perfusion with 10 column volumes of 0.3 *M* cupric sulfate aqueous solution, pH 3.9, six column volumes of distilled water, and five column volumes of the carrier solutions described below.

Protein adsorpton isotherms. Protein adsorption isotherms were determined by frontal chromatography according to the technique of Jacobson *et al.* [30] by using a 50 × 1 mm I.D. microbore column packed with Cu^{2+} charged IMAC material.

Operation of displacement chromatograph. A schematic of the displacement chromatograph system employed in this work is illustrated elsewhere [25]. In all displacement experiments, the columns were sequentially perfused with carrier, feed, displacer, and regenerant solutions. Fractions of the column effluent were collected throughout the displacement runs and were assayed by analytical chromatography.

MADC of proteins. Displacement experiments were carried out using 50 × 5 mm I.D. columns packed with Cu^{2+} charged IMAC stationary phase materials. Unless stated otherwise, the displacer was 30 mg/ml ribonuclease A (RNase A) in the mobile phase carriers described below. The regenerant was 15 column volumes of 25 m*M* phosphate buffer, pH 4.0, containing 1.0 *M* sodium chloride. All protein displacements were carried out at a flow-rate of 0.1 ml/min at 22°C.

MADC of α-chymotrypsinogen A and cytochrome c. Displacement experiments were carried out using a feed mixture containing 2 mg α-chymotrypsinogen A and 4 mg cytochrome *c* in 2 ml of a 25 m*M* phosphate buffer carrier, pH 6.0, containing 1.0 *M* sodium chloride. Sodium chloride was added to all carrier solutions in order to quench non-specific ionic adsorption. The following experiments were carried out: displacement chromatography with RNase A displacer on a Cu^{2+} charged IMAC column; displacement chromatography with RNase A displacer on a "naked" IDA column; preparative elution chromatography on a Cu^{2+} charged IMAC column.

MADC of α-chymotrypsinogen A, cytochrome c, and lysozyme. Displacement experiments with RNase A as the displacer were carried out using a feed mixture containing either 2 or 4 mg of α-chymotrypsinogen A, 4 mg of cytochrome *c*, and 4 mg of lysozyme in 2 ml of a 25 m*M* phosphate buffer carrier containing 1.0 *M* sodium chloride at pH 5.0, 6.0, and 7.0.

MADC of α-chymotrypsinogen A, cytochrome c, and lactoferrin. MADC using RNase A as the displacer was carried out on a feed mixture containing 2 mg α-chymotrypsinogen A, 4 mg cytochrome c, and 16 mg lactoferrin in 2 ml of a 25 m*M* phosphate buffer carrier, pH 6.0, containing 1.0 *M* sodium chloride.

Effect of imidazole containing carriers on MADC. Displacement experiments with RNase A as the displacer were carried out using a feed mixture containing 4 mg of cytochrome *c* and 16 mg of lactoferrin in 2 ml of a 25 m*M* phosphate buffer carrier containing 1.0 *M* sodium chloride. The following MADC experiments were carried out: pH 6.0 carrier containing 0.2, 0.5, and 3.0 m*M* imidazole; pH 7.0 carrier containing 0.2 and 0.5 m*M* imidazole.

High-performance liquid chromatographic (HPLC) analysis. Fractions collected during the displacement chromatographic runs were analyzed by gradient elution cation-exchange chromatography. A Waters Delta Prep 3000 chromatography system with Waters 600E system controller (Millipore, Milford, MA, USA), a Waters 712 WISP auto-injector, a Waters Lambda-Max Model 481 LC spectrophotometer,

and a Waters 745B integrator were assembled to carry out HPLC analysis. Protein analysis were carried out using a 100 × 4.6 I.D. SCX column (Rockland Technologies). A 6-min linear gradient of 0–1.0 *M* sodium chloride in 50 m*M* TRIS–HCl buffer, pH 8.0, was employed. Displacement fractions were diluted 10–50 fold with the first eluent buffer and 25-μl samples were injected. The flow was 2.0 ml/min. The column effluents were monitored at 280 nm. Quantitative analyses were carried out and the data was used to construct displacement chromatograms.

RESULTS AND DISCUSSION

Preliminary results from our laboratory had indicated that IMAC systems with immobilized Ni^{2+} were able to produce displacement like behavior of proteins [31]. However, relatively high levels of Ni leakage during the displacement experiments made this system impractical for protein separations. In this manuscript, we will report on MADC using a Cu^{2+} charged IMAC system which exhibits strong interactions with the proteins and is extremely stable under the displacement conditions.

MADC of two component protein mixtures

The separation of the proteins α-chymotrypsinogen A and cytochrome *c* by displacement chromatography on the IMAC system was investigated using RNase A as the displacer. The carrier contained 1 *M* sodium chloride to suppress any residual IDA functionalities on the stationary phase material. The resulting displacement chromatogram is shown in Fig. 1. Under these conditions, α-chymotrypsinogen A eluted ahead of the displacement train while the cytochrome *c* was well displaced by

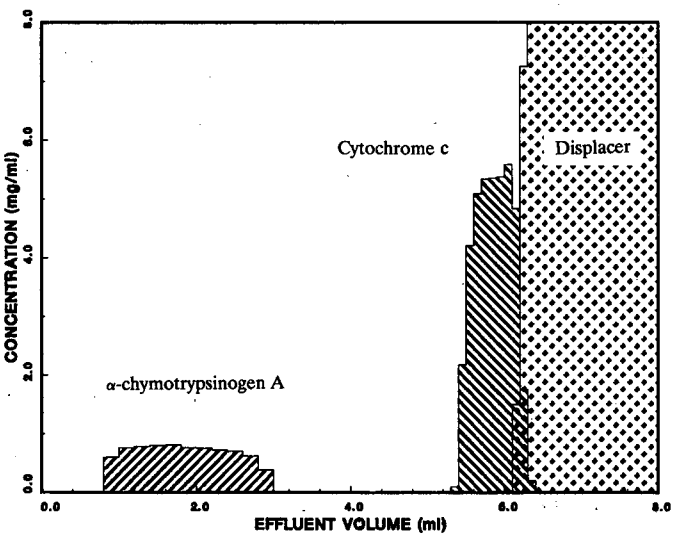

Fig. 1. Displacement chromatogram of a two-component protein mixture. Column, 50 × 5 mm I.D. Cu^{2+} charged metal chelate Superose (10 μm); carrier, 1.0 *M* sodium chloride in 25 m*M* phosphate buffer, pH 6.0; displacer, 30 mg/ml RNase A in carrier; flow-rate 0.1 ml/min; temperature 22°C; feed, 2 mg α-chymotrypsinogen A and 4 mg cytochrome *c* in 2 ml carrier; fraction volume, 100 μl.

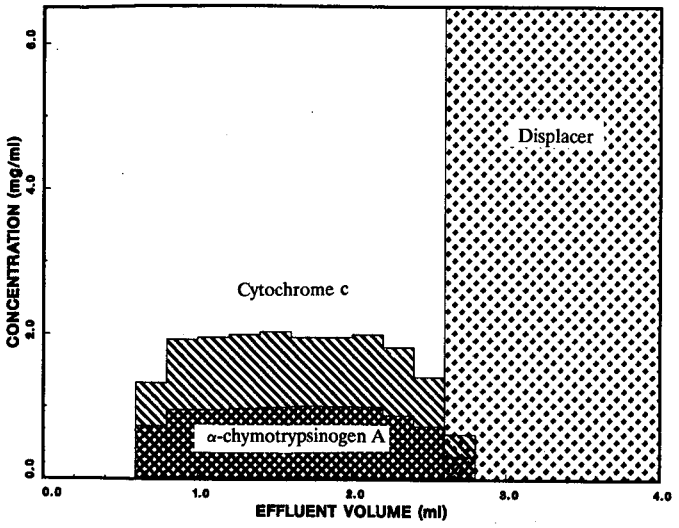

Fig. 2. Displacement chromatogram of a protein mixture on IDA support. Chromatographic conditions as stated in Fig. 1 with the exception of: column, naked IDA; fraction volume, 200 μl.

the RNase A displacer. This separation resulted in a three-fold concentration of the cytochrome *c* and produced a very sharp boundary between the displacement zones. A 95% recovery of the cytochrome *c* was achieved at a purity of 96% in this separation. The separation presented in Fig. 1 demonstrates that proteins can be employed as efficient displacers of other proteins under appropriate conditions in IMAC systems.

In order to determine whether this separation was indeed metal affinity displacement chromatography, two control experiments were carried out. The first control consisted of the same displacement separation described for Fig. 1 with the exception of using a "naked" IDA column. In the absence of the metal, the IDA column acts as a weak cation exchanger. As shown in Fig. 2, in the absence of the metal, there was complete mixing of the two feed proteins. In fact, both proteins emerged from the column at the column dead time, due to the action of the high salt mobile phase carrier. Thus, the displacement behavior demonstrated in Fig. 1 was indeed due to the specific interactions of the proteins with the immobilized Cu^{2+}.

In order to dramatize the action of the displacer in these systems, the MADC experiment was repeated in the absence of the displacer. Fig. 3 demonstrates that while the α-chymotrypsinogen A peak was unaffected by the lack of displacer, the cytochrome *c* zone emerged in the classic overloaded elution state. In contrast to the displacement shown in Fig. 1, the preparative elution presented in Fig. 3 is characterized by significant tailing and dilution of the cytochrome *c*. These results demonstrate the ability of the displacer to both concentrate and reduce the tailing of solutes in preparative metal chelate chromatography.

MADC of three component protein mixtures

In order to increase the complexity of the feed mixture, we examined the linear

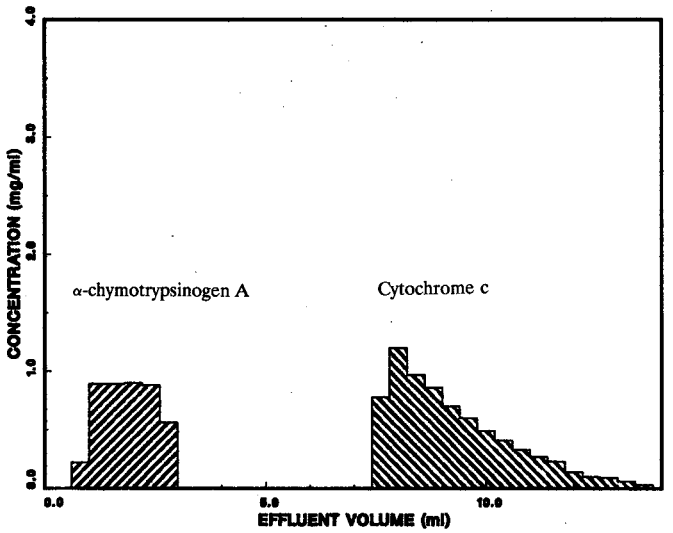

Fig. 3. Preparative elution chromatogram of a two-component protein mixture. Chromatographic conditions as stated in Fig. 1 with the absence of the displacer; fraction volume, 400 μl.

elution chromatographic behavior of a variety of proteins known to exhibit affinity for IMAC systems [9,10,13]. Affinities ranged from very strongly retained proteins such as myoglobin and concanavalin A; to intermediate affinity proteins such as RNase A, lactoferrin, and lysozyme; to relatively low affinity proteins such as cyto-

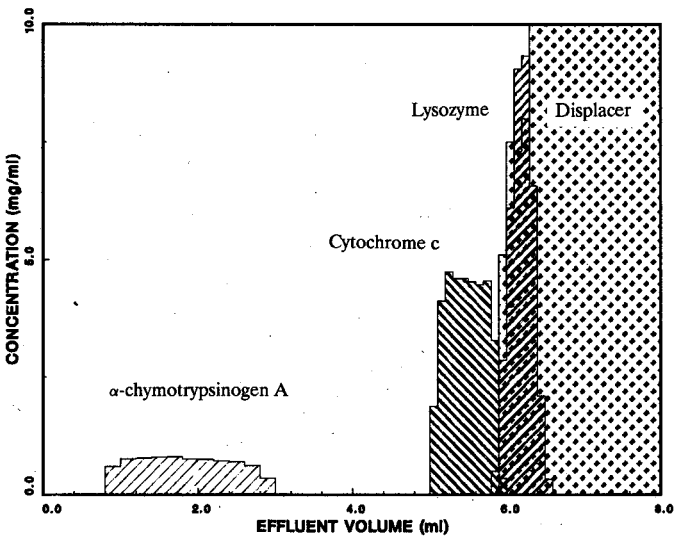

Fig. 4. Displacement chromatogram of a three-component protein mixture. Chromatographic conditions as stated in Fig. 1 with the exception of feed, 2 mg α-chymotrypsinogen A, 4 mg cytochrome *c*, and 4 mg lysozyme in 2 ml carrier.

chrome *c* and α-chymotrypsinogen A. Preliminary displacement experiments were carried out using myoglobin as the displacer. However, the limited solubility of the myoglobin (15 mg/ml) as well as the difficulty of regenerating the IMAC column following perfusion with this protein made it impractical as a displacer.

Under linear elution conditions, RNase A had a consistently stronger retention than the proteins lysozyme, cytochrome *c* and α-chymotrypsinogen A. Accordingly, MADC experiments were carried out using RNase A to displace a feed mixture containing these three proteins. The resulting chromatogram shown in Fig. 4, indicates that α-chymotrypsinogen A eluted ahead of the displacement train while cytochrome *c* was well displaced during the separation. On the other hand lysozyme emerged from the column immediately following the breakthrough of the displacer. Since RNase A exhibited a stronger retention than lysozyme under linear elution conditions this displacement behavior was indicative of the presence of crossing adsorption isotherms for these two proteins [32].

In an attempt to achieve a successful displacement, the experiment was repeated at pH 5.0 and 7.0. In both cases, the lysozyme emerged from the system after the breakthrough of the displacer. The displacement chromatogram for the pH 5.0 experiment is shown in Fig. 5. Under these conditions, the cytochrome *c* displacement zone was not fully developed and the emergence of the lysozyme in the displacer zone produced a distortion of the front.

Clearly, in order to develop appropriate displacement conditions, more detailed information on the non-linear adsorption behavior of these proteins was required. Accordingly, the adsorption isotherms of various proteins was measured using microbore frontal chromatography. The resulting adsorption isotherms are presented in Fig. 6. As expected from the displacement results shown in Figs. 4 and 5, the ad-

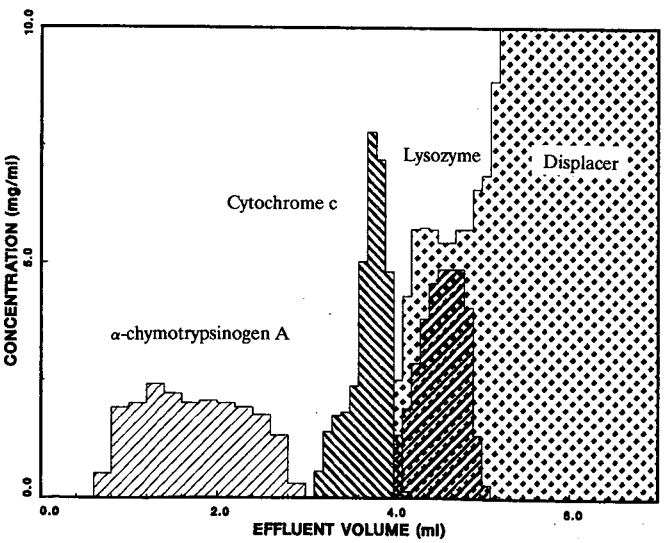

Fig. 5. Displacement chromatogram of a three-component protein mixture. Chromatographic conditions as stated in Fig. 1 with the exception of: feed, 4 mg each of α-chymotrypsinogen A, cytochrome *c*, and lysozyme in 2 ml carrier; carrier, 1.0 *M* sodium chloride in 25 m*M* phosphate buffer, pH 5.0.

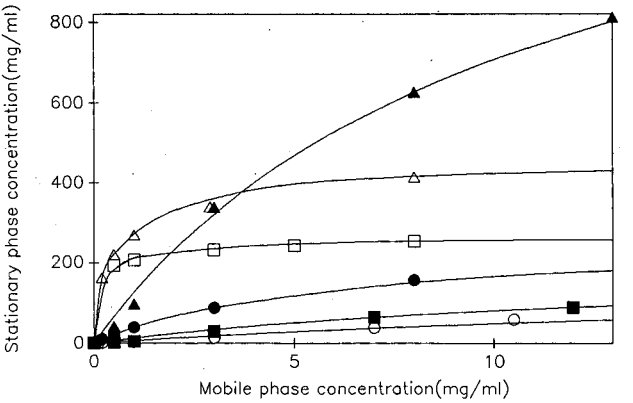

Fig. 6. Protein adsorption isotherms. Column, 50 × 1 mm I.D. Cu^{2+} charged metal chelate superose; carrier, 1.0 *M* sodium chloride in 25 m*M* phosphate buffer, pH 6.0. ▲ = Lysozyme; △ = RNase A; □ = lactoferrin; ● = cytochrome *c*; ■ = α-chymotrypsin; ○ = α-chymotrypsinogen A.

sorption isotherms of lysozyme and RNase A crossed under these carrier conditions.

All protein adsorption isotherms measured on the IMAC system satisfied the displacement requirement for concave downward isotherms [22]. The characteristic high loading capacity of IMAC systems is clearly evident in this data. These adsorption capacities are comparable to those of Belew *et al.* [33] when one takes into account differences in definitions of stationary phase volume. The relatively high capacity of IMAC systems as compared to ion-exchange and reversed-phase systems may be in part responsible for the ability to carry out displacements on relatively

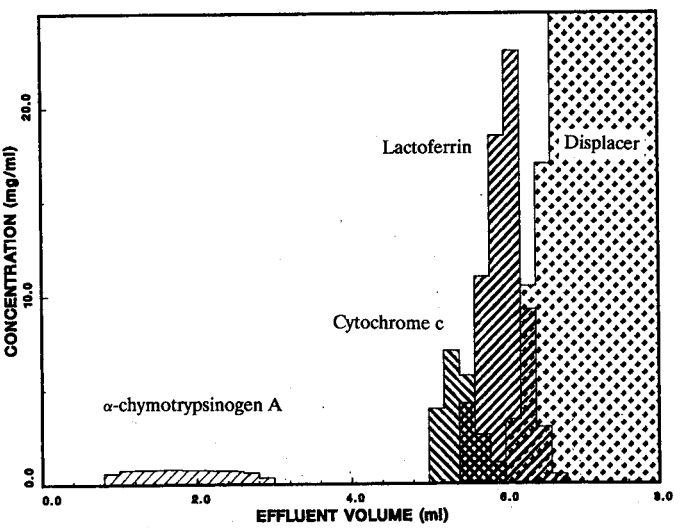

Fig. 7. Displacement chromatogram of a three-component protein mixture. Chromatographic conditions as stated in Fig. 1 with the exception of: feed, 2 mg α-chymotrypsinogen A, 4 mg cytochrome *c*, and 16 mg lactoferrin in 2 ml carrier; fraction volume, 200 μl.

short IMAC columns. In fact, the combination of high binding capacity and corresponding shorter column lengths may produce additional economic advantages for MADC systems.

As seen in Fig. 6, the adsorption isotherms of RNase A and lactoferrin are well separated at pH 6.0. Accordingly, we investigated the displacement separation of α-chymotrypsinogen A, cytochrome *c*, and lactoferrin using 30 mg/ml RNase A as the displacer. The resulting chromatogram shown in Fig. 7 indicates that the α-chymotrypsinogen A eluted from the system ahead of the displacement zones of cytochrome *c* and lactoferrin. While this separation was able to produce a three-fold concentration of the displaced proteins, the boundaries separating the displacement zones were quite diffuse. This is in contrast to the results presented in Fig. 1 where the system produced sharp boundaries. Clearly, the lactoferrin is responsible for the non-ideal behavior in this system. In fact, this type of tailing behavior has been observed in previous research in our laboratory on reversed-phase displacement systems [34].

Imidazole mobile phase modifier effects

While the exact mechanism for this tailing is not known, it is postulated that the tailing in this system is due to either slow desorption kinetics and/or steric effects due to the difference in the molecular weight of the lactoferrin (76 kilodalton) and the other proteins (12–24 kilodalton). In order to minimize the deleterious effect of slow desorption kinetics on the displacement behavior of these systems we employed imidazole as a mobile phase modifier while retaining RNase A as the displacer. Experiments were carried out with 0.2, 0.5, and 3.0 m*M* imidazole in the carrier. While 0.2 m*M* imidazole had no apparent effect on the system, 3.0 m*M* imidazole resulted in the

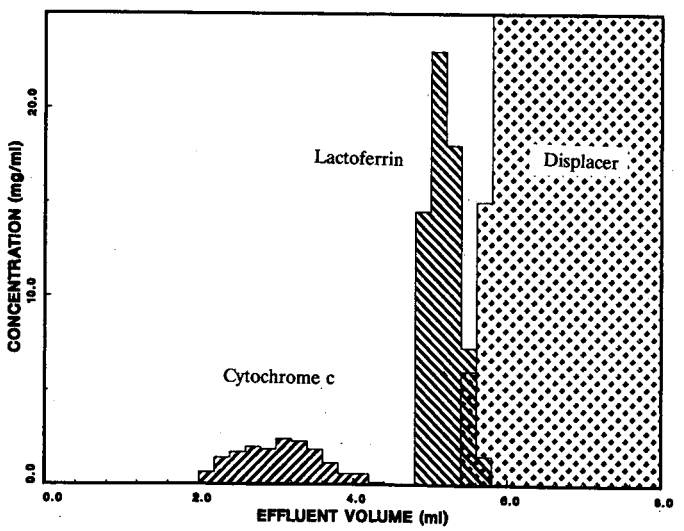

Fig. 8. Displacement chromatogram of a two-component protein mixture. Chromatographic conditions as stated in Fig. 1 with the exception of: carrier, 0.5 m*M* imidazole and 1.0 *M* sodium chloride in 25 m*M* phosphate buffer, pH 6.0; feed, 4 mg cytochrome *c* and 16 mg lactoferrin in 2 ml carrier; fraction volume, 200 μl.

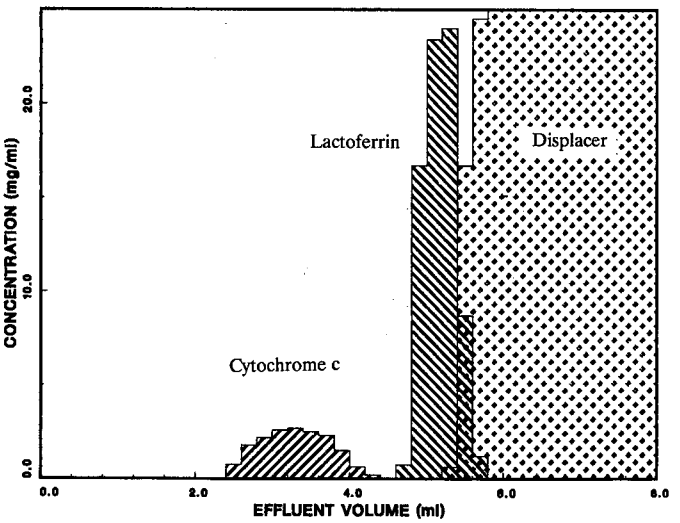

Fig. 9. Displacement chromatogram of a two-component protein mixture. Chromatographic conditions as stated in Fig. 1 with the exception of: carrier, 0.2 m*M* imidazole and 1.0 *M* sodium chloride in 25 m*M* phosphate buffer, pH 7.0; feed, 4 mg cytochrome *c* and 16 mg lactoferrin in 2 ml carrier; fraction volume, 200 μl.

elution of both cytochrome *c* and lactoferrin ahead of the RNase A displacer front. In contrast, the addition of 0.5 m*M* imidazole to the carrier resulted in significant sharpening of both the lactoferrin tail and the displacer front as shown in Fig. 8. Under these conditions, cytochrome *c* eluted from the system ahead of the displaced lactoferrin.

In an effort to produce a successful displacement of both cytochrome *c* and lactoferrin, the experiment was carried out at pH 7.0 with various imidazole concentrations. Fig. 9 shows the separation achieved at pH 7.0 using a 0.2 m*M* imidazole carrier. Again, the displacement experiment resulted in elution of the cytochrome *c* and successful displacement of the lactoferrin. Interestingly, a lower imidazole concentration was required to achieve sharp displacement of the lactoferrin at pH 7.0 as compared to pH 6.0. While these results do not establish the exact mechanism for the tailing observed in this system, they indicate that dispersion in MADC systems can be minimized by the appropriate use of imidazole as a mobile phase modifier.

CONCLUSIONS

In this report we have demonstrated that IMAC systems can be employed in the displacement mode for the simultaneous concentration and purification of proteins. This work demonstrates that proteins can be employed as efficient displacers of other proteins under appropriate conditions in IMAC systems and that the displacement behavior is due to the specific interactions of the proteins with the immobilized Cu^{2+} support. The adsorption isotherms of a variety of proteins were measured and the effect of crossing adsorption isotherms on the displacement chromatographic process was investigated. Finally, tailing observed with certain displaced proteins was signif-

icantly improved by the addition of appropriate amounts of imidazole to the carrier solution. We are currently developing alternative displacer for MADC and applying this powerful hybrid bioseparation technique for the direct purification of biopharmaceuticals from complex fermentation broths.

ACKNOWLEDGEMENTS

The gifts of stationary phase materials from Rockland Technologies (Newport, DE, USA) and chromatographic supplies and equipment from Pharmacia LKB Biotechnology (Piscataway, NJ, USA) and Waters Chromatography Division (Millipore, Milford, MA, USA) are gratefully acknowledged. This research was supported by the Eastman Kodak Company and Grant No. CTS-8900566 from the National Science Foundation.

REFERENCES

1 M. A. Vijayalakshmi, *Trends Biotechnol.*, 7 (1989) 71.
2 F. Helfferich, *Nature (London)*, 189 (1961) 1001.
3 J. Porath, J. Carlsson, I. Olsson and G. Belfrage, *Nature (London)*, 258 (1975) 598.
4 E. S. Hemdan and J. Porath, *J. Chromatogr.*, 323 (1985) 255.
5 E. S. Hemdan and J. Porath, *J. Chromatogr.*, 323 (1985) 265.
6 S. A. Margolis, A. J. Fatiadi, L. Alexander and J. J. Edwards, *Anal. Biochem.*, 183 (1989) 108.
7 T. W. Hutchens and T. T. Yip, *J. Chromatogr.*, 500 (1990) 531.
8 M. Belew and J. Porath, *J. Chromatogr.*, 516 (1990) 333.
9 E. Sulkowski, *Trends Biotechnol.*, 3 (1) (1985) 1.
10 E. Sulkowski, in R. Burgess (Editor), *Protein Purification: Micro to Macro, UCLA Symposium on Molecular and Cellular Biology, New Series*, Vol. 68, Alan R. Liss, New York, 1987, p. 149.
11 E. S. Hemdan, Y. J. Zhao, E. Sulkowski and J. Porath, *Proc. Natl. Acad. Sci. U.S.A.*, 86 (1989) 1811.
12 S. S. Suh and F. H. Arnold, *Biotechnol. Bioeng.*, 35 (1990) 682.
13 Z. El Rassi and Cs. Horváth, in K. M. Gooding and F. E. Regnier (Editors), *HPLC of Biological Macromolecules (Methods and Applications)*, Marcel Dekker, New York, 1990, p. 179.
14 B. Lonnerdal, J. Carlsson and J. Porath, *FEBS Lett.*, 75 (1) (1977) 89.
15 J. P. Salier, J. P. Martin, P. Lambin, M. McPhee and K. Hochstrasser, *Anal. Biochem.*, 109 (1980) 273.
16 J. Porath, B. Olin and B. Granstrand, *Arch. Biochem. Biophys.*, 225 (2) (1983) 543.
17 Z. El. Rassi and Cs. Horváth, *J. Chromatogr.*, 359 (1986) 241.
18 M. Belew, T. T. Yip, L. Andersson and R. Ehrnstrom, *J. Biochem.*, 164 (1987) 457.
19 J. Porath, *J. Chromatogr.*, 443 (1988) 3.
20 A. R. Sundquist and R. C. Fahey, *J. Bacteriol.*, 170 (8) (1988) 3459.
21 E. Li-Chan, L. Kwan and S. Nakai, *J. Dairy Sci.*, 73 (1990) 2075.
22 Cs. Horváth, in F. Bruner (Editor), *The Science of Chromatography*, Elsevier, Amsterdam, 1985, p. 179.
23 J. Frenz and Cs. Horváth, in Cs. Horváth (Editor), *High Performance Liquid Chromatography, Advances and Perspectives*, Vol. 8, Academic Press. Orlando, FL, 1988, p. 211.
24 S. M. Cramer and G. Subramanian, *Separation and Purification Methods*, 19 (1) (1990) 31.
25 S. M. Cramer and Cs. Horváth, *Prep. Chromatogr.*, 1 (1988) 29.
26 G. Subramanian, M. W. Phillips and S. M. Cramer, *J. Chromatogr.*, 439 (1988) 341.
27 G. Subramanian, M. W. Phillips, G. Jayaraman and S. M. Cramer, *J. Chromatogr.*, 484 (1989) 225.
28 G. Vigh, G. Quintero and G. Farkas, *J. Chromatogr.*, 484 (1989) 237.
29 G. Vigh, G. Farkas and G. Quintero, *J. Chromatogr.*, 484 (1989) 251.
30 J. Jacobson, J. Frenz and Cs. Horváth, *J. Chromatogr.*, 316 (1984) 53.
31 G. Subramanian, *Doctoral Thesis*, Rensselaer Polytechnic Institute, Troy, NY, 1990.
32 G. Subramanian and S. M. Cramer, *Biotech. Progress*, 5 (3) (1989) 92.
33 M. Belew, T. T. Yip, L. Andersson and J. Porath, *J. Chromatogr.*, 403 (1987) 197.
34 M. W. Phillips and S. M. Cramer, presented at *Annual AIChE Meeting, Chicago, IL, 1990.*

Journal of Chromatography, 549 (1991) 101–111
Elsevier Science Publishers B.V., Amsterdam

CHROM. 23 312

Two-dimensional viscous flow analysis in a micro flow-cell of an ultraviolet absorption detector for high-performance liquid chromatography

MASAO KAMAHORI*, YOSHIO WATANABE and HIROYUKI MIYAGI
Central Research Laboratory, Hitachi Ltd., 1-280 Higashikoigakubo, Kokubunji, Tokyo 185 (Japan)
and
HIROSHI OHKI and RYO MIYAKE
Mechanical Engineering Research Laboratory, Hitachi Ltd., 502 Kandatsu, Tsuchiura, Ibaraki 300 (Japan)
(First received July 5th, 1990; revised manuscript received October 30th, 1990)

ABSTRACT

Flow profiles in a Z-type 0.6-μl micro flow-cell of an ultraviolet absorption detector for high-performance liquid chromatography were evaluated. The flow profile and band broadening in the flow-cell were calculated by finite-element analysis using a supercomputer (HITAC S-810). The flow profile was Poiseuille flow following the Golay equation at flow-rates less than 0.2 ml/min. However, at flow-rates above 0.2 ml/min the flow had two types of band broadening, depending on the form of the flow-cell and the connection between the flow-cell and the connecting tubing. The first type was band broadening independent of flow velocity, including mixing broadening at flow-rates from 0.2 to 1.0 ml/min. The second was mixture-type band broadening between laminar flow broadening and mixing broadening depending on the flow velocity, which gave a Gaussian profile containing a tailing peak, at flow-rates over 1.0 ml/min. A comparison of these results and the experimental results showed good agreement.

INTRODUCTION

Extra-column contributions to band broadening are significant for overall system performance in high-performance liquid chromatography (HPLC). They become more and more critical when highly efficient fast and micro liquid chromatography using small particle packings or narrow-bore columns are employed [1]. They include volumetric broadening originating from the injector, detector flow-cell and connecting tubing and temporal broadening resulting from the response rate of the detector. In particular, the detector flow-cell is a significant source of band broadening in the chromatographic system.

Sternberg [2] reported that several sources of volumetric broadening were present in the flow-cell: the cell volume itself; laminar flow broadening; and mixing and diffusional broadening. Laminar flow broadening resulting from the laminar flow and an associated parabolic flow profile in the flow-cell has been described by Martin *et al.* [3]. It is generally recognized that when sharp diameter changes in fittings between

the flow-cell and the connecting tubing are present, in addition to abrupt bends in the flow-cell, band broadening may be caused. The band broadening is extremely difficult to describe from a purely theoretical basis, since it involves a poorly described area of hydrodynamics in the range of low Reynolds numbers, where laminar flow is normally expected. However, laminar flow broadening is usually an insignificant source of band broadening in the flow-cell because of its short length. Rather, the flow-cell often contributes to distortion or exponential tailing of a solute peak. One source may be the diffusional and mixing processes which occur within flow-cells containing a fitting and that also have abrupt bends. If the flow profile in the flow-cell is similar to that in open tubing, the flow profile in the Z-type flow-cell should be of the Poiseuille type in the main channel. This includes secondary flow or turbulence in the fitting. However, there is no theoretical explanation regarding band broadening in flow-cells that have the fitting and the abrupt bends, because the relevant Navier–Stokes differential equations for complex geometrical forms have not been solved. A careful design of the flow-cell in fast and micro HPLC requires detailed knowledge of the flow profiles and band broadening in the flow-cell.

Recently, Atwood and Golay [4,5] reported that the dispersion of a short tubing was mathematically simulated using a computer model combining a Poiseuille flow with diffusion. They studied the theory of dispersion in a sample in short, straight open tubings. However, they have not directly solved the relevant Navier–Stokes differential equations and the diffusion equation, but have used the model combining the Poiseulle flow with diffusion. It may be difficult to simulate dispersion of the Z-type flow-cell of an ultraviolet absorption detector because of its complex geometrical forms (*i.e.* an abrupt bend and a fitting with sharp changes in tubing diameter). Furthermore, it may not be possible to visualize the flow and concentration profiles in the flow-cell. In this paper, the simulation of flow profiles and band broadening in the Z-type flow cell with a direct solution of these equations by finite-element analysis using a supercomputer (HITAC S-810) is discussed.

EXPERIMENTAL

Practical measurements of band broadening in the flow cell

A Hitachi 655A-12 liquid chromatograph pump was used. The mobile phase was passed through a column (50 mm × 4 mm I.D.), packed with 2-μm glass beads, to the injector (Rheodyne 7520) by the pump. The injector was connected directly, without a separation column, to a modified Hitachi 655-51 UV monitor (with the reported 0.6-μl flow-cell [6]). The output signal from the UV detector was fed to an analyzing recorder (YEW Model 3655).

Methanol was used as the eluent, into which 0.5 μl of benzene (0.5%, v/v, dissolved in the eluent) was injected. Most of the measurements, because at very narrow band profiles, have to be carried out in less than 1 s, because practical measurements of band broadening were carried out without a separation column. We used a system that had an overall time constant of 10 ms for the detector electronics and a sampling rate of 1 ms with a 1-kHz low-pass filter for the recorder. The band broadening was defined by the standard deviation of a concentration profile, taking the width at 60.7% of the maximum height.

Two-dimensional viscous flow analysis in the flow-cell

To determine the real flow profiles in the flow-cell, it is necessary to solve a three-dimensional viscous flow analysis problem. However, it is not obvious that, to solve the relevant Navier–Stokes differential equations, a diffusion equation may be used to analyze the flow profiles in the flow-cell. Furthermore, three-dimensional viscous flow analysis is a complicated and time-consuming task. It was difficult to solve the flow analysis in this stage. In the first stage, two-dimensional viscous flow analysis, which is simpler than three-dimensional analysis but ignores the effect of flow and diffusion in the z direction (*i.e.* eddy diffusion), was applied directly to solve the flow profiles in the flow-cell. We have studied here the theory, in this case of two-dimensional flow analysis.

A computer program for two-dimensional viscous flow analysis using finite-element analysis has been developed by Ikegawa and co-workers [7–9]. A mathematical handling of the flow and concentration profiles is possible, but the chromatogram and variance (second moment) are not included in the program. We prepared a new program for calculation of the band broadening, that is the chromatogram and second moment, in the flow-cell. An outline of the calculation method is as follows.

Calculation of velocity vector

A simplified flow chart for the calculation of the velocity vector is shown in Fig. 1. The initial condition was a non-compressed viscous flow. First, potential flow in the flow-cell was calculated without the viscous effect. Secondly, the velocity vector was calculated using the results of the potential flow with the viscous effect. The flow profile was drawn using the calculated velocity vector.

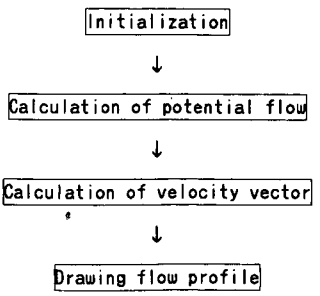

Fig. 1. Flow chart for calculation of flow profile.

Calculation of chromatogram and second moment

Fig. 2 shows a simplified flow chart for the calculation of the chromatogram and second moment. The initial condition was the input of the sample concentration profile. First, the diffusion equation was solved using the calculated velocity vector. Secondly, the chromatogram was drawn using the calculated concentration of each element in the flow-cell. Finally, the second moment was calculated.

Conditions for the calculation were as follows: number of elements, 3175; mobile phase, methanol; solute, benzene; diffusion coefficient, 0.001 mm^2/s; range of flow-rates, 0.2–2.0 ml/min.

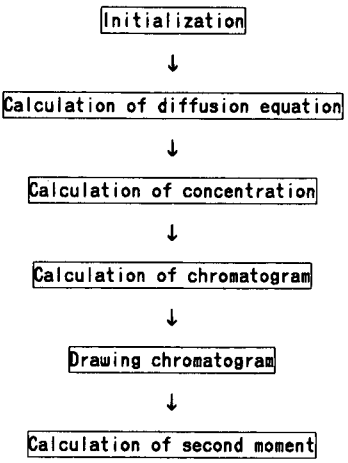

Fig. 2. Flow chart for calculation of chromatogram and second moment.

Fig. 3 shows the structure of the flow-cell for two-dimensional viscous flow analysis. Fig. 4 shows the mesh of the flow path in the flow-cell for the analysis corresponding to Fig. 3.

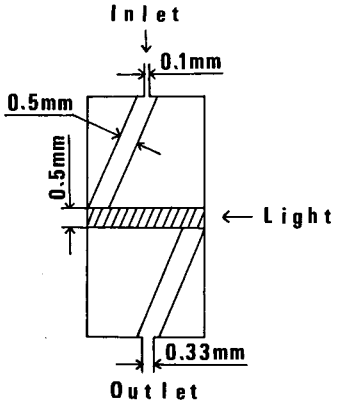

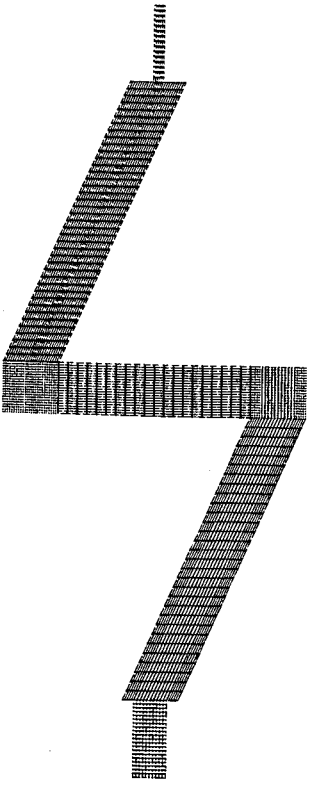

Fig. 3. Schematic diagram of flow-cell. Oblique lines indicate optical path.

Fig. 4. Mesh of flow-cell for finite-element analysis.

TABLE I

TYPES OF BAND BROADENING IN CHROMATOGRAPHIC SYSTEM

Symbols: r = cell radius; L = cell length; F = solvent flow-rate; D_m = solvent diffusion coefficient; V = cell volume.

Type of band broadening	Response function	Second moment (σ^2)
Laminar flow broadening		$\pi r^4 LF/24D_m$
Diffusional broadening		$L^4F^2/4D_m^2$
Mixing broadening		V^2

RESULTS AND DISCUSSION

Basic theory

The detector flow-cell is a significant source of band broadening within the chromatographic system. Sternberg [2] suggested that the flow-cell has several sources of volumetric broadening: the cell volume itself; laminar flow broadening; and mixing and diffusional broadening. The different types of volumetric broadening, the corresponding response functions and their second moments expressed as the volume-based variance are summarized in Table I. The listed data show that laminar flow broadening is Gaussian, and diffusional and mixing broadening are exponential.

Band broadening

Fig. 5 shows a plot of actual variance (closed circles) *versus* flow-rate for the flow-cell. Four types of band broadening phenomena exist according to the flow-rate (F): (1) $F \leqslant 0.25$ ml/min: the variance increased with increasing flow-rate; (2) 0.25 ml/min $\leqslant F \leqslant$ 0.4 ml/min: the variance decreased slightly with increasing flow-rate; (3) 0.4 ml/min $\leqslant F \leqslant$ 1.0 ml/min: the variance was constant, independent of the

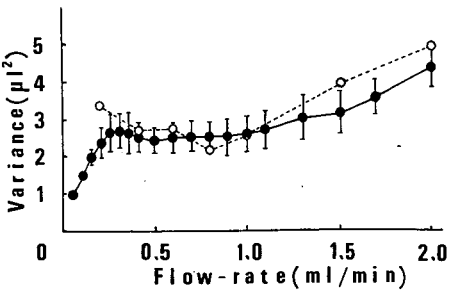

Fig. 5. Effect of flow-rate on variance. Symbols: ● = actual variance; | = standard deviation; ○ = calculated variance.

flow-rate; (4) 1.0 ml/min $\leqslant F$: the variance increased with increasing flow-rate, but the slope of the line was different from that at flow-rates less than 0.25 ml/min.

In a previous paper [6], we reported on the flow dependency in the micro flow-cell. The flow dependency found in the two studies differed. The difference may result from the injector and the connecting tubing, because the Rheodyne injector had much smaller broadening than the former one used (Tokyorika 5001). The connecting tubing in this study was 20 mm × 0.1 mm I.D. and smaller than the 20 mm × 0.25 mm I.D. tubing used in the previous study. So the flow dependency seen in the present case should be very close to the actual contribution of band broadening in the flow-cell.

Fig. 5, as mentioned before, shows a plot of the calculated variance (open circles) *versus* flow-rate for the flow cell. We have studied fast HPLC, and made a computer program for it. Therefore, there are no data for the calculated variance at flow-rates less than 0.2 ml/min in this study, because the computer program for flow analysis needs another key to solve variance for low flow-rates. Three types of band broadening phenomena were apparent: (1) 0.2 ml/min $\leqslant F \leqslant$ 0.4 ml/min: the variance decreased slightly with increasing flow-rate; (2) 0.4 ml/min $\leqslant F \leqslant$ 1.0 ml/min: the variance was constant, independent of the flow-rate; (3) 1.0 ml/min $\leqslant F$: the variance increased with increasing flow-rate.

The actual measurements and calculation of band broadening are summarized in Table II. A comparison of the experimental and calculated results showed good agreement.

TABLE II

DEPENDENCE OF BAND BROADENING ON FLOW-RATE

Flow-rate (ml/min)	Band broadening	
	Experiment	Calculation
< 0.2	Increase	–
0.2–0.4	Slightly decrease	Slightly decrease
0.4–1.0	Constant	Constant
> 1.0	Increase	Increase

Simulated flow profiles and chromatogram

Fig. 6a, b and c show the flow profile in the flow-cell at flow-rates of 0.2, 0.6 and 2.0 ml/min, respectively. Atwood and Golay [5] reported that the peak eluted from a small injection becomes markedly non-Gaussian in a short straight tubing because of insufficient velocity averaging. At the flow-rate of 0.2 ml/min, however, the flow profile was Poiseuille flow following the Golay equation [10], as shown in Fig. 6a. The band broadening was the laminar flow type. The velocity averaging (*i.e.* sample molecular averaging) requires long tubing or a high flow-rate if the tubing used is straight and round. The result of this study may indicate that the velocity averaging occured in the fitting with sharp changes in tubing diameter in spite of having short tubing with low plate numbers. In fact, the calculated chromatogram was nearly

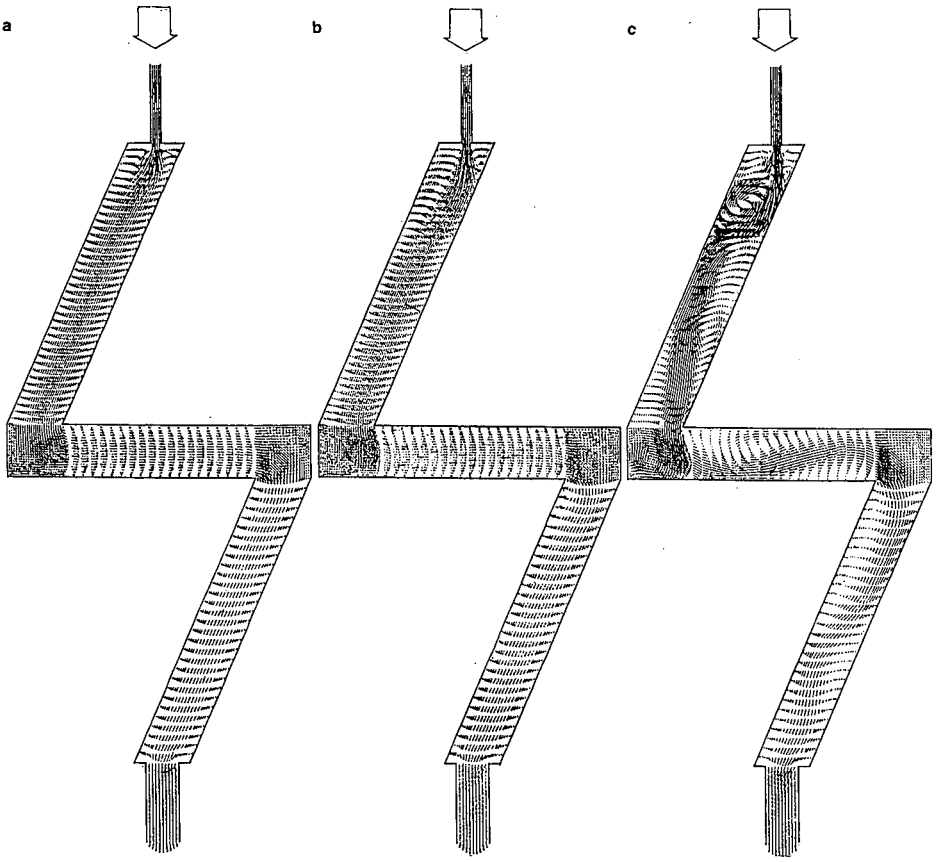

Fig. 6. Calculated flow profile in flow-cell. Flow-rates: (a) 0.2 ml/min, (b) 0.6 ml/min, (c) 2.0 ml/min.

Gaussian at the flow-rate of 0.2 ml/min (data shown later). At flow-rates from 0.2 to 1.0 ml/min, the flow had a parabolic profile in the main channel, which included an eddy current in the fitting between the flow-cell and the connecting tubing. Additionally, stagnation occurred in the bend of the flow-cell, as shown in Fig. 6b. The eddy current in the fitting expanded with increasing flow-rate, including mixing broadening. The total band broadening in the flow-cell acted not as laminar flow broadening, but as mixing broadening owing to the eddy current in the fitting and to the stagnation in the bend due to the lower flow-rate. The second moment was constant, independent of the flow-rate. At flow-rates over 1.0 ml/min, the calculated second moment increased with increasing flow-rate. It was expected that laminar flow broadening, resulting from the laminar flow, and the associated parabolic flow profile in the flow-cell may exist. However, the parabolic flow profile in the main channel was transformed, and the eddy current in the fitting and the bend were as shown in Fig. 6c. Fig. 7 shows time courses of the concentration profiles in the flow-cell at a flow-rate of 1.0 ml/min. From the concentration profiles, the concentration distribution

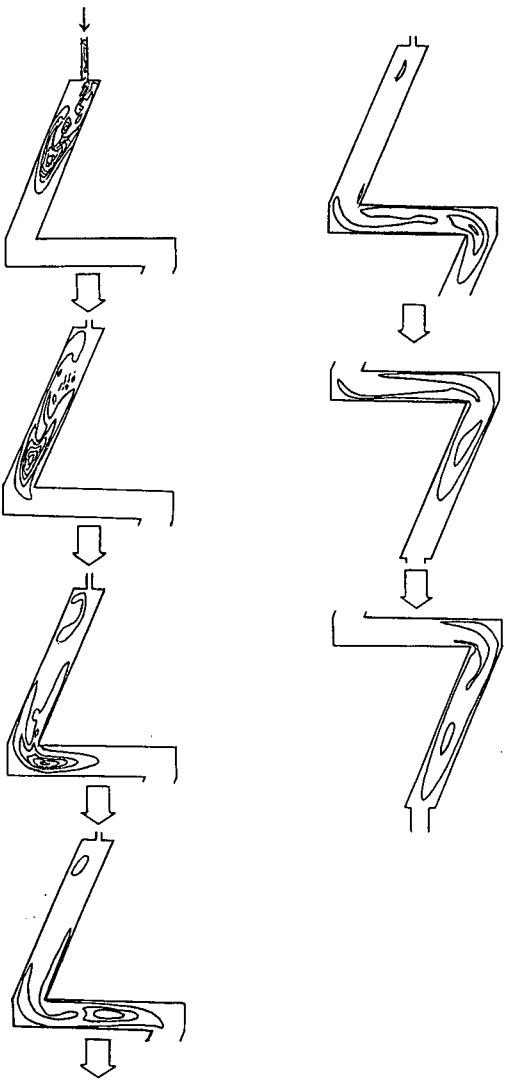

Fig. 7. Time courses of calculated concentration profiles in flow-cell.

was seen as separated, which led to a tailing peak. This case should be treated in terms of the Gaussian distribution, combined with essentially the Gaussian-broadened exponential distribution. The band broadening in such a peak would be approximated by a combination of laminar flow broadening and exponential broadening.

Fig. 8a–g shows a simulated chromatogram by finite-element analysis at flow-rate of 0.2, 0.4, 0.6, 0.8, 1.0, 1.5 and 2.0 ml/min, respectively. The calculated chromatogram at the flow-rate of 0.2 ml/min was nearly Gaussian, as shown in Fig. 8a. An increasing flow-rate led to formation of the tailing peak, which indicated enlargement

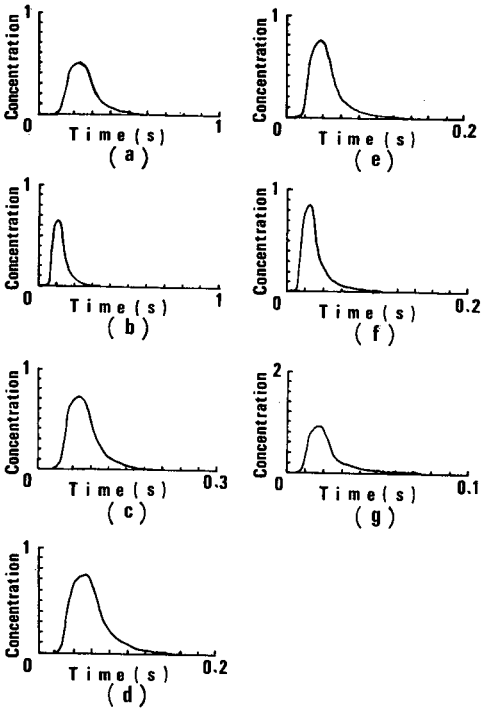

Fig. 8. Calculated chromatogram by finite-element analysis. Flow-rates: (a) 0.2 ml/min; (b) 0.4 ml/min; (c) 0.6 ml/min; (d) 0.8 ml/min; (e) 1.0 ml/min; (f) 1.5 ml/min; (g) 2.0 ml/min.

of the effect on mixing broadening caused by the eddy current and the stagnation. In particular, the calculated chromatogram at the flow-rate of 2.0 ml/min produced an exponential peak more than half that shown in Fig. 8g. In the case of the actual chromatogram, the profile generally showed an extended tailing peak with increasing flow-rate. A comparison of both results showed good agreement.

A plot of the eluted volume of the mobile phase *versus* flow-rate for the flow-cell is shown in Fig. 9. At flow-rates from 0.2 to 0.8 ml/min, the eluted volume was nearly

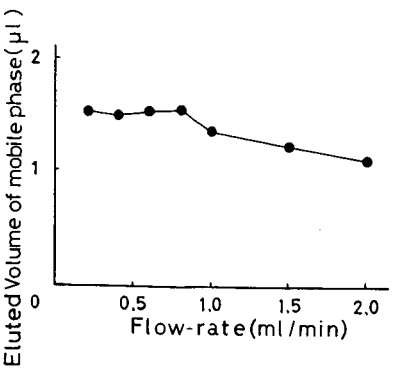

Fig. 9. Effect of flow-rate on eluted volume of mobile phase.

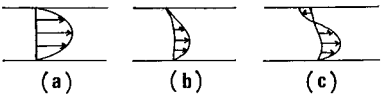

Fig. 10. Types of band broadening in flow-cell. (a) Laminar flow broadening; flow-rates less than 0.2 ml/min; (b) intermediate state; flow-rates from 0.2 to 1.0 ml/min; (c) laminar flow broadening + mixing broadening; flow-rates greater than 1.0 ml/min.

constant, independent of the flow-rate. At flow-rates greater than 1.0 ml/min, the eluted volume decreased with increasing flow-rate. An ideal laminar flow would have a Gaussian profile whose variance would decrease with increasing flow-rate. The results also indicated that the eddy current resulted in the constant variance at flow-rates from 0.2 to 1.0 ml/min, and the laminar flow controlled the variance at flow-rates greater than 1.0 ml/min.

Type of band broadening

The above-mentioned results may indicate that three types of band broadening existed in the Z-type micro flow-cell. Fig. 10a, b and c shows three types of band broadening at flow-rates less than 0.2, from 0.2 to 1.0, and greater than 1.0 ml/min. The first, Fig. 10a, was laminar flow broadening following laminar flow at flow-rates less than 0.2 ml/min. The second, Fig. 10c, was a mixture between laminar flow broadening and mixing broadening at flow-rates greater than 1.0 ml/min. The third, Fig. 10b, was an intermediate state between the first and second types at flow-rates from 0.2 to 1.0 ml/min. The intermediate state is affected by the form of the flow-cell, particularly the fitting between the flow-cell and the connecting tubing, and the bend in the flow-cell. Thus, the flow dependency in this study was suggested to be different from that in the previous study [6].

The flow-cell has more or less an exponential tail owing to the presence of tail-producing sites which lead to skewed peaks. The major source in this case was suggested to be the mixing process which occurred in the flow-cell containing the fitting and the bend. The two-dimensional viscous flow analysis can take into account band broadening in the flow-cell or even the fitting with sharp changes in tubing diameter, as well as the bend in the flow-cell.

The present numerical technique for two-dimensional viscous flow analysis by supercomputer is seen as a powerful tool for the design of various kinds of manufactured products, especially instruments in fast HPLC, which are related in design to fluid flow problems.

ACKNOWLEDGEMENT

We would like to thank Dr. M. Ikegawa (Mechanical Engineering Research Laboratory, Hitachi) for use of the finite-element analysis program and for his helpful discussions.

REFERENCES

1 M. Verzele and C. Dewaele, in F. Bruner (Editor), *The Science of Chromatography*, Elsevier, Amsterdam, 1983, pp. 435–447.
2 J. C. Sternberg, *Adv. Chromatogr.*, 2 (1966) 205–270.
3 M. Martin, C. Eon and G. Guiochon, *J. Chromatogr.*, 108 (1975) 229–241.
4 M. J. E. Golay and J. G. Atwood, *J. Chromatogr.*, 186 (1979) 353–370.
5 J. G. Atwood and M. J. E. Golay, *J. Chromatogr.*, 218 (1981) 97–122.
6 M. Kamahori, Y. Watanabe, J.Miura, M. Taki and H. Miyagi, *J. Chromatogr.*, 465 (1989) 227–232.
7 M. Ikegawa and N. Sato, *Proceedings of the 7th Symposium on Numerical Analysis in Fluid Mechanics, Tokyo, Aug. 1986*, Union of Japanese Scientists and Engineers, Tokyo, 1986, , pp. 205–212.
8 C. Kato and M. Ikegawa, *Proceedings of the 7th Symposium on Numerical Analysis in Fluid Mechanics, Tokyo, Aug. 1986*, Union of Japanese Scientists and Engineers, Tokyo, 1986, pp. 125–132.
9 C. Kato and M. Ikegawa, *Proceedings of the 1st Symposium on Computational Mechanics, Tokyo, Aug. 1987*, Union of Japanese Scientists and Engineers, Tokyo, 1987, pp. 111–118.
10 M. J. E. Golay, in D. H. Desty (Editor), *Gas Chromatography 1958*, Academic Press, New York, 1958, 36–53.

Journal of Chromatography, 549 (1991) 113–125
Elsevier Science Publishers B.V., Amsterdam

CHROM. 23 331

High-performance liquid chromatography of reaction mixtures from the oxidation and degradation of lactose

L. A. Th. VERHAAR, H. E. J. HENDRIKS, W. P. Th. GROENLAND and B. F. M. KUSTER*
Laboratorium voor Chemische Technologie, Technische Universiteit Eindhoven, P.O. Box 513, 5600 MB Eindhoven (Netherlands)

(First received December 4th, 1990; revised manuscript received February 28th, 1991)

ABSTRACT

A method is described for the high-performance liquid chromatographic analysis of reaction mixtures from the heterogeneously catalysed oxidation of lactose to lactobionate and the homogeneous alkaline oxidative degradation of lactose to β-O-D-galactopyranosyl-(1→3)-D-arabinonate. Two columns in series, a resin-based anion-exchanger in the acetate form and a resin-based cation exchanger in the H^+ form with water as the eluent, allow the quantification of the sugars without interference from the oxidation and degradation products. Occasionally an RP-18 reversed-phase column was used for the determination of lactulose in the reaction samples. A resin-based anion-exchange column in the Cl^- or SO_4^{2-} form allows the determination of the anionic oxidation and degradation products without interference from the sugars present in the reaction samples. In the analyses of the anionic oxidation and degradation products a method was developed to determine some of these products without their pure standards. The method is based on the regular behaviour in refractive index detection of members of a homologous series of aldonates.

INTRODUCTION

Lactose or milk sugar is produced from the liquid residue that remains in the process of cheese or milk protein production. This by-product can be upgraded by selective oxidations such as the heterogeneous catalytic oxidation of lactose to lactobionate [1] or the homogeneous oxidative degradation of lactose of β-O-D-galactopyranosyl-(1→3)-D-arabinonate [2]. The main reaction paths of both processes are depicted in Fig. 1 by routes 1 and 2, respectively. In both instances mixtures of sugars and alkali metal salts of oxidation and degradation products are obtained.

Sugars and their oxidation and degradation products have been analyzed by gas chromatography (GC) after derivation to their trimethylsilyl ethers [3–5]. Because the silylating agent also reacts with water, water has to be evaporated almost quantitatively before silylation can be carried out. Another complicating factor in GC can be the appearance of separate peaks for anomeric forms and ring structures.

Aqueous solutions of sugars and their ionic oxidation and degradation products have been analyzed without derivatization using liquid chromatography.

Non-ionic sugars have been chromatographed by (i) amine-modified silica gel

0021-9673/91/$03.50

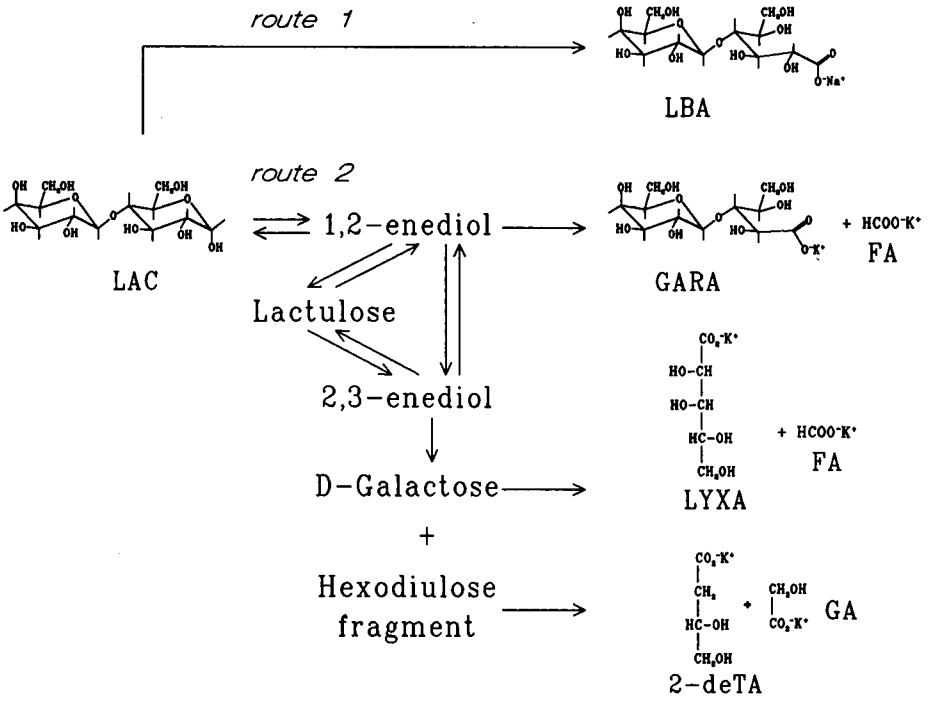

Fig. 1. Simplified reaction scheme for the heterogeneous catalytic oxidation of lactose (route 1) and homogeneous oxidative degradation of lactose (route 2). LAC = lactose; LBA = lactobionate; GARA = β-O-D-galactopyranosyl-(1→3)-D-arabinonate; LYXA = D-lyxonate; 2-deTA = 2-deoxy-D-tetronate; FA = formate; GA = glycolate.

columns [6–9], (ii) octadecyl-modified silica gel columns [10–13], (iii) anion-exchange resin columns [14–17] and (iv) cation-exchange resin columns [18–21]. In amine-modified silica gel chromatography, using acetonitrile–water mixtures as the eluent, good separations have been achieved between sugars which differ in molecular weight or structure; much lower selectivity exists between the stereoisomers. The chromatographic separation of deionized lactose–lactulose–galactose mixtures using amine-modified silica gel stationary phase was described by Parrish *et al.* [9]. However, the time-consuming deionization step, necessary to prevent coelution of the organic anions and the sugars, and the use of the toxic acetonitrile are drawbacks of this method. Chromatography on RP-18 columns with water as the eluent has been reported for sugar oligomers. The retention increases with increasing molecular weight and separate elution has been obtained for the anomeric forms. The selectivity for monosaccharides is very low and for retention of the disaccharides a subambient column temperature is necessary.

Anion-exchange chromatography based on borate complexation in combination with chemical detection methods has frequently been used in the past. Although a high selectivity for mono- and disaccharide separation can be obtained, the relatively long analysis time and the loss of resolution by the chemical detection methods

are serious drawbacks of this method. Moreover, the high pH of the borate buffer used as the eluent gives rise to isomerization of the sugars during their elution, as reported for lactose–lactulose by Carubelli [14].

Sugars have also been analysed using resin-based cation exchangers in the Ca^{2+} [18,19], Pb^{2+} [20] or H^+ form [21]. If a high column temperature was chosen or mutarotation catalysts [22,23] were used, separate peaks for the anomeric furanose and pyranose forms could be avoided. However, the usability of cation-exchange resin columns is limited by their low retention for sugars. This is caused by molecular exclusion, which is in competition with complexation forces between the polyhydroxy compounds and the immobilized cation on the resin. As a result, capacity factors lower than 2 are obtained for sugars, as can be seen from the results of Pecina *et al.* [24]. Moreover, the anionic oxidation and degradation products present in the reaction mixtures will also have a low retention [25], hampering simple and accurate sugar determinations.

The organic anions formed in the oxidation and degradation reactions are polar compounds without any apolar functionality, so a separation mechanism based on hydrophobic interactions (reversed-phase chromatography) can be excluded. However, differences in the strengths of the acids opens up the possibility of using anion-exchange chromatography [26–30]. For polyhydroxycarboxylic acids, retention increases with decreasing molecular size and, moreover, dibasic acids elute after monobasic acids of the same carbon number. The retention can be influenced by the addition of a complexing cation to the eluent. For example, the elution of oxalate and tartronate can be accelerated drastically by the addition of Mg^{2+} ions to the eluent [30]. Complexation of these organic anions by Mg^{2+} ions reduces the interaction between the organic anion and the counter ion of the resin. For all the anion-exchange systems mentioned above, non-ionic sugars were not retarded.

This paper describes a high performance liquid chromatographic (HPLC) method for the analysis of mixtures of sugars and their oxidation and degradation products, shown in Fig. 1.

The analysis of the non-ionic sugars in the presence of oxidation and degradation products is mainly performed on an anion-exchange column in the acetate (Ac^-) form in series with a cation-exchange column in the H^+ form, using water as the eluent and refractive index (RI) detection. Occassionally an RP-18 reversed phase column was used to verify the occurrence of lactulose under the reaction conditions applied.

Two independent anion-exchange columns allow the analysis of the anionic oxidation and degradation products, using serial UV and RI detection. The oxidation products could be chromatographed without interference from the sugars and *vice versa*. In the analysis of the oxidation and degradation products a method was developed to determine some products without the pure standards. The method used is based on the regular behaviour in refractive index detection for a homologous series of aldonates.

EXPERIMENTAL

Apparatus

A Spectra-Physics Type SP 8800 ternary HPLC pump in combination with an

SP 8775 autosampler, a Rheodyne Model 7010 injection valve with a 20-μl sample loop and a SP 8790 column heater were used. A Millipore–Waters Type R410 refractive index detector in series with a Spectra-Physics SP 8450 variable-wavelength UV–VIS detector operated at 212 nm and connected to a SP 4290 two-channel digital integrator allowed dual detection and peak integration for the various compounds.

Columns

Before packing a column, the resin material was washed twice with 20 equiv. of a 0.5 *M* solution of a compound of the ionic form needed. After washing, the resin was dispersed for 30 min in an ultrasonic bath and packed in the analytical column with the eluent as the liquid phase at a pressure of about 100 atm.

Five columns were used, as follows.

BA-X8 (Ac^-) column. This was a 70 × 4.6 mm I.D. Lichroma stainless-steel tube slurry packed with Benson Type BA-X8 anion-exchange resin, having quaternary ammonium functional groups attached to the polystyrene–divinylbenzene (8%) lattice and with a particle diameter of 7–10 μm, and during the packing washed overnight with 1 dm^3 of a 0.5 *M* solution of sodium acetate in water to obtain the AC^- form.

BA-X8 (Cl^-) column. This was the same as the BA-X8 (Ac^-) column, but 280 mm in length, and during the packing it was washed overnight with 1 dm^3 of a 0.2 *M* solution of sodium chloride in water to obtain the Cl^- form.

BA-X8 (SO_4^{2-}) column. This was as for the BA-X8 (Cl^-) column, but during the packing it was washed with 1 dm^3 of a 0.5 *M* solution of ammonium sulphate in water to obtain the SO_4^{2-} form.

BC-X8 (H^+) column. This was the same as the BA-X8 (Cl^-) column but slurry packed with Benson Type BC-X8 cation-exchange resin having sulphonic acid groups and during the packing washed overnight with 1 dm^3 of a 0.05 *M* solution of sulphuric acid in water to obtain the H^+ form.

RP-18 column. This was a 250 × 4.6 mm I.D. stainless-steel column obtained from Chrompack, prepacked with CP Spher C_{18}, consisting of octadecylsilane-modified silica with 5-μm spherical particles.

Pretreatment. Before use, the BA-X8 (Ac^-) and BC-X8 (H^+) columns were rinsed with water to obtain an effluent free from sodium acetate or sulphuric acid, respectively. All liquids used for preparing the columns and all eluents were filtered over a Millipore HAWP filter (0.45 μm) and degassed with helium.

Sampling

If necessary, the reaction samples were acidified with 2 *M* hydrochloric acid to pH $\approx$ 9 and diluted with water to give a maximum concentration per solute of about 0.05 *M*, and stored at *ca.* 278 K. Before analysis, the samples were filtered over a Schleicher and Schüll GC 92/RC 55 filter combination.

For kinetic measurements, the composition of the reaction mixtures was determined as a function of time; therefore, the concentrations found were corrected for all dilutions and for the effects of sampling [1,2].

RESULTS AND DISCUSSION

Analysis of sugars

Injection of a reaction sample from the oxidation of lactose to lactobionate and also from the alkaline oxidative degradation reaction of lactose to β-O-D-galactopyranosyl-(1→3)-D-arabinonate (GARA) on the BC-X8 (H^+) column with a 0.005 *M* sulphuric acid as the eluent, or the same resin in the Ca^{2+} or Pb^{2+} form with water as the eluent, resulted in complex chromatograms using refractive index detection. For all three columns, co-elution of the non-ionic sugars and the anionic reaction products took place, so quantification of the chromatograms is difficult. However, on connecting a BA-X8 (Ac^-) column upstream of the BX-X8 (H^+) column and using water as the eluent, the chromatograms shown in Fig. 2 and 3, respectively, were obtained.

The anionic products present in the samples exchange with the acetate of the BA-X8 (Ac^-) column and adsorb strongly. The exchanged acetate behaves like an injected compound whose retention depends on the properties of both columns. Hydrophobic interactions between the apolar part of the acetate molecule and the apolar resin matrix give just enough retention to the acetate for elution after the non-ionic sugars. The liberated acetate is equimolar to the amount of anions injected, so by integrating the size of the acetate peak the total amount of anions present in the reaction sample could be determined.

Although the amount of exchangeable acetate is limited, the capacity of the short BA-X8 (Ac^-) column was high enough for the injection of more than 250 samples containing 0.15 anion equivalents per dm^3 each. On the verge of exhaustion of the acetate capacity, the second weakest anion will also be liberated and influence

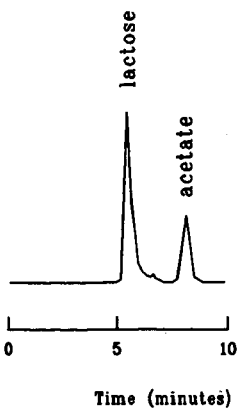

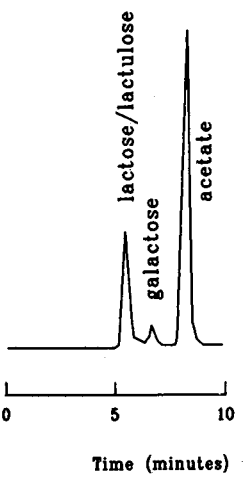

Fig. 2. Chromatogram of a sample from a reaction mixture at *ca.* 50% conversion in the heterogeneous catalytic oxidation of lactose. Analytical conditions: BA-X8 (Ac^-) column in series with a BC-X8 (H^+) column, both at 85°C; eluent, distilled water; flow-rate, 0.4 ml min^{-1}; refractive index detection.

Fig. 3. Chromatogram of a sample from a reaction mixture at *ca.* 70% conversion in the alkaline oxidative degradation reactions of lactose. Analytical conditions as in Fig. 2.

the chromatogram. Therefore, in a series of reaction samples, a few samples containing potassium chloride were included; if only the acetate peak was obtained, the system could be used for sugar determinations. If regeneration had to be carried out, both columns were disconnected and the BA-X8 (Ac^-) and BC-X8 (H^+) columns were flushed overnight with 1 dm^3 of a 0.5 *M* solution of sodium acetate in water and with 1 dm^3 of 0.05 *M* sulphuric acid, respectively. After separate conditioning by flushing with pure water, the column combination could be used again. The regeneration procedure used had no significant influence on the effectiveness of the separation.

In the heterogeneous catalytic oxidation of lactose (Fig. 1, route 1), the sugar part of the chromatogram given in Fig. 2 consists of the lactose peak only. However, in the alkaline oxidative degradation reaction of lactose (Fig. 1, route 2), the lactose isomer lactulose and the monosaccharide D-galactose will also be present, giving a more complex chromatogram. The first peak of the chromatogram in Fig. 3 belongs to the co-elution of lactose and lactulose, and the second peak belongs to D-galactose.

Because almost identical molar responses were found for lactose and lactulose with RI detection, the total concentration of lactose and lactulose could be measured. However, in experiments to study the kinetics of the oxidation and degradation reactions it is important to know their individual concentrations. The lactose–lactulose separation could not be achieved using a combination of an Ac^- column with either a Pb^{2+} or a Ca^{2+} column. Owing to the use of the Ac^- precolumn, injection broadening occurred, resulting in an unacceptable decrease in resolution.

Based on the results of Rajakylä [13] for maltose and sucrose, a solution to the problem was found by using an RP-18 column with water as the eluent. Injection of an aqueous solution of pure lactose, pure lactulose and a reaction sample on to an

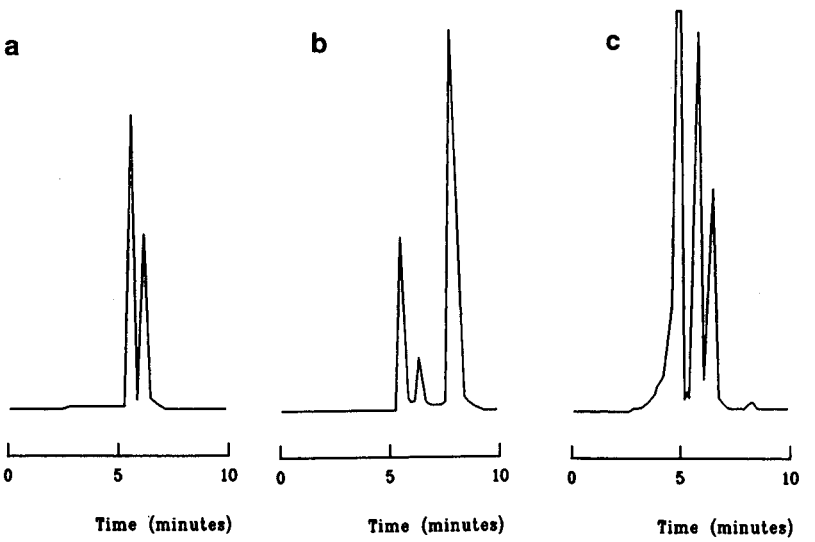

Fig. 4. Chromatograms of (a) a 32 m*M* aqueous lactose solution, (b) a 22 m*M* aqueous lactulose solution and (c) a sample from a reaction mixture at *ca.* 65% conversion in the oxidative degradation reaction of lactose. Analytical conditions: RP-18 column, ice cooled; eluent, distilled water; flow-rate, 0.5 ml min^{-1}; refractive index detection.

ice-cooled RP-18 column resulted in the chromatograms shown in Fig. 4a, b and c, respectively. In Fig. 4a two peaks are obtained for lactose with a 60:40 peak-area ratio, representing the β- and α-anomeric pyranose forms, respectively. In Fig. 4b three peaks are obtained for lactulose with a peak-area ratio of 25:7:68, probably representing the β-furanose, α-furanose and β-pyranose tautomers present in the aqueous lactulose solutions. These ratios for aqueous lactulose solutions are in good agreement with the results of Pfeffer and Hicks [31,32] obtained by ^{13}C NMR spectroscopy. The chromatograms given in Fig. 4a and b indicate co-elution of the small furanose peaks of lactulose with both the anomeric lactose peaks but a separate elution of the pyranose form of lactulose.

Attempts to activate the mutarotation reaction under analytical conditions to obtain one-peak chromatograms for both lactose and lactulose were unsuccessful; a higher column temperature resulted in a complete loss of retention and addition of sulphuric acid to the eluent did nog influence the chromatograms markedly. Under all conditions applied, D-galactose and the anionic products gave no retention and did not influence the determination of lactose and lactulose.

As can be seen in Fig. 4c, the furanose forms of lactulose co-elute with both lactose anomers and separate elution of the β-pyranose form of lactulose is obtained. Because the lactose and lactulose mutarotation equilibria mentioned above appeared to be independent of variations in pH between 5 and 9 and addition of potassium chloride at concentrations up to 150 m*M* as occurs in the reaction samples, the lactulose concentration could be determined using the peak-area ratios and the lactulose β-pyranose peak area only. Under the reaction conditions applied, the lactulose concentration was very low during the entire course of reaction, so the lactose–lactulose determination with the RP-18 column was occasionally carried out. Determination of the non-ionic sugars was mainly carried out using the BC-X8 (H^+) column connected in series with the BA-X8 (Ac^-) column, as mentioned before. In serial analysis only standard solutions of lactose and D-galactose were used for determination of the lactose–lactulose and D-galactose contents in the reaction samples.

Analysis of the anionic oxidation and degradation products

From the scheme given in Fig. 1, it can be seen that the alkaline oxidative degradation of lactose (route 2) leads to a relatively complex reaction mixture. The oxidative degradation of lactose will lead to β-O-D-galactopyranosyl-(1→3)-D-arabinonate (GARA) and an equal amount of formate; non-oxidative degradation of lactose will lead via a β-elimination to the formation of a reactive 4-deoxy-2,3-hexodiulose fragment and the more stable D-galactose [2]. Just like the lactose to GARA mechanism, D-galactose will give D-lyxonate and formate in a parallel oxidative degradation reaction whereas the hexodiulose can be oxidized easily to 2-deoxy-D-tetronate (2-deTA) and glycolate. Moreover, β-O-D-galactopyranosyl-(1→2)-D-erythronate and glycolate may be formed when enolization and oxidation occur between the C-2 and -3 of the glucose moiety in lactose.

As has been described, chromatography based on anion-exchange mechanisms can be used for the separation of the anionic oxidation and degradation products. Preliminary qualitative experiments were carried out using the BA-X8 (Ac^-) column with 0.2 *M* sodium acetate solution as the eluent. It was found for aldonic acids that the retention and resolution increase with a decrease in molecular size [33]. On the

BA-X8 (Ac^-) column a clear distance was found between the peaks of lactobionate and GARA. Corresponding to the rules described above, lactobionate eluted in front of GARA.

Following these rules, β-O-D-galactopyranosyl-(1→2)-D-erythronate was expected to elute at a clear distance after the GARA peak, but no peak was observed that can be ascribed to a significant production of β-O-D-galactopyranosyl-(1→2)-D-erythronate under the reaction conditions applied. However, owing to a strong UV-adsorption at 212 nm, aqueous acetate was not a suitable eluent for quantitative low-wavelength UV detection. Therefore, in spite of a decrease in resolution, a low UV-absorbing eluent such as aqueous chloride or sulphate was chosen. Analyses were carried out with the BA-X8 (Cl^-) column and an aqueous solution of 0.16 *M* NaCl and 0.02 *M* $MgCl_2$ as the eluent or the BA-X8 (SO_4^{2-}) column and an aqueous 0.2 *M* $(NH_4)_2SO_4$ solution as the eluent. In the latter instance, the aqueous $(NH_4)_2SO_4$ solution was made alkaline to pH $\approx$ 7.5 with a few drops aqueous ammonia. Dual detection was applied by placing the RI detector in series with the UV (212 nm) detector.

From the reactions of lactose to lactobionate and to GARA, chromatograms for the anionic products were obtained with the BA-X8 (Cl^-) system as shown in Figs. 5 and 6, respectively. The heterogeneous catalytic oxidation of lactose with a bismuth-modified palladium-on-carbon catalyst leads to an almost quantitative production of lactobionate [1] and therefore the chromatogram in Fig. 5 is simple. Be-

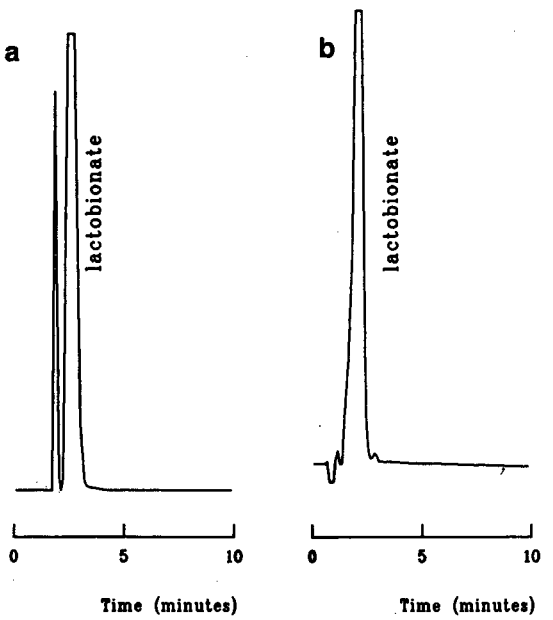

Fig. 5. Chromatograms of a sample as described for Fig. 2. Analytical conditions: BA-X8 (Cl^-) column; column temperature, 85°C; eluent, 0.02 *M* $MgCl_2$ + 0.16 *M* NaCl in water; flow-rate, 1.1 ml min^{-1}; (a) refractive index detection, (b) in series with UV (212 nm) detection.

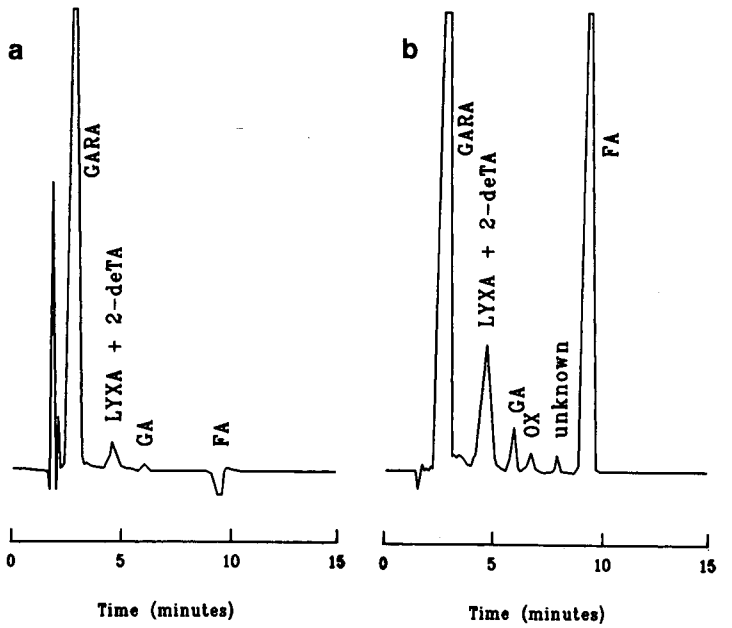

Fig. 6. Chromatograms of a sample as described for Fig. 3. Analytical conditions as in Fig. 5.

cause lactobionate was available as a pure compound and its peak areas could be integrated well, accurate quantification of this reaction product was possible.

As can be seen in Fig. 6, the chromatogram obtained form the alkaline degradation of lactose to GARA is more complex. Separate elution was obtained for GARA, glycolate and formate. The broad peak appearing in front of the peak of glycolate can be ascribed to co-elution of D-lyxonate and 2-deTA. The retention of D-lyxonate could be verified by carrying out an alkaline oxidative degradation reaction of D-galactose, wherein D-lyxonate was expected to be the main product. According to the retention rules described above, co-elution of the byproduct 2-deTA in this peak is plausible.

When the BA-X8 (SO_4^{2-}) system was used for the same reaction sample, the chromatogram shown in Fig. 7 was obtained. Separate peaks were obtained of D-lyxonate, the expected 2-deTA, glycolate and formate, but the main reaction product GARA eluted too close to the injection peak, hampering an accurate GARA peak integration. Because an accurate determination of the main product GARA was preferred, standard analyses were carried out using the BA-X8 (Cl^-) system. Occasionally analyses with the BA-X8 (SO_4^{2-}) system were carried out for byproduct determination. Comparison of the RI and UV (212 nm) detection methods leads to the conclusion that for the low-molecular-weight products UV detection is far superior in sensitivity to RI detection.

In liquid chromatography, loop injection of aqueous samples can be done with high reproducibility. Therefore, when the reaction sample components are available as pure compounds, an external standardization method can be used for quantifica-

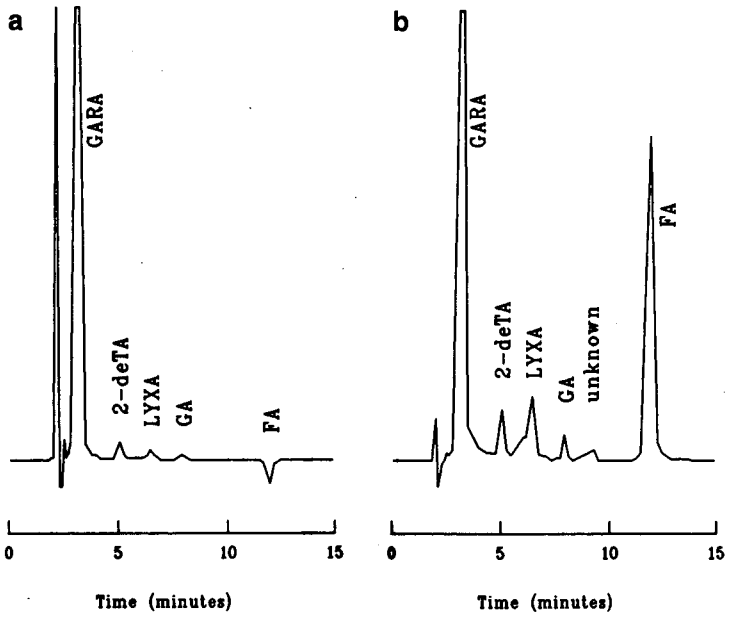

Fig.7. Chromatogram of a sample from a reaction mixture at *ca.* 85% conversion in the oxidative degradation reaction of lactose. Analytical conditons: BA-X8 (SO_4^{2-}) column; column temperature, 85°C; eluent, 0.2 *M* $(NH_4)_2SO_4$ in water; flow-rate, 1.1 ml min^{-1}; (a) refractive index detection, (b) in series with UV (212 nm) detection.

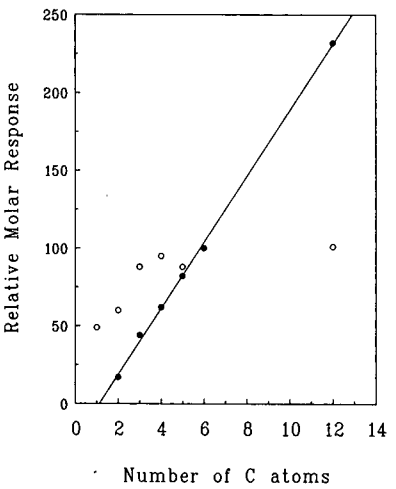

Fig. 8. (●) Refractive index and (○) UV (212 nm) responses of equimolar amounts of polyhydroxy monocarboxylic acids as a function of the number of carbon atoms in the compounds. Abscissa: 1 = formate; 2 = glycolate; 3 = D-glycerate; 4 = D-erythronate; 5 = D-arabinonate; 6 = D-glyconate; 12 = lactobionate.

tion. However, from the products formed during the alkaline oxidative degradation of lactose, GARA, D-lyxonate and 2-deTA were not available in a specified quality, so their determination had to be verified using an alternative method.

It was found in other sugar oxidation experiments that in RI detection a linear relationship is obtained for aldonates when their relative molar responses are plotted against the number of carbon atoms in a homologous series. Moreover, for stereoisomers almost identical RI responses were obtained. Such regularities were not found with UV (212 nm) detection, as can be seen in Fig. 8. It is to be expected that the RI sensitivity of GARA and D-lyxonate will conform to the same regular behaviour. Based on this regularity of the molar RI response in a homologous series, the molar RI response of GARA was defined as being equal to the lactobionate response minus one sixth of difference between the responses of lactobionate and gluconate. For D-lyxonate the relative molar response for RI detection was defined as being equal to that of its commercially available stereoisomer D-arabinonate.

Owing to its deoxy-group, 2-deTA differs in molecular structure from the aldonates, so an irregular behaviour of the relative molar RI response is to be expected. The relative molar RI responses of D-glycerate and D-lactate indicated that replacement of a hydroxy group by a deoxy group results in a substantial decrease in molar response. An almost similar difference in molecular structure exist between D-erythronate and 2-deTA. The relative molar response for 2-deTA was therefore taken as the response value for D-erythronate minus the difference between the values for D-glycerate and D-lactate.

From the above-defined relative molar RI response values for GARA, D-lyxonate and 2-deTA and the UV (212 nm)/RI ratios obtained from the "one-injection chromatograms" using dual detection, the relative molar UV (212 nm) responses could be calculated. For both RI and UV (212 nm) detection the results are summarized in Table I, including some values for relevant compounds. With these values the concentrations of the compounds present in the reaction samples for the reactions of

TABLE I

RELATIVE MOLAR UV (212 nm) REPONSES, RI RESPONSES AND UV/RI RATIOS FOR SEVERAL COMPOUNDS OBTAINED USING THE BA-X8 (SO_4^{2-}) SYSTEM AND THE BA-X8 (Cl^-) SYSTEM

Compound	BA-X8 (SO_4^{2-}) system			BA-X8 (Cl^-) system		
	UV	RI	UV/RI	UV	RI	UV/RI
Experimental values						
D-Gluconate	100	100	1.00	100	100	1.00
D-Lactate	88	26	3.33	84	27	3.05
D-Glycerate	91	38	2.39	88	44	2.00
D-Arabinonate	85	81	1.05	88	82	1.05
Lactobionate	–	–	–	101	232	0.44
Defined values						
D-Lyxonate	85	81	1.05	–	–	–
2-deTA	82	56	1.46	–	–	–
GARA	–	–	–	101	210	0.48

TABLE II

COMPOSITION OF A REACTION MIXTURE FROM THE ALKALINE OXIDATIVE DEGRADATION OF LACTOSE, GIVEN AS CONCENTRATIONS AND % OF INITIAL MOLES OF CARBON

$[LAC]_0$ = 250.0 mmol dm^{-3}.

Component	Concentration (mmol dm^{-3})	% of initial moles of carbon
Sugars		
Lactose–Lactulose	36.0	14.4
D-Galactose	8.0	1.6
Sugar acids		
GARA	188.7	69.2
D-Lyxonate	5.1	0.9
2-deTA	14.7	2.0
Glycolate	10.0	0.7
Formate	209.8	7.0
Total		95.8

lactose to lactobionate and of lactose to GARA could be calculated. For both reactions satisfactory carbon mass balances were obtained up to almost complete conversion. As an example, the product distribution of a reaction sample of the oxidative degradation of lactose to GARA is given in Table II. It clearly shows that GARA and formate are the main reaction products and, moreover, that the reaction pathway given in Fig. 1 (route 2) covers over 96% of the product mass.

ACKNOWLEDGEMENT

This investigation was carried out with support of the Dutch National Innovation Oriented Program Carbohydrates (IOP-k).

REFERENCES

1 H. E. J. Hendriks, B. F. M. Kuster and G. B. Marin, *Carbohydr. Res.*, 204 (1990) 121.
2 H. E. J. Hendriks, B. F. M. Kuster and G. B. Marin, *Carbohydr. Res.*, in press.
3 C. C. Sweeley, R. Bently, M. Makita and W. W. Wells, *J. Am. Chem. Soc.*, 85 (1963) 2497.
4 G. Petersson, H. Riedl and O. Samuelson, *Sven. Papperstidn.*, 70 (1967) 371.
5 L. A. Th. Verhaar and H. G. J. de Wilt, *J. Chromatogr.*, 41 (1969) 168.
6 J. C. Linden and C. L. Lawhead, *J. Chromatogr.*, 105 (1975) 125.
7 F. M. Rabel, A. G. Caputo and E. T. Butts, *J. Chromatogr.*, 126 (1976) 731.
8 K. Aitzetmüller, *J. Chromatogr.*, 156 (1978) 354.
9 F. W. Parrish, K. Hicks and L. Doner, *J. Dairy Sci.*, 63 (1980) 1809.
10 A. Heyraud and M. Rinaudo, *J. Liq. Chromatogr.*, 3 (1980) 721.
11 L. A. Th. Verhaar, B. F. M. Kuster and H. A. Claessens, *J. Chromatogr.*, 284 (1984) 1.
12 N. W. H. Cheetham and G. Teng, *J. Chromatogr.*, 336 (1984) 161.
13 E. Rajakylä, *J. Chromatogr.*, 353 (1986) 1.
14 R. Carubelli, *Carbohydr. Res.*, 2 (1966) 480.
15 R. B. Kesler, *Anal. Chem.*, 39 (1967) 1416.
16 E. F. Walborg and R. S. Lantz, *Anal. Biochem.*, 22 (1968) 123.
17 A. Floridi, *J. Chromatogr.*, 59 (1971) 61.

18 H. D. Scobell, K. M. Brobst and E. M. Steele, *Cereal Chem.*, 54 (1977) 905.
19 S. J. Angyal, G. S. Bethell and R. J. Beveridge, *Carbohydr. Res.*, 73 (1979) 9.
20 F. E. Wentz, A. D. Marcy and M. J. Gray, *J. Chromatogr. Sci.*, 20 (1982) 349.
21 G. Bonn and R. Pecina, *J. Chromatogr.*, 287 (1984) 215.
22 L. A. Th. Verhaar and B. F. M. Kuster, *J. Chromatogr.*, 210 (1981) 279.
23 K. Brunt, *J. Chromatogr.*, 267 (1983) 347.
24 R. Pecina, G. Bonn, E. Burtscher and O. Bobleter, *J. Chromatogr.*, 287 (1984) 245.
25 K. B. Hicks, P. C. Lim and M. J. Haas, *J. Chromatogr.*, 319 (1985) 159.
26 P. Jandera and J. Churacek, *J. Chromatogr.*, 86 (1973) 351.
27 R. Schwarzenbach, *J. Chromatogr.*, 251 (1982) 339.
28 J. D. Blake, M. L. Clarke and G. N. Richards, *J. Chromatogr.*, 312 (1984) 211.
29 P. Vratny, O. Mikes, P. Strop, J. Coupek, L. Rexova-Benkova and D. Chadimova, *J. Chromatogr.*, 257 (1983) 23.
30 P. J. M. Dijkgraaf, L. A. Th. Verhaar, W. P. T. Groenland and K. van der Wiele, *J. Chromatogr.*, 329 (1985) 371.
31 P. E. Pfeffer and K. B. Hicks, *Carbohydr. Res.*, 102 (1982) 11.
32 P. E. Pfeffer and K. B. Hicks, *Carbohydr. Res.*, 111 (1983) 181.
33 L. A. Th. Verhaar, unpublished results.

Journal of Chromatography, 549 (1991) 127–132
Elsevier Science Publishers B.V., Amsterdam

CHROM. 23 341

Column liquid chromatographic determination of saccharides with a single calibration graph using post-column enzyme reactors and coulometric detection

NOBUTOSHI KIBA*, KAZUYOSHI SHITARA, HIROSHI FUSE and MOTOHISA FURUSAWA
Department of Applied Chemistry and Biotechnology, Faculty of Engineering, Yamanashi University, Kofu 400 (Japan)
and
YOSHINORI TAKATA
Naka Works, Hitachi Ltd., Katsuta 312 (Japan)
(First received December 6th, 1990; revised manuscript received March 14th, 1991)

ABSTRACT

Immobilized enzymes were used as column reactors in a column liquid chromatographic system for the specific detection of the saccharides stachyose, raffinose and sucrose. Invertase and fructose dehydrogenase (FDH) were immobilized onto poly(vinyl alcohol) beads and porous glass beads, respectively. The oligosaccharides were separated on a cation-exchange resin column with water as the mobile phase. Invertase was capable of quantitatively hydrolysing the oligosaccharides to fructose, which reacts with the hexacyanoferrate(III) ion in the presence of FDH. The hexacyanoferrate(II) ion produced was monitored coulometrically. A single calibration graph for fructose based on the peak area was used to determine each oligosaccharide. The limits of detection for stachyose, raffinose and sucrose were 27, 5 and 2 ng (in a 50 μl sample), respectively.

INTRODUCTION

High-performance liquid chromatography (HPLC) is a useful technique for determining saccharides. Several HPLC methods have been reported, most of which make use of aminopropyl, C_{18} or ion-exchange stationary phases [1]. The detection methods used have been studied with the aim of improving the sensitivity; pulsed amperometric detection (PAD) has recently been used for the sensitive determination of saccharides in HPLC column effluents [2–5]. The sensitivity of PAD for individual members of a homologous series of oligosaccharides increases with increasing molecular mass. The immobilized glucoamylase reactor has been used as a post-column reactor for the determination of malto-oligosaccharides using a single calibration graph for glucose [6].

Invertase (β-D-fructofuranosyl fructohydrolase, EC 3.2.1.26) catalyses the hydrolysis of oligosaccharides with a terminal unsubstituted β-D-fructofuranosyl resid-

0021-9673/91/$03.50

ue to produce free D-fructose. An immobilized invertase reactor has been used for the flow-injection determination of sucrose [7,8]. Fructose dehydrogenase (FDH) [D-fructose:(acceptor) 5-oxidoreductase, EC 1.1.99.11] has been used for the specific determination of D-fructose in seminal plasma [9]. The enzyme was also immobilized and used for the amperometric flow-injection determination of fructose in foods [10,11].

In this work immobilized invertase and FDH reactors were used in tandem with cation-exchange chromatography and coulometric detection for the determination of oligosaccharides such as sucrose, raffinose and stachyose using a single calibration graph for fructose. Each saccharide was hydrolysed by the invertase and the fructose produced reacted with the hexacyanoferrate(III) ion in the immobilized FDH reactor as follows

$$\text{D-Fructose} + 2Fe(CN)_6^{3-} = \text{5-keto-D-fructose} + 2Fe(CN)_6^{4-}$$

The hexacyanoferrate(II) ion produced was monitored coulometrically.

EXPERIMENTAL

Chemicals

Invertase (from *Candida utilis*, 500 U mg^{-1}) was obtained from Sigma (St. Louis, MO, USA). FDH (from *Gluconobacter sp.*, 30 U mg^{-1} was obtained from Toyobo (Osaka, Japan). Fructose, sucrose, raffinose, stachyose, sodium gluconate and gluconic acid were from Nacalai Tesque (Kyoto, Japan). Poly(vinyl alcohol) beads (GS-520, 9 μm) were from Asahi Kasei (Tokyo, Japan). Long-chain amino-CPG (pore size, 50 nm; amount of amine, 83 μ equiv. g^{-1}; particle size, 200/400 mesh) was from Electro-Nucleonics (Fairfield, NJ, USA). The mobile phase was water and the reagent solution consisted of 0.2 *M* sodium gluconate–gluconic acid buffer (pH 5.0) and 40 m*M* potassium hexacyanoferrate(III). The counter electrode electrolyte was a potassium hexacyanoferrate(II)–potassium hexacyanoferrate(III)-potassium nitrate–potassium hydroxide solution with a concentration of 0.1 *M* of each component. All other chemicals were of analytical-reagent grade.

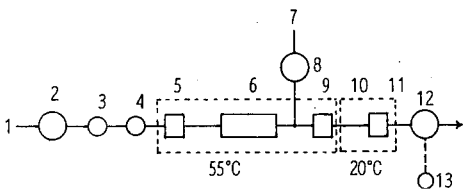

Fig. 1. Schematic diagram of a column liquid chromatographic system for the determination of stachyose, raffinose, sucrose and fructose. 1 = Mobile phase (water); 2 = pump (0.5 ml min^{-1}); 3 = damper; 4 = injector with 50-μl loop; 5 = guard column (TSKgel SCX, 5 μm, 3 cm × 7.8 mm); 6 = analytical column (TSKgel SCX, 5 μm, 60 cm × 7.8 mm); 7 = reagent solution (40 m*M* $K_3[Fe(CN)_6]$ in 0.2 *M* gluconate buffer (pH 5.0); 8 = pump (0.2 ml min^{-1}); 9 = immobilized invertase reactor (5 cm × 4 mm); 10 = cooling coil (1 m × 0.25 mm); 11 = immobilized fructose dehydrogenase reactor (5 cm × 4 mm); 12 = coulometric monitor; 13 = data processor.

Apparatus

A schematic diagram of the chromatographic configuration used in this work is shown in Fig. 1. The chromatographic system consisted of a mobile phase pump (L-6000, Hitachi, Tokyo, Japan), a pulse damper (LOD-1, Gasukuro Kogyo, Tokyo, Japan), an injection valve (7125, Rheodyne, Cotati, CA, USA) with a 50-μl loop, a guard column (30 × 7.8 mm I.D., stainless-steel), an analytical column (600 × 7.8 mm I.D., stainless-steel), a reagent solution pump (75613, Gaskuro Kogyo), two immobilized enzyme reactors (each 50 × 4 mm I.D., stainless-steel column), a coulometric monitor (655A-26, Hitachi) and a data processor (Chromatocorder II, System Instrument, Tokyo, Japan). The chromatographic columns were filled with TSKgel SCX (H^+ form) (5 μm) (Tosoh, Tokyo, Japan). The columns and the immobilized invertase reactor were kept at 55°C in a column oven and the cooling coil (1 m × 0.25 mm I.D., stainless-steel tube) and the immobilized FDH reactor were maintained at 20°C in a water-bath.

The mobile phase and the reagent solution were pumped at 0.5 and 0.2 ml min^{-1}, respectively, and mixed before entering the immobilized invertase reactor. The hydrolysis of the oligosaccharides took place in the reactor and D-fructose was produced. The fructose and hexacyanoferrate(III) reacted in the immobilized FDH reactor and the hexacyanoferrate(II) produced was monitored coulometrically at an electrolytic potential of 200 mV *versus* $Fe(CN)_6^{3-}/Fe(CN)_6^{4-}$. At the electrolytic potential, the electrolytic efficiency for hexacyanoferrate(II) reached 100%, and the background current was negligibly small.

Preparation of enzyme reactors

Invertase was immobilized onto the poly(vinyl alcohol) beads. The method of amination of the beads was similar to that used by Matsumoto *et al.* [12]. The attached amine was immobilized at a concentration of 3.2 mequiv. g^{-1} dry beads. The aminated beads were packed into a column (50 × 4 mm I.D.) by the slurry-packing method. Glutaraldehyde solution (4%) in 0.1 *M* sodium hydrogencarbonate solution was pumped through the column for 2 h at 0.2 ml min^{-1} and the column was washed with deaerated water for 15 min at 0.5 ml min^{-1}. Invertase solution [100 mg in 10 ml of 0.05 *M* phosphate buffer solution (pH 7.0)] was circulated through the column at 0.3 ml min^{-1} for 10 h at room temperature. Invertase was immobilized with a 70% yield.

FDH was immobilized onto the CPG column. FDH was dissolved at a concentration of 1 mg ml^{-1} in 0.1 *M* gluconate buffer solution (pH 5.0) and 0.1% Triton X-100. An aliquot (10 ml) of this solution was added to 0.8 g of the CPG support which was activated by glutaraldehyde and shaken for 3 h at 15°C. FDH was immobilized with a 10% yield. The immobilized FDH reactor was prepared by slurry-packing the FDH-linked support into a column (50 × 4 mm I.D.).

RESULTS AND DISCUSSION

Evaluation of enzyme reactors

The properties of immobilized FDH were first evaluated without using the guard and analytical columns nor the immobilized invertase reactor. The influence of pH on the enzymatic reaction was studied over the pH range 4.0–6.0. A standard

solution of D-fructose (50 μM) was injected onto the column and mixed with potassium ferrocyanate(III) solution buffered with 0.1 M gluconate at various pH values before the reaching reactor column. The optimum pH for the enzymatic reaction was about 5.0. The reactor was placed in a water-bath and the temperature was varied between 10 and 40°C. The reactor exhibited the highest activity at 20°C. The effect of the concentration of the hexacynoferrate(III) ion in the reactor was examined in the concentration range 5–20 mM. The peak height was constant at concentrations greater than 10 mM. The apparent Michaelis constant of the immobilized FDH for the hexacyanoferrate(III) ion was about 0.8 mM.

The peak height decreased linearly as the flow-rate was increased from 0.5 to 1.0 ml min^{-1}. With 10 mM hexacyanoferrate(III) in 0.1 M gluconate buffer solution (pH 5.0) at 20°C and a flow-rate of 0.7 ml min^{-1}, 100 μM D-fructose was converted by FDH with a 10% yield. The reactor was used for 8 h per day and was stored at 4°C in 0.1 M phosphate buffer solution (pH 7.0) when not in use. The activity remained at 80% of the initial value for 4 weeks. The plot of peak area against concentration was linear from 0.05 to 400 μM. Above 500 μM the plot began to curve. The apparent Michaelis constant for D-fructose was about 5.8 mM.

The immobilized invertase reactor was used in the flow injection analysis mode by omitting the guard and analytical columns to evaluate the efficiency of fructose production from each oligosaccharide at various temperatures. The reactor was placed in an oven and the temperature varied from 30 to 70°C in the presence of 10 mM hexacyanoferrate(III) in 0.1 M gluconate buffer solution (pH 5.0) at a flow-rate of 0.7 ml min^{-1}. The peak area of the liberated fructose was determined by injecting oligosaccharide standards (10 μM). The molar ratio of fructose produced from the oligosaccharide injected was used to calculate the reaction efficiency. An efficiency of 100% was obtained in the range 40–70°C for sucrose, 45–65°C for raffinose and 52–68°C for stachyose. A reaction temperature of 55°C was chosen for the immobilized invertase reactor. The efficiencies for sucrose, raffinose and stachyose were maintained at a constant value for 30, 15 and 8 days, respectively.

Separation of the saccharides

The separation of mixtures of fructose, sucrose, raffinose and stachyose was carried out by anion-exchange chromatography on a TSK gel SAX column (5 μm, 30 cm × 6 mm) with 0.1 M borate buffer (pH 7.5 at 70°C) or 0.1 M sodium hydroxide–0.2 M sodium acetate solution (at 50°C) as the mobile phase. The borate buffer interfered with the enzymatic reaction owing to the formation of complexes with the saccharides. The reproducibility of the analyses with the sodium hydroxide–sodium acetate mobile phase was poor as a result of the incomplete mixing of the mobile phase with the flow of the make-up solution. A cation-exchange resin column (TSK gel SCX, 5 μm, 600 × 7.8 mm I.D., H-form) was used in an attempt to separate the saccharides at 55°C with water as the mobile phase. A stable and reproducible chromatogram (peak areas) was obtained, as shown in Fig. 2. The peak area for stachyose, raffinose or sucrose was identical to that of fructose (19.3 μC for 10^{-9} mol of fructose). This made it possible to determine the saccharides using the single fructose calibration graph. As the peak area is independent of the peak dispersion which occurs within the guard and analytical columns and the immobilized enzyme reactors, and as it is also independent of the sample dilution, this method is valid only when

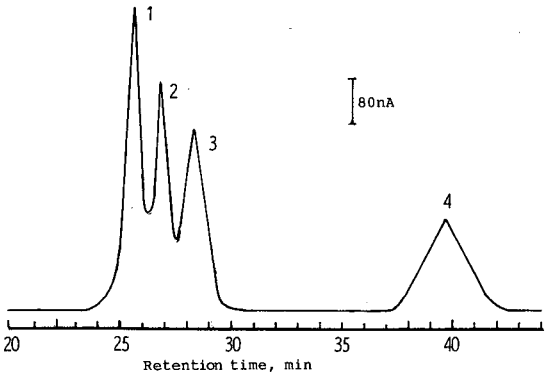

Fig. 2. Chromatogram of a standard mixture of 20 μM each of (1) stachyose, (2) raffinose, (3) sucrose and (4) fructose. Sample size 50 μl.

peak areas (coulomb) are used. The relative accuracy of the method is shown in Table I.

The peak area was plotted against the concentration of saccharides. The concentration ranges of linear response for fructose, sucrose, raffinose and stachyose were from 0.1 to 800 μM, 0.5 to 600 μM, 1.0 to 500 μM and 2.0 to 450 μM, respectively. The lower limit of the calibration graph for the oligosaccharides was governed by the efficiency of the hydrolysis. The slope of the graph was 0.965 $\pm$ 0.01 $\mu C\ \mu M^{-1}$ and the correlation coefficient was 0.9998 (21 points). The detection limits (signal-to-noise ratio 3) for fructose, sucrose, raffinose and stachyose were 0.08 (0.7), 0.1 (2), 0.3 (5) and 0.5 μM (27 ng in a 50-μl injection), respectively.

Application

This system was used to determine the amount of each saccharide found in a soybean extract. The sample was prepared by aqueous extraction according to the procedure of Kennedy *et al.* [13]. The sample was analysed under the same conditions as those described in the caption of Fig. 1. A single calibration graph for fructose was used to determine the amounts of fructose, sucrose raffinose and stachyose which

TABLE I

ACCURACY OF DETERMINATION OF THE SACCHARIDES IN THE STANDARD MIXTURE

Saccharide	Concentration in mixture (μM)	Apparent concentration (μM)[a]	Relative accuracy (%)
Fructose	200	201(2.8)[b]	0.5
Sucrose	200	199(2.1)	−0.5
Raffinose	100	101(2.0)	1.0
Stachyose	100	103(2.5)	3.0

[a] Calculated from the areas of the peaks using the calibration graph of fructose concentration *versus* fructose peak area.

[b] Values are means with the coefficient of variation (%) (n = 5) in parentheses.

TABLE II

RESULTS FOR FRUCTOSE, SUCROSE, RAFFINOSE AND STACHYOSE IN SOYBEAN EXTRACT

Saccharide	Saccharides found (%)[a]	
	Proposed method	Gas chromatography [14]
Fructose	0.50(3.5)[b]	0.48(5.4)[b]
Sucrose	5.87(2.4)	5.35(5.7)
Raffinose	0.87(3.8)	0.86(8.6)
Stachyose	3.88(2.2)	3.86(7.1)

[a] Percentage meal dry weight.
[b] Values are means with the coefficient of variation (%) (n = 5) in parentheses.

were present in the sample. The results obtained by this method and by gas chromatography [14] of the trimethylsilyl oxime derivatives of the saccharides are shown in Table II.

It is concluded that the immobilized invertase and FDH reactors are useful for the coulometric determination of sucrose, raffinose and stachyose using the single calibration graph for fructose based on peak area. This method is specific for oligosaccharides, but is not superior to anion-exchange chromatography with PAD [15] in terms of the time of analysis and limit of detection. It should be noted that the immobilized invertase reactor should be renewed every 8 days, and that this is a disadvantage of the proposed technique.

REFERENCES

1 H. Bauer and W. Voelter, in A. Henschen, K.-P. Hupe, F. Lottspeich and W. Voelter (Editors), *High-performance Liquid Chromatography in Biochemistry*, VCH, Weinheim, 1985, pp. 393–412.
2 S. Hughes and D. C. Johnson, *Anal. Chim. Acta*, 132 (1981) 11.
3 R. E. Reim and R. M. Van Effen, *Anal. Chem.*, 58 (1986) 3203.
4 K. Koizumi, Y. Kubota, T. Tanimoto and Y. Okada, *J. Chromatogr.*, 464 (1989) 365.
5 L. E. Welch, D. A. Mead, Jr. and D. C. Johnson, *Anal. Chim. Acta*, 204 (1988) 323.
6 L. A. Larew and D. C. Johnson, *Anal. Chem.*, 60 (1988) 1867.
7 B. Olsson, B. Stalbom and G. Johnsson, *Anal. Chim. Acta*, 179 (1986) 203.
8 C. A. Swindlehurst and T. A. Nieman, *Anal. Chim. Acta*, 205 (1988) 195.
9 K. Nakashima, H. Takei, O. Adachi, E. Shinagawa and M. Ameyama, *Clin. Chim. Acta*, 151 (1985) 307.
10 K. Matsumoto, O. Hamada, H. Ukeda and Y. Osajima, *Anal. Chem.*, 58 (1986) 2732.
11 K. Matsumoto, H. Kamikado, H. Matsubara and Y. Osajima, *Anal. Chem.*, 60 (1988) 147.
12 I. Matsumoto, Y. Ito and N. Seno, *J. Chromatogr.*, 239 (1982) 747.
13 I. R. Kennedy, O. D. Mwandemele and K. S. Mcwhirter, *Food Chem.*, 17 (1985) 85.
14 I. Molnar-Perl, M. Pinter-Szakacs .. Kovago and J. Petroczy, *J. Chromatogr.*, 295 (1984) 433.
15 R. D. Rocklin and C. A. Pohl, *J. Liq. Chromatogr.*, 6 (1983) 1577.

Journal of Chromatography, 549 (1991) 133–139
Elsevier Science Publishers B.V., Amsterdam

CHROM. 23 333

Improved separation of lysoglycolipids from solvolysates by reversed-phase high-performance liquid chromatography

NAOYUKI KATO, SHINSEI GASA* and AKIRA MAKITA
Biochemistry Laboratory, Cancer Institute, Hokkaido University School of Medicine, Kita-ku, N15W7 Sapporo 060 (Japan)
and
HARUHISA OGUCHI
Department of Pediatric Dentistry, School of Dentistry, Hokkaido University, Sapporo 060 (Japan)
(First received December 5th, 1990; revised manuscript received February 27th, 1991)

ABSTRACT

This paper describes the preparation of lysoglycosphingolipids by improved separation procedures. After desalting from the hydrazinolysate or alkaline hydrolysate of neutral glycolipids and sulphatide, the lipid mixtures were fractionated on a second reversed-phase high-performance liquid chromatography column to yield lysogalactosylceramide, lysolactosylceramide, lysoglobotriaosylceramide and lysoglobotetraosylceramide with a recovery rate of 50–68%. Lysosulphatide was separated from the desalted hydrazinolysate by DEAE-Sephadex column chromatography with a recovery rate of 75%. The purified lysoglycolipids were characterized by proton NMR spectrometry.

INTRODUCTION

Lysoglycosphingolipids (lysoGSLs), which are *N*-deacylated at the ceramide moiety in GSLs, accumulate in the brains of patients with glycosphingolipidoses [1–3] and in the twitcher mouse brain [4,5]. Such accumulations of lysoGSLs are suspected to be responsible for the pathological manifestations of these diseases [6], although they are also detected in minute amounts in the normal brain [7,8]. Cytotoxic lysoGSLs, such as sphingosine, are powerful inhibitors of protein kinase C [9].

LysoGSLs can be converted into artificial GSLs with a uniform carbon length that can be radiolabelled at the acyl moiety. For the laboratory preparation of lysoGSLs, intact GSLs are *N*-deacylated by saponification [10–13] or by hydrazinolysis with [14] or without [15] hydrazine sulphate as an effective catalyst. The hydrazinolysis of GSLs containing *N*-acetylhexosamine and/or sialic acid, however, yields various *N*-deacylated products, depending on the time and temperature of the reaction [14]. In many instances the reaction mixture is dialysed to remove low-molecular-mass non-lipid materials, followed by the isolation of lysoGSLs by silicic acid chromatography. With these procedures for the preparation of lysoGSLs, the recovery is generally low.

0021-9673/91/$03.50

In this paper, reversed-phase high-performance liquid chromatography (HPLC) is described as an effective procedure for the isolation of lysoGSLs from the hydrazinolysate or hydrolysate. The separated lysoGSLs were characterized by proton NMR spectrometry.

EXPERIMENTAL

Materials

Anhydrous hydrazine was purchased from Eastman Kodak (NY, USA). The Sep-Pak C_{18} cartridges and Wakosil C_{18} columns (5C18-200, 4.6 × 250 mm) were obtained from Waters (Milford, MA, USA) and Wako (Tokyo, Japan), respectively. Pre-coated thin-layer chromatography (TLC) plates (silica gel 60, 20 × 20 cm) were from Merck (Darmstadt, Germany). All other reagents were of analytical-reagent grade. Galactosylceramide (GalCer) and sulphated galactosylceramide (sulphatide) were purified from porcine brain. Lactosylceramide (LacCer) was isolated from equine erythrocytes as reported previously [16]. Globotriaosylceramide (Gb_3Cer) and globotetraosylceramide (Gb_4Cer) were prepared from porcine erythrocytes [17].

Hydrazinolysis and saponification of GSLs

The ratio of the solvent mixture is expressed by volume unless stated otherwise.

Hydrazinolysis was carried out according to the method of Suzuki *et al.* [14], except that the reaction temperature was 130°C. Briefly, 20–800 mg of GSLs, except for Gb_4Cer, were heated at 130°C for 16 h in 0.1–1.6 ml (200–500 mg/ml) of anhydrous hydrazine containing 2% (w/v) hydrazine sulphate in a glass tube (15 mm × 8 cm) with a cap sealed with PTFE tape. The hydrazinolysate was then supplemented with chloroform–methanol–water (3:48:47) until the solution became clear. Gb_4Cer (200 mg), however, was saponified with 1 *M* tetramethylammonium hydroxide in 10 ml of *n*-butanol at 100°C for 13 h according to the method of Sonnino *et al.* [13] The saponification mixture was diluted with an equal volume of water.

The diluted reaction mixture of hydrazinolysis or saponification was directly applied to Sep-Pak cartridges (15 mg or less of starting GSL per cartridge) and successively washed with the chloroform–methanol–water mixture and water [18] until the washings became negative to Nessler's reagent for hydrazinolysis, or the pH became neutral in saponification. LysoGSL and unreacted GSL were eluted completely from one cartridge with 1 ml of methanol and 5 ml of chloroform–methanol–water (60:30:4.5). The eluates were concentrated and developed by TLC with chloroform–methanol–water–acetic acid (60:40:8:1, solvent I), followed by staining with an orcinol–sulphuric acid reagent.

Isolation of lysoGSL by reversed-phase high-performance liquid chromatography or by DEAE chromatography

To isolate lysoGSL, although not lysosulphatide, the desalted sample was dried and dissolved in a minimum volume of chloroform–methanol–water (3:48:47) and applied to a reversed-phase column for HPLC. Elution was performed at a flow-rate of 1 ml/min in 1.5-ml fractions with methanol–water (6:4, 10 ml) using a linear gradient from methanol–water (6:4, 30 ml) to methanol (30 ml) for 60 min, and chloroform–methanol–water (60:30:4.5, 5 ml). Each fraction was concentrated *in vacuo* and

monitored by TLC developed with chloroform–methanol–water (60:35:8, solvent II), followed by staining with an orcinol–sulphuric acid reagent.

After the hydrazinolysate of the sulphatide (200 mg) was treated with the cartridge as described, the eluate was directly applied without concentration on a DEAE-Sephadex A-25 (1.0 × 5 cm, acetate form) column. Lysosulphatide passed through the column with 10 ml of chloroform–methanol–water (30:60:8), while unreacted sulphatide bound to the column. The unreacted sulphatide was eluted with 10 ml of 90 m*M* ammonium acetate solution in methanol followed by desalting with a Sep-Pak cartridge as described.

The fraction containing lysoGSL was combined and examined for purity on a TLC plate developed with solvent I, followed by staining with an orcinol–sulphuric acid or with ninhydrin reagent.

Proton NMR spectrometry

Proton NMR spectra of the isolated lysoGSLs (0.5–2 mg) were obtained in 0.4 ml of [$^2H_6$]dimethylsulphoxide containing 2% ^2H_2O at 90°C on a Varian JNM-GX500 spectrometer in the Fourier-transform mode. The apparatus was equipped with a JEC-980B computer which had a 48k memory capacity, and was used at the High Resolution NMR Laboratory, Hokkaido Unversity, as described previously [19]. The frequency was 500 MHz and the sweep width was 5 kHz. The chemical shifts were indicated by the distance (ppm) from tetramethylsilane as an internal standard.

RESULTS

Desalting from solvolysate

The reversed-phase cartridge technique resulted in the elution of most of the lysoGSLs with methanol–water (7:3 or 8:2) free from the bulk of hydrazine and salts, as seen when the bound and unbound fractions were examined by TLC and Nessler's

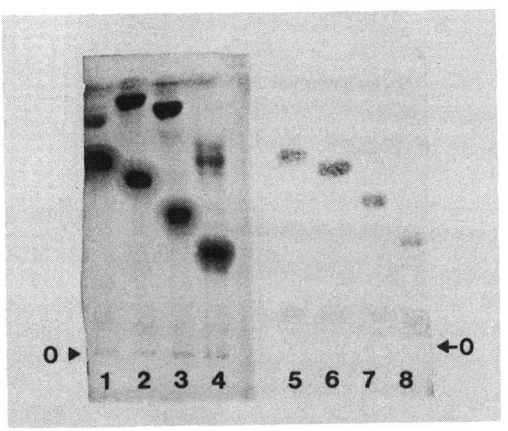

Fig. 1. TLC of hydrazinolysates of GSLs. Hydrazinolysates of GSLs were applied to a Sep-Pak C_{18} cartridge and then chromatographed on silica gel TLC developed with solvent I. Lanes: 1, 5 = hydrazinolysate of sulphatide; 2, 6 = of GalCer; 3, 7 = of LacCer; 4, 8 = of Gb_3Cer. Lanes 1–4 and 5–8 were separately stained by an orcinol–sulphuric acid reagent and a ninhydrin reagent, respectively. O = Origin.

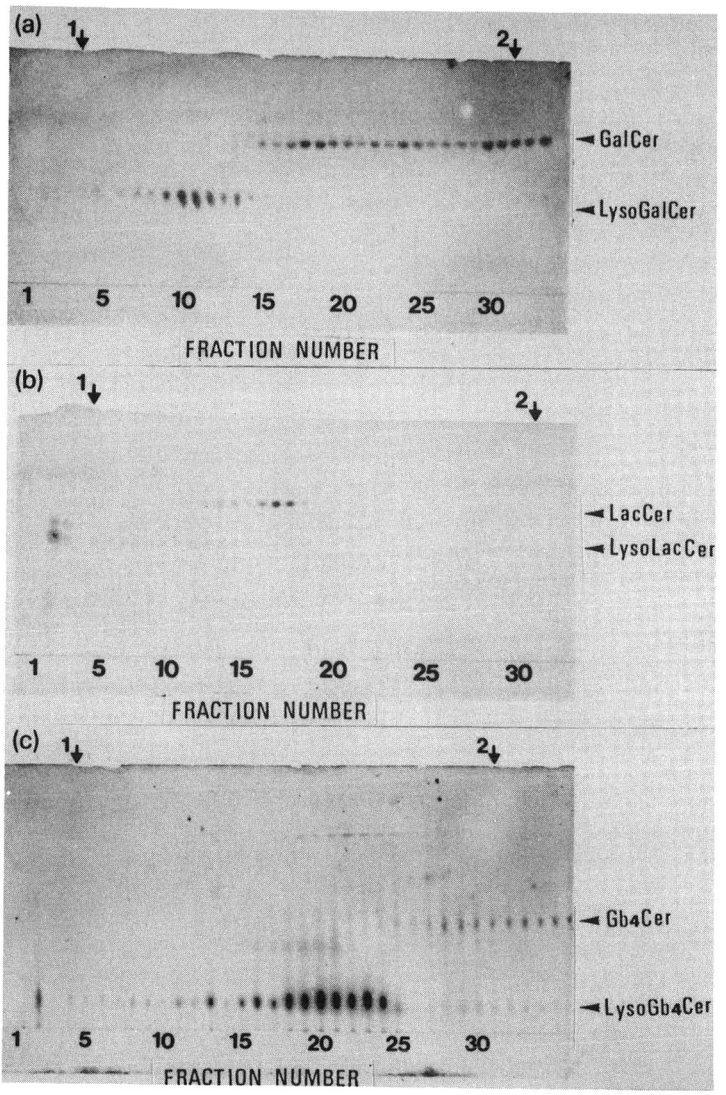

Fig. 2. Separation of lysoGSL from GSL using reversed-phase HPLC. The hydrazinolysates of sulphatide, GalCer, LacCer and Gb_3Cer, and the hydrolysate of Gb_4Cer were desalted using a Sep-Pak cartridge and were applied to a C_{18} column from HPLC as described under Experimental. After gradient elution, each fraction was concentrated and examined by TLC developed with solvent II, followed by staining with an orcinol–sulphuric acid reagent. (a) hydrazinolysate of GalCer; (b) of LacCer; (c) hydrolysate of Gb_4Cer. In each panel, the lower spots were positive for the ninhydrin reaction and the upper spots were negative. Arrows 1 and 2 indicate the start and finish points of gradient elution, respectively.

reagent. However, the co-elution of lysoGSLs with unreacted GSLs from the cartridge was unavoidable, as it was not possible to separate each of these lipids only by using the cartridge. Fig. 1 shows a thin-layer chromatogram of lipid fractions after treatment with the cartridges of hydrazinolysates of sulphatide, GalCer, LacCer and

Gb_3Cer. The slowly migrating, ninhydrin-positive spots can be assigned to the small amounts of remaining hydrazine or fatty acyl hydrazide as a result of the similar mobility of this species in every lane.

Separation of lysoGSL for GSL

When a mixture containing lysoGSL and GSL was subjected to reversed-phase HPLC, the best separation of the lipids was attained by gradient elution from methanol–water (6:4) to methanol. As shown in Fig. 2, lysoGalCer (a), lysoLacCer (b) and $lysoGb_4Cer$ (c) were clearly separated from their unreacted, native GSLs, eluting faster than the respective unreacted GSL. However, with a large initial amount (more than 800 mg) of GalCer at the hydrazinolysis step, the lysoGSL was not completely eluted, and further elution with chloroform–methanol–water (30:80:8, Fig. 2a) was necessary. This solvent system was usually also employed for generation of the column.

From 200 mg each of the GSLs, 80 mg (64% of the calculated amount) of lysoGalCer, 95 mg (68%) of lysoLacCer, 87 mg (58%) of $lysoGb_3Cer$ and 79 mg (50%) of $lysoGb_4Cer$ were obtained using these separation procedures.

For the isolation of lysosulphatide, DEAE chromatography was used instead of a second reversed-phase chromatographic separation. The lysosulphatide was recovered in the unbound fraction on the DEAE column, whereas unreacted sulphatide bound to the column, from which sulphatide was eluted with 90 m*M* ammonium acetate in methanol [20], as shown in Fig. 3. The yield of the lysosulphatide was 75%, which was fairly high compared to the separation using reversed-phase chromatography.

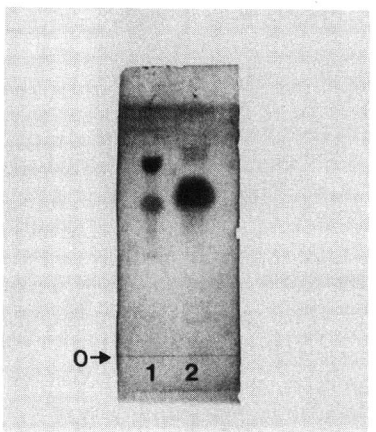

Fig. 3. Separation of lysosulphatide and sulphatide. The hydrozinolysate of sulphatide was desalted and applied directly to a DEAE–Sephadex column. The unbound and bound fractions were obtained as described under Experimental. These fractions were concentrated and separated by TLC developed with solvent I, followed by staining with an orcinol–sulphuric acid reagent. Lanes 1 and 2 demonstrate fractions bound and unbound to the ion exchanger, respectively. O = Origin.

Proton spectrometry of lysoGSLs

The lysoGSLs obtained were charaterized by proton NMR spectrometry, comparing the spectra obtained with the respective native GSLs. The spectrum of lysoGalCer shows the disappearance of a triplet either at 2.10 ppm due to the C–2 hydroxymethine proton or at 5.3 ppm due to cisoid olefinic protons of the fatty acyl group, which were predominantly α-hydroxy fatty acids of porcine brain GalCer (data not shown). Similar observations were made in the spectra of lysoLacCer, lysosulphatide and lysoGb$_4$Cer. In the lysoGSLs, although chemical shifts of the anomeric protons on the carbohydrate chains and transoid olefinic protons on the long-chain base resonated down field, these protons were retained, verifying the chemical structures of the lysoGSLs. Amide protons resonated at 7.5 ppm, and the doublet on the ceramide moiety of the GSLs [21] shifted to a higher field with a triplet in the lysoGSLs examined (data not shown).

DISCUSSION

As lysoGSLs lack one of two hydrocarbon chains and are dialysable in water, the dialysis of lysoGSLs against water is not favourable. The separation of a lysoGSL from the parent GSL by reversed-phase chromatography reported in this paper is based on the difference of hydrophobicity between these two compounds. As lysoGSLs have less mobility than intact GSLs in silicic acid chromatography, these lipids can be separated by this procedure. However, an amino group in the lysoGSL will interact with silicic acid to give tailed elution during the chromatographic separation and will consequently lead to a low recovery on the column. Therefore, reversed-phase chromatography appears to be more advantageous than silica gel chromatography for the separation of lysoGSLs. For the separation of lysosulphatide and sulphatide, the lysosulphatide, which has a neutral charge, did not bind to the DEAE column, whereas the sulphatide did bind to the column. However, the method could not be applied for the separation of monosialoganglioside and its lysoganglioside (data not shown).

Hydrazinolysis was advantageous compared to the standard procedure using alkaline hydrolysis to remove the fatty acyl group at the ceramide moiety of *N*-acetylhexosamine-lacking neutral GSL or sulphatide. The alkaline hydrolysis of sulphatide concomitantly gave a more than 20% of yield of lysoGalCer as a by-product. The hydrozinolysis of GSL containing *N*-acetylhexosamine and/or sialic acid, however, could not be used to obtain a corresponding homogenous deacylation product at the ceramide moiety, as the reaction gave a mixture containing a partially deacylated derivative at *N*-acetylhexosamine and/or the sialic acid moiety. Deacylation of *N*-acetylhexosamine could be avoided by the alkaline hydrolysis of Gb4Cer as demonstrated in this work and of gangliosides as reported previously [22].

The chemical characterization of lysoGSLs has been performed by fast atom bombardment mass spectrometry and carbon NMR spectrometry for lysoGalCer and lysoGlcCer [23] and for sulphatide [24], or by proton NMR for lysogangliosides [22,25]. These spectrometries were effective in confirming the absence of a fatty acyl group in native GSL. In the proton NMR spectum of lysoGalCer, the anomeric proton of the carbohydrate attached to sphingosine shifted to a lower field compared to that of the parent GSL, suggesting that sphingosine and ceramide have different electronegativities.

REFERENCES

1 O. Nilsson and L. Svennerholm, *J. Neurochem.*, 39 (1982) 709.
2 S. Neuenhofer, E. Conzelmann, G. Schwarzmann, H. Egge and K. Sandhoff, *Biol. Chem. Hoppe-Seyler,* 367 (1986) 241.
3 B. Rosengren, J.-E. Mansson and L. Svennerholm, *J. Neurochem.*, 49 (1987) 834.
4 H. Shinoda, T. Kobayashi, M. Katayama, I. Goto and H. Nagara, *J. Neurochem.*, 49 (1987) 92.
5 K. Tanaka, H. Nagata, T. Kobayashi and I. Goto, *Brain Res.*, 454 (1988) 340.
6 Y. A. Hannun and R. M. Bell, *Science*, 235 (1987) 670.
7 H. Igisu and K. Suzuki, *J. Lipid Res.*, 25 (1984) 1000.
8 B. Rosengren, P. Fredman, J.-E. Mansson and L. Svennerholm, *J. Neurochem.*, 52 (1989) 1035.
9 Y. A. Hannun, C. R. Loomis, A. H. Merrill and R. M. Bell, *J. Biol. Chem.*, 261 (1986) 12604.
10 T. Taketomi and T. Yamakawa, *J. Biochem.*, 54 (1963) 444.
11 G. Nonaka, Y. Kishimoto, Y. Seyama and T. Yamakawa, *J. Biochem.*, 85 (1979) 511.
12 K. M. Koshy and J. M. Boggs, *Lipids*, 7 (1982) 998.
13 S. Sonnino, G. Kirschner, R. Ghidoni, D. Acquotti and G. Tettamanti, *J. Lipid Res.*, 26 (1985) 248.
14 Y. Suzuki, Y. Hirabayashi and M. Matsumoto, *J. Biochem.*, 95 (1984) 1219.
15 H. Higashi and S. Basu, *Anal. Biochem.*, 120 (1982) 159.
16 S. Gasa, A. Makita and Y. Kinoshita, *J. Biol. Chem.*, 258 (1983) 876.
17 F. Sako, S. Gasa, A. Makita, A. Hayashi and S. Nozawa, *Arch. Biochem. Biophys.*, 278 (1990) 228.
18 M. A. Williams and R. H. McCluer, *J. Neurochem.*, 35 (1980) 266.
19 S. Gasa, M. Nakamura, A. Makita, M. Ikura and K. Hikichi, *Eur. J. Biochem.*, 155 (1986) 603.
20 S. Gasa, M.-T. Casl, A. Makita, N. Sakakibara, T. Koyanagi and T. Atsuta, *Eur. J. Biochem.*, 189 (1990) 301.
21 S. Gasa, T. Mitsuyama and A. Makita, *J. Lipid Res.*, 24 (1983) 174.
22 S. Neuenhofer, G. Schwarzmann, H. Egge and K. Sandhoff, *Biochemistry*, 24 (1985) 525.
23 A. Hara and T. Taketomi, *J. Biochem.*, 100 (1986) 415.
24 T. Taketomi, A. Hara, Y. Kutsukake and E. Sugiyama, *J. Biochem.*, 107 (1990) 680.
25 Y. Hirabayashi, M. Kimura, M. Matsumoto, K. Yamamoto, S. Kadowaki and T. Tochikura, *J. Biochem.*, 103 (1988) 1.

Journal of Chromatography, 549 (1991) 141–152
Elsevier Science Publishers B.V., Amsterdam

CHROM. 23 324

Ovine luteinizing hormone

V. Significance of flow-through peaks observed during chromatofocusing as revealed by various methods of sample preparation and application

H. EDWARD GROTJAN* and BRUCE D. SCHANBACHER
Animal Science Department, University of Nebraska, Lincoln, NE 68583-0908 (USA)
and
BROOKS A. KEEL
Department of Obstetrics and Gynecology, University of Kansas School of Medicine–Wichita, Women's Research Institute, 2903 E. Central, Wichita, KS 67214 (USA)
(First received October 3rd, 1990; revised manuscript received March 11th, 1991)

ABSTRACT

In a previous study [Keel *et al., Biol. Reprod.*, 36 (1987) 1102] the ovine luteinizing hormone (oLH) in pituitary extracts was chromatofocused on pH 10.5–7 gradients after equilibration in 25 m*M* triethylamine–HCl, pH 11.0, by gel permeation. Under these conditions, some immunoreactive oLH flowed through the columns unrestricted and this was interpreted to represent extremely basic isoforms. However, when selected flow-through peaks were re-chromatofocused, each was contaminated with other isoforms of oLH. In order to clarify this dilemma, various methods of sample preparation and application were systematically compared. Consistent with previous observations, variable amounts of the immunoreactive oLH in pituitary extracts equilibrated in triethylamine by gel permeation, dialysis, flow dialysis or ion-retardation chromatography eluted as flow-through peaks when chromatofocused. In contrast, when the ionic components in the pituitary homogenization buffer were removed by these methods as well as ultrafiltration and the proteins were applied to the resin in the elution buffer (1:45 Pharmalyte 8-10.5–HCl, pH 7.0), none of the immunoreactive oLH in pituitary extracts eluted as a flow-through peak. Thus, it appears that oLH eluting as a flow-through peak results from incomplete binding of the hormone to the chromatofocusing resin when applied in triethylamine.

INTRODUCTION

The heterogeneity of the glycoprotein hormones is abundantly documented in the scientific literature with many, if not all, exhibiting multiple-charge isomers (for examples, see Keel and Grotjan [1]). One method which has been utilized to examine the charge heterogeneity of the glycoprotein hormones is chromatofocusing [1–5]. In a previous study [2], the conditions utilized for chromatofocusing were essentially those recommended in the directions supplied with the reagents [6]. Accordingly,

0021-9673/91/$03.50

samples were applied to the resin in chromatofocusing "start" buffer (25 m*M* triethylamine–HCl, pH 11.0) after gel permeation on small columns of Sephadex G-25 Superfine [2]. Under these conditions, some of the ovine luteinizing hormone (oLH) in pituitary extracts flowed through the columns unrestricted when chromatofocused on pH 10.5–7 gradients. Furthermore, the percentage of oLH eluting as flow-through peaks was increased in the pituitaries of rams or wethers treated with androgens [2]. However, when selected flow-through peaks (designated as peak A in Keel *et al.* [2]) from several chromatofocusing profiles were dialyzed against water and re-chromatofocused (as decribed in detail in the subsequent paper [5]), it became apparent that each was contaminated with other isoforms of oLH [7]. In order to resolve this dilemma, various methods of sample preparation and application were systemically compared. During these experiments it became apparent that the buffer in which the pituitary extract was applied to the chromatofocusing column affected the percentage of oLH flowing through the columns unrestricted. When samples were applied to the resin in the elution buffer (1:45 Pharmalyte 8-10.5–HCl, pH 7.0), none of the oLH in pituitary extracts eluted as a flow-through peak.

MATERIALS AND METHODS

Purified oLH and pituitary extracts

Highly purified oLH was obtained from Dr. David Sherwood, University of Illinois, Urbana, IL, USA [8]. Ovine or bovine pituitaries were homogenized in 150 m*M* NaCl, 50 m*M* Tris (pH 7.4) containing 1% (v/v) Triton X-100 and a series of protease inhibitors (5 m*M* Na_2EDTA, 1 m*M* phenylmethylsulphonyl fluoride and 200 U/ml aprotinin), centrifuged at 100 000 *g* for 1 h and frozen at −70°C as decribed previously [2]. Selected pituitary extracts from Keel *et al.* [2] were also utilized. Purified oLH was supplemented with 2 mg cytochrome *c*, 3 mg myoglobin and 4 mg ovalbumin prior to chromatofocusing (see Figs. 4 and 5) while aliquots of pituitary extracts were supplemented with 2 mg cytochrome *c* and either 5 mg ovalbumin (see Figs. 1–3) or 3 mg myoglobin (see Figs. 6–8) prior to preparation for chromatofocusing by one of the methods subsequently described. All sample preparation and chromatographic separations were performed at 4°C.

Gel permeation

A 0.5- or 1.0-ml aliquot of a pituitary extract was equilibrated in either 25 m*M* triethylamine–HCl, pH 11.0, or 1:45 Pharmalyte 8-10.5–HCl, pH 7.0 (Pharmacia/LKB, Piscataway, NJ, USA), by gel permeation on 1.0 × 15 cm columns of Sephadex G-25 Superfine (Pharmacia/LKB). The columns were eluted at 4 ml/h and 0.5 ml fractions were collected. Columns eluted with Pharmalyte were washed with water between samples and re-equilibrated with 2–4 column volumes of Pharmalyte prior to sample application. The recovery of immunoreactive oLH from pituitary extracts prepared by gel permeation was typically >75%.

Ion-retardation chromatography

A 1.0 × 40 cm column of AG11A8 ion-retardation resin (Bio-Rad, Richmond, CA, USA) was regenerated with 1 *M* NH_4Cl and re-equilibrated in water. A 1.0-ml aliquot of a pituitary extract was loaded and eluted at 14 ml/h with water. Fractions

of 1.0 ml were collected. The void-volume material was pooled, lyophilized and dissolved in triethylamine. Recovery of immunoreactive oLH was 87%.

Dialysis and flow dialysis

A 0.5- or 1.0-ml aliquot of a pituitary extract was placed in SpectraPor1 dialysis tubing (6000–8000 mol.wt. cut off; Spectrum Medical Industries, Los Angeles, CA, USA) and dialyzed against 1–2 l water overnight. Aliquots of extracts prepared by flow dialysis were placed on one side of a SpectraPor1 membrane in a 2.5-ml Spectrum flow-dialysis apparatus. Approximately 3 l water were allowed to flow through the opposite side overnight. In both cases, the conductivity of the dialyzed sample was checked with a hand-held conductivity meter (Model CDH-53, Omega, Stamford, CT, USA) and the sample was then supplemented with a concentrated (10 ×) solution of triethylamine or Pharmalyte. Prior to chromatofocusing, samples prepared by these methods were centrifuged at 12 800 *g* for 5 min to remove any particulate matter resulting from the reduction in ionic strength and/or removal of detergent. The recovery of immunoreactive oLH from samples prepared in this manner was typically >85%.

Ultrafiltration

A 0.5- or 1.0-ml aliquot of a pituitary extract was diluted with an equal volume of water, placed in an Amicon Centricon 10 ultrafiltration device (Amicon, Beverly, MA, USA) and centrifuged three times at 5000 *g* for 30 min. Between each centrifugation a volume of water equal to the volume of the diluted extract was added. The retentate was recovered by adding 0.5 ml water, inverting the device and centrifugation at 1000 *g* for 3 min. Conductivity of the sample was assessed as described above and each was supplemented with a concentrated Pharmalyte solution prior to chromatofocusing. Samples prepared in this manner yielded immunoreactive oLH recoveries of >83%. Typically, no more than 7% of the immunoreactive oLH was present in the filtrate.

Chromatofocusing

Chromatofocusing on pH 10.5–7 gradients was performed essentially as described by Keel *et al.* [2]. Columns (20 ml, 25 × 1.0 cm I.D.) of PBE 118 resin (Pharmacia/LKB) were equilibrated in 25 m*M* triethylamine–HCl, pH 11.0. Samples prepared in triethylamine were loaded to start the run while samples prepared in Pharmalyte were loaded after 3.0 ml of the elution buffer had been applied to the column. In both cases, the pH gradient was developed with 1:45 Pharmalyte 8-10.5–HCl, pH 7.0, which was eluted at 10 ml/h and collected as seventy or eighty 3.0-ml fractions. The pH gradient was monitored with a Pharmacia pH monitor. After the lower-limiting pH had been reached, materials bound to the column were eluted with 1 *M* NaCl which was collected as an additional twenty 3.0-ml fractions. Each chromatofocusing fraction was subsequently neutralized by the addition of 0.3 ml 1.1 *M* Tris-HCl, pH 7.0. When purified oLH was analyzed, chromatofocusing buffers were supplemented with 1% (v/v) glycerol. When pituitary extracts were analyzed, chromatofocusing buffers were supplemented with 0.1% (v/v) glycerol. The addition of extra proteins and glycerol enhances the recovery of oLH [9].

Chromatofocusing on pH 9–6 gradients was performed on 20 ml PBE 94 resin

(Pharmacia/LKB) equilibrated in 25 m*M* ethanolamine–acetate, pH 9.4. An aliquot of a bovine pituitary extract was de-salted by flow dialysis against water and supplemented with a concentrated solution of Polybuffer 96–acetate, pH 6.0 (Pharmacia/LKB). After sample application, the pH gradient was developed at 10 ml/h with 1:40 Polybuffer 96–acetate, pH 6.0, and collected as eighty 3.0-ml fractions. Materials bound at the lower-limiting pH were eluted with 1 *M* NaCl which was collected as an additional twenty 3.0-ml fractions. Each fraction was neutralized with Tris as described above. The recovery of purified oLH and LH in pituitary extract from the chromatofocusing columns was 53 ± 4 and 75 ± 5%, respectively.

Radioimmunoassays

The oLH concentrations in chromatofocusing fractions were quantitated by radioimmunoassays using purified hormones obtained from Dr. D. N. Ward, Houston, TX, USA, and Dr. L. E. Reichert, Jr., Albany, NY, USA, and a polyclonal antiserum developed in rabbits against a human chorionic gonadotropin (hCG)α–oLHβ heterodimer [10]. Highly purified oLH (oLH-LER-1056-C2 or oLH-LER-1374A) was iodinated in 0.5 *M* Na_2HPO_4, pH 8.2, using a ^{125}I/oLH molar ratio of two and one Iodobead (Pierce, Rockford, IL, USA) for 15 min at room temperature. Unincorporated ^{125}I was removed by gel permeation. The immunoassay buffer contained 150 m*M* NaCl, 50 m*M* Tris–HCl (pH 7.4), 5 m*M* Na_2EDTA, 1 g/l gelatin and 0.1% (w/v) sodium azide. Purified oLH (oLH-DNW-HSN-10-124, potency = 1.7 × NIH-LH-S1) was used as the reference preparation. The relative cross reactivities of various hormones on a molar basis were: oLH 100%, oLHβ 113%, oLHα 0.14%, ovine follicle-stimulating hormone (FSH) 3.4%, porcine FSHβ <0.03%, bovine thyroid-stimulating hormone (bTSH) 2.0%, bTSHβ 0.4%, bovine growth hormone 0.5%, bovine prolactin <0.04% and porcine adrenocorticotropin <0.01%. When buffered with Tris, up to 0.2-ml aliquots of chromatofocusing fractions could be included in an immunoassay tube without significant interference from the chromatofocusing reagents. Because the molecular structure of ovine and bovine (b) LH are extremely similar [1], the LH concentrations in chromatofocusing fractions derived from bovine pituitary extracts were quantitated in the same assay system utilizing the oLH standard noted above as the reference preparation.

Titration of PBE 118 chromatofocusing resin

A volume of 10 ml of PBE 118 Resin (Lot MF 02136 with a stated capacity of 51 μmol pH $unit^{-1}$ ml^{-1}) was equilibrated in 1 *M* KCl by repeated centrifugation. The resin was diluted to a 10% (v/v) suspension in 1 *M* KCl and adjusted to a pH > 12 with 10 *M* NaOH. The resin was the titrated to a pH < 3 with 0.5 *M* HCl at room temperature. All pH measurements were obtained with a Corning Ross pH electrode and Corning pH meter.

RESULTS

In our previous study [2], ovine pituitary extracts were equilibrated in 25 m*M* triethylamine–HCl, pH 11.0 (chromatofocusing "start" buffer) by gel permeation on 15 × 1 cm I.D. columns of Sephadex G-25 Superfine. A clear separation of proteins and ionic components was achieved (Fig. 1). In order to determine if the method by

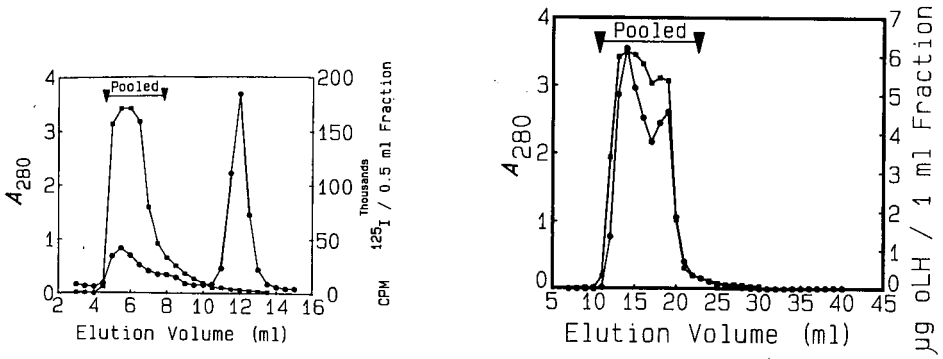

Fig. 1. Elution of proteins and ^{125}I during gel permeation on Sephadex G-25 Superfine. A 0.5-ml aliquot of an ovine pituitary extract (50 mg tissue equivalents) was supplemented with 2 mg cytochrome *c*, 5 mg ovalbumin and 520 000 cpm ^{125}I. The mixture was applied to a 15 × 1.0 cm I.D. column and eluted at 4 ml/h with 25 m*M* triethylamine–HCl, pH 11.0. Fractions (0.5 ml) were collected. (■) Elution of proteins; (●) radioactivity. When utilized to prepare pituitary extracts for chromatofocusing, the void-volume peak containing the proteins as judged by the absorbance at 280 nm was pooled (denoted by the bar).

Fig. 2. Utilization of ion-retardation chromatography to remove the ionic constituents from the proteins in a 1.0-ml aliquot of pituitary extract supplemented with 2 mg cytochrome *c* and 5 mg ovalbumin. The 40 × 1.0 cm I.D. column of AG11A8 (Bio-Rad) was eluted at 14 ml/h with water and 1.0-ml fractions were collected. All of the immunoreactive oLH (●) co-eluted with proteins as judged by the absorbance at 280 nm (■). The void-volume material was pooled, lyophilized, dissolved in triethylamine and chromatofocused (lower left-hand panel of Fig. 3). In a separate experiment performed under similar conditions, it was demonstrated that >97% of the ^{125}I was removed from the proteins in a pituitary extract to which ^{125}I was added.

which the ionic components in the pituitary homogenization buffer were separated from the proteins had any effect on the chromatofocusing elution profile of oLH, aliquots of a pool of pituitary extracts were equilibrated in triethylamine by various methods including gel permeation (Fig. 1), ion-retardation chromatography (Fig. 2), dialysis and flow dialysis. In each case, the proteins were eluted or reconstituted in 25 m*M* triethylamine and the removal of ionic components was documented by checking the conductivity. Irrespective of the method of sample preparation, a small percentage of the oLH in each extract flowed through the chromatofocusing columns unrestricted (Fig. 3). However, the percentage of immunoreactive oLH eluting in these flow-through peaks (designated as peak A in Fig. 3) was not consistent.

Because similar results, at least qualitatively, were obtained with multiple methods of sample preparation (Fig. 3) and because the proteins were applied in a buffer approximately equal to the ionic strength to the chromatofocusing reagents, at least two possible explanations existed: (1) there were indeed a small percentage of extramely basic forms of oLH in pituitary extracts; or (2) the triethylamine might not be the optimal buffer to load the oLH in a pituitary extract. The latter possibility is tantamount to stating that the chromatofocusing resin had been overloaded under the specific experimental conditions utilized. Thus, a series of experiments was conducted to determine if the columns had, in effect, been overloaded.

Highly purified oLH [8] previously demonstrated to be devoid of extremely basic forms was utilized in one series of experiments designed to examine this possibil-

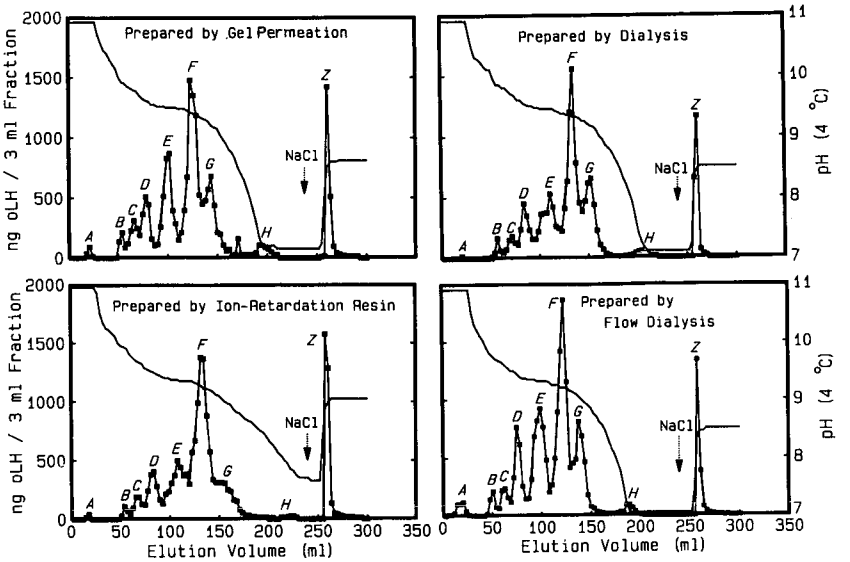

Fig. 3. Chromatofocusing elution profiles of the immunoreactive oLH in aliquots of a pool of pituitary extracts prepared by various methods. In each case, aliquots of a pool of pituitary extracts were supplemented with 2 mg cytochrome *c* and 5 mg ovalbumin. After removal of ionic components by the method indicated, samples were reconstituted in 25 m*M* triethylamine–HCl, pH 11.0, and chromatofocused on pH 10.5–7 gradients. The columns were eluted at 10 ml/h with 1:45 Pharmalyte 8-10.5–HCl, pH 7.0, and 3.0-ml fractions were collected. The oLH concentration of each fraction (□) was quantitated by radioimmunoassay and the pH gradient (solid line) was monitored with a flow-through pH monitor. Materials bound at the lower-limiting pH of 7.0 were eluted with 1 *M* NaCl and coded as peak Z. Other isoforms of oLH are coded with the letters A through H beginning with the most basic form [2,5]. See the text for additional experimental details.

ity. Similar chromatofocusing elution profiles were noted when 20 μg of purified oLH were applied to the columns in 25 m*M* triethylamine–HCl, pH 11.0 (Fig. 4); 1:45 Pharmalyte 8-10.5–HCl, pH 7.0 (Fig. 4); or 25 m*M* Tris–HCl, pH 8.0 (data not illustrated). Furthermore, the chromatofocusing elution profile of purified oLH applied in 25 m*M* NaCl was also similar to that obtained when the oLH was loaded in one of the aforementioned buffers except for an extremely small flow-through peak (Fig. 5). However, when purified oLH was dissolved in the buffer used to extract pituitary tissue (150 m*M* NaCl, 50 m*M* Tris, etc.), all of the oLH flowed through the column unrestricted (data not illustrated), presumably because of the high ionic strength in which the sample was applied. This series of experiments suggested that the buffer in which *small amounts of purified* oLH is applied to the chromatofocusing resin has a minimal effect on the elution profile *if* it is of sufficiently low ionic strength.

In order to further test whether the buffer in which samples were applied to the chromatofocusing resin was an important consideration, aliquots of a single pituitary extract were prepared by gel permeation or flow dialysis and applied to the chromatofocusing columns in either triethylamine or Pharmalyte (Fig. 6). Removal of ionic constituents was again monitored by checking the conductivity of each sample. Irrespective of the method of sample preparation, a small flow-through peak (designated as A in Fig. 6) was observed when the proteins were applied to the chromatofocusing

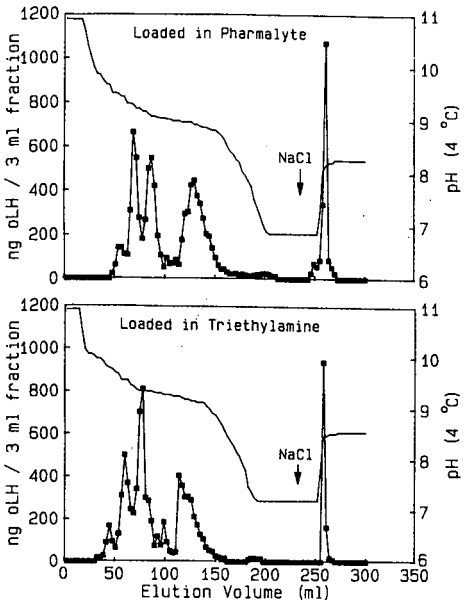

Fig. 4. Elution of 20 μg purified oLH [8] applied in 1:45 Pharmalyte 8-10.5–HCl, pH 7.0 (top panel) or 25 mM triethylamine–HCl, pH 11.0 (lower panel) on pH 10.5–7.0 chromatofocusing gradients. Each sample was supplemented with 2 mg cytochrome c, 3 mg myoglobin and 4 mg ovalbumin prior to application. Replicate samples dissolved in the above buffers as well as purified oLH dissolved in 25 mM Tris, pH 8.0, yielded similar elution profiles (data not illustrated). Additional experimental details are presented in the legend of Fig. 3 and the text.

columns in triethylamine. However, when the proteins in pituitary extracts were loaded in Pharmalyte, no flow-through peaks were observed. Likewise, no flow-through peaks were evident when pituitary extracts were prepared by ultrafiltration and loaded in Pharmalyte (data not illustrated). A small amount ($<1\%$) of the immunoreactive oLH eluted between the initial drop in the pH gradient and peak B. This peak is coded as peak A′ in Figs. 6–8 to distinguish it from peak A (exclusively used to denote

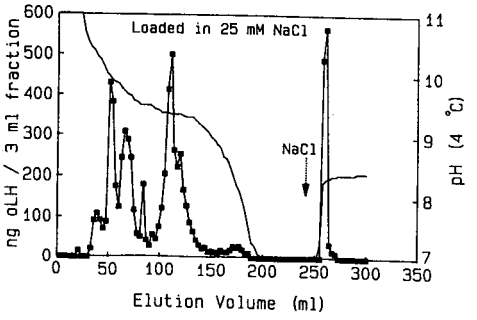

Fig. 5. Elution of 20 μg purified oLH applied in 25 mM NaCl on a pH 10.5–7.0 chromatofocusing gradient. See Fig. 4 and the text for remaining experimental details.

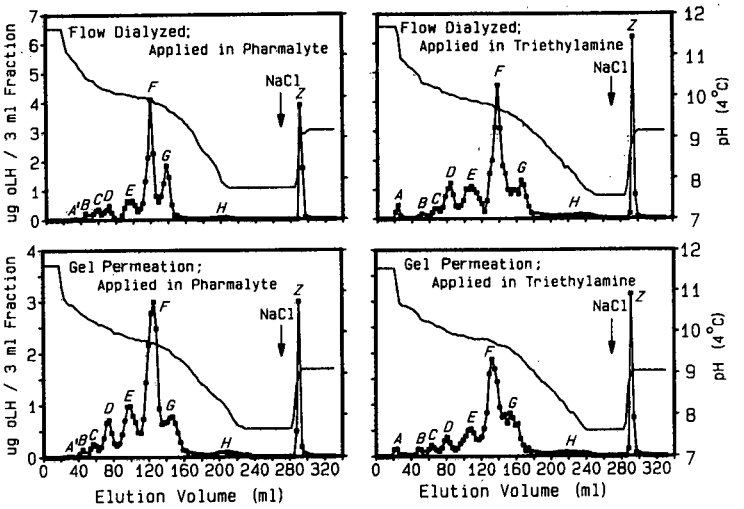

Fig. 6. Chromatofocusing elution profiles of the immunoreactive oLH in aliquots of a pituitary extract prepared by flow dialysis (upper panels) or gel permeation (lower panels) and applied to the resin in 1:45 Pharmalyte 8-10.5–HCl, pH 7.0 (left-hand panels) or 25 m*M* triethylamine–HCl, pH 11.0 (right-hand panels). Note that each sample loaded in triethylamine exhibited a small, but detectable, flow-through peak (denoted as A) but that samples applied in Pharmalyte did not. See Fig. 3 or the text for remaining experimental details.

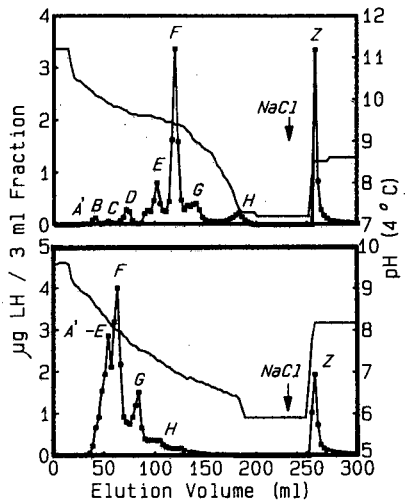

Fig. 7. Chromatofocusing elution profile of the immunoreactive LH in a bovine pituitary extract on pH 10.5–7 (top panel) and pH 9–6 (bottom panel) gradients. Aliquots (1 ml) of a pituitary extract from a steer were desalted by flow dialysis and applied in the corresponding elution buffer. Each peak of immunoreactive bLH was identified with letters beginning with the most basic isoform [2,5,10]. Note that the five most basic forms of bLH (peaks A′ to E) eluted as a shoulder on peak F when chromatofocused on a pH 9–6 gradient. See text for remaining experimental details.

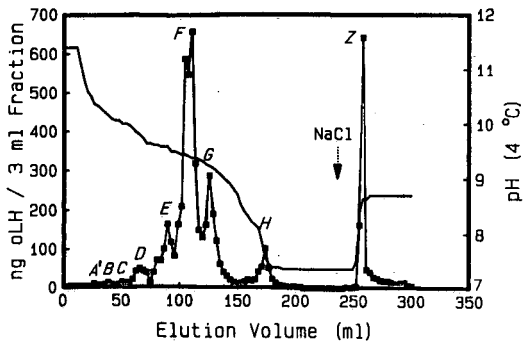

Fig. 8. Chromatofocusing elution profile of the immunoreactive oLH in the pituitary extract of a dihydrotestosterone-implanted wether [2]. Ionic components were removed by flow dialysis and the proteins were reconstituted in Pharmalyte 8-10.5–HCl, pH 7.0. Several other pituitary extracts from rams or androgen-implanted wethers [2] also were devoid of flow-through peaks when prepared by flow dialysis and applied in Pharmalyte (data not illustrated). See Fig. 3 and the text for remaining experimental details.

flow-through peaks). In addition small amounts (typically $\leqslant 3\%$) of the immunoreactive oLH eluted as the pH gradient approached its lower-limiting plateau. Forms eluting in this region are denoted as peak H in the figures. Thus, when pituitary extracts are prepared by dialysis, flow dialysis, ion-retardation chromatography, gel permeation or ultrafiltration and *applied to the chromatofocusing columns in Pharmalyte*, no immunoreactive oLH is observed as a flow-through peak. These results suggest *that the buffer in which the oLH in a pituitary extract* is applied to the chromatofocusing resin has a significant effect on the pattern of oLH isoforms observed. It also appears that the additional proteins in pituitary extracts, *versus* the 20 μg of purified oLH, contribute to the degree of binding even though both types of samples were supplemented with 7–9 mg of exogenous proteins.

The results of these experiments suggested that the PBE 118 resin exhibited a reduced binding capacity when samples were applied in triethylamine. In order to obtain additional information about the characteristics of this resin, a titration curve was prepared (Fig. 9). In the pH 10–7 range, the observed exchange capacity of the

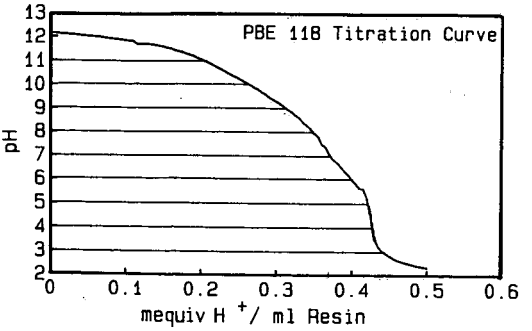

Fig. 9. Titration curve for PBE 118 chromatofocusing resin. A 10-ml volume of resin as a 10% (v/v) suspension in 1 *M* KCl was adjusted to a pH > 12 with 10 *M* NaOH and then titrated with 0.5 *M* HCl. The resulting pH was measured with a Ross pH electrode.

resin was similar to that reported by the manufacturer, *i.e.* $\approx$ 50 μmol pH unit^{-1} ml^{-1}. Nonetheless, the titration curve suggests that the amount of positive charge and hence effective binding capacity of the resin decreased as pH increased. Furthermore, above pH 11, this drop was rather rapid. Under the experimental conditions employed, the pH of the triethylamine was adjusted to 11.0 at room temperature using a Ross electrode. At 4°C, the temperature used for chromatofocusing, the pH of this buffer was approximately 11.4. Furthermore, the microenvironment of an anion exchanger may be one pH unit higher than the surrounding buffer [11]. These considerations plus the experimental observations suggest the PBE 118 chromatofocusing resin exhibits a somewhat limited binding capacity at high pH values. They also explain why proteins bound to the resin more effectively when applied in Pharmalyte at pH 7.0.

Because the above results suggested that ovine pituitary extracts contained lesser amounts of extremely basic forms of oLH than was previously thought, the possibility of substituting pH 9–6 gradients was examined (Fig. 7). Aliquots of a bovine pituitary extract, which exhibited a pattern of isohormones similar to those in ovine pituitary extracts [10,12], were utilized in this experiment. When chromatofocused on a pH 10.5–7 gradient, no bLH was observed as a flow-through peak. Similarly, no flow-through peak was observed on the pH 9–6 gradient. However, it did appear that the five most basic forms of bLH (peaks A′ through E) eluted as a shoulder on the major peak F when the pH 9–6 gradient was used. Thus, it appears that pH gradients starting at a relatively high pH are required to analyze the charge isomers of ovine and bovine LH by chromatofocusing.

In order to further clarify the presence or absence as well as the percentage of extremely basic forms of oLH in the pituitaries of rams and androgen-treated wethers [2], aliquots of samples which previously exhibited significant amounts of oLH in a flow-through peak were re-analyzed under conditions where the sample was loaded in Pharmalyte. A representative chromatofocusing profile is illustrated in Fig. 8. In each case, no immunoreactive oLH was observed as a flow-through peak (A) but a small percentage (typically $<2\%$) eluted as a peak (coded as peak A′) between the flow through and peak B. This suggests that the percentage of extremely basic forms of oLH was previously overestimated [2], in part, because of the specific experimental conditions utilized for sample preparation and chromatofocusing.

DISCUSSION

Chromatofocusing, the chromatographic analog of isoelectric focusing [13], has proven effective in analyzing the charge isomers of the glycoprotein hormones [1–5]. Both the theory and practical aspects of the technique have been described [6,13]. Nonetheless, it has been our experience that the general guidelines [6,13] do not universally apply to all pH gradients and that this is especially true for gradients starting at very basic pH values. The general instructions suggest that proteins may be applied to the chromatofocusing resin in either the "start" or elution buffer [6,13]. While true for most pH gradients [7], this study suggests that the sample application buffer is an important consideration for pH 10.5–7 gradients.

When chromatofocusing was implemented in our laboratory, gel permeation was chosen as a means to equilibrate the proteins in the desired buffer [6]. Triethyla-

mine was chosen over the elution buffer (1:45 Pharmalyte 8-10.5–HCl, pH 7.0) simply because it would be extremely expensive to routinely use diluted Pharmalyte for gel permeation. A column volume of 20 ml, with a stated capacity to handle approximately 200 mg protein [6], was selected because this yielded a theoretical capacity approximately ten-fold larger than the amount of protein to be applied to the columns (including both the endogenous proteins in pituitary extracts and the exogenous proteins added prior to sample preparation). With this approach, some of oLH in pituitary extracts flowed through the columns unrestricted and this was previously interpreted to indicate the presence of extremely basic forms [2]. The results of the present studies suggest that these flow-through peaks *do not* represent extremely basic forms but primarily result from incomplete binding of the hormone to the resin when it is applied in triethylamine. The seemingly contrasting results obtained with purified oLH and oLH in pituitary extracts can be attributed to the quantity of hormone and other basic proteins applied to the columns. Rather than simply using the stated exchange capacity to calculate column volume, it would appear desirable to experimentally determine the binding capacity of the resin at the pH of sample application.

There are also simple alternatives to verify that the separation is being effected as anticipated. For example, the addition of the colored proteins cytochrome *c* and myoglobin, which have isoelectric points of $\approx$ 10.6 and $\approx$ 7.2, respectively, provide a readily visible check on binding of the proteins to the resin. When applied in either triethylamine or Pharmalyte, cytochrome *c* was retarded slightly and eluted a few fractions after the flow-through peak. However, it generally eluted as a broader peak when applied in triethylamine. When samples were applied in Pharmalyte, the myoglobin bound tightly to the top of the column as the sample was applied. However, when applied in triethylamine, the myoglobin frequently migrated a variable distance onto the column before it began to focus. Nonetheless, its elution position was similar in both cases. Interestingly, on pH 10.5–7 gradients myoglobin elutes approximately two pH units above its true isoelectric point [14]. During chromatofocusing proteins elute according to their surface charge characteristics but not necessarily at their isoelectric points [13]. Thus, cytochrome *c* and myoglobin serve primarily to verify binding and establish reproducibility. If oLH applied in triethylamine, similar to myoglobin, migrated variable distances through the column before binding, it is likely that variable amounts of oLH in pituitary extracts simply moved completely through the column without binding and were detected as flow-through peaks.

In subsequent experiments, Grotjan and Zalesky [9] have utilized column volumes as small as 3.0 ml and noted quantitative binding (*i.e.*, no LH observed as a flow-through peak) of the LH in a 0.5-ml aliquot of an ovine or bovine pituitary extract supplemented with 2 mg each of cytochrome *c*, myoglobin and ovalbumin if the sample is applied in Pharmalyte. These observations provide further experimental evidence consistent with the above hypothesis.

In order to further characterize the revised chromatofocusing protocol, the subsequent paper [5] examines the misclassification errors associated with individual peaks for a pituitary extract prepared by flow dialysis and applied in Pharmalyte. It demonstrates that chromatofocusing is an effective method for separating the charge isomers of oLH when utilized under the slightly revised sample preparation and application conditions developed and validated herein. In view of the present findings, were are currently re-assessing the effects of castration and androgen-replacement on the pattern of oLH isohormones.

ACKNOWLEDGEMENTS

We thank Drs. O. D. Sherwood, D. N. Ward and L. E. Reichert, Jr. as well as the NIH Pituitary Hormone Distribution Program for providing the hormones utilized in this study. Excellent technical assistance was provided by Kirsten Peterson, Valarie Haack, Alycia Zalesky and Janet Glen. This study was supported, in part, by funds from the Parsons Endowment of the University of South Dakota School of Medicine and NIH grant HD18879. Published as paper No. 9382 Journal Series of the Nebraska Agricultural Research Division, Institute of Agriculture and Natural Resources.

REFERENCES

1 B. A. Keel and H. E. Grotjan, Jr., *Microheterogeneity of Glycoprotein Hormones*, CRC Press, Boca Raton, FL, 1989.
2 B. A. Keel, B. D. Schanbacher and H. E. Grotjan, Jr., *Biol. Reprod.*, 36 (1987) 1102.
3 S. C. Chappel, C. L. Bethea and H. G. Spies, *Endocrinology*, 115 (1984) 452.
4 W. F. P. Blum, G. Riegelbauer and D. Gupta, *J. Endocrinol.*, 105 (1985) 17.
5 H. E. Grotjan and D. D. Zalesky, *J. Chromatogr.*, 549 (1991) 153.
6 *Chromatofocusing with Polybuffer and PBE*, Pharmacia/LKB Technical Bulletin, 1980.
7 H. E. Grotjan, unpublished results.
8 O. D. Sherwood, H. J. Grimek and W. H. McShan, *Biochim. Biophys. Acta*, 221 (1970) 87.
9 H. E. Grotjan and D. D. Zalesky, in preparation.
10 D. D. Zalesky and H. E. Grotjan, *Dom. Anim. Endocrinol.*, 8 (1991) 179.
11 R. K. Scopes, *Protein Purification: Principles and Practice*, Springer, New York, 1982.
12 D. D. Zalesky and H. E. Grotjan, *Biol. Reprod.*, 44 (1991) 1016.
13 T. W. Hutchens, in J.-C. Janson and L. Ryden (Editors), *Protein Purification: Principles, High Resolution Methods, and Applications*, VCH, New York, 1989, Ch. 5, p. 149.
14 H. E. Grotjan, S. E. DesJarlais and S. E. Rand, in W. W. Chin and I. Boime (Editors), *Glycoprotein Hormones*, Serono Symposia, USA, Norwell, MA, 1990, Ch. 4, p. 27.

Journal of Chromatography, 549 (1991) 153–158
Elsevier Science Publishers B.V., Amsterdam

CHROM. 23 325

Ovine luteinizing hormone

VI. Analysis of the misclassification errors in the separation of intrapituitary isohormones by chromatofocusing

H. EDWARD GROTJAN* and DOUGLAS D. ZALESKY
Animal Science Department, University of Nebraska, Lincoln, NE 68583-0908 (USA)
(First received October 3rd, 1990; revised manuscript received March 11th, 1991)

ABSTRACT

Luteinizing hormone (LH) in extracts of the ovine (o) anterior pituitary gland elutes as eight or more distinct peaks when analyzed by chromatofocusing on pH 10.5–7 gradients [Keel *et al., Biol. Reprod.*, 36 (1987) 1102]. In order to examine the efficacy of this approach to identify the distinct charge isomers of oLH, a pool of pituitary extracts was de-salted by flow dialysis and chromatofocused on a pH 10.5–7 gradient. The immunoreactive oLH eluted in nine distinct peaks which were coded with letters beginning with the most basic form. The fractions corresponding to each peak were pooled, dialyzed and lyophilized. Each peak was then re-chromatofocused on a pH 10.5–7 gradient except for the immunoreactive oLH eluting in peak A′ because of the small amount present in this peak. Each peak, except for F and H, also consisted of a small percentage of immunoreactive oLH associated with adjacent peaks. This was plausible because chromatofocusing does not generally yield baseline resolution of peaks. Peak H eluted in a broad manner and was contaminated with significant amounts of isohormones F, G and Z. In contrast, peaks B, E, F, G and Z almost completely eluted in the anticipated regions. Thus, it appears that analysis of oLH charge isomers by chromatofocusing yields minimal misclassification errors and that the misclassification errors observed are associated with molecular forms which comprise a relatively small percentage of the oLH in pituitary extracts.

INTRODUCTION

Many, if not all, of the glycoprotein hormones exhibit charge heterogeneity [1–4]. One method frequently used to analyze the charge isomers of a particular glycoprotein hormone is chromatofocusing [1–4]. Although this method has been utilized by a variety of researchers, only a limited number have examined the efficacy of this approach by re-chromatofocusing each peak (for example, see Blum *et al.* [4]). In this study, we examined the ability of pH 10.5–7 chromatofocusing gradients to resolve the intrapituitary isohormones of ovine luteinizing hormone (oLH) as judged by re-chromatofocusing each peak identified in the original elution profile.

0021-9673/91/$03.50

MATERIALS AND METHODS

Extraction of anterior pituitary tissues

Anterior pituitary from ewes were extracted in a Tris-buffered saline solution supplemented with 0.5% (v/v) Triton X-100 and protease inhibitors [3]. Extracts were centrifuged at 100 000 *g*, aliquoted and frozen at −70°C. To prepare the original profile, four 0.5-ml aliquots obtained from different animals were pooled and supplemented with 3 mg cytochrome *c* and 4 mg myoglobin.

Chromatofocusing and radioimmunoassays

The pool of pituitary extract was de-salted by flow against water, diluted to 2% Pharmalyte 8-10.5–HCl, pH 7.0 (Pharmacia/LKB, Piscataway, NJ, USA), and chromatofocused on a pH 10.5–7 gradient using 20 ml of resin as previously described [3]. The immunoreactive oLH in each fraction was determined by radioimmunoassay [3]. This profile was divided into distinct peaks which were coded with letters beginning with the most basic form [1,3] (Fig. 1). The fractions corresponding to each peak were pooled, supplemented with 4 mg cytochrome *c* plus 3 mg myoglobin and dialyzed in SpectraPor 1 dialysis tubing (6000–8000 mol.wt. cut off; Spectrum Medical Industries, Los Angeles, CA, USA) against several changes of distilled water. After lyophilization, the resultant proteins from each peak were redissolved in 1:45 Pharmalyte

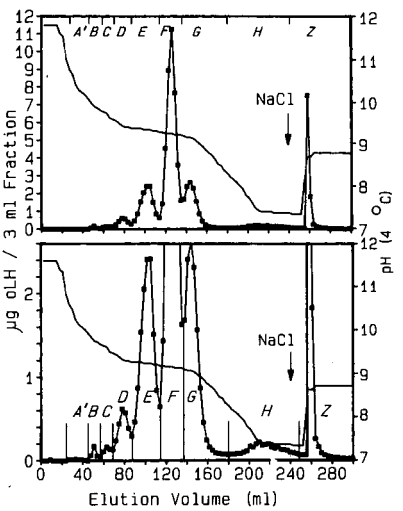

Fig. 1. Elution profile of the immunoreactive oLH in a pool of pituitary extracts chromatofocused on a pH 10.5–7 gradient. A pool of pituitary extracts (2 ml equivalent to 200 mg tissue) was supplemented with 3 mg cytochrome *c* plus 4 mg myoglobin, de-salted by flow dialysis against water and diluted to 2% Pharmalyte 8-10.5–HCl, pH 7.0. The column was eluted with diluted Pharmalyte at 10 ml/h and 3-ml fractions were collected. The oLH concentration in each fraction (■) was quantitated by radioimmunoassay and the pH gradient (solid line) was monitored with a flow-through pH monitor. Each peak of immunoreactive oLH was coded with a letter beginning with the most basic form [1,3]. Materials bound at the lower-limiting pH of 7.0 were eluted with 1 *M* NaCl and coded as peak Z. The same data is plotted in both panels except that the ordinate has been expanded to illustrate peaks with lower amounts of oLH. The distribution of oLH among the peaks is given in Table I. Remaining experimental details are presented in the text.

8-10.5–HCl, pH 7.0, and re-chromatofocused on pH 10.5–7 gradients. Columns containing 20 ml resin were utilized for peaks D–Z while columns with volumes of 10 ml resin were utilized for peaks B and C. Peak A′ was not re-chromatofocused because of the extremely small amount of immunoreactive oLH in this peak. Columns (10 ml), 26 × 0.7 cm I.D., were eluted at 4 ml/h and fractions of 1.5 ml were collected. Each fraction was neutralized with a concentrated Tris–HCl solution as described in the previous paper [3]. The oLH concentration of each fraction was again determined by radioimmunoassay [3]. In all gradients, the pH was monitored with a Pharmacia/LKB pH monitor. All dialysis and chromatographic procedures were performed at 4°C.

RESULTS AND DISCUSSION

When a pool of ovine pituitary extracts was chromatofocused on a pH 10.5–7 gradient, the immunoreactive oLH eluted in nine distinct peaks (Fig. 1). These peaks were coded with letters beginning with the most basic form [1,3]. In this experiment, 127.2 μg oLH were loaded on the column and 81.9 μg were quantitated in the various fractions for a recovery of 64%. The distribution of oLH among these peaks is given in Table I. In general terms, the distribution of immunoreactive oLH was comparable to that previously observed [1,2] when materials eluting in the flow-through region were excluded from the calculations [3].

In order to examine the efficacy of chromatofocusing to separate and identify the distinct charge isomers of oLH, each peak from the original elution profile was re-chromatofocused on a pH 10.5–7 gradient (Figs. 2–9). Because of the relatively small amounts of oLH present in peaks B and C, they were re-chromatofocused on 10- rather than 20-ml columns. More than 90% of peak B re-focused as isohormone B (Fig. 2; Table I). Approximately 75% of peaks C (Fig. 3), D (Fig. 4) and E (Fig. 5) returned in the expected regions with the remainders primarily eluting as more acidic

TABLE I

ELUTION pH VALUES AND DISTRIBUTION OF IMMUNOREACTIVE oLH IN THE ORIGINAL CHROMATOFOCUSING PROFILE AND AFTER RE-CHROMATOFOCUSING

Peak	Original profile		Upon re-chromatofocusing		
	Elution pH (4°C)	Amount eluted in this peak (%)	Elution pH (4°C)	Re-focused in this peak (%)	Immunoreactive oLH recovered (%)
A′	10.38	0.1	N.D.[a]	N.D.	N.D
B	9.87	0.4	10.17	94	87
C	9.72	0.7	9.99	74	59
D	9.42	3.1	9.36	77	101
E	9.33	15.6	9.57	68	80
F	9.24	47.8	9.33	98	97
G	9.15	15.7	9.21	89	60
H	≈7.4	3.9	≈7.9	24	72
Z	<7.40	12.5	<7.40	81	61

[a] N.D. = Not determined.

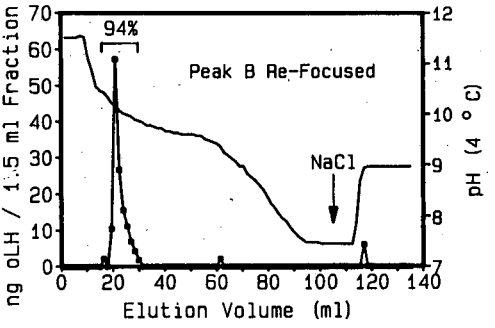

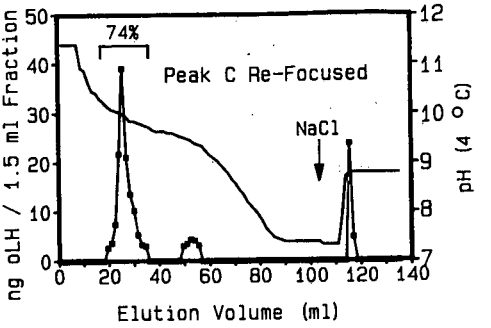

Fig. 2. Re-chromatofocusing of peak B from the original profile on a pH 10.5–7 gradient using a 10-ml column. The column was eluted at 4 ml/h and 1.5-ml fractions were collected. See the text and legend of Fig. 1 for experimental details.

Fig. 3. Re-chromatofocusing of peak C from the original profile on a pH 10.5–7 gradient using a 10-ml column. See the text and legends of Figs. 1 and 2 for experimental details.

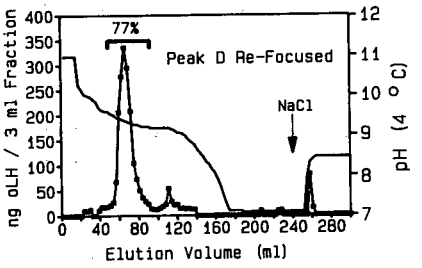

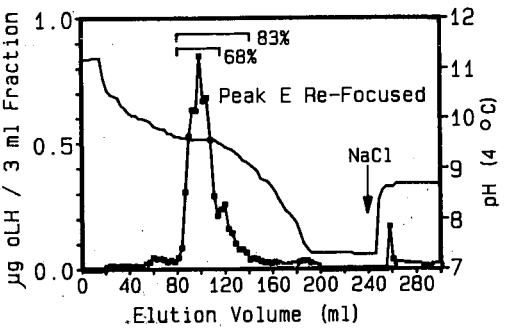

Fig. 4. Re-chromatofocusing of peak D from the original profile on a pH 10.5–7 gradient. See the text and legend of Fig. 1 for experimental details.

Fig. 5. Re-chromatofocusing of peak E from the original profile on a pH 10.5–7 gradient. See the text and legend of Fig. 1 for experimental details.

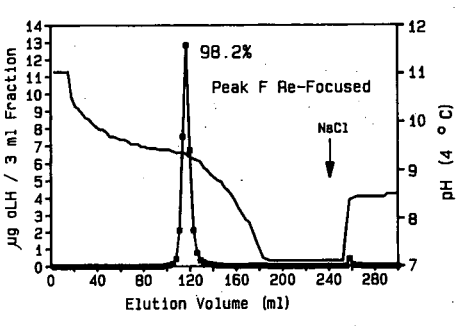

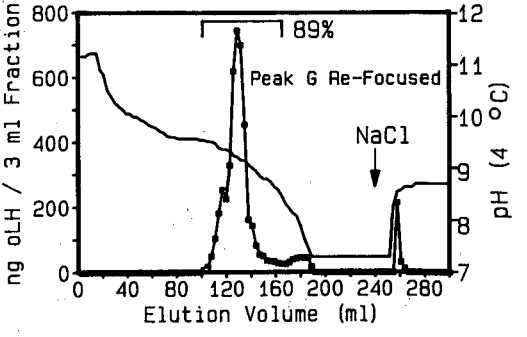

Fig. 6. Re-chromatofocusing of peak F from the original profile on a pH 10.5–7 gradient. See the text and legend of Fig. 1 for experimental details.

Fig. 7. Re-chromatofocusing of peak G from the original profile on a pH 10.5–7 gradient. See text and legend of Fig. 1 for experimental details.

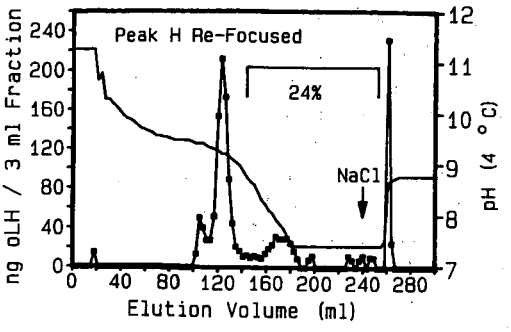

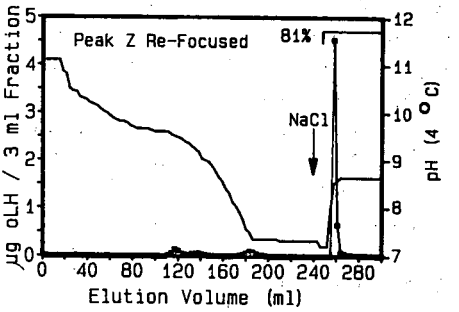

Fig. 8. Re-chromatofocusing of peak H from the original profile on a pH 10.5–7 gradient. Note that slightly less than 25% re-focused in the expected region. See the text and legend of Fig. 1 for experimental details.

Fig. 9. Re-chromatofocusing of peak Z from the original profile on a pH 10.5–7 gradient. See the text and legend of Fig. 1 for experimental details.

forms. The pH of the tube containing the highest oLH concentration in peak E was slightly higher when re-chromatofocused than in the original profile (Table I). This was attributed to slight variations in the pH gradients between chromatographic runs, particularly as monitored with a flow-through electrode at 4°C, rather than as a shift in elution position. Some of the oLH in peaks C, D and E were bound to the column when re-chromatofocused, but eluted with 1 *M* NaCl. The absolute amounts of oLH eluting in this fashion were relatively small and may represent oLH non-specifically bound to the resin at low ionic strength.

Peak F was the predominant form and comprised almost 50% of the immunoreactive oLH in the pituitary (Fig. 6, Table I). When this peak was re-chromatofocused, essentially all of the immunoreactive oLH was again recovered in a peak corresponding to the elution position in the original profile (Fig. 6). The second-most abundant form of immunoreactive oLH was peak G. When peak G was re-chromatofocused, approximately 90% eluted in the anticipated region (Fig. 7) with the remainder eluting in the more acidic peaks H and Z.

When we revised our method slightly and began loading the pituitary extracts in Pharmalyte rather than triethylamine [3], a noticeable amount of oLH eluted as the pH gradient dropped off sharply. This peak was coded as H and is the fifth most abundant form of oLH observed in the original profile (Fig. 1, Table I). Typically, peak H elutes in a broad band as the pH gradient reaches the lower limit and, frequently, some oLH continues to elute even though the pH gradient has plateaued. When the immunoreactive oLH eluting in this manner (peak H) was re-chromatofocused only about 25% again eluted in the anticipated region (Fig. 8). Peak H appears to be primarily composed of a mixture of isohormones G and Z as well as small amounts of F. As noted previously [2,5], a large majority of the materials bound to the column at the lower-limiting pH of 7.0 (peak Z) again bound when re-chromatofocused (Fig. 9).

In any chromatographic system, the possibility of selective losses exists. The recovery of the oLH in each peak of the original profile (Table I) was similar to those

typically observed (60–85%) when intrapituiraty oLH is chromatofocused [1–3,5] suggesting there were no losses of specific isoforms.

Based on the data presented above, the charge isomers of oLH are adequately resolved by chromatofocusing. Some peaks were contaminated with forms eluting in adjacent regions but this is because chromatofocusing does not generally yield baseline resolution of the peaks of immunoreactive oLH. It would appear that there are at least eight distinct charge isomers of intrapituitary oLH which elute in the peaks coded A'–G and Z in the figures. The primary peak which appears to be subject to misclassification is peak H. Only 25% of peak H re-chromatofocused in the anticipated region. Peak H is somewhat unusual because it elutes rather broadly as the pH gradient drops sharply and continues to elute even after the pH gradient has plateaued. Peak H may represent molecular forms of oLH which are weakly bound at the lower-limiting pH of 7.0 rather than a unique molecular form.

If one considers the percentage of hormone originally classified and re-chromatofocused in each respective peak, approximately 86% of the oLH was correctly classified in the original profile. Furthermore, the misclassified portion was generally associated with adjacent peaks. Thus, it appears that analysis of the charge isomers of oLH by chromatofocusing yields minimal misclassification errors and those which are observed are associated with molecular forms which comprise a relatively small percentage of the oLH in pituitary extracts. Thus, chromatofocusing is an effective method to separate the charge isomers of the glycoprotein hormones.

ACKNOWLEDGEMENTS

We thank Drs. D. N. Ward and L. E. Reichert, Jr. as well as the NIH Pituitary Hormone Distribution Program for providing the hormones utilized in this study. Excellent technical assistance was provided by Valarie Haack and Alycia Zalesky. This study was supported, in part, by NIH grant HD18879. Published as paper No. 9381 Journal Series of the Nebraska Agricultural Research Division, Institute of Agriculture and Natural Resources.

REFERENCES

1 B. A. Keel, B. D. Schanbacher and H. E. Grotjan, Jr., *Biol. Reprod.*, 36 (1987) 1102.
2 B. A. Keel and H. E. Grotjan, Jr., *Microheterogeneity of Glycoprotein Hormones*, CRC Press, Boca Raton, FL, 1989.
3 H. E. Grotjan, B. D. Schanbacher and B. A. Keel, *J. Chromatogr.*, 549 (1991) 141.
4 W. F. P. Blum, G. Riegelbauer and D. Gupta, *J. Endocrinol.*, 105 (1985) 17.
5 B. A. Keel and H. E. Grotjan, Jr., *Anal. Biochem.*, 142 (1984) 267.

Journal of Chromatography, 549 (1991) 159–174
Elsevier Science Publishers B.V., Amsterdam

CHROM. 23 342

Experimental design for the optimization of the separation of aliphatic amines by ion chromatography

J. VIALLE*, P. NAVARRO and TRAN THI NGUYET
Service Central d'Analyse du CNRS, BP 22, 69390 Vernaison (France)
P. LANTERI
Laboratoire de Synthèse Organique Appliquée–ESCIL, Université Lyon I, 43 Bd. du 11 novembre 1918, 69622 Villeurbanne Cedex (France)
and
R. LONGERAY
Service Central d'Analyse du CNRS, BP 22, 69390 Vernaison, and Laboratoire de Synthèse Organique Appliquée–ESCIL, Université Lyon I, 43 Bd. du 11 november 1918, 69622 Villeurbanne Cedex (France)
(First received March 27th, 1990; revised manuscript received March 26th, 1991)

ABSTRACT

The analysis of aliphatic amines in industrial solutions by reversed-phase chromatography presents some drawbacks owing to interferences with system peaks and other compounds in the sample. This technique is applicable only to simple mixtures. Ion chromatography, commonly used for inorganic ions, has been applied to the separation of aliphatic amines and offers the advantage of specificity for ionizable compounds and can be associated with conductivity detectors. The use of alkali metal ions as eluting ions improves the separation. The addition of an organic solvent to the aqueous mobile phase improves the efficiency for long-chain amines. Optimization using chemometric methodology is presented for the separation of alcoholamines and primary, secondary and tertiary aliphatic amines using an ion-exchange silica-based column. The influence of the various components of the mobile phase was studied.

INTRODUCTION

Industrial solutions used as descalers, corrosion inhibitors and surfactants often contain primary, secondary and tertiary amines and there is a need to know and monitor the composition of these solutions, but few analytical methods are fully satisfactory. Many high-performance liquid chromatographic (HPLC) systems used for separations without derivatization of organic compounds of an ionic character employ reversed-phase (RP) HPLC in the form of either ion-suppression or ion-pair chromatography. Both techniques are successful with acidic compounds, but their application to the separation of cationic molecules encounters many difficulties. The high-pH mobile phases necessary for ion suppression of basic compounds are incompatible with silica bonded packings, and the multiple equilibrium which governs the ion-pairing mechanism on reversed-phase packings gives rise to system peaks which often interfere with the separated peaks. Moreover, RP-HPLC is not a specific

0021-9673/91/$03.50

means of separating amines and interferences from non-ionic species can occur when analysing complex samples. Nevertheless, some examples of separations of basic compounds using these techniques have been published, particularly in the biochemistry field for catecholamines [1] and to a lesser exent amino acids [2,3].

For aliphatic amines, there are numerous examples of separations of non-ionic derivatized compounds by RP-HPLC [4–7], but in contrast very few examples of suitable separations without derivatization have been reported [8]. Very often in these instances only a small number of compounds are considered and poor efficiencies and low resolutions are obtained. Depending on the origin of the reversed-phase column packing, differences in the end-capping procedure applied to the various bonded silicas can cause variations in the quality of the separation from one column to another.

Another approach to the chromatographic analysis of amines is ion-exchange chromatography (IEC). Its use in the separation of amino acids and biogenic amines has been reported for many years using commercial devices [9–11]. However, despite reasonable analytical results, these methods were complex and tedious, the analysis time was often long and the separation was not efficient. Since the late 1970s, the performance of ion-exchange columns has greatly increased with the advent of ion chromatography (IC) for the separation of inorganic ions, but so far applications to organic ions have not been frequent.

Among the numerous HPLC methods that have been developed for the separation and determination of amino compounds, some are very well adapted for application to particular compounds, but most of the more recent ones involve a separation after precolumn derivatization. Indeed, there has always been a lack of a more general HPLC procedure for the separation of amines whatever the organic moiety in these cationic molecules. With aliphatic amines another problem is the poor detectability of these compounds owing to the absence of any chromophoric groups in the molecule.

This paper deals with the separation of primary, secondary and tertiary aliphatic amines. Amines are often present in samples containing many other organic components that can interfere with their separation. The method presented here is based on IEC as this can be a specific separation mode for these compounds. For the same reasons, conductivity is used as a specific detection mode. The influence of the various components of the mobile phase that can affect the separation of the amines was studied using a chemometric approach.

EXPERIMENTAL

Reagents

All amines and solvents were of high-purity grade from Prolabo (Paris, France) and Fluka (Mulhouse, France). Water was deionized using an Elgastat (High Wycombe, UK) Spectrum apparatus. The injected solutions were prepared by dissolving the amines in pure water if possible or in water plus an organic solvent when necessary to effect solubility.

As the mobile phase is a mixture of water and an organic solvent, any reference to pH corresponds to that of the aqueous part of the mobile phase adjusted with nitric acid. To this aqueous solution was then added the organic solvent containing nitric

TABLE I

MIXTURES ANALYSED

No.	Amine	Mixture M_1: amount (g) in 10 ml water solution	Mixture M_2: amount in 10 ml acetonitrile–water (25:75) solution
1	Ethanolamine	0.010	–
2	Methylamine	0.020	–
3	Diethanolamine	0.022	–
4	Ethylamine	0.028	–
5	Triethanolamine	0.036	0.0365
6	*n*-Propylamine	0.036	–
7	N-Methyldiethanolamine	0.042	0.042
8	*n*-Butylamine	0.044	–
9	Diethylamine	0.049	–
10	Trimethylamine	0.080	0.080
11	Cyclohexylamine	0.078	–
12	Triethylamine	0.073	0.073
13	1-Aminopropanolamine	–	0.057
14	Benzylamine	–	0.088
15	Dipropylamine	–	0.111

acid at the same concentration as in the acidified water. When necessary, alkali metal salts were then directly dissolved in the mobile phase and the amount of cation added is expressed as the volume of a 1 mol/l solution added to 1 l of mobile phase.

Amine solutions

The separation of amines was performed by studying the optimization of the separation of two different mixtures, M_1 and M_2, listed in Table I. These mixtures, which contained some amines in common, were chosen from among fifteen different compounds and they were made up so as to contain alcoholamines, primary, secondary and tertiary amines. Long-chain amines such as octylamine could not be included in these mixtures because they were poorly soluble in the mobile phases.

Choice of column

As regards organic cations, the separation of some short-chain aliphatic amines has been described using conditions similar to that used for metal cations [12], but there are few examples of amine separations depending on the length of the organic moiety [13]. Amino compounds are charged species with dimensions and a lipophilic character that make them analogous to metal complexes. Therefore, the separation of amines was performed on the same ion-exchange column as for the complex species [14,15], that is, on a high-capacity silica-based exchanger.

Mobile phase

As amines have both ionic and lipophilic character, their retention depends on two distinct mechanisms: ion exchange and lipophilic interaction with the alkyl chain bearing the ionic sites. Therefore, the mobile phase is made up in such a way as to use the two mechanisms to control the elution. As regards the ion-exchange mechanism, the strength of a simple acidic solution, even at low pH, is not sufficient to elute

amines with a suitable efficiency (see Table II, experiment 1). It is then necessary to use more strongly eluting cations than the proton and therefore alkali metal salts were added to the mobile phase. Lipophilic interactions are controlled by adding an organic solvent to the mobile phase, and methanol, tetrahydrofuran (THF) and acetonitrile were tested. It must be noted that, as conductivity detection is used, the higher the efficiency of the solvent, the less will be its amount in the mobile phase and the better will be the detection sensitivity.

Instrumentation

The ion-exchange column was a Nucleosil 5A (Macherey, Nagel & Co., Düren, Germany) column (25 cm long × 0.46 cm I.D.) of 5-μm particle size. Mobile phase was pumped at a flow-rate of 1 ml/mn by a Gilson (Villiers le Bel, France) Model 302 reciprocating pump and samples were injected via a Rheodyne Model 7010 valve equipped with a 20-μl loop. To prevent bubbling, the mobile phase was continuously degassed with helium during all the experiments.

The mobile phase conductance was measured with a Wescan 213 A conductivity detector (Techmation, Paris, France). The conductivity cell and the column were placed in a oven regulated at 30°C.

Chemometric methodology

To optimize the separation of a number of compounds, the traditional approach would consist in studying separately each factor which influences the separation. For each retained factor, the capacity factor and the selectivity would be studied for each pair of compounds. On such a basis, a recent and exhaustive study of the separation of four isomeric compounds taking into account three experimental factors led to the measurement of nearly 200 chromatograms in order to achieve a perfect routine separation of the four isomers [16].

A chemometric approach to such a problem is based on the use of an optimum (in a statistical sense) matrix of experiments which allows the simultaneous variation of all the experimental factors studied. This, associated with a methodological approach, gives rise to a number of experiments which can be drastically reduced in comparison with the traditional methodology, while providing the optimum information. Chemometric methods are based on the explicit use of a mathematical model linking the observed response Y and the influencing factors X_i. Variables are usually "coded" to have a range of variation from -1 to 1. Generally, a polynomial relationship is satisfactory. For example, the simplest model is $Y = b_0 + \sum b_i X_i$, where the b_i coefficients represent the linear effects of the factors X_i on the response Y.

In this work, the qualitative or quantitative experimental factors which are likely to control the separation of amines include the nature and amount of the solvent added to the aqueous mobile phase, the nature and concentration of the eluting cation, the nature of the anions bound to this cation and the pH. The study consisted of three parts: an exploratory study in order to define a likely experimental domain, a screening of the influential factors, including qualitative factors, and an optimization of the factors that have a quantitative effect on the separation.

RESULTS AND DISCUSSION

Preliminary study

Preliminary information on the influence of an alkali metal and on the importance of the addition of organic solvents on the retention of various amino compounds is shown in Figs. 1 and 2. However, in order to adopt a chemometric process rather than a traditional approach, a series of experiments were carried out as displayed in Table II. The factors studied were the nature and the amount of the organic solvent, the nature of the eluting cation and of the corresponding co-ion and their concentrations. As it had been found that the lower the pH, the faster is the separation (a decrease in pH from 2.6 to 2.0 give a 25% decrease in the retention time), the pH was kept at the lowest value compatible with the column, *i.e.*, 1.5.

The responses of interest in this study were the retention time of three particular amines: ethanolamine [$Y^{(a)}$], ethylamine [$Y^{(b)}$] and diethylamine [$Y^{(c)}$]. The experimental conditions and the values $Y_j^{(u)}$ (jth experiment; u = a, b or c) obtained for these preliminary experiments are shown in Table II.

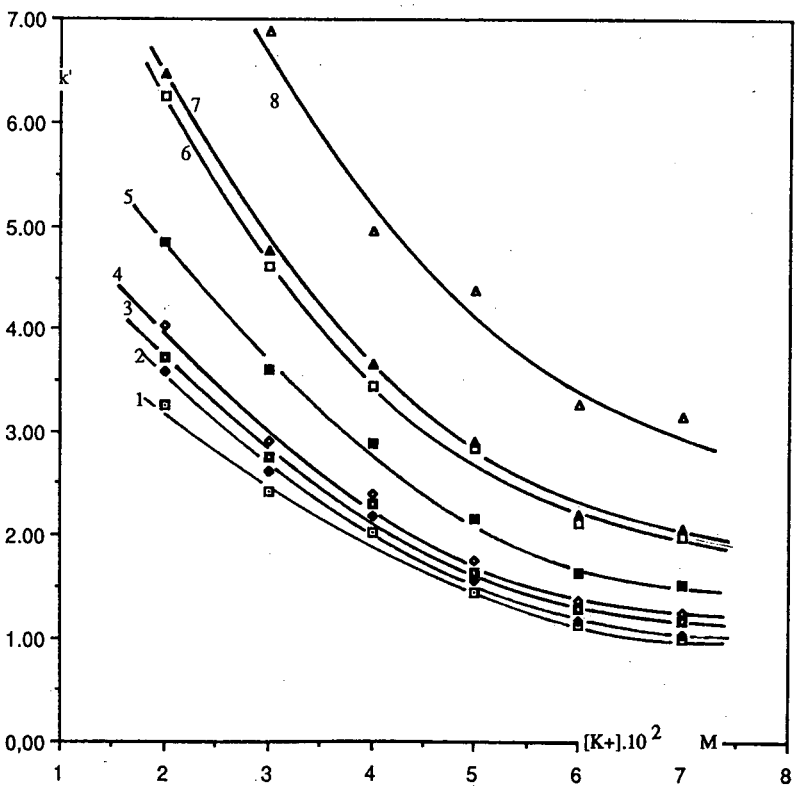

Fig. 1. Influence of K^+ concentration on the retention of amines. Mobile phase, water–methanol (64:36); KNO_3 solution pH, 1.5; column, Nucleosil SA (250 × 4.6 mm I.D.). The numbers refer to the amines in Table I.

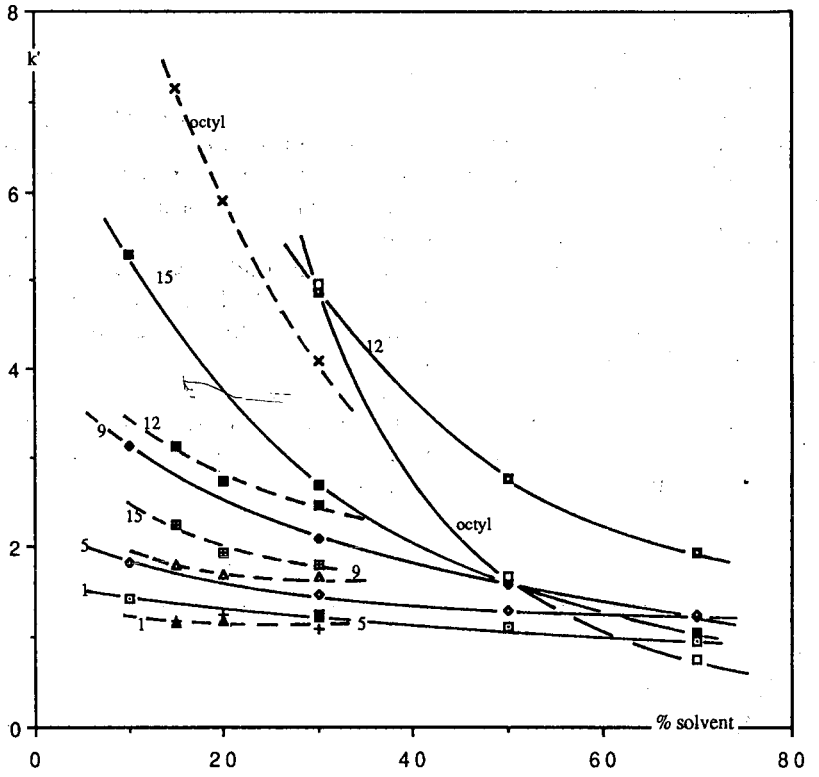

Fig. 2. Dependence of the retention of amines on the amount of methanol (solid lines) or THF (dashed lines). Mobile phase, $[KNO_3] = 5 \cdot 10^{-2}$ *M*, pH = 1.5; column, Nucleosil SA (250 × 4.6 mm I.D.). The numbers refer to the amines in Table I.

TABLE II

PRELIMINARY EXPERIMENTS

Expt. No.	Solvent	[solvent] (%)	Cation	Anion	[Eluted cation] ($\times 10^{-2}$ *M*)	Retention time (min)		
						$Y^{(a)}$	$Y^{(b)}$	$Y^{(c)}$
1	CH_3OH	10	H^+	NO_3^-	[a]	21	28	–
2	CH_3OH	10	Na^+	Ac^-	1	15.5	20.8	25
3	CH_3OH	10	Na^+	Ac^-	5	9.4	9.7	19
4	CH_3OH	30	Na^+	Ac^-	5	7.4	8.5	12.4
5	CH_3OH	50	Na^+	Ac^-	5	7.2	8	10.2
6	CH_3OH	50	Na^+	NO_3^-	5	6.9	7.7	9.8
7	CH_3OH	50	K^+	NO_3^-	5	6.1	6.5	8
8	CH_3OH	10	K^+	NO_3^-	5	6.3	7.5	12.8
9	CH_3OH	30	K^+	NO_3^-	5	6.2	7	9.6
10	THF	30	K^+	NO_3^-	5	6.1	6.5	8

[a] HNO_3: amount necessary for pH 1.5.

The interpretation of these results is as follows:

the comparison between runs 1 and 2 shows the necessity to use an eluting cation to avoid an excessive retention time;

the comparison between experiments 2 and 3 shows the effect of the concentration of eluting cation: the higher is the concentration, the shorter is the retention time, as displayed in Fig. 1;

the set of experiments 3–5 shows that increasing the methanol concentration decreases the retention time, as seen in Fig. 2;

the comparison between experiments 5 and 6 shows the influence of the nature of the co-ion: nitrate gives lower retention times than acetate;

the comparison between experiments 6 and 7 shows the influence of the nature of the eluting cation: K^+ is a stronger eluent than Na^+;

experiments 7–9 show again the effect of an increase in the methanol concentration but, with potassium nitrate, this effect is much less than with sodium acetate;

the comparison between experiments 9 and 10 shows the effect of organic solvent, THF producing shorter retention times than methanol.

Screening design

From the above results a choice of the studied factors was made: nature of the solvent, amount of solvent, amount of eluting cation and pH.

For a given response $Y^{(u)}$, the model

$$Y^{(u)} = b_0{}^{(u)} + b_1{}^{(u)} X_1 + b_2{}^{(u)} X_2 + b_3{}^{(u)} X_3 + b_4{}^{(u)} X_4$$

will allow the estimation of the effect $b_i{}^{(u)}$ in which we are interested: $b_1{}^{(u)}$ will be the effect of the type of solvent, $b_2{}^{(u)}$ the effect of the amount of solvent, $b_3{}^{(u)}$ the effect of the potassium nitrate (eluting cation) and $b_4{}^{(u)}$ the effect of pH.

A two-level fractional factorial design [17] of eight experiments would be appropriate for this problem. A 2^{4-1} fractional factorial design with the defining relation $I = -1234$ was used:

Run No.	X_1	X_2	X_3	X_4	$Y^{(u)}$ (observed response)
1	−1	−1	−1	+1	$Y_1{}^{(u)}$
2	+1	−1	−1	−1	$Y_2{}^{(u)}$
3	−1	+1	−1	−1	$Y_3{}^{(u)}$
4	+1	+1	−1	+1	$Y_4{}^{(u)}$
5	−1	−1	+1	−1	$Y_5{}^{(u)}$
6	+1	−1	+1	+1	$Y_6{}^{(u)}$
7	−1	+1	+1	+1	$Y_7{}^{(u)}$
8	+1	+1	+1	−1	$Y_8{}^{(u)}$

From this experimental matrix, an effect matrix of eight columns corresponding to the different combinations of columns 1, 2 and 3 was built:

Column	0 (−1234)	1	2	3	4 (−123)	5 (12)	6 (13)	7 (23)	$Y^{(u)}$ (response)
	+1	−1	−1	−1	+1	+1	+1	+1	$Y_1{}^{(u)}$
	+1	+1	−1	−1	−1	−1	−1	+1	$Y_2{}^{(u)}$
	+1	−1	+1	−1	−1	−1	+1	−1	$Y_3{}^{(u)}$
	+1	+1	+1	−1	+1	+1	−1	−1	$Y_4{}^{(u)}$
	+1	−1	−1	+1	−1	+1	−1	−1	$Y_5{}^{(u)}$
	+1	+1	−1	+1	+1	−1	+1	−1	$Y_6{}^{(u)}$
	+1	−1	+1	+1	+1	−1	−1	+1	$Y_7{}^{(u)}$
	+1	+1	+1	+1	−1	+1	+1	+1	$Y_8{}^{(u)}$

Our model involves only first-order terms but it is possible to compute eight various linear contrasts l_i obtained by adding together all the response values with plus signs in columns, 0, 1, 2, etc., subtracting all those with minus signs and dividing by the appropriate column divisor 8. For example,

$$l_1^{(u)} = [-Y_1^{(u)} + Y_2^{(u)} - Y_3^{(u)} + Y_4^{(u)} - Y_5^{(u)} + Y_6^{(u)} - Y_7^{(u)} + Y_8^{(u)}]/8$$

$$l_1^{(1)} = (-0.598 + 0.724 - 0.486 + 0.548 - 0.676 + 0.693 - 0.338 + 0.561)/8 = 0.428/8 = 0.0535$$

The confouding scheme is given by:

$$l_0^{(u)} = b_0^{(u)} - b_{1234}^{(u)}$$
$$l_1^{(u)} = b_1^{(u)} - b_{234}^{(u)} \qquad l_2^{(u)} = b_2^{(u)} - b_{134}^{(u)}$$
$$l_3^{(u)} = b_3^{(u)} - b_{124}^{(u)} \qquad l_4^{(u)} = b_4^{(u)} - b_{123}^{(u)}$$
$$l_5^{(u)} = b_{12}^{(u)} - b_{34}^{(u)} \qquad l_6^{(u)} = b_{13}^{(u)} - b_{24}^{(u)} \qquad l_7^{(u)} = b_{23}^{(u)} - b_{14}^{(u)}$$

where $b_i^{(u)}$ are main effects for the studied response $Y^{(u)}$, $b_{ij}^{(u)}$ are two-factor interaction effects, $b_{ijk}^{(u)}$ are three-factor interaction effects, etc.

Assuming that interactions between more than two factors are negligible, it is possible to estimate separately main effects which are confounded with three-factor interactions, and to estimate only the sum of two-factor interactions effects.

Experimental domain (factors and levels)

THF and acetonitrile (ACN) were chosen as solvents because they are better solvents than methanol for amines. The amount of solvent was varied from 5% to a upper limit of 25% to retain satisfactory mobile phase conductivity.

Potassium nitrate was chosen as the eluting species as K^+ is a stronger eluent than Na^+, and as the eluting strength effect of nitrate is higher than that of acetate. Its concentration range in the mobile phase varied from $2 \cdot 10^{-2}$ to $6 \cdot 10^{-2}$ *M*.

The influence of pH was studied between pH 2 and 5.

The experimental domain (factors and levels) in the screening experiments is given in Table III. The amounts of solvent and potassium nitrate solution added to the mobile phase are expressed as the volume added to obtain 1 l of mobile phase.

TABLE III

FACTORS AND LEVELS FOR THE FACTORIAL STUDY

Factor		Level	
		−1	+1
X_1	Nature of solvent	THF	ACN
X_2	Amount of solvent (ml)	50	250
X_3	Amount of KNO_3 solution (ml)	20	60
X_4	pH	2	5

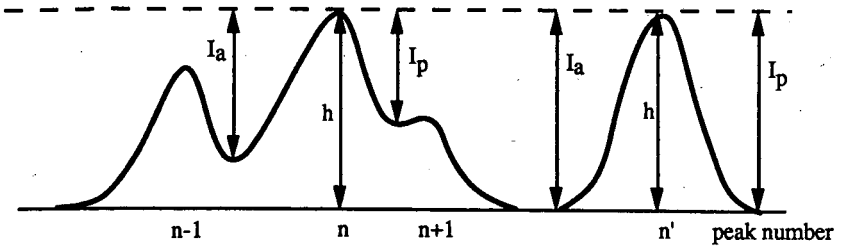

Fig. 3. Graph giving the directions for the separation index calculation.

Observed response

Chromatographic response functions (CRF) have been studied by numerous workers as reported by Lu and Huang [18]. We propose a very simple one, consistent with a limited number of experiments.

The studied response, *i.e.*, the evaluation of the quality of the separation, is made through an "overall separation index, I_s", calculated according to the directions in Fig. 3.

Each peak n is related to $y_n = 1/2\ (I_a/h + I_p/h)$, which gives $y_n = 1$ for each completely separated peak, since $I_a = I_p = h$ in that case.

To take into account the time limit of the analysis, y_n is set to 0 if the retention time is over 60 min.

For the whole set of separated peak $Y_n = \sum y_n$, and if there are N components in the analysed mixture, the overall separation index is

$$I_s = Y_n/N = \sum y_n/N = \text{the response function } Y^{(u)}.$$

According to this CRF, the nearer to 1 is the response, the better is the separation.

Analysis of results

The experimental matrices for both mixtures M_1 [vector $Y^{(1)}$] and M_2 [vector $Y^{(2)}$], in natural (experimental) variables U_i or coded variables X_i, are shown in Table IV. For each response vector $Y^{(1)}$ or $Y^{(2)}$ the calculated coefficients are given in Table V.

TABLE IV

TWO-LEVEL FRACTIONAL FACTORIAL DESIGN

Run No.	U_1	U_2	U_3	U_4	X_1	X_2	X_3	X_4	$Y^{(1)}$	$Y^{(2)}$
1	THF	50	20	5	−1	−1	−1	1	0.598	0.798
2	ACN	50	20	2	1	−1	−1	−1	0.724	0.744
3	THF	250	20	2	−1	1	−1	−1	0.486	0.621
4	ACN	250	20	5	1	1	−1	1	0.548	0.670
5	THF	50	60	2	−1	−1	1	−1	0.676	0.942
6	ACN	50	60	5	1	−1	1	1	0.693	0.703
7	THF	250	60	5	−1	1	1	1	0.338	0.556
8	ACN	250	60	2	1	1	1	−1	0.561	0.856

TABLE V

COEFFICIENTS OF THE MODEL FOR SEPARATION INDEX

Effect	$Y^{(1)}$	$Y^{(2)}$
b_0	0.578	0.736
b_1	0.053	0.007
b_2	−0.095	−0.060
b_3	−0.011	0.028
b_4	−0.034	−0.054
Confounding:		
$(b_{12}-b_{34})$	0.018	0.080
$(b_{13}-b_{24})$	0.006	0.008
$(b_{14}-b_{23})$	0.023	−0.002

Mixture M_1 [response $Y^{(1)}$]. The amount of solvent (X_2) is the factor that has the major effect [$b_2^{(1)} = -0.095$], followed by, to a lesser extent, the nature of the solvent (X_1) and the pH (X_4), while the influence of K^+ concentration (X_3) seems to be low. From the results it can be concluded that:

on average, acetonitrile gives a better separation than THF [$X_1 = 1$ with $b_1^{(1)} = 0.053$];

the lower the amount of solvent, the better is the separation [$X_2 = -1$ with $b_2^{(1)} = -0.095$];

it is better to work at pH 2 than at pH 5 [$X_4 = -1$ with $b_4^{(1)} = -0.034$];

$[K^+]$ has little effect as b_3 is small [$b_3^{(1)} = -0.011$].

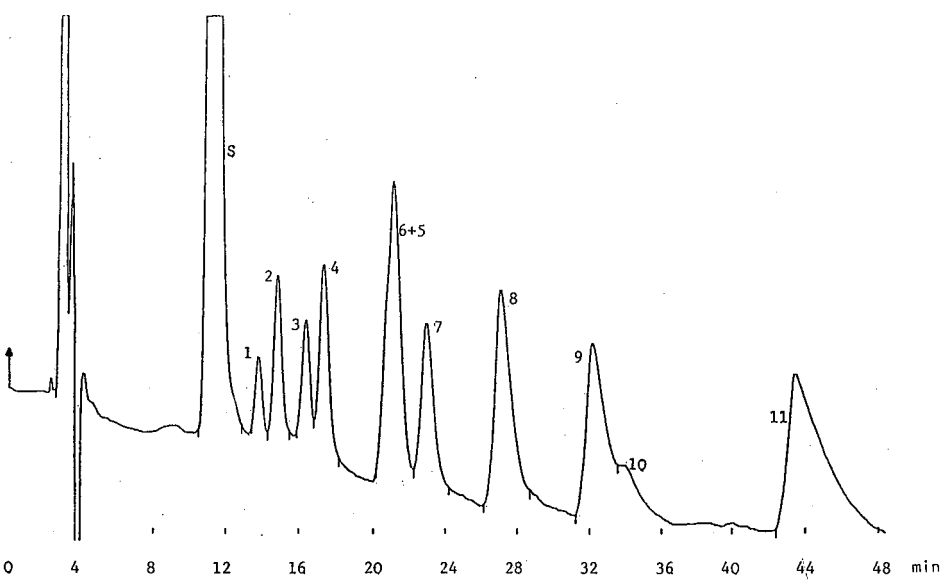

Fig. 4. Separation of mixture M_1 according to the conditions of experiment 2 (factorial design), Table IV. Flow-rate, 1 ml/min. Other conditions as mentioned in the text. The numbers refer to the amines in Table I.

Experiment 2, which fulfills the best compromise according to these constraints ($X_1 = 1$, $X_2 = X_3 = X_4 = -1$), actually gives the best separation among the eight experiments performed. Fig. 4 shows the chromatogram obtained under these conditions. The first detected peaks correspond to unretained solutes, *i.e.*, the sample solvent and the anionic solutes. The system peak which correspond to the eluting ions is then eluted as a significant peak before the analysed compounds.

It should be noted that the effect of X_3 seems to contradict the theoretical knowledge of the influence of K^+ in cation-exchange chromatography. However, it can be considered that although the effect of $[K^+]$ is low as a main effect, it can play a significant role in the interaction effects, but to estimate the b_{ij} terms without confounding, eight additional experiments would have been necessary. Nevertheless, although it is not possible to have an unconfounded estimate of all b_{ij} coefficients, an X_iX_j interaction can be discussed using the following type of diagram where the plane is divided into four quadrants by two axes X_i and X_j:

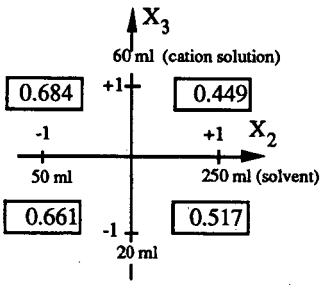

The right and upper value represents the average of the experimental response when $X_i = 1$ and $X_j = 1$ {in our example $X_2 = 1$ and $X_3 = 1$ for runs 7 and 8, and the average is $[Y_7^{(1)} + Y_8^{(1)}]/2 = (0.338 + 0.561)/2 = 0.449$}. The other three values are calculated in an analogous manner using the corresponding combinations ($X_i = -1$ and $X_j = 1$, $X_i = -1$ and $X_j = -1$, $X_i = 1$ and $X_j = -1$).

From the X_2X_3 diagram corresponding to the interaction between the percentage of organic solvent in the mobile phase (X_2) and the K^+ concentration (X_3), it can be seen that for $X_2 = -1$ (5% solvent), the response varies from 0.661 to 0.684 when X_3 goes from -1 to 1 ($[K^+]$ goes from $2 \cdot 10^{-2}$ to $6 \cdot 10^{-2}$ M). When X_2 is at the level -1 (25% solvent), the separation index decreases from 0.517 to 0.449 for the same $[K^+]$ variation. This shows that the effect of $[K^+]$ is a function of the solvent amount and *vice versa*.

It should be noted that such an observation, which shows the dependence of the influence of one factor on the levels of the other factors, could not be evidenced using the traditional optimization approach (sequential single factor at a time), despite the large number of experiments performed.

Mixture M_2 [response $Y^{(2)}$]. The conclusions are the same as for the mixture M_1 regarding the effects of X_2 and X_4, but the effects of X_1 and X_3 are different:

the influence of the nature of the solvent is of little importance [$b_1^{(2)} = +0.007$];

it is better to use a small amount of solvent [$X_2 = -1$ with $b_2^{(2)} = -0.060$];

the higher the K^+ concentration, the better is the separation [$X_3 = +1$ with $b_3^{(2)} = 0.028$];

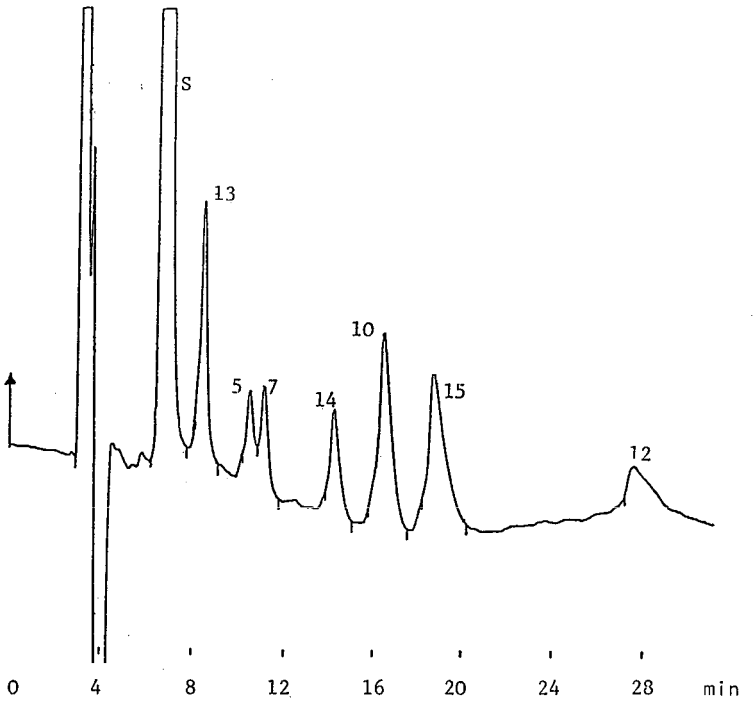

Fig. 5. Separation of mixture M_2 according to the conditions of experiment 5 (factorial design), Table IV. Flow-rate, 1 ml/min. Other conditions as mentioned in the text. The number refer to the amines in Table I.

it is better to use pH 2 than pH 5 [$X_4 = 1$ with $b_4^{(2)} = -0.054$].

Experiment 5, which fulfills the best compromise among these constraints ($X_1 = -1, X_2 = -1, X_3 = 1, X_4 = 1$), actually gives the best separation index from the eight experiments performed. The corresponding separation is shown in Fig. 5.

As above, the examination of the interaction diagrams brings additional information to the previous conclusions:

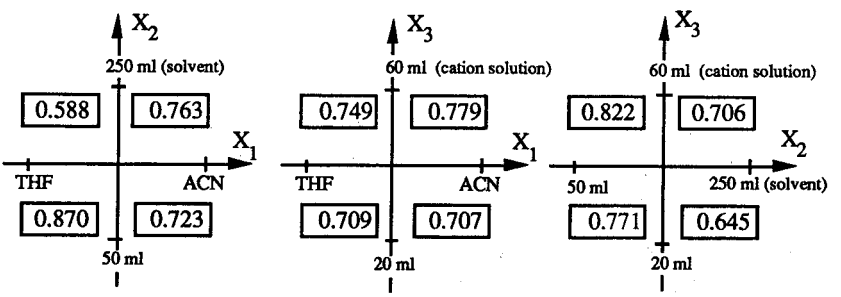

Examination of the interaction between X_1 and X_2 shows that on average the best separation is obtained either for a small amount of THF or to a lesser extent for a large amount of acetonitrile.

TABLE VI

SEQUENTIAL SIMPLEX DESIGN FOR MIXTURE M_1

Run No.	K^+ (ml)	CH_3CN (ml)	I_s	t_R[a] (min)
1	20	30	0.705	45
2	60	30	0.767	44
3	40	90	0.924	52
4	80	90	0.875	27
5	60	150	0.793	25
6	20	150	0.829	70

[a] t_R = Retention time of last peak.

From the interaction between X_1 and X_3 it appears that the best separations are obtained with $[K^+] = 6 \cdot 10^{-2}$ M, whatever the solvent. The interaction between X_2 and X_3 shows that the best separations are obtained for $[K^+] = 6 \cdot 10^{-2}$ M and for a small amount of solvent near 5%.

Simplex optimization for the twelve-amines mixture M_1

In order to simplify the problem of the separation of this mixture, we can reasonably make two final choices: use acetonitrile as the solvent, and work at pH 2, as a pH lower than 2 would risk damage to the stationary phase. As there is a high interaction level between the amount of acetonitrile and the K^+ concentration, the simplex method [19–23] is used to find the optimum combination of these two factors, with the following coded parameters:

factors	centre of the domain	variation step
ml KNO_3 (1 M solution)	40	23
ml CH_3CN	50	40

These results are given in Table VI. Runs 1, 2 and 3 correspond to the initial simplex (Fig. 6). Vertex 1 (run 1) has the worst response and vertex 3 (run 3) has the best response. Reflection is accomplished to generate the new vertex 4 (run 4). Then

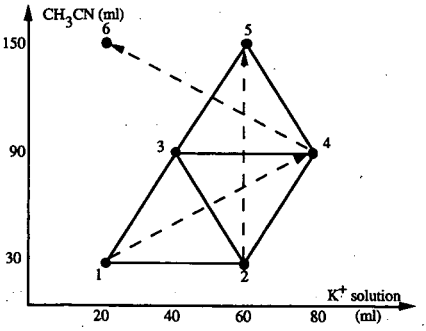

Fig. 6. Evolution of sequential simplex design.

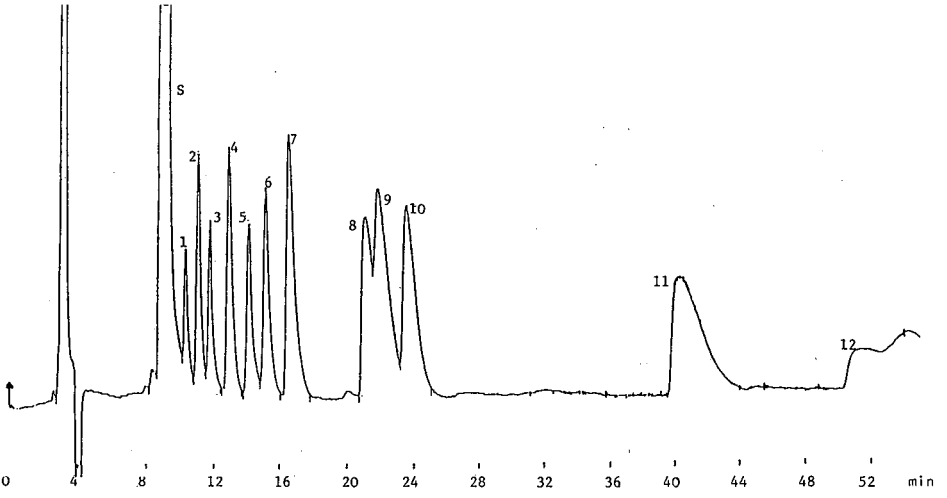

Fig. 7. Separation of mixture M_1 according to conditions of experiment 3 (simplex design), Table VI. The numbers refer the amines in Table I.

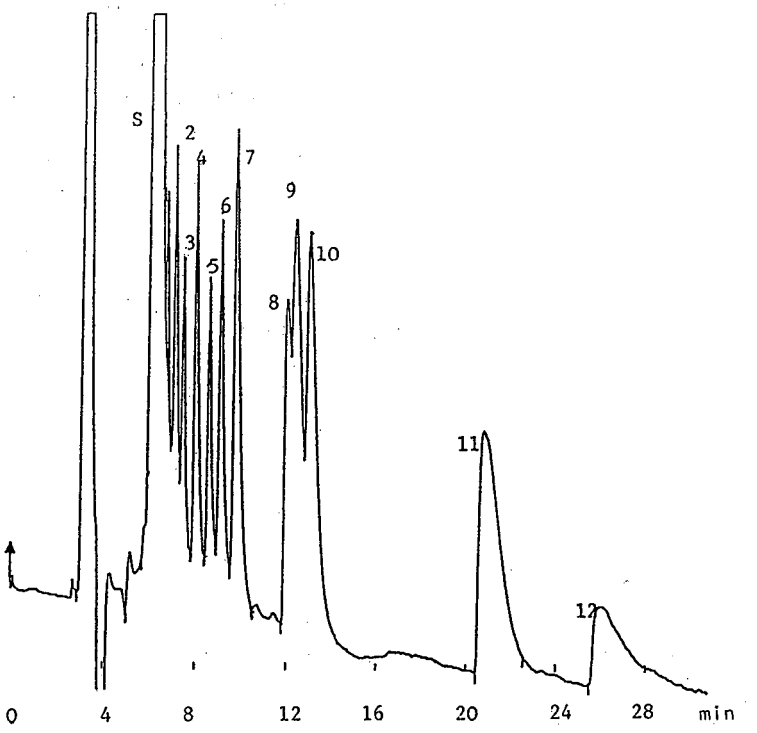

Fig. 8. Separation of mixture M_1 according to conditions of experiment 4 (simplex design), Table VI. The numbers refer to the amines in Table I.

evolution brings us to vertex 5 (run 5) and, if we apply the reflection rule, we obtain vertex 2. It is necessary to prevent oscillation about a ridge; a new vertex is obtained by rejecting the next-to-worst vertex instead of the worst vertex: vertex 6 (run 6). It seems that in this part of the domain with the elution system used, the optimum separation index is obtained with run 3. The best I_s value is 0.924. This run corresponds to an almost complete separation of the twelve compounds to be separated, as shown in Fig. 7. Only the separation between peaks 8, 9 and 10 is not fully achieved, although peak 10 is almost separated, as $y_8 = 0.639$, $y_9 = 0.613$ and $y_{10} = 0.913$.

If the analysis time is taken into account (the retention time for the last peak is t_R in Table VI), the conditions of experiment 4 can be reasonable as the separation index is 0.875 and the whole analysis time is 27 min instead of 52 min for experiment 3. This also implies that it is accepted that the first peaks be eluted on the system peak tail and that the resolution between peak 8, 9 and 10 be decreased further: $y_8 = 0.55$, $y_9 = 0.484$, $y_{10} = 0.781$. The chromatogram of experiment 4 is presented in Fig. 8.

CONCLUSIONS

A chemometric approach to the separation of aliphatic amines has allowed us to find optimum separation conditions with a limited number of experiments: for mixture of twelve amines, taking into account four elution factors, it was shown that only 24 experiments allow the study of the simultaneous variation of all the studied experimental factors and information on the interactions between the mobile phase components has been obtained that could not be obtained with a traditional approach, *i.e.*, the variation of one factor at a time.

A chromatographic system based on both an ion-exchange mechanism and a lipophilic interaction mechanism proved very efficient for separating amino compounds. However, the sensitivity of the detection of the separated compounds has not been studied, and the large amounts of organic solvent in the mobile phase necessary to elute the more lipophilic amines cause a decrease in the dissociation of the ionizable solutes, a decrease in the mobile phase conductivity and a poor detection limit for these compounds. Other detection modes such as spectrophotometry coupled with a post-column derivatization device or light-scattering detection might be preferable as such detection could allow elution gradient and perhaps further improvements of the separation of amines by this HPLC method.

REFERENCES

1 H. D. Christensen and J. L. Whitsett, in G. L. Hawks (Editor), *Biological–Biomedical Applications of Liquid Chromatography*, Marcel Dekker, New York, 1979, p. 507.
2 M. T. W. Hearn and W. S. Hancock, *N. Z. Med. J.*, 86 (1977) 352.
3 J. C. Kraak, K. M. Jonker and J. F. K. Auber, *J. Chromatogr.*, 142 (1977) 671.
4 J.-K. Lin and C.-C. Lai, *Anal. Chem.*, 52 (1980) 630.
5 G. Gubitz, R. Wintersteiger and A. Hartinger, *J. Chromatogr.*, 218 (1981) 51.
6 P. Jandera, H. Pechova, D. Tockjteinova, J. Churacek and J. Kralovsky, *Chromatographia*, 16 (1982) 275.
7 K. Shimada, M. Tanaka and T. Nambare, *J. Chromatogr.*, 280 (1983) 271.
8 J. N. Lapage and E. M. Rocha *Anal. chem.*, 55 (1983) 1360.
9 M. Roth and A. Hampai, *J. Chromatogr.*, 83 (1973) 353.
10 P. Jandera en J. Churacek, *J. Chromatogr.*, 98 (1974) 1.

11 H. Adler, M. Margosaes, L. R. Snyder and C. Spitzer, *J. Chromatogr.*, 143 (1977) 125.
12 S. A. Bouyoucos, *Anal. Chem.*, 49 (1977) 401.
13 F. C. Smith and R. C. Chang, *CRC Crit. Rev. Anal. Chem.*, (1980) 197.
14 S. Elchuk and R. M. Cassidy, *Anal. Chem.*, 51 (1979) 1434.
15 J. Vialle, M. C. Bertrand, M. Kolosky, O. Paisse and G. Raffin, *Analusis*, 17 (1989) 376.
16 E. Lesellier, C. Marty, C. Berset and A. Chapla, *J. High Resolut. Chromatogr.*, 12 (1989) 447.
17 G. E. P. Box, W. G. Hunter and J. S. Hunter, *Statistics for Experimenters*, Wiley, New York, 1978.
18 P.-C. Lu and H.-X. Huang, *J. Chromatogr. Sci.*, 27 (1989) 690.
19 W. Spendley, G. R. Hext and F. R. Himsworth, *Technometrics*, 4 (1962) 441.
20 S. N. Deming and L. R. Parker, Jr. *CRC Crit. Rev. Anal. Chem.*, (1978) 187.
21 C. Porte, W. Debreuille and A. Delacroix, *Actual. Chim.*, October (1984) 45.
22 C. Porte, W. Debreuille and A. Delacroix, *Actual. Chim.*, June–July (1986) 1.
23 C. Porte, W. Debreuille and A. Delacroix, *Actual. Chim.*, September (1987) 233.

Journal of Chromatography, 549 (1991) 175–184
Elsevier Science Publishers B.V., Amsterdam

CHROM. 23 348

Large-scale purification of the synthetic peptide fragment 163–171 of human interleukin-β by multi-dimensional displacement chromatogaphy[a]

G. C. VISCOMI*, C. CARDINALI, M. G. LONGOBARDI and A. S. VERDINI
Sclavo SpA, 1 Fiorentina, I-53100 Siena (Italy)
(First received January 14th, 1991; revised manuscript received April 3rd, 1991)

ABSTRACT

Multi-dimensional chromatography has been used successfully in the displacement mode for the purification of the synthetic peptide H–Val–Gln–Gly–Glu–Glu–Ser–Asn–Asp–Lys–OH, the fragment 163–171 of human interleukin-β. This peptide can mimic several of the *in vivo* and *in vitro* immunostimulatory activities of the entire protein, except for the inflammatory effect. A large-scale procedure has been developed to purify the synthetic peptide by reversed-phase (RP) and ion-exchange (IE) displacement chromatography (DC) in a single run without any pretreatment. Masses from 100 mg to about 35 g of the unpurified compounds synthesized by a solid-phase technique on a Merrifield-type resin and obtained by acidolytic cleavage from the solid support, can be purified in this way. In the RP-DC mode the carrier and the displacer were aqueous solutions of 0.1% trifluoroacetic acid and 50 m*M* benzyltributylammonium chloride, respectively, whereas in the IE-DC mode the carrier was water and the displacer 50 m*M* ammonium citrate solution. RP-DC and IE-DC were also performed in series by directing the effluent of the RP column onto the IE column. Peptide purities and recoveries greater than 96 and 90%, respectively, were obtained.

INTRODUCTION

Of the various biologically active substances used in drug treatments, peptides are acquiring increasing therapeutic relevance. As peptides usually show a strong effect at low doses, they need to be synthesized in the gram to kilogram range. The mild conditions required for their purification make preparative liquid chromatography the method of choice for the development of efficient process technologies [1].

Synthetic peptides obtained through homogeneous or solid-phase procedures are frequently contaminated with closely related impurities resulting from unavoidable side-reactions, such as sequence deletions, racemization, the incomplete removal of the side-chain protecting groups and the multiple addition of amino acid residues. The target peptide and most of the peptide contaminants are difficult to separate as a

[a] Part of this work was presented at the *7th International Symposium on Preparative Chromatography, Ghent, April 1990.*

0021-9673/91/$03.50

result of their chemical and structural similarities and purification to chemical homogeneity is often a very demanding task.

Generally, in preparative liquid chromatography, once the purity levels are fixed, most effort is addressed to increase the volume of production by increasing the loading capacity of the stationary phases. It has recently been shown that to maximize the throughput, the stationary phases should be considerably overloaded [2]. As column overloading favours displacement effects, displacement chromatography (DC) can be considered as a suitable purification process in the large-scale production of synthetic peptides [3].

The reported applications of DC in the peptide field have been restricted to purifications in the range of hundreds of milligrams [4–7]. This paper reports a study of the potential of this technique for the purification of the crude synthetic peptide interleukin-1-β (IL-1β)-(163–171) on the multi-gram scale. The peptide samples were used in the DC runs without prior manipulation so that they contained, in addition to the peptide impurities, salts and derivatives produced during the deblocking and the final acidolytic removal of the peptide from the polystyrene resin.

In addition to maintaining the ability of the natural protein to activate T-cell functions without inducing an inflammatory response [8], the peptide IL-1β(163–171) has been shown to act as an adjuvant of IL-1β for both the T-helper-dependent and T-helper-independent immune response [9]. Therefore, the suggested use of this peptide as an adjuvant in vaccine formulations adds further significance to the preparative purification, as large amounts of this peptide will be required for future clinical trials.

EXPERIMENTAL

Materials

Benzyltributylammonium chloride (BTBA) and trifluoroactic acid (TFA) were supplied by Fluka (Buchs, Switzerland). Methanol and acetonitrile [high-performance liquid chromatography (HPLC) grade] were purchased from Merck (Darmstadt, Germany). Diammonium hydrogencitrate, ammonium chloride and aqueous ammonium hydroxide were provided by Carlo Erba (Milan, Italy). Triammonium citrate was obtained by neutralizing the diammonium hydrogencitrate to pH 7 with ammonium hydroxide.

Water was purified with a Milli-Q system (Millipore, Bedford, MA, USA). The aqueous eluents were filtered through a 0.45-μm cellulose acetate filter and the organic eluents through a 0.5-μm PTFE filter; all the eluents were degassed with helium prior to use.

Apparatus

The analytical chromatograph was assembled from two Model 114 pumps, a System Organizer, a Model 165 UV detector and a Model 450 data/system controller (Beckman, CA, USA) and a Model BD-41 recorder (Kipp & Zonen, Delft, Netherlands). A flow diagram of a typical displacement chromatograph has been reported previously [3].

The DC runs in reversed-phase (RP) mode were carried out on a 250 × 4 mm I.D. LiChrosorb RP-18 column (10 μm, Merck) in the milligram range. The HPLC

equipment consisted of a Model M-45 pump (Waters Assoc., Milford, MA, USA) with the reservoirs of carrier, displacer and regenerant solutions connected via a four-way valve, a Model 7010 injector (Rheodyne, CA, USA) with a 10-ml loop, a PU-4025 UV detector (Pye Unicam, Cambridge, UK) to monitor the displacement chromatogram at 260 nm and a Model 2210 recorder (LKB, Bromma, Sweden). The column effluent was collected with a Model 2070 Ultrarack II fraction collector (LKB).

The RP-DC separations were carried out in the gram range on axial compression columns of 20, 40 and 80 mm I.D. (Jobin Yvon, Longjiumeau, France), packed with LiChroprep RP-18 (25–40 μm) (Merck). The pump was a Model 590 programmable HPLC pump equipped with a four-solvent selecting valve (Waters Assoc.). The effluents, monitored by a Model PU 4025 UV detector at 260 nm, were collected with a Model 2211 Superrac fraction collector (LKB).

The 4, 20, 40 and 80 mm I.D. columns were equilibrated with the carrier for 20 min at flow-rates of 0.4, 8, 32 and 128 ml/min, respectively. The same flow-rates were used to regenerate the stationary phase with methanol after the displacement runs. Taking into account the equilibration, elution and regeneration steps, the total chromatographic time for the displacement runs was about 260 min. The presence of the displacer agent in the fractions was monitored by thin-layer chromatography or spectrophotometry [10]. The displacement chromatographic run in the ion exchange (IE) mode was carried out in the milligram range on a Mono-Q 50 × 5 mm I.D. column (10 μm) with a fast protein liquid chromatography (FPLC) system equipped with three P-500 pumps and a Model Frac 100 fraction collector (Pharmacia, Uppsala, Sweden). The IE-DC on the gram scale was performed on a 350 × 10 mm I.D. column packed with Q-Sepharose Fast Flow (45–164 μm, Pharmacia). The chromatographic apparatus consisted of Model 590 pump with the four-solvent selecting valve (Waters Assoc.), a Model UV-M detector at 214 nm and a Model Rec 481 recorder (Pharmacia).

Analytical IE chromatography was performed to analyse some collected fractions and to detect the presence of the IE-DC displacer using a FPLC system with a Mono Q column.

The multi-dimensional displacement chromatographic run was monitored online by dedicated equipment as described previously [11]; a 33 × 4.6 mm I.D. Supelcosil LC-18-DB column (3 μm, Supelchem, Milan, Italy) was used under isocratic conditions with 0.1% TFA in acetonitrile–water (4:96) as the eluent.

Fast atom bombardament mass spectrometry (FAB-MS) was carried out in the Analytical Department of ENIRICERCHE (Monterotondo, Rome, Italy).

RESULTS

The analytical chromatogram of the crude mixture after the acidic cleavage of the peptide from the resin is shown in Fig. 1. Compounds of peptidic nature consitute about 50% (w/w) of the total material.

The peak at the retention time (t_R) 3.29 min corresponds to the target peptide IL-1β(163–171), whereas that at t_R 4.14 min is the peptide impurity with the glutamine residue replaced by the glutamic acid residue, (Gln)IL-1β(163–171), most probably arising from the acid-catalysed hydrolysis of the Gln side-chain carboxyamide

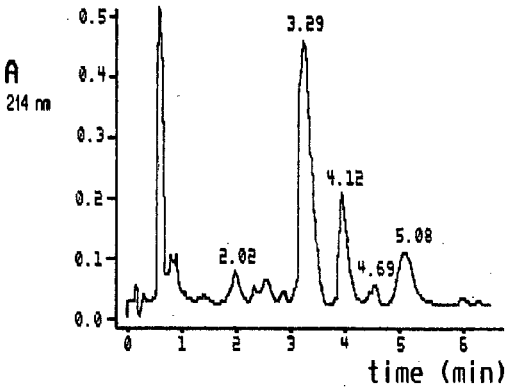

Fig. 1. RP-HPLC of crude synthetic mixture of IL-1β(163–171). Sample: 40 μg of mixture in 20 μl. Eluents: A, 0.1% TFA; B, 0.1% TFA in acetonitrile–water (60:40). Gradient: 3–6% B in 3 min, 6–3% B in 2 min, 3–3% B in 2 min. Flow-rate, 1.5 ml/min; column, 33 × 4.6 mm I.D. LC-18 DB Supelcosil.

during the peptide assembly on the solid support. The peak at t_R 4.96 min is an aminosuccinimide derivative originated from the ring closure of the aspartyl residue during the acylation step of the C-terminal lysine α-NH_2:

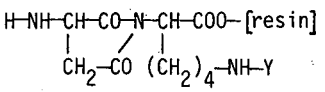

The identities of the target peptide and both peptide impurities have been assessed by FAB-MS.

The peak at t_R 2.02 min has been tentatively attributed to the Asp–Lys-β isopeptide: H–Val–Gln–Gly–Glu–Glu–Ser–Asn–NH–CH(CH_2–CO–Lys–OH)–COOH, as its area increased on treatment with 1 *M* sodium hydroxide solution with the concomitant reduction of the peak at t_R 4.96 min.

The peak at t_R 5.08 min was associated with an impurity, the identity of which has not been determined and which co-eluted with the target peptide in an analytical IE-FPLC separation carried out on a 50 × 5.0 mm I.D. Mono-Q column with a gradient from 5 to 100 m*M* of disodium hydrogenphosphate at pH 7.0 in 20 min.

The optimum conditions for a convenient purification procedure for IL-1β (163–171) in RP-DC wer first tested on a small scale using a 250 × 4.0 mm I.D. LiChrosorb RP-18 column.

The concentration of the mixture to be fed onto the column was determined in a preliminary study and it was found that the complete adsorption of the material onto the stationary phase, an essential step for the displacement mechanism, did not occur at concentrations greater than 10 mg/ml. The RP-DC was carried out by loading 100 mg of the untreated crude mixture onto the column using 0.1% TFA as the carrier and 50 m*M* BTBA as the displacer. The results obtained are shown in Fig. 2, where the histogram is constructed on the basis of the RP-HPLC analysis of the collected fractions.

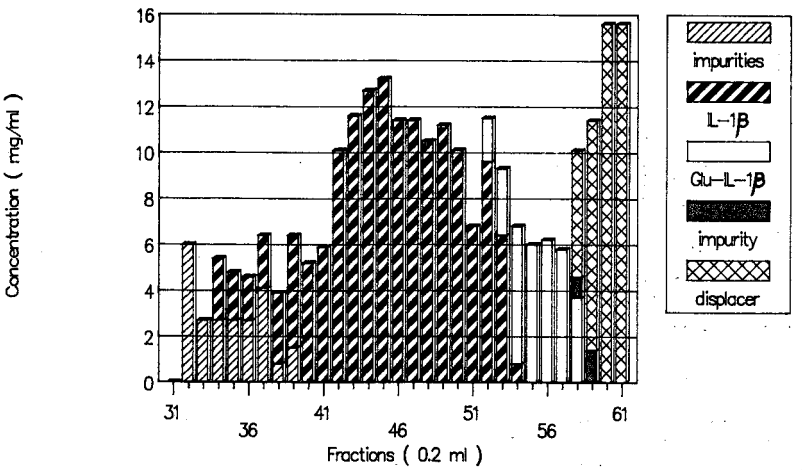

Fig. 2. Displacement histogram of RP-DC. Flow-rate, 0.1 ml/min; column 250 × 4 mm I.D. LiChrosorb RP-18; 98 mg of the mixture; pooled fractions, 40–51.

Multi-gram purification was obtained by adopting a scaling-up procedure similar to that described for the large-scale purification of the cysteine derivative Fmoc–Cys(Trt)–OH [11]. The 4.0 mm I.D. LiChrosorb RP-18 column used in the preliminary experiments was replaced in turn by 20, 40, and 80 mm I.D. LiChroprep columns, while the linear velocity of the sample and displacer solution (0.017 cm/min), the sample concentration (10 mg/ml) and the ratio of the loaded sample per gram of stationary phase (45 mg/g) were kept constant.

The results are summarized in Table I and the relative histograms are shown in Figs. 3–5. The purity levels of the desired peptide were greater than 95% in the pooled fractions collected.

The regeneration of the stationary phase after each displacement run was achieved with 2 ml of methanol per gram of stationary phase. As the relatively low yield was a result of the overlap between the bands of the target peptide and the impurity (Glu)IL-1β(163–171), which has a different net charge with respect to IL-1β (163–171), an attempt was made to improve the resolution of the bands by operating in the IE-DC mode. The run was carried out on a small scale by loading 50 mg of the

TABLE I

EFFECT OF SCALING-UP PROCEDURE ON PURIFICATION OF THE PEPTIDE

Column size (mm)	Stationary phase (g)	Loaded sample (g)	Yield[a] (%)	Peptide recovery (g)
250 × 4	1.8	0.098	78.2	0.024
260 × 20	45	2.0	78.8	0.55
260 × 40	200	9.0	81.8	2.4
260 × 80	800	35.5	78.2	8.1

[a] Calculated as collected peptide in the pure form over the total amount present in the crude mixture.

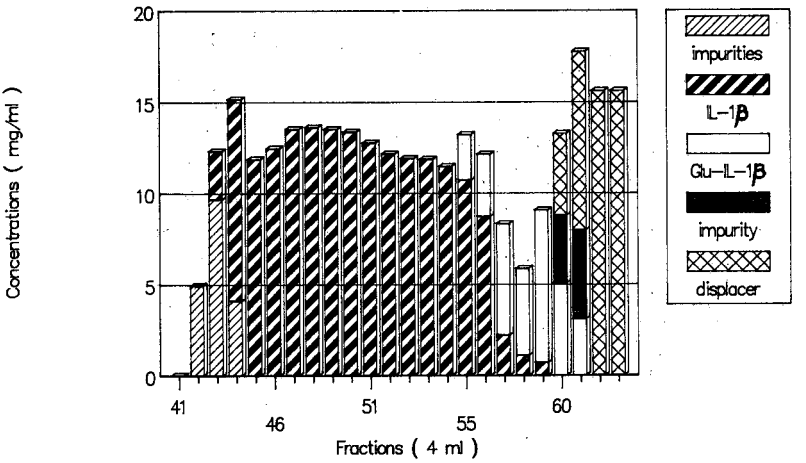

Fig. 3. Displacement histogram of RP-DC. Flow-rate, 2 ml/min; column, 260 × 20 mm I.D. LiChroprep RP-18; 2.0 g of the mixture; pooled fractions, 90–110.

material onto a 50 × 5.0 mm I.D. Mono Q column, using water (pH 7.0) as the carrier and 50 m*M* ammoniun citrate as the displacer.

The displacement separation gave a reduced overlap zone, less than 5% of the IL-1β(163–171) band, between the two eluted bands. However, as expected from the results of the analytical IE-FPLC experiments, the impurity appearing at t_R 5.08 min in Fig. 1 was present in all the fractions containing IL-1β(163–171).

However, as this impurity can easily be removed in RP-DC, it was decided to combine the advantages of both the DC modes by carrying out the purification with two columns connected in series, the first operating in the RP-DC mode and the

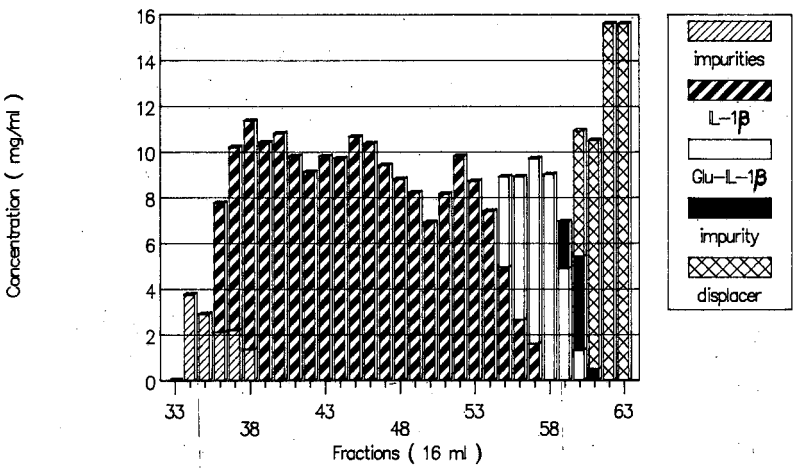

Fig. 4. Displacement histogram of RP-DC. Flow-rate, 8 ml/min; column, 260 × 40 mm I.D. LiChroprep RP-18; 9 g of the mixture; pooled fractions, 74–108.

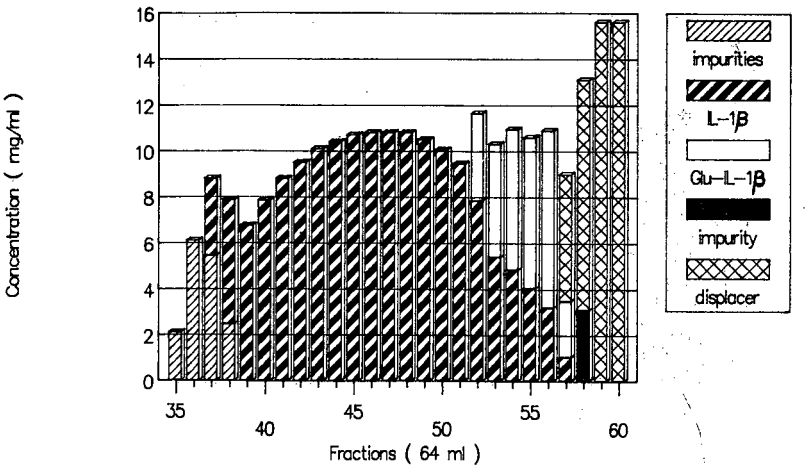

Fig. 5. Displacement histogram of RP-DC. Flow-rate, 32 ml/min; column, 260 × 80 mm I.D. LiChroprep RP-18; 35.5 g of the mixture; pooled fractions, 77–103.

second in the IE-DC mode (Fig. 6). The effluent of the 260 × 20 mm I.D. LiChroprep RP-18 column, monitored on-line, was directed, through valve 1 onto the 350 × 10 mm I.D. Q Sepharose FF column just as IL-1β(163–171) left the column. Immediately before reaching the top of the IE column, the pH of the effluent was changed from

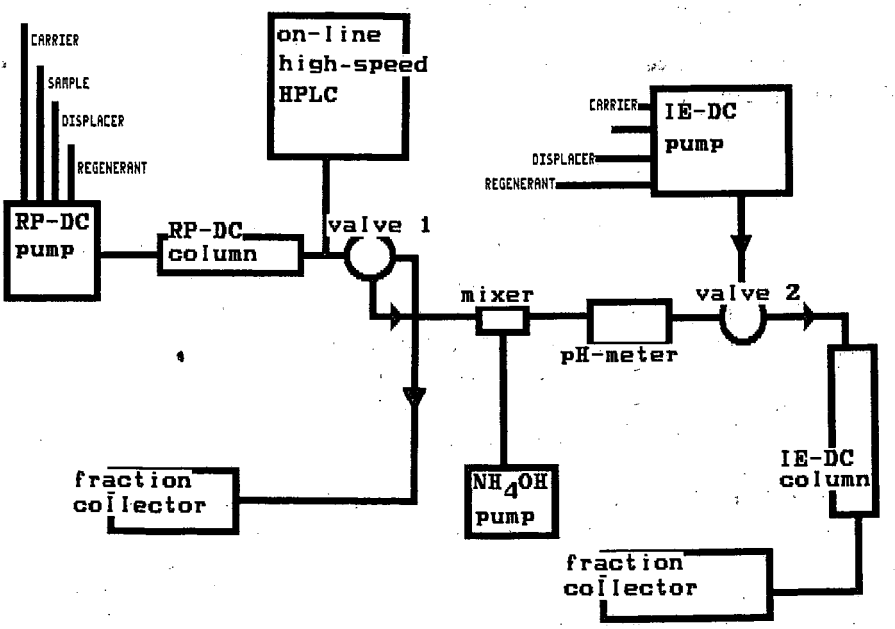

Fig. 6. Schematic diagram of chromatographic apparatus used for RP-DC and IE-DC in series.

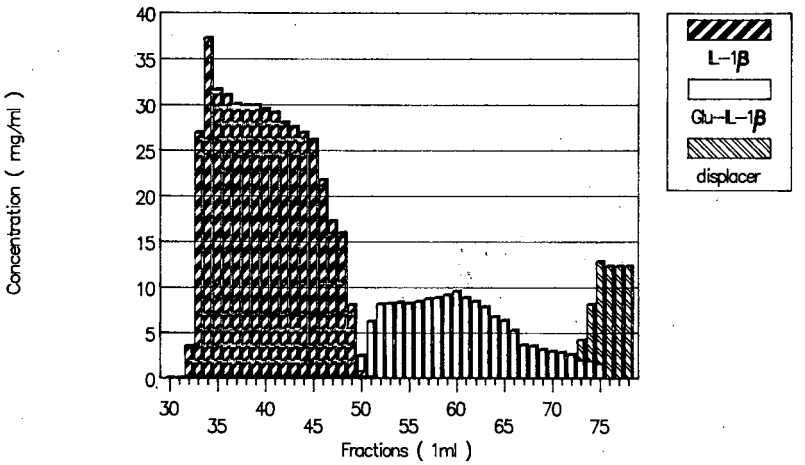

Fig. 7. Displacement histogram of IE-DC in the technique using RP- and IE-DC in series. Conditions of RP-DC as in Fig. 3. IE-DC conditions: flow-rate, 0.5 ml/min; column, 350 × 10 mm I.D. Q Sepharose Fast Flow; pooled fractions, 32–49.

3.0 to 7.0 to ensure that a complete adsorption of all the compounds onto the ion-exchange stationary phase occurred.

After the disappearance of the target peptide in the effluent and before the appearance of the unknown impurity at t_R 5.08 min, loading to the IE column was stopped and the stationary phase was conditioned with the carrier. The displacer solution was then pumped through the IE column at a linear velocity of 0.01 cm/s.

The resulting displacement histogram is given in Fig. 7. The chromatographic yield increased to over 90% and the purity of the IL-1β(163–171) recovered by lio-phylization was greater than 98%.

DISCUSSION

A straightforward scaling-up procedure has been developed for the purification of 100 mg to 35.5 g of the peptide IL-1β(163–171) using DC by simply widening the column diameters using the same conditions as in the small-scale separation of the target peptide. This result suggests that the purification of even larger amounts of crude peptide preparations could be easily achieved using DC.

Compared to the previously reported RP-HPLC purification of the same peptide in the elution mode [12], twenty times more crude material can be loaded per gram of stationary phase and a purer peptide obtained (>95% *versus* >90%) with fourteen times less solvent.

In the RP-DC experiments, 1.3 ml of eluents, included the regenerant solvent, were consumed per milligram of purified peptide. Using RP-DC and IE-DC in series, higher purity levels (>98%) and recovery (>90%) have been achieved. As reported previously stationary phases with a larger particle diameter and lower column costs do not reduce the separation efficiency of the experiments at the gram scale [11].

It is often difficult to find a suitable displacer for the DC runs; however, these

data confirm that the tetraalkylammonium halides represent a class of modulated hydrophobicity compounds that can be used advantageously for the purification of a large number of peptides in RP-DC [4–7, 13]. It is less difficult to find an IE-DC displacer as, theoretically, any compound with a net charge higher than that of the compound to be purified could be a potential displacer [14].

As far as the oligopeptides are concerned, the search for a displacer is facilitated further as conformational effects are less important or even negligible with respect to proteins. Therefore, a compound with a net charge one unit higher than that of the target compound can be used. This concept, previously applied with success to the purification of the retro-inverso tetrapeptide analogue of tuftsin, was effective for the purification of IL-1β(163–171) [15]. Triammonium citrate, an inexpensive salt with a net charge of −3 at pH 7.0 was used to displace IL-1β(163–171) (net charge −2 at the same pH). The high charge density of the citrate can perhaps also explain the displacement of the peptide impurity (Glu)IL-1β(163–171), which has the same net charge as the displacer.

It seems pertinent in this discussion to point out the remarkably mild conditions of the IE-DC experiments. Using water as the carrier and 50 m*M* ammonium citrate as the displacer, the desired product and some of the related impurities are collected in water and recovered simply by lyophylization, with clear advantages in terms of ease and the cost of product recovery.

CONCLUSIONS

As large amounts of the synthetic peptide IL-1β(163–171) are used for biological and clinical studies in this institute, DC has been adopted as a technique which is easy to scale-up, has an efficient use of the stationary phases and equipments and uses a reduced volume of eluent.

About 35.0 g of crude IL-1β(163–171), prepared by solid-phase synthesis on a Merrifield-type resin and used as such after acidic cleavage from the solid support, have been efficiently purified in a single chromatographic DC run.

In the RP mode, the superiority of DC compared to the classical preparative RP-HPLC was demonstrated by the purity of peptide obtained (>95%), the chromatographic yield (>80%), the load capacity (45 mg/g of stationary phase) and the considerably reduced consumption of solvents.

In the IE mode, DC exhibited a remarkably convenient feature, namely, the use of low concentrations (50 m*M*) of the inexpensive salt ammonium citrate as the eluent, the collection of highly concentrated fractions (up to 30 mg/ml) in water and the simple final recovery of pure IL-1β(163–171) by lyophylization.

The feasibility of using DC in series in the RP and IE modes has been demonstrated, with a evident improvement both in the purity (>98%) and total chromatographic recovery (>90%) of the target peptide.

REFERENCES

1 J. Rivier, R. McClintock, R. Galyean and H. Anderson, *J. Chromatogr.*, 288 (1984) 303.
2 S. Godbane and G. Guiochon, *J. Chromatogr.*, 444 (1988) 275.
3 Cs. Horvath, A. Nahum and J. H. Frenz, *J. Chromatogr.*, 218 (1981) 365.

4 H. Kalasz and Cs. Horvath, *J. Chromatogr.*, 215 (1981) 295.
5 Gy. Vigh, Z. Varga-Puchony, G. Szepesi and M. Gazdag, *J. Chromatogr.*, 386 (1987) 353.
6 G. C. Viscomi, S. Lande and Cs. Horvath, *J. Chromatogr.*, 440 (1988) 157.
7 G. C. Viscomi, A. Ziggiotti and A. S. Verdini, *J.Chromatogr.*, 482 (1989) 99.
8 G. Antoni, R. Presentini, F. Perin, A. Tagliabue, P. Ghiara, S. Censini, G. Volpini, L. Villa and D.Boraschi, *J. Immunol.*, 137 (1986) 3201.
9 L. Nencioni, L.Villa, A. Tagliabue, G. Antoni, R. Presentini, F. Perin, S. Silvestri and D. Boraschi, *J. Immunol.*, 139 (1987) 800.
10 E. Papp and J. Inczedy, *Talanta*, 27 (1980) 49.
11 F. Cardinali, A. Ziggiotti and G. C. Viscomi, *J. Chromatogr.*, 499 (1990) 37.
12 F. Perin, R. Presentini and G. Antoni, *J. Chromatogr.*, 397 (1987) 365.
13 Cs. Horvath, in F. Bruner (Editor) *The Science of Chromatography* (*Journal of Chromatography Library*, Vol. 32), Elsevier, Amsterdam, 1985, pp. 179–203.
14 A. W. Liao, Z. El Rassi, D. M. LeMaster and Cs. Horvath, *Chromatographia*, 24 (1987) 881.
15 A. S. Verdini, M. Pinori, M. G. Longobardi, G. C. Viscomi, L. Parente, P. Pileri, S. Peppoloni, S. Silvestri and L. Nencioni, *J. Med. Chem.*, (1991), in press.

Journal of Chromatography, 549 (1991) 185–193
Elsevier Science Publishers B.V., Amsterdam

CHROM. 23 335

Bioanalysis of the neuropeptide des-enkephalin-γ-endorphin by high-performance liquid chromatography with on-line sample pretreatment using gel permeation and solid-phase isolation

D. S. STEGEHUIS, U. R. TJADEN*, C. M. B. VAN DEN BELD and J. VAN DER GREEF
Division of Analytical Chemistry, Center for Bio-Pharmaceutical Sciences, University of Leiden, P.O. Box 9502, 2300 RA Leiden (Netherlands)
(First received December 27th, 1990; revised manuscript received March 12th, 1991)

ABSTRACT

A bioanalytical method is described that allows the determination of a number of β-endorphin-related peptides. The method is based on the application of fluorescence detection after high-performance liquid chromatography followed by post-column derivatization with *o*-phthaldialdehyde. Concentrations exceeding 10–25 ng/ml could be determined by using conventional fluorescence detection, whereas lower concentrations demand the use of laser-induced fluorescence detection. The sample pretreatment includes the use of on-line gel permeation, on-line solid-phase isolation and heart cutting of a peak from reversed-phase gradient elution. The sample pretreatment procedure does not discriminate between the dodecapeptide des-enkaphalin-γ-endorphin (DEγE) and its metabolites in order to obtain similar recoveries for all components. The final chromatographic phase system is based on ion-pair formation, which permits the separation of DEγE from its metabolites and degradation products. The optimized procedure allows the determination of these peptides in plasma at concentration levels down to about 1 ng/ml, demanding a sample volume of 1 ml.

INTRODUCTION

There is growing interest in the bioanalysis of endogenous peptides owing to their pharmacological activity at low concentration at several sites in the human body. As an example, β-endorphins play an important role in the central nervous system. For a number of these peptides immunoassays have been developed [1]. Although methods based on radiochemical techniques, such as radioimmunoassays (RIA) and radioreceptor assays (RRA), allow the determination of extremely low concentrations [2,3] directly in the biological matrix, these methods may be not sufficiently selective with respect to structurally closely related metabolites and degradation products. A practical drawback of RIA and RRA is the application of radioactive labels, demanding a laboratory equipped for radioactive measurements. Non-radioactive bioanalytical methods may therefore be attractive. In addition to immunoassays, chromatographic methods such as liquid chromatography (LC) in combination with UV absorbance or fluorescence detection can be considered. The

0021-9673/91/$03.50

peptides that have been investigated in this study, however, show poor spectrophotometric and electrochemical [4] characteristics. We focused on the peptide des-enkaphalin-γ-endorphin (DEγE) and metabolites that interfere in the RIA owing to the high cross-reactivity. In order to allow the determination of these peptides at the ng/ml or even lower plasma levels, their detectability has to be improved, *e.g.*, by employing pre-or post-column derivatisation techniques [5,6]. Further, the compounds of interest have to be separated from an excess of interferents originating from the biological matrix.

The combination of high-performance liquid chromatography (HPLC), post-column derivatization and fluorescence detection has proved to be a powerful tool in the bioanalysis of peptides. Detection limits in the picogram range could be obtained in this way [7,8]. From earlier work it is known that the sample clean-up is extremely important [9], especially when laser-induced fluorescence (LIF) detection is used [10]. A sample clean-up for DEγE has been described in a previous paper [9] and consisted of a combination of on-line dialysis and solid-phase isolation. This method resulted in a determination limit for this peptide of about 10 ng/ml in plasma, although the detection limit for the *o*-phthaldialdehyde derivative of this peptide was 100 pg/ml. The discrepancy between these two limits is mainly caused by the sample clean-up procedure, which therefore has to be improved with respect to selectivity towards the biological background. Therefore, we investigated the use of gel permeation for sample pretreatment as an alternative to on-line dialysis for the removal of macromolecular compounds, because these matrix constituents will severely interfere with the analysis of peptides [11,12]. Regarding the determination of DEγE the immediate removal or deactivation of enzymes is especially important, because they cause its degradation resulting in a half-life of about 2 min [9]. Also, the plugging and modification of the chromatographic system that can be caused by these macromolecular compounds can be very disturbing when larger sample volumes (1 ml) are introduced. Even after deproteination with trichloroacetic acid to decrease enzyme activity, an unacceptable amount of relatively high-molecular mass compounds was still present in the sample. Similar selectivities are expected from gel permeation and dialysis, as both methods have in principle the same selectivity criteria, which are based on molecular size. However, a clear advantage that can be expected from gel permeation is that, in addition to selectivity towards the higher molecular mass compounds, it also offers selectivity towards the lower molecular mass range combined with additional adsorption characteristics.

EXPERIMENTAL

Chemicals

Trichloroacetic acid (TCA) was supplied by Baker Chemicals (Deventer, Netherlands). Mercaptoethanol (ME) and *o*-phthaldialdehyde (OPA) by Fluka (Buchs, Switzerland) and LC-grade acetonitrile by Rathburn (Walkerburn, UK). Synthetic human DEγE (β-endorphin 6–17; βE 6–17) and its metabolites (βE 7–17 and βE 8–17) were donated by Organon International (Oss, Netherlands). The phosphate buffers were composed of different volumes of 0.05 *M* phosphoric acid and 0.05 *M* disodium hydrogenphosphate purchased from Brocacef (Maarssen, Netherlands). The borate buffer was prepared from 0.1 *M* sodium tetraborate.

Throughout the study deionized water obtained from a Milli-Q water purification system (Millipore, Bedford, MA, USA) and capped polypropylene vials (Greiner, Alphen a/d Rijn, Netherlands) were used for all peptide-containing solutions. Amberlite XAD-2 (Rohm and Haas, Philadelphia, PA, USA) with a particle size range of 20–30 μm and Sephadex G-50 superfine (Pharmacia, Uppsala, Sweden) were used in the gel columns.

Equipment

The HPLC gradient system consisted of two dual-piston high-pressure pumps (Spectroflow 400; Kratos, Ramsey, NJ, USA) controlled by a Spectroflow SF450 programmer. A laboratory-made high-pressure mixing device with an internal volume of about 400 μl with a stirring magnet was applied. The switching system was a MUST (Spark Holland, Emmen, Netherlands) equipped with two six-port valves (Model 7010; Rheodyne, Berkely, CA, USA). Injections were performed with a fixed-volume (100 μl) injection valve (Model 7125; Rheodyne). Fluorescence detection was performed with a Perkin-Elmer (Beaconsfield, UK) LS 4 detector using an excitation wavelength of 334 nm, an emission wavelength of 455 nm and a slit width of 5 nm for both excitation and emission. The analytical column (100 × 3.0 mm I.D.) was laboratory-packed with C_{18} Nucleosil (5 μm) (Macherey, Nagel & Co., Düren, Germany). The precolumn was a stainless-steel cartridge (30 × 2.0 mm I.D.) packed with XAD-2 (20–30 μm). The post-column derivatization device consisted of a Model P 3500 high-pressure pump (Pharmacia) and a stainless-steel reaction coil (400 μm I.D.) spirally coiled with a coil diameter of about 2 cm. The internal volume was about 0.2 ml. A stainless-steel dead-volume T-piece (Upchurch Scientific, Oak Harbor, WA, USA) was used to mix the effluent and the derivatization reagent. The continuous-flow system consisted of an autosampler (Model 1000), with Solvent Flux tubing, and a peristaltic pump (Model 2002), all from Skalar (Breda, Netherlands). The polystyrene autosampler tubes had a volume of 3.5 ml (Skalar). The dimensions of the gel column cartridge (Pharmacia) were 120 × 10 mm I.D. with a volume adaptor. The glass tube was replaced by a Plexiglas tube (laboratory-made). The fraction collector was a Model 100 from Pharmacia.

The LIF system, which is described in detail elsewhere [10], has as an excitation source a water-cooled continuous-wave argon-ion gas laser (Model 2025-03; Spectra-Physics, Mountain View, CA, USA). Operating in the UV mode, the laser emits at 351.1 and 363.8 nm with a total output power of 165 mW. A rectangular flow-through cuvette (Model 176.752 QS, 22.5 μl; Hellma, Müllheim/Baden, Germany) with an optical path length of 1.5 mm is used as detector cell. Because the laser beam was focused very close to the inlet capillary, an effective cell volume of 2 μl was realized. The fluorescence light was guided to the photomultiplier tube by a liquid light guide (1000 × 5.0 mm I.D., No. 77556; Oriel, Stratford, CT, USA) equipped with a plano-convex fused-silica lens (diameter 11 mm, focal length 19 mm; No. 41210) at each end. At the detector side, the light was collected by a plano-convex lens (as above) and directed into an interference filter (Oriel, Stratford, CT, USA). The fluorescence was detected by a blue–green-sensitive photomultiplier tube (PMT) (No. 9635B; Thorn EMI, Ruislip, Middlesex, UK) operating at 600 V, which was generated by a high-voltage supply (Model 244; Keithley Instruments, Cleveland, OH, USA). The signal was processed by a current amplifier (Model 427; Keithley Instruments).

Pretreatment

Plasma samples were obtained from a pharmacokinetic study with healthy volunteers in which the samples should be assayed by an RIA method. Because this method does not allow the presence of TCA, the samples were immediately frozen after sampling. These plasma samples were treated individually, because of the limited stability of DEγE in plasma. Spiking of the calibration samples was also applied one sample after another. The samples were defrosted individually and immediately deproteinated by adding 300 μl of 1 *M* TCA per millilitre of plasma. After deproteination, the samples were whirl-mixed for 3 s and centrifuged for 10 min at 1000 *g*. The supernatant (about 1 ml) was decanted and placed in the autosampler.

The whole sample was loaded onto the gel permeation column at a flow-rate of 0.3 ml/min. The fraction from 25 to 35 min was heart-cut (fraction I). This whole fraction (corresponding to 3 ml) was reconcentrated on an XAD-2 column with a flow-rate of 0.6 ml/min. After about 5 min, the XAD-2 columm was connected in series with the analytical column of the gradient system by switching valve 1 (Fig. 1). The gradient profile started for 5 min with 100% aqueous mobile phase and then 5 min at 15% acetonitrile, followed by 5 min at 27.5% acetonitrile. Between 15 and 16 min after starting the gradient, a second heart-cut (fraction II) was made by switching valve 2 (Fig. 1). This fraction had a volume of 0.5 ml.

Chromatography

For conventional fluorescence detection and LIF detection, two different chromatographic systems were used. Conventional fluorescence detection was applied for monitoring the chromatographic system belonging to the sample pretreatment part using a C_{18} analytical column (Nucleosil C_{18} 5 μm; 100 × 3.0 mm I.D.) with a mobile phase consisting of phosphate buffer (0.05 *M*, pH 2.4)–acetonitrile (4:1, v/v).

The LIF detector was used in the final step, where separation and determina-

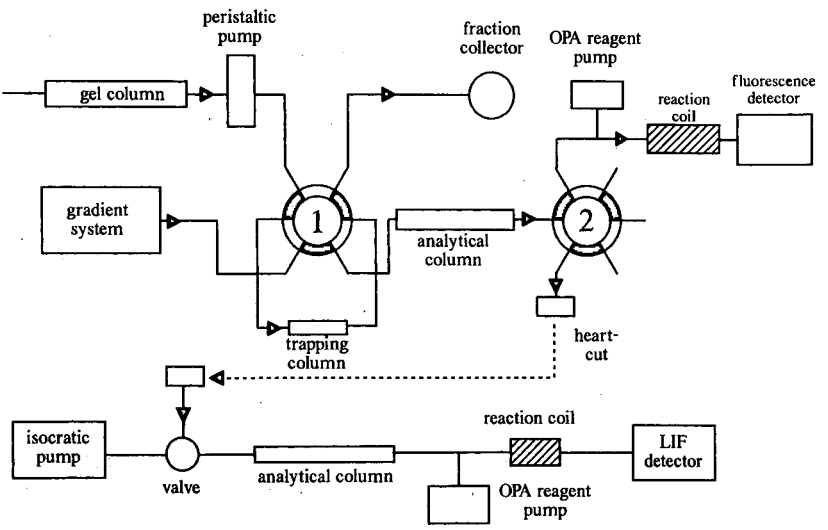

Fig. 1. Scheme of analytical system.

tion of DEγE and its metabolites took place. The chromatographic system for the LIF detector consisted of a C_{18} analytical column (see above) with a mobile phase consisting of phosphate buffer (0.01 *M*, pH 2.4)–acetonitrile–22.5 m*M* octanesulphonate (76.8:22.7:0.5, v/v/v). Two different injection methods were used. In the fluorescence detection system, the sample was diluted to an acetonitrile concentration below 10% and loaded onto an XAD-2 column. By switching valve 1 (Fig. 1), the sample was introduced into the HPLC system. In the LIF detection system, an injection loop of 1.5 ml was used, and the sample was diluted to 1.0 ml with water. After injection of the sample on the octanesulphonate system, on-column concentration took place.

Detection

Both conventional fluorescence and LIF detection, were applied, both in combination with post-column OPA derivatization. The conventional fluorescence detection system was used for the daily screening of concentrations above 10–25 ng/ml. Below this concentration, LIF detection was required to determine DEγE. In both systems, the post-column reagent was added at a flow-rate of 0.25 ml/min via a T-piece. Derivatization took place in a reaction coil with a reaction time of 15 s. The reagent solution contained 9.0 mg of OPA and 260 μl of ME in 200 ml of 0.1 *M* borate buffer (pH 9.5).

RESULTS AND DISCUSSION

In an earlier paper [9], a method was described in which on-line dialysis was used in the sample clean-up for plasma samples containing DEγE. On-line dialysis allowed the complete removal of compounds with a molecular mass above 10 000 dalton, but is not selective for plasma components with a low molecular mass. Furthermore, recoveries were relatively low (about 25%) and dependent on the dialysis time. In order to improve this method, we investigated gel permeation as a sample pretreatment technique. Gel permeation is often used as a method for separations based on molecular mass distribution [13], for example, for protein analysis [14–16] or analysis of lower molecular mass biopolymers such as peptides [17]. For gel permeation, Sephadex G-50 was chosen, because DEγE has a molecular mass of 1304 dalton and the fractionation range of this gel is between 1500 and 30 000 dalton. In principle, DEγE should be eluted within approximately one column volume but in practice is was about three void volumes. The elution profile of DEγE is given in Fig. 2. The retention volume indicates that retention is based on a combination of mechanisms. Separation of the analyte from larger molecular compounds occurs by a size-exclusion mechanism. The occurrence of capacity factors larger than the theoretical value for gel permeation implies that, in addition to size exclusion, adsorption phenomena also contribute to the retention of DEγE. The polar surface of the Sephadex stationary phase, made by cross-linking dextranes with epichlorohydrin, probably causes adsorption of the polar peptides. A similar phenomenon has been described by Schoots and Cramers [18], who compared dialysis with gel permeation for "middle molecules" with molecular masses between 300 and 1500 dalton. Because the contribution of adsorption phenomena to the retention of DEγE was very favourable regarding the selectivity of the system, no attempts were made to suppress adsorption,

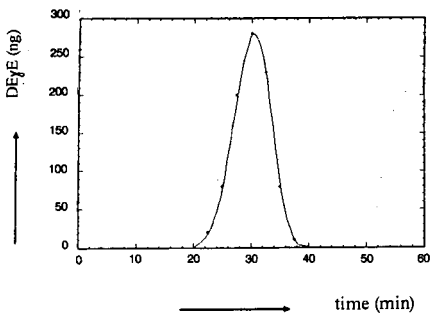

Fig. 2. Elution profile of DEγE from the Sephadex G-50 column. A 1-ml volume of solution containing 1 μg of DEγE was placed on the gel column. Fractions were analysed using conventional fluorescence detection (see text).

e.g., by adding a strong buffer to the mobile phase. DEγE also strongly adsorbs on glass surfaces; therefore, the Sephadex gel was installed in a Plexiglas tube instead of the glass tubes provided by the manufacturer.

A practical drawback in applying gel permeation in the conventional mode is the time-consuming elution procedure caused by the inherent low flow-rates. The high compressibility of the gel does not permit flow-rates higher than can usually be achieved by hydrostatic flow. This problem has been overcome by implementation of the gel column in a continuous-flow system. The gel column is connected to a peristaltic pump so that the eluent is pumped in and sucked out at the same flow-rate. In this way the flow-rate can be increased with a minimum pressure build-up and gel permeation can be performed in an on-line mode with automated fraction collection. A further advantage of this technique is an improved reproducibility of selectivity and recovery of the clean-up method. The fraction containing the highest concentration of DEγE and the lowest concentration of interfering compounds as determined in the fractions composing the profile given in Fig. 2 is used for further pretreatment. The sample, with an initial volume of 1 ml, is diluted to about 6 ml during gel permeation, from which 3 ml (fraction I) is processed further and must therefore be concentrated again. This concentration step is performed on a reversed-phase XAD-2 column. The XAD-2 material is very suitable for this application, as described previously [9], because the capacity factor of DEγE is sufficiently high to allow preconcentration of volumes up to 10 ml without breakthrough. Direct analysis of fraction I, using an isocratic ion-pairing system that permits the separation of DEγE and its metabolites, and that is compatible with LIF detection, results in disappointing determination limits and unacceptable run times. Therefore, an additional clean-up by means of a gradient elution was applied. In this step the use of ion-pair formation must be avoided because this should introduce selectivity between the individual analytes. After 15 min, a heart-cut (fraction II with a volume of 0.5 ml) was made. Fig. 3a shows a chromatogram of the gradient run of a plasma sample, where the marked area indicates the heart-cut. Fig. 3b and c show the chromatogram of the heart-cut fractions containing 400 and 40 ng, respectively. Although this fraction seems to be fairly clean, it must be realized that in this stage neither an ion-pairing agent nor LIF detection was applied. Therefore, fraction II can now be analysed by an isocratic

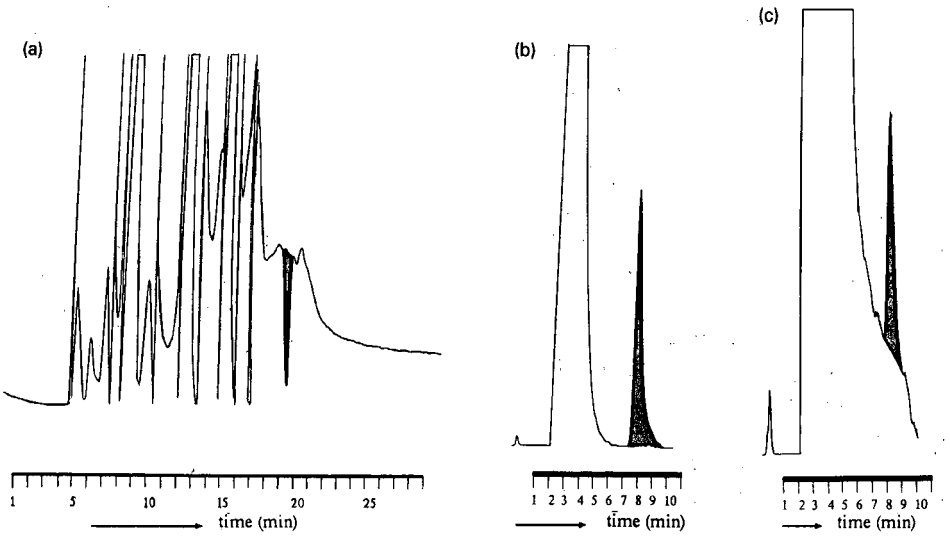

Fig. 3. Chromatogram of plasma sample after sample pretreatment with gel permeation, solid-phase concentration and gradient elution. For conditions, see text. (a) The black area indicated the location where the heart-cut was taken. Processed plasma volume, 1 ml. (b), (c) Chromatograms of heart-cut fractions (b + c); b and c are samples containing 400 and 40 ng of DEγE, respectively, added to 1 ml of plasma.

system, but first it must be diluted with water to reduce the modifier content. The diluted fraction with a volume of about 1 ml can be introduced on the isocratic system, either by concentrating the sample once again on an XAD-2 precolumn, or by injecting the sample with an injection loop of 1.5 ml applying on-column concentration.

With the ion-pairing chromatographic system DEγE can be separated from its metabolites βE 7–17 and βE 8–17 [19,20]. Because the sample pretreatment does not discriminate between DEγE and its metabolites, the recovery of these analytes is about the same. The recovery of the overall method was determined by assaying blank plasma samples that were spiked with known amounts of the compounds under investigation. The recovery for this group of peptides was about 50%. Although this recovery can be increased by selecting a larger volume after the gel permeation step, a smaller fraction was collected, because this step has been optimized with respect to the ratio between analytes and interfering compounds. Obviously, this lower recovery is due to the limited efficiencies achieved with permeation columns of the Sephadex type.

A conventional fluorescence detector was used to monitor the sample pretreatment, although of course a less sensitive method such as UV absorbance detection can also be used for this purpose. The LIF detection system has been used because pharmacokinetic profiles had to be followed down to the pg/ml range. If such low concentration levels are not involved, conventional fluorescence detection can also be used in the final separation and determination stage.

The analysis time for a single sample is about 80 min. However, a series of about 20 samples could be analysed in *ca.* 8 h. This higher throughput of samples is possible because except for the acidic deproteination and the last dilution step before

injection into the ion-pairing system, the system is automated and most steps can be operated simultaneously. Also, the two off-line steps can be integrated into the automated procedure, which can be realized by either robotics or continuous-flow techniques, although the former would more suitable for implementation.

Quantitative aspects

In order to generate calibration graphs, blank plasma samples were spiked with DEγE at concentration of 1, 5, 10, 50 and 100 ng/ml and analysed according to the procedure with LIF detection as described above. A typical correlation coefficient and equation of the curve were 0.997 and $y = 1.85\ (\pm 0.05)x + 2.54\ (\pm 2.48)$, respectively, in which the standard deviation of the slope and the intercept are given in parentheses. The fluorescence signal is expressed in arbitrary fluorescence units. The determination limit was 1 ng/ml plasma.

The accuracy of the method was determined by analysing a series of ten blank plasma samples spiked with 100 ng/ml of DEγE using conventional fluorescence detection. The accuracy was characterized as the relative difference between added and found concentrations and appeared to be -7%. This relatively high bias is certainly caused by the limited stability of the peptide. Degradation of DEγE was observed not only in biological matrices but also in buffered solutions (pH 2.4, 0.01 *M*, in demineralized water and in purified water sometimes unpredictable and unexplainable degradation was observed.

The day-to-day variation was determined on four different days, resulting in a relative standard deviation of 4.9% at a level of 100 ng/ml and 9.7% at 10 ng/ml.

Application to biological samples

The applicability of the method was demonstrated by assaying a number of plasma samples originating from a pharmacokinetic experiment. In Fig. 4a and b the chromatograms are shown of an extract of plasma from a healthy volunteer before and after intramuscular administration of 20 mg of DEγE. It can be seen that DEγE is

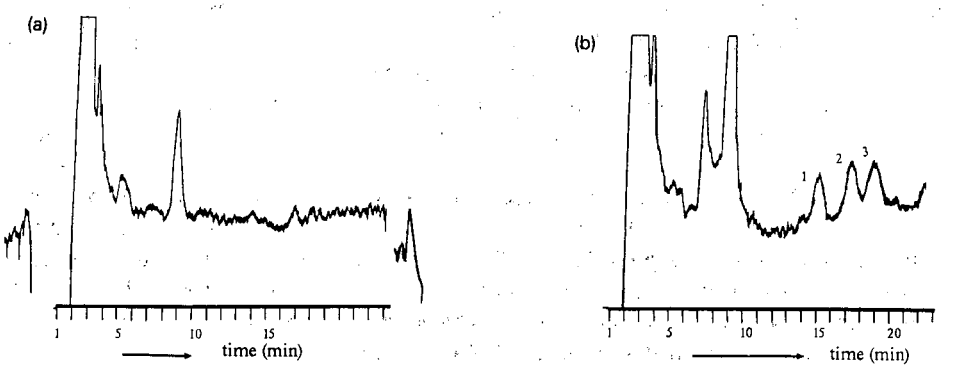

Fig. 4. (a) Analysis of human plasma sample before intramuscular injection of DEγE; 1 ml of plasma was analysed. (b) Analysis of human plasma sample taken 8 min after intramuscular injection of 20 mg of DEγE; 1 ml of plasma has been analysed. The peaks correspond to about (1) 4 ng/ml of DEγE, (2) 4 ng/ml of βE 7–17 and (3) 4 ng/ml of βE 8–17.

well separated from its main metabolites βE 7–17 and βE 8–17. The pretreated samples were measured with the LIF detection system. The metabolites of DEγE were determined from the calibration graphs for DEγE. This is possible only because the OPA derivatization takes place at the same amino function of peptides. The metabolic degradation took place at the C-terminus of the peptides [1]. Hence the fluorescence intensities of the OPA derivatives of DEγE and its metabolites can be considered to be equal.

CONCLUSIONS

The method presented is suitable for the determination of DEγE and its metabolites βE 7–17 and βE 8–17 at concentrations down to 1 ng/ml in complex biological matrices such as plasma. The method is more sensitive and selective than previously described methods such as on-line dialysis [9] and RIA [1]. The on-line dialysis method could not reach the same determination levels and the RIA method could not achieve the same selectivity.

A major problem common to all methods is the instability of DEγE in biological matrices at concentrations below 100 ng/ml. The risk of this instabiliy can be reduced to a minimum by extremely careful handling of the samples and peptide solutions. Peptide stock solutions were more stable in acidic buffers, but also in this environment degradation was sometimes observed.

REFERENCES

1 J. C. Verhoef, H. Scholtens, E. G. Vergeer and A. Witter, *Peptides*, 6 (1985) 467.
2 G. H. Fridland and D. M. Desiderio, *J. Chromatogr.*, 379 (1986) 251.
3 D. Liu and D. M. Desiderio, *J. Chromatogr.*, 422 (1987) 61.
4 L. H. Fleming and N. C. Reynolds, Jr., *J. Chromatogr.*, 432 (1988) 65.
5 M. Kai, J. Ishida and Y. Ohkura, *J. Chromatogr.*, 430 (1988) 271.
6 M. Ohno, M. Kai and Y. Ohkura, *J. Chromatogr.*, 490 (1989) 301.
7 T. Miyazki, M. Kai and Y. Ohkura, *J. Chromatogr.*, 490 (1989) 43.
8 G. R. Rhodes and V. K. Boppana, *J. Chromatogr.*, 444 (1988) 123.
9 D. S. Stegehuis, U. R. Tjaden and J. van der Greef, *J. Chromatogr.*, 511 (1990) 137.
10 C. M. B. van den Beld, H. Lingeman, G. J. van Ringen, U. R. Tjaden and J. van der Greef, *Anal. Chim. Acta*, 205 (1988) 15.
11 G. B. Irvine, *J. Chromatogr.*, 404 (1987) 213.
12 N. Hirata, M. Kasai, Y. Yanagihara and K. Noguchi, *J. Chromatogr.*, 434 (1988) 71.
13 M. E. Himmel, K. Tatsumoto and K. Grohmann, *J. Chromatogr.*, 498 (1989) 93.
14 E. Lacey and K. L. Snowdon, *J. Chromatogr.*, 525 (1990) 71.
15 J. P. Sion, M. Laureys, E. Gerio and Gorus, *J. Chromatogr.*, 496 (1989) 91.
16 T. van Gent and A. van Tol, *J. Chromatogr.*, 498 (1989) 93.
17 J. M. Piot, D. Guillochon and D. Thomas, *Chromatographia*, 25 (1988) 307.
18 A. C. Schoots, C. A. M. G. Cramers, *J. Chromatogr.*, 497 (1989) 79.
19 P. S. Janssen, J. W. van Nispen, P. A. T. A. Melgers and R. L. A. E. Hamelinck, *Chromatographia*, 212 (1986) 461.
20 C. M. B. van der Beld, U. R. Tjaden, N. J. Reinhoud, D. S. Stegehuis and J. van der Greef, *J. Controlled Release*, 13 (1990) 129.

Journal of Chromatography, 549 (1991) 195–205
Elsevier Science Publishers B.V., Amsterdam

CHROM. 23 346

Mobile phase effects in the high-performance affinity purification of thermolysin

MORENO ZAMAI[a]
Department of Organic Chemistry, University of Padova, Padova (Italy)
and
GIORGIO FASSINA*
Protein Engineering Unit, Tecnogen ScpA, Via Ampere 56, 20131 Milan (Italy)
(First received August 7th, 1990; revised manuscript received February 13th, 1991)

ABSTRACT

The dependence on solvent composition of the affinity of thermolysin (E.C. 3.2.24.4) for an immobilized inhibitor was characterized using zonal, competitive and frontal analytical high-performance liquid affinity chromatography (HPLAC). Affinity, measured as the extent of thermolysin retardation on inhibitor (Gly-D-Phe) columns, was strongly affected by variations in the pH, ionic strength, nature of buffering salts and the presence of organic solvents such as 2-propanol in the eluting buffer. While zonal elution experiments allowed the determination of the influence of the mobile phase composition on the overall process, frontal elutions identified specific effects on the individual affinity properties of the enzyme and the immobilized inhibitor. In agreement with data determined previously completely in solution, the interaction on the solid phase was driven mainly by hydrophobic interactions and was affected negatively by organic salts. Based on these results, more efficient elution conditions for the purification of thermolysin by affinity chromatography were established.

INTRODUCTION

Binding between biological macromolecules usually occurs between structurally well defined entities with a number of specific side-chain groups involved in providing various interactions to stabilize the forming complex. The medium plays an essential role in favouring or unfavouring such interactions. Ionic/hydrophilic contributions to the interaction can be distinguished from hydrophobic contributions by determining the effect of increasing concentrations of salts and organic solvents on the system binding affinity, under conditions that do not alter the three-dimensional structure of the folded macromolecule.

The study of solvent effects on binding processes is also of extreme importance when a careful design of affinity purification methods has to be made. Very often, milder conditions than chaotropic elution can be devised simply by selecting an elut-

[a] Present address: Farmitalia Carlo Erba, Nerviano (MI), Italy.

0021-9673/91/$03.50

ing buffer composition that reduces the system binding affinity constant by only one or two orders of magnitude.

In this study, the affinity properties of the protease thermolysin with respect to its inhibitor Gly-D-Phe were characterized under different solvent conditions by analytical high-performance liquid affinity chromatography (HPLAC) using zonal, competitive and frontal elutions [1,2].

Thermolysin is a thermostable metallo endopeptidase which catalyses the hydrolysis of proteins and synthetic peptide substrates [3,4]. The interaction with its inhibitor Gly-D-Phe has been previously characterized in solution [5] from enzymatic inhibition data, providing an equilibrium binding constant of 16 m*M*. The three-dimensional structure of the enzyme is also known [6], and it has been shown that the interaction with the inhibitor Gly-D-Phe is mainly hydrophobic in nature [7]. Affinity chromatography of thermolysin has been carried out previously using various ligands immobilized on soft gels [8–10], eluting bound thermolysin by raising the buffer pH to 9.0.

The effect of different buffer compositions on the binding affinity of the protease/inhibitor interaction was evaluated to determine whether useful information about the interaction process could be obtained by analytical HPLAC and used to devise new procedures for more efficient affinity purifications of thermolysin.

EXPERIMENTAL

Materials

Thermolysin from *Bacillus thermoprotheolyticus* (Rokko), N^{α}-(furylacryloyl) glycyl-L-leucinamide (FAGLA) and Gly-D-Phe were obtained from Sigma (St. Louis, MO, USA) High-performance liquid chromatographic (HPLC)-grade water, acetonitrile and 2-propanol from Fisher Scientific (Fair Lawn, NJ, USA) and trifluoroacetic acid (TFA) from Pierce (Rockford, IL, USA). The epoxy-preactivated affinity support Eupergit C30 N was obtained from Rohm & Haas (Weiterstadt, Germany). Glass columns for packing the derivatized affinity support were purchased from Omni (Cambridge, UK). HPLC and HPLAC separations were performed on a LKB HPLC system. Analytical reagent grade solvents and chemicals were used throughout.

Immobilization of Gly-D-Phe on Eupgergit C30 N

Eupergit C30N (1.5 g) was washed twice with 50 ml of deionized water on a sintered-glass funnel. The resin was then washed twice with 50 ml of coupling buffer (pH 8.0) containing 0.1 *M* sodium hydrogen carbonate and 0.5 *M* sodium chloride, and sucked dry by vacuum aspiration. The resin was then suspended in 45 ml of coupling buffer containing 600 mg of Gly-D-Phe and incubated at room temperature for 2 h with shaking. Excess liquid was decanted, 940 mg of glycinamide dissolved in 40 ml of the above coupling buffer were added and the suspension was shaken for 1 h at room temperature. The derivatized resin was washed twice with 50 ml of coupling buffer and twice with 50 ml of water and then dried under vacuum. The column used for frontal analysis experiments was prepared with a lower loading, coupling 40 mg of Gly-D-Phe on 1.0 g of Eupergit C30 N. Solutions used in the derivatization procedure were first sterilized by passing them through a 0.22-μm filter.

High-performance liquid affinity chromatography

Derivatized support was dry-packed into a 150 × 6.6, 100 × 6.6 or 50 × 3 mm I.D. glass column. For chromatography, the columns were connected to an LKB liquid chromatograph equipped with a Model 2151 variable-wavelength UV detector. All buffers used for chromatographic elutions were prepared with HPLC-grade water, filter sterilized and degassed under vacuum prior to use.

Enzyme activity

The activity of thermolysin was measured by monitoring the decrease in absorbance of FAGLA at 345 nm at 25°C. The assay solution (3 ml) contained FAGLA (1 m*M*) in 10 m*M*) in 10 m*M* Tris (pH 7.0), 10 m*M* calcium chloride and 10^{-5} *M* zinc acetate, and the catalytic reaction was initiated by adding an enzyme solution (5–50 μl). The decrease in absorbance at 345 nm was followed as a function of time.

Theoretical

Dissociation constants for the interaction of thermolysim with immobilized Gly-D-Phe were obtained by two methods: zonal elution and continuous (broad zone) elution. In the former instance, the column was equilibrated with an appropriate buffer (see Results), monitoring the effluent by measuring the UV absorbance at 280 nm, until a stable baseline was observed. Zones containing different amounts of thermolysin were then injected and the elution profile was recorded. The elution volume of the zone, V, can be related to the concentration of thermolysin in the zone by

$$\frac{1}{V-V_0} = \frac{K_{M/P}}{M_T} + \frac{[P]}{M_T} \tag{1}$$

where V_0 is the unretarded elution volume (determined with injections of blue dextran), $K_{M/P}$ is the dissociation constant of the immobilized inhibitor–thermolysin complex and M_T is the total amount of immobilized inhibitor. During zonal elution [P] is not easily defined and is not determined. However, is possible to plot the initial concentration of P in the zone, namely $[P]_0$, against $1/(V-V_0)$ and calculate the $K_{M/P}$ value from the intercept at $[P]=0$. Competitive elutions were also carried out by injecting zoned of thermolysin on the inhibitor column equilibrated with buffers containing different Gly-D-Phe concentrations, $[L]_T$. The variation of V with $[L]_T$ was evaluated by the equation

$$\frac{1}{V-V_0} = \frac{K_{M/P} + [P]}{M_T} + \frac{K_{M/P}[L]_T}{K_{P/L}M_T} \tag{2}$$

where $K_{P/L}$ represents the dissociation constant between the mobile Gly-D-Phe and thermolysin. Total amount of active, immobilized Gly-D-Phe was determined from frontal elution experiments. To the equilibrated column, solutions containing different concentrations of affinity-purified thermolysin were applied continuously and the effluent was monitored by measuring the UV absorbance until a plateau was observed. The variation of the elution volume of the front, V, was plotted according to the equation

$$\frac{1}{[P]_T(V-V_0)} = \frac{K_{M/P}}{M_T} \cdot \frac{1}{[P]_T} + \frac{1}{M_T} \tag{3}$$

From a plot of the first term of eqn. 3 against $1/[P]_T$ it is possible to calculate $1/M_T$ from the intercept at $1/[P]_T = 0$.

RESULTS

Characterization of thermolysin–Gly-D-Phe interaction by analytical HPLAC

The zonal elution affinity chromatography approach was used to evaluate quantitatively the binding process between immobilized Gly-D-Phe and soluble thermolysin. Zones containing different amounts of thermolysin were injected onto the [Gly-D-Phe]Eupergit column equilibrated with 50 m*M* Tris (pH 7.0), and the elution profile was recorded (Fig. 1). The extent of retardation was found to be linearly dependent on the amount applied (Fig. 1, inset), in agreement with eqn. 1.

Amino acid analysis of the Gly-D-Phe-derivatized affinity support indicated the presence of 500 μmol of immobilized inhibitor. Assuming this to be a correct value for the functional capacity, M_T, a chromatographically calculated dissociation constant of 14 m*M* is obtained. To verify the absence of aspecific interactions on the column, competitive elutions of thermolysin were carried out on the [Gly-D-Phe]Eupergit column with different amounts of Gly-D-Phe dissolved in the eluting buffer. According to eqn. 2, under these conditions it is possible to obtain not only $K_{M/P}$, but also $K_{P/L}$, the dissociation constant for the interaction between soluble Gly-D-Phe and thermolysin. The results are summarized in Fig. 2. The chromatographically calculated value of $K_{M/P}$ (14 m*M*) agrees fairly well with the $K_{P/L}$ value (16 m*M*), both calculated under the same conditions, indicating that aspecific interactions with the support, if they occur, are negligible. These values agrees well also with the inhibition constant of

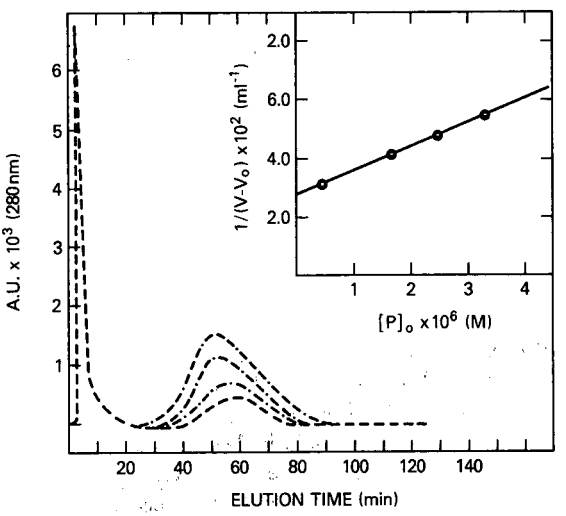

Fig. 1. Zonal elution HPLAC analysis of thermolysin binding to immobilized Gly-D-Phe. Zones (200 μl) containing different amounts of HPLAC-purified thermolysin were eluted on the [Gly-D-Phe]Eupergit column (75 × 6.6 mm, M_T 500 μmol) equilibrated with 20 m*M* Tris–10 m*M* $CaCl_2$ (pH 7.1) at a flow-rate of 0.5 ml/min. The inset shows the variation of *V* with the amount of thermolysin in the applied zone. Data are plotted according to eqn. 1.

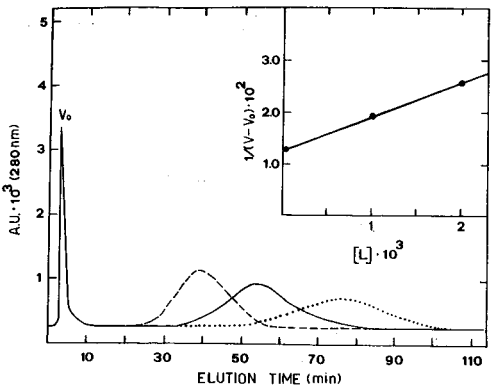

Fig. 2. Competitive zonal elution HPLAC analysis of thermolysin binding to Gly-D-Phe. Zones of 28 μg of HPLAC-purified thermolysin in 200 μl were eluted on the [Gly-D-Phe]Eupergit column (6.6 × 150 mm I.D., M_T 1 mmol) equilibrated with 20 mM Tris–10 mM $CaCl_2$ (pH 7.1) at a flow-rate of 1.0 ml/min containing soluble Gly-D-Phe at concentrations of 0, 1 and 2 mM. Data are plotted according to eqn. 2.

soluble Gly-D-Phe for soluble thermolysin (K_i = 16 mM), determined completely in solution [5]. The lower affinity observed for the interaction in solution may well reflect the previously reported diminished inhibition of thermolysin enzymatic activity by dipeptides with free α-amino groups [5].

Dependence of mobile phase composition on thermolysin–inhibitor interaction

The extent of thermolysin retardation on the [Gly-D-Phe]Eupergit column was strongly dependent on the composition of the eluting buffer (Fig. 3). An increase in the Tris concentration in the buffer negatively affected the binding, reducing the interaction strongly. Similarly, but to smaller extent, 4-(2-hydroxyethyl)-1-piperazineethanasulphonic acid (HEPES) influenced the retardation. Inclusion of 2-propanol also reduced the binding, indicating that hydrophobic interaction phenomena play an essential role in the process, as lowering of the surface tension in an aqueous phase on inclusion of an organic solvent has been shown to reduce greatly hydrophobic interactions between molecules [11].

Determination of column capacity

Although with the zonal approach a convenient determination of equilibrium binding constants is provided, no information about the accessibility of the immobilized inhibitor can be obtained. This information is critical when evaluation of the mobile phase composition has to be made. Frontal elutions allow the determination of the amount of functionally active inhibitor immobilized on the column and at the same time also equilibrium binding constants. The dependence of chromatographically calculated M_T values on the concentration of (A) Tris and (B) HEPES is illustrated in Fig. 4. From the graphical analysis, the intercept according to eqn. 2 corresponds to the reciprocal of the column capacity, M_T, and the slope is function both of $K_{M/P}$ and M_T. In the presence of Tris, the capacity of the column, M_T, decreases with increasing Tris concentration, whereas in the presence of HEPES it remains unaffected, even if the reduction in the binding constant is evident from the change in

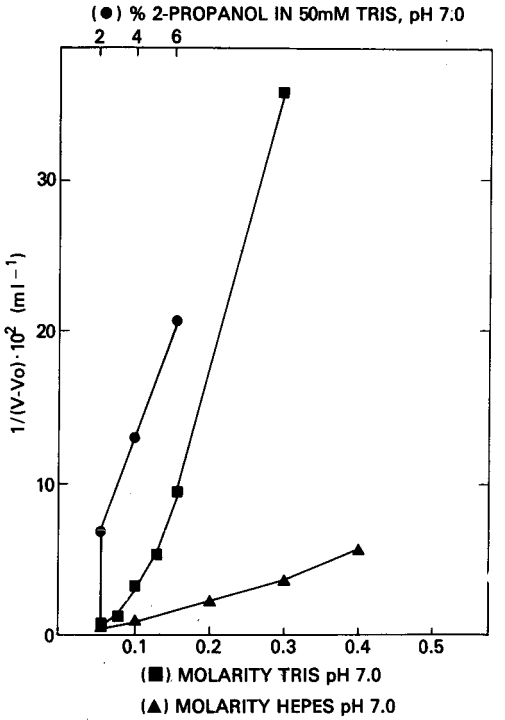

Fig. 3. Affinity dependence on the composition of the mobile phase. Extent of binding is expressed as $1/(V-V_0)$ obtained by extrapolation to [P]= 0. The [Gly-D-Phe]Eupergit column was equilibrated at a flow-rate of 1.0 ml/min with (●) 50 m*M* Tris–10 m*M* $CaCl_2$ (pH 7.0) and various concentrations of 2-propanol, (■) 10 m*M* $CaCl_2$ (pH 7.0) and various concentrations of Tris and (▲) 10 m*M* $CaCl_2$ (pH 7.0) and various concentrations of HEPES.

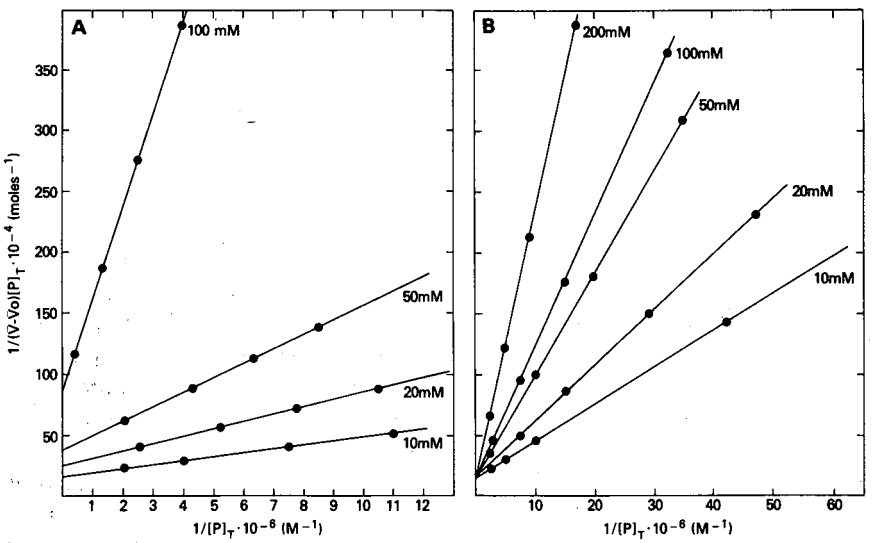

Fig. 4. Frontal analysis of the dependence of the interaction on the mobile phase composition on the [Gly-D-Phe]Eupergit column (50 × 5 mm I.D., M_T 56 μmol) equilibrated at a flow-rate of 0.5 ml/min with 10 m*M* $CaCl_2$ (pH 7.0) and (A) various concentrations of Tris and (B) various concentrations of HEPES. Data are plotted according to eqn. 3 to calculate values of M_T by extrapolation to 1/[P] = 0.

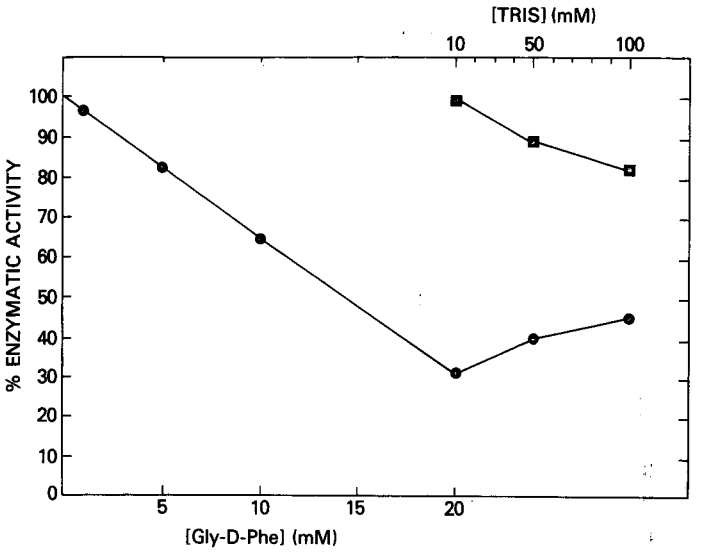

Fig. 5. Effect of Tris on the enzymatic activity of thermolysin. The decrease in enzymatic activity of thermolysin in the presence of Gly-D-Phe was measured in 10 m*M* Tris–10 m*M* $CaCl_2$ (pH 7.0). When the activity had decreased to 20% of the original value, the Tris content was raised and the variation in activity monitored (●). The effect of Tris on the enzymatic activity of TLN was also monitored in the absence of inhibitor (■).

slope. From these results it is clear that the large reduction in binding affinity in the presence of Tris is due mainly to a reduction in the amount of functionally active inhibitor (*i.e.*, functional capacity) and minimally to an effect on the protease.

Dependence of thermolysin enzymatic activity on Tris concentration

To verify that the effect of increasing Tris concentration on the thermolysin–Gly-D-Phe interaction is not limited to the solid phase, an evaluation of enzymatic activity of thermolysin towards its substrate FAGLA in the presence of inhibitor and Tris was carried out, as shown in Fig. 5. The thermolysin activity decreased with increasing Tris concentration, but in the presence of Gly-D-Phe as inhibitor the overall effect is an increase in enzymatic activity, at least in the range of Tris concentrations tested.

Preparative HPLAC purification of thermolysin

Purification of thermolysin has been carried out previously by affinity chromatography mainly on soft gels with immobilized inhibitors [8–10]. Elution of bound protease from the support is usually achieved by a buffer pH change to 9.0, disrupting the thermolysin salt bridges His-231/Asp-226 and His-142/Asp-170, which are an integral part of the active site of the enzyme [12].

The possibility of using different elution conditions, based on the previously observed effects of the mobile phase on the binding affinity, was evaluated in order to establish milder and more convenient ways to purify the protease. Commercially obtained thermolysin was first adsorbed on the column equilibrated with 10 m*M*

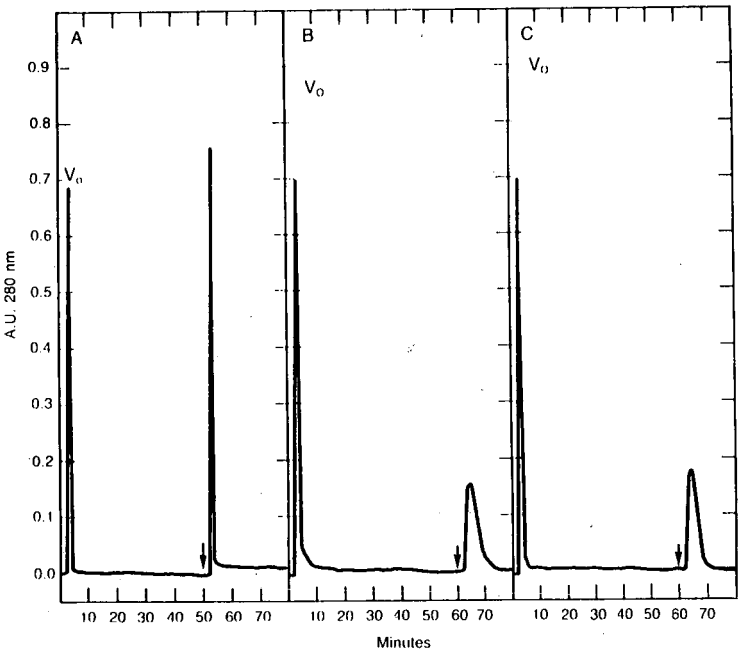

Fig. 6. Preparative HPLAC purification of commercial thermolysin on [Gly-D-Phe]Eupergit. The columm (150 × 10 mm I.D.) was equilibrated at a flow-rate of 1.0 ml/min with 10 m*M* $CaCl_2$ (pH 7.0) and 4.0 mg of commercial thermolysin dissolved in 200 μl of eluting buffer were injected. At the points indicated by the arrows, the eluent was changed to (A) 0.1 *M* Tris–10 m*M* $CaCl_2$ (pH 9.0); (B) 5% 2-propanol–10 m*M* Tris–10 m*M* $CaCl_2$ (pH 7.0); (C) 0.4 *M* Tris–10 m*M* $CaCl_2$ (pH 7.0).

Tris–10 m*M* calcium chloride (pH 7.0). Elution of bound protein was achieved by a buffer change to disfavour, or strongly reduce, the binding process. Fig. 6 shows typical chromatograms obtained for the purification of 4 mg of crude thermolysin. Bound protein was eluted by (A) of pH change to 9.0, (B) the inclusion of 5% 2-propanol and (C) 0.4 *M* Tris (pH 7.0). At pH 9.0 the affinity between thermolysin and Gly-D-Phe is completely abolished and bound protease is eluted as a sharp, narrow peak. Elution with 5% 2-propanol or 0.4 *M* Tris allows the recovery of thermohysin in a much wider peak, reflecting the residual binding affinity under these conditions. The presence of contaminants or autolytic products in the purified thermolysin preparations was then checked by reversed-phase HPLC [13] (Fig. 7). While the purified thermolysin preparation obtained by elution with 5% 2-propanol and 0.4 *M* Tris (pH 7.0) are essentially contaminant free, the small amount of degradation products in the pH 9.0-eluted thermolysin preparation were derived from the slow autolysis of the protease occurring at pH values above neutrality [14]. Consequently, the specific activity of the protease purified using neutral buffers was also higher than that from pH 9.0 purification (Table I). In any case, the recovery of activity was high under all the conditions employed. The same column has been used for more than 50 runs with no apparent loss of capacity.

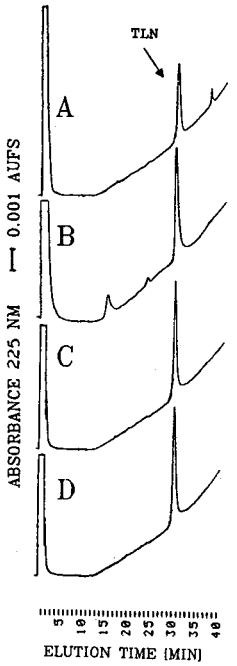

Fig. 7. Reversed-phase HPLC profiles of commercial thermolysin (A), and affinity-purified thermolysin eluted by (B) 0.1 *M* Tris–10 m*M* $CaCl_2$ (pH 9.0), (C) 10 m*M* Tris–10 m*M* $CaCl_2$–5% 2-propanol (pH 7.0) and (D) 0.4 *M* Tris–10 m*M* $CaCl_2$ (pH 7.0).

TABLE I

RECOVERY OF ACTIVITY OF HPLAC-PURIFIED THERMOLYSIN

Elution conditions[a]	Activity recovery[b] (%)	Specific activity[c] [(mg/ml)$^{-1}$s^{-1}]
(A) 0.1 *M* Tris (pH 9.0)	78	0.43
(B) 0.4 *M* Tris (pH 7.0)	83	0.48
(C) 10 m*M* Tris (pH 7.0)–5% 2-propanol	90	0.55

[a] Containing 10 m*M* $CaCl_2$.
[a] Determined using FAGLA as substrate.
[c] Specific activity of the commercial thermolysin sample was 0.4 (mg/ml)$^{-1}$s^{-1}.

CONCLUSIONS

Examination of solvent effects is of great importance in studying binding processes, as preliminary information can be obtained on the mechanisms involved in the interaction.

Analytical HPLAC leads to detailed information that does not require the interaction to be studied to produce secondary effects, such as enzymatic activity or

chromophoric transitions. In this particular instance, equilibrium binding constants determined on the solid phase by analytical HPLAC for thermolysin–Gly-D-Phe interaction were in good agreement with those determined completely in solution [5]. The effect of organic salts on the enzymatic activity of thermolysin has been previously studied in solution [15] using the neutral substrate FAGLA. While K_{cat} is affected negatively, K_m remains essentially unaltered, thus indicating that the thermolysin–neutral substrate interaction is not influenced by the presence of organic salts. In our study, the affinity properties of thermolysin for its inhibitor Gly-D-Phe, immobilized through its amino group on the solid support and thus with a free carboxyl group, are strongly influenced by the presence of Tris in the buffer. This effect is mainly due to the reduction of accessible inhibitor, and minimally to a reduction in the binding properties of the protease. Frontal elution data indicated that in the presence of 50 m*M* Tris only half to the total amount of immobilized Gly-D-Phe is accessible to the protease. Hence the Tris molecule is competing with thermolysin for the immobilized inhibitor, with an equilibrium binding dissociation constant of *ca.* 50 m*M*. The mechanism of this interaction can be postulated as an ionic interaction between the free carboxyl group of the inhibitor and the charged amino group of the Tris moiety. The same effect was observed in solution by evaluating the influence of Tris on the enzymatic activity of thermolysin towards FAGLA in the prensence and absence of Gly-D-Phe as inhibitor. The Tris molecule has a limited effect on the enzymatic activity, whereas the inhibition by Gly-D-Phe is effectively decreased by the presence of increasing concentrations of this organic salt. In agreement with data obtained on the solid phase by zonal and frontal analytical HPLAC, the interaction between thermolysin and Gly-D-Phe is also inhibited in solution by the Tris molecule. Finally, the evaluation of the effect of solvent composition on the thermolysin–Gly-D-Phe interaction indicated that an efficient reduction in binding affinity could be obtained by including 5% 2-propanol or 0.4 *M* Tris in the eluting buffer. These conditions could be used for affinity purification of thermolysin, appearing to be more convenient than elution by pH alteration, as the protease at pH values above neutrality slowly undergoes to autolytic processes leading to fragmentation [14].

ACKNOWLEDGEMENTS

The authors are grateful to Simona Germani for excellent technical assistance and to Professor Giovanni Cassani for his support.

REFERENCES

1 I. M. Chaiken (Editor), *Analytical Affinity Chromatography*, CRC Press, Boca Raton, FL, 1987.
2 G. Fassina and I. M. Chaiken, *Adv. Chromatogr.*, 27 (1987) 247.
3 K. Morihara, H. Tsuzuki and T. Oka, *Arch. Biochem. Biophys.*, 123 (1968) 572.
4 J. Feder and J. M. Schuck, *Biochemistry*, 9 (1974) 2784.
5 J. Feder, L. R. Brougham and B. S. Wildi, *Biochemistry*, 13 (1974) 1186.
6 B. W. Matthews, L. H. Weaver and W. R. Kester, *J. Biol. Chem.*, 249 (1974) 8030.
7 B. Holmquist and B. L. Vallee *Biochemistry*, 15 (1976) 101.
8 N. Nishino and J. C. Powers, *Biochemistry*, 18 (1979) 4340.
9 T. Komiyama, T. Aoyagi, T. Takeuchi and H. Umezawa, *Biochem. Biophys. Res. Commun.*, 65 (1975) 352.

10 N. K. Pangburn, Y. Burstein, P. H. Morgan, K. A. Walsh and H. Neurath *Biochem. Biophys. Res. Commun*, 54 (1973) 371.
11 C. J. Van Oss, D. R. Absolm and A. W. Neumann, in T. L. Gribnau, J. Visser and R. J. R. Nivard (Editor), *Affinity Chromatography and Related Techniques*, Elsevier, Amsterdam 1982, p. 29.
12 P. M. Colman, J. N. Jansonius and B. W. Matthews, *J. Mol. Biol.*, 70 (1972) 701.
13 G. Fassina, C. Vita, D. Dalzoppo, M. Zamai, M. Zambonon and A. Fontana, *Eur. J. Biochem.*, 156 (1986) 221.
14 A. Fontana, G. Fassina, C. Vita, D. Dalzoppo, M. Zamai and M. Zambonin *Biochemistry*, 25 (1986) 1847.
15 M. Fukuda and S. Kundugi, *Biocatalysis*, 2 (1989) 225.

Journal of Chromatography, 549 (1991) 207–215
Elsevier Science Publishers B.V., Amsterdam

CHROM. 23 340

High-performance liquid chromatography of synthetic oligonucleotides

A new affinity protecting group[a]

R. K. GAUR[b]
Department of Chemistry, University of Delhi, Delhi-110 007 (India)
(Received February 1st, 1991)

ABSTRACT

The use of triphenylmethyl (trityl) protecting groups with long alkyl chain substituents, *viz.*, (4-hexadecyloxyphenyl)diphenylmethyl and (4-decyloxyphenyl)diphenylmethyl, as affinity handles in the purification of oligonucleotides results in significant depurination of oligonucleotides, while removing these protecting groups from the high-performance liquid chromatographically purified oligonucleotides in 80% acetic acid. Excellent resolution of solid-phase synthesized medium- to large-size oligonucleotides using the 4-methoxy-4'-octyloxytrityl (MOTr) group is demonstrated. Moreover, the MOTr group is removed neatly under conditions identical with those used for the deprotection of the dimethoxytrityl group, and hence is less prone to depurination.

INTRODUCTION

Automated solid-phase methods have made the syntheses of oligonucleotides rapid and allowed their widespread employment in molecular biology. The last few years have seen a tremendous improvement in the methods used to prepare modified oligonucleotides [1–4]. Oligonucleotides synthesized by means of these methods have to be purified from by-products after detachment from the solid support.

Many techniques have been used for the purification of chemically synthesized oligonucleotides, including thin-layer (TLC) [5], paper [6], gravity-fed column [7] and high-performance liquid chromatography (HPLC) in ion-exchange [8], normal- [5] and reversed-phase [9] modes. Polyacrylamide gel electrophoresis (PAGE) is also a commonly used technique of purification [10]. However, reversed-phase (C_{18}) column chromatography has become more popular than the others. The reversed-phase

[a] Presented at the *International Symposium on Chromatography (CIS'89), Tokyo, October 17–20, 1989.* The majority of the papers presented at this symposium have been published in *J. Chromatogr.*, Vol. 515 (1990).

[b] Present address: Department of Biochemistry and Molecular Biology, St. Louis University School of Medicine, 1402 South Grand Boulevard, St. Louis, MO 63104, USA.

0021-9673/91/$03.50

HPLC (RP-HPLC) separation takes advantage of the fact that the conventional 5′-protecting group, *viz.*, dimethoxytrityl (DMTr) (trityl = triphenylmethyl), is a hydrophobic moiety and rather than resolving oligomers differing by a single base, the separation involves resolving 5′-DMTr-DNA from 5′-hydroxy-DNA.

The DMTr group has been found to be suitable for the purification of DNA fragments up to 30 nucleotides in length [11]. However, larger oligonucleotides are difficult to purify using the DMTr group as an affinity handle. In order to overcome the limitations of DMTr group, the use of trityl protecting groups with long alkyl chain substituents, *e.g.*, (4-hexadeacyloxyphenyl)diphenylmethyl (HTr) and (4-decyloxyphenyl)diphenylmethyl (DTr) groups was recommended by Seliger and co-workers [12–14]. Recently,it was observed [15] that the HTr group causes most oligonucleotides to be retained too strongly on C_{18} stationary phase. In general, the main impurities obtained in oligonucleotide synthesis are due to either incomplete capping or 5′-protected failure sequences that are usually shorter than the desired product. These failure sequences seem to be produced by a depurination reaction occurring during the acid treatment used to cleave the DMTr group following each nucleotide addition. The quantitative elution of such small nucleotides with substituents that have too long alkyl chains was either difficult or required a change of solvent. In fact, monomeric HTr-dT was not eluted at all with acetonitrile, but required carbon tetrachloride as eluent.

It has been observed that HPLC-purified oligonucleotides terminated by either an HTr or a DTr group require prolonged exposure to 80% acetic acid in order to remove these protecting groups, thus resulting in significant depurination of the oligonucleotides. It is well documented [16] that the complete removal of the monomethoxytrityl group in 80% acetic acid takes 90 min at 27°C, which is 4.5 times longer than that for the DMTr group (20 min). In view of the above limitations and based on earlier work [17], it was decided to investigate the use of a moderately hydrophobic disubstituted trityl protecting group with 4-methoxy and 4′-octyloxy substituents.

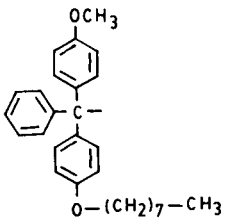

MOTr Group

Model studies demonstrated the utility of the 4-methoxy-4′-octyloxytrityl (MOTr) group as an affinity handle for the purification of medium- to large-size oligonucleotides useful for total gene synthesis and other applications in molecular biology.

EXPERIMENTAL

Reagents

Acetic acid, triethylamine and aluminium oxide were purchased from E. Merck

(India), HPLC-grade acetonitrile from Spectrochem (India) and DMTr-dT from the CSIR Centre for Biochemicals (India). A 0.1 *M* triethylammonium acetate (TEAA) buffer was used in all HPLC analyses, and was prepared by dilution of a 1 *M* stock solution, which was prepared in the following manner: 5.0 g of aluminium oxide was added to 75 ml of triethylamine and the suspension was stirred for 15 min. Then 20 ml of acetic acid were added to 69.7 ml of aluminium oxide-treated triethylamine and distilled water was added to 400 ml. The pH was adjusted to 7.0 with acetic acid. The solution was diluted to 500 ml with distilled water and filtered with 0.22-μm Millipore Durapore filter.

Column

HPLC was performed using either a μBondapak C_{18} column (300 × 3.9 mm I.D., 10 μm) from Waters Assoc. (Milford, MA, USA) or a Zorbax ODS column (250 × 4.6 mm I.D., 5 μm) from DuPont (Wilmington, DE, USA). Both columns were equipped with a precolumn (30 × 8 mm I.D.) packed with Nucleosil 7 C_{18}.

Apparatus

A Model LC-4A HPLC system (Shimadzu, Kyoto, Japan) consisting of a dual-plunger reciprocating pump, a helium degassing unit, an SPD-2AS UV spectrophotometric detector and a C-R3A data processor, was used for all purifications.

*Synthesis of 5'-O-(4-methoxy-4'-alkoxytrityl)thymidine (**3a–e**)*

4-Methoxy-4'-alkoxytrityl groups were selectively introduced at the 5'-hydroxyl position of thymidine by a known method [13] with a slight modification (Fig. 1). In each instance a yield of 85–92% was obtained. The intermediates were characterized by their NMR and UV spectra ($\lambda_{max} \approx \lambda_{max}$ of parent nucleoside).

*Synthesis of 5'-O-(4-methoxy-4'-octyloxytrityl)thymidine-3'-O-(methyl-N,N-diisopropylamino)phosphoramidite (**4**)*

The phosphoramidite **4** was synthesized essentially according to the method reported in the literature [18,19]. 5'-O-(4-Methoxy-4'-octyloxytrityl)thymidine (1.0 g, 1.5 mmol) was reacted with chloro-N,N-diisopropylaminomethoxyphosphine (0.45 ml, 2.3 mmol) in dichloromethane (5 ml) containing diisopropylethylamine (1.1 ml, 6.2 mmol) as an acid scavenger. After work-up, **4** was obtained as a white foam in 89% yield; TLC [dichloromethane–ethyl acetate–triethylamine (45:45:10)], R_F = 0.76.

Removal of 4-methoxy-4'-alkoxytrityl group

The kinetics of the hydrolysis of the 4-methoxy-4'-alkoxytrityl group in **3a–e** in 80% acetic acid was studied in the following manner. A solution of **3a** (4.58 mg) in 1 ml of 80% acetic acid was kept at room temperature with occasional swirling. Aliquots were removed at 1-min intervals and applied to a TLC plate (Fluka precoated plates with fluorescent indicator, 254 nm). The TLC plate was developed with chloroform–methanol (9:1) and spots were revealed under UV light or by spraying with perchloric acid solution with subsequent heating of the plate at 100°C. In each instance hydrolysis was essentially complete in 15–20 min.

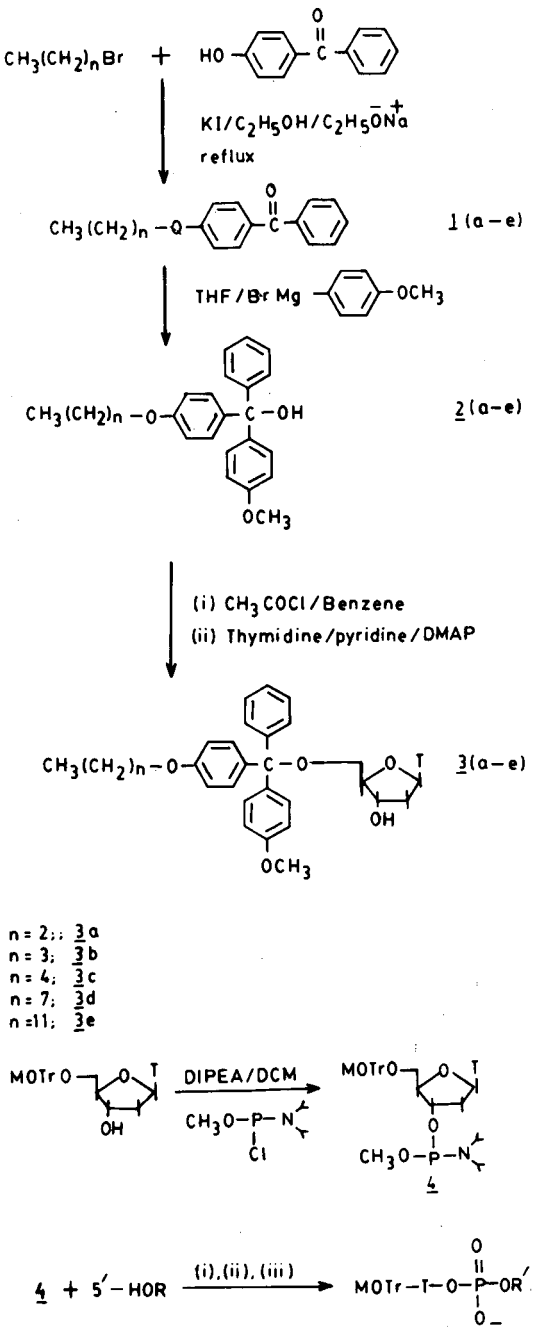

Fig. 1. Scheme for the synthesis of 5'-O-(4-methoxy-4'-alkoxytrityl)thymidines and 5'-O-(4-methoxy-4'-octyloxytrityl)thymidine-3'-O-(methyl-N,N-diisoproylamino)phosphoramidite. In the bottom reaction, (i) = tetrazole; (ii) = aqueous iodine; (iii) = 25% aqueous ammonia, 60°C for 16 h. R = protected oligonucleotide; R' = deprotected oligonucleotide.

Oligonucleotide synthesis and deprotection

Oligonucleotides were synthesized following solid-phase (controlled-pore glass supports) phosphoramidite chemistry [18,19] on a Pharmacia Gene Assembler [20] using methyl or 2-cyanoethyl phosphoramidite derivatives. Oligonucleotides with up to 30 bases were prepared using methyl phosphoramidite and a 60-mer sequence was synthesized with 2-cyanoethyl phosphoramidite. The synthesis was carried out on a 1.3-μmol scale of support-bound first nucleoside. For the synthesis of oligonucleotides with a 5′-MOTr group, in the last coupling step 5′-O-(4-methoxy-4′-octyloxytrityl)thymidine-3′-O-(methyl-N,N-diisopropylamino)phosphoramidite was used. In this final coupling step, no changes to the coupling time or the solvent were made. After the synthesis of the required sequence, the MOTr group was kept intact. The internucleotide methyl phosphate protecting groups were removed with ammonium thiophenoxide [21] treatment. Removal of the exocyclic base protecting groups together with the cleavage of the oligonucleotide from the support was achieved with 25% aqueous ammonia at 60°C for 16 h. With oligo-dT, the support was treated with aqueous ammonia (25%) at room temperature only. The crude oligonucleotides terminated by either DMTr or 4-methoxy-4′-octyloxytrityl groups were then purified by HPLC.

Sample preparation for HPLC purification

After completion of the synthesis, deprotection and cleavage from the support, the ammonia solution containing the crude oligonucleotide was evaporated to dryness in a Savant Speed Vac concentrator. The residue was dissolved in 0.1 *M* TEAA buffer (pH 7.0) and desalted on a Bio-Gel P-2 column using the same buffer as eluent. The desalted product was collected and concentrated and the residue was dissolved in 0.1 *M* TEAA buffer (pH 7.0) (200 μl) and *ca.* 20 μl were applied to the column for HPLC purification.

*HPLC of 5′-O-(4-methoxy-4′-alkoxytrityl)thymidine (**3a–e**)*

The thymidine derivatives **3a–e** were purified on a reversed-phase C_{18} column (μBondapak) using tetrahydrofuran–water–metanol (3:2:2) as the eluent. The pure product peaks were collected and lyophilized. A mixture consisting of HPLC-purified thymidine derivatives, *viz.*, **3a–e** and DMTr-dT, was injected under identical conditions onto the reversed-phase column.

RESULTS AND DISCUSSION

4-Methoxy-4′-alkoxytrityl groups were selectively introduced at the 5′-hydroxyl position of thymidine by a known method [13] with a slight modification (Fig. 1). In each instance, a yield of 85–92% was obtained. The TLC R_F values of 5′-O-(4-methoxy-4′-alkoxytrityl)thymidine derivatives (**3a–e**) obtained on silica gel with chloroform–methanol (9:1) increase with increase in the carbon chain length of the alkoxy function (Fig. 2). This reflects that the increase in the carbon chain length of the alkoxy function increases the hydrophobicity of the 5′-protected thymidine derivatives.

The chromatogram (Fig. 3) obtained by simultaneous injection of **3a–e** and DMTr-dT (used as a reference) onto a C_{18} reversed-phase column shows that the

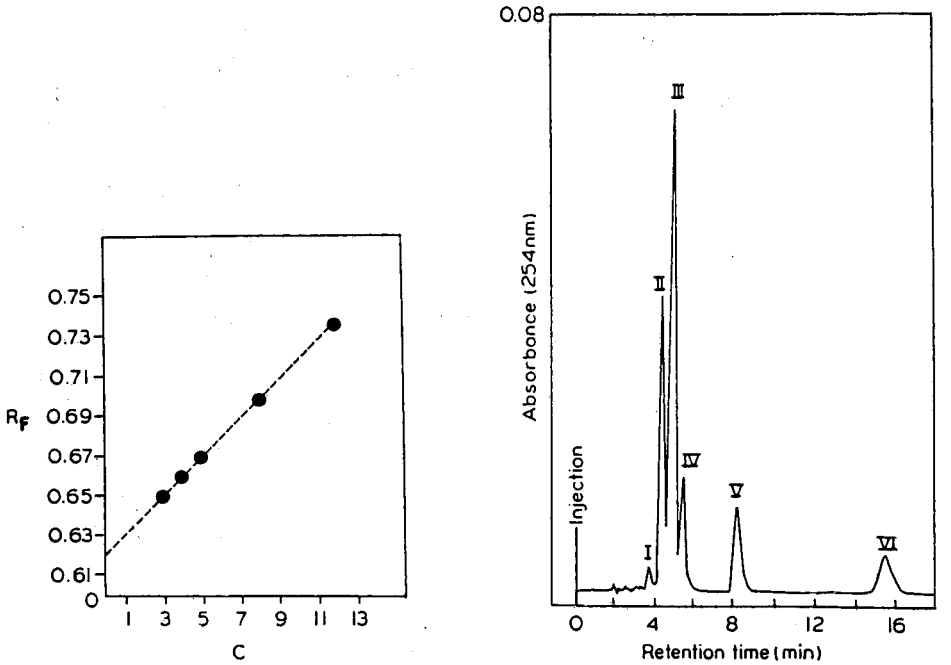

Fig. 2. Dependence of R_F values on the alkyl chain length, C, of compounds **3a–e** on silica gel TLC with chloroform–methanol (9:1).

Fig. 3. HPLC profile of a mixture of **3a–e** and DMTr-dT. Column, μBondapak C_{18} (300 mm × 3.9 mm I.D.); tetrahydrofuran–water–methanol (3:2:2); flow-rate, 1 ml/min. Peaks: I = DMTr-dT; II = **3a**; III = **3b**; IV = **3c**; V = **3d**; VI = **3e**.

retention times of these derivatives increase with increase in the carbon chain length of the alkoxy function. This, however, is contrary to their behaviour on a silica gel TLC plate. This can be explained in terms of hydrophobic interactions between the substituted trityl groups with similar alkyl chains bound to the reversed phase of the column.

The rationale of using a disubstituted trityl group (MOTr) for the affinity purification of oligononucleotides was that a very long alkyl chain substitution in the trityl group would make it much too hydrophobic and hence short nucleotides, *i.e.*, monomers or dimers resulting from incomplete capping or depurination, would be retained on the C_{18} column for a longer time or might not be eluted at all from the column. This has already been reported with the HTr group [15]. Further, with a monosubstituted trityl group (HTr or DTr), the time required for the removal of these protecting groups from the HPLC-purified oligonucleotide was found to be very long, which can cause significant depurination of the purified oligonucleotides. The 4-methoxy-4′-octyloxytrityl group is moderately hydrophobic in comparison with the HTr and DTr groups and, being disubstituted, it can be removed from the HPLC-purified oligonucleotides under conditions identical with those used for the deprotection of the DMTr group.

Fig. 4 shows the elution profile of a mixture consisting of DMTr-d(T_9C),

DMTr-d(T_{19}C) and DMTr-d(T_{29}C) on a C_{18} reversed-phase column. The difference in the retention times of the truncated sequences and the desired oligonucleotide decreases with increase in the oligonucleotide length, because as the length of the oligonucleotide increases the net hydrophobic contribution of the DMTr group to the oligonucleotide is counterbalanced by polar nature of the polyanionic chain. Hence, in oder to obtain a better resolution between the truncated sequence and the desired oligonucleotide, a reasonably hydrophobic group was required.

The limitations of the DMTr group were further demonstrated by injecting a mixture consisting of MOTr-d(T_9C), MOTr-d(T_{19}C) and MOTr-d(T_{29}C) (Fig. 5) under conditions identical with those used for the analysis of a mixture of DMTr-d (T_9C), DMTr-d-(T_{19}C) and DMTr-d(T_{29}C) (Fig. 4). As can be seen from the retention times, the proportion of acetonitrile in the mobile phase required to elute MOTr-d(T_{29}C) is still greater than that required for DMTr-d(T_9C). Hence, under identical conditions, the retention time of an oligomer bearing a 5′-MOTr group is much higher than that for the corresponding oligomer bearing a 5′-DMTr group (see further Figs. 4 and 5). This demonstrates that, although an increase in the length of the oligonucleotide reduces the retention time, the overall retention time conferred by the longer alkyl substituent far exceeds the influence of the polyanionic chain.

The utility of the MOTr group for the purification of polynucleotides was further demonstrated by synthesizing a longer sequence, *viz.*, MOTr-d(T)$_{60}$. Fig. 6

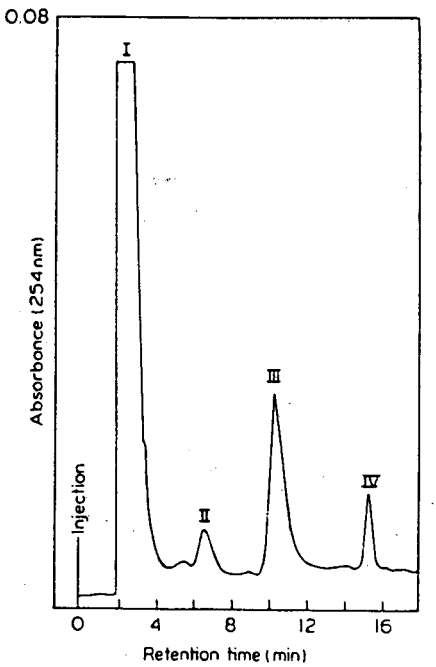

Fig. 4. HPLC profile of a mixture of DMTr-d(T_9C), DMTr-d(T_{19}C) and DMTr-d(T_{29}C). Column, Zorbax ODS (25 mm × 4.6 mm I.D.); flow-rate 1 ml/min; gradient from 20 to 40% B in 20 min, with solvent A = 0.1 *M* TEAA (pH 7.0) and solvent B = acetonitrile. Peaks: I = truncated sequences; II = DMTr-d (T_{29}C); III = DMTr-d(T_{19}C); IV = DMTr-d(T_9C).

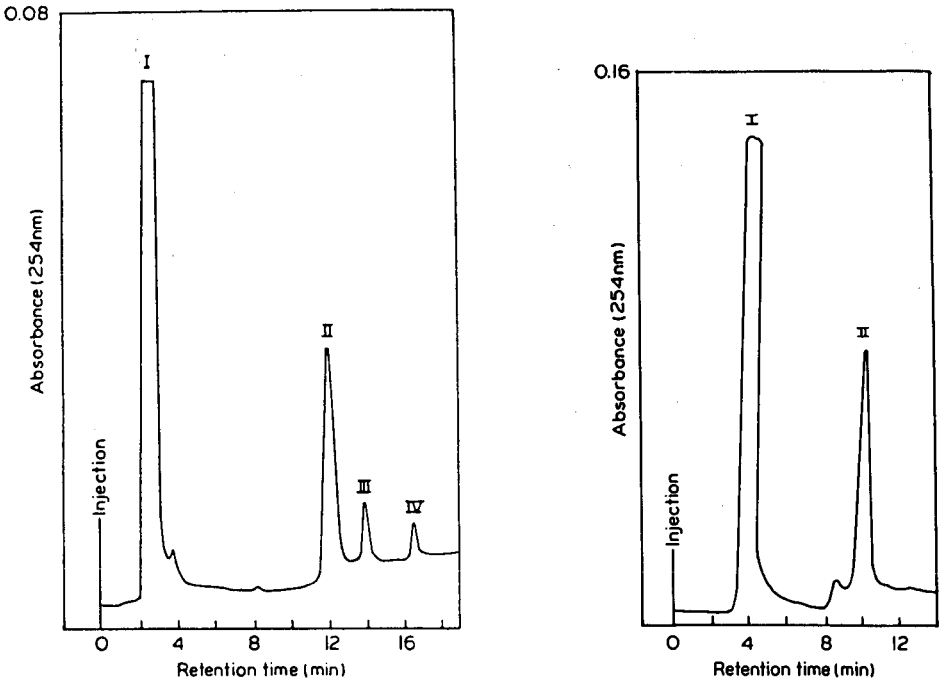

Fig. 5. HPLC profile of a mixture of MOTr-d(T_9C), MOTr-d($T_{19}C$) and MOTr-d($T_{29}C$). Conditions as in Fig. 4. Peaks: I = truncated sequences; II = MOTr-d($T_{29}C$); III = MOTr-d($T_{19}C$); IV = MOTr-d(T_9C).

Fig. 6. HPLC purification of MOTr-d$(T)_{60}$. Column, Zorbax ODS (25 mm × 4.6 mm I.D.); flow-rate, 1 ml/min; gradient from 10 to 70% B in 40 min, with solvent A = 0.1 *M* TEAA (pH 7.0) and solvent B = acetonitrile. Peaks: I = truncated sequences; II = MOTr-d$(T)_{60}$.

shows the HPLC purification profile of MOTr-d$(T)_{60}$. Even with this chain length the desired peak is well resolved from the truncated sequences. The near baseline separation and symmetry of the peak indicated the purity of the product. The product peak was collected, concentrated and reinjected under identical conditions. Again a single peak was obtained, showing the purity of the product.

These results demonstrate that the DMTr group is suitable as an affinity handle for the purification of oligonucleotides. However, the resolution of large oligonucleotides is poor. The MOTr group has been used successfully for the purification of a model polynucleotide, d$(T)_{60}$. The MOTr group is easy to introduce and, being disubstituted, can be removed under conditions identical with those used for the removal of the conventionally used DMTr group, thereby, minimizing the depurination of the HPLC-purified product.

ACKNOWLEDGEMENTS

I am grateful to Professor M. Atreyi (Department of Chemistry) and Dr. K. C. Gupta (CSIR Centre for Biochemicals) for constructive discussions throughout the course of this work. I am also grateful to the Scientist-in-Charge (CSIR Centre for

Biochemicals) and Head, Department of Chemistry, for providing the necessary facilities. Thanks are due to Mr. Abdual Raheem for expert technical assistance. Financial support from CSIR is gratefully acknowledged.

REFERENCES

1 R. K. Gaur, P. Sharma and K. C. Gupta, *Nucleic Acids Res.*, 17 (1989) 4404.
2 K. C. Gupta, P. Sharma, S. Sathyanarayana and R. K. Gaur, presented at the *58th Annual Meeting of the Society of Biological Chemists, Izatnagar, Oct. 1989.*
3 B. A. Connolly, *Nucleic Acids Res.*, 15 (1987) 3131.
4 B. S. Sproat, B. Beijer, P. Rider and P. Neuner, *Nucleosides Nucleotides*, 7 (1988) 651.
5 K. K. Ogilvie and M. J. Nemmer, *Tetrahedron Lett.*, 21 (1980) 4159.
6 A. F. Turner and H. G. Khorana, *J. Am. Chem. Soc.*, 81 (1959) 4651.
7 H. G. Khorana and J. P. Vizsolyi, *J. Am. Chem. Soc.* 83 (1961) 675.
8 T. G. Lawson, F. E. Regnier and H. L. Weith, *Anal. Biochem.*, 133 (1983) 85.
9 A. F. Markham, M. D. Edge, T. C. Atkinson, A. R. Greene, G. R. Heathcliffe, C. R. Newton and D. Scanlon, *Nucleic Acids Res.*, 8 (1980) 5193.
10 K. Itakura, J. J. Rossi and R. B. Wallace, *Annu. Rev. Biochem.*, 53 (1984) 323.
11 C. S. Craik, *Biotechniques*, 3 (1985) 12.
12 H. Seliger, M. Holupirek and H.-H. Gortz, *Tetrahedron Lett.*, (1978) 2115.
13 H.-H. Gortz and H. Seliger, *Angew. Chem., Int. Ed. Engl.*, 20 (1981) 681.
14 H. Seliger and G. Schmidt, *J. Chromatogr.*, 397 (1987) 141.
15 H. Seliger, A. Herold, U. Kotschi, J. Lyons and G. Schmidt, in K.S. Bruzik and W. J. Stec (Editors), *Biophosphates and Their Analogues, Synthesis, Structure, Metabolism and Activity*, Elsevier, Amsterdam, 1987, p. 43.
16 H.Schaller, G. Weimann, B. Lerch and H. G. Khorana, *J. Am. Chem. Soc.*, 85 (1963) 3821.
17 R. K. Gaur, *Ph.D. Thesis*, University of Delhi, Dehli, 1989.
18 S. P. Adams, K. S. Kavka, E. J. Wykes, S. B. Holder and G. R. Galluppi, *J. Am. Chem. Soc.*, 105 (1983) 661.
19 L. J. McBride and M. H. Caruthers, *Tetrahedron Lett.*, 24 (1983) 245.
20 *Gene Assembler Manual*, Pharmacia Fine Chemicals, Uppsala.
21 G. W. Daub and E. E. van Tamelen, *J. Am. Chem. Soc.*, 99 (1977) 3526.

Journal of Chromatography, 549 (1991) 217–220
Elsevier Science Publishers B.V., Amsterdam

CHROM. 23 317

Separation and simultaneous high-performance liquid chromatographic determination of benzocaine and benzyl benzoate in a pharmaceutical preparation

BÁRBARA GIGANTE, ANA M. V. BARROS, ADRIANO TEIXEIRA and M. J. MARCELO-CURTO*

Laboratório Nacional de Engenharia e Tecnologia Industrial, Departamento de Tecnologia de Indústrias Químicas, Estrada das Palmeiras, 2745 Queluz (Portugal)

(First received January 21st, 1991; revised manuscript received March 8th, 1991)

ABSTRACT

A simple reversed-phase high-performance liquid chromatographic method suitable for the simultaneous determination of benzocaine and benzyl benzoate in dermatological preparations is described. An internal standard method was employed, using a C_{18} "bonded phase" silica column and a mobile phase consisting of acetonitrile–water (40:60, v/v), with absorption of the column effluent monitored at 254 nm. No sources of interference were observed. The simultaneous determination of both compounds by the method described is rapid and accurate.

INTRODUCTION

Benzyl benzoate, a potent acaricide, and benzocaine (ethyl *p*-aminobenzoate), a local anesthetic, are formulated together in dermatological preparations used against scabies and pediculosis. No methods have been reported for the quantification of benzyl benzoate, and although several methods have been described for the quantification of benzocaine [1–3] none is suitable for the simultaneous determination of both compounds. In this paper, we describe a high-performance liquid chromatographic (HPLC) procedure in which both compounds can be quantified simultaneously under the same chromatographic conditions.

EXPERIMENTAL

Chemicals

HPLC-grade methanol and acetonitrile were used (Merck, Darmstadt, Germany). Water was purified with a Millipore filtration unit (deionized, $< 10 \mu\Omega$).

Reference standards and standard solutions

Benzocaine, benzyl benzoate and benzophenone (internal standard) were analytical-grade reagents (Merck); Neo-Escabenzil and other dosage forms were kindly donated by Companhia Portuguesa Higiene (Lisbon, Portugal).

0021-9673/91/$03.50

An internal standard stock solution of benzophenone in methanol at a concentration of 1.5 mg/ml was used. The reference stock solution was prepared by accurately weighing about 0.02 g of benzocaine and 0.15 g of benzyl benzoate and dissolving with methanol in a 10-ml volumetric flask. The reference solution was prepared by measuring 1.0 ml of the reference stock solution and 1 ml of internal standard stock solution into a 10-ml volumetric flask and diluting with methanol.

Standard solutions for calibration graphs. Appropriate volumes were measured out of the reference solution, mixed with the internal standard and diluted to 10 ml with methanol. The calibration was carried over a concentration range of 0.01–0.5 mg/ml for benzocaine and 0.07–0.30 mg/ml for benzyl benzoate.

Apparatus

A Spectra-Physics (San Jose, CA, USA) high-performance liquid chromatograph equipped with a Rheodyne 10-μl loop injector valve, a double stage pump Ioschrom LC and a variable-wavelength UV detector Spectra-Chrom 100 were used. The wavelength was set at 254 nm. The chromatographic peaks were recorded with a Spectra-Physics SP 4270 computing integrator connected to the spectrophotometer, with an operating voltage of 10 mV and chart speed of 10 mm/min. A 22 × 0.46 cm I.D. stainless-steel column containing C_{18} "bonded phase" silica, 5 μm, with a 3 cm guard column (Brownlee Labs., Santa Clara, CA, USA) and a 10-μl injector loop were employed. The injection volume was 50 μl. A flow-rate of 2 ml/min eluted benzocaine and benzyl benzoate in 1.8 and 4.5 min, respectively. All analyses were performed at room temperature.

Mobile phase and stability of chromatographic system

The mobile phase consisted of acetonitrile–water (60:40, v/v), filtered through a 0.2-μm PTFE membrane and degassed first in an ultrasonic bath and then by helium flow. The column was equilibrated with mobile phase at a flow-rate of 2 ml/min.

Sample preparation

The sample solution was prepared by accurately weighing about 0.05 g of the sample, mixing with 5 ml of internal standard stock solution and diluting with methanol in a 50-ml volumetric flask. The injection solution was prepared by accurately measuring 1 ml of the sample solution and diluting with methanol in a 10-ml volumetric flask. This solution was filtered through a 0.45-μm PTFE membrane prior to HPLC analysis.

RESULTS AND DISCUSSION

Although other HPLC methods have been described for the quantification of benzocaine [1–3], trials to separate benzocaine and benzyl benzoate simultaneously by the methods reported were unsuccessful.

Fig. 1 depicts a chromatogram of the commercial formulation Neo-Escabenzil, typically containing 2% benzocaine and 15% benzyl benzoate, showing the HPLC method proposed here to be suitable for the simultaneous determination of both compounds. Benzocaine and benzyl benzoate were eluted in 1.8 and 4.5 min, respectively, from standard and sample solutions.

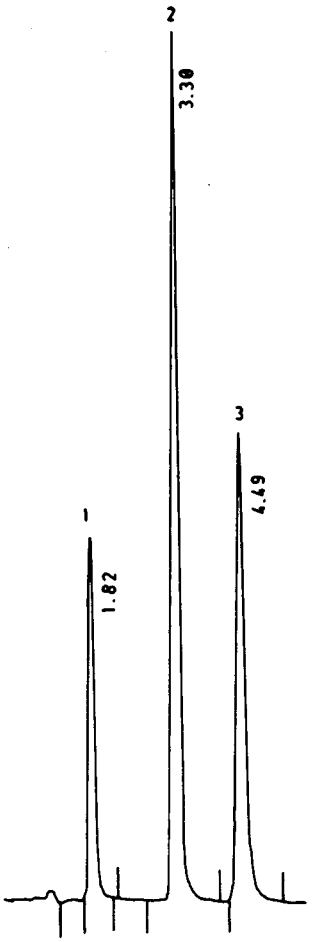

Fig. 1. Chromatogram of a sample of Neo-Escabenzil at 254 nm. Peaks: 1 = benzocaine (0.022 mg/ml; retention time 1.82 min); 2 = benzophenone (internal standard, 1.5 mg/ml; retention time 3.30 min); 3 = benzyl benzoate (0.157 mg/ml; retention time 4.49 min).

Adequate separation of benzocaine and benzyl benzoate was achieved with a mobile phase consisting of acetonitrile–water (60:40, v/v), pH adjustment being unnecessary to reach optimum chromatographic conditions. The column was equilibrated with mobile phase at a flow-rate of 2 ml/min. The relative standard deviation (R.S.D.) of five replicate injections of a standard was not more than 1.8%.

The wavelength of 254 nm was selected for detection according to the absorbance maxima of benzocaine, benzyl benzoate and their concentrations in the sample solution.

An internal standard method was employed, with benzophenone as the internal standard. No interference from additives or diluents was detected upon application of the analytical procedure to commercial formulations.

Linearity of detector response to variations in concentration was determined

TABLE I

CALIBRATION DATA FOR ANALYSIS

Compound	Concentration range (mg/ml)	Correlation coeffient ($n=5$) ± R.S.D. (%)	Slope	Intercept	Retention time (min)
Benzocaine	0.01–0.50	0.9991 ± 0.038	0.0094	0.0073	1.80
Benzyl benzoate	0.07–0.30	0.9994 ± 0.180	0.0023	0.0002	4.50

over a range of 0.01–0.50 mg/ml for benzocaine with a correlation coefficient of 0.9991 ($n=5$) and 0.07–0.30 mg/ml for benzyl benzoate with a correlation coefficient of 0.9994 ($n=5$). Calibration graphs were constructed of peak area *versus* concentration; the slope and intercept obtained by linear regression analysis are listed in Table I and the results show the low R.S.D. values between analysis. The reproducibility of the method was tested with repeated analysis of samples ($n=11$) corresponding to the average weight of the samples.

The accuracy of the method was determined by calculating the recovery of known amounts of the authentic sample solution added to the average weight of the assay samples. Recoveries were in the range 100–103% for benzocaine and 97–100% for benzyl benzoate.

This method is simple, specific, accurate and reproducible and therefore can be applied to various commercial pharmaceutical preparations.

REFERENCES

1 I. Jane, A. McKinnon and R. J. Flanagan, *J. Chromatogr.*, 323 (1985) 191.
2 R. Gill, R. W. Abbott and A. C. Moffat, *J. Chromatogr.*, 301 (1984) 155.
3 M. Bhuze, S. Fregert and B. Gruvberger, *Photodermathology*, 1 (1984) 277.

Journal of Chromatography, 549 (1991) 221–228
Elsevier Science Publishers B.V., Amsterdam

CHROM. 23 334

Stability-indicating high-performance liquid chromatographic assay for α-methyldopa in sustained-release capsules

MOHAMMED EL-SAYED METWALLY

Department of Analytical Chemistry, Faculty of Pharmacy, Mansoura University, El-Mansoura 35516 (Egypt)

(First received January 9th, 1991; revised manuscript received March 19th, 1991)

ABSTRACT

A stability-indicating high-performance liquid chromatographic assay has been developed for the analysis of α-methyldopa (MD) in sustained-release capsules and in the presence of MD decomposition products and an MD industrial impurity, 3-O-methyl-methyldopa (MMD). The method utilizes reversed-phase chromatography (cyano-bonded column), an acidic mobile phase containing sodium heptanesulphonate as ion-pairing reagent and UV detection. Detector responses were linear in the ranges 0.5–200 μg/ml for MD and 0.2–100 μg/ml for MMD. The mean recoveries of MD from authentic sample and sustained-release capsules were 100.09 ± 0.38 and 100.38 ± 0.46%, respectively. The recovery of MD added to degraded MD were 99.69% by the proposed method and 153.13% by the US Pharmacopeial (USP) spectrophotometric method. The method is sensitive, accurate and rapid and can be used in routine analysis for MD.

INTRODUCTION

L-α-Methyldopa [L-3-(3,4-dihydroxyphenyl)-2-methylalanine] (MD) is a competitive inhibitor of DOPA-decarboxylase and is used in the management of hypertension [1]. Owing to the various routes used for the synthesis of MD, there are a number of by-products that might be present as impurities in the final product [2]. 3-O-Methyl-methyldopa (MMD) is one of the by-products that is difficult to separate from the parent compound owing to the similar solubility characteristics and chemical properties. In addition to the presence of impurities, MD dosage forms degrade easily under unfavourable storange conditions [3] and can undergo oxidation in alkaline media to a polymeric melanin-like pigment [4].

In spite of these inherent difficulties, there has been no reliable stability-indicating assay of MD in pharmaceutical dosage forms. Gupta and Gupta [3] used the official US Pharmacopeial (USP) method [5] to study the effect of storage of MD tablets in counting machines. MD has been determined in dosage forms by fluorimetry [6,7], ultraviolet (UV) spectrophotometry [8], spectrophotometry [9–12], proton magnetic resonance spectroscopy [13], potentiometry [14] and thin-layer chromatography [15]. These methods are not specific or they may require rigid experimental conditions such as pH adjustment and temperature control. The method described by

0021-9673/91/$03.50

Chu [16] using ion-exchange chromatography is lengthy and time consuming. The high-performance liquid chromatographic (HPLC) method described by Ting [17] was tested in our laboratory and cannot be used for the separation of MD from its degradation products. Using the ion-pair HPLC method described by Ghanekar and Das Gupta [18], one of the MD degradation products interfered seriously with MMD. A gas chromatographic method for the determination of MD in tablets and raw material was developed by Watson and Lawrence [2], but requires a lengthy derivatization step.

Several methods for the determination of MD in combination with thiazide [16,17], hydrochorothiazide [18–20] and catecholamines [21] in pharmaceutical preparations have also been reported. These methods suffer from peak tailing, multiple peaks for the same compound or incomplete separation of combined drugs [7].

This paper describes the development of an ion-pair HPLC method for the determination of MD in sustained-release capsules and in the presence of MD degradation products and the industrial impurity MMD. The proposed method is accurate, sensitive and rapid and can be easily applied for routine quality control.

EXPERIMENTAL

Chemicals

USP reference standards of MD and MMD were used. MD bulk material (checked according to the USP [22]) and MD sustained-release microcapsules were supplied by Elan Pharmaceutical Research (Gainesville, GA, USA). Methanol (HPLC grade), acetonitrile (HPLC-grade), acetic acid and sodium heptanesulphonate acid were purchased from Aldrich (Milwaukee, WI, USA). All other chemicals were of high purity and used as received.

Liquid chromatograph

A Rheodyne (Berkeley, CA, USA) Model 7125 injection system with a 20-μl loop was used. A Waters Assoc. (Milford, MA, USA) Model 590 solvent pump and a Spectroflow Model 757 variable-wavelength detector (Schoëffel Instrument, Westwood, NJ, USA) set at 280 nm were used. A Hewlett-Packard (Avondale, PA, USA) Model 3392A integrator was used for integrating the eluted peaks. A 250 mm × 4.6 mm I.D. Phenomenex (Rancho Palos Verdes, CA, USA) CN 5-μm analytical column was used.

Methanol–water (20:80, v/v) containing 2% (v/v) acetic acid and 0.005 *M* sodium 1-heptanesulphonate was used as the mobile phase. The pH of the solutions was adjusted to 2.60 ± 0.05. The mobile phase was filtered by passing it through a Millipore 0.45-μm filter and degassed before use. The mobile phase flow-rate was 1.6 ml/min. The temperature was ambient.

Determination of water content

The water content was determined in MD bulk powder and in the MD sustained-release capsules using the official USP method [22] recommended for MD. The water contents were found to be 12.3 and 13.0%, respectively.

Preparation of stock solutions

Stock solutions (0.10%) of MD and MMD were prepared in 0.1 *M* sulphuric acid.

Degradation of MD

Volumes of 5.0 ml of the MD stock solution were mixed with 5.0 ml of 0.10 or 1.0 *M* sodium hydroxide solution at 25°C. After an appropriate period, the reaction mixture was quenched by adding 5 ml of sulphuric acid of appropriate concentration (0.1 or 1 *M*). The mixture was adjusted to volume (100.0 ml) with deionized water.

Extraction of MD from sustained-release microcapsules

Beads equivalent to 500 mg of MD were ground to a fine powder and transferred to a 100-ml volumetric flask, then 50 ml of 0.05 *M* sulphuric acid were added. The flask was sonicated for 15 min and then the solution was adjusted to volume with 0.05 *M* sulphuric acid and filtered. The first 10.0 ml of the filtrate were rejected and 10 ml of the clear filtrate were diluted to 100.0 ml with 0.05 *M* sulphuric acid.

Preparation of calibration graphs

An accurately weighed 50-mg sample of USP MD or USP MMD was transferred into a 100-ml volumetric flask and 50 ml of 0.05 *M* sulphuric acid were added. The flask was sonicated for 15 min and then the solution was adjusted to volume with 0.05 *M* sulphuric acid. Serial dilutions of MD or MMD standards were made. Concentrations of MD and MMD were determined in the acidified aqueous solutions using the HPLC conditions given above, and the peak heights of the standards (calibration graphs) were recorded. The plots of the peak height *versus* concentration were linear over the range 0.5–200 μg/ml for MD with a regression coefficient of 0.999 and over the range 0.2–100 μg/ml for MMD with a regression coefficient of 0.992.

Quantification

All measurements were made using peak heights. Concentrations of sample solutions containing MD were calculated using the slope and the intercept of the calibration graph prepared under the above conditions. The slope and the intercept of the calibration graph were obtained by linear regression of peak height *vs.* concentration ($y = ax + b$), where a is the slope, b is the intercept and y is the response of the analyte.

RESULTS AND DISCUSSION

It has been reported that MD may undergo partial or complete degradation under unfavourable conditions [3]. Initial attempts to apply a C_{18} reversed-phase column with different mobile phases [17,18] failed. Ion-pair HPLC using a CN-bonded column was very useful for separating MD from its degradation products (Fig. 1), or from excepients that are present in the sustained release capsules (Fig. 2). Fig. 3 illustrates the analytical separation of a synthetic mixture of MD from MMD, together with MD decomposition products. Under the above-mentioned experimental conditions, the retention times were MD 4.5, MMD 6.03 and MD decomposition products 1.5, 1.69, 1.9, 2.28, 2.63, 2.84, 3.09 and 6.74 min. Peaks with retention times of 1.85 and 2.58 in Fig. 2 are due to excepients, namely shellac and fumaric acid, respectively.

Methanol was chosen as an organic solvent modifier where all the degradation peaks were successfully separated from MD and MMD, whereas the use of aceto-

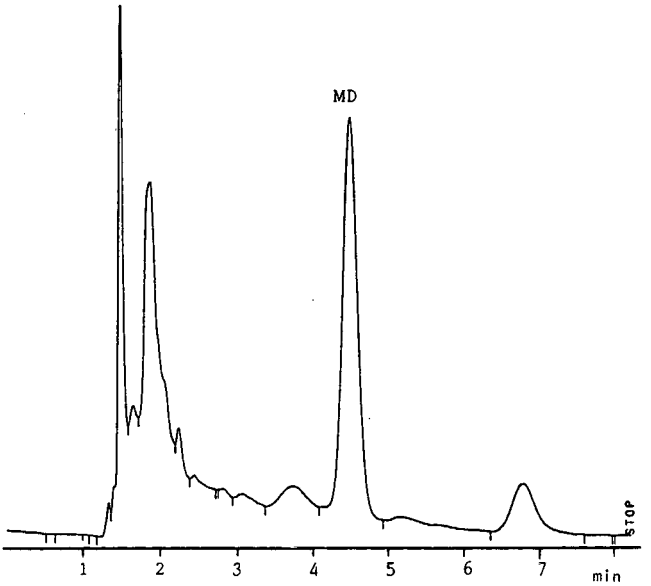

Fig. 1. Chromatogram obtained from a mixture of MD (10 μg/ml, t_R = 4.5 min) and degraded MD (100 μg/ml, 2 h degradation time in 0.1 *M* NaOH at 25°C, t_R = 1.5, 1.69, 1.9, 2.28, 2.63, 2.84, 3.09 and 6.74 min). Chromatographic conditions: column, 250 × 4.6 mm I.D. Phenomenex CN, 5 μm; mobile phase, methanol–water (20:80, v/v) containing 2% (v/v) acetic acid and 0.005 *M* sodium 1-heptanesulphonate; pH, 2.60 ± 0.05; flow-rate, 1.6 ml/min; detector wavelength, 280 nm.

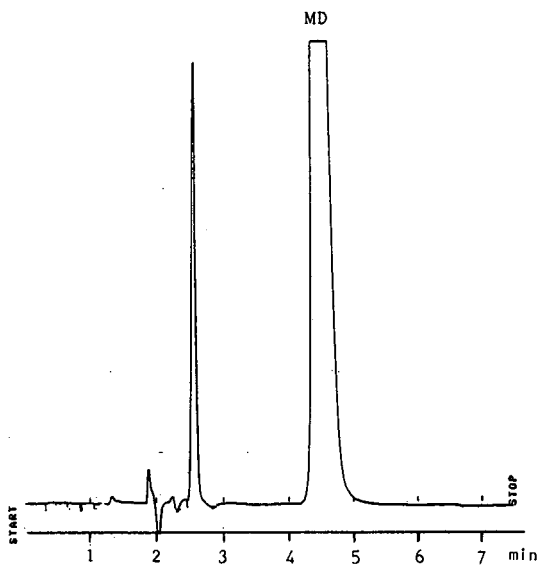

Fig. 2. Chromatogram obtained for MD sustained-release capsules (t_R = 4.5 min, 90 μg/ml). Chromatographic conditions as in Fig. 1.

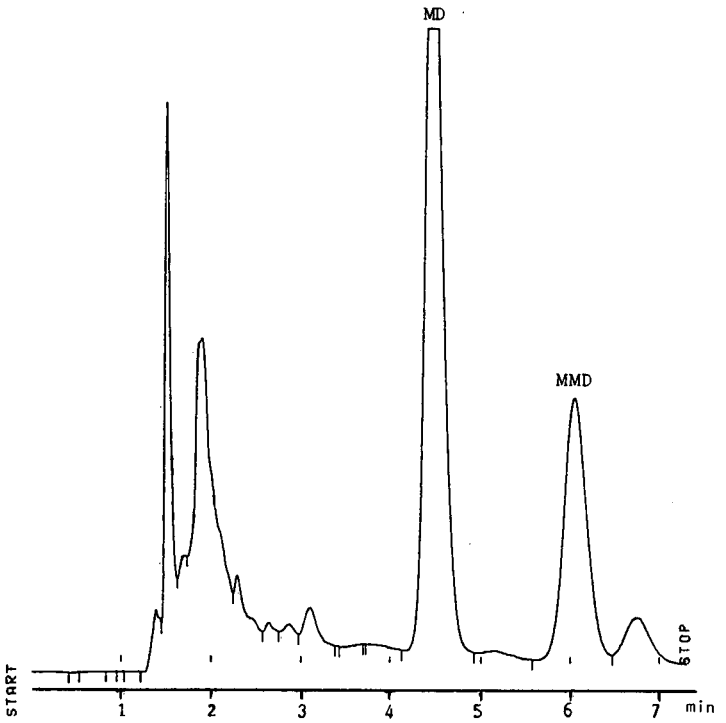

Fig. 3. Chromatogram obtained from a mixture of MD (10 μg/ml, t_R = 4.5 min), MMD (10 μg/ml, t_R = 6.03) and degraded MD (100 μg/ml, 2 h degradation time in 0.1 *M* NaOH at 25°C, t_R = 1.5, 1.69, 1.9, 2.28, 2.63, 2.84, 3.09 and 6.74 min). Chromatographic conditions as in Fig. 1.

nitrile as an organic modifier resulted in overlapping one of the peaks of degradation products of MD with that of MMD. Under identical chromatographic conditions and without using the ion-pairing reagent, separation of MD from either its degradation products or from MMD was not possible.

Conversion of MD to oxidized products [18] under alkaline conditions was followed by HPLC, and was shown to proceed via pseudo-first-order kinetics [23]. The degradation rate constant (k_{obs}) in 0.1 *M* sodium hydroxide solution at 25°C was 1.28×10^{-2} min^{-1}, with a half-life of 58.60 min. An overnight decomposition of MD gave zero recovery of MD by the proposed method and a 53.13% recovery of MD by the USP spectrophotometric method [22], an indication of the selectivity of the proposed method. These results are in good agreement with those reported by Ghanekar and Das Gupta [18].

Based on the peak-height responses of standards, the proposed method is linear in the ranges 0.5–200 μg/ml for MD and 0.2–100 μg/ml for MMD. The standard deviations based on ten injections of the standard solutions were estimated to be 0.34% for MD and 0.45% for MMD.

Accuracy was determined by recovery studies of added MD to sustained-release capsules (Table I). The average recoveries obtained were 100.38 ± 0.46% by the proposed HPLC method and 100.87 ± 0.54% by the USP spectrophotometric meth-

TABLE I

RECOVERY OF MD ADDED TO DIFFERENT BATCHES OF SUSTAINED-RELEASE CAPSULES USING THE PROPOSED HPLC METHOD AND THE USP SPECTROPHOTOMETRIC METHOD [22]

Batch[a]	Sample (μg/ml)	Claimed (μg/ml)	Added (μg/ml)	HPLC method		USP method	
				Found (μg/ml)	Recovery (%)	Found (μg/ml)	Recovery (%)
C821	13.70	8.10	13.69	21.63	98.85	21.87	100.61
	29.00	17.14	19.91	37.20	100.75	36.99	99.70
	125.50	74.17	30.43	104.29	98.97	105.32	102.35
C934	8.13	4.63	2.01	6.65	100.62	6.62	99.12
	54.23	30.87	50.10	81.92	101.90	81.92	101.90
	140.10	79.75	90.10	171.34	101.66	171.87	102.25
C1040	35.90	20.63	4.02	24.59	98.56	24.58	98.31
	75.12	43.16	40.20	84.01	101.61	84.29	102.31
	100.23	57.59	100.09	158.20	100.52	159.00	101.32
Mean					100.38		100.87
S.D.					0.46		0.54

[a] Batch C821 contained 58.710% MD, batch C934 58.75% MD and batch C1040 58.46% MD (see Table III).

od. The accuracy of the method was also tested by adding different amounts of completely degraded solution of MD to solutions containing the corersponding amount of non-degraded drug (Table II). A plot of the amount of MD added *versus* the amount recovered gave a slope of nearly unity, within experimental error (1.004), an intercept near zero (−0.037) and correlation coefficient near unity (0.999). Recov-

TABLE II

DETERMINATION OF MD IN THE PRESENCE OF ITS DEGRADATION PRODUCTS USING THE PROPOSED HPLC METHOD AND THE USP SPECTROPHOTOMETRIC METHOD [22]

MD added[a] (μg/ml)	HPLC method		USP method	
	Found	Recovery (%)[b]	Found	Recovery (%)[b]
1.500	1.467	97.800	2.243	149.500
5.000	4.990	99.800	7.635	152.700
10.000	10.010	100.100	15.250	152.500
25.010	24.860	99.400	38.340	153.300
50.210	50.612	100.800	77.775	154.900
100.030	100.260	100.230	155.917	155.870
Mean		99.688		153.128
S.D.		0.945		2.018

[a] Each solution contained an equivalent concentration of a completely degraded solution.
[b] Based on three determinations.

TABLE III

DETERMINATION OF MD IN DIFFERENT BATCHES OF SUSTAINED-RELEASE CAPSULES USING THE PROPOSED HPLC METHOD AND THE USP SPECTROPHOTOMETRIC METHOD [22]

Calculations are not based on anhydrous bases.

Batch	Sample weight (μg/ml)	HPLC method		USP method	
		Found (μg/ml)	Recovery (%)	Found (μg/ml)	Recovery (%)
C821	10.02	5.89	58.78	5.79	57.78
	40.91	24.08	58.86	23.79	58.15
	75.45	44.38	58.82	43.19	57.24
	100.31	58.47	58.29	59.29	59.11
	150.20	88.24	58.81	87.98	58.58
C934	5.98	3.45	57.69	3.54	59.20
	25.05	14.76	58.92	14.21	56.73
	40.97	23.98	58.53	23.95	58.46
	80.21	47.01	58.61	46.23	57.64
	175.23	100.76	57.50	100.21	57.19
C1040	10.29	5.90	57.34	6.00	58.31
	45.47	26.79	58.92	26.80	58.94
	50.17	29.58	58.96	29.47	58.74
	115.80	68.10	58.81	68.03	58.75
	136.40	78.50	57.55	77.20	56.60
	217.90	129.00	59.20	128.10	58.79
21B/11	20.09	11.50	57.24	11.82	58.84
	85.05	49.90	58.67	50.03	58.82
	126.60	74.10	58.53	73.42	57.99
	152.30	87.60	57.52	86.89	57.05
	205.20	117.98	57.50	119.12	58.05
Mean			58.34		58.14
S.D.			0.65		0.80

eries for the six spiked samples tested ranged from 97.80 to 100.80% (mean 99.69%, S.D. = 0.94%) These data indicate that the method is both selective and accurate. This was further confirmed by analysing the previous solutions of MD using the USP spectrophotometric method for tablets [22]. The results were overestimated and demonstrated that the USP method was not stability indicating. The observed high recovery with the USP method is due to the interference of the MD degradation products at the recommended wavelength for MD–iron(II) tartrate complex (550 nm).

Application to the determination of MD in raw samples at different concentrations covering the whole calibration graph was successfully made with a mean recovery of 100.09 ± 0.38%. The results were compared with those obtained using the USP spectrophotometric method [22] for MD tablet. Comparison with the USP non-aqueous titration method for MD raw materials was not possible owing to the high detection limit of the USP method.

In Table II, the percentage of the label claim values obtained when the pro-

posed HPLC method was applied to the determination of MD in sustained-release capsules at different dosage levels in four different batches are compared with those obtained with the USP spectrophotometric method [22]. No noticeable discrepancies were observed. No MMD was found in any analysed sustained-release batches.

The HPLC method eliminates the need to determine MD, MMD and MD degradation products by separate methods. The separation without the ion-pairing reagent was very poor. In addition, excipients (citric acid, fumaric acid, sodium lauryl sulphate, non-pariels, talc polyvinylpyrrolidone, and shellac) did not interfere in the determination of MD in the sustained release capsules. Moreover, the sensitivity of the method is such that it can be used as purity-indicating test to ascertain the presence of as little as 0.2% of MMD in MD (based on 125 mg MD per dosage form [22]), as well as a stability-indicating assay for MD.

In conclusion, the proposed method is accurate, rapid, selective and precise. It gave results for MD in sustained-release capsules which were in excellent agreement with those obtained by the compendial method. The method was superior, however, in separating MD from its degradation products. This advantage is being explored in kinetic studies on MD.

ACKNOWLEDGEMENTS

The author thanks Professor Dr. M. I. Walash, Professor Dr. M. M. Salem Rizk and Professor Dr. S. M. Hassan for their assistance during the preparation of the manuscript. The author also thanks the Quality Control Department at Elan Pharmaceutical Research (Gainesville, GA, USA) for supplying MD raw material, MMD raw material and MD sustained-release capsules.

REFERENCES

1 A. G. Gilman, L. S. Goodman and A. Gilman, *The Physiological Basis of Therapeutics*, Macmillan, New York, 6th ed., 1980, pp. 795–803.
2 J. R. Watson and R. C. Lawrence, *J. Chromatogr.*, 103 (1975) 63–70.
3 V. S. Gupta and A. Gupta, *Am. J. Hosp. Pharm.*, 36 (1979) 1539–41.
4 T. E. Young, B. W. Babbitt and L. A. Wolfe, *J. Org. Chem.*, 45 (1980) 2899–2902.
5 *The United States Pharmacopoeia, XIXth Revision*, United States Pharmacopoeial Convention, Rockville, MD, 1975, p. 320.
6 R. Leverty and K. M. Tylor, *Anal. Biochem.*, 22 (1968) 269–279.
7 B. K. Kim and R. T. Koda, *J. Pharm. Sci.*, 68 (1977) 1632–1634.
8 R. G. Bhatkar and V. N. S. Nevreckar, *Indian Drug Pharm. Ind.* 15 (1980) 45–47.
9 S. K. Wahba-Khalil and R. B. Salma, *J. Pharm. Pharmcol.*, 26 (1974) 972–974.
10 N. El-Rabbat and N. M. Omer, *J. Pharm. Sci.*, 67 (1978) 779–781.
11 M. I. Walash, A. A. Abou Ouf and F. B. Salem, *J. Assoc. Off. Anal. Chem.*, 68 (1985) 91–95.
12 P. B. Issopoulos, *Fresenius' Z. Anal. Chem.*, 336 (1990) 124–128.
13 A. M. Farina, M. A. Iorio and A. Doldo, *Spectrosc. Lett.*, 21 (1988) 455–487.
14 E. M. Athanasiou-Malaki and M. A. Koupparis, *Anal. Chim. Acta*, 161 (1984) 349–353.
15 J. Martens, K. Guenther and M. Schickedanz, *Arch. Pharm: (Weinheim, Ger.)*, 319 (1986) 572–574.
16 R. Chu, *J. Assoc. Off. Anal. Chem.*, 54 (1971) 603–608.
17 S. Ting, *J. Assoc. Off. Anal. Chem.*, 66 (1983) 1436–1442.
18 A. G. Ghanekar and V. Das Gupta, *J. Pharm. Sci.*, 67 (1978) 1247–1250.
19 I. L. Honigberg, J. T. Stewart, A. P. Smith and D. W. Hester, *J. Pharm. Sci.*, 64 (1975) 1201–1204.
20 V. Das Gupta and A. B. Dhruv, *Drug Dev. Ind. Pharm.*, 12 (1986) 691–700.
21 G. R. Rao, S. Raghaveer and K. R. Mohan, *Indian Drugs*, 19 (1982) 328–330.
22 *The United States Pharmacopoeia, XXIInd Revision*, United States Pharmacopoeial Convention, Rockville, MD, 1990, pp. 865–867.
23 M. E.-S. Metwally, in preparation.

Journal of Chromatography, 549 (1991) 229–236
Elsevier Science Publishers B.V., Amsterdam

CHROM. 23 315

High-performance liquid chromatographic determination of atrazine, deisopropylatrazine and deethylatrazine in soils from corn fields

GEORG KARLAGANIS* and ROLAND VON ARX
Federal Office of Environment, Forests and Landscape, Hallwylstrasse 4, CH-3003 Berne (Switzerland)
HANS ULRICH AMMON
Federal Research Station for Plant Production, Reckenholz, CH-8046 Zurich (Switzerland)
and
RUDOLF CAMENZIND
ILB Laboratories, Birkenweg 6, 3123 Belp (Switzerland)
(First received September 18th, 1990; revised manuscript received March 20th, 1991)

ABSTRACT

A reversed-phase high-performance liquid chromatographic (HPLC) assay of atrazine, deisopropylatrazine and deethylatrazine in soil samples from corn fields (treated with atrazine) is described. Soil (50 g) was homogenized, treated in an ultrasonic bath and extracted with methanol. The extract was purified on an aluminium oxide column, Sep-Pack C_{18} cartridges (atrazine only) and acrodisc filters. HPLC was performed on a LiChrosorb RP-18 5 μm column using a mobile phase of acetonitrile–water (35:65, v/v for atrazine and 20:80, v/v for the metabolites). The method was validated by ultraviolet diode-array spectroscopy and verified by capillary gas–liquid chromatography–mass spectrometry. The method is suitable for monitoring atrazine concentrations in soil from corn fields; it may also be used for routine measurements and for controlling correct atrazine dosing to avoid the misuse of the pesticide.

INTRODUCTION

The intense use of pesticides in agriculture and along roads, railway tracks and in public areas has led to an increasing awareness of the risks of contamination of the environment by xenobiotics. Monitoring programmes in Switzerland indicate that several groundwater and drinking water sources contain pesticide residues [1,2]. Atrazine is among the most commonly found substances. An assessment of the origin of this compound is rather difficult, as the fate of atrazine in soil depends on complex interactions between mass flow, diffusion, hydrodynamic dispersion, routes of water and solutes in the soil, pesticide stability and sorption on soil particles and pesticide stability and sorption on to soil organic matter. Hence measurements of atrazine residues in soils will help to achieve a better understanding of the fate of this compound and to detect possible sources of groundwater contamination. Until now mon-

0021-9673/91/$03.50

itoring progammes have only been based on measurements of residues in groundwater.

Numerous analytical procedures for determining herbicide residues have been described. For the analysis of triazine herbicides the conventional method by gas chromatography (GC) with nitrogen–phosphorus detection [3–6], liquid chromatography [3,7–9] and GC–mass spectrometry (MS) [10–15] have been applied successfully. Recently enzyme-linked immunosorbent assay has also been shown to be a useful method for the determination of triazine herbicide residues [16]. Residues of herbicides in soil samples have been measured [17–19]. The persistence of these substances in soil with respect to possible crop rotation problems [20–23] has been investigated.

This paper describes a high-performance liquid chromatography (HPLC) method for the determination of atrazine residues and metabolites in soil, which may be used for routine monitoring programmes. The sampling and analytical reproducibilities for atrazine have been determined.

MATERIALS AND METHODS

Collection of soil samples

Soil samples were collected at two different sites, Wasterkingen and Reckenholz, from plots treated with five different doses of atrazine (Table I). Each treatment included four plots (repetitions) of either 80 or 10 m^2. The time between the last atrazine application and the sampling data ranged from 109 days to over 3 years, and the doses were between 0 and 1.50 kg of atrazine per ha per year (Table I). From each plot (repetition) 20 subsamples were collected from a depth of 20 cm with a soil sampler (diameter 5 cm) and these were subsequently mixed by hand. The soil samples were stored immediately in a cold room at 2–4°C and then frozen at −20°C until analysis.

Reagents

All solvents were of analytical-reagent grade, with the exception of solvents for

TABLE I

ATRAZINE RESIDUES IN SOIL SAMPLES FROM A CORN FIELD EXPOSED TO DIFFERENT ATRAZINE APPLICATIONS AS DETERMINED BY HPLC

Sampling reproducibility based on four samples per treatment.

Treatment	Location	Atrazine application rates (kg active ingredient/ha/year)		Last atrazine application (days before sampling)	Mean atrazine residue (ppb)	Standard deviation (ppb)
		1984–1986	1987			
A	Wasterkingen	0.625	1.25	161	20.5	5.8
B	Wasterkingen	0.625	0	>360	8.0	5.9
C	Reckenholz	0	1.00	109	21.5	9.5
D	Reckenholz	0	1.50	136	10.4	4.1
E	Reckenholz	0	0	>1140	>2.0	–[a]

[a] Below limit of determination of 2 ppb.

HPLC (HPLC grade). Aluminium oxide (basic, W200, Woelm No. 04571) was dried for 5 h at 650°C. Water (19 ml per 100 g) was added, mixed and equilibrated at room temperature overnight. Sep-Pack C_{18} cartridges (Water Assoc., Milford, MA, USA) were washed with 10 ml of methanol and 10 ml of water before use. No plastic containers were used to avoid contamination of the samples with phthalates.

Isolation of atrazine from soil

The frozen soil samples (about 500 g each) were stored overnight at room temperature on aluminium foil washed with acetone and hexane. Large pieces were disintegrated mechanically with a shovel. The soil sample was pulverized by repeated division and recombination. From each sample 100 g were dried at 105°C overnight for the determination of dry matter. Another 50-g aliquot of the homegenized soil was suspended in 100 ml of methanol and treated for 10 min in an ultrasonic bath. This procedure was repeated once more, and the combined methanol extract was diluted with 250 ml of water and 50 ml of saturated sodium chloride solution and then extracted three times with 50 ml of methylene chloride. The lower phase was separated, dried with sodium sulphate and filtered. The combined methylene chloride extracts were evaporated at 40°C and the residue immediately redissolved with 5 ml of toluene.

The solution was applied to a chromatography column (22 × 1.8 cm) containing 20 g of aluminium oxide and 2 g of a top layer of anhydrous sodium sulphate. This purification step was necessary for the removal of interfering soil components, especially in the case of soil samples with high humus contents. The column was rinsed with 100 ml of hexane, which was then discarded. The atrazine was eluted with 100 ml of a mixture of hexane–diethyl ether (2:1, v/v), the eluate was evaporated to dryness at 35°C and the residue was immediately redissolved in 5 ml of distilled water and treated in an ultrasonic bath. The aqueous solution was passed through an acrodisc filter and a Sep-Pak C_{18} cartridge, both attached to a glass syringe. Atrazine was eluted with 0.5 ml of methanol and 2 ml of methanol–methylene chloride (3:7, v/v). The combined eluates were evaporated to dryness at 45°C, redissolved in 5 ml of acetonitrile–water (35:65, v/v), treated in an ultrasonic bath and filtered through an acrodisc filter (1.2 μm) into a vial of the HPLC autosampler. This extract was stored at 4°C until determination by HPLC.

Isolation of deethylatrazine and deisopropylatrazine

Another 50 g of the homogenized soil sample was suspended in 100 ml of methanol and treated for 10 min in an ultrasonic bath. The suspension was filtered through a paper filter containing a spoonfull of anhydrous sodium sulphate. The sample was extracted a second time with 100 ml of fresh methanol, as described in the preceding section. The filter was then rinsed with 20 ml of methanol. The combined methanol extracts were evaporated to dryness at a temperature not exceeding 45°C. The residue was immediately dissolved in 5 ml of toluene using an ultrasonic bath for a few seconds. The solution was applied to a chromatography column (22 × 1.8 cm) containing 20 g of aluminium oxide. The column was rinsed in portions with a total of 100 ml of hexane, which was then discarded. The two metabolites were eluted with 100 ml of a mixture of diethyl ether–methanol (2:1, v/v). The eluate was evaporated to dryness at 45°C; it was then immediately redissolved in 5 ml of acetonitrile–water

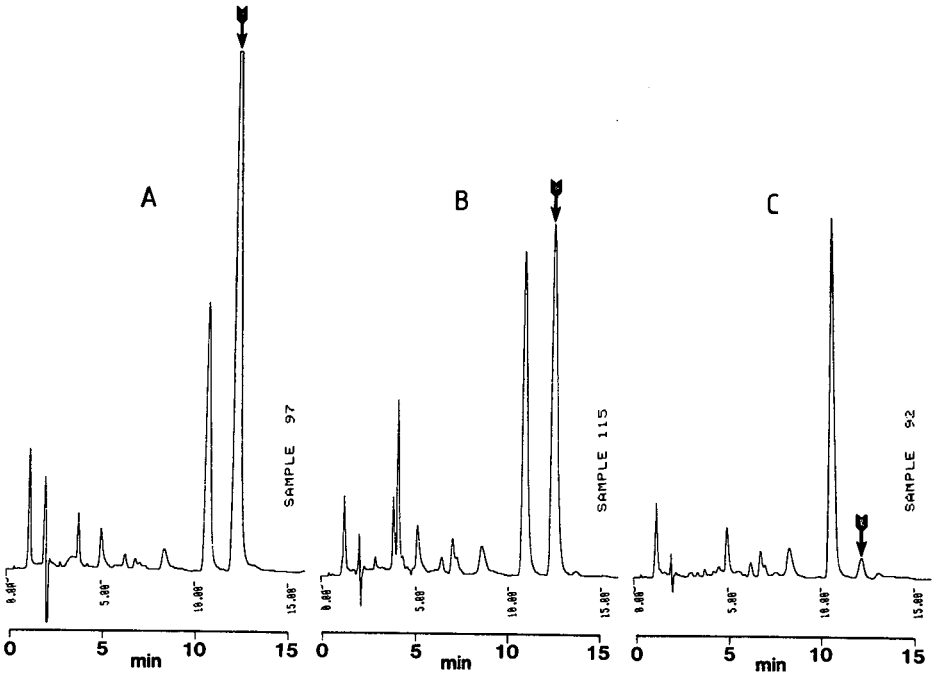

Fig. 1. High-performance liquid chromatogram of atrazine in soil from a corn field. Samples A, B and C correspond to different atrazine concentrations (146, 80 and 5 ppb, respectively). The atrazine peak elutes after 12 min, as indicated by the arrows.

(20:80, v/v) and filtered through an acrodisc filter [chemical resistance (CR), 1.45 μm] into a vial of the HPLC autosampler.

High-performance liquid chromatography

A LiChrosorb RP-18 column (250 × 4 mm, particle size 5 μm; E. Merck, Darmstadt, Germany) was used together with a LiChrosorb RP-18 pre-column (5 μm particle size). The mobile phases were acetonitrile–water (35:65, v/v) for atrazine and acetonitrile–water (20:80, v/v) for the metabolites at a flow-rate of 1.2 ml/min and a pressure of approximately 13 MPa. The injection volume was 20 μl and the solution was pumped with a Waters Model 510 pump. Detection was achieved with a Spar-Holland SPH 125 autosampler (Emmen, Netherlands) and LDC-Milton Roy UV detector (Riviera Beach, FL, USA) at 222 nm, with integration by a Waters 740 delta module integrator. Residues were calculated as ppb[a] wet soil.

RESULTS AND DISCUSSION

Fig. 1 shows three HPLC chromatograms of soil samples from corn fields

[a] Throughout this article, the American billion (10^9) is meant.

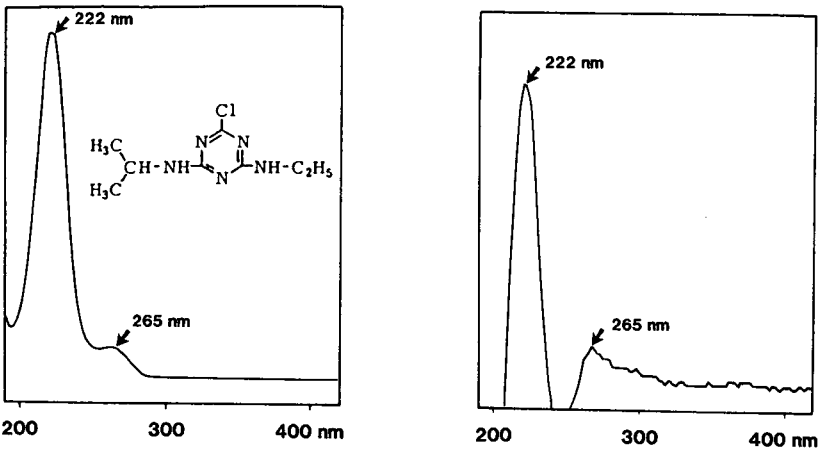

Fig. 2. UV spectra (HPLC–diode array) of atrazine from a standard solution (left) and from an extract of a soil sample (right). Both spectra show the same absorption maxima (222 nm) and shoulders (265 mn).

TABLE II

ANALYTICAL REPRODUCIBILITY (INTRA-DAY) OF ATRAZINE, DEETHYLATRAZINE AND DEISOPROPYLATRAZINE DETERMINATION BY HPLC

Compound	Sample number	Number of determinations (*n*)	Mean (ppb)	Standard deviation (ppb)	Coefficient of variation (%)
Atrazine	1	6	18.12	1.21	6.66
	2	6	9.48	1.18	12.45
	3	6	5.37	0.55	10.18
Deethylatrazine	4	6	7.37	0.72	9.77
Deisopropylatrazine	5	6	6.75	0.31	4.59

TABLE III

MEAN RECOVERY (STANDARD DEVIATION) OF ATRAZINE DEETHYLATRAZINE AND DEISOPROPYLATRAZINE FROM SPIKED SOIL SAMPLES AS DETERMINED BY HPLC (n = 6)

Compound	Amount added (ppb)	Amount recovered (ppb)	Percentage recovered
Atrazine	10	6.53 ± 0.12	65.3
	100	61.00 ± 3.06	61.0
Deethylatrazine	10	7.37 ± 0.72	73.7
	40	33.17 ± 5.23	82.9
Deisopropylatrazine	10	6.75 ± 0.31	67.5
	40	33.33 ± 5.13	83.3

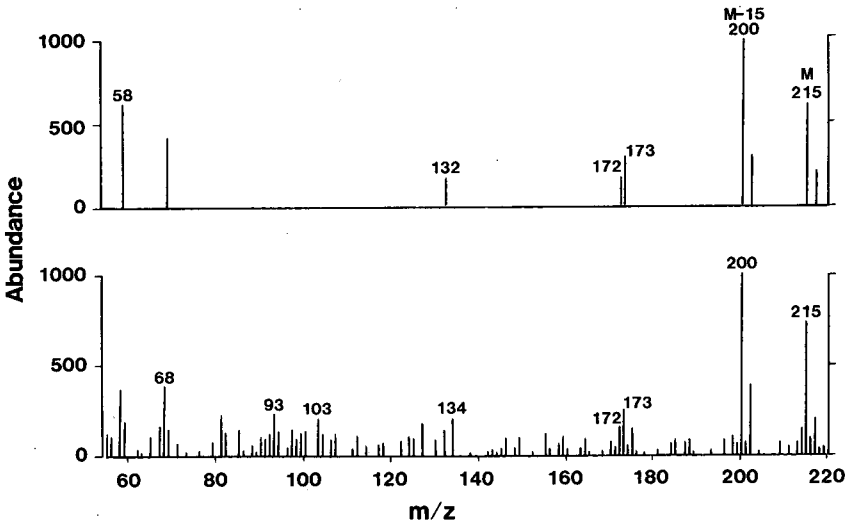

Fig. 3. Mass spectra of atrazine (capillary GC–EI-MS) from a standard solution (top) and from an extract of a soil sample (bottom). A Hewlett-Packard GC–MS system HP-5790A/HP-5970A was used equipped with a 30 m × 0.25 mm I.D. fused-silica capillary column DB-1 (methyl silicone) at 60°C, programmed at 20°C/min to 260°C column temperature.

containing atrazine. Baseline separation was achieved within 15 min. Phthalates may appear as additional peaks, therefore plastic containers should not be used during the extraction procedures. The identity of the peak with a 12 min retention time was confirmed by diode-array UV spectroscopy (Fig. 2).

The variability of atrazine determination in soil is dependent on the analytical method and the heterogeneity of atrazine distribution within the corn field. The intra-day reproducibility of the assay in soil samples with low atrazine concentrations ranged from 6.7 to 12.5% (Table II). The recoveries were 61–65% for atrazine, 74–

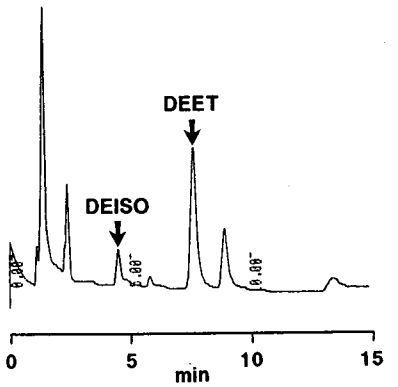

Fig. 4. High-performance liquid chromatogram of atrazine metabolites in soil from a corn field. Deisopropylatrazine (DEISO) elutes after 4.9 min (soil concentration 3 ppb); deethylatrazine (DEET) elutes after 8.5 min (12 ppb).

83% for deethylatrazine and 68–83% for deisopropylatrazine (Table III). Every fifth sample of the assays was a spiked soil sample to check the recovery. The limits of detection were 0.5 ppb for atrazine, 0.5 ppb for deethylatrazine and 0.5 ppb for deisopropylatrazine (signal-to-noise ratio 4:1).

The drying of soil samples before extraction in a heated place should be avoided. Drying of a soil sample for 15 h at 60°C reduces the atrazine content by 24% (n = 6). The HPLC method was validated by capillary GC–electron impact (EI)–MS. The mass spectra from a standard solution and from an extract of a soil sample were comparable (Fig. 3), yielding a molecular ion of m/z 215 and a base peak of m/z 200 (M − 15).

Atrazine metabolites are biologically active and it is therefore important to be able to monitor their concentrations in soil. Fig. 4 shows a chromatogram of the two primary metabolites of atrazine in a soil from a corn field.

Table I gives the sum of sampling and analytical reproducibility for atrazine and shows the atrazine content after different treatments. Four samples per treatment were taken. It is clear that the coefficient of variation is higher (compared to Table II) as a result of the variation of atrazine concentrations in the four soil samples taken within the corn field. However, the soil samples in Table I were taken in November and have low atrazine concentrations of up to 100 ppb (normal dose), or up to 500 ppb (overdose).

This method was developed for controlling atrazine dosing to avoid the misuse of the pesticide. It can be adapted for other similar compounds.

ACKNOWLEDGEMENTS

The authors are grateful to Mr. H. J. Laska and to Mr. A. Litscher for skilfull technical assistance and to Mrs. T. J. Lindt for help with the preparation of the manuscript.

REFERENCES

1 H. R. Kühni *Bericht über das SGCI-Untersuchungsprogramm (Febr. 1987–Febr. 1988), Pflanzenbehandlungsmittel im Grundwasser*, Fachgruppe Agrar der SGCI, Basle (1988) 41 pp.
2 U. Müller *Jahresbericht 1987*, Kantonales Laboratorium, Berne 1988, pp. 123–129.
3 M. Popl, Z. Voznakova, V. Tatar and J. Strnadova, *J. Chromatogr. Sci.*, 21 (1983) 39–42.
4 T. G. Steinheimer and M. G. Brooks, *Int. J. Environ. Anal. Chem.*, 17 (1984) 97–111.
5 T. G. Kreindl, H. Malissa and K. Winsauer, *Mikrochim. Acta*, 1 (1986) 1–13.
6 P. C. Bardalaye and W. B. Wheeler, *Int. J. Environ. Anal. Chem.*, 25 (1986) 105–113.
7 E. Smolkova and V. Pacakova, *Chromatographia*, 11 (1978) 698.
8 A. Di Corcia, M. Marchetti and R. Samperi, *J. Chromatogr.*, 405 (1983) 357–363.
9 I. G. Ferris and B. M. Haigh, *J. Chromatogr. Sci.*, 25 (1987) 170–173.
10 B. A. Karlhuber, W. D. Hörmann and K. A. Ramsteiner, *Anal. Chem.*, 47 (1975) 2450–2452.
11 F. Mangani and F. Bruner, *Chromatographia*, 17 (1983) 337–380.
12 V. Lopez-Avila, P. Hirata, S. Kraska, M. Flanagan and J. H. Taylor, Jr., *Anal. Chem.*, 57 (1985) 2797–2801.
13 E. Davoli, E. Benefati, R. Bagnati and R. Fanelli, *Chemospere*, 16 (1987) 1425–1430.
14 W. E. Pereira, C. E. Rostad and T. J. Leiker, *Anal. Chim. Acta*, 228 (1989) 69–75.
15 L. Q. Huang, *J. Assoc. Off. Anal. Chem.*, 72 (1989) 349–354.
16 E. M. Thurman, M. Meyer, M. Pomes, Ch. A. Perry and P. Schwab, *Anal. Chem.*, 62 (1990) 2043–2048.
17 K. Ramsteiner, W. D. Hörmann and D. O. Eberle, *J. Assoc. Off. Anal. Chem.*, (1974) 192–201.

18 T. H. Byast, E. G. Cotterill and R. J. Hance, *Technical Report*, Vol. 15, Agricultural Research Council Weed Research Organization, Oxford, 2nd ed., 1977.
19 W. D. Hörmann, *Rückstandsanalytik von Pflanzenschutzmitteln, Mitteilung VI der Senatskommission für Pflanzenschutz-, Pflanzenbehandlungs- und Vorratsschutzmittel, Methodensammlung der Arbeitsgruppe "Analytik", 1. Lieferung*, VCH Verlagsgesellschaft, Weinheim, 1985, Nr. 6-A, pp. 1–7; Nr. 6-B, pp. 1–7.
20 L. Stalder and W. Pestemer, *Weed Res.*, 20 (1980) 341.
21 W. Pestemer, L. Stalder and B. Eckert, *Weed Res.*, 20 (1980) 349.
22 W. Pestemer, V. Radulescu, A. Walker and L. Ghinea, *Weed Res.*, 24 (1984) 359.
23 W. Pestemer, *Mitt. Schweiz. Landwirtschaft*, 1/2 (1988) 2.

Journal of Chromatography, 549 (1991) 237–245
Elsevier Science Publishers B.V., Amsterdam

CHROM. 23 332

Carrier effect in the analysis of phenylurea herbicides using high-performance liquid chromatography–particle beam-mass spectrometry

M. J. INCORVIA MATTINA

Department of Analytical Chemistry, The Connecticut Agricultural Experiment Station, 123 Huntington Street, New Haven, CT 06511 (USA)

(First received November 27th, 1990; revised manuscript received March 5th, 1991)

ABSTRACT

The structural similarity between phenylurea and the herbicides diuron, linuron, and monuron is exploited to enhance the analysis for the chlorophenylureas using high-performance liquid chromatography–particle beam-mass spectrometry. Phenylurea functions as the analyte "carrier" through the particle beam interface, improving the detection limits and the linearity of the calibration curves for the cited compounds of the herbicide class. Combined with solid phase extraction the method provides a rapid and reliable analysis for the chlorophenylureas in water matrices.

INTRODUCTION

The phenylurea herbicides, diuron, linuron, and monuron, which function by inhibiting photosynthesis [1], are used in field applications for pre- and post-emergence weed control in a wide variety of crops. Their widespread agricultural use, toxicity, and possible carcinogenicity [2] have stimulated the development of methods for the detection of the phenylureas at low concentration levels in water, soil, and food. Because these compounds are thermally labile, determination based on gas chromatography (GC) is usually preceded by derivatization [3,4]. The derivatization step may be circumvented by the use of liquid chromatography (LC) coupled with electrochemical detection [5], UV detection [6], photoconductivity detection [7], or thermospray mass spectrometry [8–10].

All of the LC detectors enumerated above lack either specificity and/or sensitivity. The particle beam (PB) interface for coupling high-performance liquid chromatography (HPLC) with mass spectrometry (MS) [11] provides the opportunity to develop methods featuring classical electron impact (EI) and chemical ionization (CI) MS with their inherent specificity. However, the detection limits frequently associated with this interface fall short of ideal values [12].

The method presented here couples several techniques to achieve a rapid, sensi-

0021-9673/91/$03.50

tive, and specific analysis for diuron, linuron, and monuron. Solid-phase extraction (SPE) is used to extract and concentrate the analytes from a water matrix. Reversed-phase HPLC with acetonitrile–water as the eluent separates the compounds in under 6 min on a C_{18} column. The PB interface introduces the LC eluate into a quadrupole mass spectrometer operated in selected ion monitoring (SIM) mode under methane enhanced electron capture negative ion (ECNI) conditions. The addition of phenylurea (PHU) to the mobile phase as the analyte carrier significantly improves the detection limits to the low ppb (ng/ml) level for each of the compounds in the original water solution. For one of the target analytes, diuron, the absolute sensitivity achievable is 160 pg injected on-column in the presence of PHU. Additionally, PHU in the mobile phase results in linear calibration curves over a greater-than-ten-fold concentration range.

EXPERIMENTAL

Reagents

Diuron, linuron and monuron (see Table I) at 99% purity were obtained from the US Environmental Protection Agency's (EPA) Pesticides & Industrial Chemicals Repository (Research Triangle Park, NC USA) or from the EPA Pesticide Reference Standards Laboratory (Beltsville, MD, USA) and were used without further purification. Phenylurea was purchased from American Tokyo Kasei (Portland, OR, USA). Solvents were Baker HPLC grade or Resi-analyzed grade (J. T. Baker, Phillipsburg, NJ, USA). Water was distilled prior to being passed through a Barnstead (Newton, MA, USA) NANOpure II system followed by 0.2 μm filtration. SPE cartridges were C_{18} high-capacity 6-ml cartridges from J. T. Baker, catalogue No. 7020-07.

Helium gas for the nebulizer on the PB interface was ultra-high-purity grade (Union Carbide–Linde Division, Danbury, CT, USA) and was filtered through an Oxyclear Disposable Gas Purifier (Labclear, Oakland, CA, USA), followed by a Supelco OMI-1 filter (Bellefonte, PA, USA). The methane enhancement gas was also Linde ultra-high-purity grade and was filtered through both an Oxyclear purifier and an OMI-1 filter.

TABLE I

PHENYLUREA HERBICIDES

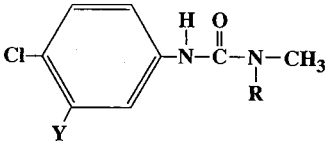

Herbicide	Mol. wt.	Y	R
Monuron	198	H	CH_3
Diuron	232	Cl	CH_3
Linuron	248	Cl	OCH_3

Apparatus

The LC column was a Waters (Milford, MA, USA) 300 mm × 2.1 mm stainless-steel μBondapak 10 μm C_{18} column, protected by a Supelco LC18 guard column. A Hewlett-Packard (Palo Alto, CA, USA) 1090 liquid chromatograph, fitted with a Rheodyne (Cotati, CA, USA) 7010 injector equipped with a Rheodyne 7012 loop-filler port and a 20-μl loop, was coupled to a Hewlett-Packard 5988A quadrupole mass spectrometer through the HP 59980A PB interface. Data acquisition and processing were under the control of the HP 59970C MS Pascal ChemStation (Rev. 3.2).

Procedure

Calibration. Separate stock solutions of diuron, linuron and monuron in methanol were prepared at 10 ng/μl concentration, from which working standards of each herbicide were prepared by serial dilution. Five methanolic calibration solutions were then prepared, each of which contained a mixture of the three herbicides, at increasing concentration from lowest concentration to highest concentration for each herbicide. The concentration of the herbicides in the calibration solutions ranged from 0.020 to 2.5 ng/μl for diuron, 0.100 to 2.5 ng/μl for linuron and 1.00 to 3.5 ng/μl for monuron. To generate the calibration curves duplicate injections of each calibration solution were made in random order onto the LC column.

SPE Recovery. Each of three 100-ml samples of tap water and three 100-ml samples of distilled, deionized (DI/DI) water were spiked with a mixture of 1000 ng of diuron (10 μg/l), 4000 ng of linuron (40 μg/l) and 6000 ng of monuron (60 μg/l). Two unspiked tap water samples and two unspiked DI/DI water samples were carried through the SPE procedure as blanks. Each water sample was extracted using an SPE cartridge, which had been conditioned with ethyl acetate, methanol, and DI/DI water under a gentle vacuum and was not permitted to run dry before the sample was applied. After the sample had completely drained through the cartridge, the cartridge was washed with approximately 5 ml of DI/DI water and air dried for 5 min. The herbicides were then eluted from the cartridge with 2 ml of methanol under a very gentle vacuum.

Liquid chromatography. An isocratic mobile phase composed of acetonitrile–water (68:32) at a flow-rate of 0.4 ml/min was used. The acetonitrile contained phenylurea at a concentration of 2.90 ng/μl.

Particle beam. The desolvation chamber temperature was set to 50°C and the helium nebulizer pressure was set at 35 p.s.i.

Mass spectrometer. The mass spectrometer was operated under methane enhanced ECNI conditions. The source temperature was 250°C; the methane pressure was 0.5 Torr, as read on the GC–MS interface thermocouple gauge. For quantitation SIM mode was used with simultaneous monitoring of the *m/z* 198, 232 and 218 ions for monuron, diuron and linuron, respectively.

RESULTS AND DISCUSSION

Fig. 1 shows the typical SIM chromatograms for a calibration curve solution (diuron at 2.50 ng/μl; linuron at 2.50 ng/μl; monuron at 3.50 ng/μl) recorded using the LC and PB settings described above with the mass spectrometer operated under

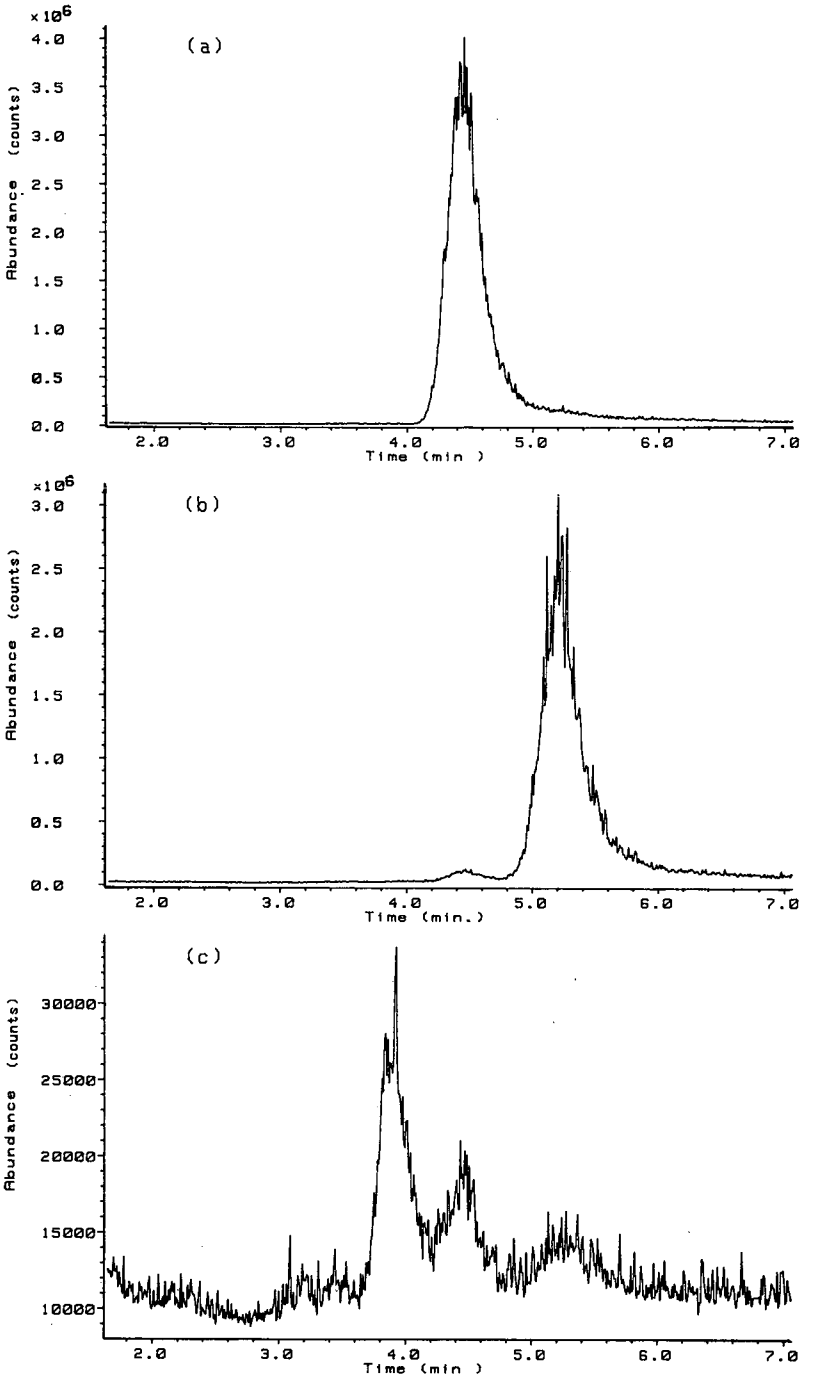

Fig. 1. LC–PB-MS chromatograms for: (a) 50 ng of diuron; (b) 50 ng of linuron; and (c) 70 ng of monuron under SIM methane-enhanced ECNI conditions.

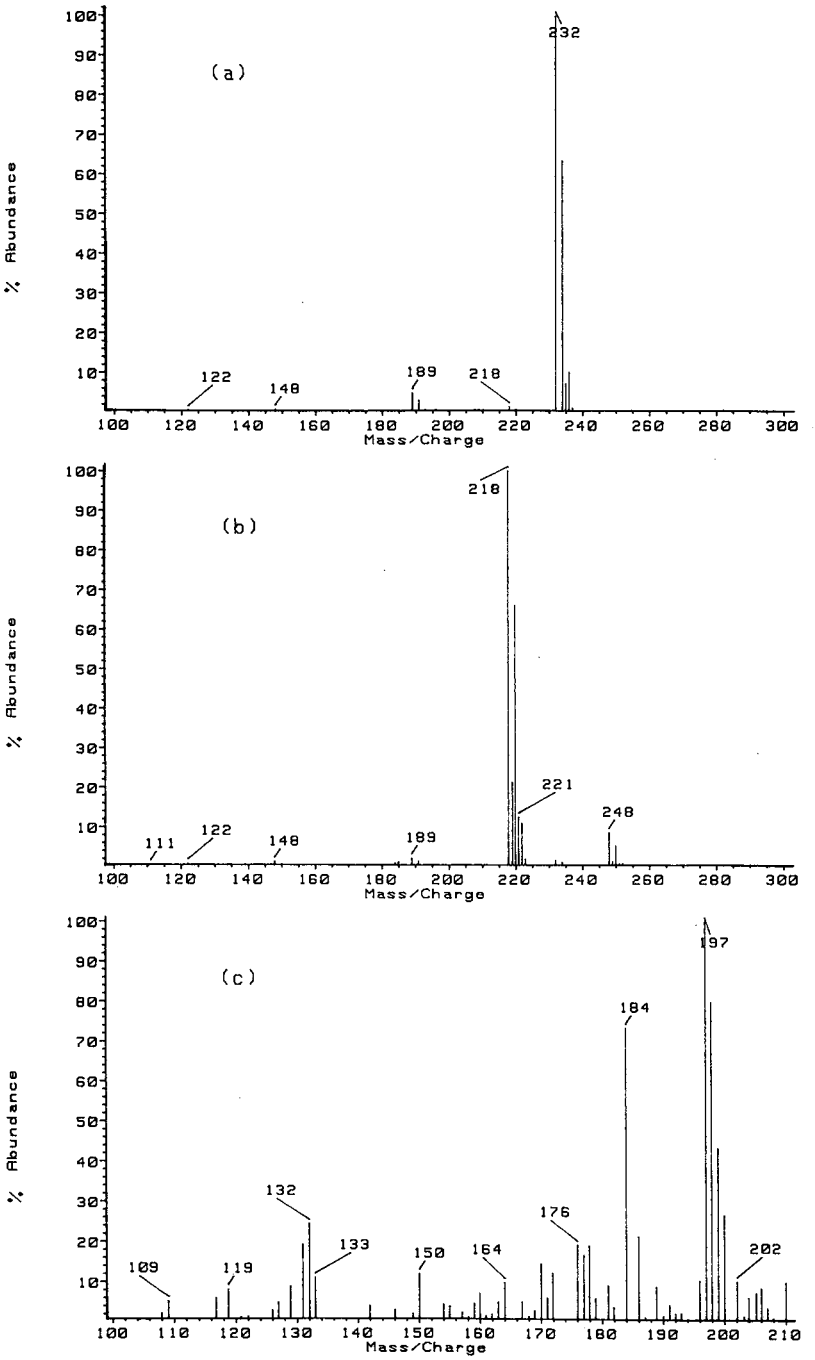

Fig. 2. Full-scan mass spectra acquired under methane-enhanced ECNI conditions for (a) diuron, (b) linuron and (c) monuron.

methane-enhanced ECNI conditions. It has been demonstrated that the molar response factors for diuron and linuron are larger under methane-enhanced ECNI conditions than under EI conditions [13]. The retention times observed for monuron, diuron and linuron are 3.9, 4.5 and 5.3 min, respectively. Under full-scan conditions the particle beam methane enhanced ECNI mass spectra for 160 ng of diuron, 160 ng of linuron, and 200 ng of monuron injected on-column are shown in Fig. 2a, b and c, respectively. The quantitation ion for diuron and monuron corresponds to the $M^{-\cdot}$ molecular ion and for linuron to the $[M-OCH_2]^{-\cdot}$ fragment ion. The base peaks recorded in the HPLC–PB-methane enhanced ECNI mass spectra for diuron and linuron correspond to the base peaks for both these compounds observed under HPLC–MS negative ion conditions using a direct liquid introduction (DLI) interface [14].

The addition of a carrier to the LC mobile phase either pre- or post-column to improve the operation of the particle beam interface has been demonstrated [15–19]. Carriers such as ammonium acetate [16], malic acid [17], or the isotopically labelled analogue of the analyte of interest [18] serve to enhance transport efficiency of the analyte through the PB interface. Improved transport efficiency results in lower detection limits for the analytes as well as linear calibration curves. The carrier, phenylurea, selected in the current experiments for the LC–PB-MS analysis of diuron, linu-

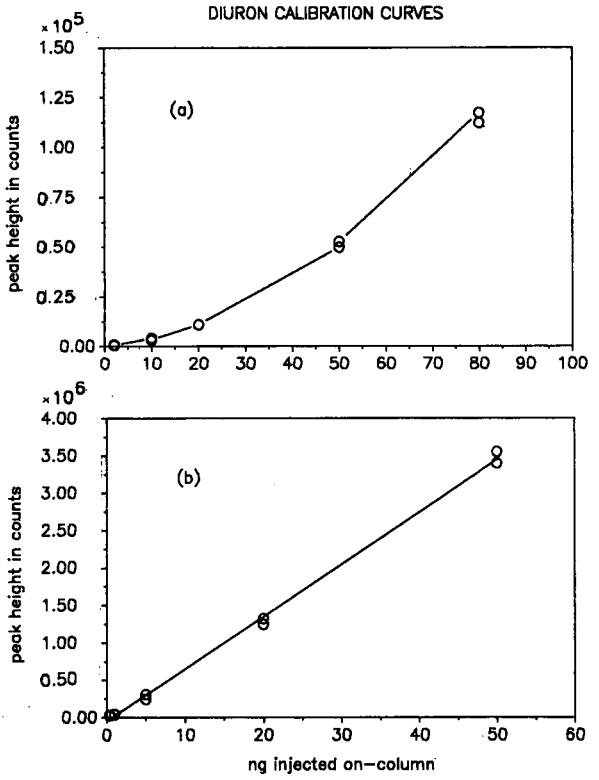

Fig. 3. Diuron calibration curves: (a) without phenylurea and (b) with phenylurea in the mobile phase.

ron and monuron, is structurally similar to the target analytes. Employing the structural similarity between a carrier and the analytes of interest to enhance transport efficiency has been demonstrated previously for the analysis of chlorophenoxy acid herbicides [19]. The improvement in both sensitivity and calibration curve linearity produced by the addition of 2.90 ng/μl PHU to the acetonitrile of the mobile phase is illustrated for diuron in Fig. 3a and b. If no PHU is present in the mobile phase or if 0.01 *M* ammonium acetate is present, the calibration curve shown in Fig. 3a is typically generated and the detection limit for diuron under methane-enhanced ECNI SIM conditions is 2 ng injected on-column. With the PHU carrier in the mobile phase the diuron calibration curve shown in Fig. 3b is generated having a correlation coefficient of 0.999. The detection limit improves to 160 pg injected on-column with a signal-to-noise ratio of 3:1.

Similar results are obtained for linuron. For the linuron calibration curve shown in Fig. 4a, generated with PHU in the mobile phase, the correlation coefficient is 0.980 and a detection limit of 500 pg injected on-column is achieved. These optimum detection limits cannot be achieved if the concentration of the phenylurea in the mobile phases drops below the 2.90 ng/μl specified above.

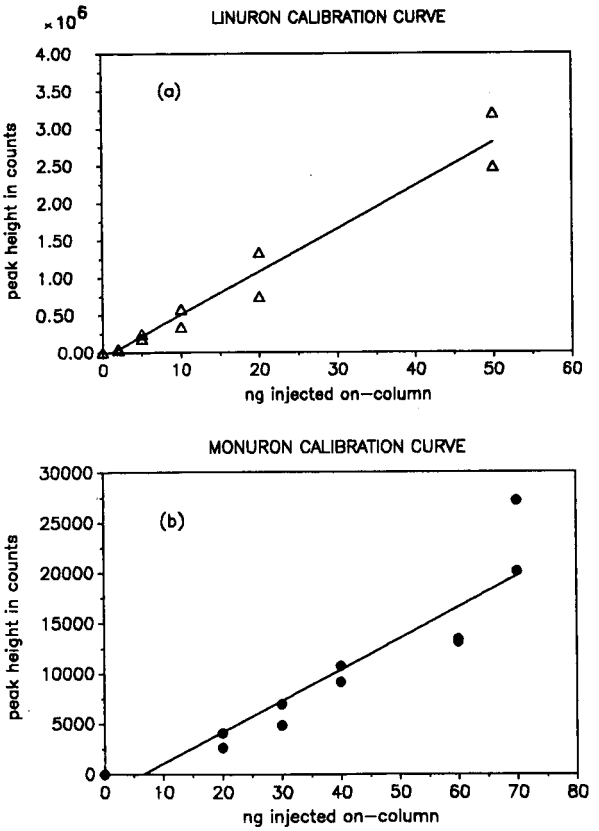

Fig. 4. Calibration curves with phenylurea present in the mobile phase for (a) linuron and (b) monuron.

TABLE II

SPE RECOVERY OF PHENYLUREA HERBICIDES FROM WATER DETERMINED BY HPLC–PB-METHANE-ENHANCED ECNI-MS

Herbicide	Spiking level	Recovery (%)	Matrix
Diuron	10 μg/l	136 ± 13 (n = 6)	Tap
	10 μg/l	126 ± 8 (n = 6)	DI/DI[a]
	0 μg/l	0 (n = 4)	Tap
	0 μg/l	0 (n = 4)	DI/DI
Linuron	40 μl/l	104 ± 11 (n = 6)	Tap
	40 μg/l	102 ± 16 (n = 6)	DI/DI
	0 μg/l	0 (n = 4)	Tap
	0 μg/l	0 (n = 4)	DI/DI
Monuron	60 μg/l	151 ± 18 (n = 6)	Tap
	60 μg/l	109 ± 14 (n = 6)	DI/DI
	0 μg/l	0 (n = 4)	Tap
	0 μg/l	0 (n = 4)	DI/DI

[a] Distilled, deionized water as described in the text.

The calibration curve for monuron generated with PHU in the mobile phase is shown in Fig. 4b. The correlation coefficient for this curve is 0.932.

Table II summarizes the SPE recovery data. For each sample duplicate injections of the SPE eluate onto the LC column were performed in random order. There are two possible explanations for the poor recovery data for monuron from the tap water samples. First, the molar response factor for monuron under methane-enhanced ECNI conditions is much smaller than that for diuron and linuron (compare Fig. 1a and b with Fig. 1c). Monuron sensitivity improves under EI conditions [20]. Second, for the tap water samples an unidentified substance(s) elutes from the C_{18} column at retention time 3.4 min, which interferes with the monuron peak at 3.9 min.

The detection limits for diuron (160 pg on-column) and for linuron (500 pg on-column) translate into optimum detectable concentrations of 160 ng/l (0.160 ppb) and 500 ng/l (0.500 ppb), respectively, for an original water sample size of 100 ml with SPE concentration to 2 ml.

The experimental results reported here support our earlier observation that the use of an appropriate generic carrier for a class of analyte compounds can render LC–PB-MS a sensitive technique for quantitation of target analytes in water matrices. When SPE is employed to extract and concentrate the analytes, a rapid, reliable, and relatively simple method is available for the determination of two classes of polar, thermally labile compounds, the chlorophenoxy acid herbicides and the phenylurea herbicides. Experiments are in progress to improve the LC resolution of the phenylurea herbicides and to extend the method to additional compounds in this class.

REFERENCES

1 J. R. Corbett, K. Wright and A. C. Baille, *The Biochemical Mode of Action of Pesticides*, Academic Press, New York, 2nd ed., 1984, p. 56.
2 R. E. Gosselin, R. P. Smith and H. C. Hodge, *Clinical Toxicology of Commercial Products*, Williams and Wilkins, Baltimore, 5th ed., 1984, pp. II–330.
3 J. F. Lawrence, *J. Assoc. Off. Anal. Chem.*, 59 (1976) 1061.
4 U. A. Th. Brinkman, A. De Kok and R. B. Geerdink, *J. Chromatogr.*, 283 (1984) 113.
5 G. Chiavari and C. Bergamini, *J. Chromatogr.*, 346 (1985) 369.
6 A. De Kok, Y. J. Vos, C. van Garderen, T. De Jong, M. van Opstal, R. W. Frei, R. B. Geerdink and U. A. Th Brinkman, *J. Chromatogr.*, 288 (1984) 71.
7 E. W. Zahnow, *J. Agric. Food Chem.*, 35 (1987) 403.
8 L. M. Shalaby, in J. D. Rosen (Editor), *Applications of New Mass Spectrometry Techniques in Pesticide Chemistry*, Wiley, New York, 1987, Ch. 12, p. 161.
9 D. Barceló, in M. A. Brown (Editor), *Liquid Chromatography/Mass Spectrometry: Applications in Agricultural, Pharmaceutical, and Environmental Chemistry*, American Chemical Society, Washington, DC 1990, Ch. 4, p. 48.
10 D. Barceló, *Org. Mass Spectrom.*, 24 (1989) 219.
11 R. C. Willoughby and R. F. Browner, *Anal. Chem.*, 56 (1984) 2626.
12 B. M. Hughes, D. E. McKenzie, J. Doi, C. K. Trang, R. G. Orth and R. W. Noble, in R. Caprioli (Editor), *Proc. 38th ASMS Conference on Mass Spectrometry and Allied Topics, Tucson, AZ, June 3–8, 1990*, American Society for Mass Spectrometry, East Lansing, MI, 1990, p. 1228.
13 M. J. I. Mattina, in R. Caprioli (Editor), *Proc. 38th ASMS Conference on Mass Spectrometry and Allied Topics, Tucson, AZ, June 3–8, 1990*, American Society for Mass Spectrometry, East Lansing, MI, 1990, p. 1091.
14 R. D. Voyksner, J. T. Bursey and E. D. Pellizzari, *J. Chromatogr.*, 312 (1984) 221.
15 T. D. Behymer, T. A. Bellar and W. L. Budde, *Anal. Chem.*, 62 (1990) 1686.
16 T. A. Bellar, T. D. Behymer and W. L. Budde, *J. Am. Soc. Mass Spectrom.*, 1 (1990) 92.
17 I. S. Kim, F. I. Sasinos, R. D. Stephens and M. A. Brown, *J. Agric. Food Chem.*, 38 (1990) 1223.
18 L. McLaughlin, T. Wachs, R. Pavelka, G. Maylin and J. Henion, presented at the *1990 Pittsburgh Conference and Exposition on Analytical Chemistry and Applied Spectroscopy, New York, NY, March 5–9, 1990.*
19 M. J. I. Mattina, *J. Chromatogr.*, 542 (1991) 385.
20 M.J. I. Mattina, unpublished results.

Journal of Chromatography, 549 (1991) 247–256
Elsevier Science Publishers B.V., Amsterdam

CHROM. 23 369

Separation and identification of sulfurized alkylphenols in oil by high-performance liquid chromatography with evaporative light scattering and mass spectrometric detection

EVAN N. CHEN, Jr. and VINCENT P. NERO
Texaco Research and Development, P.O. Box 509, Beacon, NY 12508 (USA)
(First received January 23rd, 1991; revised manuscript received April 16th, 1991)

ABSTRACT

Sulfurized alkylphenols, intermediates for the production of detergents, were separated from undesired reaction side products and base oil on a γ-cyclobond II column by high-performance liquid chromatography (HPLC) with evaporative light scattering detection (ELSD), and then identified by direct electron exposure mass spectrometry techniques. This technique was successful in monitoring the quality of the alkylphenols prior to producing the final product. ELSD proved to be superior over other conventional HPLC detection methods in the analysis of sulfurized alkylphenols.

INTRODUCTION

Various types of detergent additives such as alkoxides, sulfonates, phenates and carboxylates have been used in lubricating oils in order to reduce or remove deposits formed by the burning of fuel. In addition, these detergent additives may also function as antioxidants and antiwear agents. The preparation of overbased detergents, in which a large amount of metal base is incorporated, have become important in the petroleum industry [1–4]. During the combustion process, the formation of harmful acidic components has led to the degradation of the lubricating oil and to the corrosion of metal bearings and engine parts. For this reason, overbased detergents have been employed to neutralize these acidic by-products.

Recently, the use of neutralized and overbased phenate detergents has increased since, in addition to acting as detergents, they exhibit increased high-temperature stability properties [5]. This is an important feature since modern automobile engines work harder and generate higher temperatures. The physical characteristics of these detergent additives are highly dependent upon the quality of sulfurized alkylphenols, the reaction intermediates. Specifically, sulfurized dodecylphenols have been used in the production of phenate detergents [6–9].

The analysis of detergent in lubricating oils by high-performance liquid chromatography (HPLC) has been well documented in the literature [10–17]. However,

0021-9673/91/$03.50

these analyses need to be extended to the reaction intermediates. The composition of sulfurized alkylphenols has been previously determined by a combination of gas chromatography (GC) and polarography [18] and by mass spectral techniques in conjunction with mathematical processing [19].

The use of evaporative light scattering detection (ELSD), an improved universal detection method for HPLC, has been investigated because of its increased sensitivity, stability from ambient temperature effects and operation with multiple solvent gradients [20–22]. This detector is an excellent candicate for the analysis of sulfurized alkylphenols due to its success in the determination of coal derivatives [23], heavy oil petroleum fractions [24], and surfactant additives [25].

This paper reports the development of an HPLC method that allows for routine determination of sulfurized dodecylphenols in oil. In addition, undesirable reaction side products that can reduce the quality of the detergent additive can be easily monitored.

EXPERIMENTAL

Apparatus

HPLC was performed on a Waters chromatography system (Waters, Milford, MA, USA) equipped with two 590 programmable pumps, a 480 automated gradient controller, a U6K injector and a 490 programmable UV detector. An ELS detector (Varex Corporation, Rockville, MD, USA) was connected in series after the UV detector. The chromatographic data were processed using the PE Nelson 2600 chromatography system (PE Nelson, Cupertino, CA, USA).

Materials

Hexane and unstabilized tetrahydrofuran (THF) (EM Science, Gibbstown, NJ, USA) were of HPLC-reagent grade. The mobile phase was continuously degassed by dry-grade helium (Linde, Danbury, CT, USA).

Chromatographic procedure

The Waters modular HPLC system was set up for gradient elution with the ELS detector connected in series after the UV detector. The solvents were thoroughly degased with helium and the system allowed to equilibriate for at least 20 min. The gradient program used to elute the components is shown in Table I.

The separation was performed on a γ-cyclobond II column (Astec, Whipanny, NJ, USA, 25 cm × 4.6 mm I.D., 5-μm spherical particle size) which can be thermally controlled by a column heater or some insulating wrap. This column was capable of separating sample into oil, sulfurized dodecylphenol, undesirable side products and unreacted material.

Upon equilibration, 10 μl of a 2.0% (w/v) sample in hexane was injected into the HPLC system. All samples were filtered through a 0.45-μm Millex-HV filter (Millipore, Bedford, MA, USA).

Each sample component was collected using 1-ml conical sample vials (Alltech, Deerfield, IL, USA) for further analysis by mass spectrometry (MS).

TABLE I

GRADIENT ELUTION PROGRAM FOR THE SEPARATION OF SULFURIZED ALKYLPHENOLS

Time (min)	Flow (ml/min)	Hexane (%)	Tetrahydrofuran (%)	Curve[a]
Initial	1	70	30	–
2	1	70	30	7
3	1	50	50	7
4	1	50	50	6
6	1	0	100	6
9	1	0	100	6
12	1	70	30	6

[a] Curves are generated by the automated gradient controller (AGC).

HPLC detection

The sample components were monitored by the UV detector (set at 280 nm), then by ELSD. The operating conditions for ELSD were optimized for sensitivity and baseline stability by adjusting the drift tube temperature and the carrier gas flow. The best detector response was achieved at an exhaust temperature of approximately 55°C and a nitrogen flow of 12 p.s.i. The range was set at 10×.

HPLC RESULTS AND DISCUSSION

Cyclodextrin bonded phases

The use of cyclodextrin stationary phases for HPLC has gained increased attention due to their versatility in normal and reversed-phase modes and their ability to form inclusion complexes to effect a variety of chemical separations [26–28]. Cyclobond columns are packed with silica gel material which is covalently bonded to the cyclodextrin molecules via a stable, non-hydrolytic, non-nitrogen-containing silane linkage [29].

The α-, β- and γ-cyclodextrins are cyclic oligosaccharides that contain 6, 7 or 8 glucopyranose units, respectively, and are arranged in the shape of a hollow truncated cone. The interior cavity is hydrophobic, being primarily comprised of methylene and 1,4-glucoside linkages. The exterior, on the other hand, is hydrophilic due to the primary and secondary hydroxyl groups [30].

The most unique characteristic of cyclodextrins is their ability to selectively form inclusion complexes with a variety of organic and inorganic molecules within their hydrophobic cavity [29]. In addition to the size and shape of the analyte, the mechanism of separation is dependent upon other factors such as dipole–dipole interactions and hydrogen bonding.

ELSD

The principle of operation involves converting the column effluent into a very fine mist after passing through a nebulizer. A stream of carrier gas then directs this

mist into a temperature-controlled drift tube where the mobile phase is vaporized leaving the fine particles of interest in the carrier gas. These sample particles are then passed through the path of a laser light source and the light that is scattered is detected by a photodetector system.

ELSD is an improved universal detection method compared to the widely used refractive index (RI) detection method. It is capable of operating free from ambient temperature effects and with multiple solvent gradients without detectable baseline drift. The detector response is a function of the mass of the solute passing through the detector, unlike most HPLC detectors whose response is based upon the concentration of the solute. These characteristics make ELSD and excellent candidate over RI detection for the analysis of sulfurized alkylphenols.

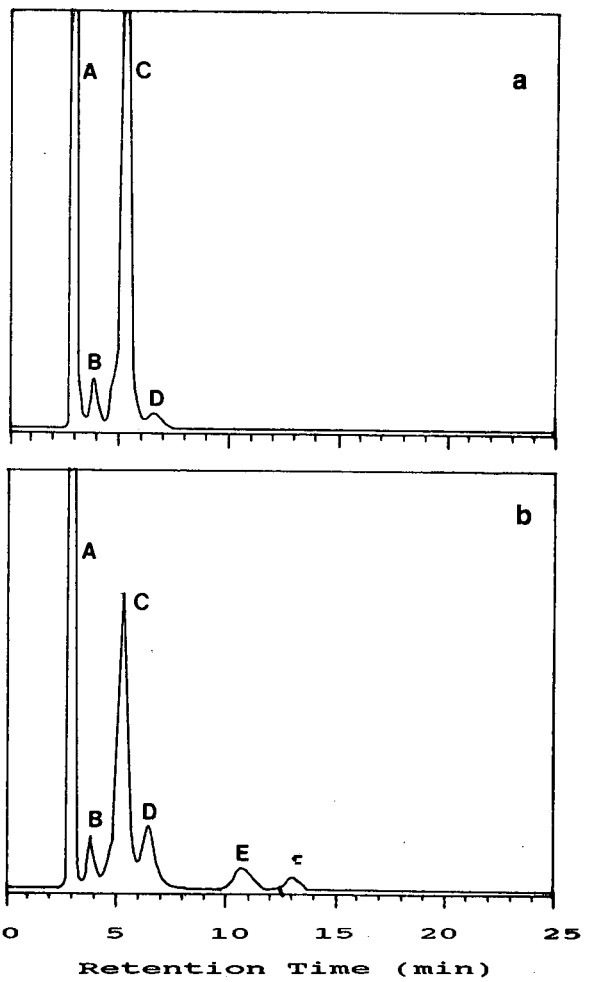

Fig. 1. (a) HPLC analysis by ELSD of a sulfurized dodecylphenol which met engine test specifications and (b) one which had failed the engine tests. See text for explanation.

Analysis of sulfurized dodecylphenols

Two sulfurized dodecylphenols were separated from undesirable reaction side products and oil by the normal-phase chromatographic method summarized in Table I. The signals from each separated component were then monitored and compared by both UV and ELS detection.

This multi-detector gradient HPLC system, in conjunction with mass spectral identification of the isolated components, was designed to monitor those intermediates which may or may not meet the standard engine test specifications. The first sample, shown in Fig. 1a, was previously determined to have met engine test specifications, while the second sample, shown in Fig. 1b, had failed the engine tests.

It can be seen from the resulting chromatograms that the first sample contained

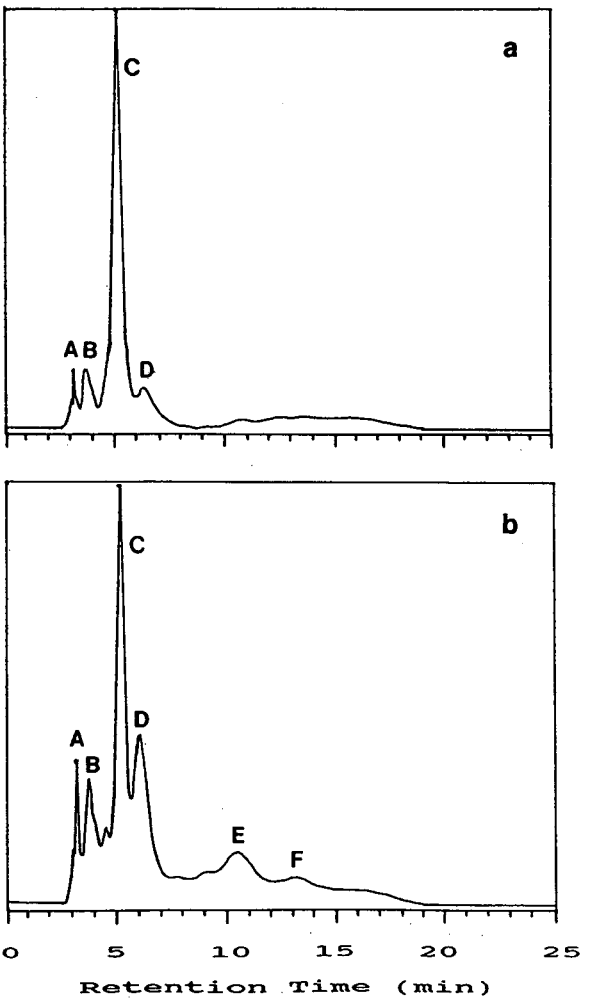

Fig. 2. (a) HPLC analysis by UV detection of sample in Fig. 1a and (b) of sample in Fig. 1b. See text for explanation.

a larger amount of the desired product (peak C) compared to the second sample. Also, the second sample contained more prominent undesirable reaction side products and unreacted material (peaks B, D–F). This method was also successful in isolating the base oil (peak A) from the other components. The significant differences between these two chromatograms demonstrated that the HPLC–ELSD system was an excellent technique for effective quality control monitoring of these types of samples.

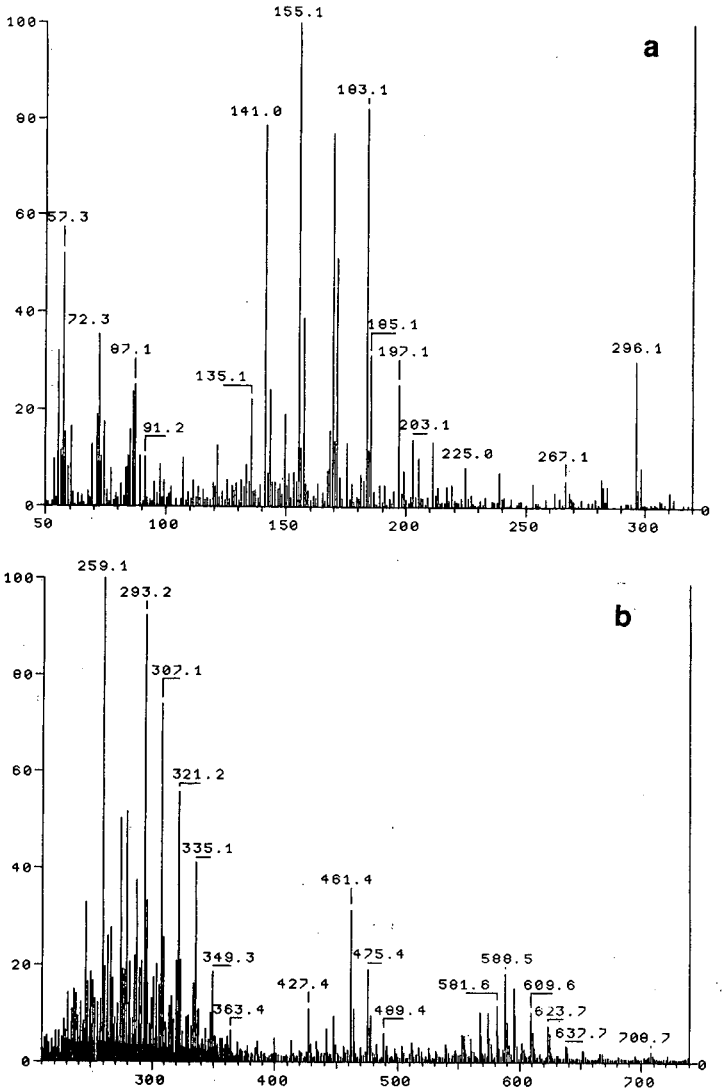

Fig. 3. (a) Mass spectra of dodecylchlorophenol **1** (peak B in Fig. 1b) and (b) dodecylhydroxyphenyl didodecylhydroxyphenyl sulfide **2** and dodecylhydroxyphenyl dodecylchlorohydroxyphenyl sulfide **3** (both also contained in peak B, Fig. 1b).

The mechanism of separation for the sulfurized dodecylphenols was more likely to be partition rather than the formation of inclusion complexes. In this case, the diameter of the solutes was too large to form complexes with the interior cavity of the cyclodextrin molecule. Since both mobile phases, hexane and THF, had strong affinities for the hydrophobic cabity, solute retention was probably due to the adsorption of the component on the outer hydrophilic portion of the cyclodextrin [30]. In addition, hydrogen bonding to the surface hydroxyls and other electrostatic interactions may have played a role in the separation process.

The corresponding UV detector chromatograms of the first and second samples are shown in Fig. 2a and b, respectively. Both chromatograms had poor resolution between peaks and noticeable baseline drift due to the interfering THF mobile phase. In addition, only a small response was observed for the non-UV absorbing base oil peak. In spite of these major disadvantages, the complementary nature of the UV detector was quite useful. Several injections were made in order to obtain repeatable and accurate retention times necessary for the collection of each sample component for mass spectral identification. The repeatability for the desired major product was found to be ± 0.03 min. This could not be accomplished with ELSD because of its destructive design.

This technique was successful in monitoring the quality of sulfurized dodecylphenols prior to producing the final detergent additive. Also, ELSD was capable of operating with multiple solvent gradients without solvent interferences.

MASS SPECTRAL EXPERIMENTAL AND IDENTIFICATIONS

Approximately 1 ml of each major HPLC fraction was collected in a conical 1-ml vial, and then concentrated by evaporation to about 0.1 ml using a gentle nitrogen stream just prior to mass spectrometric analysis. The fraction was then deposited onto the rhenium wire filament of a direct insertion probe and allowed to dry. The probe was inserted into the source of a Finnigan-MAT TSQ 70 quadrupole mass spectrometer in close proximity to the transverse electron beam. The sample was rapidly volatilized into the source by linearly heating the probe filament from 20 to 1150°C over a 1-min time period. The source temperature was held at 150°C. Its ion current was 200 μA at 70 eV. The first quadrupole was scanned from 50 to 900 u at 1 scan per 0.75 s.

The HPLC chromatogram of the first sample, which had previously met engine test specifications, resulted in four well-defined peaks (Fig. 1a). All of these peaks were identifiable by their mass spectra. The first chromatographic peak (designated A in Fig. 1a) represented the base oil in which the sulfurized alkylphenol was dissolved during the manufacturing process. The second peak (B) contained several components, mainly dodecylchlorophenol **1** along with some dodecylhydroxylphenyl didodecylhydroxylphenyl sulfide **2** and dodecylhydroxyphenyl dodecylchlorohydroxyphenyl sulfide **3**, all of which were apparently minor side products. The third peak (C) was identified solely as the desired major product, di(dodecylhydroxyphenyl) sulfide **4**. Finally, the last peak (D) was determined to be di(dodecylhydroxyphenyl) disulfide **5**.

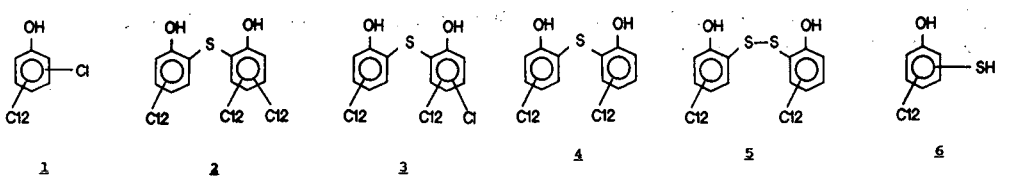

1 2 3 4 5 6

The mass spectra of these compounds are shown in Fig. 3 and 4. The dodecylchlorophenol **1** and its isomers volatilized more readily from the other components in the HPLC fraction representing peak B, and therefore produced a relatively clean mass spectrum, as shown in Fig. 3a. The molecular ion, *m/z* 296, and the major fragment ions, *m/z* 141, 155, 169 and 183, resulting from the losses on the dodecyl chain, were the major ions observed. The corresponding chlorine isotope peaks were also observed at the expected intensities. Since compounds **2** and **3** simultaneously

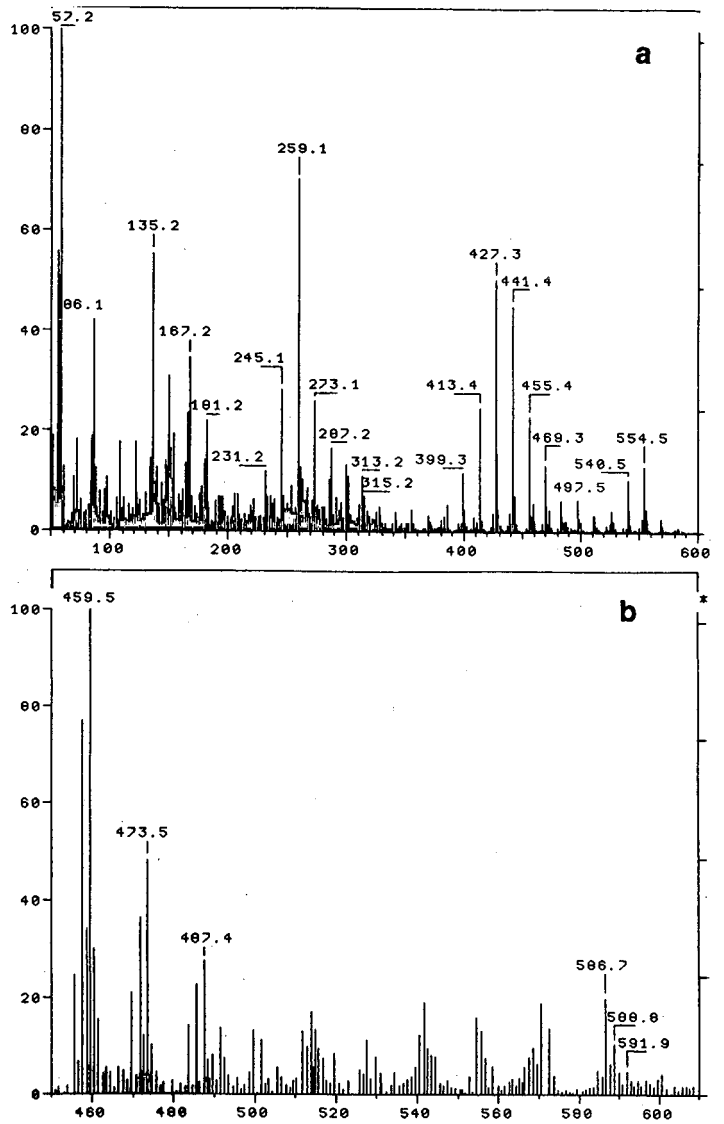

Fig. 4. (a) Mass spectra of di(dodecylhydroxyphenyl) sulfide **4** (peak C in fig. 1b) and di(dodecylhydroxyphenyl) disulfide **5** (peak D in fig. 1b).

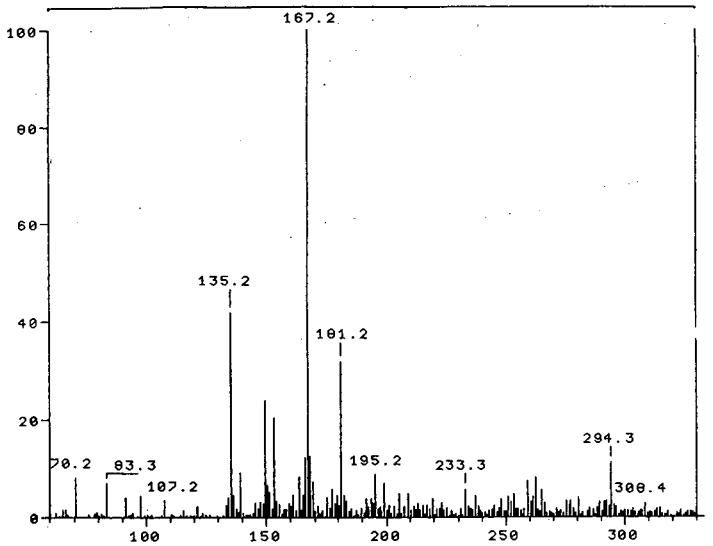

Fig. 5. Mass spectrum of dodecylmercaptophenol **6** (peak E in Fig. 1b).

volatilized, they produced a common mass spectrum shown in Fig. 3b. Furthermore, both compounds consisted of a homologous series with a range of approximately four carbons. Homologs of compound **2** had weak molecular peaks at *m/z* 680, 694, 708 and 722. Major fragmentation peaks at *m/z* 581, 595, 609 and 623 resulted from the losses from the alkyl chain. Homologs of compound **3** had molecular ion peaks at *m/z* 574, 588 and 602 with corresponding chlorine isotope peaks. These molecules had major fragmentation ions at *m/z* 279, 293, 307, 321, 461, 475 and 489. The mass spectrum in Fig. 4a represents di(dodecylhydroxyphenyl) sulfide **4**. It had homologous molecular ions at *m/z* 526, 540, 554 and 568. Fragmentation produced major ions at *m/z* 245, 259, 273, 413, 427 and 441. The corresponding disulfide **5** had a molecular ion at *m/z* 586 and fragment ions at *m/z* 459, 473 and 487, as shown in Fig. 4b.

The second sample, which had failed the engine test, contained six well-defined HPLC chromatographic peaks (see Fig. 1b). The first four peaks had the same retention times and mass spectra as the first sample, differing only in intensities. The fifth HPLC fraction, representing peak E in Fig. 5, was identified by its mass spectrum to be dodecylmercaptophenol **6**. It had a molecular ion peak at *m/z* 294 and corresponding fragment peaks at *m/z* 153, 167, 181 and 195 from losses along the alkyl chain. The last peak (F) was not identified.

CONCLUSIONS

The coupling of HPLC procedures with both ELSD and MS provided excellent results in the analysis of sulfurized dodecylphenols in oil. ELSD provided highly resolved peaks and was capable of operating with multiple solvent gradients and free from ambient temperature effects unlike other conventional HPLC detection meth-

ods. Complementary mass spectral identification demonstrated its effectiveness in characterization of the sample components. This HPLC–ELSD method was rapid and successful in monitoring the quality of sulfurized alkylphenols prior to producing the final detergent product.

REFERENCES

1 A. R. Sabol, E. W. Blaba and C. G. Brannen, *US Pat.*, 3 609 076 (1971).
2 R. W. Watson, E. E. Richardson and A. R. Sabol, *US Pat.*, 3 492 230 (1970),
3 J. M. King and N. Bakker, *US Pat.*, 3 932 289 (1976).
4 J. J. Valcho, F. J. Slama, J. S. Strukl and C. M. Park, *US Pat.*, 4 614 602 (1986).
5 N. Benfaremo and C. S. Liu, *Lubrication*, 76 (1990) 1.
6 A. D. Abbott and N. L. Allphin, *US Pat.*, 3 367 867 (1968).
7 L. C. Rogers and M. W. Hunt, *US Pat.*, 3 718 589 (1973).
8 R. L. Sung, H. Chafetz, B. H. Zoeleski and W. D. Foucher, *US Pat.*, 3 969 235 (1976).
9 V. C. E. Burnop, *US Pat.*, 4 104 180 (1978).
10 M. Kudoh, H. Ozawa, S. Fudano and K. Tsuji, *J. Chromatogr.*, 287 (1984) 337.
11 H. R. Menez and C. L. Perez, *J. High Resol. Chromatogr.*, 12 (1989) 562.
12 G. R. Bear, C. W. Lawley and R. M. Riddle, *J. Chromatogr.*, 302 (1984) 65.
13 G. R. Bear, *J. Chromatogr.*, 371 (1986) 387.
14 R. J. Hwang and M. Stauffer, *J. Liq. Chromatogr.*, 10(4) (1987) 601.
15 D. R. Zornes, G. P. Willhite and M. J. Michnick, *Soc. Pet. Eng. J.*, 18(3) (1978) 207.
16 P. L. Desbene, B. Desmazieres, J. J. Basselier and L. Minssieux, *Chromatographia*, 24 (1987) 588.
17 B. F. Nilsson and O. Samuelson, *J. Chromatogr.*, 198 (1980) 267.
18 S. V. Monin, A. Y. Levin, L. O. Kogan and A. R. Lipshteyn, *Khim. Tekhnol. Topl. Masel*, 5 (1986) 30.
19 A. A. Polyakova, L. O. Kogan, G. V. Vasilenko, L. G. Nekhamkina, G. B. Belan, Y. D. Muchinskiy, M. S. Khots and R. N. Semanyuk, *Tr.-Mezhdunar. Kongr. Poverkhn.-Akt. Veshchestvam, 7th Meeting*, 1 (1977) 450.
20 A. Stolywo, H. Colin and G. Guiochon, *J. Chromatogr.*, 265 (1983) 1.
21 A. Stolywo, H. Colin and G. Guiochon, *J. Chromatogr.*, 57 (1985) 1342.
22 T. H. Mourey, *J. Chromatogr.*, 357 (1986) 101.
23 K. D. Bartle, M. J. Mulligan, N. Taylor, T. G. Martin and C. E. Snape, *Fuel*, 63 (1984) 1556.
24 S. Coulombe, *J. Chromatogr. Sci.*, 26 (1988) 1.
25 G. R. Bear, *J. Chromatogr.*, 459 (1988) 91.
26 E. Smolkova-Keulemansova, *J. Chromatogr.*, 251 (1982) 17.
27 H. J. Issaq, *J. Liq. Chromatogr.*, 11 (1988) 2131.
28 E. Smolkova-Keulemansova, *J. Chromatogr.*, 184 (1980) 347.
29 D. W. Armstrong, *US Pat.*, 4 539 399 (1985).
30 *Cyclobond Handbook —A Guide to Using Cyclodextrin Bonded Phases*, Astec Inc., Whippany, NJ, 1987.

Journal of Chromatography, 549 (1991) 257–264
Elsevier Science Publishers B.V., Amsterdam

CHROM. 23 336

Simultaneous analysis of anions and cations by single-column ion chromatography

RAAIDAH SAARI-NORDHAUS* and JAMES M. ANDERSON, Jr.
Alltech Associates Inc., 2051 Waukegan Road, Deerfield, IL 60015 (USA)
(First received January 14th, 1991; revised manuscript received March 26th, 1991)

ABSTRACT

A new technique for the simultaneous analysis of anions and cations is described. The technique involves the use of the existing single column ion chromatography equipment with the addition of a switching valve. An anion and a cation column are used as the separator column. Three eluents are developed to allow simultaneous separation of anions and monovalent cations or anions and divalent cations. A simultaneous analysis of anions such as fluoride, chloride, nitrite, bromide, nitrate, phosphate, sulfate, and cations such as sodium, ammonium, potassium, rubidium, magnesium, calcium, and barium can be accomplished in approximately 20 to 30 min depending on the number of ions present in the sample. The detection limits for most ions are less than 500 μg/l.

INTRODUCTION

Ion chromatography, as originally developed by Small *et al.* [1], has been used extensively in many laboratories for the determination of inorganic anions and cations. The majority of the anion and cation analyses have been performed using separate columns and eluents. Recently, the simultaneous analysis of both anions and cations has been explored. One technique uses a dual channel instrument with two different eluents, injectors, columns, and detectors [2]. A single injection, with dual columns and a single detector on a dual channel instrument, has also been used [3]. Another technique utilizes one injector, one eluent, several columns (anion, cation and an anion suppressor column) and two detectors connected in various configurations [4,5]. This enables the detectors to independently monitor the anions and cations as they elute from the respective columns.

A single column approach for the simultaneous analysis of anions and cations has also been used. One technique uses a complexing agent as the eluent [6,7]. Using this method, metal ions are converted into anionic complexes and are separated along with the other inorganic anions on an anion separator column. Another technique uses a mixed bed ion-exchange column. Pietrzyk and Brown [8] used a column containing alumina and silica microparticles. At the eluent pH used, alumina provides anion-exchange sites and silica provides cation-exchange sites, thus allowing simultaneous separation of anions and cations. A mixed bed ion-exchange column contain-

0021-9673/91/$03.50

ing polystyrene divinyl benzene resin with quaternary amine and sulfonic acid functionalities has also been used [9]. By using an eluent that contains both anion and cation eluting ions, the simultaneous separation of inorganic anions and cations can be performed with one injection, one pump, one column and one detector. The advantage of this approach is that the analysis can be accomplished using existing single-column ion chromatography (SCIC) systems without the need for additional equipment. However, experiments in our laboratory indicated that one major problem with this technique is the difficulty in manufacturing a reproducible column when a new batch of material is used. The ion-exchange capacity of the anion and cation exchangers varies from batch to batch. Therefore, the ratio of the anion to the cation exchanger has to be modified each time a new batch of material is used.

The technique presented here uses one injection, one pump, an anion column, a cation column, a switching valve, and a conductivity detector. The configuration of the system is shown in Fig. 1. By changing the eluent composition, the simultaneous analysis of anions and monovalent cation, or anions and divalent cations can be achieved.

EXPERIMENTAL

The ion chromatograph used in this work was an Alltech/Wescan metal-free ion chromatography system (Alltech, Deerfield, IL, USA). It consists of an Alltech

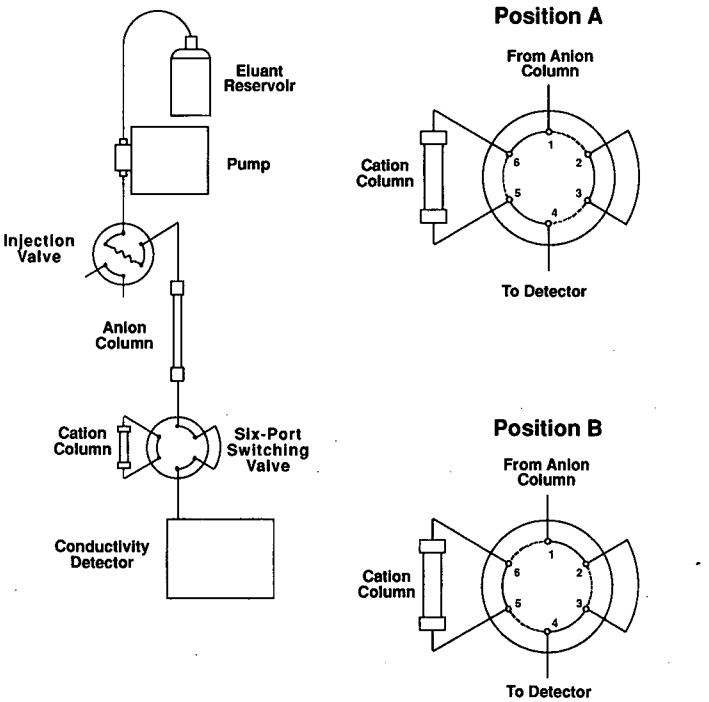

Fig. 1. Instrument configuration for the simultaneous analysis of anions and cations. At position A, the eluent is passed through both anion and cation columns. At position B, the cation column is bypassed.

Model 325 metal-free pump, a Rheodyne 9125 metal-free injection valve(100-μl sample loop), a Alltech Model 320 conductivity detector, and a Timberline column heater. The temperature of the column heater and the conductivity detector cell was maintained at 35°C. A Rheodyne Model 9000 metal-free switching valve combined with the Alltech universal valve actuator was used to direct the eluent flow through or around the cation separator column. All data were recorded on a Spectra-Physics (Santa Clara, CA, USA) SP 4400 Chromjet integrator. The Alltech Universal Anion Column (150 × 4.6 mm I.D.) and the Wescan Cation/R Column (100 × 3.2 mm I.D.) were used as the separator columns.

Reagents

Only reagent-grade chemicals (Aldrich, Milwaukee, WI, USA) were used for standard and eluent preparations.

Three different eluents were used: lithium *p*-hydroxybenzoate, lithium hydrogenphthalate, and lithium hydrogenphthalate–ethylenediamine combination. Stock solutions of *p*-hydroxybenzoic acid (pHBA) (100 m*M*) and phthalic acid (100 m*M*) were prepared by dissolving the ACS-reagent-grade chemicals in methanol. Lithium *p*-hydroxybenzoate eluent was prepared by diluting the stock solution to 5 m*M* and adjusting to pH 7.8 with lithium hydroxide. Lithium hydrogenphthalate eluent was prepared by diluting the stock solution to 4 m*M* and adjusting to pH 4.5 with lithium hydroxide. Lithium hydrogenphthalate–ethylenediamine eluent was prepared by diluting the stock solution to 4 m*M*, adding concentrated solution of ethylenediamine to make 1 m*M* ethylenediamine solution, and adjusting the pH to 4.5 with lithium hydroxide.

Procedure

Fig. 1 shows the system configuration. This technique involves three steps. Step 1, at position A where the eluent is passed through both anion and cation columns, a sample is injected. Since cations are not retained on the anion column, they will rapidly pass through the anion column. Step 2, once the cations reach the inlet of the cation column, the valve is switched to position B, where the cation column is bypassed, trapping the sample cations at the inlet of the cation column. All the anions are separated and detected by the conductivity detector. Step 3, when all the anions have eluted from the anion column, the valve is switched back to position A to separate the cations that are retained on the inlet of the cation column.

The timing of step 2 is very important. If the valve is switched too early, the cations may not reach the cation column. The cations that do not reach the cation column will not be separated and pass rapidly through the anion column in the void volume. If the timing is delayed too long, the cations may be separated on the cation column and eluted along with the other anions. This may cause peak overlapping (anion and cation) and inaccurate results. The exact time to switch the valve in step 2 can be determined easily by injecting an anion standard on an anion column (the cation column is bypassed, or both the cation column and the switching valve may be removed from the system). Since cations are not retained on the anion column, they will pass rapidly through the anion column in the column void volume along with other non-retained components. The first peak (solvent peak) on a chromatogram is attributed to these non-retained components. The retention time at which the solvent

peak returns to baseline is used as the exact time to switch the valve from position A to position B. The timing for step 3 is not as critical as step 2. The valve may be switched at any time after all the anions are eluted from the anion column. The retention time for the cations (and the whole analysis time) is dependent on the timing of step 3. If the valve is switched immediately after all the anions are eluted, the retention times for the cations (and the whole analysis time) will be shorter. If it is delayed, the retention times and the whole analysis time will be longer. The switching valve may be operated manually, or once the proper timing is determined, an electronically actuated switching valve and data system may be used.

RESULTS AND DISCUSSION

The goal of this work was to develop a simple method for simultaneous separation of anions and cations using existing SCIC equipment. Since using a mixed-bed column is unreliable due to the poor column to column reproducibility, separate anion and cation columns were used. A switching valve was added to the system to direct flow of the eluent.

Three eluents were developed to separate anions and monovalent cations, and anions and divalent cations. Fig. 2 shows the chromatograms of the anion and cation standards using these eluents. By using 5 m*M* lithium *p*-hydroxybenzoate, pH 7.8, fluoride, chloride, nitrite, bromide, nitrate, phosphate, sulfate, sodium and potassium are separated and detected simultaneously. The valve is switched from position A to position B at 1 min 50 s and switched back to position A after all the anions are eluted from the column. *p*-Hydroxybenzoate was chosen as the eluent for anions because it is one of the most useful eluents in SCIC. It has lower equivalent conductance than most inorganic anions and is capable of eluting both monovalent and divalent anions in one run. Lithium was chosen as the cation eluent because its selectivity for the resin is close to that of sodium, ammonium and potassium. Also, lithium is not commonly found in most samples. Due to the pH of the eluent, ammonia exist in the molecular (neutral) form and was not retained on the cation column or detected by the conduc-

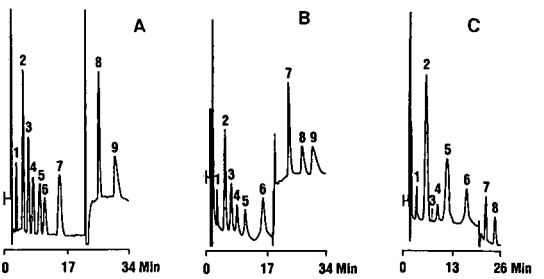

Fig. 2. Chromatograms of standard ions using various eluents. (A) 5 m*M* lithium *p*-hydroxybenzoate, pH 7.8; peaks: 1 = fluoride; 2 = chloride; 3 = nitrite; 4 = bromide; 5 = nitrate; 6 = phosphate; 7 = sulfate; 8 = sodium; 9 = potassium. (B) 4 m*M* lithium hydrogenphthalate, pH 4.5; peaks: 1–5 as in (A); 6 = sulfate; 7 = sodium; 8 = ammonium; 9 = potassium. (C) 4 m*M* lithium hydrogenphthalate–1 m*M* ethylenediamine, pH 4.5; peaks: 1–5 as in (A); 6 = sulfate; 7 = magnesium; 8 = calcium. Column: Alltech Universal Anion Column (150 × 4.6 mm I.D.) and Wescan Cation/R column (100 × 3.2 mm I.D.). Eluent flow-rate: 1.0 ml/min. Detector: conductivity.

tivity detector. Since ammonium is not detected, it is possible to detect sodium and potassium ions in the presence of high concentrations of ammonium.

In order to determine ammonium simultaneously with the anions, another eluent, 4 m*M* lithium hydrogenphthalate, pH 4.5 was developed. At pH 4.5, all the ammonia present is in the ammonium form, with the necessary charge for retention on the cation column and detection by the conductivity detector. Using this eluent, fluoride, chloride, nitrite, bromide, nitrate, sulfate, sodium, ammonium and potassium can be analyzed simultaneously, as shown in Fig. 2. The valve is switched from position A to position B at 2 min 10 s and switched back to position A after all the anions are eluted from the anion column. Like pHBA, phthalate was chosen because of its low equivalent conductance and is capable of eluting both monovalent and divalent anions in one run. Since the pH of the eluent is low, phosphate is eluted in the column void volume (solvent peak).

Since lithium is a monovalent cation, it is capable of eluting monovalent cations only at the concentration used in these eluents. To analyze anions and divalent cations, a lithium hydrogenphthalate–ethylenediamine combination was developed. Ethylenediamine was chosen as the eluent for cations because it is a commonly used eluent for separating divalent cations in SCIC [10]. Phthalate is the eluent for anions. Lithium hydroxide was added to bring the pH of the eluent to 4.5 since phthalic acid, pH 4.5 is the commonly used eluent for separating anions on the anion column used for this study. Since the equivalent conductance for magnesium and calcium are lower than the equivalent conductance of ethylenediamine, the peaks are detected as negative peaks (decrease in conductance). The polarity of the detector is reversed after the valve is switched in step 3 to make the magnesium and calcium peaks positive. By using this eluent, fluoride, chloride, nitrite, bromide, nitrate, sulfate, magnesium and calcium can be analyzed simultaneously as shown in Fig. 2C. The valve is switched from position A to position B at 2.00 min and is switched back to position A after all the anions are eluted from the anion column. At the same time, the polarity of the detector is reversed.

The position of the anion and cation columns may be reversed. As shown in Fig. 3, the cations are eluted first if the cation column is placed before the anion column. In this analysis, the valve is switched from position A to position B at 1 min 30 s.

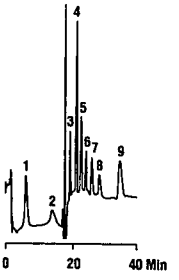

Fig. 3. Chromatogram of standard ions using lithium *p*-hydroxybenzoate after the position of the anion and cation columns is reversed. Other chromatographic conditions are shown in Fig. 2. Peaks: 1 = sodium; 2 = potassium; 3 = fluoride; 4 = chloride; 5 = nitrite; 6 = bromide; 7 = nitrate; 8 = phosphate; 9 = sulfate.

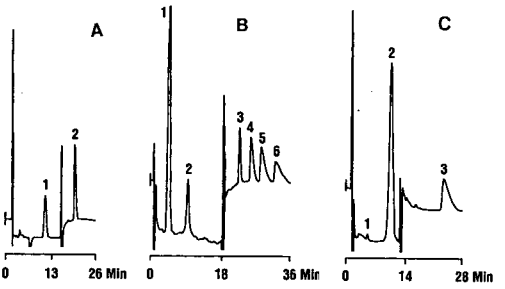

Fig. 4. Simultaneous separations of anions and cations. (A) Pharmaceutical pentapeptide sample using lithium *p*-hydroxybenzoate eluent; peaks: 1 = phosphate; 2 = sodium. (B) Working standard containing rubidium ion using lithium hydrogen phthalate eluent; peaks: 1 = chloride; 2 = nitrate; 3 = sodium; 4 = ammonium; 5 = potassium; 6 = rubidium. (C) Barium nitrate solution using lithium hydrogenphthalate–ethylenediamine eluent; peaks: 1 = chloride; 2 = nitrate; 3 = barium. Other chromatographic conditions are shown in Fig. 2.

Fig. 4 shows the separation of a pharmaceutical sample (pentapeptide) and standard solutions containing additional ions. In addition to the common inorganic anions and cations, the determination of rubidium and barium are also possible as shown in Fig. 4B and C, respectively.

A slight baseline shift occurs when the cation column is switched in and out of the flow data. This baseline shift may be due to differences in the distribution coefficient for the eluent components on the anion and cation stationary phases [11]. When the cation column is bypassed, an ion-exchange equilibrium is established between the anion driving ion (*p*-hydroxybenzoate or phthalate) and the anion exchanger. When the valve is switched, a second equilibrium is established between the cation driving ion (lithium and/or ethylenediamine) and the cation exchanger, thus, a baseline shift results. However, this shift does not adversely effect the linearity or precision of this method. Linear regression analyses and simple correlation coefficients of the calibration plots of peak area against ionic concentration for sodium nitrate using lithium hydrogen phthalate eluent are listed in Table I. These results are comparable to the well known analysis of anions and cations using separate columns and eluents.

A standard solution containing various anions and cations was analyzed to determine the reproducibility of the method using one of the eluents developed. Table

TABLE I

LINEAR REGRESSION ANALYSES AND SIMPLE CORRELATION COEFFICIENTS OF THE SODIUM NITRATE CALIBRATION PLOTS

Lithium hydrogenphthalate was used as eluent.

Ions	Regression equation[a]	Correlation coefficient (r)
Nitrate	$y = -0.024 + 0.011 C_{\text{Nitrate}}$	0.998
Sodium	$y = -0.005 + 0.010\ C_{\text{Sodium}}$	0.999

[a] y represents the peak area and C represents the concentration of ions (ppm).

TABLE II

REPRODUCIBILITY OF THE SIMULTANEOUS SYSTEM USING LITHIUM HYDROGENPHOSPHATE ELUENT

Ions	Concentration (ppm)	R.S.D. (%)[a]
Fluoride	10	2.27
Chloride	20	0.76
Nitrite	20	1.58
Bromide	20	1.46
Nitrate	20	0.89
Sulfate	30	1.24
Sodium	45	0.38
Ammonium	5	1.16
Potassium	19	2.00

[a] Relative standard deviation, $n = 9$.

II lists the relative standard deviations (R.S.D.) (%) for nine replicate injections using lithium hydrogenphthalate eluent. The R.S.D. ranged from 0.38 to 2.27%. This is comparable to SCIC analysis of anions and cations using separate columns and eluents.

The detection limits for various ions (expressed as minimum detectable concentration) with the three eluents developed in this study are shown in Table III. The numbers were obtained based on a 100 μl injection volume and were calculated as a threefold signal-to-noise ratio at the baseline ($S/N = 3$). The detection limits for most ions are less than 0.5 ppm.

Since the valve can be switched from position B back to position A immediately after all the anions are eluted from the anion column, this technique allows the analyst to minimize the run time depending on the nature of the sample. For example, if the sample contains only chloride and sodium, the valve may be switched from

TABLE III

DETECTION LIMITS WITH VARIOUS ELUENTS

Ions	Lithium *p*-hydroxybenzoate (ppm)	Lithium hydrogenphthalate (ppm)	Lithium hydrogenphthalate–ethylenediamine (ppm)
Fluoride	0.15	0.12	0.17
Chloride	0.12	0.17	0.16
Nitrite	0.14	0.15	0.16
Bromide	0.43	0.40	0.54
Nitrate	0.40	0.40	0.41
Phosphate	1.50	–	–
Sulfate	0.67	0.96	1.04
Sodium	0.38	0.25	–
Ammonium	–	0.12	–
Potassium	0.40	0.36	–
Magnesium	–	–	0.13
Calcium	–	–	0.30

position B to position A after the chloride peak and the total run time will be reduced from 25 min to approximately 10 min.

The main area of application of this technique will be the analysis of water samples [rain water, tap water, ground water, well water, and seawater (brine)], pharmaceutical samples, food products, and any other matrix where information on the anionic and cationic fractions of the sample are required. Instead of performing two chromatographic analyses using two different eluents, this technique offers a simpler and faster method for the simultaneous determination of anions and cations.

CONCLUSIONS

The system described here simplifies the simultaneous determination of anions and cations, requiring only conventional IC equipment with the addition of a switching valve. Various ions can be determined in 20 to 30 minutes depending on the number of ions present in the sample. Using lithium *p*-hydroxybenzoate eluent, fluoride, chloride, nitrite, bromide, nitrate, phosphate, sulfate, sodium and potassium can be analyzed simultaneously. Since ammonium is not detected, it is also possible to detect sodium and potassium ions in the presence of high concentrations of ammonium. Fluoride, chloride, nitrite, bromide, nitrate, sulfate, sodium, ammonium and potassium can be analyzed using lithium hydrogen phthalate eluent. Lithium hydrogenphthalate–ethylenediamine eluent allows for the determination of anions (fluoride, chloride, nitrite, bromide, nitrate and sulfate) and divalent cations (magnesium, calcium and barium). This technique allows the analyst to minimize the run time depending on the nature of the sample.

REFERENCES

1 H. Small, T. S. Stevens and W. C. Baumann, *Anal. Chem.*, 47 (1975) 1801.
2 J. S. Fritz, D. T. Gjerde and C. Pohlandt, *Ion Chromatography*, Hüthig, New York, 1982, Ch. 5.
3 N. P. Barkley, G. L. Contner, M. Malanchuk, in J. D. Mulik and E. Sawicki (Editors), *Ion Chromatographic Analysis of Environmental Pollutants*, Vol. 2, Ann Arbor Sci. Publ., Ann Arbor, MI, 1979, p. 115.
4 V. K. Jones and J. G. Tarter, *J. Chromatogr.*, 312 (1984) 456.
5 V. K. Jones, S. A. Frost and J. G. Tarter, *J. Chromatogr. Sci.*, 23 (1985) 442.
6 M. Yamamoto, H. Yamamoto and Y. Yamamoto, *Anal. Chem.*, 56 (1984) 832.
7 S. Matsushita, *J. Chromatogr.*, 312 (1984) 327.
8 D. J. Pietrzyk and D. M. Brown, *J. Chromatogr.*, 466 (1989) 291.
9 D. J. Pietrzyk and D. M. Brown, *Anal. Chem.*, 58 (1986) 2254.
10 D. T. Gjerde and J. S. Fritz, *Ion Chromatography*, Hüthig, New York, 2nd ed., 1987, Ch. 9.
11 D. T. Gjerde and J. S. Fritz, *Ion Chromatography*, Hüthig, New York, 2nd ed., 1987, Ch. 4.

Journal of Chromatography, 549 (1991) 265–272
Elsevier Science Publishers B.V., Amsterdam

CHROM. 23 305

Ion chromatography of inorganic iodine species using C_{18} reversed-phase columns coated with cetyltrimethylammonium

KAZUAKI ITO*, EIJI SHOTO and HIROSHI SUNAHARA

Department of Environmental Science, Faculty of Engineering, Hiroshima Univeristy, 1-4-1 Kagamiyama, Higashi-Hiroshima 724 (Japan)

(First received November 13th, 1990; revised manuscript received March 5th, 1991)

ABSTRACT

Low-capacity anion-exchange columns were developed by sorption of cetyltrimethylammonium on two types of C_{18} reversed-phase columns which were coated with 1 m*M* cetyltrimethylammonium in water–methanol mixtures (57:43, v/v, to 45:55, v/v) at 20°C. The exchange capacities of the columns were estimated by three methods. The high separation efficiency for anions was performed by using a 0.1 *M* sodium chloride–5 m*M* sodium phosphate buffer (pH 5.8) as mobile phase. An ion chromatographic system for iodide consisted of the column (polymer-coated silica packing) coated with 1 m*M* cetyltrimethylammonium in water–methanol (56:44%, v/v), the sodium chloride mobile phase, and ultraviolet or amperometric detection. Good chromatograms for iodide in surface sea waters were obtained without interference by an excess of salts.

INTRODUCTION

Anion separation has been carried out by using low-capacity anion-exchange columns [1–4] and reversed-phase columns [5–15]. For the latter, some alkylammoniums have been added to mobile phases [6,13–15] or coating solutions [8–12]. For the preparation of coated columns, long-chain quaternary ammoniums such as cetyltrimethylammonium (CTA^+) have been employed [8–12]. The coated columns have a wide applicability for anion determination, because anion-exchange capacities can be controlled by using various coating conditions for practical purposes. However, this technique and its advantage have rarely been applied to real samples.

Direct determination of trace-level nitrite and nitrate in sea water by use of coated column has previously been reported by the authors [11]. The ion chromatographic system employed consisted of C_{18}-silica (silicone-coated packing material) columns coated with CTA^+ which had higher exchange capacity, 0.1 *M* sodium chloride–5 m*M* sodium phosphate (sodium hydrogenphosphate–sodium dihydrogenphosphate) buffer (pH 5.8) as mobile phase, and UV or amperometric (AMP) detection. The interference of an excess of Cl^- in sea water could be removed by use of a high concentration of sodium chloride in the mobile phase because there was no retention of Cl^- on the column in the Cl^- form. Further, the mobile phase stabilized

0021-9673/91/$03.50

the retention of CTA^+ on the column and did not disturb UV and AMP detection. This system (mobile phase, detection method) was also applied to direct determination of iodide in sea water using a low-capacity anion-exchange column [3,4]. However, the coated columns with high capacity could not be applied to sensitive detection of iodide because of a larger retention volume.

The separation of iodide on C_{18} reversed-phase columns has been achieved using the mobile phases acetonitrile–2 m*M* tetrabutylammonium hydroxide–40 m*M* phosphate buffer (pH 6.0) (5.0:47.5:47.5) [13] and 0.01 *M* octylamine adjusted to pH 6.2 with orthophosphoric acid [14]. The column coated with tridodecylmethylammonium and the mobile phase 0.2 *M* sodium dihydrogenphosphate–0.039 *M* sodium phosphate (pH 6.4) was also effective [12].

In this study, the column efficiency of the coated columns with low capacity, which were coated with methanol-rich solutions of 1 m*M* CTA^+, by the use of 0.1 *M* sodium chloride mobile phase was investigated in order to extend the usefulness of the coated columns. The results were compared with the previous results obtained by using a conventional ion chromatography column [3,4]. Further, the system was applied to detection of iodine species (I^- and $I^- + IO_3^-$; IO_3^- was reduced to I^- [16,17]) in sea water.

EXPERIMENTAL

Apparatus

The ion chromatographic system employed in this study was identical to that described previously [11]: (a) a Tosoh Model CCPM pump; (b) a Rheodyne 7125 injector (100-μl sample loop); (c) a Hitachi Model L-4200 UV detector; Yanagimoto Models VMD-101A and P-1000 amperometric (AMP) detectors using a glassy carbon working electrode; (d) a Tosoh CP-8000 chromatoprocessor.

Column

Two types of C_{18} reversed-phase columns were Capcellpak C_{18} (Shiseido, 150 × 4.6 mm I.D., particle size 5 μm, octadecyl-bonded silica gel coated with silicone polymer [18,19] and TSKgel ODS-80T_M (Tosoh, 150 × 4.6 mm I.D., particle size 5 μm, octadecyl-bonded silica gel). The columns were equilibrated with 1 m*M* cetyltrimethylammonium chloride (CTAC, used as received) in various water–methanol mixtures [methanol concentration 43–55% (v/v), HPLC grade] at 20 ± 0.05°C. The solutions were pumped through the columns at a flow-rate of 0.5 ml/min. The methods for (a) determination of completion of the column coating and (b) determination of amount of sorbed CTA^+ were identical to those described previously [11]. After washing with water, the columns were used for the separation of inorganic anions. The mobile phase used was 0.1 *M* sodium chloride–5 m*M* sodium phosphate buffer (pH 5.8) and the flow-rate was maintained at 1.0 ml/min. Separations and measurements were carried out at room temperature (*ca.* 25°C).

Reagent

All inorganic salts were of analytical reagent grade. Inorganic sodium salts were used for the preparation of stock solutions of each anion (10–50 g/l) and the mobile phase (0.1 *M* sodium chloride). Artificial sea waters (salinity 0–45‰) were prepared

according to the Lyman–Fleming formula [20]. All solutions were prepared in distilled, deionized water and filtered through a 0.45-μm membrane filter before use.

Analysis of iodine species in sea water

For iodide, surface sea waters of the Seto Inland Sea, which were sampled near Hiroshima City, were filtered through a 0.45-μm membrane filter within 24 h of collection, pretreated by passage through a Sep-Pak C_{18} cartridge (Waters Assoc.), and directly injected [UV (226 nm) and AMP (+1.0 V *vs.* Ag/AgCl) detection]. For total inorganic iodine (I^- + IO_3^-), 0.02 *M* ascorbic acid (0.25 ml) and 3 *M* acetic acid (0.25 ml) were added to the samples (24.5 ml) for reduction of iodate to iodide. The samples, which were shaken for 2 min, were injected (UV detection). The iodide and total iodine were determined from the peak area with reference to calibration standards (35‰ artificial sea water) and its solutions containing the reductants, respectively.

RESULTS AND DISCUSSION

Preparation of columns with low capacity

The amounts of sorbed CTA^+ on two C_{18} reversed-phase columns, Capcellpak C_{18} and TSKgel ODS-80T_M, could be easily controlled by the addition of methanol in 1 m*M* CTAC coating solutions. Fig. 1 shows the variation of the amount of sorbed CTA^+ with methanol concentration (40–55%, v/v) in coating solutions. The amount of sorbed CTA^+ decreased rapidly with increasing amount of methanol. The anion-exchange capacities of the coated columns with 43 and 45% (v/v) methanol were estimated by three methods: (1) the amount of sorbed CTA^+; (2) the determination of nitrate onto anion-exchange sites; (3) the breakthrough volume of salicylate [11]. The results are summarized in Table I. They indicate that the sorbed CTA^+ almost works

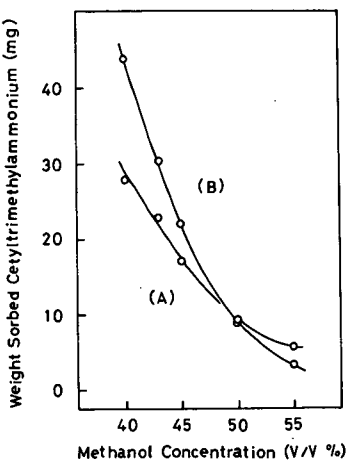

Fig. 1. Variation of amount of sorbed cetyltrimethylammonium with concentration of methanol in coating solution. C_{18} reversed-phase column: (A) Capcellpak C_{18} and (B) TSKgel ODS-80T_M. Coating conditions are given in the Experimental section.

TABLE I

ANION-EXCHANGE CAPACITIES OF COLUMNS COATED WITH CTA^+

Solution water–methanol (%, v/v)	Column	Exchange capacity (mequiv. per column)		
		CTA^+ sorbed	Salicylate	Nitrate
57:43	Capcellpak C_{18}[a]	0.073	0.068	0.059
	TSKgel ODS-80T_M[a]	0.098	0.083	0.088
55:45	Capcellpak C_{18}	0.059	0.050	0.046
	TSKgel ODS-80T_M	0.077	0.068	0.065
–	TSKgel IC-Anion-PW[b]	–	–	0.066

[a] The columns were coated with 1 m*M* CTAC in water–methanol mixtures at 20°C.
[b] The supplier's value was 0.07 mequiv. per column.

as an anion-exchange site and the anion-exchange capacities are similar to a conventional IC column, TSKgel IC-Anion-PW.

Separation of iodide

Fig. 2 shows the corrected retention volumes of seven inorganic anions on two columns coated with methanol-rich solutions. The anions (1 mg/l each) were separated by using a mobile phase of 0.1 *M* sodium chloride–5 m*M* sodium phosphate buffer (pH 5.8). The same results as regards retention volumes were also obtained using other columns. Sodium chloride in the mobile phase at a concentration of 0.1 *M*

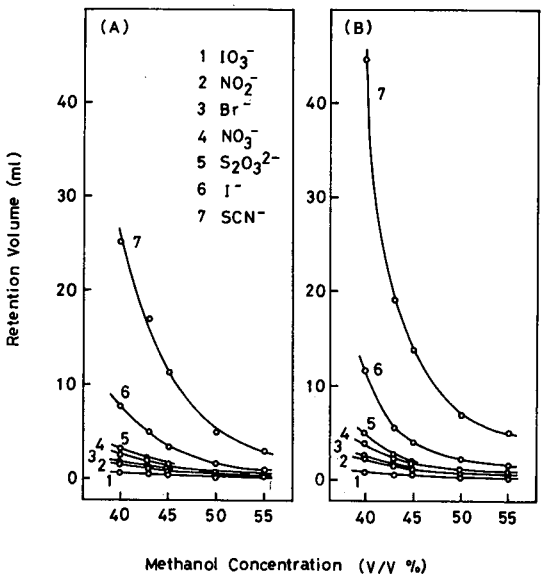

Fig. 2. Variation of retention volume of inorganic anions with concentration of methanol in coating solution. Conditions: column, (A) Capcellpak C_{18} and (B) TSKgel ODS-80T_M; mobile phase, 0.1 *M* sodium chloride–5 m*M* sodium phosphate buffer (pH 5.8).

stabilized the sorbed CTA^+, probably because of the reduction of ionic repulsion among CTA^+s and enhancement of hydrophobic interactions of CTA^+s with octadecyl groups [11]. In this study, the retention volumes of anions on columns coated with 44% methanol were constant for a successive flow (30 h; flow-rate of 1.0 ml/min), and the coated column (Capcellpak C_{18}) could be used for a series of studies without coating (2 weeks).

For both columns the retention volume of each anion decreased with increasing methanol concentration, *i.e.* decreasing the amount of sorbed CTA^+. The retention volumes of anions on Capcellpak C_{18} were small compared with those on TSKgel ODS-80T_M over the methanol concentration studied. However, the amount of sorbed CTA^+ (Capcellpak C_{18}) was similar to TSKgel ODS-80T_M for 50% methanol and larger for 55% methanol (Fig. 1). For 40–45% (v/v) methanol, iodide was well separated from hydrophilic anions (iodate, nitrite, bromide, nitrate and thiosulfate) and thiocyanate with lower hydration energy. Thus, it was found that the separation system (the coated column and mobile phase) for iodide is reasonable.

Fig. 3A and B show separation of inorganic anions on Capcellpak C_{18} coated with a water–methanol (56:44, v/v) solution. Good chromatograms and flat baselines were obtained by both UV (226 nm) and AMP (+1.0 V *vs.* Ag/AgCl) detection. The column which is coated with silicone polymer gains resistance to the alkaline solution (up to pH 10) [18,19] and has been already applied to the determination of nitrite and nitrate in sea water (*ca.* pH 8) [11]. The elution order of singly charged anions on the Capcellpak C_{18} was identical to that on TSKgel IC-Anion-PW [3,4]. A longer retention volume of SCN^- with lower hydration energy on Capcellpak C_{18} may be due to matrix effects such as carbon-chain length on quaternary ammonium groups and surface properties.

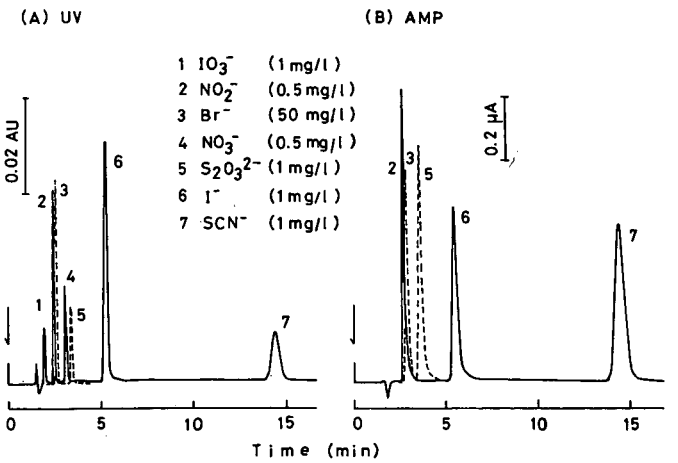

Fig. 3. Ion chromatograms of inorganic anions. Conditions: column, Capcellpak C_{18} coated with 1 m*M* CTA^+ in water–methanol (56:44%, v/v); mobile phase, 0.1 *M* sodium chloride–5 m*M* sodium phosphate buffer (pH 5.8). Detection, (A) UV = 226 nm, (B) AMP = +1.0 V (*vs.* Ag/AgCl). Flow-rate, 1.0 ml/min. Sample volume, 100 μl.

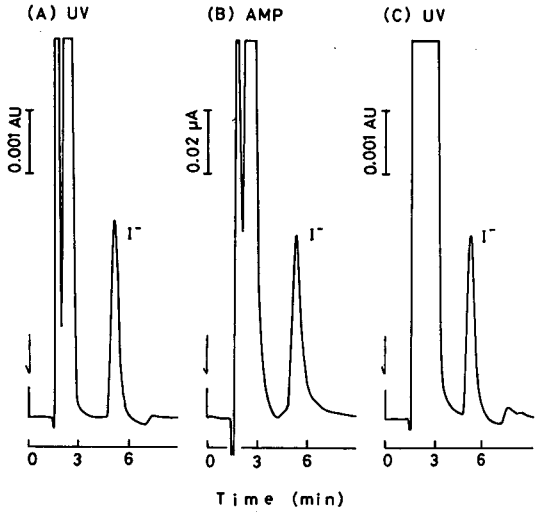

Fig. 4. Ion chromatograms of iodide (0.2 mg/l) in artificial sea water (salinity 35‰). (A) UV = 226 nm; (B) AMP = +1.0 V; (C) UV = 226 nm (iodate was reduced to iodide). Other conditions were the same as in Fig. 3.

Detection of iodine species in artificial sea water

Detection of trace-level iodine species in solutions containing an excess of salts was examined. Fig. 4A and B show ion chromatograms of iodide (0.2 mg/l) in artificial sea water (salinity 35‰) by UV and AMP methods, respectively. A good iodide peak was obtained without interference by an excess of anions; Cl^- = 17 300 mg/l, SO_4^{2-} = 2710 mg/l, HCO_3^- = 142 mg/l and Br^- = 67 mg/l.

However, the iodate peak was masked by the coexisting ions. Therefore, the optimum condition for reduction of iodate to iodide was examined by the addition of ascorbic acid and acetic acid [17] in 35‰ artificial sea water. Ascorbic acid, $2 \cdot 10^{-4}$ *M*, and 0.03 *M* acetic acid in the solution were appropriate for the completion of the reaction. Fig. 4C shows an ion chromatogram with UV detection of 0.2 mg/l IO_3^- in the artificial sea water under the reaction conditions. A good iodide peak, which was a little broad compared with Fig. 4A, was obtained. However, the peak could not be obtained by using TSKgel IC-Anion-PW, because of interference by the reductants. In the course of experiment, by the way, it was necessary to remove an AMP detector from the chromatographic system because the detector strongly responded to the reductants.

The peak heights of iodide (0.2 mg/l) in salinity 35‰ with the UV and AMP detection decreased to 45 and 50% of those in pure water, respectively. The broadness of iodide peak may be due to the self-elution of this solution and a reduction in self-diffusion of iodide in the salt solution. However, the peak areas were almost constant for eight solutions (salinity 0–45‰); the relative standard deviation (R.S.D.) was 3.8 and 3.6% with UV and AMP detection, respectively.

The calibration graphs obtained by the peak-area method for iodide (0.01–0.2 mg/l) in 35‰ artificial sea water showed downward curvatures for both methods of detection. Similar curvature was obtained in the artificial sea water containing reduc-

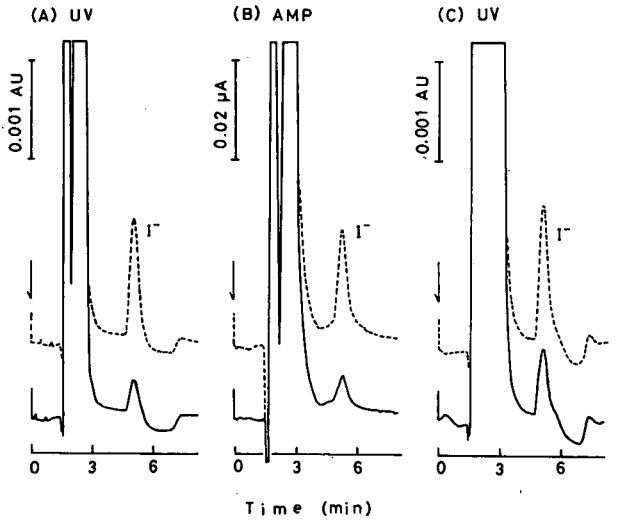

Fig. 5. Ion chromatograms of a sea water sample (Table II, No. 1). Solid lines, a real sample; dashed lines, the sample spiked with 0.05 mg/l I^- (A and B) and IO_3^- (C). (A) UV = 226 nm; (B) AMP = +1.0 V; (C) UV = 226 nm (iodate was converted to iodide). Other conditions were the same as in Fig. 3.

tants. The addition of salinity in samples was effective for the stability of baseline and reduction of peak noise. The detection limits (signal-to-noise ratio = 2) were 5 and 5 μg/l for iodide by the UV and AMP methods, respectively, and 10 μg/l for iodide (reduced from iodate) by the UV method. Thus, good reproducibility of ten replicate injections of 0.2 and 0.05 mg/l I^- in artificial sea water was obtained: the R.S.D. was 0.7% (0.2 mg/l) and 2.5% (0.05 mg/l) for UV detection, and 0.6% (0.2 mg/l) and 2.2% (0.05 mg/l) for AMP detection. For I^- (from IO_3^-) by the UV method, the R.S.D. was 0.9% (0.2 mg/l)and 2.3% (0.05 mg/l).

TABLE II

ANALYTICAL RESULTS OF I^- AND I^- + IO_3^- IN SEA WATER BY UV AND AMP DETECTION

Sample No. (Seto Inland Sea)	*n*	I^-: UV (AMP)			I^- + IO_3^-: UV		
		Added (mg/l)	Found (mg/l)	Recovery (%)	Added (mg/l)	Found (mg/l)	Recovery (%)
1	4	–	0.021 ± 0.003	–	–	0.051 ± 0.004	–
		(–)	(0.017 ± 0.004)	(–)	0.050	0.102 ± 0.003	102
		0.050	0.070 ± 0.005	98			
		(0.050)	(0.068 ± 0.003)	(102)			
2	4	–	0.025 ± 0.002	–	–	0.052 ± 0.002	–
		(–)	(0.023 ± 0.004)	(–)	0.050	0.101 ± 0.007	98
		0.050	0.078 ± 0.003	106			
		(0.050)	(0.072 ± 0.004)	(98)			

Application to iodine species in sea waters

Fig. 5 shows the ion chromatograms of a sea water sample (solid line) and the sample spiked with 0.05 mg/l I^- (Fig. 5A and B) and 0.05 mg/l IO_3^- (Fig. 5C) (dashed line). The chromatograms were in good agreement with those of artificial sea water in Fig. 4. The results obtained are summarized in Table II. Good agreement between the UV and AMP methods was obtained. Moreover, quantitative recoveries were obtained.

CONCLUSION

C_{18} reversed-phase columns coated with cetyltrimethylammonium, which have a low capacity, and a sodium chloride mobile phase were found to be effective for iodide separation as an alternative to a conventional IC column system. Dissolution of sorbed CTA^+ was not observed. A good iodide peak in sea water was obtained. Further, the columns may enable the detection of iodide and thiocyanate in concentrated salt solutions.

REFERENCES

1 H. Small, T. S. Stevens and W. C. Bauman, *Anal. Chem.*, 47 (1975) 1801.
2 O. Shpigun and Yu. A. Zolotov, *Ion Chromatography in Water Analysis*, Ellis Horwood, Chichester, 1988, p. 44.
3 K. Ito and H. Sunahara, *Bunseki Kagaku*, 37 (1988) 292.
4 K. Ito and H. Sunahara, *J. Chromatogr.*, 502 (1990) 121.
5 P. K. Dasgupta, in J. G. Tarter (Editor), *Ion Chromatography*, Marcel Dekker, New York, 1987, p. 253.
6 P. G. Rigas and D. J. Pietrzyk, *Anal. Chem.*, 58 (1986) 2226.
7 L. M. Warth and J. S. Fritz, *J. Chromatogr.*, 462 (1989) 165.
8 D. L. Duval and J. S. Fritz, *J. Chromatogr.*, 295 (1984) 89.
9 D. J. Barkley, T. E. Dahms and K. N. Villeneuve, *J. Chromatogr.*, 395 (1987) 631.
10 T. Takeuchi and E. S. Yeung, *J. Chromatogr.*, 370 (1986) 83.
11 K. Ito, Y. Ariyoshi, F. Tanabiki and H. Sunahara, *Anal. Chem.*, 63 (1991) 273.
12 R. M. Cassidy and S. Elchuk, *Anal. Chem.*, 54 (1982) 1558.
13 H. Nagashima and K. Nakamura, *J. Chromatogr.*, 324 (1985) 498.
14 N. E. Skelly, *Anal. Chem.*, 54 (1982) 712.
15 F. J. Gustafson, C. G. Markell and S. M. Simpson, *Anal. Chem.*, 57 (1985) 621.
16 E. C. V. Butler and R. M. Gershey, *Anal. Chim. Acta*, 164 (1984) 153.
17 E. Nakayama, T. Kimoto and S. Okazaki, *Anal. Chem.*, 57 (1985) 1157.
18 Y. Ohtsu, Y. Shiojima, T. Okumura, J. Koyama, K. Nakamura, O. Nakata, K. Kimata and N. Tanaka, *J. Chromatogr.*, 481 (1989) 147.
19 T. Kanda, J. Koyama, K. Nakamura, Y. Ohtsu and T. Ohta, *Nippon Kagaku Kaisi*, (1989) 702.
20 J. Lyman and R. H. Fleming, *J. Mar. Res.*, 3 (1940) 134.

Journal of Chromatography, 549 (1991) 273–281
Elsevier Science Publishers B.V., Amsterdam

CHROM. 23 220

Gas chromatographic properties of organoammonium exchanged montmorillonites

I. Tetraalkylammonium cations

G. A. EICEMAN* and A. S. LARA
Department of Chemistry, New Mexico State University, Las Cruces, NM 88003 (USA)
(First received June 28th, 1990; revised manuscript received January 28th, 1991)

ABSTRACT

The retention of aliphatic hydrocarbons, benzene, and substituted benzenes was determined by gas chromatography with R_4N^+ treated montmorillonite in a OV-101 film. Columns were modified with four R_4N^+ cations for R = CH_3, C_2H_5, *n*-C_3H_7 and *n*-C_4H_9; Na^+ and NH_4^+ exchanged montmorillonites were used in control columns. The $(CH_3)_4N^+$ tailored montmorillonite showed thermal stability and enhanced retentive properties *versus* control columns. Relative retention of substitutional isomers of benzene suggested a steric component in separations. Analyses by gas chromatography–mass spectrometry of decomposition products of other, thermally instable, R_4N^+ montmorillonites was consistent with a base promoted elimination reaction. Organoammonium tailoring agents with β-hydrogens including Bentone-34 should all exhibit thermal instability in treated montmorillonites.

INTRODUCTION

Montmorillonite is a 2:1 layered type of phyllosilicate with negative charges of 0.25–0.6/unit cell from isomorphic substitution of Mg^{2+} for Al^{3+} in octahedral layers of the aluminosilicate. Sodium is the natively abundant counterion in the interlamellar region and exchange by organic ammonium cations may impart characteristic adsorptive properties to montmorillonite. In most investigations, alkyl- or arylamine cations based on $R_{(4-x)}NH_x^+$ for x = 0–3 have been utilized to alter clay properties. While coulombic forces promote cation exchange, the alkyl substituents are attracted to the basal plane and other alkyl chains (if sufficiently long) through Van der Waals interactions. Presumably, the alkyl groups affect adsorption or retention of compounds by these tailored clays [1–4].

In the mid-1950s, stationary phases based upon natural solids including zeolites, clays, silicas, and others received attention as packings for gas–solid chromatography (GSC). A few organoammonium montmorillonites of the form $R_2N^+R'_2$ (R = CH_3 and R′ = $C_{18}H_{37}$) or $RN^+R'_3$ (R = CH_3 and R′ = $C_{16}H_{35}$) were examined between 1957–1968 [5–8] and the octadecyl form was deemed useful in separating

0021-9673/91/$03.50

substituted benzene isomers. A commercial product, Bentone-34, eventually became available and a steric component to separation was tacitly suggested but not explored.

In 1971, Tarramasso [9] demonstrated that montmorillonite could be tailored to impart specific chromatographic properties and proposed that basal spacings of 24–26 Å would allow compounds to enter the interlamellar region. The elution order via partition or adsorption mechanisms for isomers of trimethylbenzene was 1,3,5- 1,2,4- and 1,2,3-trimethylbenzene. This order was reversed with tailored montmorillonite [9,10] and steric models were invoked to explain the reversal in retention order. The interlamellar distances for montmorillonite with the following tailoring agents are [11,12]: TMA [$(CH_3)_4N^+$], 4.3 Å; TEA [$(C_2H_5)_4N^+$], 4.5 Å; TPA [$(C_3H_7)_4N^+$], 5.0 Å; and TBA [$(C_4H_9)_4N^+$], 6.7 Å. Thus, the interlamellar region is sufficient to accept and retain small molecules and possibly allow some separation based upon adsorbate geometry or size. Specific interactions should be weak and retention should be governed by adsorbate size and geometry for non-polar molecules. Thus, retention might be anticipated in the order of increasing R from CH_3 to C_4H_9 where the basal space is incrementally enlarged and the interlamellar region is available for adsorption.

An objective of this and a following investigation was to systematically examine the retention properties of several organoammonium tailored montmorillonites. A model for retention with tailored clays in gas chromatography (GC) will be proposed and could provide a basis for predicting tailoring agents for improved GSC performance. The simplest organoammonium cation family to initiate this investigation was the R_4N^+ for carbon numbers of 1–4 for the alkyl group, R.

EXPERIMENTAL

Instrumentation

A Hewlett-Packard Model 5890A gas chromatograph was equipped with a flame ionization detector, heated injector port, and HP Model 3392A integrating recorder. The inlet was modified with a 0–100 p.s.i. pressure gauge (Ashcroft–Duragauge) which permitted continuous inspection and measurement of inlet pressures (0.5 p.s.i. precision). Column flows were measured at the detector with a soap-bubble meter.

Materials and reagents

Montmorillonite was obtained in sodium form from a commercially available clay, Aquagel, also known as Wyoming Bentonite, through purification and isolation as summarized in Table I. Tailored montmorillonites were prepared from purified sodium montmorillonite and aqueous solutions of appropriate ammonium salts. Typically, tailoring agent was added to 1 g of sodium montmorillonite in 1000-fold excess of the estimated cation-exchange capacity, stirred with paddles at 30 rpm for 8–10 h, and isolated by decanting after a 2 h period for settling. The clay was air-dried at ambient temperature for 24 h and then heated at 100°C for 2 h. A 115-mesh fraction was added to a solution of OV-101 and packings were prepared through rotary evaporation of solvent. Ratios of packing, liquid phase and clay are given in Table II.

TABLE I

PURIFICATION OF WYOMING BENTONITE (AQUAGEL) TO SODIUM MONTMORILLONITE (25 g)

Step	Treatment
1	Add 250 ml of a sodium acetate buffer, pH 5, 70°C; stir gently for 1 h
2	Centrifuge, decant and mechanically remove black grit
3	Add in order: 200 ml solution of 0.3 *M* sodium citrate, 25 ml of 1 *M* $NaHCO_3$, 5 g of sodium dithionite; then stir for 1 h
4	Centrifuge, decant and remove grit
5	Add 100 ml of 30% H_2O_2 and stir 1 h
6	Centrifuge and decant
7	Resuspend with 250 ml of water and floc with sodium chloride
8	Filter solid and dry at 90°C for 48 h

Procedures

Since retention was particularly sensitive to compound and column temperature, a temperature gradient of 5°C/min from 50°C was regarded as a reasonable vehicle to characterize retention for a large number of compounds. The retention times, t_r and retention time for an unretained solute, t_m, in this instance methane, were obtained under identical conditions for all columns and compounds. Sufficient ambiguities existed in the exact mechanism of retention, *i.e.* partition, adsorption, or steric exclusion, that use of more elementary terms such as specific retention volumes or partition coefficients was considered premature and experimentally intractable. Consequently, reliance was made on daily reproducibility of column flows and inlet pressures to facilitate comparisons of retention. An aliquot of 1 μl of 0.01 *M* solutions of compounds in carbon disulfide was introduced into the GC apparatus simultaneously with the start of the temperature program.

TABLE II

CHARACTERISTICS OF PACKINGS FOR TAILORED MONTMORILLONITES

Column	Form of tailoring agent	Column packing mass (g)	Clay adsorbent mass (g)
Composition of individual columns			
TMA	Cl^- salt	2.5082	0.0502
TEA	Br^- salt	2.4851	0.0497
TPA	Br^- salt	2.6226	0.0525
TBA	Br^- salt	2.7488	0.0550
Composition of packing (w/w): 96% solid support: Chromosorb W-AW 2% liquid phase: OV-101 2% tailored montmorillonite			

Vapors from thermal decomposition of tailored montmorillonite solids were analyzed using a Hewlett-Packard 5995A gas chromatography–mass spectrometer with a 30-m SuperOx II capillary column. An inlet liner was packed with 0.3–0.8 mg of solid and inserted in the GC–mass spectrometric (MS) injection port. The capillary column had previously been set to −10°C in order to cryogenically focus highly volatile decomposition products. The inlet (250°C) was operated in splitless mode for *ca.* 10 s and reset to split mode with the start of the oven temperature program. This program consisted of initial temperature, −10°C; initial time, 5 min; program rate, 6°C/min; and final temperature, 200°C or lower. The mass spectrometer was started after 1 min to allow the venting of air and then was operated from m/z of 35 to 600 at 600 a.m.u./s.

RESULTS AND DISCUSSION

GC retention properties for R_4N^+-montmorillonites

Retention behavior of montmorillonite tailored with TMA, TEA, TPA, and TBA for alkanes from pentane to nonane is shown in Fig. 1. In comparison, control columns (Na^+ or NH_4^+ tailored montmorillonite in 2% OV-101) exhibited retention

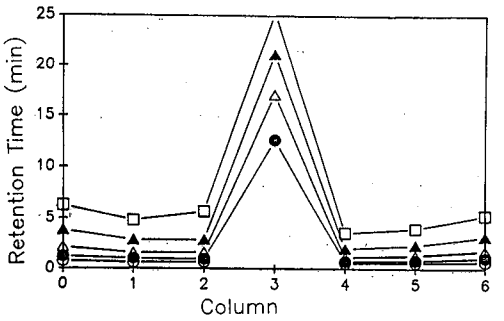

Fig. 1. Retention times and trends for *n*-alkanes on controls and tetraalkylammonium exchanged montmorillonite. Columns: 0 = No clay; 1 = Na^+; 2 = NH_4^+; 3 = TMA; 4 = TEA; 5 = TPA; 6 = TBA. *n*-Alkanes: ○ = pentane; ● = hexane; △ = heptane; ▲ = octane and □ = nonane.

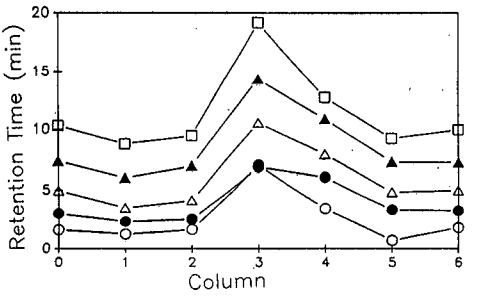

Fig. 2. Retention times and trends for monosubstituted benzenes on controls and tetraalkylammonium exchanged montmorillonite. Columns as in Fig. 1. Monosubstituted benzenes: ○ = benzene; ● = toluene; △ = ethylbenzene; ▲ = propylbenzene; □ = butylbenzene.

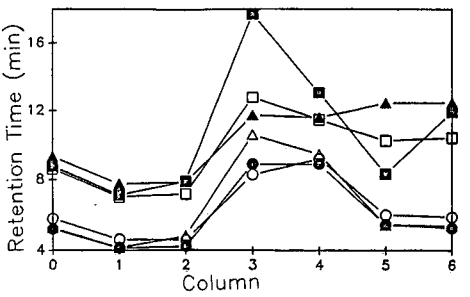

Fig. 3. Retention times and trends for disubstituted benzenes on controls and tetraalkylammonium exchanged montmorillonite. Columns as in Fig. 1. Disubstituted benzenes: ○ = *o*-xylene; ● = *m*-xylene; △ = *p*-xylene; ▲ = *o*-dichlorobenzene; □ = *m*-dichlorobenzene; ■ = *p*-dichlorobenzene.

times of 0.8 to 6 min for pentane and nonane, respectively. Thus, only the TMA montmorillonite exhibited retention significantly larger than that for controls and was inconsistent with an expected trend of TBA > TPA > TEA > TMA. Similarly, monosubstituted benzenes (Fig. 2) were retained better on TMA than on controls, TEA, TPA, and TBA packings. In the retention times for xylenes and dichlorobenzenes (Fig. 3), the TMA column showed enhanced retention over all other phases where retention times were inversely proportional to vapor pressures. Thus, retention in controls and packings, except TMA, occurred through general dispersion interactions with no obvious steric component. The retention order for disubstituted benzenes with non-specific liquid phases has been determined [9] as *ortho* > *meta* > *para*. However, this trend was inverted with both dichlorobenzenes and xylenes on TMA suggesting some control over retention through a steric mechanism.

Column efficiencies for various analytes ranged from acceptable to poor for packed columns. For example, an average number of theoretical plates was *ca.* 400 or height equivalent for a theoretical plate of 0.5 cm for a 2-m column. While this performance cannot be regarded as analytical grade behavior, the emphasis in this work was the coverage of active sites and mechanical integrity of the column. Thus, the use of thin films of montmorillonite not in a supporting liquid phase might be expected to impart column efficiency better than that observed here.

Thermal stabilities of tailored montmorillonites

The failure of TEA, TPA, and TBA packing to exhibit comparable, if not better, retention than TMA might originate with thermal decomposition of the R_4N^+ pillars and collapse of the montmorillonite layers to a H^+ or NH_4^+ exchanged form. Thermal instability of tailored montmorillonite was seen as excessive column bleed for TEA, TPA, and TBA packings and corresponded with decreases in retention times. In contrast, retention behavior for the TMA phase was unaffected by conditioning at temperatures up to 200°C. Estimated upper temperature limits for conditioning columns without degradation were: TEA, 180°C; TPA, 160°C; and TBA, 130°C. Previously, comparably tailored montmorillonites were shown to undergo decomposition to alkenes, olefins, and alkanes [13] lending credence to the concept of a collapsed interlamellar region for TEA, TPA, and TBA.

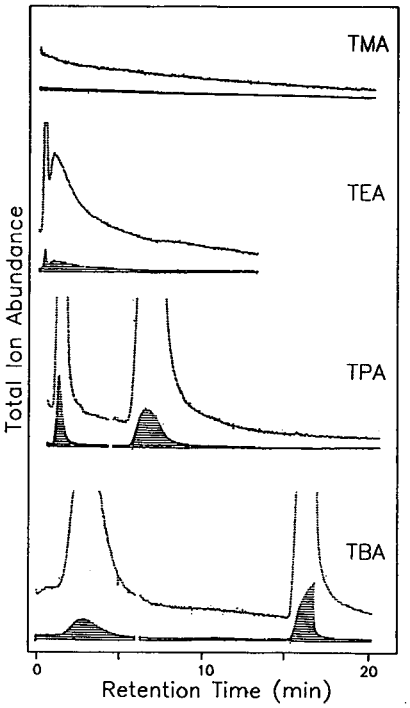

Fig. 4. Total ion chromatograms from GC–MS analysis of thermal decomposition products from tetraalkylammonium exchanged montmorillonites.

The total ion chromatograms (TIC) from GC–MS analysis of gases from heated TMA, TEA, TPA, and TBA packings are shown in Fig. 4. Thermal decomposition of TMA was not observed in the TIC which was essentially free of any detectable components. In contrast, TICs for TEA, TPA, and TBA showed large amounts of components in simple chromatograms. In every instance, the peak eluting second in the TIC (retention times of 2.64, 7.16, and 16.96 min for TEA, TPA, and TBA, respectively) was identified as R_3N, presumably derived from R_4N^+. The first peak in each TIC was identified as a bromine substituted hydrocarbon from the R branch of the particular ammonium cation R_4N^+, namely RBr. Mass spectra were matched favorably to catalogued mass spectra [14] and retention times were checked with authentic standards.

Reactions of tetraalkylammonium cations have been reported [11,12,15,16] and could occur via a halide substitution reaction (eqn. 1) or through a Hofmann elimination (eqn. 2):

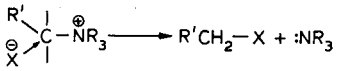

(1)

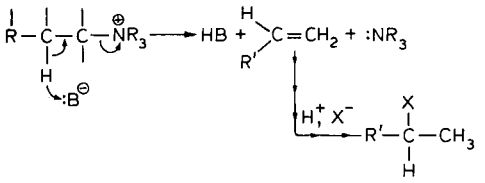

(2)

A substitution in the interlamellar region would require a halide anion, the nucleophile, to substitute for the leaving group, the free amine (II), as shown in eqn. 3:

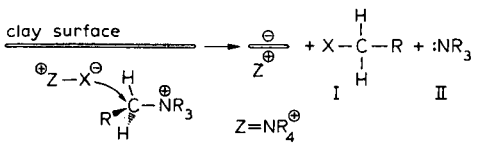

(3)

The products of this reaction, I and II, were consistent with the GC–MS findings (Fig. 4) and could originate with treatment of clays with bromide and iodide salts (*i.e.* $R_4N^+Br^-$). The exception, TMA, was introduced as the chloride salt and differences may be associated with a lower nucleophilic strength of Cl^- *versus* Br^-. This possibility was examined with GC–MS studies on decomposition of TMA^+Br^- and TMA^+I^- salts. Small levels of methylhalides were observed and trimethylamine was not detected. This suggested that an elimination mechanism and not nucleophilic attack caused decomposition of the tailoring agent. A reservoir of X^- in the interlamellar region was unexpected and could arise from excess tailoring salt not washed from the montmorillonite.

Consequences from thermal degradation of tailoring agent will leave the clay with H^+ in place of R_4H^+ and adsorbate molecules would be sterically blocked from entering the interlamellar region. Thus, the chromatographic properties of the decomposed tailored montmorillonites should resemble those for untailored material as was observed in Figs. 1–3. The findings suggest that tailored montmorillonites undergo degradation through an adaptation of a Hofmann elimination [17–19]; an exact proof is presently impossible since products from a halide substitution and an elimination reaction will be the same.

A point that supports a Hofmann elimination is the availability of basic reactant sites on clays. The Al–O octahedrally coordinated layer framework contains two coordinated hydroxyl groups for each Al–O octahedron. These hydroxyl groups protrude into the hexagonal holes created by the Si–O tetrahedra of the outermost layer. The hydrogens on these Al–OH groups vary in acidity due to uneven distribution of charge density, degree of isomorphic substitution of metal cations, and the ratio of dioctahedral to trioctahedral sites in the Al–O layer. Consequently, protons from the OH group become delocalized and migrate to neighboring OH groups forming OH_2^+ and loss of water occurs. The remaining oxide, O^-, then coordinates with a vacant Al site [20] as shown (eqn. 4):

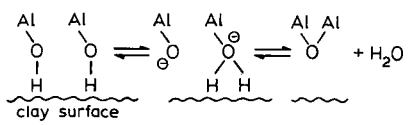

(4)

Dehydroxylation has been recognized for inorganic cation clays [21,22] and is promoted by low humidities and high temperatures as would be experienced in a purified nitrogen stream of a GC column. The temperatures needed to promote dehydroxylation are large (250–700°C) relative to GC elution temperatures with the organic ammonium pillars. Another factor that promotes dehydroxylation is interlamellar dimensions and in general, dehydration rates increase with increases in the interlamellar distance. Organoammonium ions may be expected to dehydroxylate and decompose at relatively low temperatures (130–180°C) since escape routes for water molecules will be enhanced with organoammonium montmorillonites.

The basic nature of the clay interlamellar region was probed with the thermal instability of two tailoring agents each without β-hydrogens. A column prepared with a tailoring agent of high pK_a, 1,4-diazabicyclo[2.2.2]octane · $2H^+$ (DABCO) with a first pK_a of 8.6 exhibited stable retention properties. However, a column prepared with pyrazines (pK_a = 0.65) was very unstable. Neither could decompose through a β-elimination indicating the presence of a reasonably basic site on the clay surface.

The last consideration for bimolecular eliminations is the generation of alkenes rather than RBr as observed in the GC–MS analyses; a subsequent hydrobromination addition to the alkene would have to occur with Hofmann eliminations. Hydrobromination of alkenes in montmorillonites or related materials is unreported and this final step of the thermal decomposition must be regarded as problematic; however, proton additions to alkenes to produce carbocations are known [23] for DABCO-montmorillonite.

In summary, a principle argument against a substitution mechanism is that despite the availability of a halide ion and the similarity of $:N(CH_3)_3$ and $:N(CH_2CH_3)_3$ as leaving groups, decomposition of TMA did not occur under these conditions. If substitution was the degradation mechanism, then the TMA clay should have undergone a thermal decomposition to free amine and halogenated alkane.

Significance for GSC stationary phases

Few reports on chromatographic properties of alkylamine salts as modifying agents for montmorillonite could be found with the exception of the early chromatographic studies with long chained amines from the 1950s and early 1960s. A commercial material based on dimethyldioctadecylammonium clay is available as a packing under the trade name Bentone-34 and has a recommended upper temperature limit of 150°C. Since Bentone-34 has hydrogens on two β-carbons, decomposition reactions as observed with TEA, TPA and TBA should be observed chromatographically as a declining drift in retention times with prolonged exposure to high temperatures and as elution of free amines in decomposition vapors released from packing at 200°C. Instability in retention times was noted but not systematically documented. However, the GC–MS analysis of decomposition vapors for Bentone-34 produced six major and *ca.* seven minor constituents that were detected and were identified with mass spectra as alkanes and alkenes with carbon numbers greater than 16. Identifications based upon manual interpretation and comparisons to data bases included: hexadecene, heptadecane, octadecane, dodecene, and tetradecene. This supported the general concept that instability in such packings is related to the tailoring agent and is consistent with a Hofmann elimination via a proton on a β-carbon with base promotion from the clay surface.

CONCLUSIONS

No comparable reports on chromatographic retention of alkylammonium modified montmorillonites exist with the exception of the early chromatographic studies with long-chained amines from the 1950s and early 1960s. Findings here are helpful in rationalizing the upper temperature limit and column instability of a commercially available dimethyldioctadecyl-ammonium clay, Bentone-34. Evidently the Bentone 34 also experienced thermal degradation consistent with the findings from R_4N^+-montmorillonites. Should elimination reactions dominate the cause for thermal instability in such tailoring agents, the existence of β-hydrogens portends poor thermal properties for all such tailoring agents. Only agents in which there are no β-hydrogens should be viewed as viable tailoring agents with packings at elevated temperatures.

ACKNOWLEDGEMENT

Support from National Science Foundation Grant No. RII-8604030 and 8904982 is gratefully acknowledged.

REFERENCES

1 J. M. Serratosa, *Clays Clay Min.*, 14 (1966) 385–391.
2 G. W. Brindley and R. W. Hoffmann, *Clays Clay Min.*, 9 (1960) 546–556.
3 R. Greene-Kelly, *Trans. Faraday Soc.*, 51 (1955) 412–430.
4 R. Greene-Kelly, *Trans. Faraday Soc.*, 52 (1956) 1281–1286.
5 C. F. Raley and J. W. Kaufman, *Anal. Chem.*, 40 (1968) 1371–1372.
6 E. W. Cieplinksi, *Anal. Chem.*, 37 (1965) 1160–1161.
7 J. V. Mortimer and P. L. Gent, *Anal. Chem.*, 36 (1964) 754–756.
8 M. van der Stricht and J. van Rysselberge, *J. Gas Chromatogr.*, 1 (1963) 29–33.
9 M. Taramasso, *J. Chromatogr.*, 58 (1971) 31–38.
10 J. V. Mortimer and P. L. Gent, *Nature (Londen)*, 197 (1963) 789–790.
11 B. K. G. Theng, *The Chemistry of Clay–Organic Reactions*, Wiley, New York, 1974, p. 220.
12 R. M. Barrer, *Zeolites and Clay Minerals as Sorbents and Molecular Sieves*, Academic Press, New York, 1978, p. 464.
13 B. K. G. Theng, *The Chemistry of Clay–Organic Reactions*, Wiley, New York, 1974, pp. 128, 289.
14 *Eight Peak Index of Mass Spectra*, Mass Spectrometry Data Centre, UK, 2nd ed., 1974.
15 B. K. G. Theng, *The Chemistry of Clay–Organic Reactions*, Wiley, New York, 1974, pp. 129, 286.
16 R. M. Barrer, *Zeolites and Clay Minerals as Sorbents and Molecular Sieves*, Academic Press, New York, 1978, p. 460.
17 J. March, *Advanced Organic Chemistry*, Wiley, New York, 3rd ed., 1985, pp. 906–909.
18 A. C. Cope, N. A. LeBel, P. T. Moore and W. R. Moore, *J. Am. Chem. Soc.*, 83 (1961) 3861–3865.
19 A. C. Cope and A. S. Mehta, *J. Am. Chem. Soc.*, 85 (1963) 1949–1952.
20 G. W. Brindley and J. Lemaitre, in A. C. D. Newman (Editor), *Chemistry of Clays and Clay Minerals*, Wiley, New York, 1987, p. 324.
21 J. D. Russell and A. R. Fraser, *Clays Clay Min.*, 19 (1971) 55–59.
22 S. Yariv and L. Heller-Kallai, *Clays Clay Min.*, 21 (1973) 199–200.
23 J. M. Thomas and Ch. R. Theocharis, in R. Scheffold (Editor), *Modern Synthetic Methods*, Springer, Berlin, 1989, p. 292.

Journal of Chromatography, 549 (1991) 283–295
Elsevier Science Publishers B.V., Amsterdam

CHROM. 23 221

Gas chromatographic retention properties of organoammonium exchanged montmorillonites

II. $CH_3N^+H_3$, $(CH_3)_4N^+$, $(CH_3)_3N^+CH_2C_6H_5$ and 1,4-diazabicyclo[2.2.2]octane · $2H^+$

A. S. LARA* and G. A. EICEMAN
Department of Chemistry, New Mexico State University, Las Cruces, NM 88003 (USA)
(First received June 28th, 1990; revised manuscript received January 28th, 1991)

ABSTRACT

The gas chromatographic retention properties of four organoammonium tailored montmorillonites were characterized using 68 probe molecules. The retention patterns favored a steric model in which retention was governed by three parameters: adsorbate dimensions and orientation, interlamellar plate separation distance, and inter-cation volumes in the interlamellar region. Tailored montmorillonites are limited in steric selectivity at large interlamellar plate distances by swelling and acceptance of oversized molecules.

INTRODUCTION

Tetramethylammonium exchanged montmorillonite showed gas chromatographic selectivity implicative of steric mechanisms in retention and excellent thermal stability from ambient to 200°C. In contrast, the tetraethyl- to tetrabutylammonium montmorillonites were thermally unstable [1]. When heated to temperatures above 100°C, these packings decomposed to corresponding free amines and halogenated alkanes. A central factor believed responsible for this thermal instability was acidic hydrogens located β to the nitrogen rendering the cation susceptible to an elimination reaction. Thus, attempts to probe retention properties of and construct retention models for organoammonium tailored montmorillonites were thwarted. In this report, organoammonium cations *without β-hydrogens* were evaluated in order to examine an anticipated relationship between interlamellar distance in modified montmorillonite and retention in gas chromatography (GC). This was accomplished using 68 probe compounds comprising six chemical classes and four tailoring agents. A preliminary model of retention in tailored montmorillonites includes interlamellar distance and cation volumes within the interlamellar region.

0021-9673/91/$03.50

EXPERIMENTAL

Details of preparation of columns, retention measurements, and data reduction were given in the preceding article [1]. The tailoring agents used in the current work were methylamine · HCl (MA), tetramethylammonium chloride (TMA), benzyltrimethylammonium iodide (BTMA) and 1,4-diazabicyclo[2.2.2]octane · 2 HCl (DABCO) and the probe compounds are listed in Table I. All compounds were obtained in the highest quality readily available and generally were reagent or analytical grade.

Retention was expressed in terms of capacity factor (k') or corrected retention time (t_r') as conventionally defined since retention in the tailored montmorillonite compounds was a mixture of partition, adsorption, and steric sieving. However, control columns were used to delineate trends in retention to determine relative importance of the steric component. A column temperature program was used to simplify data collection since small differences in structures caused large differences in elution

TABLE I

RETENTION TIMES FOR PROBE COMPOUNDS ON TAILORED CLAY COLUMNS

Compound	Column			
	MA	TMA	BTMA	DABCO
Alkanes				
Pentane	0.758	0.591	0.740	0.676
Hexane	7.404	13.070	7.821	0.894
Heptane	11.895	18.041	13.551	1.356
Octane	16.646	22.323	17.014	2.438
Nonane	20.843	26.680	20.549	10.035
Dodecane	30.923			18.167
2,2-Dimethylbutane	0.592	0.550	0.746	0.719
2,3-Dimethylbutane	0.599	0.594	0.741	0.799
2-Methylpentane	0.604	0.646	0.767	0.806
3-Methylpentane	0.604	0.636	0.816	0.839
Isooctane	1.701	1.048	10.005	1.255
Alkenes and alkynes				
1-Hexene	6.400	14.588	10.870	0.878
cis-2-Hexene	5.213	8.548	9.448	0.966
trans-2-Hexene	6.988	15.059	11.233	1.046
1-Hexyne	9.577	13.371	12.626	1.151
Cycloalkanes and cycloalkenes				
Cyclopentane	0.601	4.029	0.749	0.782
Cyclohexane	1.377	4.162	7.201	1.103
Cyclohexene	2.727	2.556	9.681	1.224
Methylcyclopentane	1.818	6.209	5.600	0.968
Methylcyclohexane	3.956	7.545	9.760	1.466
1,3-Cyclohexadiene	4.459	2.464	13.306	6.600
1,4-Cyclohexadiene	5.383	3.799	16.545	12.011
1-Methyl-1,4-cyclo-hexadiene	10.534	6.864	14.299	11.924
cis-Decalin	10.600	11.689	21.230	13.538
trans-Decalin	14.600	20.625	21.614	13.780
Dicyclohexyl	21.178	26.778	28.087	19.167

TABLE I (*continued*)

Compound	Column			
	MA	TMA	BTMA	DABCO
Aromatics				
Benzene	6.266	6.301	19.495	12.600
Toluene	10.196	6.138	17.381	11.384
o-Xylene	13.758	8.003	11.731	6.592
m-Xylene	15.013	8.931	16.754	12.281
p-Xylene	16.225	17.257	20.445	14.952
Ethylbenzene	14.399	9.745	20.528	14.284
n-Propylbenzene	18.201	14.406	24.919	17.019
Isopropylbenzene	16.721	11.980	22.180	14.276
n-Butylbenzene	22.732	18.956	28.401	19.454
Isobutylbenzene	20.716	16.551	26.659	18.154
sec-Butylbenzene	20.403	15.701	25.141	16.938
tert.-Butylbenzene	12.400	11.578	22.463	14.056
Di-*tert.*-butylbenzene	21.000	23.768		18.950
1,3,5-Trimethylbenzene	22.443	14.522	11.970	6.882
1,2,3-Trimethylbenzene	21.711	14.756	13.496	8.351
1,2,4-Trimethylbenzene	21.804	14.753	15.781	11.474
Polycyclic aromatic hydrocarbons				
Biphenyl	31.765	30.233		
Naphthalene	23.416	18.885	24.513	
Fluorene	34.128	30.049	26.786	
Halogenated alkanes				
Methylene chloride	6.400	8.200	0.763	0.739
Chloroform	7.894	10.788	0.751	1.055
Carbon tetrachloride	0.796	3.400	0.768	1.134
1-Chlorobutane	11.453	15.070	11.885	1.242
2-Chlorobutane	7.698	9.967	8.989	0.988
1-Bromobutane	13.356	17.523	14.458	2.518
2-Bromobutane	8.000	11.597	11.309	1.449
Halogenated benzenes				
Chlorobenzene	12.239	9.276	21.400	18.528
o-Dichlorobenzene	21.474	12.193	15.832	12.768
m-Dichlorobenzene	20.888	13.228	22.064	18.981
p-Dichlorobenzene	21.912	17.050	27.523	
Fluorobenzene	6.901	6.797	20.848	14.268
o-Difluorobenzene	14.143	6.134	17.162	9.893
m-Difluorobenzene	11.896	5.278	16.759	9.842
p-Difluorobenzene	14.264	10.926	24.934	17.800
1,2,4-Trifluorobenzene	21.202	10.471	18.200	10.148
1,2,4,5-Tetrafluorobenzene	28.144	15.655	16.900	7.723
1,2,3,5-Tetrafluorobenzene	26.499	14.084	7.800	1.076
1,2,3,4-Tetrafluorobenzene	28.394	15.879	10.906	1.501
Perfluorobenzene	40.000	25.400	15.000	0.940
a,a,a-Trifluorotoluene	7.562	6.810	17.591	10.974
Bromobenzene	14.509	11.214	23.673	20.063
Solvent				
Carbon disulfide	0.617	0.623	0.799	0.746

at fixed temperatures on the montmorillonite columns. The large number of probe compounds necessitated the simplicity offered by a temperature program.

RESULTS AND DISCUSSION

Thermal stability and reproducibility

The four quaternary ammonium cations including MA, TMA, BTMA, and DABCO exhibited thermal stability with upper temperature limits of 220°C (MA and TMA); 180°C (BTMA); and 140–150°C (DABCO). Unfortunately, this upper temperature limit effectively restricted studies to molecules no larger than *ca.* 150 a.m.u. Nonetheless, columns could be made reproducibly from fresh batches of sodium montmorillonite to within 10% relative standard deviation on relative retentions. The columns exhibited low chromatographic efficiency [1] in current mechanical configurations. Finally, the tailored montmorillonites showed chromatographic retention patterns diametrically opposed to those observed with general (non-specific partition) interactions and with gas–solid adsorption in control columns [1].

TABLE II

ln k' FOR PROBE COMPOUNDS ON MODIFIED CLAY PHASES AND CONTROL COLUMNS

The largest value for ln k' is given in italics in each compound series and for each column. Values are emphasized where isomers exhibit identical retention within a series.

Compound	Column[a]								
	OV-101	Na-Clay	TBA	TPA	TEA	MA	TMA	BTMA	DABCO
Dimethylbenzenes									
o-Xylene	*5.6*	*4.4*	*5.3*	*5.5*	*5.9*	6.2	5.9	6.2	5.6
m-Xylene	5.4	4.3	5.2	5.4	5.8	6.3	6.1	6.6	6.3
p-Xylene	5.4	4.3	5.2	5.4	5.9	*6.4*	*6.7*	*6.8*	*6.5*
Dichlorobenzenes									
o-Dichlorobenzene	*6.1*	*5.0*	*6.1*	*6.3*	6.2	6.7	6.4	6.6	6.4
m-Dichlorobenzene	6.0	4.9	5.9	6.1	6.2	6.6	6.5	6.9	6.8
p-Dichlorobenzene	6.0	4.9	6.1	5.8	*6.4*	*6.7*	*6.7*	*7.1*	+[d]
Trimethylbenzenes[b]									
1,3,5-Trimethylbenzene	5.9	4.8	5.6	5.8	5.9	**6.7**	**6.6**	6.3	5.7
1,2,3-Trimethylbenzene						**6.7**	**6.6**	6.4	5.9
1,2,4-Trimethylbenzene						**6.7**	**6.6**	*6.6*	*6.2*
Decalins[c]									
cis-Decalin						5.9	6.3	**6.9**	**6.4**
trans-Decalin						*6.3*	*6.9*	**6.9**	**6.4**

[a] Findings for columns of ammonium, piperazine, pyrazine, and hexamethylenediamine were comparable to the sodium clay and OV-101 in magnitude and order of elution.

[b] 1,2,3-Isomer yielded greatest ln k' values on columns of RSL-150, piperazine, pyrazine, and hexamethylenediamine.

[c] *cis*-Decalin yielded greatest ln k' values on columns of RSL-150, piperazine, pyrazine, and hexamethylenediamine.

[d] Indicates a peak that was strongly retained and flattened in shape so that a retention time measurement was problematic.

TABLE III

ln k' FOR FLUORINATED BENZENES AND NON-AROMATIC RING COMPOUNDS ON TAILORED CLAY COLUMNS

The elution order is ranked in bold numbers adjacent to the ln k' values.

Compound	Column				
	RSL-150	MA	TMA	BTMA	DABCO
Fluorinated benzenes					
Fluorobenzene	1.43 **6**	5.5 **1**	5.8 **3**	6.8 **6**	6.5 **6**
m-Difluorobenzene	1.40 **4**	6.1 **2**	5.5 **1**	6.6 **4**	6.1 **5**
o-Difluorobenzene	1.58 **9**	6.2 **3**	5.7 **2**	6.6 **4**	6.1 **5**
p-Difluorobenzene	1.46 **7**	6.3 **4**	6.3 **5**	7.0 **7**	6.7 **7**
1,2,4-Trifluorobenzene	1.42 **5**	6.7 **5**	6.2 **4**	6.7 **5**	6.1 **5**
1,2,3,5-Tetrafluorobenzene	1.30 **2**	6.9 **6**	6.5 **6**	5.8 **1**	3.3 **2**
1,2,4,5-Tetrafluorobenzene	1.38 **3**	7.0 **7**	6.6 **7**	6.6 **4**	5.8 **4**
1,2,3,4-Tetrafluorobenzene	1.48 **8**	7.0 **8**	6.6 **8**	6.2 **2**	3.8 **3**
Perfluorobenzene	1.20 **1**	7.3 **9**	7.1 **9**	6.5 **3**	3.0 **1**
Non-aromatic ring compounds					
Cyclopentane	0.13 **1**	1.44 **1**	5.20 **4**	2.43 **1**	2.56 **1**
Cyclohexane	0.33 **3**	3.52 **2**	5.24 **5**	5.73 **3**	3.33 **3**
Methylcyclopentane	0.24 **2**	3.93 **3**	5.67 **6**	5.46 **2**	3.08 **2**
Methylcyclohexane	0.55 **7**	4.89 **5**	5.88 **8**	6.06 **5**	3.81 **5**
Cyclohexene	0.38 **5**	4.45 **4**	4.68 **2**	6.05 **4**	3.52 **4**
1,3-Cyclohexadiene	0.35 **4**	5.02 **6**	4.64 **1**	6.38 **6**	5.65 **6**
1,4-Cyclohexadiene	0.49 **6**	5.23 **7**	5.14 **3**	6.61 **8**	6.29 **8**
1-Methyl-1,4-cyclohexadiene	0.84 **8**	5.95 **8**	5.78 **7**	6.46 **7**	6.28 **7**

Retention properties

Retention times for the probe analytes on the four columns are tabulated in Table I and selected results for k' from all columns including controls are shown in Tables II and III. Both k' and elution orders for disubstituted benzenes on tailored montmorillonite *versus* control columns (Table II) suggested that retention was due not only to non-specific partitioning. For example, the *para* isomer of disubstituted benzenes ($C_6H_4X_2$, where X = Cl and CH_3) showed retention times longer than the *ortho*- and *meta*-isomers on those clay columns which were thermally stable. In contrast, the *para*-isomer eluted first from non-polar OV-101 and sodium or ammonium control columns and on clay columns believed to decompose to ammonium forms [1]. Inversions of trends were also observed with the trimethylbenzenes (Table II) and comparisons within clay phases is suggestive of subtle effects (*vide infra*). A final example of retention inversion was the geometric isomers of decalin. *cis*-Decalin was retained longer than *trans*-decalin on non-polar and control columns while the reverse was observed for MA and TMA (Table II). These isomers had comparable retention times on BTMA and DABCO columns indicating an absence of steric selectivity.

Specific patterns in retention and energetics of intercalation

Plots of t'_r for 68 probe compounds and four tailored clays are shown in Fig. 1 and can be compared to the retention of *n*-alkanes and *n*-alkylbenzenes on control

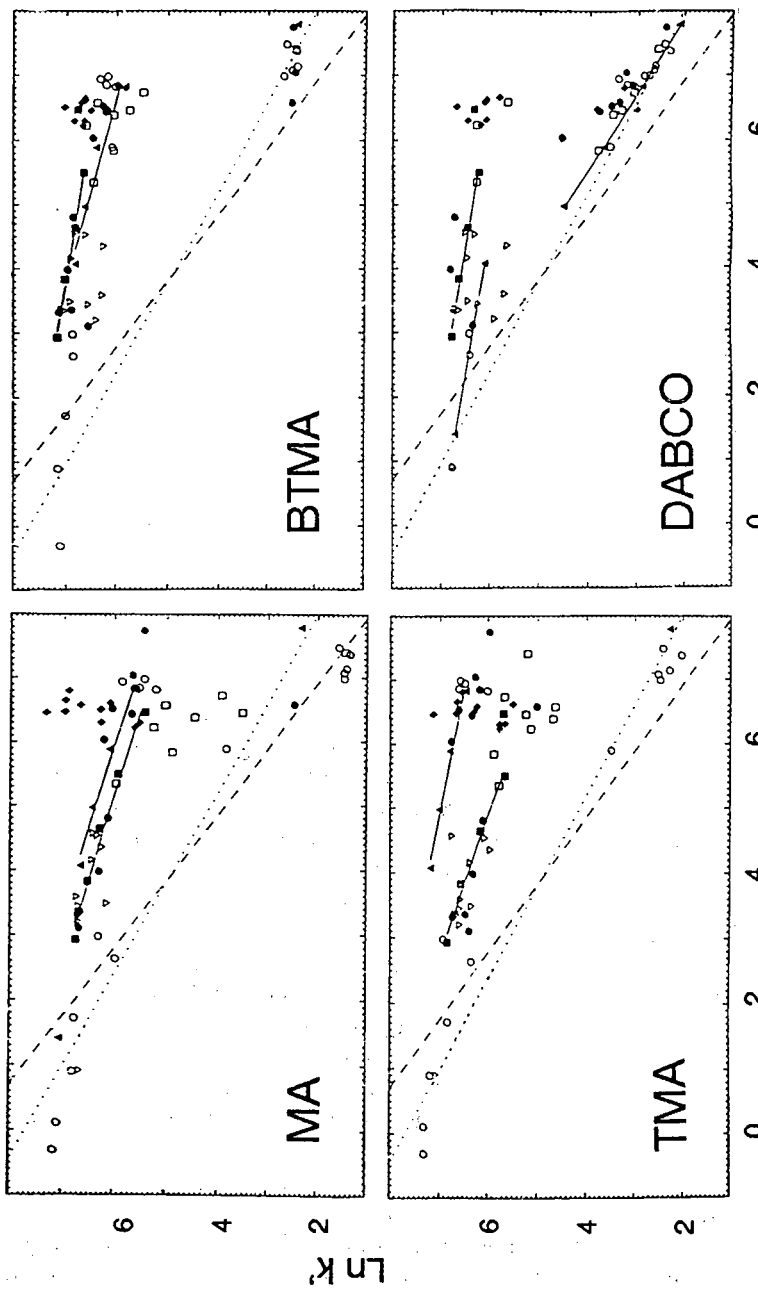

Fig. 1. Plots of ln k' *versus* ln vapor pressure (at 75°C) for organic compounds on MA, TMA, BTMA, and DABCO tailored montmorillonite. The dashed line depicts the retention of *n*-alkanes on control columns. The dotted line depicts the retention of *n*-alkylbenzenes on control columns. Legend: ▲ = *n*-alkanes, ■ = *n*-alkylbenzenes, ◆ = fluorobenzenes, □ = non-aromatic rings, ● = halogenated hydrocarbons, ▽ = polysubstituted benzenes.

columns. Adsorbate retention was generally greater with the tailored clays than on the control columns and the *n*-alkanes and *n*-alkylbenzenes were particularly affected. Since this increase could not be attributed to dipole-induced dipole interactions, hydrogen bonding, or liquid phase partitioning on the coated clay surface, adsorbates evidently were migrating into the interlamellar plate region created by the cations where known distances are [2]: NH_4, 1.0–1.2 Å; MA, 2.1–2.6 Å; TMA, 4.1 Å; DABCO, 5.4 Å. These distances represent plates at low potential energy and the distances can be increased, if justified by energies, through imbibing compounds. For example, a benzene ring and an alkane group are 3.7 Å and 4.0 Å thick, respectively and MA must expand the interlamellar region if a molecule is to enter this region and undergo retention. The TMA tailored clay could accept, without expansion, the *n*-alkanes, *n*-alkylbenzenes, and cyclopentane. Nearly all other compounds, in particular the branched methylalkanes and neo-alkanes, necessitate expansion to 5.9 Å. Ammonium and sodium forms with interlamellar distances of 1.0–1.2 Å and *ca.* 0 Å respectively showed no retention while the MA and TMA forms did exhibit retention. Thus, plate distances of 1.2–2.1 Å represent a region of transition from no expansion to partial expansion of the clay layers or plates.

Binding energies between clay plates arise from dispersion and electrostatic cohesion and dispersion forces may be substantially due to the large surface areas of adjacent sheets. Electrostatic cohesion forces exist due to the Coulombic interactions between positive charged counterions and negative charged clay sheets. When sheets are in close proximity (Na^+ and NH_4^+ forms) these energies are comparatively large. However, when sheets or plates are separated by 5.5 Å (DABCO) or 4.1 Å (TMA), the electrostatic forces are relatively weak. In order to retain adsorbate molecules which are larger than the dimensions of the interlamellar region, the plates must be separated and seemingly occurred with TMA and DABCO. Adsorption of comparable compounds on Na^+ and NH_4^+ forms with strong plate interactions might be anticipated as unlikely. Thus, space in sodium and ammonium forms of the clay should be unavailable to probe molecules and experimentally these inorganic montmorillonite showed low retention. In instances where the tailoring agent was suspected of thermal degradation to ammonium forms, comparable behavior was observed. In contrast, oversized molecules were retained by the MA and TMA organoammonium tailored clays indicating lessened inter-plate strengths of attraction.

These dynamic GC measurements have static sorption precedent [3] where the sorption/desorption curves with MA and TMA were observed as hysteresis loops and the extent of separation between loops was indicative of further swelling that the clay experiences in intercalating a molecule. Except for water, all analytes created hysteresis in sorption–desorption lines with MA and this was pronounced with bulky compounds such as cyclohexane and isoalkanes. This remarkable agreement supports the interpretation of these GC measurements and the conclusion that intercalation of guest molecules by the tailored clays was occurring.

Comparisons of tailored montmorillonites

Of the four tailored clays that showed chromatographic retention, the MA and TMA had permanent plate separations less than DABCO and BTMA. Correspondingly, the MA and TMA columns displayed behavior different from that for DABCO and BTMA columns and this difference was not simply an augmentation of the trends

seen with MA and TMA columns. For example, the MA and TMA columns retained *n*-alkanes to a larger extent than the aromatic hydrocarbons while this trend was reversed with DABCO and BTMA columns (Fig. 1). A reversal was also observed with the two sets of chromatographic adsorbents (MA and TMA *versus* BTMA and DABCO) in the elution order for *cis*- and *trans*-isomers of decalin.

The differences in elution orders for the two pairs (MA and TMA *versus* DABCO and BTMA) can be rationalized using models for the interlamellar pillars. The original consideration was expansion of the distance vertical to the plates through large and rigid molecules. However, charge densities of the clay affect cation exchange and the extent and quantity of pillar formation. Cation-exchange capacities (CEC) and charge densities for batches of montmorillonites are unique within a range. In tailored clays, the charge density directly governs the average area per cation permitted in the interlamellar region and thus will control the average lateral free or available distance between cation sites. Depending on the lateral size of a fixed pillar cation, a lateral distance between ions will be empty and will be unique to a clay and a cation. Montmorillonites, with DABCO as the exchanged cation, have average free distances of *ca.* 6 Å [2]. In contrast, for the same clay, MA and TMA must have lateral distances > 6 Å. Thus, for the retention of cyclopentane, benzene, cyclohexane, and cyclopentane on DABCO clay, the molecules had to assume an orientation normal to the plate surface (Fig. 2) and these dimensions favored retention of the aromatic molecules. These aromatic compounds could also be accomodated with MA and TMA at the expense of energy to swell the interlamellar distance. The cyclic guest analytes assumed a flat position which is reasonable considering charge densities. Since BTMA showed retention properties much like DABCO, the expectation is that BTMA should have an interlamellar region much like DABCO.

The *n*-alkanes were retained on all columns except DABCO. Some swelling in MA was needed to physically allow penetration of alkanes into the region in a zigzag manner with the chain parallel to the plate. Swelling with TMA is not needed for alkanes to enter the interlamellar region and once the alkanes are intercalated in MA and TMA columns, close contact between the adsorbate and the clay surfaces should promote maximum interactions via Van der Waals forces. The BTMA column also retained the alkanes significantly and molecular dimensions suggest that perpendicular slots were just large enough to accept the adsorbate for intercalation. This close contact promoted Van der Waals attractions. In contrast to the trends for MA, TMA, and BTMA, alkanes of all sizes until nonane were not appreciably retained on DABCO. Presumably, the distances between cations in DABCO were large enough that the alkanes were capable of entering and leaving the interlamellar region without geometric constraints promoting strong Van der Waal interactions.

Support for this model of combined lateral and vertical parameters in tailored montmorillonites arises from the retention behavior of branched alkanes. All four structural isomers of *n*-hexane eluted early on every column indicating little or no retention and correspondingly, no penetration into the interlamellar space. The MA and TMA columns exhibited low retention for all branched alkanes *versus* that for DABCO and BTMA columns. Isooctane was not retained by MA and TMA but was retained by BTMA and may be a gauge of a certain critical size. Certainly the cavity in DABCO is large enough to intercalate a *tert.*-butyl group and perhaps large enough not to experience significant interactions between guest and tailoring agent.

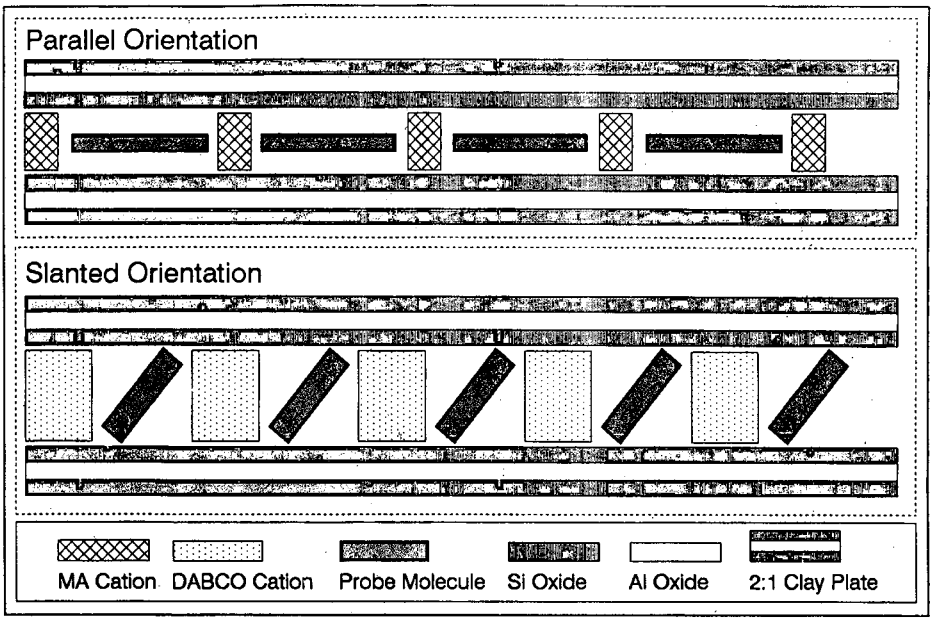

Fig. 2. Schematic of insertion of molecules into interlamellar region of tailored montmorillonite for a small (MA) and large (DABCO) cation.

The *tert.*-butyl group was active in selective retention for the alkylaromatic hydrocarbons. Retention of *tert.*-butylbenzene was low for MA and TMA but was comparable in retention to the corresponding *n*-alkylbenzenes for DABCO and BTMA. Olefins were retained much like their *n*-alkane counterparts in all columns.

The *cis*-and *trans*-isomers of decalin also seemed to be sensitive indicators of the differences in lateral and vertical spaces in the interlamellar region (Table II). Retention times for *cis*-decalin were 10.6, 11.7, 21.2, and 13.5 min for MA, TMA, BTMA, and DABCO, respectively. In contrast and under identical conditions, respective times for *trans*-decalin were 14.6, 20.6, 21.6, and 13.7 min. Greater expansion of the plates was required for the *cis*-isomer than for the *trans*-isomer and was evident in the retention times with MA and TMA where plate expansion would be costly in electrostatic energy. The difference in retention times was fully 9 min on TMA relative to MA despite similar physical properties for the isomers. On a non-polar column based on solubility but non-specific, dispersion interactions, the retention order was reversed to *trans* before *cis* and retention times showed minor differences. The retention of the decalins on BTMA and DABCO was significant compared to MA and TMA but no selectivity for the geometric isomers was exhibited. The dimensions of cavities for the interlamellar region in BTMA and DABCO tailored clays were sufficiently large to permit unobstructed access by each isomer with the ring intercalated perpendicular to the plates. Moreover, in this orientation, the limiting dimensions of the isomers were identical (Table II).

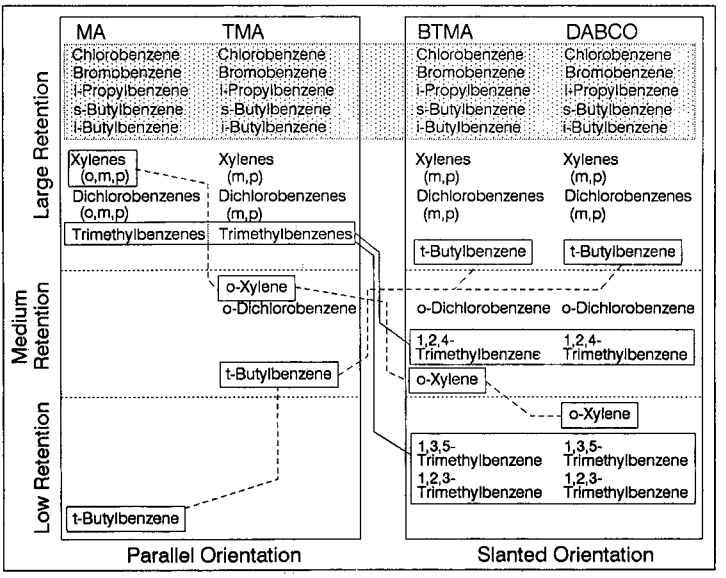

Fig. 3. Trends in retention for four columns of tailored montmorillonites. The compounds in the shaded box were unaffected by changes in cation. The trends suggest differences in orientation of intercalation or orientation as designated.

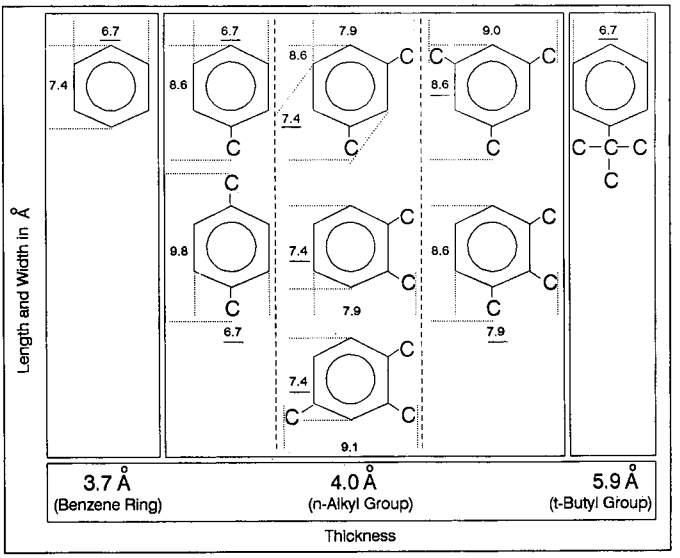

Fig. 4. Calculated molecular length, width and thickness for substituted benzenes from Barrer [5]. The underlined dimension represents the smallest and controlling dimensions for intercalation.

Retention for alkyl and fluorine substituted benzenes

Originally, the substituted benzenes were considered molecular probes of the steric requirements associated with the substituent group. Retention can be divided into three rows or zones per Fig. 3. The top row was for the substituted benzenes that were retained as well as corresponding *n*-alkylbenzenes. The bottom row was for those substituted benzenes that did not show intercalation or retention. Intermediate behavior is shown in a middle row. These results can be discussed through an evaluation of calculated dimensions of the various guest molecules as shown in Fig. 4.

The only molecule of the alkylated and fluorinated benzenes not retained by the MA and TMA columns was *tert.*-butylbenzene which has a thickness of *ca.* 5.9 Å from the butyl group *versus ca.* 4.2–4.5 Å for an alkane in either zigzag orientation (α // or $\alpha \perp$). The cumene substituent, an isobutyl moiety, and a *sec.*-butyl moiety were of comparable thickness when they underwent intercalation with the chain lengthened and parallel to the montmorillonite surface. The xylenes, dichlorobenzenes, and trimethylbenzenes were intermediate sizes and were all only 4 Å or less in thickness. The MA column behaved ideally in that all of the compounds except *tert.*-butylbenzene were intercalated and retained according to Van der Waals interactions. The TMA column showed retention trends identical to those for MA with slightly improved resolution in xylene and dichlorobenzene isomers. Slightly smaller unoccupied lateral distances in TMA than in MA may have contributed to enhanced interactions and slightly improved resolution.

In contrast to the generally unselective MA and TMA, BTMA and DABCO were selective to size with respect to length and breadth of molecules if not so much to the thickness of compounds. Consequently, *tert.*-butylbenzene was highly retained in comparison to other butylbenzene isomers and cumene. These molecules were essentially benzenes with single substituents and thicknesses of 4.6 Å or less. Trimethylbenzene isomers were remarkably excluded from intercalating on BTMA and DABCO and showed low retention times. The ring width for the 1,2,4-isomer was slightly smaller (7.4 Å) than the other two isomers (7.9 and 8.6 Å) and insertion of molecules into the interlamellar space, with rings perpendicular to the clay plates, was shown to be sensitive to this dimension (Table II). One of the distinguishing features between the adsorbent pairs of MA/TMA and BTMA/DABCO was the overall inversion of retention times between alkanes and aromatic compounds (Fig. 1). For MA and TMA, both classes of molecules can enter the interlamellar region parallel to the stacked layer planes. In this manner, alkanes can undergo favorable Van der Waals interactions and show strong retention on MA and TMA.

Fluorinated aromatic and non-aromatic controls

A series of fluorinated benzenes were used to refine this chromatographic model and the discussion below can be referenced to the relative retention of these compounds on a non-polar RSL-150 capillary column (Table III). The retention of these compounds on the MA columns did not parallel the non-polar column pattern and trends were unequivocal. The highly fluorinated benzenes were highly retained and this was especially evident with the TMA column. The simplest possibility was that the fluorine atoms inductively reduced the π electron density of the aromatic ring and thus allowed the fluorinated benzenes to intercalate in a flat orientation on the MA and TMA columns.

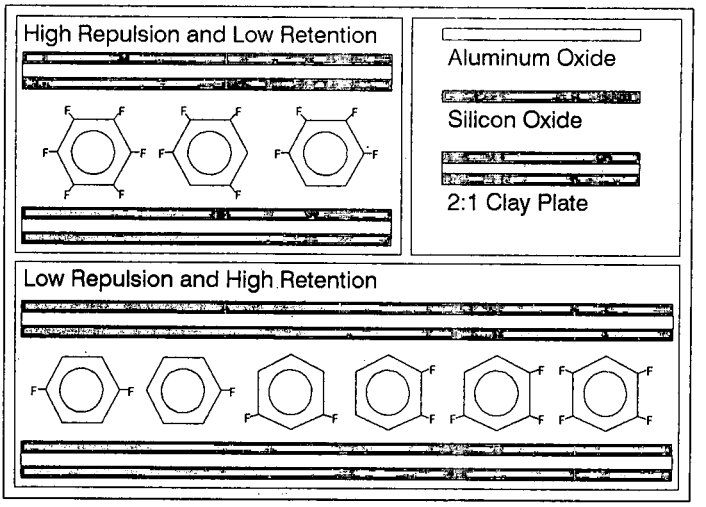

Fig. 5. Model for electrostatic repulsions for fluorinated aromatics in interlamellar layers.

The retention order of these compounds on DABCO columns also did not parallel trends seen in the RSL-150 column or on MA/TMA. In particular, the retention of 1,2,3,4-tetrafluorobenzene, 1,2,3,5-tetrafluorobenzenes, and perfluorobenzene were moderated presumably by vapor pressure and the concept of vertical slots. Fluorinated benzenes that exhibited extremely low retention times *versus* those that were well retained on BTMA or DABCO are depicted in Fig. 5. Those compounds that were retained could intercalate into vertical slots without locating a fluorine atom toward the clay surface. Moreover, those fluorobenzenes that were not retained and likely did not intercalate, were not able to squeeze into a vertical slot without forcing a fluorine atom toward or against the montmorillonite surface. The overall negative charge on the plate surfaces presumably caused Coulombic repulsions and forced an exclusion of those fluorinated benzenes with structures as shown in Fig. 5.

Another analyte series for consideration was the five and six-carbon, non-aromatic rings and retention times for these are shown in Table III. All columns except TMA exhibited trends like those in the non-polar RSL-150 column. That is, non-specific dispersion forces were the effective mechanism of retention and this paralleled simple vapor pressure trends.

The retention behavior of non-aromatic unsaturated rings and halogenated alkanes suggest that the steric model is not complete and a second moderating factor may exist. For example, on MA and TMA, 2-bromobutane, 2-chlorobutane, 1-bromobutane and 1-chlorobutane were retained strongly whereas the four isomers of saturated hexane were not retained. From a strictly steric exclusion perspective, this behavior should not have occurred. The halogenated analytes and the unsaturated rings were the only test compounds with some degree of polarity or high electron density and these aberrations were noted for a limited test set of compounds. Thus, the concept of another controlling parameter for highly polar organic compounds seemed reasonable though not highly developed from these limited results and should be anticipated. The main source of adsorption for non-polar compounds should be attributed to steric considerations with organoammonium tailored montmorillonites.

CONCLUSIONS

The core concept in this model is that of two-dimensional intercalating cavities. Vertical dimensions in the interlamellar region do not suffice alone as a predictor of chromatographic retention or of resolution with tailored montmorillonites in agreement with static models [4]. Retention of non-polar molecules on montmorillonite tailored with organoammonium cations was due to three parameters including the interlamellar distance, the lateral free-volume or distance between exchanged cations, and the CEC and surface area.

ACKNOWLEDGEMENT

Support from National Science Foundation Grant No. RII-8604030 and 8904982 is gratefully acknowledged.

REFERENCES

1 G. A. Eiceman and A. S. Lara, *J. Chromatogr.*, 549 (1991) 273.
2 R. M. Barrer, *Zeolites and Clay Minerals as Sorbents and Molecular Sieves*, Academic Press, New York, 1978, pp. 460, 464, 473.
3 R. M. Barrer, *Zeolites and Clay Minerals as Sorbents and Molecular Sieves*, Academic Press, New York, 1978, p. 465.
4 R. M. Barrer, *Clays Clay Min.*, 37 (1989) 385–395.
5 R. M. Barrer, *Zeolites and Clay Minerals as Sorbents and Molecular Sieves*, Academic Press, New York, 1978, p. 742.

Journal of Chromatography, 549 (1991) 297–311
Elsevier Science Publishers B.V., Amsterdam

CHROM. 23 217

Evaluation of gas chromatography–Fourier transform infrared spectroscopy–mass spectrometry for analysis of phenolic compounds

DAVID T. WILLIAMS*
Environmental Health Centre, Health and Welfare Canada, Tunney's Pasture, Ottawa, Ontario K1A 0L2 (Canada)
QUANG TRAN and PHILLIP FELLIN
Concord Scientific Corporation, 2 Tippett Road, Toronto, Ontario M3H 2V2 (Canada)
and
KENNETH A. BRICE
Atmospheric Environment Service, Environment Canada, Downsview, Ontario M3H 5T4 (Canada)
(Received October 18th, 1990)

ABSTRACT

A gas chromatography (GC)–infrared (IR) spectroscopy–mass spectrometric (MS) system was evaluated for the identification and quantitation of 50 target phenolic compounds. Six columns of varying polarities were tested to achieve optimum chromatographic resolution of the phenolic compounds. The low polarity columns (HP-1, DB-5) gave resolution of 41 of the 50 phenolics; higher polarity columns (DB-17, DB-1701, DB-210, Nukol) were not as effective. Standard solutions containing 50 target phenolic compounds with concentrations in the range of 10 to 600 ng/μl were prepared. The solutions were injected into the selected column (HP-1) using cool on-column injection with a retention gap and with the IR detector and mass spectrometer run in the full scan mode. Fully resolved peaks could be easily identified and quantitated by either IR spectroscopy or MS. For co-eluting compounds spectral subtraction (IR) or selected ion (MS) techniques were employed as appropriate to identify the individual phenolics.

INTRODUCTION

A recent report [1] detailed a method for the determination of alkylated phenolics in air. Analysis of the final extract was performed using fused-silica capillary column gas chromatography (GC) with flame ionisation detection (FID) or mass spectrometric (MS) detection. The method was deemed adequate but the results indicated a clear need for increased specificity in the identification and quantitation of phenolic compounds. Although GC–MS is a powerful technique the mass spectra for positional isomers are usually virtually identical and hence, without good chromatographic separation, compound identification cannot be definitive. In contrast, the infrared (IR) spectra of such isomers can be very different, allowing unambiguous compound identification [2,3], and overlapping chromatographic peaks can be re-

0021-9673/91/$03.50

TABLE I

CAPILLARY COLUMNS, SUPPLIERS AND OPTIMUM TEMPERATURE PROGRAMS

Column	Description	Supplier	Ramp 1					Ramp 2			Ramp 3		
			Initial T (°C)	Hold Time (min)	Rate (°C/min)	Final T (°C)	Hold Time (min)	Rate (°C/min)	Final T (°C)	Hold Time (min)	Rate (°C/min)	Final T (°C)	Hold Time (min)
HP-1	25 m × 0.20 mm I.D., 0.5-μm film	Hewlett-Packard	55	1	2	124	0	5	170	0	10	280	1
DB-5	30 m × 0.25 mm I.D., 0.25-μm film	J & W Scientific	50	1	4	164	0	40	280	3	NA[a]	NA	NA
DB-17	30 m × 0.25 mm I.D., 0.25-μm film	J & W Scientific	50	4	4	178	0	25	280	2	NA	NA	NA
DB-1701	30 m × 0.25 mm I.D., 0.25-μm film	J & W Scientific	50	4	5	180	0	15	280	1	NA	NA	NA
DB-210	30 m × 0.25 mm I.D., 0.25-μm film	J & W Scientific	60	1	4	140	0	10	250	0	NA	NA	NA
Nukol	20 m × 0.25 mm I.D., 0.25-μm film	Supelco	50	1	20	150	14	3	200	0	10	230	22

[a] NA = Not applicable.

solved into the two components using spectral subtraction techniques [4]. The combination of the two techniques (GC–IR–MS) is especially powerful [5,6].

Direct gas chromatography of parent phenols is now feasible with the advent of fused-silica capillary columns and avoids the problems encountered in derivatisation of phenolic compounds. The present study evaluates the use of cool on-column sample injection–fused-silica capillary GC (employing a variety of stationary phases) coupled with tandem IR spectroscopy and MS for the identification and quantitation of 50 target phenolic compounds.

EXPERIMENTAL

Materials and instrumentation

Pure phenolic compounds. The phenolic kit supplied by Supelco Canada contained 49 compounds. 2,3,5,6-tetramethylphenol was provided by Varian Canada. Methanol (99.7%) supplied by Fisher Scientific and chloroform (99.7%) supplied by Caledon Labs. were used as solvents for the phenolic compound standards.

Fused silica capillary columns. Table I presents information on the six fused-silica capillary columns and the suppliers.

Gas chromatography–flame ionisation detection. An HP-5890 gas chromatograph equipped with a flame ionisation detector was used for initial investigation of phenolics separation by six capillary columns of varying stationary phase polarity. A cool on-column injection port with a 26 gauge steel needle guide (HP P/No. 19245-20540) was used for sample introduction, which allowed the application of an auto sampler/auto injecter system (HP 7673A). The column was connected to the injector via a fused-silica retention gap (1.0 m × 0.53 μm) coated with 0.1 μm of methyl silicone (HP P/No. 19095-10050). The connection of the retention gap and the column was made possible by using an appropriate press-fit glass connector (HP P/No. 4041-2173). The GC oven conditions were varied with each type of column. Other parameters were: helium flow-rate, 1.5 ml/min (column) and 35 ml/min (make up gas); hydrogen flow-rate, 30 ml/min; air flow-rate, 320 ml/min; injector, cold on-column; detector, 280°C; injection; 1 μl solution for each GC run.

Gas chromatography–infrared–mass spectrometry. The Hewlett-Packard GC–IR–MS system consisted of an HP 5890 GC connected to an HP 5965A Fourier transform (FT) IR detector and to an HP 5970B MS detector. The central control of the IR detection was the HP 59970C Chemstation which was installed with the HP 59965 IR operating software and equipped with an HP 7957 Winchester drive (80 Mb) and an HP 9144 tape drive (80 Mb). The MS detector was controlled by an HP 59970 MS Chemstation with an HP 9133 drive. The column connections to the GC were similar to those used in the GC–FID system. The flow from the GC capillary column entered the IR detector through a heated interface, passed through the light pipe and returned to the GC oven through a second interface. The IR detector exit interface was lined with a fused-silica capillary transfer line (0.1 mm I.D.) which extended through the heated interface of the MS detector to the ion source. Operational conditions for the GC–IR–MS were: IR light pipe, IR and MS interface temperatures, 290°C; ion source temperature, 230°C; electron impact, 70 eV; electron multiplier, 1800 V; scan-rate MSD (40–300 a.m.u./s); FT-IR scan-rate, 3.3 scans/s (4000–750 wave numbers); optical resolution, 8 wave numbers. Helium sweep gas (0.5

ml/min) was introduced at the inlet and outlet of the IR light pipe interface to minimize peak tailing resulting from dead volume effects in the sample path. The total gas flow-rate through the light pipe was approximately 2 ml/min and the total flow-rate at the second interface was therefore 2.5 ml/min. The flow-rate allowed to enter the MS detector was approximately 0.5 ml/min, the remaining 2.0 ml/min flow was vented to a charcoal collector tube.

Procedures

This section describes the protocols used for different tests using the analytical systems. The objective was to evaluate available analytical components and optimise conditions for resolution and detection of phenolic compounds.

Purity tests for 50 phenolic compounds

The individual standards of phenolics were prepared in chloroform (about 200 ng/μl) and stored in the dark at 4°C. All standards were analysed on HP-1, DB-5, DB-17, DB-1701, DB-210 or Nukol columns using GC–IR–MS and GC–FID. Only one peak was detected for each compound injected into the system. The MS and IR spectra of each phenolic compound were compared to the spectra of the National Bureau of Standards (MS) and the US Environmental Protection Agency (IR) libraries to assess compound purity. The results indicated no evidence of contamination in the standard solutions of the 50 phenolic compounds.

MS and IR library synthesis. To minimise search time MS and IR libraries for the 50 phenolics were prepared using the individual phenolic standard solutions (about 200 ng/μl) and the DB-5 column.

Preparation of quantitation mixtures of phenolics. The 50 target phenolics were divided into five groups each containing ten completely resolved phenolics as determined by GC–FID fitted with the DB-5 column. For each group twelve quantitative mixtures were prepared initially in methanol but later in chloroform at concentrations from 5 to 1000 ng/μl per component. Ten composite quantitative solutions of all 50 phenolics were also prepared at concentrations from 10 to 600 ng/μl. For the dinitrophenol and 3,4,5-trichlorophenol compounds the concentrations were up to 1500 ng/μl due to their low detectabilities by the GC–IR–MS system.

Optimisation of GC temperature program. For each column, at least six temperature programs were evaluated to determine the best conditions for separation of the target phenolics. The composite quantitative mixture of all phenolics with concentration of 100 ng/μl each was used. The identification of peaks in each chromatogram was performed using both IR and MS library searches. To verify peak identity the five solutions containing ten phenolic compounds were injected into the system using the same temperature program. Table I presents the optimum temperature program for each column.

Calibration tests. The HP1 column was selected to investigate the linear range and the detection and quantitation limits of the MS and IR detectors for each phenol. Since the presence of possible interferences of overloading effects were unknown, the calibrations for individual phenolic compounds were performed using the ten compound mixture standards. These results were compared to the results from the mixtures containing all 50 target phenolics. The calibration was performed using the full scan mode for the IR and MS detectors. Three methods of quantitation were used: (i)

for fully resolved peaks calibration curves were established based upon the total responses of the IR and MS detectors, (ii) for peaks containing co-eluting isomers (*e.g.* 3- and 4-methylphenol, 2,4- and 3,5-dimethylphenol and 3- and 4-ethylphenol), the IR data were selected since spectral subtraction could be reliably performed. The IR spectra for each phenolic compound at different concentrations were abstracted and used for measuring the adsorption at different wavenumbers. The calibration curves of these phenolics were established based upon the relationship between absorption and concentration for each phenol at each selected wavelength according to the Lambert–Beer law. If the unknown chromatographic peak was a mixture of two isomers (*e.g.*, 3- and 4-methylphenol), the 4-methylphenol contribution to absorption intensity was subtracted from the mixture's intensity to give the intensity that was attributable to the pure spectrum of 3-methylphenol. From this pure spectrum, the absorption at a suitable wavelength was measured and the concentration of 3-methylphenol was calculated based upon the previous calibration, (iii) for peaks of co-eluting phenolics for which the mass spectra are different, selected MS ion chromatograms of characteristic mass ranges of each compound were used to establish the calibration curves.

Unknown tests. Sixteen samples containing mixtures of phenolic compounds which were unknown to the analyst were prepared. The GC–IR–MS, equipped with an HP-1 column, was used for the identification and quantitation of the 16 samples. Samples 1 and 10 were analyzed in triplicate. The identification of unknown compounds was based on retention time and the analysis of IR and MS spectra. For quantitation of unknowns one of the above three quantitation methods was used; in all cases quantitation was carried out relative to known standards analysed under similar conditions.

RESULTS AND DISCUSSION

Solvent effect

Initial use of methanol as solvent resulted in peak splitting which was not resolved by use of a retention gap. Grob [7] has indicated that the retention gap technique fails if the injected liquids do not wet the surface of the column inlet. Chloroform was tested as a substitute for methanol and was found to be suitable for all target phenolic compounds. Testing on the GC–IR–MS with six different columns confirmed the elimination of peak splitting phenomena by using chloroform as the solvent.

Column performance

The column performance was evaluated based on the number of phenolics that could be eluted and the number of well resolved peaks from a chromatogram of the mixtures of 50 phenolic compounds. IR and MS identifications are greatly simplified if components of complex mixtures can be resolved by use of an appropriate chromatographic column. Six capillary columns of varying polarity were evaluated for the separation of the 50 component phenolic mixture. Six or more different temperature programs were tested for each column. Table II indicates the retention times using the optimum temperature program for each column. It is apparent that the HP-1 and DB-5 columns gave the greatest number of resolved peaks (resolution defined as 20%

TABLE II

RETENTION TIMES OF 50 PHENOLIC COMPOUNDS ON SIX DIFFERENT CAPILLARY COLUMNS WITH OPTIMUM TEMPERATURE PROGRAMS

No.	Compound	Retention time (min)					
		HP-1	DB-5	DB-17	DB-1701	DB-210	Nukol
1	Phenol	18.364	9.436	16.05	19.148	8.173	27.471
2	2-Methylphenol	23.286	11.951	18.978	20.637	9.885	27.226
3	3-Methylphenol	24.840	12.721	19.794	21.722	10.845	31.159
4	4-Methylphenol	24.761	12.691	19.824	21.722	10.810	30.807
5	2,3-Dimethylphenol	32.186	16.458	24.191	24.180	13.095	33.462
6	2,4-Dimethylphenol	30.040	15.346	22.601	23.117	12.503	30.616
7	2,5-Dimethylphenol	30.218	15.405	23.150	23.131	12.590	30.474
8	2,6-Dimethylphenol	26.952	13.827	21.148	21.086	11.600	22.484
9	3,4-Dimethylphenol	33.262	17.014	24.698	25.056	14.797	36.443
10	3,5-Dimethylphenol	31.610	16.129	23.329	24.222	13.791	34.585
11	2,3,5-Trimethylphenol	38.643	19.852	27.343	26.473	16.261	36.365
12	2,3,6-Trimethylphenol	36.044	18.400	26.045	24.616	15.257	28.915
13	2,4,6-Trimethylphenol	34.110	17.390	24.631	23.702	14.050	26.859
14	2-Ethylphenol	29.288	14.957	22.247	22.943	11.654	30.139
15	3-Ethylphenol	31.600	16.142	23.533	24.393	13.329	34.856
16	4-Ethylphenol	31.328	16.028	23.447	24.333	13.186	34.594
17	2-Chlorophenol	19.060	9.699	15.907	16.880	8.255	19.775
18	3-Chlorophenol	33.630	17.134	24.690	26.951	13.956	42.581
19	4-Chlorophenol	33.477	17.155	25.180	26.968	14.442	42.409
20	2,3-Dichlorophenol	32.016	16.341	24.135	23.025	13.388	35.606
21	2,4-Dichlorophenol	31.454	16.013	23.213	23.488	12.922	35.041
22	2,5-Dichlorophenol	31.702	16.102	23.150	23.586	12.895	35.678
23	2,6-Dichlorophenol	33.804	17.300	25.278	23.787	14.990	32.314
24	3,4-Dichlorophenol	44.917	24.761	33.405	33.096	20.706	59.649
25	3,5-Dichlorophenol	44.188	23.955	31.333	32.581	18.925	55.805
26	2,3,4-Trichlorophenol	43.151	23.153	31.676	29.804	19.236	45.678
27	2,3,5-Trichlorophenol	41.822	21.972	29.428	28.821	17.389	44.114
28	2,3,6-Trichlorophenol	43.786	23.723	32.273	29.446	20.328	43.851
29	2,4,5-Trichlorophenol	42.890	22.822	30.511	29.803	18.741	45.768
30	2,4,6-Trichlorophenol	42.543	22.644	30.396	28.454	18.885	41.614
31	3,4,5-Trichlorophenol	50.289	30.741	38.772	36.306	24.893	ND
32	2,3,4,5-Tetrachlorophenol	48.995	29.128	37.342	ND[a]	23.541	ND
33	2,3,5,6-Tetrachlorophenol	48.862	29.004	37.213	33.073	23.744	ND
34	Pentachlorophenol	52.859	32.240	40.532	ND	26.775	ND
35	2-Chloro-5-methylphenol	26.418	13.377	19.816	19.987	11.072	23.765
36	4-Chloro-2-methylphenol	38.294	19.787	27.940	28.230	16.787	42.034
37	4-Chloro-3-methylphenol	39.404	20.458	28.605	29.024	17.307	44.250
38	2-Bromophenol	24.221	12.370	19.805	19.414	10.120	25.913
39	3-Bromophenol	39.173	20.292	28.812	29.611	16.583	47.789
40	4-Bromophenol	39.027	20.287	29.200	29.635	17.060	47.049
41	2,4-Dibromophenol	42.017	22.297	31.272	28.619	18.030	43.629
42	2,6-Dibromophenol	43.319	23.394	32.971	28.618	19.942	40.808
43	2-Nitrophenol	28.255	14.726	22.758	20.735	15.873	19.143
44	3-Nitrophenol	46.620	26.812	36.638	35.011	25.475	ND
45	4-Nitrophenol	48.010	28.569	38.277	36.123	26.775	57.577
46	2,4-Dinitrophenol	46.934	27.628	37.575	ND	27.810	ND
47	2,5-Dinitrophenol	45.079	26.312	36.547	ND	26.984	ND
48	2,6-Dinitrophenol	48.214	29.506	39.281	34.621	28.927	ND
49	3,4-Dinitrophenol	55.344	33.839	ND	ND	ND	ND
50	2,3,5,6-Tetramethylphenol	42.884	22.877	30.663	27.940	18.680	34.747

[a] ND = Not detected.

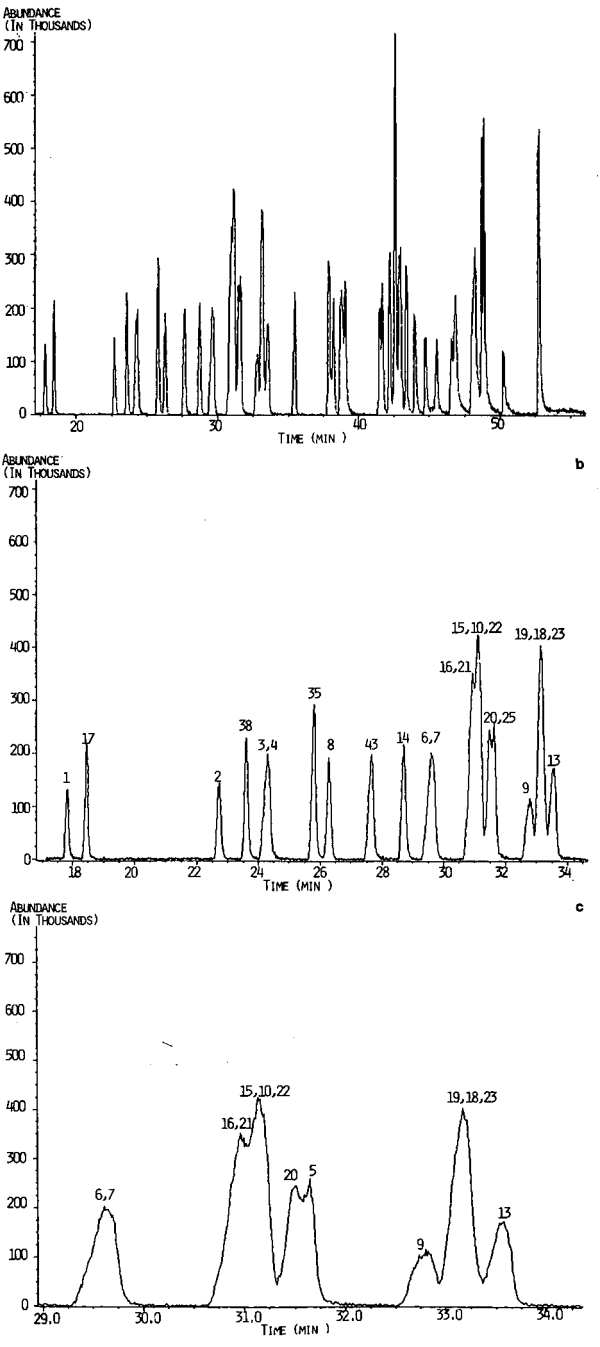

Fig. 1.

(*Continued on p. 304*)

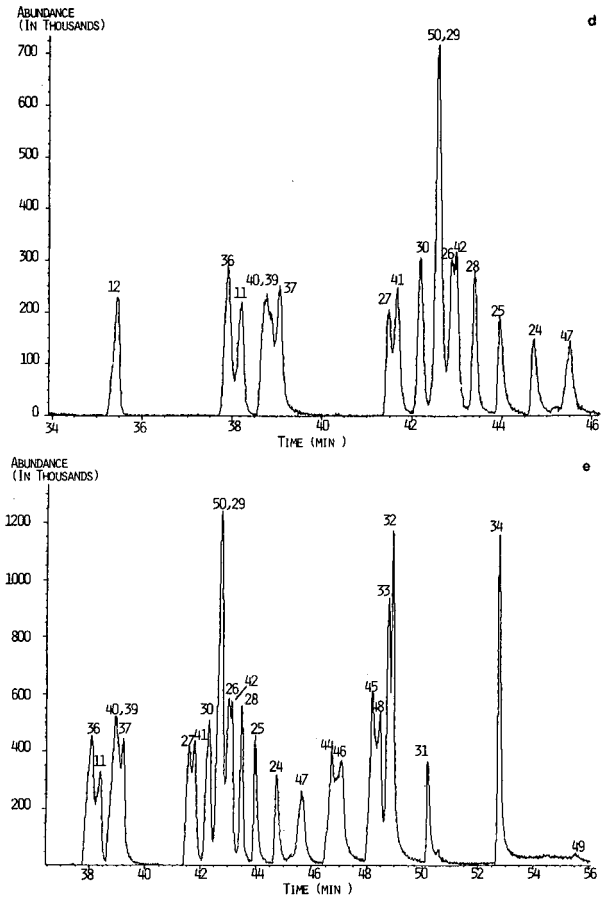

Fig. 1. Standard (a) and expanded (b–e) chromatograms of the 50 phenolics analysed on the HP-1 column using the optimum temperature program. TIC = Total ion chromatogram.

peak to valley); slightly superior peak resolution favoured the use of the HP-1 column. Both columns operate primarily on the principle of dispersive interactions; with each the maximum number of peaks observed at the 100 ng injection level was found to be 41 when 50 compounds were injected. Co-elution was still a problem in that some compounds could not be resolved (*e.g.* 3- and 4-methylphenol, 2,4- and 2,5-dimethylphenol, 2,3,5,6-tetramethylphenol and 2,4,5-trichlorophenol) and some other compounds were only partially resolved. A typical chromatogram for the HP-1 column is shown in Fig. 1. The added selectivity afforded by use of other columns with potential dipole, and acid–base phase interactions proved useful in providing separation of some of the compounds; however, these interactions also resulted in losses of significant numbers of highly polar phenolics. This effect is demonstrated by the results of the high polarity Nukol column tested which gave the worst performance of all the columns in terms of the number of compounds lost during chromatography. These findings are consistent with those of Korhonen [8,9]. He reported on

TABLE III

DETECTION LIMITS (ng/μl) AND LINEAR DYNAMIC RANGE FOR TARGET PHENOLIC COMPOUNDS FROM STANDARDS PREPARED AS TEN COMPOUND MIXTURES

No.	Compound	IR		MS	
		High	Low[a]	High	Low
1	Phenol	200	40	400	20
2	2-Methylphenol	500	50	500	20
3	3-Methylphenol	500	20	500	20
4	4-Methylphenol	450	40	450	40
5	2,3-Dimethylphenol	500	30	300	20
6	2,4-Dimethylphenol	400	20	400	10
7	2,5-Dimethylphenol	200	50	400	10
8	2,6-Dimethylphenol	350	40	350	10
9	3,4-Dimethylphenol	600	50	600	40
10	3,5-Dimethylphenol	400	50	400	10
11	2,3,5-Trimethylphenol	400	50	400	10
12	2,3,6-Trimethylphenol	500	20	500	10
13	2,4,6-Trimethylphenol	600	20	600	10
14	2-Ethylphenol	300	20	300	20
15	3-Ethylphenol	600	20	300	10
16	4-Ethylphenol	500	70	500	20
17	2-Chlorophenol	400	30	400	10
18	3-Chlorophenol	400	50	400	10
19	4-Chlorophenol	300	50	400	40
20	2,3-Dichlorophenol	600	40	700	20
21	2,4-Dichlorophenol	400	40	500	30
22	2,5-Dichlorophenol	400	40	400	20
23	2,6-Dichlorophenol	400	30	400	20
24	3,4-Dichlorophenol	300	70	300	60
25	3,5-Dichlorophenol	400	40	500	20
26	2,3,4-Trichlorophenol	400	50	400	40
27	2,3,5-Trichlorophenol	400	50	400	50
28	2,3,6-Trichlorophenol	250	20	600	20
29	2,4,5-Trichlorophenol	300	70	450	70
30	2,4,6-Trichlorophenol	700	50	700	10
31	3,4,5-Trichlorophenol	1200	30	1000	70
32	2,3,4,5-Tetrachlorophenol	300	70	600	50
33	2,3,5,6-Tetrachlorophenol	200	50	500	50
34	Pentachlorophenol	600	80	600	60
35	2-Chloro-5-Methylphenol	400	30	400	20
36	4-Chloro-2-Methylphenol	250	60	400	20
37	4-Chloro-3-Methylphenol	250	40	500	30
38	2-Bromophenol	300	20	700	20
39	3-Bromophenol	600	50	600	40
40	4-Bromophenol	400	40	400	20
41	2,4-Dibromophenol	600	50	600	40
42	2,6-Dibromophenol	300	40	400	30
43	2-Nitrophenol	400	20	500	40
44	3-Nitrophenol	400	50	400	70
45	4-Nitrophenol	400	70	600	80
46	2,4-Dinitrophenol	800	100	800	120
47	2,5-Dinitrophenol	800	100	800	150
48	2,6-Dinitrophenol	1200	100	1200	170
49	3,4-Dinitrophenol	600	300	600	300
50	2,3,5,6-Tetramethylphenol	150	30	320	20

[a] Signal-to-noise ratio 3.

TABLE IV

METHODS OF CALIBRATION FOR 50 PHENOLICS COMPOUNDS

No.	Compound	Method
1	Phenol	Total response of IR and MS
2	2-Methylphenol	Total response of IR and MS
3	3-Methylphenol	IR method, absorption *vs.* concentration at a single wavelength (1600 or 1156 cm^{-1})
4	4-Methylphenol	IR method, absorption *vs.* concentration at a single wavelength (1515 or 1174 cm^{-1})
5	2,3-Dimethylphenol	MS: mass range: 106.5–122.5
6	2,4-Dimethylphenol	IR method, absorption *vs.* concentration at a single wavelength (3656 or 2933 cm^{-1})
7	2,5-Dimethylphenol	IR method, absorption *vs.* concentration at a single wavelength (1515 or 1230 cm^{-1})
8	2,6-Dimethylphenol	Total response of IR and MS
9	3,4-Dimethylphenol	MS: mass range: 106.5–122.5
10	3,5-Dimethylphenol	MS: mass range: 120.5–121.5
11	2,3,5-Trimethylphenol	Total response of IR and MS
12	2,3,6-Trimethylphenol	Total response of IR and MS
13	2,4,6-Trimethylphenol	MS: mass range: 106.5–122.5
14	2-Ethylphenol	Total response of IR and MS
15	3-Ethylphenol	IR method, absorption *vs.* concentration at a single wavelength (1600 of 1155 cm^{-1})
16	4-Ethylphenol	IR method, absorption *vs.* concentration at a single wavelength (1514 or 1174 cm^{-1})
17	2-Chlorophenol	Total response of IR and MS
18	3-Chlorophenol	MS: mass range: 127.5:128.5
19	4-Chlorophenol	MS: mass range: 127.5–128.5
20	2,3-Dichlorophenol	MS: mass range: 125.5–164.5
21	2,4-Dichlorophenol	MS: mass range: 125.5–164.5
22	2,5-Dichlorophenol	MS: mass range: 125.5–164.5
23	2,6-Dichlorophenol	MS: mass range: 161.5–164.5
24	3,4-Dichlorophenol	Total response of IR and MS
25	3,5-Dichlorophenol	Total response of IR and MS
26	2,3,4-Trichlorophenol	MS: mass range: 195.5–198.5
27	2,3,5-Trichlorophenol	MS: mass range: 195.5–198.5
28	2,3,6-Trichlorophenol	Total response of IR and MS
29	2,4,5-Trichlorophenol	MS: mass range: 195.5–198.5
30	2,4,6-Trichlorophenol	MS: mass range: 195.5–198.5
31	3,4,5-Trichlorophenol	Total response of IR and MS
32	2,3,4,5-Tetrachlorophenol	Total response of IR and MS
33	2,3,5,6-Tetrachlorophenol	Total response of IR and MS
34	Pentachlorophenol	Total response of IR and MS
35	2-Chloro-5-Methylphenol	Total response of IR and MS
36	4-Chloro-2-Methylphenol	Total response of IR and MS
37	4-Chloro-3-Methylphenol	MS: mass range: 106.5–142.5
38	2-Bromophenol	Total response of IR and MS
39	3-Bromophenol	MS: mass range: 171.5–174.5
40	4-Bromophenol	MS: mass range: 171.5–174.5
41	2,4-Dibromophenol	MS: mass range: 251.5–254.5
42	2,6-Dibromophenol	MS: mass range: 251.5–254.5
43	2-Nitrophenol	Total response of IR and MS
44	3-Nitrophenol	MS: mass range: 138.5–139.5
45	4-Nitrophenol	MS: mass range: 138.5–139.5
46	2,4-Dinitrophenol	MS: mass range: 183.5–184.5
47	2,5-Dinitrophenol	Total response of IR and MS
48	2,6-Dinitrophenol	MS: mass range: 183.5–184.5
49	3,4-Dinitrophenol	Total response of IR and MS
50	2,3,5,6-Tetramethylphenol	MS: mass range: 134.5–150.5

the unsuitability of OV-351 and free fatty acid phase column liquid phases for the analysis of phenolic compounds, particularly the chloro substituted phenolics; these columns are similar to the Nukol column in terms of polarity. The column related losses were highlighted by 3,4-dinitrophenol which proved universally difficult to analyze due to poor peak shape and tailing. The low sensitivity to this compound is likely due to significant losses of the compound occurring in the chromatographic column or on the detector surfaces rather than the inherent detector limitations. Interesting features of the Nukol column were its ability to resolve completely two pairs of isomers, 3- and 4-methylphenol, 3- and 4-ethylphenol and to resolve partly 2,4- and 2,5-dimethylphenol compounds which are not easily resolved with the other columns. This revealed the advantage offered by the more polar Nukol column for separation of certain phenolic isomers. Unfortunately, other groups of phenolics appeared to remain unresolved with this column.

System calibration

Calibration of the GC–IR–MS system was performed by injection of working standard solution prepared as ten compound mixtures. The total ion chromatogram (MS) and the total response chromatogram (IR) were used to set up the calibration curves. Because of the limitation on carrier gas flow (0.5 ml/min) to the MS only about 20% of the amount injected was transmitted to the MS. The linear range observed for each compound is given in Table III; the detection limits for each phenolic were estimated based on the calibration curves and on a signal-to-noise ratio of three. These values represent the identification and quantitation limits for each phenolic. Essentially all compounds gave linear calibration with MS over the range indicated. Non-zero intercepts were evident indicating that some adsorption of phenolic compounds may have occurred in the chromatographic system. Many of the phenolics showed linear calibration with the IR, but some exhibited complex deviations from linearity. In part, these are explainable by light absorption which deviated from the Lambert–Beer law. Calibration tests with the 50 compound mixtures gave similar results except that the co-elution of certain phenolics complicated the method of quantitation and gave somewhat narrower dynamic ranges and higher detection limits. For co-eluting compounds with similar mass spectra but unique IR features, the method of choice for determination of concentration was based on the IR response. In this method the total IR absorption spectrum is obtained first and the spectral subtraction was performed to obtain the pure IR spectrum. For example, the IR spectrum of coeluted 3,5-dimethylphenol and 3-ethylphenol, which have similar mass spectra, was subtracted by the 3,5-dimethylphenol spectrum to obtain a pure spectrum of 3-ethylphenol. The wavelength unique for the specific compound was selected to generate a response relationship. These are generally characterized by non-zero intercepts, a narrow linear range and a saturation of response at higher concentrations. Where co-elution of non-isomeric phenolic compounds occurred the phenols generally exhibited unique mass spectra. Hence a characteristic mass for the compound could be selected and its response utilized to generate a calibration curve. The calibration curves for these compounds were generally linear. For compounds that were chromatographically resolved, calibration was based on the total ion chromatogram (MS) or the total response chromatogram (IR) depending on which gave optimum response. In general these compounds gave linear relationships. Table IV summarises the selected detector and method of calibration for each phenol.

TABLE V

RESULTS OF UNKNOWN SAMPLE ANALYSES

Sample No.	Compound identification	Quantitation (ng/μl)			
		IR Result	MS Result	Design concentration	Detection limit
1	3-Methylphenol	100/98/106	–[b]	100	60
	2,4-Dimethylphenol	82/90/104	–	100	30
	2,4,6-Trimethylphenol	–	57/58/58	100	30
	3-Chlorophenol	ND/ND/ND[a]	ND/ND/ND	100	30
2	Blank solvent	ND	ND	ND	–
3	2-Methylphenol	538	502	500	20
	2,6-Dimethylphenol	57	40	40	20
	4-Ethylphenol	578	–	500	70
	2,6-Dichlorophenol	–	117	100	20
	3-Bromophenol	–	198	250	30
	2,4,6-Trichlorophenol	–	100	100	30
	3,4-Dichlorophenol	ND	ND	40	50
	2,4-Dinitrophenol	–	105	250	120
4	2-Methylphenol	380	240	250	20
	4-Ethylphenol	72	–	40	70
	3-Bromophenol	–	64	100	30
	3,4-Dichlorophenol	906	375	500	50
5	Phenol	100	98	100	20
	3-Methylphenol	75	–	100	60
	2-Bromophenol	102	110	100	20
	3-Bromophenol	–	58	100	30
	4-Chloro-3-Methylphenol	–	41	100	30
6	2-Methylphenol	ND	ND	10	20
	2,6-Dimethylphenol	ND	ND	0.8	20
	4-Ethylphenol	ND	–	10	70
	2,6-Dichlorophenol	–	ND	2	20
	3-Bromophenol	–	ND	5	30
	2,4,6-Trichlorophenol	–	ND	2	30
	3,4-Dichlorophenol	ND	ND	0.8	50
	2,4-Dinitrophenol	–	ND	5	120
7	2-Methylphenol	470	630	500	20
	2,6-Dimethylphenol	35	53	40	20
	4-Ethylphenol	549	–	500	70
	2,6-Dichlorophenol	–	120	100	20
	3-Bromophenol	–	230	250	30
	2,4,6-Trichlorophenol	–	130	100	30
	3,4-Dichlorophenol	ND	ND	40	50
	2,4-Dinitrophenol		270	250	120
8	2-Methylphenol	96	98	100	20
	2,6-Dimethylphenol	300	260	250	20
	2,6-Dichlorophenol	–	510	500	20
	2,4,6-Trichlorophenol	–	460	500	30
	2,4-Dinitrophenol	–	ND	40	120

TABLE V (*continued*)

Sample No.	Compound identification	Quantitation (ng/μl)			
		IR Result	MS Result	Design concentration	Detection limit
9	2-Methylphenol	ND	ND	40	20
	3-Bromophenol	–	ND	40	30
	2,4-Dinitrophenol	–	ND	100	120
10	3-Ethylphenol	141/146/145	–	100	90
	2,3,5,6-Tetramethylphenol	–	118/129/123	100	30
	2,4,5-Trichlorophenol	–	93/88/92	100	70
11	2,6-Dimethylphenol	80	94	100	20
	4-Ethylphenol	100	–	100	70
	2,6-Dichlorophenol	–	240	250	20
12	2-Methylphenol	604	400	500	20
	2,6-Dimethylphenol	26	38	40	20
	4-Ethylphenol	530	–	500	70
	2,6-Dichlorophenol	–	82	100	20
	3-Bromophenol	–	120	250	30
	2,4,6-Trichlorophenol	–	86	100	30
	3,4-Dichlorophenol	ND	ND	40	50
	2,4-Dinitrophenol	–	140	250	120
13	Phenol	103	84	100	20
	3-Ethylphenol	94	–	100	90
	3,5-Dimethylphenol	–	88	100	30
	2,3,5,6-Tetramethylphenol	–	69	100	30
14	2,6-Dimethylphenol	600	500	500	20
	2,6-Dichlorophenol	–	40	40	20
	2,4,6-Trichlorophenol	–	46	40	30
	3,4-Dichlorophenol	58	67	100	50
	2,4-Dinitrophenol	–	380	500	120
15	2-Methylphenol	ND	ND	25	20
	2,6-Dimethylphenol	ND	ND	2	20
	4-Ethylphenol	ND	–	25	70
	2,6-Dichlorophenol	–	ND	5	20
	3-Bromophenol	–	ND	12.5	50
	2,4,6-Trichlorophenol	–	ND	5	30
	3,4-Dichlorophenol	ND	ND	2	50
	2,4-Dinitrophenol	–	ND	12.5	120
16	4-Ethylphenol	300	–	250	70
	3-Bromophenol	–	360	500	50
	2,4,6-Trichlorophenol	–	240	250	30
	3,4-Dichlorophenol	210	160	250	50

[a] ND = Not detected in sample.
[b] Not quantitated in sample.

Unknown test results

The ability of the GC–IR–MS system to identify and quantitate co-eluting phenolics was assessed by analysis of sixteen check samples fortified with compounds/

concentrations unknown to the analyst. Optimum HP-1 column conditions were used and quantitation was based on calibration data derived from composite standard solutions containing all 50 target phenolics using the method of quantitation outlined in Table IV. The phenolics present in the check samples were identified by retention time and by use of the spectral libraries. For co-eluting compounds the spectral subtraction technique (IR) or selected ion method (MS) were employed as appropriate to identify the individual phenolics; quantitation of the phenolics was based on the method reported in Table IV.

The composition and concentrations of the check samples are given in Table V together with the results obtained by IR and MS analysis. Sample 2 was a solvent blank and samples 3, 7 and 12 were replicate aliquots of the same solution. In general the phenolic compounds were correctly identified in the check samples when the compounds were present at concentrations substantially above the detection limit. No false positives were reported and no phenolics were reported in the blank solvent (sample 2) or in samples (6 and 15) in which fortification of the phenols was at levels at or below the instrument detection limit. The quality of the quantitative data varied from compound to compound and to some extent depended on the method of quantitation. Good agreement was obtained between sample data and the design concentration for 2,6-dimethylphenol (samples 3, 6–8, 11, 12, 14 and 15) which had good chromatographic resolution and which was quantitated using total response of the two detectors. MS data were somewhat more accurate than IR data in the 40 to 500 ng/μl range and for the replicate samples (3, 7 and 12) fortified at 40 ng/μl the precision of the MS data (43.7 $\pm$ 8.1 ng/μl) was better than the precision of the IR data (39.3 $\pm$ 15.9 ng/μl). 3,4-Dichlorophenol is not reported as present in samples (3, 6, 7, 12 and 15), however, when present at twice the detection level or higher (samples 4, 14 and 16) it is correctly identified. Quantitation, however, indicate a consistently low bias for this compound of approximately 30%. When quantitation was carried out by selected mass MS, data for 2,4,6-trichlorophenol showed good accuracy in the 40 to 500 ng/μl range (samples 3, 6–8,12 and 14–16), and for the replicate samples (3, 7 and 12) fortified at 100 ng/μl the precision was reasonable (105 $\pm$ 23 ng/μl). When quantitation was carried out by single wavelength IR, data for 4-ethylphenol showed good accuracy in the 100 to 500 ng/μl range (samples 3, 4, 6, 7, 11, 12, 15 and 16) and for the replicate samples (3, 7 and 12) fortified at 500 ng/μl the precision was good (552 $\pm$ 24 ng/μl). For replicate samples (3, 7 and 12) accuracy and precision for 2-methylphenol (IR, 537 $\pm$ 67 ng/μl; MS, 511 $\pm$ 115 ng/μl), 3-bromophenol (MS, 183 $\pm$ 57 ng/μl) and 2,4-dinitrophenol (MS, 172 $\pm$ 87 ng/μl) was the least satisfactory. Its poor detection limit (120 ng/μl) and losses in the system are probable reasons for poor results found with 2,4-dinitrophenol. The poor performance with 2-methylphenol and 3-bromophenol is not as easily understood however. The reproducibility of analysis within the same sample is demonstrated by the triplicate analyses performed on samples 1 and 10 (precision was better than $\pm$ 10%).

CONCLUSIONS

The data clearly indicate the utility of a GC–IR–MS system for the identification and quantitation of phenolic compounds although detection limits determined with the system are higher than those found using GC–FID or GC–MS alone. Identi-

fication/quantitation of the phenolic compounds was faster using MS data analyses compared to using IR data analysis but IR detection was superior in identification of unknowns, especially for isomeric compounds. The coupling of the two detectors with the GC is a great advantage for the analysis of phenolic compounds.

ACKNOWLEDGEMENTS

Appreciation is expressed to Dr. D. Kane, Cap. D. Vanloon and Cpl. L. Baylis of DCIEM (Defence and Civil Institute for Environmental Medecine) for their support and assistance during the experiment. We thank DCIEM for provision of analytical instrumentation.

REFERENCES

1 *Report No. J1199*, Concord Scientific Corporation, Toronto, Oct., 1987.
2 W. Duncan and W. H. Soine, *J. Chromatogr. Sci.*, 26 (1988) 521–526.
3 M. I. Selala, J. J. Janssens, V. Coucke, S. Andries and P. J. C. Schepens, *J. Chromatogr.*, 489 (1989) 51–56.
4 C. J. Wurrey, *Trends Anal. Chem.*, 60 (1989) 52–58.
5 J. R. Cooper and C. L. Wilkins, *Anal. Chem.*, 61 (1989) 1571–1577.
6 D. F. Gurka, I. Farnham, B. B. Potter, S. Pyle, R. Titus and W. Duncan, *Anal. Chem.*, 61 (1989) 1584–1589.
7 K. Grob, *On-Column Injection in Capillary Gas Chromatography: Basic Technique, Retention Gaps, Solvent Effects*, Hüthig, Heidelberg, Basel, New York, 1987.
8 I. O. O. Korhonen, *Chromatographia*, 17 (1983) 195–199.
9 I. O. O. Korhonen, *J. Chromatogr.*, 303 (1984) 197–205.

Journal of Chromatography, 549 (1991) 313–324
Elsevier Science Publishers B.V., Amsterdam

CHROM. 23 326

Gas chromatographic determination of nitrophenols in atmospheric liquid water and airborne particulates

ROLAND HERTERICH
Lehrstuhl für Hydrologie, Universität Bayreuth, Postfach 101251, W-8580 Bayreuth (Germany)
(First received November 26th, 1990; revised manuscript received March 20th, 1991)

ABSTRACT

A method for the determination of nitrophenols in fogwater and atmospheric particles is presented. The gas chromatographic (GC) performances of the underivatized pure compounds and their corresponding acetate esters were compared using four fused-silica columns with three alternative detection modes, *viz.* mass-selective detection, nitrogen-specific detection and electron-capture detection (ECD). Splitless injection of pure nitrophenols suffered from adsorption in the GC system causing unacceptable imprecision in the quantification of semi-volatile nitrophenols. The separation of nitrophenols as their corresponding acetates and ECD improved the GC performance and the analytical results. Acetylation with acetic anhydride in alkaline aqueous solution was found to be a very specific, uncomplicated and rapid method of derivatization. Its high sensitivity and accuracy and excellent suitability for analysing complex aqueous samples such as fogwater is demonstrated in detail as part of a multi-residue procedure.

INTRODUCTION

In 1976, Noijma *et al.* [1] reported the identification of nitrated phenols as secondary pollutants in the urban atmosphere. In their study, and subsequently more intensively [2,3], smog chamber experiments provided evidence for the photochemical generation of nitrated phenols from primary emissions such as aromatic hydrocarbons and nitrogen oxides. However, these is also sufficient evidence for direct emissions from cars [4,5]. In view of the toxic potential of nitrophenol (some dinitrophenols have been used as pesticides with a broad application), it is surprising that the potential for formation of nitrophenols in the atmosphere has not yet been thoroughly investigated. Also, monitoring data have only sporadically been published [5–10]. In connection with research on forest decline, attention has recently been focused on high concentrations of nitrated phenols in atmospheric liquid water [5–8]. Concentrations in cloud- and fogwater exceeding 1 μmol l^{-1} for 4-nitrophenol and 0.5 μmol l^{-1} for highly phytotoxic dinitrophenols[4] raise the questions of the sources, the fate and also the possible toxic effects of these compounds in the corresponding forest ecosystems. Expecting more research activity in this field, we see a need for sophisticated and time-effective analytical schemes by which nitrophenols can be determined reliably in complex matrices such as fogwater, air samples, humic soils or foliage. Many analytical procedures published in recent years [11–14] (see Böhm *et al.* [14] for more

0021-9673/91/$03.50

literature) did not solve this analytical problem satisfactorily with respect to extraction efficiency, sensitivity and selectivity of detection.

Unlike polycyclic aromatics and semivolatile organochlorine pollutants, which can be efficiently extracted from water and separated from the more polar fraction of airborne organics with the help of silica or Florisil columns, similar procedures seem more complicated for polar nitrophenols. Among the great number of organic acids, phenols and carbonyls present in atmospheric samples, nitrophenols can only be separated by means of highly selective detection and/or a distinctive sample preparation taking into account their moderate vapour pressures [15]. With nitrophenols, high-performance liquid chromatography coupled with UV detection, preferably applied for the analysis of phenolic compounds, does not achieve the resolution capacity and selectivity of detection [14] that is achieved in modern gas chromatography (GC). Moreover all isomeric nitrophenols in the atmosphere must be properly identified first, partly without authentic standards. Therefore, it seemed most useful to develop a procedure with the option of GC coupled with mass selective (MS) detection.

In the past, the conversion of phenols to methyl, silyl and pentafluorobenzyl ethers or acetyl derivatives has widely been used to improve their GC performance [13,16,17]. Owing to progress in column manufacture, good chromatographic behaviour is now also claimed for acidic and highly polar underivatized nitrophenols [6] (see also technical notes of column manufacturers). In the first part of this paper pure nitrophenols and their corresponding acetates are compared with respect to their GC performance. Subsequently a modified procedure is presented for the derivatization of nitrophenols with acetic anhydride.

EXPERIMENTAL

Reagents and apparatus

Nitrophenol standards were purchased from Fluka and Aldrich internal standards 2,3,4,5-Tetrachlorophenol (TClP) and aldrin from Promochem. Technical-grade solvents were distilled twice before use. Stock standard solutions of individual nitrophenols of 2 g l^{-1} were prepared in acetone. Standard mixtures for the determination of recoveries and demonstration runs were prepared in pentane–acetone (5:1) (organic standard solution, Table I) and in 0.1 *M* potassium carbonate, referred to as an aqueous standard solution. Calibration samples consisted of an appropriate dilution of this aqueous standard solution in 1.95 ml of 0.1 *M* potassium carbonate. Internal standard solutions containing 10 μmol l^{-1} of TClP in 0.1 *M* potassium carbonate denoted quantification standard (IS_{TClP}), and 0.41 μmol l^{-1} of aldrin in hexane (injection standard, IS_{ALD}) were used. Nitrophenols and internal standards and their concentrations used in demonstration runs are given in Table I.

Bistabil continuous liquid–liquid extraction apparatus and centrifuge tubes were purchased from Brand (Wertheim, Germany). Modified frits of porosity 1 with a cylindrical reservoir 50 mm × 20 mm I.D.) were manufactured by Brand according to our design. GC-analysis was performed on a Varian 3700 instrument with electron-capture (ECD) and nitrogen thermionic-specific detection (TSD). GC–MS runs were made on a Hewlett-Packard HP 5890 gas chromatograph directly coupled to a Model 5790 mass-selective detector. New GC columns from Durabond (DB 5, and DB 17, both 30 m × 0.25 mm I.D., 0.25 μm) J & W (SE-54, 30 m × 0.25 mm I.D. 0.25 μm)

TABLE I

IDENTIFICATION NUMBERS OF NITROPHENOLS AND INTERNAL STANDARDS (IS)

Concentration of pure nitrophenols in the organic standard solution used in demonstration runs in Figs. 1a, 1b and 2a.

Identification number	Compound	Abbreviation	Concentration (μmol l^{-1})
1	2-Nitrophenol	2-NP	3.63
2	3-Methyl-2-nitrophenol	3M-2NP	1.91
3	4-Methyl-2-nitrophenol	4M-2NP	3.32
4	5-Methyl-2-nitrophenol	5M-2NP	1.90
5	2,6-Dinitrophenol	2,6-DNP	0.85
6	3-Nitrophenol	3-NP	6.27
7	2,4-Dinitrophenol	2,4-DNP	11.2
8	4-Nitrophenol	4-NP	5.27
9	4-Methyl-2,6-dinitrophenol	4M-2,6DNP	1.81
10	3-Methyl-4-nitrophenol	3M-4NP	4.44
11	6-Methyl-2,4-dinitrophenol	6M-2,4DNP	4.57
12	2,6-Dimethyl-4-nitrophenol	2,6dM-4NP	4.36
13	2,3,4,5-Tetrachlorophenol	IS_{TCIP}	0.50
14	Aldrin	IS_{ALD}	0.41

and Hewlett-Packard (Ultra 2, 25 m × 0.2 mm I.D., 0.33 μm) were tested. Injection sleeves were freshly silanized prior to the injection of pure nitrophenols.

Procedure

The analytical scheme is organized in six steps as follows: (1) sample extraction; (2) concentration; (3) dissolution in hexane; (4) acid–base partitioning; (5) derivatization with acetic anhydride; and (6) extraction of the acetylated nitrophenols into 1 ml of hexane.

Sample extraction. Atmospheric liquid water is continuously liquid–liquid extracted as follows: pour 80 ml of CH_2Cl_2 into a 250-ml Bistabil liquid–liquid extractor, carefully overlay the solvent with 250 ml of the sample containing 20 g of dissolved NaCl and allow most of the solvent to rinse down into the boiling reservoir. Wash the sample vessel with 30 ml of purified water and add the washings to the sample. Pour more water into the extraction apparatus until the solvent layer is about 20 mm high. Acidify with 0.4 ml of concentrated H_2SO_4, insert the frit, wash the empty sample vessel with 20 ml of CH_2Cl_2, and add the washings to the extractor. In some instances it may be necessary to improve the operation of the frits with the help of a small layer of sea sand in the solvent reservoir of the frits. Run the extraction for 5 h with moderate heat, keeping a flow of about 4 drops s^{-1} from the reflux condenser. After extraction, the solvent underlying the aqueous sample is combined with the solvent in the boiling reservoir. Atmospheric particles filtered from 50–500 m^3 of air on a glass-fibre filter are extracted ultrasonically with 80 ml of CH_2Cl_2. The extract is cleaned from the filter material by centrifugation or filtration over anhydrous Na_2SO_4.

Concentration. Extracts of CH_2Cl_2 are concentrated to about 3 ml by means of a rotary evaporator. The extract is transferred to a 10-ml narrow-bottomed cen-

trifuge tube. At this point storage is recommended until the number of samples has reached 20 or more, allowing the following steps to be done more efficiently.

Solvent exchange. Reduce the volume of CH_2Cl_2 extracts obtained after the previous step to 0.3 ml under a gentle stream of nitrogen with the tubes maintained at room temperature by means of a water bath. Fill to 4 ml with hexane and blow down to 3 ml.

Acid–base partitioning. Add 2.0 ml of 0.1 *M* K_2CO_3 buffer solution of the sample using a transfer pipette, shake vigorously, centrifuge to improve phase separation and transfer 1.95 ml of the buffer extract into a 10-ml round-bottomed centrifuge tube with the help of a transfer pipette and disposable plastic tips.

Derivatization. After atmospheric samples and calibration samples have been spiked with 50 μl of IS_{TCIP}, add exactly 75 μl of acetic anhydride using a transfer pipette, quickly seal the tube and shake it immediately, then open the tube.

Extraction of acetylated phenols. After completion of derivatization of all samples and standards, add 1 ml of IS_{ALD} (reaction time is not critical and hydrolysis of esters has not been observed). In order to drive out CO_2 and suppress coextraction of underivatized acids and phenols, add *ca.* 0.5 g of a mixture of K_2HPO_4 and KCl (2:1), raising the pH to *ca.* 6–7. Shake vigorously for about 10 s. Store the sample at −20°C until analysis within 1 week or remove the hexane extract from the frozen aqueous layer when further concentration or storage over several months is required.

RESULTS AND DISCUSSION

GC performance and detection of nitrophenols

Underivatized nitrophenols. Some pure nitrophenols have been reported to be successfully separated and quantified on suitable fused-silica capillary columns [6].

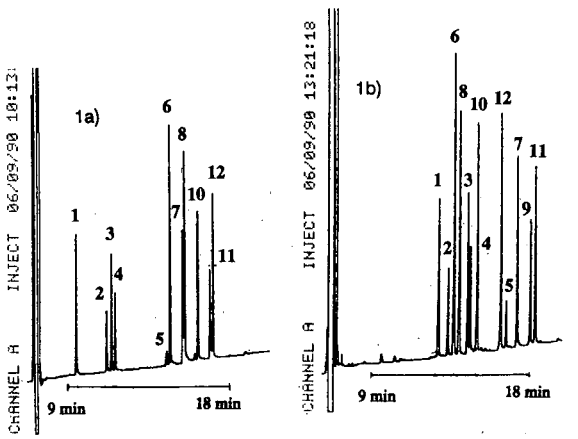

Fig. 1. GC performance of (a) pure nitrophenols and (b) corresponding nitrophenyl acetates on a new Ultra 2 column as specified with nitrogen-specific detection (TSD). Temperature programme: 50°C, held for 1 min, increased at 8°C min^{-1} to 270°C, held for 3 min. (a) Splitless injection of 2 μl of organic standard solution. Peak identification and concentrations as given in Table I. (b) The analytical procedure was started in step 4 (see *Procedure*), after 1 ml of organic standard solution had been redistributed in 3 ml of pentane. If complete derivatization and extraction are assumed, the concentrations of nitrophenyl acetates correspond to those listed in Table I.

Our efforts to determine pure, semi-volatile nitrophenols without the help of labelled standards, however, were not very encouraging, as shown in Fig. 1 and Table II. Comparing the chromatographic performances of underivatized nitrophenols on an HP Ultra 2 column (the most suitable for pure nitrophenols) with that of the corresponding acetates reveals better separation and better peak shapes of lower volatile 4-nitrophenols after acetylation. The precision of quantification (s_w) for underivatized 4-nitrophenols, 4-nitrocresols and dinitrophenols, referred to as semi-volatile nitrophenols (SVNP), turned out to be unsatisfactory, whereas more volatile 2-nitrophenols and 2-nitrocresols (VNP) exhibited excellent reproducibilities.

It must be noted that for demonstration purposes the concentrations of dinitrophenols were set disproportionately high in comparison with mononitrophenols (Table I). In real atmospheric samples 4-nitrophenol loadings normally exceed those of dinitrophenols considerably [5,8]. The low sensitivity for dinitrophenols (response factor, $RF_{TSD} = 2.55$) and high imprecision of quantification for all SVNPs indicate uncontrolled adsorption in the GC system. This is most valid for 2,4-DNP with the most acidic hydroxyl group ($pK_A = 3.91$) [15]. Theoretically the response factor of dinitrophenols on a nitrogen-specific detector should be $RF_{TSD} = 0.5$ if related of 2-NP. These great deviations between expected and measured TSD response factors suggest severe losses in the chromatographic system. Adsorption to active OH sites, existing in the GC inlet and on the column, is well known for semi-volatile polar compounds and for some nitrophenols in particular. This becomes obvious by a low specific response of dinitrophenols, their decreasing abundance with impurities in the inlet, column age and by parabolic calibration graphs (disproportionate response with increasing concentrations). Taking less volatile 3-NP as a reference compound for SVNPs hardly reduced the imprecision. Hence, shortcomings of injecting pure nitrophenols as described above can only be solved with the help of labelled standards. As critical SVNPs behave very differently in the chromatographic system one standard for each nitrophenol is necessary.

Nitrophenyl acetates. As is shown in Table II, acetylation improved the precision of quantification of SVNPs whereas it remained the same for VNPs. A similar quality of data was obtained for MS detection of acetylated mononitrophenols (not shown). Surprisingly, severe losses in sensitivity have been observed in MS detection of acetylated dinitrophenols. As we conclude from runs with TSD, this low sensitivity is not caused by incomplete derivatization of dinitrophenols alone (see below). Obviously dinitrophenyl acetates produce much less stable ions (*e.g.*, for 2,4-dinitrophenyl acetate the most abundant ions are $m/z = 226$, 184, 168 and 154) than acetylated mononitrophenols. Owing this disadvantage GC–MS quantification of nitrophenols as their acetates is of limited application.

Unacceptably high standard deviations for dinitrophenyl acetates measured with TSD (Table II) may be caused by uncontrolled discrimination in the injection port. Splitless injection and TSD of acetylated nitrophenols also showed severe deviations from linearity in calibration runs covering one order of magnitude. These sources of error, often lying in the injection port, can be substantially suppressed with on-column injection or injection in the split mode and quantitative analysis within a narrow range of concentration, *e.g.*, one order of magnitude. Split injection does not impair the sensitivity for acetylated nitrophenols if highly sensitive ECD is employed. However, in order to use ECD, prior effective sample clean-up is necessary.

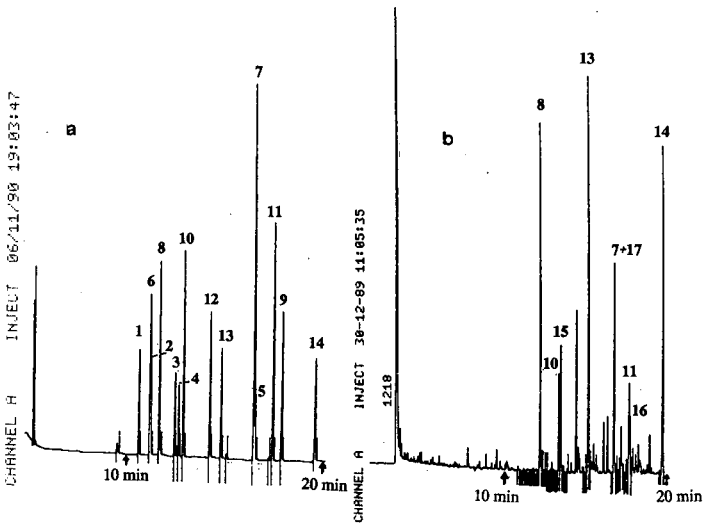

Fig. 2. GC–ECD of nitrophenyl acetates on a DB-17 column as specified. Chromatographic conditions and sensitivity as used in routine analysis: column temperature increased from 110 to 270°C at 6°C min^{-1}, splitting ratio 1:20, injection volume 2 μl. (a) Standard mixture obtained as decribed for Fig. 1b, diluted 1:2 prior to injection, giving *ca.* 0.4 pmol of 4-NP acetate on the column. (b) Moderately polluted cloudwater sample. Peaks: 15 = 2-M-4-NP; 16 = nitrated phenol (not further identified); and 17 = most probably 3-M-2,4DNP.

TABLE II

RESPONSE FACTORS (*RF*) IN RELATION TO 2-NP AND IMPRECISION (s_w, n = 4) OF VARIOUS PURE NITROPHENOLS AND THEIR CORRESPONDING ACETATES WITH NITROGEN TSD, MS AND ECD

s_w = (Standard deviation/mean value) · 100%.

Compound	Pure phenols[a]				Nitrophenyl acetates[b]			
	RF_{MS}	s_w (%)	RF_{TSD}	s_w (%)	RF_{TSD}	s_w (%)	RF_{ECD}	s_w (%)
2-NP	1.00	–	1.00	–	1.00	–	1.00	–
3M-2NP	2.59	6	1.09	1	1.09	2	[c]	
4M-2NP	0.84	4	1.02	1	0.97	2	0.94	1
5M-2NP	0.87	4	0.98	1	0.93	2	0.70	1
2,6-DNP	[d]		[d]		0.87	13	[c]	
3-NP	1.46	13	1.05	14	0.95	2	[c]	
2,4-DNP	4.45	29	2.55	38	2.83	17	0.75	4
4-NP	1.73	17	0.96	18	1.04	2	0.74	2
4M-2,6DNP	[d]		[d]		0.69	6	0.31	2
3M-4NP	2.74	14	1.03	16	1.02	2	0.58	1
6M-2,4DNP	1.44	25	1.64	29	1.23	6	0.46	2
2,6dM-4NP	0.65	19	0.94	6	0.96	7	0.78	3

[a] Concentration of organic standard solution as shown in Table I and used for Fig. 1a.
[b] For concentrations see Table I and legend of Fig. 1b.
[c] Coelution with another compound.
[d] Peak area to small.

Fortunately in alkaline solution acetic anhydride reacts preferably with phenolate anions to form corresponding acetates. This offers the opportunity of combining an acid–base extraction with a specific derivatization procedure in order to discriminate neutral compounds and organic acids. Fig. 2 may demonstrate that this easy and rapid fractionating leads to smooth chromatograms where all relevant aqueous phase nitrophenols can properly be quantified in a short run of 20 min. In samples of fogwater and atmospheric particles the peak of 2,4-DNP exactly combines with that of another nitrated phenolic compound, either 3-M-2,4-DNP or 5-M-2,4-DNP. These dinitrophenols (2,4-DNP, 2,6-DNP and *n*-M-2,4-DNP) are sufficiently separated on an SE-54 or an Ultra 2 column as specified. Despite a similar coating, the DB 5 column exhibited unacceptable peak tailing for nitrophenyl acetates.

Analysis of nitrophenols as nitrophenyl acetates

Derivatization and calibration graphs. The absolute recovery of the analytical procedure, starting in step 4 with 5 nmol of 4-nitrophenol in 3 ml of hexane, was measured to be 81%. This value is related to an equally concentrated standard solution of 4-nitrophenyl acetate in hexane. Incomplete extraction of the esters into 1 ml of hexane accounts for most of these losses. In contrast, extraction of nitrophenols from hexane into the K_2CO_3 solution (volume corrected as 1.95 ml out of 2 ml of buffer solution are recovered) and the yield of derivatization were determined for 4-nitrophenol to be close to 100%. Almost equal response factors of other mononitrophenols on a nitrogen-specific detector (RF_{TSD}) indicate a similar behaviour of all mononitrophenols in the acetylation procedure and the CG system. On the other hand considerably lower RF_{TSD} values for 6-M-2,4-DNP and most striking for 2,4-DNP (Table II) suggest incomplete acetylation. In addition, incomplete derivatization of dinitrophenols is also proved by coextraction of pure dinitrophenols and the remaining yellow colour of highly loaded buffer extracts after acetic anhydride has been added. It is also worth mentioning that the derivatization yields were higher for 4-M-2,6-DNP and 2,6-DNP than for 2,4-dinitrophenols.

In alkaline solution acetylation proceeds via a nucleophilic attack of the phenolate species on an acetyl C atom, producting acetic acid. Acetylation of phenols in alkaline media has to compete with the consumption of acetic anhydride by OH^- first, and with the final depression of pH to about 4 (using 75 μl of acetic anhydride for 2 ml of 0.1 *M* K_2CO_3). The derivatization yield should, therefore, depend greatly on the individual reaction velocity of the deprotonated species. Acetylation of phenolate anions with strong nucleophilic properties (indicated by high pK_A values of the corresponding acid) keeps pace with the pH depression and removal of acetic anhydride. This explanation fits well with increasing yields of acetylation in the order 4-NP (pK = 7.08) > 6-M-2,4-DNP (pK = 4.31) > 2,4-DNP (pK = 3.94).

Efforts to increase the derivatization yield included the use of different molarities of the K_2CO_3 buffer solution, replacement of K_2CO_3 with $KHCO_3$, variable amounts of acetic anhydride, elevated reaction temperatures and reaction times lasting from 1 min to several hours, but with no significant success. Parameters governing reproducibility of the derivatization reaction were found to be a constant volume of buffer solution and acetic anhydride and rapid mixing of the reactants. These conditions can be easily controlled in this micro-derivatization technique to give a linear and reproducible derivatization within a concentration range spanning at least one order of magnitude (Fig. 3).

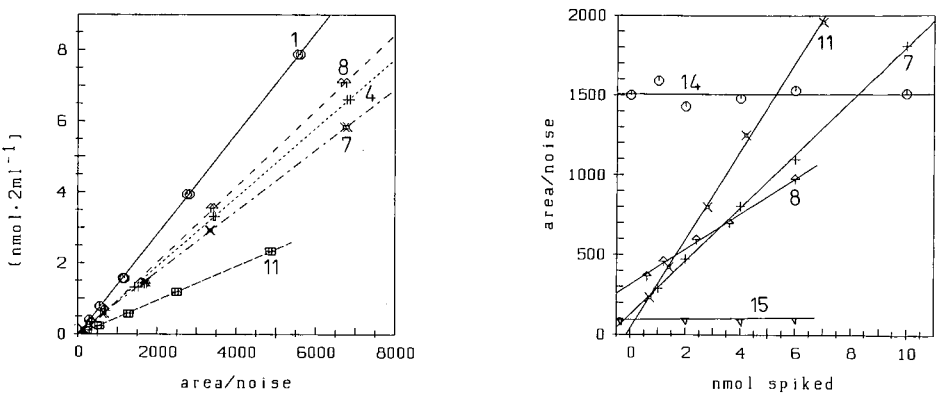

Fig. 3. Calibration lines for selected nitrophenyl acetates. Concentrations given refer to pure nitrophenols in calibration samples (1.95 ml of aqueous standard mixture plus 50 μl of IS_{TCIP}) ready to be derivatized. Noise calculated by the automatic peak threshold function of a Spectra-Physics integrator in front of the 2-NP peak.

Fig. 4. Determination of calibration data for a diluted fogwater sample using the standard addition method. 15 = Relative abundance of 2-M-4P (not spiked) in relation to the quantification standard IS_{TCIP}; 14 = relative abundance of Aldrin in relation to IS_{TCIP}.

Matrix effects. Incomplete derivatization may lead to variable yields of acetylation at different concentrations or from sample to sample. However, despite the incomplete conversion of dinitrophenols, acetylation proceeds rigorously, and is not affected by the addition of 1 ml of hexane, 0.1 g of NaCl, 10 μmol of benzoic acid and 10 μmol of *p*-cresol to 2 ml of buffer solution; note that these amounts are 1000 times higher than the nitrophenol content. Although none has been observed so far, any irregularity with the derivatization step can be readily checked for each individual sample by calculating the relative abundance of a neutral compound and one or more phenolic internal standards. Equal peak-height ratios of the quantification standard IS_{TCIP} (Fig. 4), which is acetylated and coextracted together with nitrophenols and the injection standard IS_{ALD} added after the derivatization step indicate the absence of concentration and matrix effects. Also some smaller peaks, *e.g.*, 2-M-4-NP, retain their initial peak area irrespective of the total amounts of phenols to be derivatized. Consequently, the results of quantitative analysis of a sample using response factors obtained from standard solutions did not deviate significantly from the concentrations measured by internal standard addition (Table III, Fig. 4). This check for matrix effects was applied to difficult samples such as samples of high inversion fogs and of canopy throughfall with no interference.

Recovery experiments and determination limits. Recoveries of analytical standards from spiked drinking water were determined for moderately concentrated samples (Table IV) and at a recommended lower limit of determination of one tenth of the concentration listed. Individual recoveries refer to the concentrations of nitrophenols in 1.95 ml of buffer solution obtained after step 4 (see *Procedure*), and do not include the losses in the derivatization reaction and the final extraction step. These losses are the same of calibration samples which are also prepared in 1.95 ml of buffer solution.

TABLE III

CONCENTRATION OF NITROPHENOLS IN THE BUFFER EXTRACT OF A DILUTED FOG-WATER SAMPLE OBTAINED AFTER STEP 4

Determined using calibration graphs for pure standards (= external calibration) and by means of the standard addition method. Two parellels were combined before injection. See also Fig. 4. H = sensitivity = dx/dc, where x = peak area/baseline noise in calibration runs of pure standards and c = concentration.

Compound	External calibration		Standard addition	
	μmol l^{-1}	H	μmol l^{-1}	H
4-NP	2.6	123	2.8	111
3M-4NP	0.81	174	0.75	167
2,4-DNP	0.63	152	0.67	149
6M-2,4DNP	0.15	271	0.15	276

As is shown, the total recovery, including buffer extraction, concentration and extraction from water, is excellent, Slightly higher standards deviations for dinitrophenols extracted from artificial aqueous samples are due to the derivatization reaction and the GC performance of these compounds. As the defined lower limit of determination in spiked drinking water the recovery was almost the same, with an imprecision still lower then 12% for SVNPs. At this level peak-to-noise ratios greater then 50:1 indicate that the overall sensitivity of this method is not fully exhausted.

Considerable losses occur in the extraction of VNPs from aqueous samples because of their coevaporation during the extraction and concentration step. However, this is not a problem as atmospheric liquid water usually shows VNP concentrations lower than 5 nmol l^{-1} and mostly less than 1% of 4-nitrophenol loadings [5,8,19]. Moreover, using this method the higher baseline noise in real rain- and fogwater samples impairs the proper determination of VNPs at their naturally occurring concentrations in rural areas. Apart from this, standard-derived imprecision

TABLE IV

RECOVERY FROM 250 ml OF SPIKED DRINKING WATER AND IMPRECISION (s_w, n = 5) OF THE OVERALL ANALYTICAL PROCEDURE

Compound	Level (nmol l^{-1})	Recovery (%)	s_w (%)
2-NP	20	61	23.0
4M-2NP	24	69	21.0
3M-2NP	10	80	15.0
5M-2NP	10	75	23.0
4-NP	22	98	3.4
3M-4NP	6	99	3.1
2,6dM-4NP	10	99	4.4
2,4-DNP	8	94	6.5
6M-2,4DNP	4	102	5.5

data and consequently lower limits of determination rarely apply for real samples. We also note that accurately defined limits of detection and determination imply reliable verification of the compounds measured. This rule, however, is often violated in highly sensitive but rather unspecific ECD and UV detection, if detection limits are calculated as a multiple of peak-to-noise ratios in calibration runs and peaks are identified from their retention times only. In view of this limitation, attention should be directed to the replicate analysis of real samples (Table V). At these low amounts compounds still can be verified in the individual sample using MS or TSD.

Quantitative analysis of a routine basis. Owing to the characteristics of ECD (high sensitivity but a narrow linear range), high-quality results necessitate multiple point calibration and a narrow span of concentrations. Dissociated nitrophenols exhibit an intense yellow colour, which offers the possiblity of dilution of unexpected highly loaded samples at this stage of the analytical scheme. As the individual composition of one kind of sample does not vary much from that of another, the concentration of the most abundant nitrophenols can be visually estimated within one order of magnitude. Hence one can adjust the concentration of the buffer extract to fit into the range of calibration samples. Addition of the quantification standard IS_{TCIP} after step 4 (see *Procedure*) also produces an equal abundance of the standard compound in calibration runs and samples to be measured. For many quantification problems in highly sensitive GC analysis, equal peak areas of the quantification standard should always be aimed at because a dependence of response factors on total amounts of the injected compound is a common observation. For this reason, addition of a quantification standard prior to the extraction and an optional dilution step is not generally recommended. However, such a compound with a known concentration in the sample, *e.g.*, 3-NP or *n*-M-3-NP, should be added to reveal accidental errors during sample preparation.

Whereas the sensitivity for mononitrophenyl acetates remained constant over several months and hundreds of runs, a substantial deterioration was observed for 2,4-dinitrophenyl derivatives owing to impurities in the injector and column ageing. Although linearity is not seriously hampered, replacement of sleeves and column

TABLE V

REPLICATE ANALYSIS OF SAMPLES OF CLOUDWATER AND ATMOSPHERIC PARTICLES AT DIFFERENT CONCENTRATION LEVELS

A1–4 = particulate matter collected with a single high-volume sampler. Filter cut up as indicated by given air volumes. CWa–d = cloudwater. CH_2Cl_2 extract of one sample divided into aliquots of corresponding water volumes.

Sample	Volume	2-NP	4M-2NP	4-NP	3M-4NP	2,4-DNP	6M-2,4DNP	Units (data)
A1	160 m^3	<0.5	<0.5	28	4.0	1.8	1.3	pmol m^{-3}
A2	80 m^3	<0.5	<0.5	30	4.2	2.0	1.2	(03/12/90)
A4	40 m^3	<0.5	<0.5	31	4.6	1.7	1.2	
CWa	125 ml	<2	<2	89	11.1	45	7.6	nmol l^{-1}
CWb	125 ml	<2	<2	88	10.6	41	7.6	(12/11/89)
CWc	25 ml	<2	<2	93	12.1	44	7.8	
CWd	15 ml	<2	<2	82	11.2	39	7.5	

shortening after about 100 injections proved useful. It is also good analytical practice to determine the calibration graph using standard mixtures that have been derivatized together with the samples.

Some applications with limited sample material, *e.g.*, dew, or difficult matrices, such as humic soil or plant material, demand an even lower measuring range than proposed. As the limits of determination mostly depend on the precision of extraction from water and the final GC quantification, enhanced sensitivity can be achieved by concentrating the final hexane extract prior to injection. Vapour pressures of the 2-nitrophenol acetates are significantly lower than for pure 2-nitrophenols, allowing a further concentration of the final hexane extract.

CONCLUSIONS

Quantitative extraction of water-soluble phenols from water using batch liquid–liquid extraction has always been unsatisfatory. Therefore, continuous liquid–liquid distribution and solid-phase adsorption techniques such as the use of anion-exchange resins, XAD columns [18] and more recently reversed-phase resins [11,19] have been employed. Reversed-phase extraction of nitrophenols from water seems to be the method of choice as is promises high recoveries also for volatile 2-nitrophenols and the omission of the time-consuming evaporation of the organic solvent. However, if large volumes of water ($V > 100$ ml) must be extracted, the effort required for complete and constant recoveries increases disproportionately. In addition, if a multi-residue procedure is employed, continuous liquid–liquid extraction proved to be more time effective.

The efficiency of extraction was found to be considerably dependent on the size and number of solvent droplets produced in the extraction apparatus. The original frits operated inefficiently and had to be modified. With this improvement the described procedure showed remarkably good results for the simultaneous extraction of nitrophenols ($4 < pK_A < 7.5$) and atrazine ($pK_A = 1.68$) [20]. To measure atrazine, the organic phase remaining after step 4 represents a purified extract which can be concentrated and injected into a GC-TSD of GC–MS system.

Adsorption of pure, semi-volatile nitrophenols in the inlet and active sites of the column was confirmed as giving serious problems in their GC determination. High-quality results might be obtained only by using labelled standards, which unfortunately are not yet commercially available. Even if this proves to be the case in the future, it must be emphasized that different physico-chemical properties of pure semi-volatile nitrophenols and excessive concentration and the injection of unpurified extracts, as practised in GC–MS analysis, will require one labelled standard for each compound of be measured.

Alternatively, nitrophenols can be determined as their nitrophenyl acetates with nitrogen-specific detection or highly sensitively with ECD without extra time-consuming clean-up steps. Good separation and determination of the seven most abundant nitrophenols, *i.e.*, 4-NP, 2-M-4-NP, 3-M-4-NP, 2,4-DNP, 6-M-2,4-DNP and two other N-methyl-2,4-dinitrophenols, in atmospheric liquid water and suspended particulate matter of the polluted and unpolluted atmosphere have been accomplished. With an additional purfication step this procedure also proved suitable for determining nitrophenols in humic soils and foliage. Vapour-phase measurements

using solid absorbents, however, require detailed investigations of possible artefact formation during sampling [5,21].

ACKNOWLEDGEMENTS

This investigation was funded by the Bayerisches Staatsministerium für Ernährung, Landwirtschaft und Forsten. I thank Ms. Christine O'Flynn for reading the English manuscript.

REFERENCES

1 K. Nojima, K. Fukaya, S. Fukui, S. Kanno, S. Nishiyama and Y. Wada, *Chemosphere*, 1 (1976) 25.
2 M. W. Gery, D. L. Fox, R. M. Kamens and L. Stockburger, *Environ. Sci. Technol.*, 21 (1987) 339.
3 D. Grosjean, *Atmos. Environ.*, 18 (1984) 1641.
4 R. Herterich, unpublished results.
5 R. Herterich and R. Herrmann, *Environ. Technol.*, 11 (1990) 961.
6 C. Leuenberger, J. Czuczwa, J. Tremp and W. Giger, *Chemospere*, 17 (1988) 511.
7 G. Rippen, E. Zietz, R. Frank, T. Knacker and W. Kloepffer, *Environ. Technol. Lett.*, 8 (1987) 475.
8 H. Richartz, A. Reischl, F. Trautner and O. Hutzinger, *Atmos. Environ.*, 24A (1990) 3067.
9 K. Kawamura and I. R. Kaplan, *Atmos. Environ.*, 22 (1986) 115.
10 C. Leuenberger, M. P. Ligocki and J. F. Pankow, *Environ. Sci. Technol.*, 19 (1985) 1053.
11 E. Chladek and R. S. Marano, *J. Chromatogr. Sci.*, 22 (1984) 313.
12 R. T. Coutts, E. E. Hargesheimer and F. M. Pasutto, *J. Chromatogr.*, 195 (1980) 105.
13 S. J. Theron and D. W. Hassett, *Water SA*, 12 (1986) 31.
14 H. B. Böhm, J. Feltes, D. Volmer and K. Levsen, *J. Chromatogr.*, 478 (1989) 399.
15 R. P. Schwarzenbach, R. Stierä, B. R. Folsom and J. Zeyer, *Environ. Sci. Technol.*, 22 (1988) 83.
16 J. Drozd, *Chemical Derivatization in Gas Chromatography*, Elsevier Amsterdam, 1981, p. 215.
17 E. Tesarova and V. Pacakova, *Chromatographia*, 17 (1983) 269.
18 C. D. Chriswell, R. C. Chang and J. S. Firtz, *Anal Chem.*, 47 (1975) 1325.
19 U. Kern, *Masters Thesis*, University of Bayreuth, 1990, p. 91.
20 G. Rippen, *Handbuch der Umweltchemikalien*, Ecomed, Landsberg, Lech, 1984, p. 202.
21 R. Herterich, in preparation.

Journal of Chromatography, 549 (1991) 325–333
Elsevier Science Publishers B.V., Amsterdam

CHROM. 23 338

Improved method for prediction of gas chromatographic retention indices of C_9–C_{12} alkylbenzenes

N. DIMOV*
Chemical Pharmaceutical Institute, Kl. Okhridsky Street 3, 1156 Sofia (Bulgaria)
and
E. MATISOVÁ
Department of Analytical Chemistry, Faculty of Chemical Technology, Slovak Technical University, 812 37 Bratislava (Czechoslovakia)

(First received November 14th, 1990; revised manuscript received March 26th, 1991)

ABSTRACT

The positive identification of higher alkylbenzene isomers is a difficult task even with a mass spectral detector. A preliminary calculative identification could serve for a better orientation in the obtained mass spectra as well as acting as a complementary and independent identification tool. An accurate equation for the prediction of retention indices of C_9–C_{12} alkylbenzenes and their temperature coefficients, dI/dT, on OV-101 is given. The basic parameter is the molecular mass, while tuning parameters include the kind of substitution and the carbon chain of the substituents. The correlation coefficient obtained for 94 alkylbenzenes is 0.9995 and the mean standard deviation is 2.7 units. The predictive possibilities of the equation are demonstrated by inter- and extrapolative calculations of the retention indices of certain isomers with experimentally measured retention data, but without the mass spectral assignment of the positions of substituents.

INTRODUCTION

Aromatic hydrocarbons are important in the petrochemical and related industries and in the environment. C_6–C_{15} aromatics represent the major part of the monoaromatic fraction of natural and synthetic hydrocarbon mixtures [1]. The positive identification of higher hydrocarbon isomers is difficult even with mass spectral detection. The role of capillary gas chromatography (GC) and combiend GC–mass spectrometry (GC–MS) for the identification of alkylbenzenes in multi-component hydrocarbon mixtures has been discussed in a recent review [2]. In that paper much space was devoted to the interlaboratory reproducibility of retention data. The best reproducibility was achieved on non-polar squalane and silicone stationary phases. However, owing to the low-temperature stability of squalane and therefore the long analysis times of alkylbenzenes above C_9, non-polar silicones such as SE-30, OV-101 and DB-1 are much more preferable. The limited number of practically significant non-polar stationary phases with very similar chromatographic properties makes the need for tabulated correct retention data (retention indices, I) of greater importance.

0021-9673/91/$03.50

Isothermal retention indices on OV-101 [3–9] and SE-30 [10,11] for alkylbenzenes up to C_{10} have been published. Whereas for C_6–C_8 and even C_9 arenes the different published data agree very well, for higher alkylbenzenes, particularly alkylbenzenes with short alkyl chains in the aromatic ring, the published retention data on OV-101 [3,6,7,9] are very far complete and the determination of reproducibility is not possible.

The most widely used combined technique, capillary GC–MS with electron impact ionization, can unambiguously identify alkylbenzenes of lower molecular mass. However, because of some drawbacks of this technique in the differentiation of higher structural isomers and the lack of standard materials, a preliminary, calculative identification seemed to be of great benefit. The so-called "chemometric" identification can contribute to identification and/or to a better understanding of quantitative structure–retention relationship of alkylbenzenes [10,12–20]. Some of the calculative methods are valid for homologous series only. The most accurate [21,22] need at least four members, which is almost impossible for higher isomers. The homomorphic factor [23], used in several papers, also shows ambiguous results for the higher isomers. The use of topological and/or electronic indices [15,16,19,20,24–26] has mostly applied to C_6–C_{10} alkylbenzenes.

A more versatile calculation method which could cover a large number of different isomers would be of greater importance. The aim of this paper is to present an accurate calculation method for the prediction of retention indices, I, and their temperature gradients, dI/dT, for C_9–C_{12} alkylbenzenes. The adequacy of the equation is assessed by comparison with experimentally measured retentions on an OV-101 capillary column [9] and is proved by comparison of inter- and extrapolative calculations of I values for certain isomers with experimentally measured retention data, but without the assignment of the positions of substituents. The most possible structures of these compounds are proposed.

THEORY

To overcome the lack of standard substances, the alkylation of benzene and its homologous under fixed conditions was performed [27]. The compound identification was based on combination of GC with MS, taking into account quantum-chemical kinetic calculations of the yields of different isomers and using homomorphic factors.

In this investigation we use another approximation of quantitative structure–retention relationships, published elsewhere [28]. The calculation is based on the following concepts:

(1) there are solute properties with the most significant influence on the retention on non-polar stationary phases; usually these are molecular mass (M_m), boiling point (T_b), vapour pressure (p_i), topological indices and other more or less extensive properties;

(2) there are specific solute properties (structure, charges, etc.), which tune the value of calculated basic retention and approximate it to the experimental value

$$R = f(B_i, T_j) \tag{1}$$

where R is the corresponding retention (in this study I), B_i are basic contributors (in

this study M_m) and T_j are tuning contributors (in this study the number, positions and C-chain of the substituents in the alkylbenzenes studied). Every statistically significant deviation of $I_{calc.}$ from $I_{exp.}$ is considered as the result of some tuning effects that have not been taken into account. Therefore, one is able to search for very specific solute feature(s) such as the known from practice *ortho* effect or the so-called propyl effect.

The experiments and the experimentally obtained retention data used in this investigation have been published elsewhere [9,27].

RESULTS AND DISCUSSION

The formulation of the regression equations was based on a linear model [28]. The molecular mass, M_m, is the only available extensive property of the higher isomers studied, which is why it is accepted as the B factor in eqn. 1. Structural parameters instead of topological and/or quantum-chemical indices are preferred as tuning contributors as the chemical interpretation in this instance is easier and clearer. Therefore, ten tuning parameters presenting all possible substitutions in the benzene ring (mono-, *o*-, *m*-, *p*-, etc.) are added as T factors in eqn. 1. The presence of a given substitution is denoted by 1 and its absence by 0. The regression analysis now shows the important influence of C-chain branching [9]. An eleventh tuning parameter accounting for this effect was also added. The general appearance of the final equation is

$$I_{calc.} = b_o + b_1 \cdot M_m + \Sigma b_n \cdot (i,j, \ldots, s) + b_{12} \cdot (\text{Corr.}) \quad (2)$$

where b_o–b_{12} are parameter estimates, M_m is the molecular mass of the corresponding alkylbenzene, $i,j, \ldots, s$ are the corresponding positions of the substituents in the benzene ring (mono-, 1,2-, ..., 1,2,3,4-, etc.) and the last tuning correction, Corr., is calculated on the basis of the following rules:

(1) the presence of one *tert.*-butyl group diminishes the relative retention expected on a M_m basis and instead of 1 for parameter evaluation a value of -4 is arbitrarily assigned. The presence of one isopropyl or sec.-butyl group is denoted by -2, for the same reason;

(2) the *ortho* location of the above groups with respect to an existing substituent demands additionally an increase in the correction and it becomes -5 and -3 respectively;

(3) the presence of normal-chain substituents increases the expected relative retention and for an ethyl group the necessary correction is $+0.3$, for an *n*-propyl group $+1$, for an *n*-butyl group $+3$ and for an *n*-pentyl group $+5$;

(4) additionally a correction of -1 is necessary if the normal-chain substituents have an inner *ortho*-location in a multi-substituted benzene.

The following examples illustrate the rules. 1,3-Diethyl-4-methylbenzene has two ethyl groups and the correction is $0.3 + 0.3 = 0.6$. One of the ethyl groups is between two other substituents and in an *ortho* position with respect to one of them; therefore, -1 is added. The final correction is -0.4. 1,3,5-Triethylbenzene has three ethyl groups and the correction is $3 \times 0.3 = 0.9$. 1-Ethyl-3-isopropylbenzene has one ethyl group ($+0.3$) and one isopropyl group, which need a correction of -2. The

final correction is −1.7. 1-Ethyl-4-*n*-butylbenzene has one ethyl and one butyl substituent and the correction is 0.3 + 3 = 3.3.

Eqn. 2 has a correlation coefficient $r = 0.998$, variance $s^2 = 26$ and $F = 29\,226$. The greatest discrepancy was found to be 10.5 i.u. This equation, hoewever, is not correct from a mathematical point of view, because the presence of a given substitution eliminates the other possibilities. That is why the values of the parametric estimates are constants only for M_m and Corr. factors while the values for the substitution factor depend on the number of compounds included in the regression.

To overcome this shortcomming, we introduce the relative value of the substitution factor, called the relative contribution, *RC*. Independent on the number of the compounds included in the regression, this relative contribution to the retention always shows the same importance of the different substitution positions. For 94 alkylbenzenes, the values of the relative contributions (monosubstitution taken as 1.0) are: 1,2-substitution = 1.892; 1,2,3-substitution = 3.242 and 1,2,3,4-substitution = 4.761. For *meta* substitution the value is 1.446 and for 1,3,5-substitution it is 1.8. *Para*-substitution has a distinct differentiation; for methylalkyl substituents it is 1.55 (alkyl means here number of C atoms in the substituent >2) and for alkylalkyl substituents, it is 1.7.

For 1,2,4- and 1,3,4-trisubstituted benzenes the value of *RC* is 2.532, for 1,2,3,5-tetrasubstituted benzenes 3.828 and for 1,2,4,5-tetrasubstituted benzenes 3.615. The following exact equation is created with the above-mentioned values of *RC*:

$$I_{calc.} = 237.33 + 5.5898M_m + 32.384RC + 9.249\text{Corr.} \quad (3)$$

with $r = 0.9995$ ($F = 108\,157$), variance $s^2 = 7.3$ and standard deviation only 2.7 i.u.

Using the corrections calculated above for 1,3-diethyl-4-methylbenzene, 1-ethyl-3-isopropylbenzene, 1,3,5-triethylbenzene and 1-ethyl-4-*n*-butylbenzene the following values of $I_{calc.}$ are obtained: 1,3-diethyl-4-methylbenzene (No. 55, Table I), $M_m = 148$, Corr. = −0.4, 1,3,4-substitution $RC = 2.532$, $I_{calc.} = 1143$, $I_{exp.} = 1149$; 1-ethyl-3-isopropylbenzene (No. 20, Table I), $M_m = 148$, Corr. = −1.7, *meta* substitution $RC = 1.446$, $I_{calc.} = 1095.7$, $I_{exp.} = 1092$; 1,3,5-triethylbenzene (No. 71, Table I), $M_m = 162$, Corr. = 0.9, 1,3,5-substitution $RC = 1.8$, $I_{calc.} = 1209.4$, $I_{exp.} = 1206$; 1-ethyl-4-*n*-butylbenzene (No. 39, Table I), $M_m = 162$, Corr. = 3.3, *para*-substitution $RC = 1.7$, $I_{calc.} = 1228.4$, $I_{exp.} = 1232$. The calculated results are compared with the experimental data in Table I. The highest discrepancy in all instances studied is 6 i.u.

The accuracy of the calculated indices is extremely good. Obviously the values obtained for the relative contribution to the retention represent clearly and in a quantitative manner the well known from practice *ortho* effect. Additionally, there is a linear regression between the values of *RC* for *ortho* substitution and the number of *ortho*-positions in the benzene ring. This allows us to calculate the *RC* value for pentasubstituted benzenes, −6.165 ± 0.002, and we are able to predict the *I* values of 1,2,3,4,5-pentamethylbenzene and 1,2,3,4-tetramethyl-5-ethylbenzene by extrapolation. The $I_{calc.}$ values coincide well with the experimental values (see Nos. 93 and 94 in Table I).

The values of the relative contributions show that there are also other effects: (i) a *meta* effect is clearly evident; (ii) branching of the substituent C-chain markedly

TABLE I

COMPARISON OF $I_{exp.}$ AND $dI/dT_{exp.}$ WITH $I_{calc.}$ AND $dI/dT_{calc.}$ VALUES AND THE DIFFERENCE $\Delta = I_{exp.} - I_{calc.}$

The experimental values are rounded to 1.0 and the calculated data to 0.1.

No.	Alkylbenzene[a]	$I_{exp.}$	$I_{calc.}$	Δ	$dI/dT_{exp.}$	$dI/dT_{calc.}$
1	iPrB	920	921.9	−1.9	0.280	0.281
2	nPrB	949	949.7	−0.7	0.265	0.300
3	tertBuB	987	981.7	5.3	0.310	0.300
4	secBuB	1005	1000.2	4.8	0.310	0.300
5	nBuB	1047	1046.4	0.6	0.270	0.300
5a	12DMB	–	–	–	0.290	0.310
6	1M2EB	973	972.1	0.9	0.305	0.310
7	12DEB	1051	1053.1	−2.1	0.310	0.310
8	1M2nPrB	1057	1056.8	0.2	0.334	0.310
8a	1M2iPrB	–	–	–	0.292	0.291
9	1E2iPrB	1098	1100.9	−2.9	0.314	0.291
9a	1E2PrB	–	–	–	0.284	0.310
10	1M2nPrB	1134	1137.9	−3.9	–	–
11	1M2nBB	1153	1153.6	−0.6	0.328	0.310
12	1iPrB2nPrB	1180	1185.6	−5.6	0.275	0.310
13	1M2nPeB	1249	1250.3	−1.3	0.310	0.310
14	12DiPrB	1150	1148.6	1.4	0.255	0.272
15	1E2secBuB	1177	1179.1	−2.1	–	–
15a	13DMB	–	–	–	0.245	0.259
16	1M3EB	955	957.7	−2.7	0.250	0.259
17	1M3iPrB	1013	1014.6	−1.6	0.235	0.240
18	1M3nPrB	1042	1042.4	−0.6	0.272	0.259
19	13DEB	1040	1038.7	1.3	0.244	0.259
20	1E3iPrB	1092	1095.7	−3.7	0.230	0.240
21	1M3secBuB	1093	1092.9	0.1	0.281	0.259
23	1M3nBuB	1140	1139.2	0.8	0.249	0.259
24	13DnPrB	1209	1208.2	0.8	0.260	0.259
25	1E3nBuB	1221	1220.2	0.8	0.250	0.259
26	1E3secBuB	1170	1173.9	−3.9	0.272	0.259
27	1nPr3iPrB	1176	1180.4	−4.4	0.238	0.240
28	1M3nPeB	1235	1235.9	−0.9	0.245	0.259
28a	14DMB	–	–	–	0.250	0.279
30	1M4iPrB	1016	1018	−2	0.263	0.260
31	1M4nPrB	1046	1045.8	0.2	0.280	0.279
32	14DEB	1046	1046.9	−0.9	0.265	0.279
33	1M4secBuB	1100	1096.3	3.7	0.282	0.279
34	1E4iPrB	1103	1103.9	−0.9	0.260	0.260
35	1M4nBuB	1146	1142.5	3.5	0.280	0.279
36	1E4secBuB	1185	1182.2	2.8	0.310	0.279
37	1nPr4iPrB	1190	1188.6	1.4	0.268	0.260
38	14DiPrB	1160	1160.9	−0.9	0.248	0.241
39	1E4nBuB	1232	1228.4	3.6	0.302	0.279
40	1M4nPeB	1241	1239.3	1.7	0.267	0.279
40a	14DnPrB	–	–	–	0.297	0.279
41	123TMB	1015	1013.1	1.9	0.370	0.341
42	12DM3EB	1094	1094.1	−0.1	0.360	0.341
42a	13DM2nPrB	–	–	–	0.303	0.341
43	12DE3MB	1170	1165.9	4.1	–	–
44	12DM3nPrB	1177	1178.8	−1.8	0.371	0.341

(*Continued on p. 330*)

TABLE I (*continued*)

No.	Alkylbenzene[a]	$I_{exp.}$	$I_{calc.}$	Δ	$dI/dT_{exp.}$	$dI/dT_{calc.}$
45	12DM3nBuB	1274	1275.6	−1.6	0.311	0.341
46	123TEB	1246	1246.9	−0.9	0.310	0.341
47	124TMB	987	990.1	−3.1	0.310	0.290
48	14DM2EB	1067	1061.8	5.2	0.300	0.290
49	13DM4EB	1069	1071.1	−2.1	0.310	0.290
50	12DM4EB	1074	1071.1	2.9	0.318	0.290
51	14DM2iPrB	1119	1118.8	0.2	0.255	0.270
52	13DM4iPrB	1123	1118.8	4.2	0.285	0.270
53	12DM4iPrB	1130	1128.1	1.9	0.287	0.270
54	14DM2nPrB	1148	1146.6	1.4	0.297	0.290
55	13DE4MB	1149	1143	6	0.305	0.290
56	13DM4nPrB	1152	1155.8	−3.8	0.302	0.290
56a	12DE4MB	–	–	–	0.300	0.290
56b	14DE2MB	–	–	–	0.305	0.290
57	12DM4nPrB	1158	1155.8	2.2	–	–
58	14DM2secBuB	1191	1197.1	−6.2	0.260	0.290
59	12DM4tertBuB	1192	1187.8	4.2	0.310	0.290
60	13DM4secBuB	1198	1197.1	0.9	0.312	0.290
61	12DM4secBuB	1210	1206.3	3.7	0.285	0.290
62	13DM4nBuB	1249	1252.6	−3.6	0.280	0.290
63	12DM4nBuB	1254	1252.6	1.4	–	–
64	124TEB	1223	1223.9	−0.9	0.288	0.290
65	14DM2nBuB	1243	1243.3	−0.3	–	–
66	135TMB	963	966.4	−3.6	0.240	0.228
67	13DM5EB	1048	1047.4	−0.6	0.240	0.228
68	13DM5iPrB	1103	1104.4	−1.6	0.215	0.209
69	13DE5MB	1130	1128.4	1.6	0.240	0.228
70	13DM5nPrB	1133	1132.1	0.9	0.235	0.228
71	135TEB	1206	1209.4	−3.4	0.195	0.228
72	13DM5secBuB	1179	1182.6	−3.6	0.227	0.228
73	13DM5nBuB	1229	1228.9	0.1	0.208	0.228
74	1234tMB	1139	1140.5	−1.5	0.440	0.424
75	124TM3EB	1215	1212.3	2.7	0.431	0.424
75a	124TM3nPrB	–	–	–	0.422	0.424
76	123TM4EB	1222	1221.5	0.5	–	–
77	1235tMB	1109	1110.3	−1.3	–	–
78	135TM2EB	1183	1182.1	0.9	0.324	0.331
79	125TM3EB	1184	1182.1	1.9	0.327	0.331
80	123TM5EB	1193	1191.3	1.7	0.340	0.331
81	135TM2nPrB	1263	1266.8	−3.8	0.346	0.331
82	125TM3nPrB	1277	1276	1	0.335	0.331
83	123TM5nPrB	1279	1276	3	–	–
84	135TM5iPrB	1238	1239	−1	–	–
85	123TM5iPrB	1246	1248.3	−2.3	0.295	0.312
86	1245tMB	1106	1103.4	2.5	0.347	0.352
87	124TM5iPrB	1233	1232.2	0.8	–	–
87a	124TM5EB	–	–		0.355	0.352
87b	124TM5nPrB	–	–		0.347	0.352
88	13DnPrB	1209	1208.2	0.8	–	–
89	14DnPrB	1221	1216.4	4.6	–	–
90	12DM35DEB	1264	1263.1	0.9	0.315	0.331
91	124TM3nPrB	1297	1297	0	–	–

TABLE I (*continued*)

No.	Alkylbenzene[a]	$I_{exp.}$	$I_{calc.}$	Δ	$dI/dT_{exp.}$	$dI/dT_{calc.}$
92	12DEEMB	1170	1165.9	4.1	–	–
93	12345pMB	1260	1264.2	−4.2	–	–
94	1234tM5EB	1344	1345.3	−1.3	–	–

[a] M = Methyl; E = ethyl; Pr = propyl; Bu = butyl; B = benzene; i = iso-; n = *n*-; sec = *sec.*-; tert = *tert.*-; D = di-; T = tri-; t = tetra-.

influences the retention (see also ref. 29); and (iii) the presence of an *ortho* substitution decreases the relative retention in both branched or normal C-chains equally.

Eqn. 3 is the most accurate given so far in the literature and it can be applied for predictive calculations. To increase the probability of the identification, however, we studied also the regression between the temperature increment of I (dI/dT) and the structure. Applying the same approach the following equation is obtained:

$$dI/dT_{calc.} = 196.63 + 103.57RC - 19.2(iPr) \quad (4)$$

with $r = 0.93$, $F = 520$ and the mean standard deviation = 0.017 i.u. for 89 alkylbenzenes, where (iPr) accounts for the presence (+1) or absence (0) of an isopropyl group. As seen from eqn. 4, in this instance the molecular mass does not play a significant role and the kind of substitution is the most important factor.

Using eqns. 3 and 4 we shall create hypotheses for the structural assignment of the alkylbenzenes, as mass spectra do not allow a positive identification [27] of positional isomers. Such a group of alkylbenzenes is the dimethyldiethylbenzenes (DiMeDiEtB). We found that all 1,2,3,4-tetrasubstituted DiMeDiEtB should have $I_{calc.}$ values between 1284 and 1302 i.u. and a dI/dT value of $0.424I$/°C. None of the experimental index values correspond to these values. Hence, *ortho*-tetrasubstituted DiMeDiEtB are not present in the mixture.

Other experimental I values are assigned as in Table II.

The other examples are presented with unpublished retention data. Among methylethyl-*n*-propylbenzenes (MeEtnPrB), 1-Me-2-Et-3-nPrB, 1-Me-3-Et-2-nPrB and 1-Me-2-Et-6-nPrB have $I_{calc.}$ values higher than any of the $I_{exp.}$ values obtained.

TABLE II

I VALUES FOR DIMETHYLDIETHYLBENZENES

Compound	$I_{calc.}$	$I_{exp.}$	$dI/dT_{calc.}$	$dI/dT_{exp.}$
1,2-DiMe-3,5-DiEtB	1272	1274.7	0.33	0.38
1,3-DiMe-2,5-DiEtB	1263	1262.9	0.33	0.23
1,3-DiMe-4,5-DiEtB	1263	1263.6	0.33	0.30
1,4-DiMe-2,6-DiEtB	1263	1258.4	0.33	0.29
1,2-DiMe-4,5-DiEtB	1256	1255.7	0.35	0.31
1,4-DiMe-2,5-DiEtB	1256	1257.3	0.35	0.34
1,3-DiMe-4,6-DiEtB	1265	1263.9	0.35	0.30

TABLE III

I VALUES FOR METHYLETHYL-*n*-PROPYLBENZENES AND DIMETHYL-*tert.*-BUTYLBENZENES

	$I_{calc.}$	$I_{exp.}$	$dI/dT_{calc.}$	$dI/dT_{exp.}$
1-Me-2-Et-4-nPrB	1228	1228.1	0.29	0.28
1-Me-3-Et-4-nPrB	1228	1232.2	0.29	0.28
1-Me-3-Et-6-nPrB	1236	1236.2	0.29	0.30
1-Me-4-et-2-nPrB	1228	1238.5	0.29	0.29
1-Me-4-Et-3-nPrB	1228	1228.1	0.29	0.28
1-Me-3-Et-5-nPrB	1213	1211.7	0.23	0.21
1,2-DiMe-3-tertBuB	1211	1211.2	0.34	0.47
1,3-DiMe-2-tertBuB	1211	1213.8	0.34	0.38
1,2-DiMe-4-tertBuB	1188	1192	0.29	0.31

Again, no *ortho*-trisubstituted MeEtPrB are present in the mixture. For the other isomers, the data in Table III are proposed. The greater difference in the case of 1-Me-4-Et-2-nPrB shows that either the experimental value or the proposed structure is uncorrect.

The illustrated coincidence between the calculated and experimental data for retention indices and the acceptable accuracy of the dI/dT values show that preliminary calculative identification is possible and we expect this to be of help in mass spectral identification. The proposed model evaluates quantitatively the relative influence of substitution in the benzene ring and branching in the alkyl substituent. Hence one can obtain both a qualitative and a quantitative understanding of the retentions of different alkylbenzenes in GC on non-polar stationary phases and can use the experimental data for structure elucidation.

REFERENCES

1 B. Kumar, R. K. Kuchhal, P. Kumar and P. L. Gupta, *J. Chromatogr. Sci.*, 24 (1986) 99.
2 E. Matisová, *J. Chromatogr.*, 438 (1988) 131.
3 V. A. Gerasimenko, A. V. Kirilenko and V. M. Nabivach, *J. Chromatogr.*, 208 (1981) 9.
4 V. A. Gerasimenko and V. M. Nabivach, *Zh. Anal. Khim.*, 37 (1982) 110.
5 J. A. Lubek and D. L. Sutton, *J. High Resolut. Chromatogr. Chromatogr. Commun.*, 6 (1983) 328.
6 St. Boneva, D. Papazova and N. Dimov, *Godishnik VHTI "Prof. Dr. As. Zlatarov"–Burgas (Bulgaria)*, 18 (1983) 143.
7 N. Dimov and St. Bonvea, *Chromatographia*, 21 (1986) 697.
8 W. Engewald, I. Topalova, N. Petsev and Chr. Dimitrov, *Chromatographia*, 23 (1987) 561.
9 E. Matisová, E. Kovačičová, Pham Thi Ha, E. Koelk and W. Engewald, *J. Chromatogr.*, 475 (1989) 113.
10 V. Svob and D. Deur-Siftar, *J. Chromatogr.*, 91 (1974) 677.
11 T. Tóth, *J. Chromatogr.*, 279 (1983) 157.
12 N. Dimov and D. Papazova, *J. Chromatogr.*, 137 (1977) 265.
13 D. Papazova and N. Dimov, *J. Chromatogr.*, 216 (1981) 321.
14 J. Bermejo, J. J. Canga and O. M. Gayol, *Int. J. Environ. Anal. Chem.*, 11 (1982).
15 J. Bermejo and M. D. Guillén, *Chromatographia*, 17 (1983) 664.
16 J. Bermejo, J. J. Canga, O. M. Gayol and M. D. Guillén, *J. Chromatogr. Sci.*, 22 (1984) 252.
17 F. Wang, *Sepu*, 4 (1986) 258; *C.A.*, 105 (1986) 218094a.
18 S. Miertuš, V. Jakuš and E. Matisová, *Chromatographia*, 30 (1990) 144.

19 N. Dimov and Ov. Mekenyan, *Anal. Chim. Acta*, 212 (1988) 317.
20 N. Dimov and Ov. Mekenyan, *J. Chromatogr.*, 471 (1989) 227.
21 R. Golovnya and O. Grigoryeva, *Zh. Anal. Khim.*, 40 (1985) 316.
22 R. Golovnya, *J. Chromatogr.*, 364 (1986) 193.
23 G. Schomburg, *J. Chromatogr.*, 23 (1966) 1.
24 J. Bermejo and M. Guillén, *J. Environ. Anal. Chem.*, 43 (1985) 88.
25 D. Bonchev, Ov. Mekenyan, G. Protič and N. Trinajstič, *J. Chromatogr.*, 176 (1979) 149.
26 K. Héberger, *Chromatographia*, 25 (1988) 725.
27 E. Matisová, M. Rukríglová, J. Krupčík, E. Kovačičová and Š. Holotík, *J. Chromatogr.*, 455 (1988) 301.
28 N. Dimov, *Anal. Chim. Acta*, 201 (1987) 217.
29 N. Dimov and D. Papazova, *Chromatographia*, 12 (1979) 720.

Journal of Chromatography, 549 (1991) 335–344
Elsevier Science Publishers B.V., Amsterdam

CHROM. 23 356

Continuous automatic monitoring of volatile organic compounds in aqueous streams by a modified purge-and-trap system

JOSEPH G. SCHNABLE*, MARIO B. CAPANGPANGAN and IRWIN H. (MEL) SUFFET
Department of Chemistry and Environmental Studies Institute, Drexel University, Philadelphia, PA 19104 (USA)

(First received December 11th, 1990; revised manuscript received April 8th, 1991)

ABSTRACT

A new inexpensive modification approach enabled continuous on-line automatic analysis of volatile organic compounds (VOCs) in small (0.1–70 ml/min) sample streams while maintaining all capabilities on a purge-and-trap system. Commercially available automated VOC analyzers require large (liters-per-hour) sample streams. VOCs in laboratory experiments and small sample streams are usually monitored by grab analysis. This paper evaluates the performance of continuously and automatically monitoring VOCs in small sample streams on a modified purge-and-trap system. A 1 ml/min stream with 30 ppb (10^9) trichloroethane and 260 ppb tetrachloroethene aqueous standards was monitored unattended for 3 days with 2–3% relative standard deviations. The competitive breakthrough of VOCs through liquid chromatography carbon minicolumns was studied.

INTRODUCTION

Convenient, versatile, reliable and inexpensive on-line automatic monitoring of volatile organic compounds (VOCs) in aqueous streams is a basic need of environmental analytical chemistry since these chemicals are regulated pollutants. Commercially available on-line sampling systems include a Tekmar (Cincinnati, OH, USA) Model 6000 process stream sampler/LSC-2 purge-and-trap/gas chromatography (GC) system [1]; a Tekmar automatic process sampler/LSC2000 purge-and-trap/GC system [1]; and a Siemens (ES Industries, Voorhees, NJ, USA) P101 process chromatograph which uses dynamic headspace analysis with multidimensional GC [2–4]. These instruments are designed for large liters-per-hour aqueous sampling streams. The Tekmar 6000 automatically samples water from a flowing stream at programmable time intervals or on a sequential stream basis [1]. Because the sample flows through 1.3-cm poly(vinyl chloride) tubing in the Tekmar 6000 sample module, a sample flow of several liters-per-hour is recommended. An automatic process sampler accessory available for the Tekmar LSC2000 [1] purge-and-trap system, which interfaces to a gas chromatograph, also requires liters-per-hour sample streams.

Water sources and waste streams have also been continuously and automatical-

0021-9673/91/$03.50

ly monitored using a Siemens P101 dynamic headspace analyzer [2–4]. The Siemens analyzer has sensitivity, accuracy and precision comparable to purge-and-trap systems, a fast cycle time (15 min for a few compounds) and requires a sample flow of at least 4 l/h [2–4].

In another approach, VOCs in a sample stream with a flow of 20 ml/h have been continuously monitored based on permeation of VOCs through a silicone polycarbonate membrane [5]. VOCs permeate from the sample water matrix to an inert gas stream. Detection limits in the low parts-per-billion (ppb)[a] range, and precision comparable to purge-and-trap methods, were reported.

Presently, commercially available automated VOC analyzers utilize expensive field samplers for large (liters-per-hour) sample streams. VOCs in laboratory experiments and small sample streams are usually monitored by grab analysis.

This paper evaluates the performance of continuous automatic on-line analysis of small (0.1–70 ml/min) sample streams, approximately hourly, for days at a time, on a modified purge-and-trap system. The purge-and-trap system used, a Tekmar LSC-2 orginally designed for one-at-a-time analysis of grab samples, maintained 100% of its original capabilities after these modifications. The gas chromatograph was a Varian 3300 with a 2.5-m 1% SP1000 packed column, a flame ionization detector, and a Hewlett-Packard 3292 integrator. The modified system was designed to monitor the breakthrough of trace (ppb) aqueous VOCs from a granular activated carbon (GAC) laboratory liquid chromatography (LC) column for as long as 3 weeks. A Varian 3250 liquid chromatograph with a 5-l PTFE bag reservoir pumped samples through the LC column filled with 100/230 mesh Filtrasorb 400 GAC.

EXPERIMENTAL

Original purge-and-trap/GC system

A standard LSC-2/4000 purge-and-trap system is designed for one-at-a-time analysis of grab samples. An LSC-2/4000 has a manual 3-way sample valve for opening the sparging vessel to the sample inlet or drain solenoid. Fig. 1a–c shows the sequence of events when a grab sample is analyzed on a standard LSC-2/4000 purge-and-trap system running in the fully automatic mode: during PURGE–READY a 5-ml sample is manually injected into the sparge sampler (Fig. 1a), the 3-way sample valve is turned and a start button is pushed to start each automatic cycle. During PURGE (Fig. 1b) volatiles are trapped. During DESORB (Fig. 1c) the drain solenoid opens emptying the sparge sampler, and the trap is heated to desorb volatiles to the gas chromatograph. During BAKE volatiles are vented from the hot trap. Finally, the system cools and returns to PURGE–READY, and the process can be repeated with the next sample.

Modified purge-and-trap/GC system

With the addition of a custom "T" connector, a 3-way solenoid and an electronic interface, the system maintained 100% of its original capabilities and gained the ability to continuously and automatically monitor small (0.1–70 ml/min) sample streams, on-line, unattended, for days at a time. Fig. 1d–f show that the added 3-way

[a] Throughout this article, the American billion (10^9) is meant.

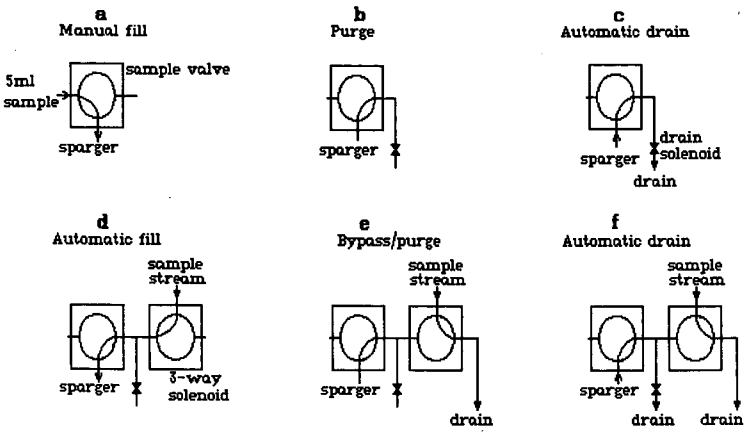

Fig. 1. On the original LSC-2 purge-and-trap, a grab sample is manually injected (a), purged (b) and can be automatically drained (c). After modifications, the system maintained 100% of its original capabilities and can continuously monitor small sample streams. Sample streams can automatically fill the sparger (d) or bypass the sparger (e) and (f). The original drain solenoid automatically drains the sparger (c) and (f).

solenoid directs the sample stream to enter or bypass the sparge sampler. The original 3-way sample valve is left in the one position shown. The original drain solenoid continues to drain the sparge sampler during DESORB.

Piping interface

Fig. 2 shows the interconnection of the original sample valve and drain solenoid, and the added custom "T" connector and 3-way solenoid: A is the 1/4-28 flanged fitting on the original drain line. The "T" connector was made from 2.5 cm of

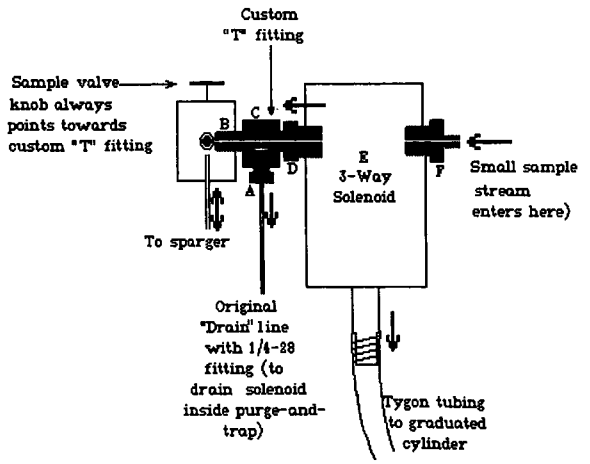

Fig. 2. Layout of the original sample valve and drain line, and added custom "T" fitting and 3-way solenoid on the modified purge-and-trap system. Arrows show all directions the sample can flow. See text for explanation.

1/4-28 threaded brass rod B (cut from a bolt), a 2-cm brass cube C, and a 1/8-in. national pipe thread (NPT) to 10-32 adapter D, after drilling and tapping C, soldering B, C, and D together, and drilling a 1.6-mm "T" path. F is also a 1/8-in. NPT to 10-32 adapter. Both 1/8-in. NPT to 10-32 adapters came with 3-way solenoid E (Allenair No. EA-5-S-120/60HZ or Tekmar part No. 14-1098-000). English 1/4-28 threads are equal to metric M6.35-1.10 threads. The 3-way solenoid has a B engraved on the influent side. The arrows in Fig. 2 show all directions the sample could flow.

Electronic interface

An electronic interface was designed to control the 3-way solenoid which allows the sample stream to enter the sparge sampler during PURGE–READY and bypass the sparge sampler at all other times. During PURGE–READY, sample enters the sparge sampler for a programmed "fill time", and then the system advances to PURGE (the automatic cycle starts, and the original drain valve drains the sparge sampler during DESORB).

Sockets 1 and 2 on the Tekmar LSC-2/4000 computer interface are an optocoupled npn transistor collector and emitter, respectively, which conduct during PURGE–READY. Sockets 4 and 5 on the LSC-2/4000 computer interface are the cathode and anode, respectively, of an optocoupled light-emitting diode which, if pulsed, advances the purge-and-trap to PURGE. The interface designed senses a transistor–transistor logic (TTL) low on sockets 1 and 2 during PURGE–READY, energizes the 3-way solenoid (to fill the sparge sampler) during PURGE–READY, and starts a timer. After the programmed time has elapsed, a TTL pulse on pins 4 and 5 advances the purge-and-trap to PURGE, the timer resets and the 3-way solenoid is off (the sample stream bypasses the sparge sampler). Note: all connections are made to the computer interface, not screw terminals on the Tekmar.

The circuit used a 7406 hex inverter and two 4020 decade counters (clocked at line frequency), a relay for the 3-way solenoid, power supply and rotary switch for selecting fill times from 4 to 2184 s. Technical details including a schematic diagram and parts list are available from the authors.

RESULTS AND DISCUSSION

Fill time

"Fill time" has been defined as the length of time that the purge-and-trap remains on PURGE–READY and sample enters the sparge sampler. Fill times of 4.27, 8.53, 17.1, 34.1, 68.3, 137, 273, 546, 1092 or 2184 s could be selected with the circuit used.

Fill volume

"Fill volume" is the volume that enters the sparge sampler. We used a 1.05-ml/min influent and a fill time of 273 s. The actual volume that enters the sparge sampler had a relative standard deviation (R.S.D.) of *ca.* 0.6% (*i.e.*, fill volumes were 4.60, 4.66, 4.67, 4.67, 4.64, 4.60, 4.62 ml; the average and standard deviation were 4.64 $\pm$0.03 ml). The average fill volume did not change after months of continuous use.

Dead volume

In the above example, the influent rate was 1.05 ml/min, and the fill time was 273 s. During filling, (1.05 × 273/60) 4.78 ml passed through the influent solenoid, but only about 4.64 ml entered the sparge vessel. The difference (0.14 ml) is dead volume, which remains in the piping between analyses. Some of this dead volume is blown out between analyses during automatic draining. Blowing out of the dead volume between analyses reduces carry-over between samples. As with the original system, sample carry-over is slight, and most noticeable after switching from very high to very low concentration samples.

Sample carry-over test

The interface circuit was modified to allow the sparge sampler to alternately fill with sample and dry blanks. When compounds of approximately 10–100 ppb were analyzed, peak areas during the dry blanks usually were about 0–5% of the sample peak areas. This much carry-over seems acceptable when monitoring concentrations which do not change much between successive runs. Carry-over can be decreased by running more than one dry blanks between samples. Fig. 3 shows the chromatographic results of the analysis of two compounds in a sample stream, with automatic dry blanks between alternate analyses.

Compatibility with original system: fill/drain modes

If the electronic interface is unplugged (or the fill time is set to infinity), the 3-way solenoid is de-energized and a sample stream would bypass the purge-and-trap system. The purge-and-trap system would maintain 100% of its original capabilities, including automatic draining. If effluent (*i.e.*, from a liquid chromatograph) is monitored for days at a time, the sample stream can be temporarily bypassed and the purge-and-trap could be tested with an ordinary calibration standard. With the original or modified purge-and-trap system, the user can manually remove a sample through the original sample inlet.

The following are possible fill-and-drain modes on the original LSC-2:

(A1) manual fill with manual drain;

(A2) manual fill with automatic drain.

With the modified system, the following fill-and-drain modes are possible:

(B1) manual fill with manual drain;

(B2) manual fill with automatic drain;

(B3) automatic fill with manual drain (we do not recommend this for continuous monitoring);

(B4) automatic fill with automatic drain.

Manual fill with manual drain, before and after instrument modification (mode A1 vs. mode B1)

On the original or modified purge-and-trap system, sample can be manually injected, the sample valve can be turned to isolate the sparge sampler from the drain line/solenoid (and any added components) during purging, and sample can be manually drained after purging.

On the original purge-and-trap system, standard can be purged this way and then with automatic drain, to test for leaks in the drain line or drain solenoid.

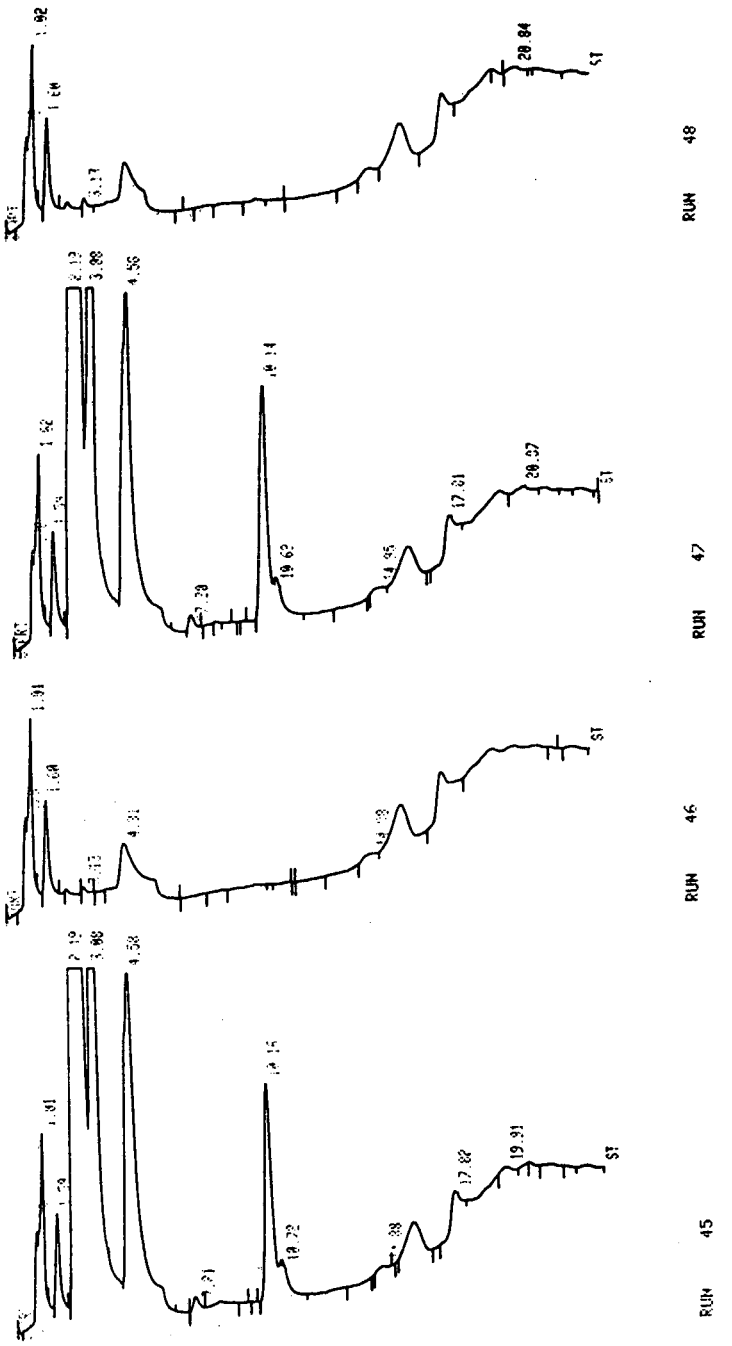

Fig. 3. Sample carry-over was tested by continuously and automatically alternating between the analysis of compounds in LC effluent (runs 45 and 47) and dry blanks (runs 46 and 48), to test the small-volume effluent monitor for sample carry-over. The LC effluent contained TCA (retention time 4.58 min), PCE retention time 10.14–10.16 min) and other VOCs. During automatic dry blanks, a small amount of sample carry-over is visible. Numbers at peaks indicate retention times in min.

On the modified purge and trap system, a standard can be purged with the sample valve isolating the custom "T"/drain line/drain solenoid/3-way solenoid. The same standard can be analyzed with automatic drain to check for analyte loss due to leaks, dead volume, etc.

Manual fill with manual drain vs. manual fill with automatic drain (mode B1 vs. mode B2)

On the modified system, fill and drain combinations B1 and B2 were compared to determine if a significant amount of VOCs are lost in the custom "T"/drain line/drain solenoid/3-way solenoid headspace area. Replicate samples of 36 ppb 1,1,1-trichloroethane (TCA) and 338 ppb tetrachloroethene (PCE) were analyzed on the modified purge-and-trap system. All samples were manually injected with a 5-ml Luer-Lok syringe. Table I shows replicate analyses of TCA and PCE with alternating manual drain and automatic drain on the modified purge-and-trap system.

(A 5-ml sample was purged 11 min, desorbed for 4 min, and the trap was baked for 12 min. A 2.5-m 1% SP1000 GC column ran isothermally at 160°C.) No significant amount of VOCs were lost using the automatic drain on the modified system, compared to manual drain with the sample valve shutting off the modified piping.

Manual fill with manual drain vs. automatic fill with automatic drain (mode B1 vs. mode B4)

A comparison was made between manually analyzing a standard with the sample valve always isolating all modifications made to the purge-and-trap (mode B1), and continuously pumping the standard at 1.05 ml/min through an LC blank column, and into the automatic small-sample-stream monitor for 69 h. A calibration curve was made by diluting a stock solution of TCA and PCE, and injecting 4.64 ml of standard into the purge-and-trap, with manual filling and manual draining and the sample valve always blocking the modified portion of the purge-and-trap (mode B1). For the TCA calibration curve, standards ranged from 5 to 100 ppb and had a

TABLE I

REPLICATE TCA AND PCE ANALYSES ON THE MODIFIED PURGE-AND-TRAP SYSTEM WITH MANUAL DRAIN (SAMPLE VALVE CLOSING OFF MODIFIED PIPING) AND AUTOMATIC DRAIN

	Manual fill, manual drain	Manual fill, automatic drain	Manual fill, manual drain	Manual fill, automatic drain
Mode	B1	B2	B1	B2
Compound	TCA	TCA	PCE	PCE
Ppb	36	36	338	338
Purged (ml)	5.0	5.0	5.0	5.0
Peak area	1590	1609	13028	12929
Peak area	1605	1635	12523	13089
Peak area	1657	1612	12908	12957
Average	1617	1618	12820	12992
Recovery		100% of mode B1		101% of mode B1
R.S.D. (%)	2.2	0.9	2.1	0.7

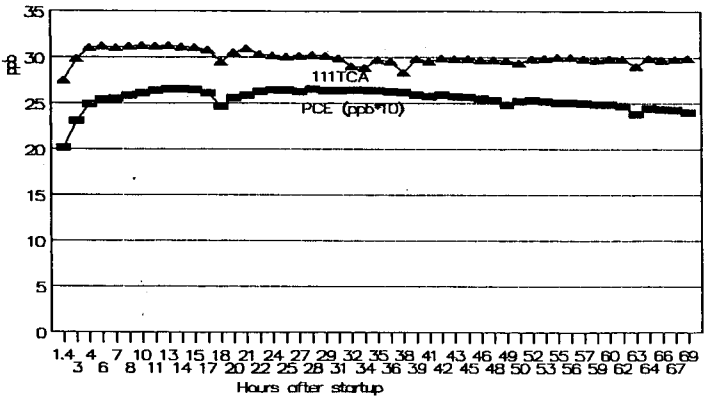

Fig. 4. A liquid chromatograph pumped 30 ppb TCA and 300 ppb PCE at 1.05 ml/min through an empty column and into the small-volume effluent monitor. TCA was detected with 100% recovery and a R.S.D. of 2.2% over 69 h. PCE was simultaneously detected with 85% recovery and R.S.D. of 2.9%.

coefficient of correlation $r = 0.997$. For the PCE calibration curve, standards ranged from 20 to 400 ppb and had a coefficient of correlation $r = 0.987$.

A 5-l volume of 30 ppb TCA and 300 ppb PCE standard (from the same stock solution and mixed in a 5-l PTFE sampling bag) was attached to liquid chromatograph and pumped at 1.05 ml/min through an empty column into the automatic small-sample-stream monitor. The purge vessel automatically filled with 4.64 ml (± 0.03 ml) of sample, and was automatically drained during desorb (mode B4). Sample purged for 11 min, desorbed for 4 min, and the column was baked for 57 min (1.4 h elapsed between each analysis). A 1% SP1000 column was run isothermally at 160°C. Fig. 4 shows TCA and PCE concentrations entering the modified purge-and-trap system *vs.* time. Table II summarizes the results of this study, excluding the first analysis after the system started up.

There was some loss of PCE, which is less polar and much more volatile than TCA. PCE loss (14.6%) was probably due to PCE adsorbing to or escaping from the

TABLE II

REPLICATE DETERMINATIONS OF TCA AND PCE IN NATURAL WATER

	TCA	PCE
Conc. supplying LC system (ppb)	30	300
Number of analyses	49	49
Time between analyses (h)	1.4	1.4
Time span (h)	69	69
Flow-rate (ml/min)	1.05	1.05
Minimum conc. (ppb)	28.4	239
Average conc. (ppb)	30.0	256
Maximum conc. (ppb)	31.3	265
R.S.D. of conc. (%)	2.2	2.9
Recovery (%)	100	85.4

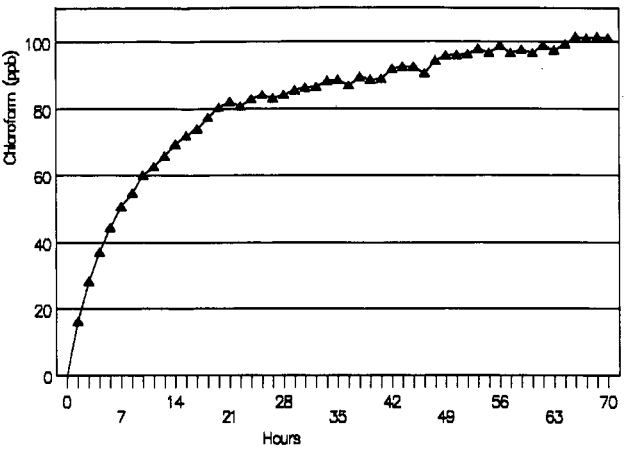

Fig. 5. The small-scale effluent monitor continously monitored a 1.05-ml/min effluent for breakthrough of chloroform from a LC microcolumn packed with activated carbon. Chloroform concentrations were determined every 1.5 h for 70 h.

PTFE bag, tubing, etc., during the 69 h of automatic monitoring. The reproducibility of the system was excellent (R.S.D. of 2.2% for TCA and 2.9% for PCE) for 69 h of sampling time.

Application

Micro carbon columns containing 50 mg of granular activated carbon were used to study the removal of VOCs from drinking water. Contaminated-surface and well-water samples were continuously pumped through micro carbon columns for as long as two weeks, and the effluent from the carbon columns was monitored via the small sample stream monitor. Fig. 5 shows a 1.05 ml/min effluent from a micro carbon column that was analyzed on the small-sample-stream monitor for 3 days. The chloroform concentration in the influent to the micro column was approximately 100 ppb. Chloroform concentrations in effluent from the micro column ranged from 0 to *ca.* 100 ppb over *ca.* 70 hours. As activated carbon becomes saturated, contaminants breakthrough carbon columns [6–11]. In subsequent studies we monitored the competitive breakthrough of several VOCs, approximately hourly, depending on the temperature program necessary to resolve the compounds.

As mentioned before, the system could alternate between samples and blanks as quality assurance. Continuous automatic alternating analyses between two different LC systems, feeding one purge-and-trap system, was tested. A second influent solenoid and electronics were added to alternately flip-flop between activating either one of two influent solenoids during PURGE–READY. Alternating sample switching between two sample streams worked. Because the second LC system for this experiment consisted only of a 5-l sample bag, a less expensive stand-alone low-volume pump, and a GAC LC column, the flow-rate of the second small-stream system was not precise enough for further LC1/LC2 purge-and-trap GC experiments.

Reliability

Because the on-line continuous and automatic monitoring system developed uses a sparge sampler to isolate VOCs from the aqueous matrix, salts and small particles in natural water samples did not cause any downtime in our purge-and-trap or GC system. The continuous small-sample-stream monitor has run continuously for one to two weeks at a time, for eleven months, with no electronic or piping problems in this interface. Traps in the purge-and-trap were replaced every few months. The seals on the LC system for the above study were replaced twice.

Modifying a Tekmar Model 4000 or LSC-2000

Continuous monitoring of small sample streams should also be possible with a Tekmar Model 4000 (it has the same sample valve and computer interface as the LSC-2), or with a Tekmar LSC-2000 (it has a compatible computer interface and a sample valve which is a mirror image of the one on the LSC-2).

CONCLUSIONS

After low-cost modifications to a Tekmar LSC-2 purge-and-trap system which was connected to a GC analysis system, the modified system had 100% of its original capabilities, and the ability to monitor low-volume (0.1–70 ml/min) sample streams. The reproducibility of determined concentrations remained excellent after days of automatic monitoring (*i.e.*, R.S.D. values of 2.2 and 2.9%). Loss of analyte through an LC pumping system was small but consistent. With very volatile compounds, analyte loss is significant (*i.e.*, 15% loss of PCE) and should be taken into consideration when doing critical quantative work. There were no reliability problems with these modifications to the purge-and-trap system after eleven months of heavy use, with normal maintenance of the rest of the system.

REFERENCES

1 *Tekmar 1990 Catalog*, Rosemount Analytical Inc., Tekmar Company, Cincinnati, OH, 1990, p. 61.
2 P. Maitoza, J. A. Valada and W. T. Madigan, *Am. Lab.*, 21 (1989) 23.
3 J. G. Schnable, I. H. Suffet and C. D. Hertz, *Proceedings from the American Water Works Association, Water Quality Technology Conference, St. Louis, MO, November 17, 1989*, American Water Works Association, Denver, CO, 1990, p. 823.
4 J. G. Schnable, B. Dussert, I. H. Suffet and C. D. Hertz, *J. Chromatog.*, 513 (1990) 47–54.
5 R. D. Blanchard and J. K. Hardy, *Anal. Chem.*, 58 (1986) 1529–1532.
6 L. J. Bilello and B. A. Beaudet, in M. J. McGuire and I. H. Suffet (Editors), *Treatment of Water by Granular Activated Carbon (Advances in Chemistry Series*, No. 202), American Chemical Society, Washington, DC, 1983, pp. 213–246.
7 P. C. Chrostowski, A. M. Dietrich, I. H. Suffet and R. S. Chrobak, in M. J. McGuire and I. H. Suffet (Editors), *Treatment of Water by Granular Activated Carbon (Advances in Chemistry Series*, No. 202), American Chemical Society, Washington, DC, 1983, pp. 481–502.
8 J. C. Crittenden, J. K. Berrigan and D. W. Hand, *J. Water Pollut. Control Fed.*, 58 (1986) 312–319.
9 D. W. Hand, J. C. Crittenden, J. M. Miller and J. L. Gehin *Technical Report Data, EPA Report No. EPA/600-2-88/053*, Environmental Protection Agency, Cincinnati, OH, 1988.
10 M. J. McGuire and I. H. Suffet *J. Am. Water Works Assoc.*, 70 (1978) 621–636.
11 R. J. Baker, I. H. Suffet and T. L. Yohe, in I. H. Suffet and P. MacCarthy (Editors), *Aquatic Humic Substances: Influence on Fate and Treatment of Pollutants (Advances in Chemistry Series*, No. 219), American Chemical Society, Washington, DC, 1989, pp. 533–548.
12 *Owners Manual for Tekmar LSC-2 Purge and Trap System*, Tekmar Company, Cincinnati, OH, 1986.
13 J. O. Grote and R. G. Westendorf, *Am. Lab.*, 11 (1979) 61–66.
14 R. G. Westendorf, J. O. Grote, and J. A. Borer, presented at *the 1981 Pittsburgh Conference on Analytical Chemistry and Applied Spectroscopy, March 9–13, 1981, Atlantic City, NJ.*

Journal of Chromatography, 549 (1991) 345–355
Elsevier Science Publishers B.V., Amsterdam

CHROM. 23 339

Quantitative analysis in capillary zone electrophoresis with conductivity and indirect UV detection

M. T. ACKERMANS, F. M. EVERAERTS and J. L. BECKERS*
Eindhoven University of Technology, Laboratory of Instrumental Analysis, P.O. Box 513, 5600 MB Eindhoven (Netherlands)
(First received January 26th, 1991; revised manuscript received March 19th, 1991)

ABSTRACT

An interesting point in quantitative capillary zone electrophoresis, when applying conductivity detection or indirect UV detection with non-UV absorbing components, is the existence of a relationship between effective mobilities and peak area, independent of the kind of ionic species. This relationship is theoretically considered for fully ionized monovalent ions resulting in a linear relationship, passing through the origin, between temporal peak area and the product of a correction factor (dependent only on the effective mobilities of the ionic species) and migration time for an equimolar sample composition. A good correlation between theory and practice could be established by applying experimental measured data.

INTRODUCTION

Huang *et al.* [1] reported on the unique advantage of quantitative capillary zone electrophoresis (CZE) using conductivity detection that the use of an internal standard allows the accurate determination of absolute concentrations in a mixture without separate calibration of the response for each component and they found a direct relationship between peak area and migration times. Further consideration of the principle of the measured conductivity shows, however, that although a relationship exists between peak area and migration time it is nearly linear only over a small mobility range. In this paper, the relationship between peak area and effective mobility for conductivity and indirect UV detection in CZE is considered for fully ionized monovalent ions.

THEORETICAL

Assuming only the presence of fully ionized monovalent ionic constituents, the electrophoretic separation mechanism can approximately be described by Kohlrausch's regulation function:

$$\sum_i c_i/m_i = \omega \qquad (1)$$

0021-9673/91/$03.50

where c_i and m_i represent the ionic concentrations and absolute values of the effective ionic mobilities of all ionic constituents and the numerical value of the Kohlrausch function ω is locally invariant with time [2]. If a volume element of the capillary is originally filled with a carrier electrolyte AB (consisting of a co-ion A and counter ion B) at a concentration c_A, it will contain after some time a mixture of sample components and carrier electrolyte when sample components pass, but finally the original situation will be restored again. If a mixture of a component i and the carrier electrolyte AB passes through such a volume element, the following equation is valid:

$$c_A^C = c_A^S + c_i^S k_i \tag{2}$$

with

$$k_i = \frac{m_i + m_B}{m_A + m_B} \cdot \frac{m_A}{m_i}$$

The superscripts C and S refer to the composition of the pure carrier electrolyte AB zone and the sample zone, respectively. The concentration of the counter ion B is determined by the electroneutrality condition.

For the zone conductivity σ can be derived:

$$\sigma^S = \sigma^C + c_i b_i \tag{3}$$

where

$$b_i = F(m_i + m_B)(1 - m_A/m_i)$$

Applying a conductivity detector in capillary electrophoresis, a detector response, directly related to σ^S-σ^C, can be expected being linearly proportional to $b_i c_i$ and hence the spatial [3] peak area will be proportional to the product of b_i and the injected amount Q_{inj}.

Generally, the measured peak area will be expressed on a temporal basis [3] and it can be expected that for CZE both without and with electroosmotic flow (EOF) the measured peak area A_i will be proportional to:

$$b_i Q_{inj} t_i \tag{4}$$

As the migration time t_i is reversely proportional to m_i and $m_i + m_{EOF}$ (without and with EOF, respectively) at a given voltage the measured peak area A_i will be proportional to:

$$b_i Q_{inj}/m_i \text{ or } b_i Q_{inj}/(m_i + m_{EOF}) \tag{5}$$

The relationship between measured peak area A_i and b_i/m_i, $b_i/(m_i + m_{EOF})$ or $b_i t_i$ must be linear, passing through the origin, whereas the products $A_i m_i/b_i$, $A_i(m_i + m_{EOF})/b_i$ and $A_i/b_i t_i$ should be a constant for all different ionic species for an equimolar sample composition. It must be remembered that generally in chromatographic

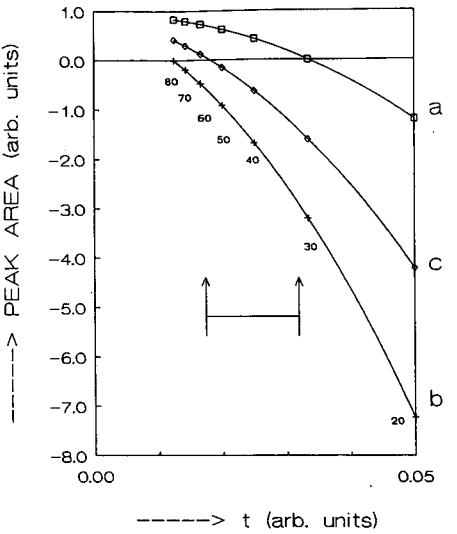

Fig. 1. Calculated relationship between temporal peak area and migration time (t, arbitrary units) for ionic species with effective mobilities of $80 \cdot 10^{-5}$ to $20 \cdot 10^{-5}$ cm^2/V · s assuming effective mobilities for co- and counter ions of (a) $30 \cdot 10^{-5}$ and $30 \cdot 10^{-5}$, (b) $80 \cdot 10^{-5}$ and $30 \cdot 10^{-5}$ and (c) $55 \cdot 10^{-5}$ and $30 \cdot 10^{-5}$ cm^2/V · s. The numbers refer to the effective mobilities, $m \cdot 10^5$ cm^2/V · s, of the ionic species.

techniques one has to work with spatial peak area as the components move with equal speed through the detector.

In Fig. 1 the peak areas (arbitrary units), calculated according to eqn. 5 (without EOF) for a given Q_{inj}, are given as a function of the migration times for ionic species with effective mobilities varying from $80 \cdot 10^{-5}$ to $20 \cdot 10^{-5}$cm^2/V · s and assuming effective mobilities for m_A and m_B of (a) $30 \cdot 10^{-5}$ and $30 \cdot 10^{-5}$, (b) $80 \cdot 10^{-5}$ and $30 \cdot 10^{-5}$ and (c) $55 \cdot 10^{-5}$ and $30 \cdot 10^{-5}$ cm^2/V · s. It can be clearly seen from Fig. 1 that the peak area changes sign at a mobility m_i equal to m_A and increases with larger differences between m_i and m_A. Further, the relationship is not linear,

TABLE I

MEASURED PEAK AREAS A_i (ARBITRARY UNITS), MIGRATION TIMES t_i (s) AND RATIOS c_i/c_{st} CALCULATED WITH THE EQUATION ACCORDING TO REF. 1

Carrier electrolyte: (I) 0.01 *M* MES–histidine at pH 6; (II) 0.005 *M* chloride–Tris at pH 7.1

Ionic species	I			II		
	A_i	t_i	c_i/c_{st}	A_i	t_i	c_i/c_{st}
Formate	53.1	113	1.83	10.5	280	0.14
Acetate	37.0	148	1.67	26.7	338	0.42
Propionate	29.4	164	1.46	33.8	369	0.58
Butyrate	25.5	175	1.36	39.1	390	0.70
Pentanoate	20.6	185	1.16	42.4	405	0.79
Hexanoate	16.9	195	1.00	51.0	425	1.00

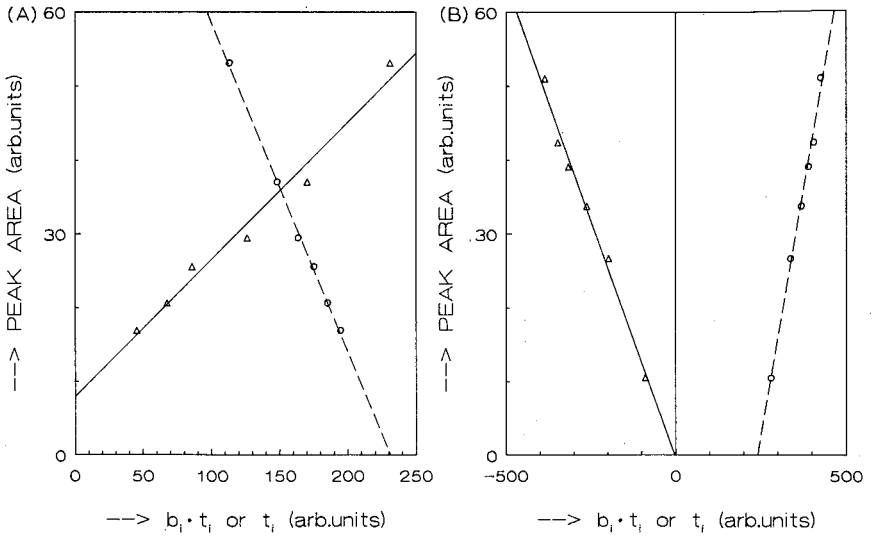

Fig. 2. Relationship between measured peak area [1] and $b_i t_i$ (solid line) and t_i (dashed line) for the electrolyte system (A) 0.01 *M* MES adjusted to pH of 6 by adding histidine and (B) 0.005 *M* HCl adjusted to pH 7.1 by adding Tris. The sample consisted of a mixture of formate, acetate, propionate, butyrate, pentanoate and hexanoate. Applying the correction factor b_i a linear relationship passing through the origin is obtained according to eqn. 4.

although for a fairly small mobility range (the arrows indicate broadly the mobility range of formate to hexanoate) it is nearly linear.

Table I gives the measured peak areas and migration times according to Huang *et al.* [1] and the calculated ratios c_i/c_{st}, with hexanoate considered as a standard (st), using the equation $c_i = c_{st} A_i t_i / A_{st} t_{st}$ as used by Huang *et al.* [1]. It can be concluded from Table I that this equation cannot be used in general, as the quotients have to be unity for an equimolar sample composition.

In Fig. 2A and B the relationships between peak area, as measured by Huang *et al.* [1], and the calculated $b_i t_i$ or t_i are given. We applied eqn. 4 (and not eqn. 5) because we did not know if the EOF was fully suppressed by the addition of tetradecyltrimethyl ammonium bromide (TTAB). It can be clearly seen that the linear relationship between temporal peak area and migration time (dashed line), as measured by Huang *et al.* changes into a linear relationship nearly passing through the origin on applying the correction factor b_i (solid line), as expected from theory. The results in Fig. 2B are better than those in Fig. 2A (large intercept on the ordinate) because the accuracy of the effective mobility 2-(N-morpholino)ethanesulphonic acid (MES) is very critical to the calculated value of b_i. In the calculation of the factor b_i the mobilities have been corrected according to the Debye–Hückel–Onsager theory.

It is obvious that a relationship between peak area A_i and retention time t_i, not linear and not passing through the origin, is not practical to be used for an internal standard, in contrast with the use of the relationship between peak area A_i and the product $b_i t_i$.

For a UV detector the measured absorbance A will be

$$A = \varepsilon c l \tag{6}$$

where ε is the molar absorption coefficient (l/mol · cm) and l is the effective path length in the detector (cm). For the carrier electrolyte this means

$$A^{C} = (\varepsilon_A + \varepsilon_B) c_A^{C} l \tag{7}$$

For a sample zone the absorbance will be

$$A^{S} = (\varepsilon_A + \varepsilon_B) c_A^{S} l + (\varepsilon_B + \varepsilon_i) c_i^{S} l \tag{8}$$

The UV signal of a sample zone, using eqn. 2, will be

$$A = A^{C} - A^{S} = c_i^{S} l[(\varepsilon_A + \varepsilon_B) k_i - (\varepsilon_i + \varepsilon_B)] \tag{9}$$

For non-UV-absorbing counter ions and sample ions, applying indirect UV detection with UV-absorbing co-ions, the UV signal is proportional to $c_i k_i$.

Analogously to conductivity detection, the spatial peak area will be proportional to $k_i Q_{inj}$ and the measured peak area A_i on a temporal basis to $k_i Q_{inj} t_i$. Further, the expression $A_i / k_i t_i$ has to be a constant in a given electrolyte system for all components at an equimolar sample composition.

EXPERIMENTAL

Instrumentation

For all quantitative experiments with a conductivity detector we used a laboratory-built capillary electrophoresis system with an on-column conductivity detector as described previously [4]. As the apparatus is a closed system, the EOF is fully suppressed. The sampling takes place into a broadened part of the capillary tube (0.55 mm I.D.) connected with two feeders (0.4 mm diameter), perpendicular to the capillary tube. A constant d.c. power supply with a maximum potential of 20 kV was used. Peak areas were determined using the integration program CAESAR. The detector electronics were connected with an IBM XT PC via a LabMaster (Scientific Solutions, Solon, USA).

For all quantitative CZE experiments with a UV detector we used the P/ACE System 2000 HPCE (Beckman, Palo Alto, CA, USA) applying UV detection at 254 nm. All experiments were carried out at 25°C using an original Beckman capillary of 57 cm, with a distance between injection and detection of 50 cm and an I.D. of 75 μm.

For all zone electrophoretic separations the injection took place at the inlet side. In the anionic mode the cathode was placed at the inlet and the anode at the outlet side, and *vice versa* for the cationic mode.

Reagents and samples

All chemicals were of analytical-reagent grade. Before preparing the sample solutions, all chemicals were dried at 105°C.

TABLE II

EFFECTIVE MOBILITIES $-m_i \cdot 10^{-5}$ ($cm^2/V \cdot s$), CALCULATED FACTORS b_i (ARBITRARY UNITS), MEASURED PEAK AREAS A_i (ARBITRARY UNITS) AND CALCULATED VALUES OF K ($= A_i m_i / b_i$) FOR DIFFERENT BACKGROUND ELECTROLYTES

Component	m_i	b_i	A_i	K
0.01 M MES + imidazole (pH 7)				
Chloride	74.45	79.30	218.47	205.1
Chlorate	62.61	65.00	209.08	201.4
Fluoride	53.22	52.75	201.93	203.7
Formate	52.43	51.68	200.34	203.3
Acetate	38.54	30.50	163.76	206.9
Propionate	33.36	20.94	136.66	217.7
Benzoate	29.93	13.75	112.66	245.2
0.01 M acetic acid + imidazole (pH 7)				
Chloride	74.17	56.84	122.71	160.1
Chlorate	62.35	40.93	103.74	158.0
Fluoride	52.97	26.87	78.77	155.3
Formate	52.18	25.62	72.51	147.7
Propionate	33.13	−12.19	−53.70	145.9
Benzoate	29.71	−21.61	−100.35	137.9
0.01 M HCl + imidazole (pH 7)				
Chlorate	62.35	−20.14	−31.74	98.3
Fluoride	52.97	−38.88	−68.82	93.8
Formate	52.18	−40.60	−72.95	93.8
Acetate	38.31	−77.67	−180.98	89.3
Propionate	33.13	−96.60	−253.93	87.1
Benzoate	29.71	−111.75	−316.45	84.2

RESULTS AND DISCUSSION

In order to check the relationship between temporal peak area and mobilities for both conductivity (eqn. 5) and indirect UV detection (eqn. 9), we measured the temporal peak area with conductivity detection and indirect UV detection, in both the anionic and cationic modes.

In Table II, the effective mobilities, m_i, calculated factors, b_i, temporal peak areas, A_i (measured with a closed CZE apparatus with an on-line conductivity detector [4]), and calculated values of K are given. The factors K ($= A_i m_i / b_i$) are virtually constant in the three different electrolyte systems, although a disadvantage of the sample injection used in our apparatus is that although linear calibration graphs are obtained for both isotachophoretic and CZE experiments, the effective injection volumes for the different components are not completely identical [4], and moreover the separation power of the apparatus used was too small to separate the whole sample mixture in a single experiment. Of course the values of the factors K for the different systems are different due to different circumstances. The three different electrolyte systems consisted of the co-ions MES, acetate and chloride at a pH of 7 adjusted by adding imidazole (anionic mode, constant electric current 10 μA). The sample components were chloride, chlorate, fluoride, formate, acetate, propionate and benzoate at a concentration of $5 \cdot 10^{-4}$ M.

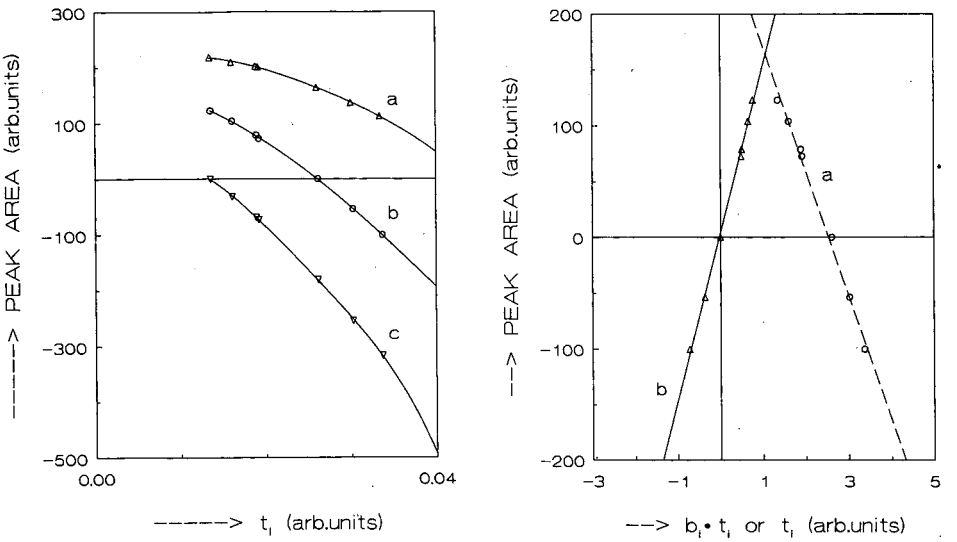

Fig. 3. Relationship between measured peak area and t_i for conductivity detection in a closed system, for three different electrolyte systems. The sign of the peak area changes at an effective mobility equal to that of the co-ion, confirming the theory (see Table II for data). Background electrolyte: (a) MES, (b) acetic acid and (c) hydrochloric acid, all at pH 7 adjusted by adding imidazole.

Fig. 4. Relationship between measured peak area and (a) t_i and (b) $b_i t_i$ for the electrolyte system 0.01 *M* acetic acid adjusted to pH 7 by adding imidazole. The sample consisted of a mixture of chloride, chlorate, fluoride, acetate, propionate and benzoate ($5 \cdot 10^{-4}$ *M*). It can be clearly seen that the relationship between peak area and t_i (dashed line) changes to a linear relationship passing through the origin if the correction factor b_i is used (solid line).

In Fig. 3 the measured peak areas in Table II are given as a function of time. The similarity with Fig. 1 is obvious.

In Fig. 4 the measured peak areas of one of the electrolyte systems in Table II are given as a function of both (a) the migration time t_i and (b) $b_i t_i$. It can be clearly seen that relationship (a) changes into (b), a linear relationship passing through the origin.

To check the relationship between peak area and mobilities for indirect UV detection with non-UV-absorbing components and counter ions, experiments were carried out in both the anionic and cationic modes. In the anionic mode we used three background electrolytes, 0.01 *M* benzoic acid, 0.01 *M* nicotinic acid and 0.01 *M* sulphosalicylic acid adjusted to pH 8 by adding Tris [tris(hydroxymethyl)aminomethane]. The sample mixture consisted of chloride, chlorate, fluoride, acetate, propionate and MES ($5 \cdot 10^{-4}$ *M*), applying pressure injection times of 5, 10 and 15 s. All experiments were carried out with a constant voltage of 25 kV. In order to supress the EOF for the greater part, 0.05% methylhydroxyethylcellulose (MHEC) was added to all solutions.

In Table III the calculated effective mobilities and calculated factors k_i, the measured migration times t_i, measured peak areas A_i and calculated values of K ($= A_i/k_i t_i$) are given. The factor K should be a constant for all components in the same

TABLE III

EFFECTIVE MOBILITIES $-m \cdot 10^5$ ($cm^2/V \cdot S$), CALCULATED FACTORS k_i ACCORDING TO EQN. 2, MEASURED MIGRATION TIMES t_i (min), MEASURED TEMPORAL PEAK AREAS A_i (ARBITRARY UNITS) AND CALCULATED VALUES OF K ($= A_i/k_i t_i$) FOR THREE DIFFERENT PRESSURE INJECTION TIMES

Wavelength of UV detection, 254 nm; capillary length, 57 cm; distance between injection and detection, 50 cm; constant voltage, 25 kV.

Background electrolyte	Component			Pressure injection time								
				5 s			10 s			15 s		
		m_i	k_i	t_i	A_i	K	t_i	A_i	K	t_i	A_i	K
0.01 *M* benzoic acid adjusted to pH 8 with Tris	Chloride	74.17	0.722	3.13	3.85	1.70	3.17	7.42	3.24	3.18	11.11	4.84
	Chlorate	62.35	0.757	3.87	4.83	1.65	3.92	9.85	3.32	3.92	14.29	4.81
	Fluoride	52.97	0.796	4.67	5.90	1.59	4.73	11.64	3.09	4.71	17.78	4.74
	Acetate	38.31	0.896	7.34	11.02	1.68	7.38	21.73	3.29	7.26	32.30	4.97
	Propionate	33.13	0.952	9.09	14.25	1.65	9.11	28.26	3.26	8.90	41.15	4.86
	MES	24.24	1.104	15.96	26.95	1.53	15.76	55.51	3.19	14.97	79.90	4.83
	Average					1.63			3.23			4.84
	Standard deviation					0.063			0.082			0.075
0.01 *M* nicotinic acid adjusted to pH 8 with Tris												
	Chloride	74.17	0.733	3.46	3.51	1.38	3.39	6.98	2.81	3.36	10.99	4.46
	Chlorate	62.35	0.769	4.38	4.87	1.45	4.26	9.45	2.89	4.20	14.18	4.39
	Fluoride	52.97	0.808	5.41	6.23	1.42	5.21	11.94	2.84	5.12	17.80	4.30
	Acetate	38.31	0.909	9.34	12.58	1.48	8.62	23.05	2.94	8.30	33.43	4.43
	Propionate	33.13	0.966	12.37	16.92	1.42	11.07	30.63	2.86	10.50	44.10	4.35
	MES	24.24	1.121	27.21	43.37	1.42	23.07	72.24	2.79	20.34	98.11	4.30
	Average					1.43			2.85			4.37
	Standard deviation					0.034			0.055			0.066
0.01 *M* sulphosalicylic acid adjusted to pH 8 with Tris	Chloride	74.17	0.890	3.59	1.32	0.41	3.34	3.16	1.06	3.25	4.51	1.56
	Chlorate	62.35	0.934	4.68	1.70	0.39	4.24	4.01	1.01	4.09	5.42	1.42
	Fluoride	52.97	0.982	5.95	2.34	0.40	5.22	5.09	0.99	4.98	7.14	1.46
	Acetate	38.31	1.105	11.61	5.00	0.39	8.93	9.49	0.96	8.18	12.45	1.38
	Propionate	33.13	1.174	17.16	7.91	0.39	11.93	13.36	0.95	10.64	17.33	1.39
	Average					0.40			1.00			1.44
	Standard deviation					0.0089			0.044			0.073

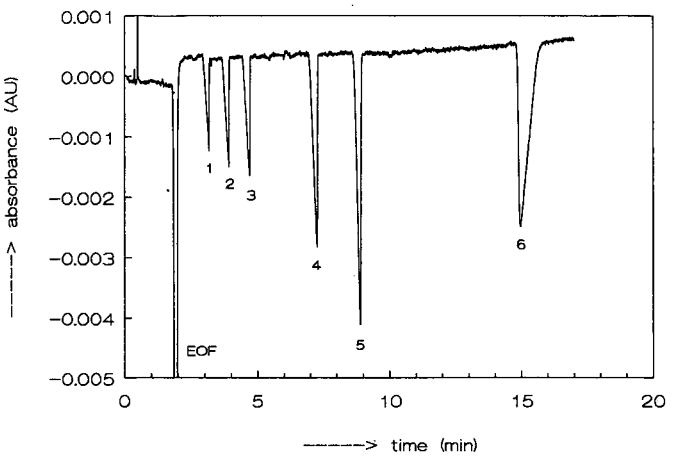

Fig. 5. Electropherogram for the separation of (1) chloride, (2) chlorate, (3) fluoride, (4) acetate, (5) propionate and (6) MES in the indirect UV mode ($5 \cdot 10^{-4}$ *M*, pressure injection time 15 s). Carrier electrolyte, 0.01 *M* benzoic acid adjusted to pH 8 by adding Tris; wavelength, 254 nm; anionic mode, applied voltage 25 kV.

TABLE IV

CALCULATED EFFECTIVE MOBILITIES $-m_i \cdot 10^5$ ($cm^2/V \cdot s$), CALCULATED FACTORS k_i ACCORDING TO EQN. 2, MEASURED MIGRATION TIMES t_i (min), MEASURED TEMPORAL PEAK AREAS A_i (ARBITRARY UNITS) AND CALCULATED VALUES OF K ($= A_i/k_i t_i$) FOR THREE DIFFERENT PRESSURE INJECTION TIMES

Pressure injection time (s)	Component	m_i	k_i	t_i	A_i	K
5	Hexanoate	26.09 (0.115)	1.064 (0.002)	4.69 (0.017)	11.54 (0.181)	2.31 (0.038)
	Pentanoate	27.65 (0.112)	1.035 (0.002)	4.88 (0.015)	11.72 (0.181)	2.32 (0.035)
	Butanoate	29.51 (0.119)	1.003 (0.002)	5.12 (0.019)	12.20 (0.089)	2.37 (0.019)
	Propionate	32.58 (0.099)	0.959 (0.001)	5.58 (0.021)	13.34 (0.200)	2.49 (0.037)
	Acetate	37.31 (0.102)	0.905 (0.001)	6.49 (0.029)	15.12 (0.133)	2.57 (0.025)
	Formate	51.67 (0.112)	0.803 (0.001)	12.71 (0.127)	24.01 (0.625)	2.35 (0.054)
	Average					2.40 (0.105)
10	Hexanoate	26.50 (0.050)	1.056 (0.001)	4.61 (0.032)	23.53 (0.262)	4.83 (0.074)
	Pentanoate	28.05 (0.035)	1.028 (0.001)	4.79 (0.032)	23.97 (0.292)	4.87 (0.076)
	Butanoate	29.73 (0.068)	1.000 (0.001)	5.00 (0.039)	24.94 (0.306)	4.99 (0.080)
	Propionate	32.59 (0.064)	0.959 (0.001)	5.41 (0.046)	26.86 (0.374)	5.18 (0.100)
	Acetate	37.21 (0.064)	0.906 (0.001)	6.23 (0.060)	29.96 (0.370)	5.31 (0.078)
	Formate	51.38 (0.082)	0.804 (0.000)	11.64 (0.224)	48.20 (0.731)	5.15 (0.162)
	Average					5.06 (0.189)
15	Hexanoate	26.76 (0.109)	1.051 (0.002)	4.63 (0.010)	35.61 (1.480)	7.31 (0.302)
	Pentanoate	28.28 (0.088)	1.024 (0.002)	4.81 (0.010)	36.08 (1.004)	7.33 (0.203)
	Butanoate	29.84 (0.092)	0.998 (0.001)	5.01 (0.013)	37.49 (0.985)	7.50 (0.190)
	Propionate	32.56 (0.113)	0.959 (0.001)	5.40 (0.013)	40.02 (0.760)	7.73 (0.141)
	Acetate	37.17 (0.116)	0.907 (0.001)	6.21 (0.017)	44.90 (1.423)	7.97 (0.250)
	Formate	51.54 (0.097)	0.804 (0.001)	11.71 (0.083)	72.40 (3.469)	7.69 (0.323)
	Average					7.59 (0.256)

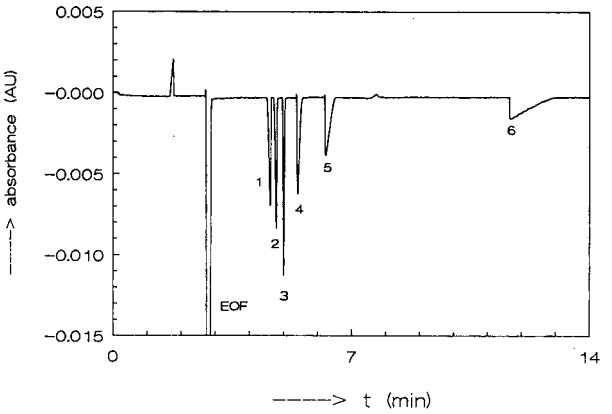

Fig. 6. Electropherogram for the separation of (1) hexanoate, (2) pentanoate, (3) butanoate, (4) propionate, (5) acetate and (6) formate in the indirect UV mode ($5 \cdot 10^{-4}$ *M*, pressure injection time 10 s). Carrier electrolyte, 0.01 *M* benzoic acid adjusted to pH 8.5 by adding Tris; wavelength, 254 nm; cationic mode, applied voltage 25 kV.

carrier electrolyte. It can be concluded from Table III that the factor K is indeed a constant for all components and is linearly related to the amount of the components injected.

Fig. 5 gives an example of the separation of a mixture (in the anionic mode, pressure injection time 15 s) with indirect UV detection. The carrier electrolyte was 0.01 *M* benzoic acid at pH 8. The sample consisted of (1) chloride, (2) chlorate, (3) fluoride, (4) acetate, (5) propionate and (6) MES at a concentration of $5 \cdot 10^{-4}$ *M*. In order to obtain an impression of the velocity of the EOF (remember that the EOF is suppressed for the greater part by the addition of 0.05% MHEC to all solutions), we created an EOF peak directed from outlet to inlet by injecting water at the outlet side by electromigration injection at 10 kV for 5 s (the length from injection to detection is only 7 cm for this EOF marker; m_{EOF} is about $14 \cdot 10^{-5}$ cm^2/V · s; without MHEC m_{EOF} is about $67 \cdot 10^{-5}$ cm^2/V · s). Note the fronting and tailing shapes of the peaks with high and low effective mobilities, respectively.

In the cationic mode we applied an electrolyte system consisting of 0.01 *M* benzoic acid adjusted to pH 8.5 by adding Tris. The applied voltage was 25 kV. The sample consisted of formate, acetate, propionate, butanoate, pentanoate and hexanoate at a concentration of $5 \cdot 10^{-4}$ *M*, applying pressure injection times of 5, 10 and 15 s. In Table IV the effective mobilities and calculated factors k_i, the measured migration times t_i, measured peak area A_i and calculated factors K ($=A_i/k_i t_i$) are given. The effective mobilities of the components are calculated from the migration times of the EOF and of the components as described previously [5].

In order to study the reproducibility of the method, all experiments were carried out five times and the average values are given in Table IV. Standard deviations are given in parentheses. It can be concluded from these data that the reproducibility is good for the migration times and the calculated effective mobilities and factors k_i. The reproducibility of K values is poorer (standard deviation *ca.* 1–2%) owing to the

inaccuracy of the measured peak areas, possibly caused by the injection method and/or inaccuracy of the peak-area determination.

Fig. 6 gives an example of the separation of the mixture in Table IV (in the cationic mode, pressure injection time 10 s) in the indirect UV mode. The carrier electrolyte was 0.01 *M* benzoic acid at pH 8.5 adjusted by adding Tris. The strong tailing effect for formate due to the absence of a self-correcting effect of the zones in CZE can be clearly seen.

CONCLUSIONS

For conductivity and indirect UV detection (for non-UV-absorbing components, applying a non-UV-absorbing counter ion and a UV-absorbing co-ion) there is a defined relationship between measured temporal peak areas and effective mobilities, independent of the kind of ionic species. Data measured for several components in several electrolyte systems confirmed the derived relationship.

The relationship between temporal peak area and the product of a correction factor (b_i for conductivity detection and k_i for indirect UV detection) and migration time t_i is linear, passing through the origin. Applying an internal standard, this relationship can be used in quantitative CZE analysis with calibration graphs being superfluous.

ACKNOWLEDGEMENTS

The authors express their gratitude to the State Institute for Quality Control for Agricultural Products (RIKILT, Netherlands) for financial support of this investigation and to Mr. B. J. Wanders for placing at their disposal the CAESAR data acquisition and analysis program.

REFERENCES

1 X. Huang, J. A. Luckey, M. J. Gordon and R. N. Zare, *Anal. Chem.*, 61 (1989) 766.
2 F. E. P. Mikkers, *Thesis*, University of Technology, Eindhoven, 1980.
2 X. Huang, W. F. Coleman and R. N. Zare, *J. Chromatogr.*, 480 (1989) 95.
4 Th. P. E. M. Verheggen, J. L. Beckers and F. M. Everaerts, *J. Chromatogr.*, 452 (1988) 615.
5 J. L. Beckers, F. M. Everaerts and M. T. Ackermans, *J. Chromatogr.*, 537 (1991) 407.

Journal of Chromatography, 549 (1991) 357–366
Elsevier Science Publishers B.V., Amsterdam

CHROM. 23 357

Quantitation of insulin injection by high-performance liquid chromatography and high-performance capillary electrophoresis

MARK LOOKABAUGH*
US Food and Drug Administration, Winchester Engineering and Analytical Center, Winchester, MA 01890 (USA)
MANJU BISWAS
Milligen Division of Millipore, Burlington, MA 01803 (USA)
and
IRA S. KRULL
Department of Chemistry and Barnett Institute, Northeastern University, Boston, MA 02115 (USA)
(First received November 9th, 1990; revised manuscript received April 8th, 1991)

ABSTRACT

High-performance capillary electrophoresis (HPCE) was evaluated as a potential technique for the regulatory analysis of commercial dosage forms of insulin. A comparison was made to a liquid chromatographic analysis presently being proposed as an official monograph in the United States Pharmacopeia. The salient points of this comparison were accuracy, precision and ease of use. Both authentic (*i.e.* single blind, spiked) samples and commercial pharmaceutical formulations (injections) were examined.

Chromatographic analyses of both commercial formulations and authentic samples were characterized by good precision, with accuracy being supported by results from authentic (spiked) samples. Conventional HPCE (by which is meant a *non-micellar* electrolyte used with an *uncoated, unmodified* fused-silica capillary) achieved reasonable accuracy, but less than impressive precision, when applied to authentic samples. When used for commercial formulations, this type of HPCE did not produce a level of accuracy suitable for regulatory purposes, even with the use of an internal standard.

INTRODUCTION

High-performance chromatography (HPLC) is currently the most widely used technique for the quantitative analysis of pharmaceutical products in finished dosage form. Capillary electrophoresis, using a different separation mechanism, can also be applied to many pharmaceutical analyses now done by HPLC. With the advent of commercial high-performance capillary electrophoresis (HPCE) systems, a comparison of the two methods is appropriate.

There now exists a formidable body of literature devoted to HPCE. Since the publication of the seminal studies, first by Mikkers, *et al.* [1] and then by Jorgenson and Lukacs [2], well over 100 reports have appeared describing applications of capil-

0021-9673/91/$03.50

lary zone electrophoresis, capillary gel electrophoresis, and micellar electrokinetic capillary chromatography (MECC) [3].

However, the articles dealing specifically with quantitative analysis are limited. MECC has been used by Fujiwara and Honda to quantitate antipyretic/analgesic dosage forms [4]. In a previous paper these authors had employed free solution capillary electrophoresis (FSCE) to determine cinnamic acid analogues in canine plasma [5]. In that paper they mentioned the scarcity of reported applications of HPCE for quantitation and cited, as the only apparent example to that time, the measurement of nucleotide concentration in biological tissue by Tsuda *et al.* [6]. Recently Huang *et al.* [7] described the determination of low molecular weight carboxylic acids using FSCE.

All four of these reports relied upon the internal standard technique as a means of calibration and injection by siphoning for introduction of sample into the capillary. Except for Huang *et al.* [7], who employed conductivity detection, all the authors chose ultraviolet absorbance as a detection scheme.

Since insulin is a protein of great pharmaceutical and hence, regulatory significance, it was selected as an analyte upon which a comparison between HPLC and HPCE could be meaningfully based. HPCE separation conditions were established using buffer systems already described in the literature [8–11]. The HPLC procedure has been issued as an in-process revision in Pharmacopeial Forum and, according to the U.S. Pharmacopeial Convention (Rockville, MD, USA), has been collaboratively validated by insulin manufactures [12].

EXPERIMENTAL

Instrumentation

Capillary electrophoresis was performed using a Model M-1200 HPCE system (Microphoretic Systems, Sunnyvale, CA, USA) equipped with a polyimide-clad (exterior coating) fused-silica capillary approximaterly 65 cm in total length (60 cm effective length) with an internal diameter of 75 μm (Polymicro Technologies, Phoenix, AZ, USA). Schwartz *et al.* [13] have described this instrumentation and its performance characteristics in considerable detail. Electrokinetic injection was used exclusively, with typical parameters consisting of an application of 5 kV for 10 s. A running potential of 25 kV, generating roughly 70 μA of background current, was used for analytical determinations. Ultraviolet absorbance at 213 nm was employed for detection.

A modular HPLC system was assembled using, as components, a WISP 710B autosampler (Waters Chromatography Division/Millipore, Milford, MA, USA), a Waters/Millipore Model 6000A solvent delivery system (pump), a Model 7960 HPLC column heater (Jones Chromatography USA, Littleton, CO, USA), a Spectroflow 757 variable wavelength UV detector (Kratos Analytical Instruments, Ramsey, NJ, USA), and a Model SP4270 recording integrator (Spectra-Physics, San Jose, CA, USA). An Ultremex silica-based, 5-μm octadecylsilane column (Cat. No. 00G-00049-B0, Phenomenex, Rancho Palos Verdes, CA, USA) was used for HPLC separations.

Chemicals, reagents and solvents

Reference standards of human, pork, and beef insulin were obtained from the United States Pharmacopeial Convention. Samples of insulin injection were collected

for investigational purposes only from normal channels of commercial distribution. Morpholine and tricine were purchased from Chemical Dynamics Corporation (South Plainfield, NJ, USA). Reagent grade potassium chloride and sodium sulfate were obtained from Fisher Scientific (Fairlawn, NJ, USA). Acetonitrile (HPLC grade) was supplied by J. T. Baker, (Phillipsburg, NJ, USA). Dansyl-l-phenylalanine and dansyl-l-glutamine (internal standards) were available from Sigma (St. Louis, MO, USA). Distilled water was produced in our laboratory using a Corning MP 6A distillation system (Corning, NY, USA).

Procedure for electrophoresis

Prior to its initial use, a fused-silica capillary was prepared by successive washings with 0.1 *M* sodium hydroxide, distilled water, and finally the running electrolyte. Once prepared, the capillary was flushed with running electrolyte between every injection. The M-1200 unit could be programmed to perform these functions automatically. The running electrolyte's composition was 10 m*M* tricine–5.8 m*M* morpholine–20 m*M* potassium chloride with an observed pH of between 8.0 and 8.1. The reference standard was dissolved in this buffer and samples of insulin injection were also diluted with it. The final concentration of both standard and sample preparations was approximately 0.15 mg/ml, corresponding to a 1:25 dilution for samples having a label declaration of 100 units (of biological activity) per ml. Lot F of USP Reference Standard Insulin (Pork), for example, had a declared activity of 26.2 units/mg. Thus, a sample of insulin injection, manufactured using bulk drug of this activity and formulated at a dosage level of 100 units/ml, would be equivalent to 3.817 mg of insulin per ml. Since there is no absolute guarantee that the insulin in a sample will possess the same biological activity (on a per-unit-of-weight basis) as a particular lot of reference standard, the actual and determined concentrations of insulin were expressed in terms of mg/ml. For those instances in which an internal standard was used, an appropriate aliquot (*e.g.* 3.0 ml of a 0.25 mg/ml solution of the internal standard) was combined with the sample aliquot prior to final dilution (to 25.0 ml) with buffer.

Procedure for HPLC

As previously mentioned, the method utilized in our studies has been published as an in-process revision [12]. The assay portion of this proposed monograph revision employs isocratic reversed-phase HPLC (25-cm, silica-based octadecylsilane column, maintained at 40°C.) with detection at 214 nm. The actual composition of the mobile phase is acetonitrile–0.2 *M* sodium sulfate (26:74), with the sodium sulfate component having been adjusted to a pH of 2.3 beforehand. Standard and sample preparation remained essentially the same as for HPCE, again with working concentrations of about 0.15 mg/ml, and either the tricine buffer or 0.01 *M* hydrochloric acid as a diluent.

RESULTS AND DISCUSSION

HPCE optimization

Nielsen *et al.* [9] have described an optimized buffer system for the characterization of human insulin, growth hormone, their derivatives, and related proteins.

Upon initial evaluation, this system proved to be suitable for our intended purposes (see Experimental Section). Hence no real optimization studies had to be conducted. We found that we were able to omit the morpholine component and obtain essentially

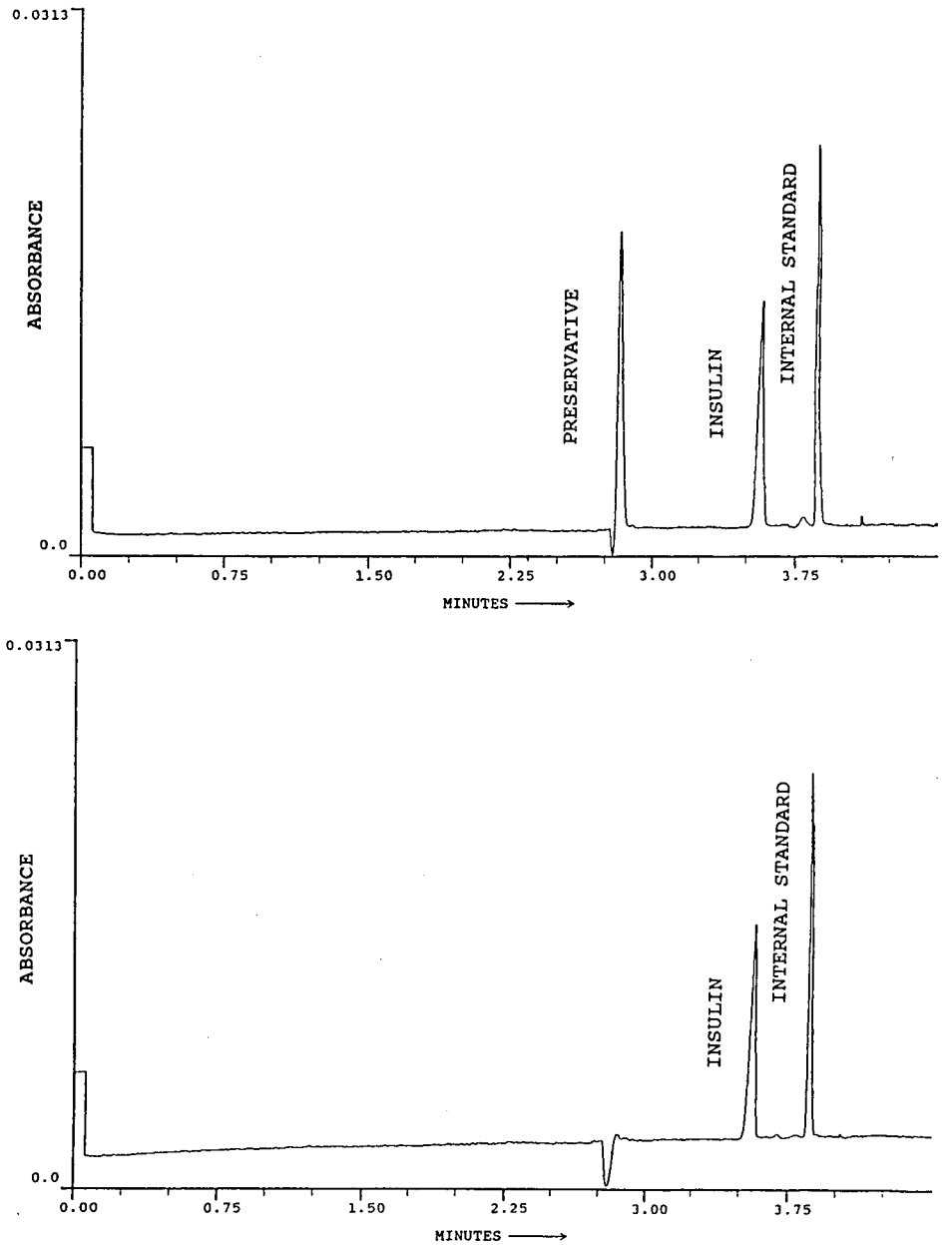

Fig. 1. Sample (upper) and standard (lower) electropherograms. Conditions are listed in Table I. Internal standard is dansyl-phenylalanine.

similar electropherograms of insulin. However, the addition of 0.1 *M* potassium hydroxide (to adjust the pH to 8.0–8.1) also produced elevated background current levels relative to the buffer containing morpholine. Little or no pH adjustment was necessary when the buffer was prepared using morpholine. Furthermore, since the lower background current required less heat to be dissipated from the capillary, we decided to include morpholine as a component. A typical set of electropherograms for a sample of insulin injection and the corresponding reference standard is presented in Fig. 1. In the case of the sample solution, the peak eluting at or near the electroosmotic flow front is attributable to phenol which is added to the formulation as a preservative.

Efficiency and replication of injection

For the purpose of our study, the choice between elecktrokinetic *vs.* vacuum injection centered on the two issues of efficiency and replication of injection. It simply proved to be the case that with our HPCE instrument superior peak shape and more reproducible peak response were observed for electrokinetic injection. As has been pointed out, analytes are introduced during electrokinetic injection with a bias based on differences in electrophoretic mobility [14]. Another point to keep in mind with this technique of sample introduction, is the fact that solutions being compared should be of similar composition and conductivity. Significant differences will result in different electric field strengths being generated by the sampling voltage, and hence different amounts of analyte being introduced into the capillary [15]. For this reason, samples were always diluted (a minimum of 25-fold) with running electrolyte prior to analysis. In Table I a representative series of electrokinetic injections for insulin standard and sample preparations are presented. It was our experience that, with a

TABLE I

REPRODUCIBILITY OF ELECTROKINETIC INJECTION FOR STANDARD AND SAMPLE PREPARATIONS OF INSULIN

65 cm × 75 μm I.D. fused-silica capillary, 5 kV/10 s injection, 25 kV running potential, 10 m*M* tricine–5.8 m*M* morpholine–20 m*M* potassium chloride buffer, 3 min purge with buffer between injections, detection at 213 nm, injection from 2 ml sample volume, *ca.* 0.15 mg/ml insulin.

	Migration time, t_m (min)		Peak response (area)	
	Standard	Sample	Standard	Sample
	3.08	3.06	16754	16741
	3.07	3.07	16023	16139
	3.04	3.06	16380	16733
	3.07	3.05	16146	16381
	3.05	3.07	16104	16121
	3.04	3.07	16537	16433
	3.05	3.07	16947	16859
	3.03	3.09	16952	16460
	3.05	3.06	16489	16844
Average	3.05	3.07	16481	16523
R.S.D. (%)	0.54	0.36	2.41	1.72

TABLE II

ANALYSIS OF AUTHENTIC (SINGLE-BLIND, SPIKED) SAMPLES OF INSULIN (PORK) REFERENCE STANDARD [a] BY HPCE

Sample	Insulin content (mg/ml)	Average calculated value ($n=3$)
1	2.510	2.458 (97.9%, R.S.D. = 12.4%)[b]
2	2.692	2.612 (97.0%, R.S.D. = 13.1%)
3	2.823	2.801 (99.2%, R.S.D. = 0.44%)

[a] Instrumental conditions as in Table I, except for injection from 200 μl volume.

[b] Figures in parentheses represent % of actual amount (mg) in spiked sample, and relative standard deviation of replicate analyses. Single-level, external standard calibration.

well equilibrated system (the apparatus does not feature a thermostat), migration times exhibited a relative standard deviation (R.S.D.) on the order of 1% or less and peak responses were reproducible within roughly 2% R.S.D. These figures represent injections made from vials containing roughly 2 ml of solution. The apparatus also permits sampling from a 96-site microtiter tray. The sample wells in this tray can accommodate a maximum of about 200 μl of liquid. Replicate injections from this volume of solution resulted in reproducibility on the order of 5% R.S.D. for peak response and 2% R.S.D. for migration time. A typical efficiency (number of theoretical plates, $N = 5.54\, t_R^2 W_{1/2}^{-2}$, where t_R is the migration time for the peak of interest and $W_{1/2}$ is the peak width at half-height) for the insulin peak (65 cm × 75 μm I.D. capillary, 25 kV) was at least 40 000.

Quantitation

Our initial results at quantitation of commercial dosage forms of insulin (*i.e.* injection) were disappointing. A total of seven samples, six with a label declaration of 100 units (*ca.* 3.8 mg) per ml and one with a 500 unit/ml declaration, were examined. Overall results ranged from a low of 85.8% of declaration to a high of 108.1%. Compendial limits for this product are 95.0–105.0% of label claim. Even more discouraging was the poor repeatability of results. Triplicate analysis of one particular injection (discrete sample preparations) yielded results of 85.8%, 91.4% and 108.1%. Single level external standard calibration had been used for these determinations. A study of authentic (single blind, spiked) solutions of insulin reference standard produced a much more plausible, if not readily explicable outcome. The results of this study are summarized in Table II. Analytical accuracy was good in all three cases, but in only one instance was accuracy accompanied by an acceptable level of precision. Since accurate HPCE results were obtained only with single blind, spiked solutions (samples in which no matrix effects whatsoever existed) the poor accuracy encountered with commercial samples may be attributable to minor differences between standard and sample preparations.

In an effort to improve precision, we next investigated the use of an internal standard. Our sample preparation did not require isolating insulin from a complex sample matrix, and merely involved diluting injections to a suitable level. For this reason we did not concern ourselves with identifying as an appropriate internal standard a compound with nearly identical physical properties (molecular weight, solu-

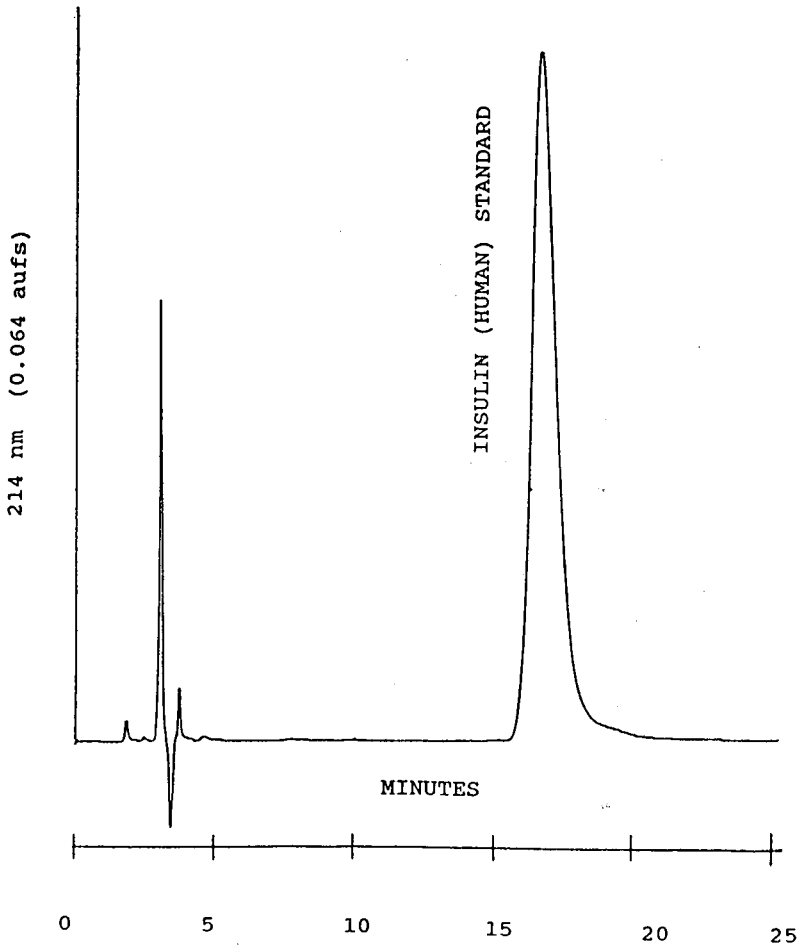

Fig. 2. Chromatogram of insulin (human) standard with UV detection (20 μl injection). Ultremex (Phenomenex) 5-μm C_{18} column, 25 cm × 0.46 cm I.D. Mobile phase: acetonitrile–0.2 *M* (pH 2.3) sodium sulfate (26:74). Flow-rate: 0.9 ml/min. Temperature: 40°C.

bility, isoelectric point) to those of insulin. We would be employing an internal standard for the express purpose of ascertaining whether its use resulted in improved analytical precision and accuracy. Two dansyl amino acids, dansyl-glutamine and dansyl-phenylalanine, were found to exhibit appropriate migration times relative to insulin and were commercially available in sufficiently pure form. Five of the pharmaceutical formulations were subjected to replicate analysis using the internal standard technique.

These samples were then reanalyzed by the previously described HPLC procedure in order to obtain comparative data. A typical chromatogram of insulin is presented in Fig. 2. Triplicate determinations were performed with single level external standard calibration being the only modification to the method. A statistical analysis of these results (omitting sample 399, the data for which were generated by

TABLE III

ANALYSIS OF INSULIN INJECTION BY HPCE VIA INTERNAL STANDARD TECHNIQUE

Sample	Species	Label claim (units/ml)	Amount found		R.S.D.[b] (%)
			mg/ml	units/ml[a]	
394	Human	100	3.359	89.01	2.51
395	Human	100	3.447	91.35	0.50
397	Pork	100	3.518	92.17	1.98
398	Pork	100	3.424	89.71	0.64
399	Human	100	3.678	97.47	1.33
399[c]	Human	100	3.572	94.66	0.37

[a] Based on assumed activities of 26.2 and 26.5 units per mg of pork and human insulin, respectively.
[b] Relative standard deviation, $n = 3$ (minimum).
[c] This series of analyses is based upon samplings from microtiter tray (200 μl volume). Otherwise, instrumental parameters as in Table I. Dansyl-*l*-phenylalanine internal standard.

TABLE IV

COMPARISON OF DETERMINATIONS OF INSULIN INJECTION (100 UNITS/ml) BY HPCE AND HPLC

Sample	Species	Amount found	mg/ml and [units/ml][a]				
		HPLC			HPCE		
394	Human	3.574	(0.91)	[94.71]	3.359	(2.51)	[89.01]
395	Human	3.719	(0.24)	[98.55]	3.447	(0.50)	[91.35]
397	Pork	3.871	(0.72)	[101.4]	3.518	(1.98)	[92.17]
398	Pork	3.662	(0.73)	[95.94]	3.424	(0.64)	[89.71]
399	Human	3.560	(2.99)	[94.34]	3.678	(1.33)	[97.47]
399	Human[b]				3.572	(0.37)	[94.66]

[a] Single level external standard calibration for HPLC data. Figures in parentheses represent relative standard deviation ($n = 3$). Based on assumed activities of 26.2 and 26.5 units per mg of pork and human insulin, respectively.
[b] This series of analyses is based upon samplings from microtiter tray (200 μl nominal volume). Otherwise, instrumental parameters are as in Table I. Dansyl-l-phenyl-alanine used as internal standard for HPCE.

TABLE V

COMPARATIVE ANALYSES OF AUTHENTIC, SINGLE-BLIND SPIKED SAMPLES[a]

Sample	Insulin content	Amount found, mg/ml, (R.S.D.), [% of actual content]					
		HPLC			HPCE		
1	2.07	2.077	(0.71)	[100.3]	2.019	(1.94)	[97.5]
2	1.19	1.172	(0.53)	[98.5]	1.219	(5.13)	[102.4]
3	4.25	4.309	(0.53)	[101.4]	4.160	(3.10)	[97.9]

[a] Single-level external standard calibrations for HPLC and HPCE. Relative standard deviation values based on 4 determinations per sample. HPCE conditions as in Table I. Refer to text for details of HPLC procedure.

sampling from two different size reservoirs) was carried out [16]. Critical values for t (Student's t-test) were exceeded (with at least a 95% confidence level) in each instance, indicating a statistically significant difference in results obtained by the two approaches, HPLC and HPCE. Tables III and IV summarize these findings.

Our final study involved a repetition of the comparison between HPLC and HPCE, but this time in a single blind format using authentic samples. The samples were prepared independently, using USP reference standard insulin (human) as the analyte and tricine buffer as the diluent. In generating the HPCE data we chose not to repeat the use of an internal standard, as it had been of no obvious advantage in improving accuracy. As Table V indicates, we were able to achieve reasonable accuracy using HPCE, although HPLC exhibited a clear advantage in terms of both accuracy and precision. Statistical evaluation revealed however that critical t-values for the two sets of data were not exceeded (95% confidence level) for any of the three samples. From a statistical standpoint then, the data are equivalent. It is worthy of note however, that relative standard deviation and variance are directly related. Since variance figures prominently in the calculation of t-values, it is in fact the relative imprecision of the data obtained by HPCE that results in a finding of statistical equivalence between the two sets of analyses.

CONCLUSIONS

Our experience —based upon the results in Tables II and V— with the analysis of single-blind spiked samples has shown that with identical standard and sample matrices, single level external standard calibration can provide reasonable accuracy (97.0% to 102.4%) at a sacrifice in precision (R.S.D. as high as 13.1%). The addition of an internal standard —refer to Tables III and IV— does impart added precision (R.S.D. of 2.51% or less) to HPCE with electrokinetic injection. At least in the case of actual sample determinations however, where even 25-fold dilution with running electrolyte leaves some disparity between standard and sample matrices, the internal standard technique did not achieve high accuracy.

It is our intention to pursue and more fully understand the issues of accuracy and precision in the FSCE of proteins. Modifications of the capillary surface (to overcome or minimize the problem of adsorption–desorption) are one possible approach to this problem. Such modifications could be either dynamic (achieved with additives, *e.g.* surfactants, to the electrolyte) or permanent (involving actual chemical transformations in order to produce a deactivated surface). It may prove necessary to use MECC rather than FSCE to resolve insulin types of different mammalian origin. In this report however, we have chosen not to focus on these matters. If indeed these issues are ever fully resolved, they clearly would merit publication in their own right. Our purpose in this study was first to examine the question of quantitation of proteins using FSCE in its simplest form.

ACKNOWLEDGEMENTS

We wish to acknowledge the assistance of several individuals within both the U S Food and Drug Administration (FDA) and Northeastern University who have assisted in the preparation of single-blind, spiked samples, especially P. Mackill, A.

Bourque, and L. Dou. Gratitude is expressed to R. Brownlee and H. Schwartz of Microphoretic Systems for the loan of the HPCE instrumentation and ancillary data station. The FDA has been most supportive in allowing M. L. and M. B. to undertake these studies within its laboratories. Constructive comments and suggestions for the eventual improvement of the manuscript were provided by B. L. Karger at Northeastern University, for which we remain grateful. I. S. K. is a current Science Advisor to the Winchester Engineering and Analytical Center of FDA.

This is contribution N. 477 from the Barnett Institute at Northeastern University.

REFERENCES

1 F. E. P. Mikkers, F. M. Everaerts and Th. P. E. M. Verheggen, *J. Chromatogr.*, 169 (1979) 1–10.
2 J. W. Jorgenson and K. D. Lukacs, *Anal. Chem.*, 53 (1981) 1298–1302.
3 *Capillary Electrophoresis Applications, A Bibliography of Selected References Published Through September 1989*, Beckman Instruments, Palo Alto, CA, 1989.
4 S. Fujiwara and S. Honda, *Anal. Chem.*, 59 (1987) 2773–2776.
5 S. Fujiwara and S. Honda, *Anal. Chem.*, 58 (1986) 1811–1814.
6 T. Tsuda, G. Nakagawa, M. Sato and K. Yagi, *J. Appl. Biochem.*, 5 (1983) 330–336.
7 X. Huang, J. A. Luckey, M. J. Gordon and R. N. Zare, *Anal. Chem.*, 61 (1989) 776–770.
8 H. H. Lauer and D. McManigill, *Anal. Chem.*, 58 (1986) 166–170.
9 R. G. Nielsen, G. S. Sittampalam and E. C. Rickard, *Anal. Biochem.*, 177 (1989) 20–26.
10 Y. Walbroehl and J. W. Jorgenson, *J. Microcolumn Sep.*, 1 (1989) 41–45.
11 P. D. Grossman, J. C. Colburn, H. H. Lauer, R. G. Nielsen, R. M. Riggin, G. S. Sittampalam and E. C. Rickard, *Anal. Chem.*, 61 (1989) 1186–1194.
12 *Pharmacopeial Forum*, Vol. 16, No. 1; US Pharmacopeial Convention, Rockville, MD, Jan.–Feb. 1990.
13 H. E. Schwartz, M. Melera and R. G. Brownlee, *J. Chromatogr.*, 480 (1989) 129–139.
14 X. Huang, M. J. Gordon and R. N. Zare, *Anal. Chem.*, 60 (1988) 375–377.
15 P. D. Grossman, H. H. Lauer, S. E. Moring, D. E. Mead, M. F. Oldham, J. H. Nickel, J. R. P. Goudberg, A. Krever, D. H. Ransom and J. C. Colburn, *Am. Biotechnol. Lab.*, 8 (1990) 35–43.
16 R. L. Anderson, *Practical Statistics for Analytical Chemists*, Van Nostrand Reinhold, New York, 1987, pp. 76–78.

Journal of Chromatography, 549 (1991) 367–373
Elsevier Science Publishers B.V., Amsterdam

CHROM. 23 344

Application of micellar electrokinetic capillary chromatography to the determination of flavonoid drugs

P. G. PIETTA* and P. L. MAURI
Dipartimento di Scienze e Tecnologie Biomediche, Sezione Chimica Organica, Via Celoria 2, 20133 Milan (Italy)
A. RAVA
Istituto Biochimico Pavese, Viale Certosa 10, 27100 Pavia (Italy)
and
G. SABBATINI
Applied Biosystems, Via Darwin 22, 20143 Milan (Italy)
(First received January 22nd, 1991; revised manuscript received March 25th, 1991)

ABSTRACT

The use of micellar electrokinetic capillary chromatography is described for the determination of flavonol-3-O-glycosides. A 72-cm fused-silica capillary column and a 50 m*M* sodium dodecyl sulphate–20 m*M* sodium borate running buffer (pH 8.3) were used for the electrophoretic separations. The samples were injected onto the capillary column in the range 10–1000 pg. Results are given for quercetin-, kaempferol- and isorhamnetin-3-O-glycosides and for a standardized *Ginkgo biloba* extract. The results are compared with those obtained by reversed-phase high-performance liquid chromatography.

INTRODUCTION

Capillary electrophoresis (CE) [1] is becoming increasingly recognized as an important analytical separation technique as a result of its speed, reproducibility, accuracy and potential for automation. In addition, CE does not require any staining procedure, and the sample bands subsequent to separation are detected by on-line ultraviolet (UV) detection in the same way as for high-performance liquid chromatography (HPLC). From a review of the literature it is clear that a large variety of compounds, including amino acids [2], peptides [3], proteins [4], oligonucleotides [5], DNA fragments [6], vitamins and drugs [7] have been separated and analysed by CE. However, this technique has not yet been applied to the separation of flavonoids. These compounds are widely distributed plant metabolites, with structures based on 2-phenylbenzopyrone and differing one from another in the pattern of hydroxylation, degree of unsaturation and type and position of sugar links. Although the flavonoids are weak acids (phenols), they are best separated on the basis of their hydrophobic differentiation, that is, by reversed-phase (RP) HPLC. CE in the micellar mode pro-

0021-9673/91/$03.50

vides an alternative to RP-HPLC, as in a micellar system ionic detergents are added directly to the mobile phase buffer to generate aggregates consisting of a hydrophobic interior and a charged surface.

Extending the previous study [8] on developing methods for the analysis of flavonoid drugs, micellar electrokinetic capillary chromatography (MECC) was used for the separation of a number of flavonol-3-O-glycosides which are commonly present in medicinal plants. This approach represents a new and powerful tool, as it allows a rapid, reproducible, high resolution and sensitive determination of flavonol-3-O-glycosides, as confirmed by the results presented in this paper.

EXPERIMENTAL

Materials

The reference compounds (Fig. 1, I-VII and IX) were obtained from Extrasynthese (Genay, France). Compound VIII was already available in this laboratory [9]. A standardized *Ginkgo biloba* extract was purchased from Laboratories IPSEN.

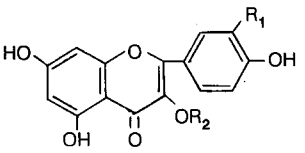

	R_1	R_2
Rutin (I)	OH	Rutinose
Isoquercitrin (II)	OH	Glucose
Hyperosid (III)	OH	Galactose
Quercitrin (IV)	OH	Rhamnose
Avicularin (V)	OH	Arabinose
Kaempferol-3-O-rutinoside (VI)	H	Rutinose
Isorhamnetin-3-O-rutinoside (VII)	OMe	Rutinose
Astragalin (VIII)	H	Glucose
Isorhamnetin-3-O-glucoside (IX)	OMe	Glucose

Fig. 1. Structures of the flavonol-3-O-glycosides.

All the other chemicals were of HPLC grade.

Apparatus

MECC. All separations were performed using an Applied Biosystems 270A CE apparatus (San Jose, CA, USA) equipped with a 72-cm fused silica capillary column (50 μm I.D.). The analysis buffer was 20 m*M* sodium borate (pH 8.3) and 50 m*M* sodium dodecyl sulphate (SDS). The other conditions were: voltage, +20 kV (+277 V/cm); temperature, 27°C; injection, 1 s aspiration (4 nl); and detection, 260 nm. All buffers were filtered using a Sigma (St. Louis, MO, USA) 0.2 μm filter. To maintain the capillary conditions, fresh buffer was introduced into the capillary between each run. This was achieved by a 2 min (approximately two volumes) aspiration of the running buffer.

The data were collected and analysed on a Shimadzu CR6A data processor (Kyoto, Japan).

HPLC. The liquid chromatograph consisted of a Model U6K universal in-

jector, two Model 510 pumps, a Model 680 automated gradient controller and a Model 480 Lambda-Max UV variable-wavelength detector (all from Waters Assoc., Milford, MA, USA). The data were collected and analysed on a Shimadzu CR3A data processor (Shimadzu, Kyoto, Japan). The column was a C_8 Aquapore RP-300 (7 μm spherical cartridge, 220 × 4.6 mm I.D.) with an Aquapore RP-300 guard column (7 μm spherical cartridge, 30 × 4.6 mm) from Applied Biosystems. Eluent A was water–2-propanol (95:5) and eluent B 2-propanol–tetrahydofuran(THF)–water (40:10:50). The gradient profile was linear from 20 to 60% B in 40 min at a flow-rate of 1 ml/min; detection was at 260 nm.

Calibration graphs

Compounds I–IX were dissolved in methanol (0.15 mg/ml); these stock solutions were diluted with 30% aqueous methanol to obtain reference solutions containing 2–250 μg/ml.

Sample preparation

The standardized *Ginkgo biloba* extract (5 mg) was dissolved in 1 ml of 30% aqueous methanol and filtered through Spartan 13 filters (0.45 μm, Schleicher and Schuel, Dassel, Germany).

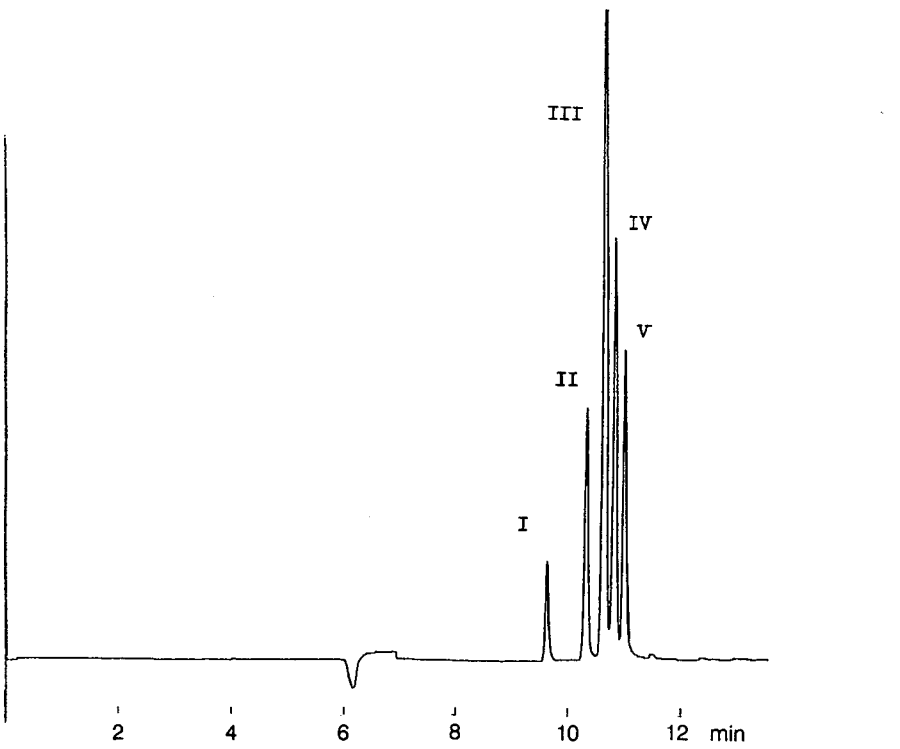

Fig. 2. MECC separation of quercetin-3-O-glycosides (20–100 pg; compounds I–V). See Fig. 1 for peak identification. Conditions: capillary, 72-cm fused silica (50 μm I.D.); voltage, 277 V/cm; buffer, 50 m*M* SDS–20 m*M* borate (pH 8.3); injection, 1 s aspiration; detection, 260 nm; attenuation 16 (mV/full scale).

RESULTS AND DISCUSSION

Of the flavonol-3-O-glycosides the most common are the quercetin, kaempferol and isorhamnetin derivatives (Fig. 1). Their determination has been traditionally carried out by RP-HPLC, whereas electrophoresis finds a limited application in the recognition of charged species, such as sulphates and glucuronides [10]. By using MECC, it has been possible for the first time to determine the flavonol-3-glycosides. According to the MECC technique, SDS was added to the running buffer (50 m*M* SDS–20 m*M* sodium borate, pH 8.3) to generate the micelles. At this pH, the electroendosmotic flow is sufficiently strong to overcome the tendency for negatively charged glycosides to migrate away from the detector, and separation takes place as a result of differences in partitioning into and out of the hydrophobic core of the micelles.

A typical electropherogram of a standard mixture of quercetin-3-O-glycosides (I–IV) is shown in Fig. 2. The five compounds gave well resolved peaks within a 14

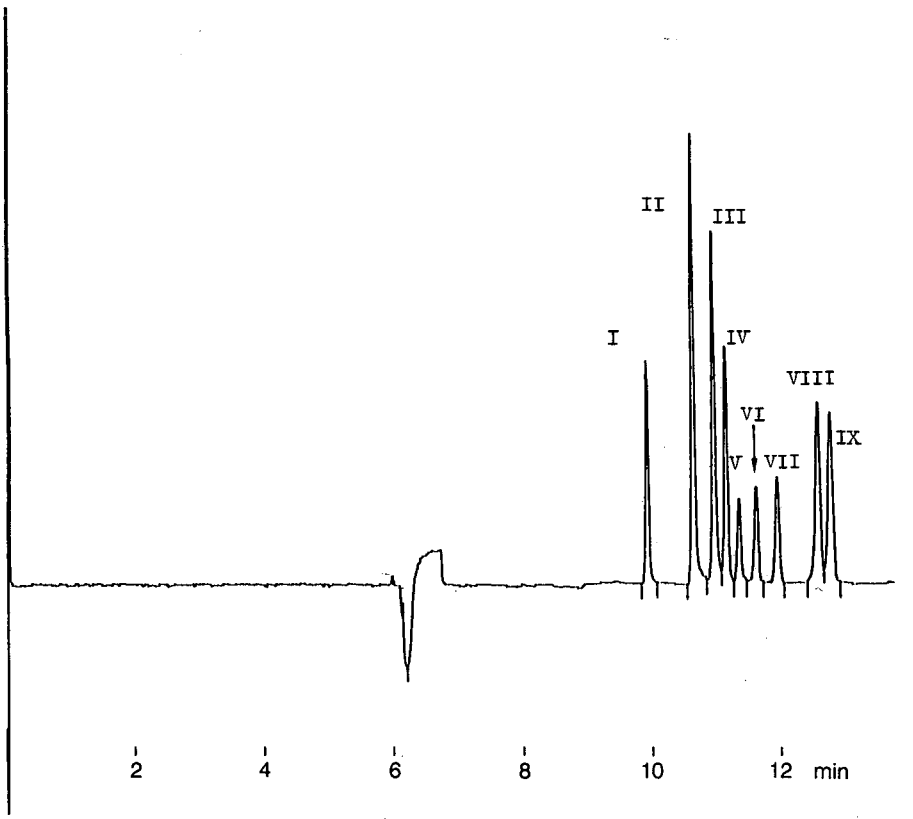

Fig. 3. MECC separation of quercetin-3-O-glycosides (compound I–V), kaempferol-3-O-glycosides (compounds VI, VIII) and isorhamnetin-3-O-glycosides (compounds VII, IX). See Fig. 1 for peak identification. Conditions as in Fig. 2.

TABLE I

MIGRATION (CE) AND RETENTION (HPLC) TIMES

Peak	CE (min)	HPLC (min)
I	9.90	11.76
II	10.61	13.92
III	10.93	13.92
IV	11.13	18.61
V	11.32	15.14
VI	11.61	15.73
VII	11.94	14.57
VIII	12.57	17.74
IX	12.76	16.52

min analysis time, and the standard deviations of the migration times were 0.4% (n = 40) and 0.7% (n = 10) for intra- and inter-day assays, respectively.

To the authors' knowledge, there is no isocratic HPLC system which allows the same separation, and a possible gradient approach is less rapid and simple. Analogous results were obtained for kaempferol- and isorhamnetin-3-O-glycosides. Although their simultaneous occurrence in medicinal plants is not frequent, a mixture of

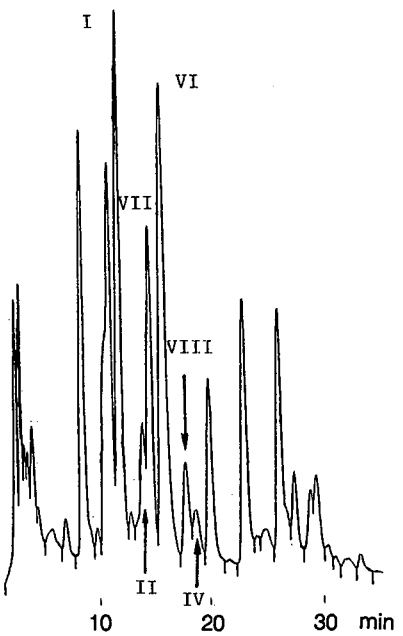

Fig. 4. RP-HPLC separation of standardized extract of *Ginkgo biloba* leaves. Conditions: column, C_8 Aquapore RP-300, 7 μm; eluent A, water–2-propanol (95:5); eluent B, water–THF–2-propanol (50:10:40); gradient profile, from 20 to 60% B in 40 min; flow-rate, 1 ml/min; detection, 260 nm. See Fig. 1 for peak identification.

all the glycosides (I–IX) was also analysed, and a sharp baseline separation was obtained (Fig. 3).

The elution order is slightly different from that found in RP-HPLC, as in addition to the hydrophobic interaction with the micelles, electrophoretic mechanisms are also occurring (Table I).

The detector response was linear over the range 10–1000 pg (15–1500 fmol), the regression coefficient being between 0.995 and 0.999 (n = 20; S.D. = 1.2 and 1.9% for intra- and inter-day, assays, respectively).

By injecting 4 nl of the sample solutions (1.5 μg/ml) in 30% methanol, amounts as low as 6 pg were detected. The percentage of organic solvent was of prime importance, as higher concentrations resulted in a poor resolution.

To confirm its validity, this technique was applied to a particularly complex matrix, *i.e.* to *Ginkgo biloba* extract, the analysis of which by RP-HPLC (Fig. 4) in the gradient mode has been previously reported [11]. As shown in Fig. 5, MECC yielded a high baseline resolution within 14 min. Of the peaks, I, II, IV, VI, VII and VIII were identified by comparison with standard.

From these results, it can be reasonably deduced that MECC is a promising tool for the determination of flavonoids. It has a greater resolving power and is faster than RP-HPLC. The level of sensitivity compared to HPLC (about 50 ng) is also

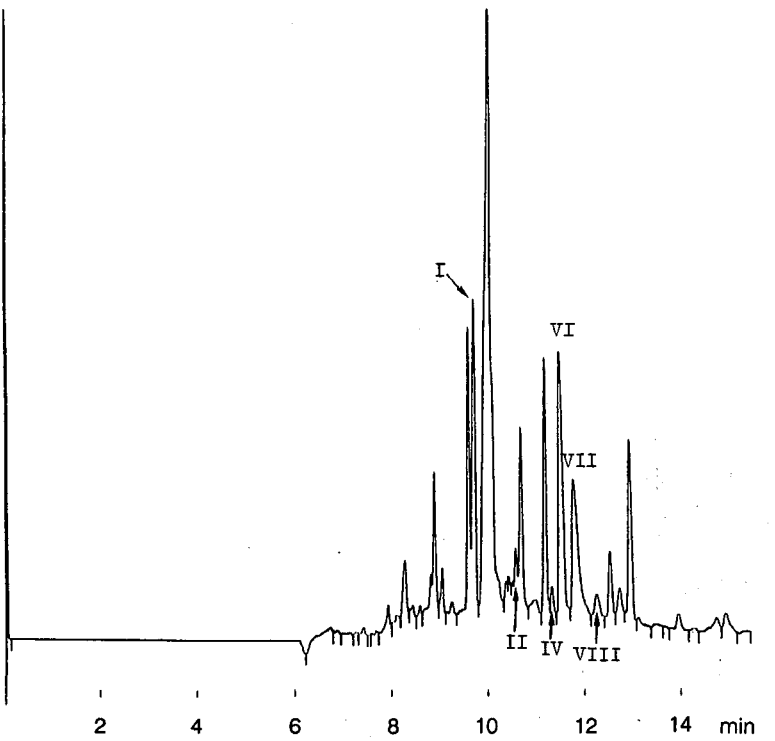

Fig. 5. MECC separation of a standardized extract of *Ginkgo biloba* leaves. For peak identification see Fig. 1. Conditions as in Fig. 2.

higher; in addition, MECC has the advantages of very low solvent consumption and the data analysis capabilities of HPLC. Owing to its complementary value with RP-HPLC, the described procedure will be extended to other flavonoids (flavones, isoflavones, flavanoids, biflavones, anthocyanins and proanthocyanins) with the aim of developing an MECC based 'finger printing' technique for medicinal plants.

ACKNOWLEDGEMENTS

The authors are grateful to CNR-P.S. "Innovazione produttiva nella P&MI" for providing funds for this work.

REFERENCES

1 J. W. Jorgerson, *Anal. Chem.*, 58 (1986) 754A.
2 N. J. Dovichi and Y. F. Cheng, *Am. Biotechnol. Labs.*, 7 (1989) 10.
3 R. M. Caprioli, W. J. Moore, M. Martin, B. B. Dague, K. Witson and S. Moring, *J. Chromatogr.*, 480 (1989) 247.
4 G. J. M. Bruin, J. P. Chang, R. H. Kuhlman, K. Zegers, J. C. Kraak and H. Poppe, *J. Chromatogr.*, 471 (1989) 429.
5 T. Wang, R. A. Hartwick and P. B. Champlin, *J. Chromatogr.*, 462 (1989) 147.
6 P. L. Mauri, P. G. Pietta and M. Pace, *J. Chromatogr.*, 566 (1991) 327.
7 H. Nishi and S. Terabe, *Electrophoresis*, 11 (1990) 691.
8 P. G. Pietta, P. L. Mauri, E. Manera and P. L. Ceva, *J. Chromatogr.*, 513 (1990) 397.
9 P. G. Pietta, P. L. Mauri, C. Gardana, F. R. Maffei and M. Carini, *J. Chromatogr.*, 537 (1991) 459.
10 K. R. Markham, *Biochem. System. Ecol.*, 8 (1980) 11.
11 P. G. Pietta, P. L. Mauri, A. Bruno, A. Rava, E. Manera and P. L. Ceva, *J. Chromatogr.*, 553 (1991) 223.

Journal of Chromatography, 549 (1991) 375–385
Elsevier Science Publishers B.V., Amsterdam

CHROM. 23 186

Separation of seven tricyclic antidepressants using capillary electrophoresis

KAREN SALOMON*, DEAN S. BURGI and JOHN C. HELMER
Varian Research Center, 3075 Hansen Way, Palo Alto, CA 94304–1025 (USA)
(First received October 25th, 1990; revised manuscript received January 9th, 1991)

ABSTRACT

Seven tricyclic antidepressants, protriptyline, desipramine, nortriptyline, nordoxepin, imipramine, amitriptyline and doxepin, were separated using capillary electrophoresis. Because the tricyclic antidepressants were similar in structure and mass, careful manipulation of the electroosmotic flow and the electrophoretic mobilities was required for an optimal separation. In the systematic approach we have developed, the differential electrophoretic mobilities were first maximized by adjusting pH. Next, increasing the buffer concentration improved the separation at the expense of migration times by reducing the electroosmotic flow. Full resolution was achieved by the addition of methanol to the buffer which decreased both the electroosmotic flow and the electrophoretic mobilities of the samples.

INTRODUCTION

Capillary electrophoresis (CE) is a separation technique that has become popular in many areas. Ease of operation and rapid analysis time are two attractive features of CE. Selectivity is based on differences in electrophoretic mobilities between samples. Applications range from the separation of metal cations [1,2] to the resolution of proteins [3–7].

Some of the more elegant work in CE involves the separation of species that are nearly identical, such as isomeric compounds or isotopically substituted species. To effect full resolution, the electroosmotic flow or the electrophoretic mobilities are carefully adjusted. Fujiwara and Honda [8] were able to separate positional isomers of substituted benzoic acids after adding methanol to their buffer to decrease the electroosmotic flow. Grossman *et al.* [9] were able to separate peptides containing seven amino acids that differed in the order of linkage by working at a low pH. Terabe *et al.* [10] were able to separate oxygen-isotopic benzoic acids by carefully adjusting the pH of the buffer to a value close to the pK_a of benzoic acid; hydroxypropyl cellulose was added to the buffer to suppress the electroosmotic flow. Bushey and Jorgenson [11,12] were able to separate dansylated methylamine and dansylated [$^2H_3$]methylamine in a buffer containing micelles by adding 20% methanol to change the capacity factor as well as to reduce the electroosmotic flow.

While there are many ways to improve separations, we are interested in

0021-9673/91/$03.50

providing a systematic approach to separating compounds that are closely related in mass and structure. In the present study we have investigated the effect of buffer pH, buffer concentration and the addition of organic modifiers on the separation of seven tricyclic amines. We are particularly interested in how the electroosmotic flow and the electrophoretic mobilities are affected. We first optimized the differential mobilities by adjusting the pH to a value close to the pK_a values of the seven amines. Increasing the buffer concentration decreased the electroosmotic flow while leaving the electrophoretic mobilities unaltered. Adding methanol to the buffer had the most significant effect on the resolution, decreasing both the electroosmotic flow and the electrophoretic mobilities. The increase in viscosity due to the methanol could not quantitatively account for the changes observed. It appeared that the changes in the dielectric constant affected the degree of dissociation of the protonated samples making them appear more neutral and decreasing the electrophoretic mobility.

EXPERIMENTAL

Instrumentation

The research CE instrument used was similar to those described previously [7,13,14]. A fused-silica capillary column, 1 m × 75 μm I.D. was suspended between two buffer reservoirs. A 30-kV Glassman (Whitehouse Station, NJ, USA) high-voltage power supply was used to apply voltage across the platinum electrodes resting in the buffer reservoirs. Samples were detected on-column using a modified Jasco UV detector set to 210 nm with an 0.05-s time constant. A detector window was fashioned in the column 75 cm from the injection end by burning off a section of the polyimide coating on the capillary column. Injections were done in a hydrodynamic fashion by dipping the injection end of the column into the sample reservoir for 5 s while it rested 3 in. above the detection end reservoir. All separations were run at 30 kV for maximum resolution and minimum migration times. The current did not exceed 20 μA.

The column was etched with 0.1 *M* NaOH for 30 min at the start of each day. Water was used to rinse the column and then the buffer was introduced and allowed to equilibrate with the silica capillary. The column was flushed with buffer after each run.

Chemicals

The buffer used was 3-(cyclohexylamino)-2-hydroxy-1-propanesulfonic acid (CAPSO) with a pK_a of 9.6 and was purchased from Sigma (St. Louis, MO, USA). NaOH obtained from J. T. Baker (Phillipsburg, NJ, USA) was used to adjust the buffer pH to values between 9.0 and 10.0. For the studies in which the pH was varied, a 50-m*M* CAPSO buffer with variable concentrations of NaOH was used. For the studies in which the buffer concentrations were varied, both the CAPSO and the NaOH concentrations were changed while keeping the pH constant at 9.55. For the studies where methanol was added, 0.5933 g of CAPSO were dissolved in 50 ml of the appropriate water–methanol mixture and then the pH was adjusted to 9.55 with NaOH.

The samples used in our study were protriptyline, desipramine, nortriptyline, nordoxepin, imipramine, amitriptyline and doxepin obtained from Alltech (Deerfield, IL, USA). Samples were prepared individually in a 50% pH 4.4 phosphate buffer and 50% methanol solution and then mixed together so that the final concentration was

0.14 m*M*. The methanol in the sample solution was used as a neutral marker to monitor the electroosmotic flow with each run.

RESULTS AND DISCUSSION

We have chosen a sample of seven tricyclic amines; the detection and quantitation of tricyclic amines is important because of the wide use of these compounds for the treatment of depression [15]. The structures of the compounds are shown in Fig. 1. Protriptyline (mol.wt. 263.37), desipramine (mol.wt. 266.37), nortriptyline (mol.wt. 263.37) and nordoxepin (ml.wt. 265.37) are all secondary amines that differ from each other only by the substitution of nitrogen or oxygen for a carbon in the ring. Protriptyline and nortriptyline are positional isomers. The pK_a values of these compounds are close to 10.7 [16]. The other three, imipramine (mol.wt. 280.40), amitriptyline (mol.wt. 277.39) and doxepin (mol.wt. 279.37) are tertiary amines that differ from each other only in the substitution of nitrogen or oxygen for a carbon in the ring. The pK_a values of these amines are close to 9.8 [16].

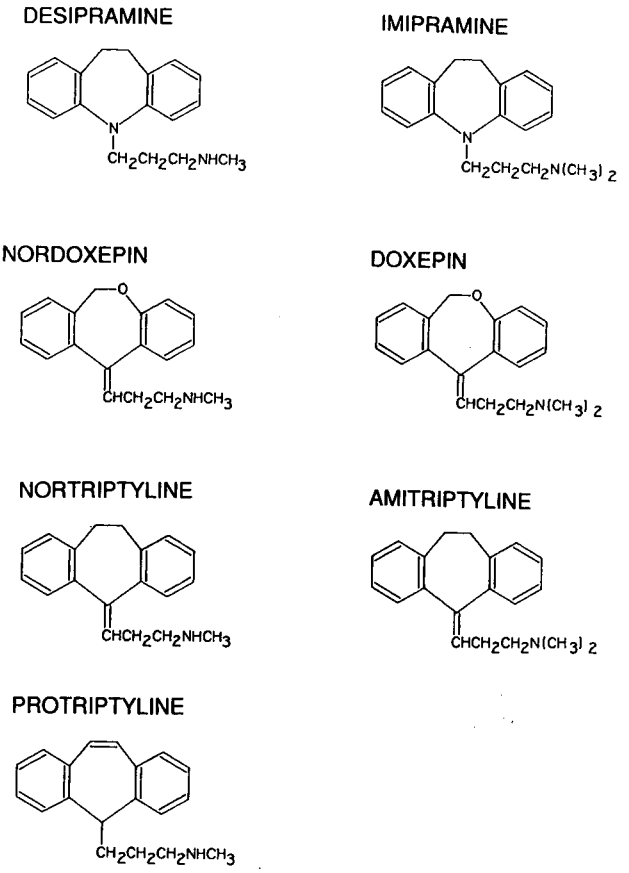

Fig. 1. Structures of the seven tricyclic amines.

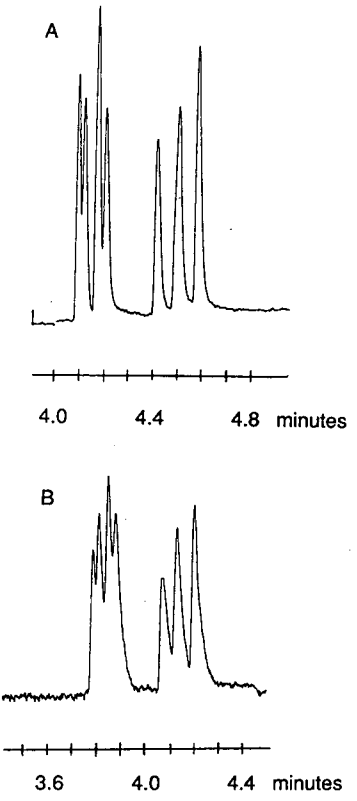

Fig. 2. (A) Separation of the seven tricyclic amines at pH 9.55, 50 m*M* CAPSO–12.5 m*M* NaOH; the order of elution is: protriptyline, desipramine, nortriptyline, nordoxepin, imipramine, amitriptyline and doxepin; (B) separation of the seven tricyclic amines at pH 9.55, 10 m*M* CAPSO–2.7 m*M* NaOH. The order of elution is the same as that for (A); the period of injection has been reduced to 3 s here.

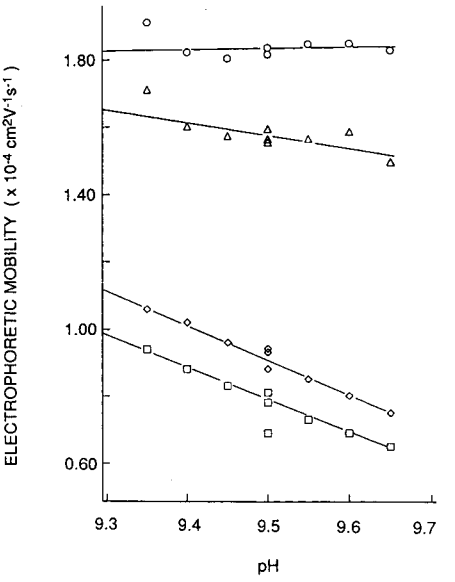

Fig. 3. Electrophoretic mobilities of protriptyline (○), nordoxepin (△), amitriptyline (◇) and doxepin (□) plotted as a function of pH for a 50 m*M* CAPSO buffer. Lines are drawn to emphasize the differences in μ_{ep} between the different compounds.

Effect of pH

At pH 6, all the amines were fully protonated; an electrophoretogram run at this pH resulted in only two peaks, each corresponding to the two different mass groupings. At pH 9.2, the three tertiary amines were baseline resolved, while the four secondary amines eluted as three peaks. At pH 9.4, the secondary amines eluted as four peaks although they were not completely separated. The resolution improved up to pH 9.55 (Fig. 2A); at pH 9.6, the amitriptyline and doxepin peaks began merging together.

Changing the pH from 9.0 to 9.65 had only a negligible effect on the electroosmotic flow (μ_{eo}); however, the change in the elctrophoretic mobilities (μ_{ep}) was pronounced. A plot of the electrophoretic mobilities of protriptyline, nordoxepin, amitriptyline and doxepin *vs.* pH is shown in Fig. 3. With the exception of the electrophoretic mobility of protriptyline (which eluted first), μ_{ep} decreased as the pH was raised.

According to the Stokes–Einstein relationship [17]

$$\mu_{ep} = \frac{q}{6\pi\eta a} \tag{1}$$

where q is the charge of a particular solute (positively charged in this case), a is the hydrodynamic radius of the solute and η is the viscosity of the solution through which the solute moves. If one assumes that the viscosity and the effective radius did not change over the pH region studied, then the observed change in μ_{ep} can be attributed to a change in the charge of the sample. A functional form for the change in the electrophoretic mobility with the degree of protonation of a species is given below [10]

$$\mu_{ep} = f\mu_{ep}(0) \tag{2}$$

where f is the fraction of a compound in its protonated form and $\mu_{ep}(0)$ is the mobility of the solute in its completely protonated form. The largest influence of the pH on the fraction protonated occurs when the pH is close to the pK_a of the solute.

Because the electrophoretic mobilities of all the samples except protriptyline decreased as the pH was raised from 9.0 to 9.6, the differential electrophoretic mobilities, $\Delta\mu_{ep}$, also changed. As the degree of protonation was altered, the differences in electrophoretic mobilities between two compounds became more or less pronounced and the resolution was affected. Resolution, R_s, is directly proportional to the differential electrophoretic mobilities according to the following equation [7,10]

$$R_s = \frac{1}{4}\left(\frac{V}{2D}\right)^{1/2}\left(\frac{l}{L}\right)^{1/2}\frac{\Delta\mu_{ep}}{[\mu_{ep}(\text{ave}) + \mu_{eo}]^{1/2}} \tag{3}$$

where V is the applied voltage, l is the length of the column to the detector window, L is the length of the column, D is the diffusion coefficient, and $\mu_{ep}(\text{ave})$ is the average electrophoretic mobility of the two components being separated. For the secondary amines, protriptyline and nordoxepin, $\Delta\mu_{ep}$ increased at higher pH values and an improvement in resolution was observed. For the tertiary amines, amitriptyline and doxepin, $\Delta\mu_{ep}$ became somewhat smaller at pH values >9.5 leading to poorer resolution of these two samples. The change in $\Delta\mu_{ep}$ with pH appeared to provide a window of optimal separation.

According to Terabe *et al.* [10], the optimum pH value for a CE separation lies below the pK_a values of the species being separated. Terabe *et al.* postulated that the optimum pH of a separation of compounds of comparable pK_a values was equal to pK_a − log 2. Assuming that the pK_a of the tertiary amines was close to 9.8, the optimal separation should have been at pH 9.5. Experimentally, pH 9.55 was found to give the best resolution of the tertiary amines which is in fairly good agreement with the theory of Terabe *et al.*

Other studies in the literature on the electrophoretic mobilities measured in a CE system as a function of pH show some dependence of μ_{ep} on pH if the pH is close to the pK_a or pI of the species being separated [18–20]. Overall, our results are consistent with the idea that the separation of similar compounds can be influenced by charge differentiation induced by an adjustment of the pH near the pK_a values of the compounds of interest.

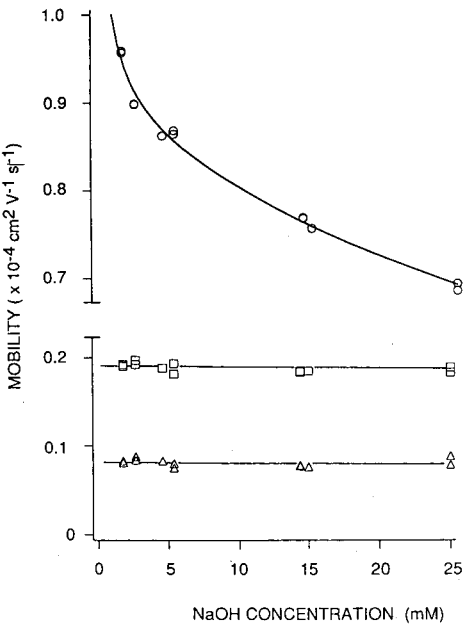

Fig. 4. Electroosmotic flow (□) and electrophoretic mobilities of protriptyline (○) and doxepin (△) as a function of NaOH concentration, at pH 9.55. The solid line drawn through the data points for the electroosmotic mobility are the result of a fit to eqn. 8.

Effect of buffer concentration

The change in the resolution of the seven tricyclic amines with buffer concentration can be seen in Fig. 2. At 10 m*M* CAPSO–2.7 m*M* NaOH, the seven peaks were much less resolved than at 50 m*M* CAPSO–14 m*M* NaOH; the pH is equivalent in both systems. The electroosmotic flow decreased as the buffer concentration increased; a plot of μ_{eo} *vs.* NaOH concentration is shown in Fig. 4. Also shown in Fig. 4 are plots of the electrophoretic mobilities of protriptyline and doxepin as a function of buffer concentration. Unlike the electroosmotic flow, the electrophoretic mobilities were invariant over the concentration range studied. Since the differential mobilities were unchanged, the observed improvement in resolution with increasing buffer concentration must be due to the reduction in the electroosmotic flow (eqn. 3).

The decrease in the zeta potential (which is proportional to μ_{eo}) with increasing buffer concentration is well known in colloid chemistry [21] and it has also been observed in capillary electrophoresis [19,22–27] although an exact relationship between μ_{eo} and buffer concentration had not been formulated. Tsuda *et al.* [22] observed a decrease in the electroosmotic flow with an increase in phosphate buffer concentration and linked it to a decrease in the double-layer thickness which is inversely proportional to the square root of the buffer concentration. However, we were unable to fit their equation to our data.

We have recently derived a relationship between the electroosmotic mobility and

the concentration of monovalent cations (*conc*) in the buffer [28]. We started with the following expression for the electroosmotic mobility

$$\mu_{eo} = \frac{Qx}{\eta} \tag{4}$$

where Q is the charge per unit area at the interface between the capillary wall and the buffer and x is the thickness of the counter-ion layer. We have postulated that the counter-ion layer consists of two regimes: one being a compact layer, the thickness of which is fixed; the other a diffuse layer in which the ions are randomly oriented and which can be described by a Gouy–Chapman model. In such a case, the thickness of the compact layer is defined as d_0 and is not concentration dependent; while the thickness of the diffuse layer is equal to $1/K'(\text{conc})^{1/2}$, where K' is a constant with a value of $3.2 \cdot 10^9\ \text{m}^{-1}\ M^{-1/2}$ (for a monovalent, dilute aqueous buffer at 25°C). The thickness of the counter-ion layer can then be written as:

$$x = d_0 + \frac{1}{K'\sqrt{(conc)}} \tag{5}$$

The charge per unit area at the interface, Q, is also dependent on the buffer concentration. As the buffer concentration is increased, more cations are adsorbed onto the silica surface, leading to a decrease in the charge at the interface. The equilibrium constant K_{wall}, for this process can be written as:

$$K_{wall} = \frac{[\text{SiO}^-\text{M}^+]}{[\text{M}^+][\text{SiO}^-]} \tag{6}$$

where SiO^- is simply Q, M^+ is a monovalent cation, and SiO^-M^+ is a silanol group with an adsorbed cation. Q can then be written in the following form [28]

$$Q = \frac{Q_0}{1 + [K_{wall}(conc)]} \tag{7}$$

where Q_0 is the sum of $[\text{SiO}^-]$ and $[\text{SiO}^-\text{M}^+]$ and corresponds to the concentration of ionized groups on the capillary surface. Substituting the above expressions for Q and x into eqn. 4, one obtains an equation for the electroosmotic mobility in terms of the buffer concentration

$$\mu_{eo} = \left(\frac{Q_0}{\eta}\right)\frac{d_0 + \dfrac{1}{K'\sqrt{(conc)}}}{1 + [K_{wall}(conc)]} \tag{8}$$

Our data was fit to the above equation and the resulting curve was plotted in Fig. 4. Values of the above parameters were found to be: $Q_0 = 1.3 \cdot 10^{16}$ charged sites/m^2; $d_0 = 3.8 \cdot 10^{-8}$ m; and $K_{wall} = 0.0093\ \text{m}M^{-1}$. In our model, the decrease in μ_{eo} with

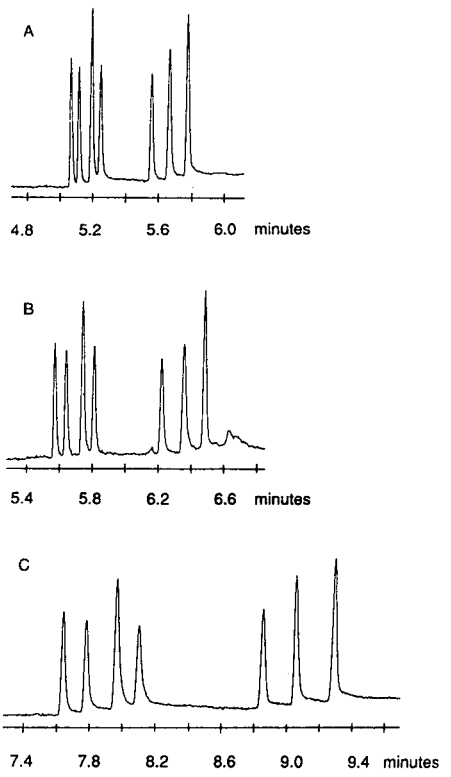

Fig. 5. Separation of seven tricyclic amines as a function of methanol concentration. (A) 4.0% (w/w) methanol; (B) 7.9% (w/w) methanol; (C) 15.8% (w/w) methanol. The order of elution is the same as that for Fig. 2A. Buffer pH 9.55; buffer concentration given in Table I.

increasing buffer concentration is linked to both a decrease in counter-ion layer thickness as well as an increase in the coverage of sites on the silica surface which reduces the charge per unit area at the interface between the capillary wall and the buffer.

Addition of methanol to the buffer

The addition of methanol to the buffer greatly improved the resolution of the seven tricyclic amines as seen in Fig. 5. At 4.0% methanol, only nortriptyline and nordoxepin were not baseline resolved; at 7.9% all peaks were baseline resolved. The resolution was further improved at 15.8% and on up to 23.7% (not shown). There was no change in the order of elution.

One factor in the improved resolution (eqn. 3) was the decrease in the electroosmotic flow (Table I). The decrease in μ_{eo} with the addition of methanol has been noted by others [8,12,27] and attributed to changes in the zeta potential, as well as changes in the viscosity and the dielectric constant of the buffer. Viscosity alone was not responsible for the reduction in μ_{eo}; if it were, the product of μ_{eo} and viscosity would be a constant according to eqn. 4. Values of the product are tabulated in Table I and are seen to decrease with increasing methanol concentration. Another factor

TABLE I

ELECTROOSMOTIC FLOW, μ_{eo}, VISCOSITY, η, AND DIELECTRIC CONSTANT, ε, FOR VARIOUS CONCENTRATIONS OF WATER–METHANOL MIXTURES

Methanol (%, w/w)	[NaOH] (mM)	μ_{eo} ($cm^2\ V^{-1}\ s^{-1}$)	η^a (cP)	ε^b	$\mu_{eo}\eta$ ($cP\ cm^2\ V^{-1}\ s^{-1}$)
0.0	12.5	$7.95 \cdot 10^{-4}$	1.00	80	$7.96 \cdot 10^{-4}$
2.0	13.0	$7.23 \cdot 10^{-4}$	1.07	–	$7.72 \cdot 10^{-4}$
4.0	13.8	$6.47 \cdot 10^{-4}$	1.13	–	$7.30 \cdot 10^{-4}$
5.9	15.5	$6.15 \cdot 10^{-4}$	1.19	–	$7.34 \cdot 10^{-4}$
7.9	16.2	$5.66 \cdot 10^{-4}$	1.26	76	$7.14 \cdot 10^{-4}$
15.8	18.0	$4.16 \cdot 10^{-4}$	1.50	–	$6.23 \cdot 10^{-4}$
23.7	19.8	$3.22 \cdot 10^{-4}$	1.69	71	$5.45 \cdot 10^{-4}$

[a] From. ref. 16.
[b] From ref. 30.

contributing to the reduction in the electroosmotic flow includes the increased NaOH concentrations needed to maintain the buffer at pH 9.55 as the percentage of methanol is increased.

In order to explore more fully the factors controlling the decrease in the electroosmotic flow with increasing methanol concentration, we have measured μ_{eo} as a function of NaOH concentration at a fixed percentage of methanol and fitted the results to eqn. 8. Experiments were conducted at pH 9.55 in CAPSO–NaOH buffers of 7.9% methanol; the concentration of NaOH was varied from 4.5 to 45 mM. A good fit of eqn. 8 with data was obtained with the following values: $K_{wall} = 0.011\ mM^{-1}$; $d_0 = 1.33 \cdot 10^{-8}$ m; and $Q_0 = 2.94 \cdot 10^{16}$ charged sites per square meter. Compared to the values derived without methanol in the buffer, it can be seen that the equilibrium constant between the sodium ions and the wall did not change. However, the value of d_0 decreased when methanol was present in the buffer. It is possible that the presence of methanol in the buffer aided in the solvation of the ions in the buffer and reduced the thickness of the compact layer next to the interface. The initial charge at the wall, Q_0, increased when methanol was present in the buffer; the presence of methanol may have minimized the repulsion between SiO^- groups on the capillary surface, thus allowing more of them to exist in a given area than if methanol were not present in the buffer. The reduction of d_0 as well as the increase in the viscosity and cation concentration are primarily responsible for the decrease in μ_{eo}. We have not found any evidence for changes in the equilibrium constant between the cations and the silica surface.

The electrophoretic mobilities also decreased as the buffer became more concentrated in methanol, leading to an improvement in resolution according to eqn. 3. Part of the decrease could be attributeed to an increase in viscosity as the percentage of methanol was increased. However, if viscosity were the only parameter controlling the electrophoretic mobility, then the product of the electrophoretic mobility and the viscosity would have been a constant at different methanol concentrations according to eqn. 1. We have found experimentally that this is not the case as shown in Fig. 6 for four of the tricyclic amines. For protriptyline which eluted first, the plot sloped downward only slightly. For nordoxepin which eluted fourth, the downward slope was more distinct. For imipramine and doxepin which eluted fifth and seventh, respective-

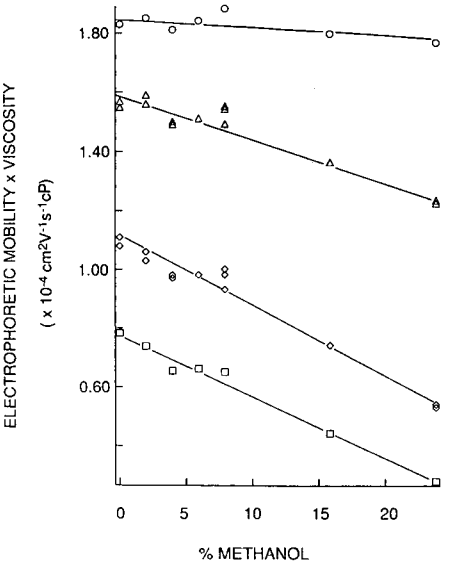

Fig. 6. Plots of the electrophoretic mobility times viscosity as a function of methanol concentration for protriptyline (○), nordoxepin (△), imipramine (◇) and doxepin (□) at pH 9.55. Lines are drawn to emphasize the differences between data sets.

ly, the downward slope was even more pronounced. Clearly, viscosity alone was not responsible for the reduction in the electrophoretic mobilities.

Another factor important in the reduction of the electrophoretic mobilities was the decrease in the degree of protonation as the percentage of methanol was increased. The dielectric constant (Table I) of water–methanol mixtures decreased as the percentage of methanol increased, and the reduction in dielectric constant would favor the more neutral side of the equilibrium between the protonated amines and their neutral bases.

$$RNH^+ + OH^- \rightleftharpoons RN: + H_2O \quad (9)$$

The equilibrium constant would then increase such that the fraction of the solute in the protonated form would decrease. Such a decrease in the concentration of the protonated amine would lead to the observed decrease in electrophoretic mobility according to eqn. 2.

Detection limits

Detection limits were obtained for all seven antidepressants. The detection limits are: 1.1 μg/ml for protriptyline; 1.0 μg/ml for desipramine, nortriptyline and nordoxepin; 0.9 μg/ml for imipramine; 0.8 μg/ml for amitriptyline; and 0.4 μg/ml for doxepin. Some of the differences in detection limits can be attributed to differences in the absorption spectra of the compounds. The detection limits in our CE apparatus are poorer than those in high-performance liquid chromatography (HPLC) which are on

the order of 2–10 ng/ml [29]. The difference in performance is in large part due to differences in the optical path. The inside diameter of a CW column is 75 μm as opposed to 4.6 mm for an HPLC column. Improvements in detection limits for a CE analysis of antidepressants may be achieved by further modifying the detectors specifically for narrow-bore capillary tubes.

CONCLUSIONS

We have shown that it is possible to separate a mixture of seven tricyclic amines that did not differ greatly in structure or molecular weight. In the systematic approach we have developed, the differential mobilities were maximized by adjusting the pH to a value slightly below the pK_a values of the samples being separated. Working at a high buffer concentration was beneficial due to the reduction in the electroosmotic flow. Further improvements in resolution were obtained upon the addition of methanol to the buffer which lead to a reduction in both the electroosmotic flow and the electrophoretic mobilities. The reduction in the electrophoretic mobilities appeared to arise from changes in the sample pK_a values in the methanol-water matrix.

REFERENCES

1 X. Huang, T.-K. J. Pang, M. Gordon and R. N. Zare, *Anal. Chem.*, 59 (1987) 2747–2749.
2 J. L. Beckers, Th. P. E. M. Verheggen and F. M. Everaerts, *J. Chromatogr.*, 452 (1988) 591–600.
3 A. S. Cohen and B. L. Karger, *J. Chromatogr.*, 397 (1987) 409–417.
4 R. M. McCormick, *Anal. Chem.*, 60 (1988) 2322–2328.
5 H. H. Lauer and D. McManigill, *Anal. Chem.*, 58 (1986) 166–170.
6 P. D. Grossman, J. C. Colburn, H. H. Lauer, R. G. Nielsen, R. M. Riggin, G. S. Sittampalam and E. E. Rickard, *Anal. Chem.*, 61 (1989) 1186–1194.
7 J. W. Jorgenson and K. D. Lukacs, *Science (Washington, D.C.)*, 222 (1983) 266–272.
8 S. Fujiwara and S. Honda, *Anal. Chem.*, 59 (1987) 487–490.
9 P. D. Grossman, K. J. Wilson, G. Petrie and H. H. Lauer, *Anal. Biochem.*, 173 (1988) 265–270.
10 S. Terabe, T. Yashima, N. Tanaka and M. Araki, *Anal. Chem.*, 60 (1988) 1673–1677.
11 M. M. Bushey and J. W. Jorgenson, *J. Microcolumn Sep.*, 3 (1989) 125–130.
12 M. M. Bushey and J. W. Jorgenson, *Anal. Chem.*, 61 (1989) 491–493.
13 S. L. Pentoney, Jr., X. Huang, D. S. Burgi and R. N. Zare, *Anal. Chem.*, 60 (1988) 2625–2629.
14 M. J. Gordon, X. Huang, S. L. Pentoney and R. N. Zare, *Science (Washington, D.C.)*, 242 (1988) 224–228.
15 P. J. Orsulak, M. C. Haven, M. E. Burton and L. C. Akers, *Clin. Chem.*, 35/7 (1989) 1318–1325.
16 R. C. Weast (Editor), *Handbook of Chemistry and Physics*, CRC Press, Cleveland, OH, 55th ed., 1974, p. D-128.
17 A. S. Cohen, A. Paulus and B. L. Karger, *Chromatographia*, 24 (1987) 15–24.
18 K. D. Altria and C. F. Simpson, *Chromatographia*, 24 (1987) 527–532.
19 G. J. M. Bruin, J. P. Chang, R. H. Kuhlman, K. Zegers, J. C. Kraak and H. Poppe, *J. Chromatogr.*, 471 (1989) 429–436.
20 J. Liu, K. A. Cobb and M. Novotny, *J. Chromatogr.*, 468 (1989) 55–65.
21 A. Adamson, *Physical Chemistry of Surfaces*, Wiley, New York, 1990, p. 445.
22 T. Tsuda, K. Nomura and G. Nakagawa, *J. Chromatogr.*, 248 (1982) 241–247.
23 K. D. Altria and C. F. Simpson, *Anal. Proc.*, 25 (1988) 85.
24 S. Fujiwara and S. Honda, *Anal. Chem.*, 58 (1986) 1811–1814.
25 V. Dolnik, J. Liu, J. F. Banks, Jr., M. V. Novotny and P. Bocek, *J. Chromatogr.*, 480 (1989) 321–330.
26 B. B. Van Orman, G. G. Liversidge, G. L. McIntire, T. M. Olefirowicz and A. G. Ewing, *J. Microcolumn Sep.*, 2 (1990) 176–180.
27 J. Gorse, A. T. Balchunas, D. F. Swaile and M. J. Sepaniak, *J. High Resolut. Chromatogr. Chromatogr. Commun.*, 11 (1988) 554–558.
28 K. Salomon, D. S. Burgi and J. C. Helmer, *J. Chromatogr.*, 559 (1991) in press.
29 F. A. Beierle and R. W. Hubbard, *Ther. Drug Monit.*, 5 (1983) 279–292.
30 L. Meites (Editor), *Handbook of Analytical Chemistry*, McGraw-Hill, New York, 1963.

Journal of Chromatography, 549 (1991) 387–399
Elsevier Science Publishers B.V., Amsterdam

CHROM. 23 345

Rapid and sensitive method for the quantitation of non-polar lipids by high-performance thin-layer chromatography and fluorodensitometry

MICHAEL J. KURANTZ*, ROBERT J. MAXWELL, RAYMOND KWOCZAK and FRANK TAYLOR

U.S. Department of Agriculture, ARS, Eastern Regional Research Center, 600 E. Mermaid Lane, Philadelphia, PA 19118 (USA)

(First received October 31st, 1990; revised manuscript received April 3rd, 1991)

ABSTRACT

Non-polar lipids were separated by high-performance thin-layer chromatography on silica gel plates and detected by use of a new reagent that induced fluorescence in the separated components. Developed thin-layer plates are dipped into a solution of sulfuric acid–ethanol–hexane (1:35:64, v/v), heated and the lipid classes are quantified by fluorescence densitometry. This technique allowed detection of certain standard lipids at the 5-ng level, is well suited for the rapid and efficient analysis of large numbers of samples and offers distinct advantages over other *in situ* fluorescence inducing methods. The method was successfully applied to the analysis of the non-polar lipids that occur in enzymatically hydrolyzed beef tallow.

INTRODUCTION

Thin-layer chromatography (TLC) has been used extensively for the analysis of lipids [1] and more recently, high-performance TLC (HPTLC) has been supplanting tradional TLC methodology. While extremely useful for lipid separations, broad applications of thin-layer techniques have been limited due to a lack of reliable quantitation of separated components [2]. This limitation was addressed by the development of quantitative methods such as absorbance densitometry of charred [3,4] or reagent-stained [5,6] thin layers, which did allow quantitation, but at the expense of many of the intrinsic advantages of TLC such as speed, sensitivity, minimal sample and plate pretreatment and reproducibility. In addition, absorbance/reflectance densitometry has been shown to yield non-linear calibration curves which have the potential to introduce large errors into a quantitative method [7].

Thin-layer chromatography combined with fluorodensitometric detection obviates many of the difficulties associated with absorbance TLC quantitation and has been used in a number of variations to analyze a broad range of components [8]. A vapor-phase fluorimetric procedure for the *in situ* derivatization of organic compounds on thin-layer plates was developed by Segura and Gotto [9] and this method has been applied to the analysis of lipids [10]. In other work, Schmitz and Assman [11]

0021-9673/91/$03.50

made use of a reagent mixture that induced fluorescence of lipids after immersion and subsequent heat treatment of developed TLC plates. While the advantages of fluorescence detection, such as superior reproducibility, lower detection limits and linear response of calibration standards are obtained with these techniques, they are somewhat complex and time consuming to perform and not conducive for use in routine analysis or large scale studies.

In this report, we present a method for the analysis of neutral lipids by HPTLC and fluorodensitometry. We developed this method for the analysis of product streams from immobilized lipase reactors designed for the hydrolysis of beef tallow [12]. Tallow is composed primarily of triacylglycerides, minor amounts of cholesterol and partial glycerides and typical lipase reactor products are mixtures of unreacted triacylglycerides, free fatty acids, diacylglycerides and monoacylglycerides. We required a simple and accurate method of analysis that could quantitate all of the above components found in partially hydrolyzed tallow that would be amenable to the large number of samples required for engineering studies of this process system. The HPTLC method described here appears to satisfy these requirements and would appear to be applicable in the quantitation of many other types of analytes. We have also found, in comparative studies, that this method is more sensitive than those previously reported for the induced fluorescence of lipids [8,11]. Because of this sensitivity the method would appear to be especially suitable for use in studies where only minute amounts of lipid are available for analysis.

EXPERIMENTAL[a]

HPTLC plates

Precoated HPTLC plates, 10 × 10 cm, silica gel 60 (Merck, Darmstadt, Germany), without fluorescent indicator, were used for all experiments.

Standards

For method development, commerical lipid-class standards, all with the same fatty acid substitution were used. These were: triolein, oleic acid, 1,2-diolein, 1,3-diolein and monoolein (Nu Chek Prep, Elysian, MN, USA).

Reagents

Hexane and methanol used in this work were HPLC grade (Burdick and Jackson, Muskegon, MI, USA), diethyl ether was analytical-reagent grade (Mallinckrodt, Paris, KT, USA), ethyl alcohol was USP dehydrated 200 proof (Pharmco, Bayonne, NJ, USA) and sulfuric acid was ACS reagent grade (J. T. Baker, Phillipsburg, NJ, USA). The tallow used in this study was edible-grade beef tallow (Ed Miniat, Chicago, IL, USA).

Fluorescence detection

Fluorescence detection of HPTLC-separated components was obtained with a TLC scanner II (Camag, Muttenz, Switzerland) equipped with a mercury lamp.

---

[a] Mention of brand or firm names does not constitute an endorsement by the US Department of Agriculture over others of a similar nature not mentioned.

Plates were scanned in the fluorescence/reflectance mode at a rate of 0.5 cm/min using an excitation wavelength of 366 nm with a 400-nm cutoff filter in place before the photomultiplier detector. The scanning beam was set at a 2-mm thickness and a 6-mm beam width. Sensitivity of the instrument was set manually at 200 arbitrary units (a.u.) and a span of 25 a.u. For automatic scanning of HPTLC lanes the instrument was programmed to scan at 1.0-cm intervals. Fluorescence output was monitored with an SP 4290 integrator (Spectra-Physics, San Jose, CA, USA) operated in the peak-height mode for the integration of detected peaks.

Plate cleaning

HPTLC plates were placed into a 10 × 10 cm TLC development tank containing approximately 400 ml of methanol and immersed for 5 min. Plates were removed, drained of excess solvent and dried in an 80–85°C oven for 15 min and stored until needed in a closed dessicator box that contained no dessicant or other chemicals [13]. Two plates were immersed into the methanol at the same time and the methanol was replenished after cleaning 20–24 plates.

Separation of lipids

Initial studies were conducted with mixtures of commercial lipid standards, dissolved in chloroform and applied to precleaned HPTLC plates with a 1.0-μl syringe ((Hamilton, Reno, NV, USA). Aliquots of 1.0 μl of lipid solutions, in the concentration range of 1–100 ng/component, were spotted to test the reproducibility and sensitivity of the method. Spots were applied at a distance of 1.5 cm from the bottom edge of the plate and a line was etched across the plate at a distance of 9.0 cm from the plate bottom. Spots were placed exactly 1.0 cm apart with a maximum of eight spots per 10 × 10 cm plate in order to conform to the TLC scanner lane interval setting for autoscanning.

The spotted HPTLC plates were placed in a developing tank (15 × 30 cm), that was preequillibrated for 10–15 min with hexane–diethyl ether–formic acid (80:20:2, v/v) and solvent was allowed to migrate to a distance of 3.0 cm from the bottom edge of the plate. Plates then were removed, air-dried (10 min) and returned to the development tank, containing the same solvent mixture, until the solvent migrated to the 9.0-cm line. Developed plates were allowed to air-dry (10 min) before the fluorescence induction treatment.

Induction of fluorescence

Fluorescence of the separated components was effected by immersion of the air-dried, developed plate into a mixture of sulfuric acid–absolute ethanol–hexane (1:35:64, v/v). The plate was quickly dipped into this mixture (1–2 s), removed and reimmersed a second time (1–2 s). After this treatment excess solvent was allowed to evaporate from the plate surface. The treated plates were then heated in a forced-air-type oven at 110°C for exactly 45 min.

Tallow standards

Lipids from partially hydrolyzed tallow were purified by preparative TLC on 20 × 20 cm, 500 μm, silica gel G plates (Analtech, Newark, DE, USA). The solvent system for initial class separation of the lipids was hexane–diethyl ether–acetic acid

(70:30:1, v/v) [14]. Diacylglyceride fractions from this separation were purified using benzene–ethyl acetate–diethyl ether–acetic acid (80:10:10:0.2, v/v) [15]. Lipid-class standards applied to the preparative plates were used to identify the separated components. Purified components were combined to form mixed standards, of known concentrations, that correspondend with the lipid-class composition of partially hydrolyzed tallow obtained from the lipase-reactor treatment of beef tallow.

Other methods

Two methods for the induced fluorescence detection of lipids were compared with the method presented in this report. Vapor-phase induction of fluorescence with ammonium bicarbonate was carried out as described by Segura and Gotto [9] in a modified heating chamber developed by Maxwell [16]. Fluorescence was also induced using a reagent comprised of manganese chloride–methanol–sulfuric acid–water described by Schmitz and Assman [11].

Estimates of the free fatty acid composition of partially hydrolyzed tallow as determined using the new HPTLC method were compared with the results obtained with a pH stat titration method described by Taylor [17].

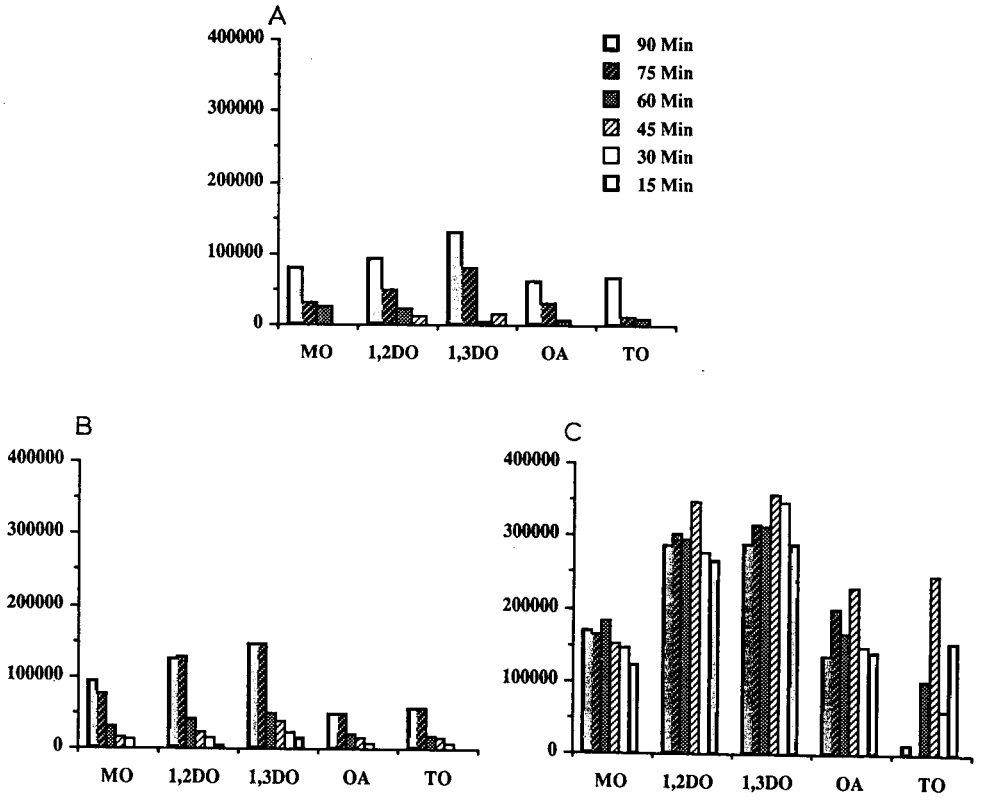

Fig. 1. Effect of temperature and time on the fluorescent response of lipid standards. Triolein (TO) 0.56 μg, oleic acid (AO) 8.97 μg, 1,3-diolein (1,3DO) 7.45 μg, 1,2-diolein (1,2DO) 6.66 μg, monoolein (MO) 6.18 μg. A = 90, B = 100, and C = 110°C.

RESULTS

Optimization of lipid detection

The solvent system of hexane–diethyl ether–formic acid (80:20:2, v/v) was arrived at after examining the more widely used hexane–diethyl ether–acetic acid solvent systems for lipid separation [1]. The solvent mixture that contained acetic acid provided a complete separation of the major lipid classes (monoacylglycerides, diacylglycerides, sterols, free fatty acids, triacylglycerides and sterol esters) but resulted in plates containing a line at the approximate R_F of the free fatty acid region after fluorescence induction. When these plates were scanned in the fluorescence mode this line interfered with the readings obtained for the free fatty acids in the test mixtures. By substituting formic acid, which is more volatile, for acetic acid, this interference was eliminated and the resolution of the major lipid classes remained unaltered.

Developed HPTLC plates, containing lipid standards and treated with the sulfuric acid–ethanol–hexane reagent, were heated at three temperatures, 90, 100 and 110°C, over a time range of 15–90 min (Fig. 1). With the exception of monoolein, optimal fluorescence was detected for all other lipids after heating at 110°C and 45 min (Fig. 1C). Monoolein appeared to give an optimum response after heating at 110°C and 60 min; however, the 45-min response was sufficient for quantitative purposes. This observation plus the fact that the response of the other test compounds decreased significantly when heated beyond 45 min led us to select the 45-min time interval and 110°C oven temperature as the optimum conditions for fluorescence induction with the new reagent. At oven temperatures greater than 110°C the fluorescent response decreased dramatically and charring of the spots became evident.

Comparisons between the use of gravity ovens and forced-air-type ovens for the heating stage, revealed that reproducible results and optimum fluorescence can only be obtained in the uniform temperature environment of the forced-air oven.

Sensitivity and linearity

Chloroform solutions of the commercial lipid standards in the concentration range of 1–100 ng/μl were applied to HPTLC plates, developed and fluorescence was

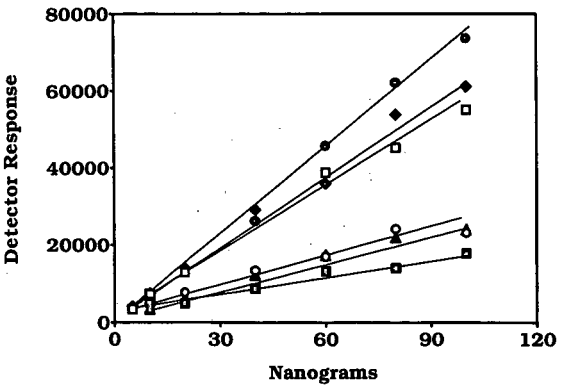

Fig. 2. Effect of concentration on the fluorescent response of lipid standards. See Table I for abbreviation code. ● = TO; ◆ = CHOL; □ = 1,3DO; ○ = 1,2DO; ▲ = OA; and ■ = MO.

TABLE I

SENSITIVITY AND LINEARITY OF STANDARD LIPIDS

The lower limit of detectability and correlation coefficients for each regression line fit shown in Fig. 2 for standard lipids. TO = Triolein; CHOL = cholesterol; 1,3DO = 1,3-diolein; OA = oleic acid; 1,2DO = 1,2-diolein; MO = monoolein.

Lipid standard	Lower limit of detection (ng)	Correlation coefficient
TO	20	0.988
CHOL	5	0.991
1,3DO	5	0.992
OA	10	0.981
1,2DO	10	0.975
MO	10	0.969

induced using the optimum conditions described above. A plot of the fluorescent response *versus* concentration (Fig. 2) revealed that the detected fluorescence differed for each class of standard lipid in this concentration range, the highest quantum yield produced by triolein and the least by monoolein. It is clear from these results that for each lipid class tested, the fluorescent response is distinct and dependent upon the structural properties of each lipid class. Table I lists the lower detectable limit, which is the minimum amount that could be accurately quantitated, for each lipid standard and the correlation coefficient for each regression line generated in the plot shown in Fig. 2. A linear relationship between fluorescence and concentration was found in the range starting at the lower limit of detection to 100 ng for all of the lipid standards analyzed using this method of fluorescence induction. The coefficients of variation for the fluorescent response of triplicate samples of the standard lipids were 2.8% for triolein, 2.3% for cholesterol, 3.4% for 1,3-diolein, 1.6% for oleic acid, 3.7% for 1,2-diolein and 2.6% for monoolein. Comparisons of values obtained for known amounts of standard lipid from standard curves resulted in an accuracy that was within 5% of the known amount spotted when calibration standards and test samples were run on separate HPTLC plates. Duplicate plates, each spotted with four samples of mixed lipid standards at the 40-ng level, showed a plate-to-plate variation in the fluorescent response of $\leqslant$ 2.9%. These results, however, were obtained when plates were cleaned together and treated with the same batch of dipping reagent. When changes are made, such as replenishment of cleaning solvent or dipping reagent, a significant difference in similarly spotted plates was noted. Due to these observations it is recommended that for maximum accuracy standards should be included on the same plate as the samples.

Effect of fatty acid composition

The effect of fatty acid unsaturation on the fluorescent response obtained after reagent treatment and heat is illustrated in Fig. 3A. The response of stearic acid (18:0) was very low but the mono-unsaturated oleic acid (18:1), at the same concentration, had a quantum yield over eighteen times greater than the saturated fatty acid. The

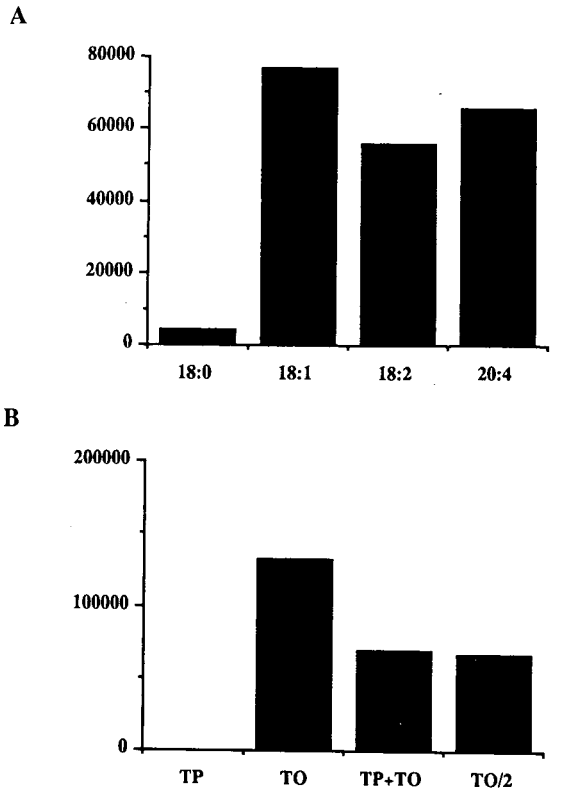

Fig. 3. Effects of unsaturation and lipid class on fluorescent response. (A) 1.0 μg of stearic acid (18:0), oleic acid (18:1), linoleic acid (18:2) and arachidonic acid (20:4). (B) 0.58 μg of tripalmitin (TP), triolein (TO), tripalmitin + triolein; 1:1, w/w mixture (TP + TO), triolein response divided by two (TO/2).

di-unsaturated linoleic acid (18:2) produced fluorescence that was 27% less than oleic acid and the polyunsaturated arachidonic acid (20:4) yielded fluorescence at a response that was 15% less than that of oleic acid. These results indicate that saturated fatty acids will probably produce the least fluorescence but that the fluorescent response is not directly proportional to the degree of unsaturation of the fatty acid.

The effect of fatty acid composition on triacylglyceride response is illustrated in Fig. 3B. Tripalmitin (16:0) failed to produce measurable fluorescence, while triolein (18:1), at the same concentration (0.58 μg), produced a significant response. A 1:1 (w/w), mixture of triolein and tripalmitin (TP + TO) produced a response slightly better than half (51.4%) of the triolein response (TO/2, theoretical 1/2 of the triolein response) and indicates that the fluorescence induced is attenuated, almost directly, in the (TP + TO) mixture, by the amount of nonfluorescent tripalmitin. This suggests that the fluorescent response obtained by this procedure for the tested triacylglycerides is dependent upon the fatty acid composition of the triacylglyceride.

Comparisons with two other induced fluorescence detection methods

Duplicate HPTLC plates containing standard mixtures were prepared and de-

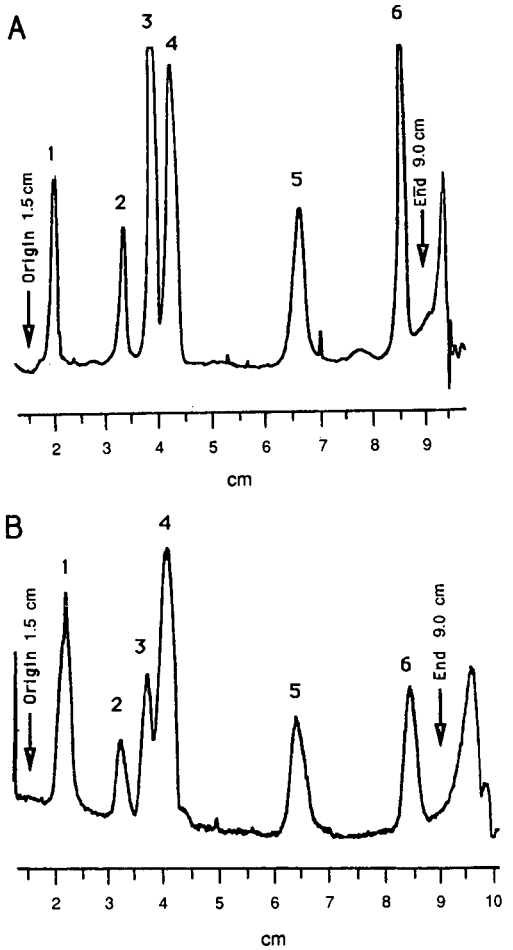

Fig. 4. A concentration of 0.4 μg of each standard was applied and plates were developed with hexane–diethyl ether–formic acid (see text). Peaks: 1 = monoolein; 2 = 1,2-diolein; 3 = 1,3-diolein; 4 = cholesterol; 5 = oleic acid; 6 = triolein. Fluorescence was induced by (A) the sulfuric acid–ethanol–hexane reagent or (B) the manganese chloride–methanol–sulfuric acid–water reagent.

veloped as described previously and fluorescence induction was accomplished with the sulfuric acid–ethanol–hexane (1:35:64, v/v) reagent and the manganese chloride–methanol–sulfuric acid–water reagent described by Schmitz and Assman [11]. For all of the compounds tested at the three different heating intervals, the sulfuric acid–ethanol–hexane reagent resulted in higher fluorescent responses, as illustrated in the histograms, than the manganese chloride–methanol–sulfuric acid–water reagent. In addition, to better overall sensitivity, the new reagent-produced fluorodensitograms with less baseline noise and peak resolution was superior (Fig. 4A) to that obtained with the manganese chloride-based reagent (Fig. 4B).

We next compared the new method with the vapor-phase fluorescence-induction technique of Segura and Gotto [9], wherein fluorescence is induced by heating the

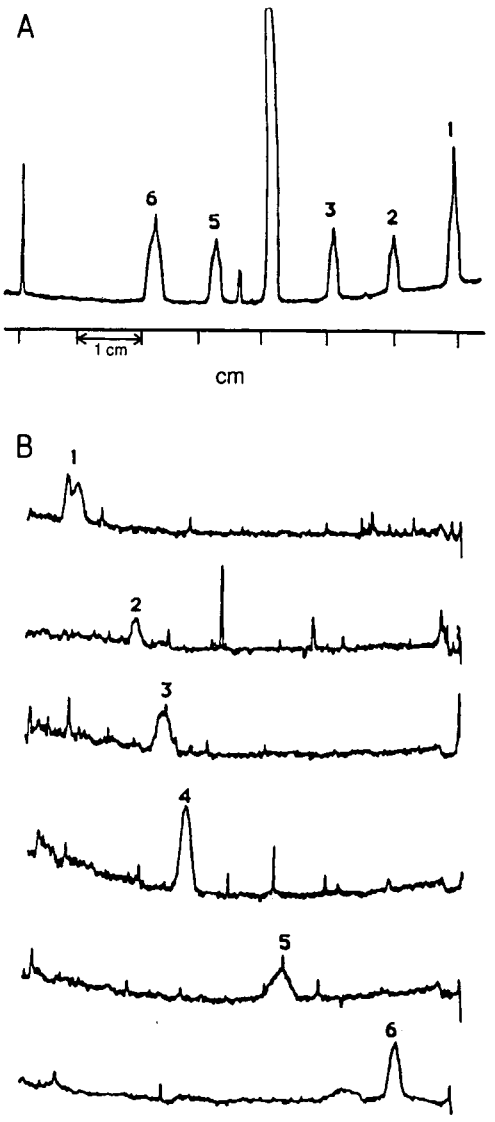

Fig. 5. A concentration of 0.125 μg of each standard applied to HPTLC plates. (A) Static spots and (B) plates developed as described in text. Detection by vapor-phase fluorescence induction. Peaks: 1 = monoolein, 2 = 1,2-diolein, 3 = 1,3-diolein, 4 = cholesterol, 5 = oleic acid and 6 = triolein.

HPTLC plate in a chamber containing an atmosphere of ammonium bicarbonate. With the vapor-phase method, standard lipids were not detectable at levels less than 1.25 μg per component on normally developed plates. When static spots of lipid standards (1.25 μg per component) were subjected to the vapor-phase treatment, they could be detected (Fig. 5A) but the response was found to be greatly deminished if the lipids spotted on HPTLC plates were allowed to migrate by the normal solvent development procedure (Fig. 5B). For detection of lipids on developed HPTLC plates, the

vapor-phase method, as tested here, lacked sensitivity and produced variable responses at the lipid concentrations used in this study.

Fluorescence stability

We examined the stability of the fluorescence induced with the sulfuric acid–ethanol–hexane reagent over time during the course of this work. For most of the tested lipids (monoolein, 1,2-diolein, 1,3-diolein, oleic acid and cholesterol) fluorescence decreased by an average of 49.8% after 24 h and was further reduced by 56.5% of the original response after three days. Triolein, however, lost only 12.0 and 36.7% of the original fluorescence after one and three days, respectively. At twelve days after fluorescence induction an average of only 5% of the original fluorescence could be detected; however, fluorescent spots could still be detected using a hand-held 254 nm light source. Because of the inconsistent degradation of the fluorescence over time, scans for quantitative determinations should be performed as soon as possible after heat treatment.

Reagent stability

The stability of the sulfuric acid–ethanol–hexane reagent was examined over time and after repeated use of the reagent for the induction of fluorescence in standard lipids on HPTLC plates. When the same 250-ml batch of reagent was used to treat a small number of plates (1 plate per day, 8 plates total) over a one-week period, the resulting fluorescence obtained was approximately the same for all of the test plates. When large numbers of plates (10 per day) were treated similarly, the reagent, based on the fluorescent response obtained, became exhausted after three days of use (30 plates total). Since sulfuric acid is the active ingredient in this reagent mixture (ethanol and hexane did not induce fluorescence), it may become diminished by reaction with components on the HPTLC plates or absorption into the silica gel sorbent layer to a level where it is no longer effective.

Analysis of tallow lipids

Calibration standards for the analysis of tallow samples were obtained by preparative TLC fractionation of partially hydrolyzed beef tallow obtained from a lipase reactor process [12]. The separated fractions of monoacylglycerides, 1,2-diacylglycerides, 1,3-diacylglycerides, free fatty acids and triacylglycerides were dissolved in chloroform and combined to form mixed standards of known concentration. The tallow-derived standards, in the concentration range of 0.1–0.8 μg/component, were subjected to HPTLC and fluorescence induction, as outlined previously. Plots of detector response *versus* concentration of each lipid class resulted in a linear relationship over the tested concentration range. Regression analysis of the calibration data yielded correlation coefficients $r = 0.994$, monoacylglycerides; $r = 0.967$, 1,2-diacylglycerides; $r = 0.959$, 1,3-diacylglycerides; $r = 0.998$, free fatty acids; and $r = 0.973$, triacylglycerides.

Samples of lipase-hydrolyzed beef tallow of unknown composition were dissolved in chloroform to give solutions of approximately 2.0 μg/μl concentrations and 1.0-μl aliquots were applied to HPTLC plates. Plates were developed and fluorescence was induced as described earlier. A fluorodensitogram of a typical sample of partially hydrolyzed tallow is presented in Fig. 6. The response of purified tallow lipid stan-

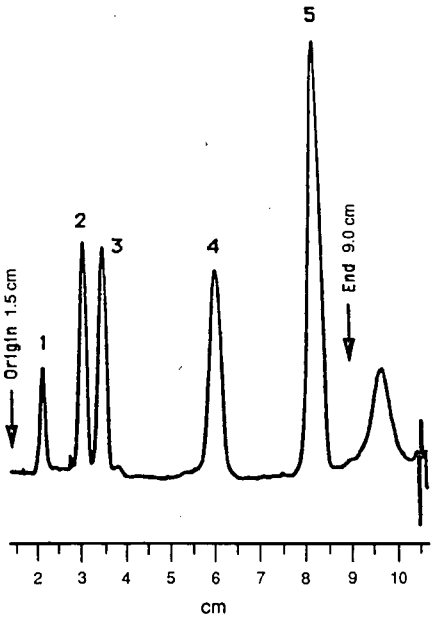

Fig. 6. Fluorodensitogram of 2.10 μg of partially hydrolyzed tallow. Plate was developed and lipids were detected as noted in text. Peaks: 1 = monoacylglycerides, 2 = 1,2-diacylglycerides, 3 = 1,3-diacylglycerides, 4 = free fatty acids, 5 = triacylglycerides.

dards was used to calculate the amount of each lipid class in the unknown samples and the weight percent of each lipid class was derived from this data. The amounts of free fatty acids present in 46 unknown partial tallow hydrolysates were calculated from the weight percent free fatty acids as determined by HPTLC. These data were compared with the free fatty acid amount determined separately, on each of the 46 samples, by a pH stat titration method [17]. Fatty acid values determined by the pH stat method *versus* the HPTLC procedure showed a good correlation between the separate determinations (r = 0.960).

DISCUSSION

The analysis of non-polar lipid mixtures by HPTLC and fluorodensitometry after fluorescence induction with the proposed reagent, is a simple and sensitive method for the quantitation of these compounds. This reagent (sulfuric acid–ethanol–hexane, 1:35:64, v/v) was initially developed for use with a class of antibiotics known as polycyclic ethers [18] and various mixtures of the three reagents were tested before arriving at the final combination. This previous work revealed that a volume of 35% ethanol was required to allow solubility of the sulfuric acid and ethanol in hexane. The use of hexane as a carrier solvent for the sulfuric acid offered the advantage of rapid and uniform drying of the plate surface following the immersion step. In addition, hexane lowers the polarity of the dipping reagent which prevents the elution of separated components into the dipping reagent and reduces spot spreading.

We applied this reagent to the analysis of lipids when the need to analyze large numbers of partially hydrolyzed tallow samples arose. At this time, we noted in the literature that Schmitz and Assman [11] reported the use of a reagent for the induced fluorescence of lipids and although the two reagents appear similar, our comparative studies revealed many major differences between them. This water-containing reagent (manganese chloride–sulfuric acid–ethanol–water) dries slowly and blemishes the plate surface. This resulted in poor quality and dereased sensitivity in fluorodensitograms due to background noise caused by surface distortions. In addition, the protracted time of plate immersion recommended with this reagent, appeared to cause spreading of separated spots that resulted in an apparent loss of resolution as observed in the fluorodensitogram.

Vapor-phase induction of fluorescence with ammonium bicarbonate, as originally described by Segura and Gotto [9], proved to be ineffective, as tested here, on solvent-developed HPTLC plates. At the 1.25 μg/component levels used in this study, suitable fluorescence appeared to be induced only when lipids were statically spotted. Migration of sample components into the adsorbent layer during plate irrigation may cause a net reduction in the amount of excitation energy available to the separated components [19]. This could result in a reduction of overall fluorescence relative to the static-spot case, where sample components are situated closer to the surface of the adsorbent layer. The vapor-phase method also requires a long period of heating at high temperature (10 h, 150°C), as well as the use of a gas-tight apparatus to maintain the ammonium bicarbonate atmosphere, thus limiting the sample number and turn-around time for analysis. Both of the methods discussed above relied upon an excitation wavelength of 366 nm to generate a fluorescent response; we utilized the same excitation wavelength for this work in order to directly compare the various methods. Since satisfactory results were obtained with lipid standards and samples, we made no effort to further optimize this parameter and caution that this wavelength may not be the optimum excitation wavelength for maximum fluorescence.

The proposed method for the analysis of non-polar lipids is relatively simple and sensitive, allowing the detection of certian lipid standards at the 5-ng level and the routine determination of 100-ng levels of naturally occurring tallow lipids. The sensitivity of this method compares well with the reported lower detectable limits obtained by the use of such fluorescent indicators as 6-*p*-toludino-2-naphthalene [20], Rhodamine G and 2,7-dichlorofluoresceine [21]; however, no direct comparative studies were conducted at this time.

In this work our interest was primarily in the development of a simple and rapid method to monitor lipase reactor products (partially hydrolyzed tallow) that would allow efficient processing of large numbers of samples. The present method satisfied this purpose as evidenced by the correlation between independent determinations of free fatty acids in samples of the various reactor products. Since sample amounts were not limited in this work, we did not attempt, at this time, to determine the lowest level of lipase reactor products that could be accurately quantitated. The method does, however, appear to be suitable for applications in which high sensitivity is required as evidenced by the comparative studies and literature comparisons, outlined above. The data does indicate, however, that the composition and structure of an analyte will have a significant influence on the fluorescent response obtained with this method. Because of this, sensitivity, calibration and accuracy determinations should be per-

formed in order to evaluate the effectiveness of this method for use with a particular analyte.

CONCLUSIONS

The HPTLC method presented here for the analysis of non-polar lipids relies upon a relatively simple plate-cleaning step and a new reagent for the induction of fluorescence on developed HPTLC plates. The procedure is rapid and sensitive and is well suited for use in large-scale studies or in routine analysis where large numbers of samples are involved. Since the mechanism of the *in situ* fluorescence induction used here appears to be relatively non-specific, the method should be applicable for the detection of a broad range of analytes that are separable by normal-phase TLC.

REFERENCES

1 R. J. Hamilton and J. B. Rossel (Editors), *Analysis of Oils and Fats*, Elsevier Applied Science, London, New York, 1986, Ch. 6, p. 243.
2 E. W. Hammond, *J. Chromatogr.*, 203 (1981) 397.
3 L. J. Nutter and O. S. Privett, *J. Chromatogr.*, 35 (1968) 519.
4 L. J. Mancal, R. K. Yu and S. Ando, *K. Lipid Res.*, 24 (1983) 1243.
5 J. Sherma and S. Bennett, *J. Liq. Chromatogr.*, 6 (1983) 1193.
6 I. Rustenbeck and S. Lenzen, *J. Planar Chromatogr.*, 2 (1989) 470.
7 C. F. Poole, S. K. Poole, T. A. Dean and N. M. Chirco, *J. Planar Chromatogr.*, 2 (1989) 180.
8 W. R. G. Baeyens and B. L. Ling, *J. Planar Chromatogr.*, 1 (1988) 198.
9 R. Segura and A. M. Gotto Jr., *J. Chromatogr.*, 99 (1974) 643.
10 I. R. Kupke and S. Zeugner, *J. Chromatogr.*, 146 (1978) 261.
11 G. Schmitz and G. Assman, *J. Chromatogr.*, 307 (1984) 65.
12 F. Taylor, C. C. Panzer, J. C. Craig and D. J. O'Brien, *Biotechnol. Bioeng.*, 28 (1986) 1318.
13 R. J. Maxwell, S. W. Yeisley and J. Unruh, *J. Liq. Chromatogr.*, 13(10) (1990) 2001.
14 H. B. White and S. S. Powell, *Biochim. Biophys. Acta*, 764 (1984) 316.
15 J. E. Storry and B. Tucklsy, *Lipids*, 2 (1967) 501.
16 R. J. Maxwell, *J. Planar Chromatogr.*, 1 (1988) 345.
17 F. Taylor, *Anal. Biochem.*, 148 (1985) 149.
18 R. J. Maxwell and S. W. Yeisley, unpublished results.
19 S. S. J. Ho, H. T. Butler and C. F. Poole, *J. Chromatogr.*, 281 (1983) 330.
20 M. Jones, R. W. Keenen and P. Horowitz, *J. Chromatogr.*, 237 (1982) 522.
21 D. W. Judge, D. E. Mullins and J. L. Eaton, *J. Planar Chromatogr.*, 2 (1989) 442.

Journal of Chromatography, 549 (1991) 400–403
Elsevier Science Publishers B.V., Amsterdam

CHROM. 23 223

Short Communication

Detection of octopamine in an insect ganglion by high-performance liquid chromatography–native fluorescence

FUMIO MIYAGAWA and YUTAKA TSUCHIDA
Special Reference Laboratories (SRL) Inc., Komiya, Hachioji, Tokyo 192 (Japan)
and
TOSHIAKI SHIMIZU*
Department of Medical Entomology, The National Institute of Health, Kamiosaki, Shinagawa, Tokyo 141 (Japan)
(First received September 19th, 1990; revised manuscript received February 14th, 1991)

ABSTRACT

Biogenic amine levels in the suboesophageal ganglion of the cabbage armyworm larvae, *Mamestra brassicae* (Lepidoptera; Noctuidae), were investigated by high-performance liquid chromatography with native fluorescence detection. The procedure involves direct injection of the sample onto a silica-octadecylsilane high-performance liquid chromatography column with the eluted fractions detected using a dual-fluorescence detector. The suboesophageal ganglion of wandering-stage larvae contained dopa, octopamine, tyramine, tyrosine and related metabolites. Fluorometric detection offers an alternative to laboratories that do not have access to electrochemical detection systems.

INTRODUCTION

High-performance liquid chromatography (HPLC) with dual-channel coulometric electrochemical detection (ED) is now the technique of choice for analysis of phentolamines [1]; however, the technique has not been applied extensively to analysis of the monohydroxy analogues of catecholamines [2]. The infrequent use of HPLC–ED for determination of phentolamines is due in part to the high electrode potentials that are required to effect electro-oxidation of these compounds [3].

On the other hand, HPLC with native dual-fluorescence detection is suitable for simultaneous analysis of both indolealkylamines (λ_{em} 350 nm) and catecholamines (λ_{em} 315 nm) in the same biological sample with excitation at 280 nm.

The biogenic amine octopamine occurs in the suboesophageal ganglion (SG) and has been measured by radioenzymic assay in the larvae of two species of Lepidoptera, the noctuid moth *Spodoptera littoralis* and the sphingid moth *Manduca*

0021-9673/91/$03.50

sexta [4]. This report describes the first use of HPLC–fluorescence detection for analysis of monoamines in Lepidoptera.

EXPERIMENTAL

Insects

The larvae of the cabbage armyworm, *Mamestra brassicae*, were reared at 20°C on an artificial diet [5] under a 16 h light–8 h dark photoperiod. Wandering-stage larvae were used in all experiments.

Sample preparation of suboesophageal ganglia

The SG were excised from female and male larvae ($n = 30$) at constant time of the diurnal cycle. They were rinsed well in Ringer solution [240 m*M* sodium chloride, 2.7 m*M* potassiumchloride, 0.4 m*M* calciumchloride and 2.38 m*M* 4-(2-hydroxyethyl)-1-piperazineethanesulphonic acid (HEPES)] to eliminate contamination from octopamine in the haemolymph. The pH of the solution was adjusted to 7.2 with sodium hydroxide. Tissues were gently homogenized in 0.1 *M* hydrochloric acid solution in a cooled microhomogenizer with a glass pestle, and the resulting homogenate centrifuged at 10 000 *g* for 10 min. The remaining supernatant was then filtered and dried using a rotary evaporator with reduced vacuum pressure. Dry samples were reconstituted with a known volume of 0.1 *M* phosphate buffer solution (pH 2.5) so that a 70-μl aliquot provided an appropriate sample for injection onto the HPLC column. The estimate of recovery of extracted amines was precisely checked. It was found that no loss of sample occured during the extraction, centrifugal filtration (UFC3 OHV, Millipore) and drying process.

HPLC apparatus

The chromatographic system (Japan Spectroscopic, Hachioji, Japan) consisted of two BIP-I liquid chromatography pumps, a system controller (801-SC), an autosampler (850-AS), an 829-01 column selection unit, a two-pen recorder and a two-wavelength fluorimetric detector (FP-540 D). A 15 cm × 6 mm I.D. analytical column packed with silica-octadecylsilane (ODS) (ERC-1161 A, Erma, Japan) was used. Two kinds of HPLC mobile phases (solvent) were used. As external standard, a mixture of reference compounds including 3,4-dihydroxyphenylethyleneglycol (DOPEG), noradrenaline (NA), adrenaline (A), 3,4-dihydroxyphenylacetic acid (DOPAC) and dopamine (DA) (100 ng/ml of each) was also prepared.

Chemicals and reagents

Chemicals for analyses were of analytical reagent grade. All amines and related compounds were purchased from Sigma (St. Louis, MO, USA).

RESULTS AND DISCUSSION

Typical chromatograms obtained from standard compounds and from extracted SG are illustrated in Fig. 1A and B. The HPLC with native fluorescence detection procedure demonstrated that dopa (DOPA), octopamine (OA), tyrosine (TYR), tyramine (TYRA) and related metabolites could be measured readily in the SG. The

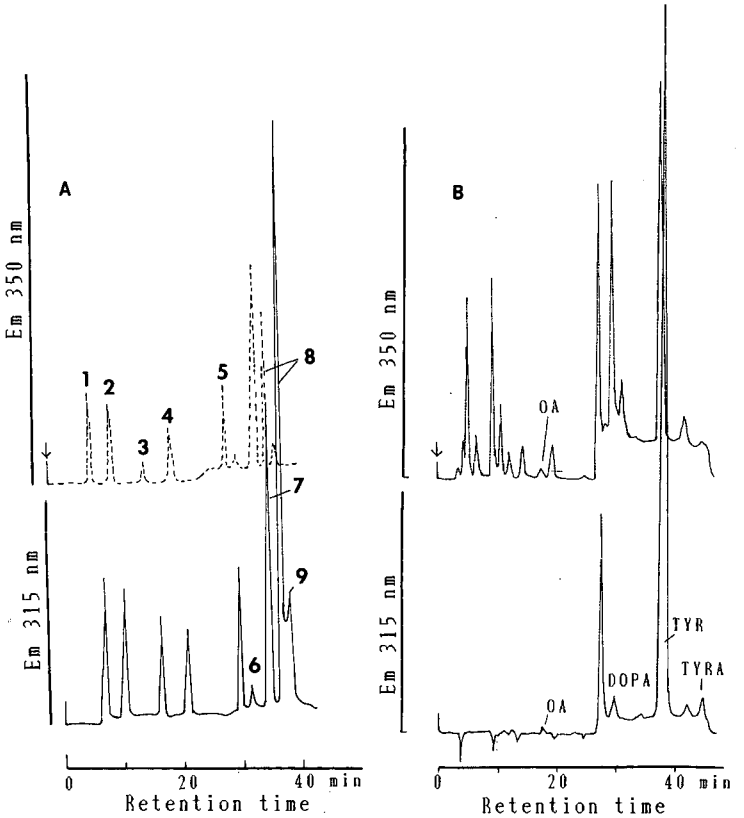

Fig. 1. Representative chromatograms of HPLC with native fluorescence detection. Analytical solvent elution time for stepwise gradient was 20 min (pump A) and 40 min (pump B), sequentially. The mobile phase 1 (pump A) consisted of 120 mg 1-octanesulphonic acid sodium salt and 50 mg disodium EDTA in 0.1 *M* phosphate buffer (pH 2.5), and solvent 2 (pump B) was prepared by adding 37 ml of acetonitrile to 1 l of solvent 1. The flow-rate was 0.8 ml/min, and injection volumes solvent were 100 μl. (A) Chromatogram of standard compounds. Peaks: 1 = DOPEG, 5 ng; 2 = NA, 5 ng; 3 = OA, 5 ng; 4 = A, 5 ng; 5 = DOPA, 5 ng; 6 = DOPAC, 15 ng; 7 = DA, 10 ng; 8 = TYR, 1000 ng; 9 = TYRA, 5 ng. (B) Typical chromatogram of the suboesophageal ganglion (n = 30).

response at 315 nm for the octopamine standard is better than at 350 nm (Fig. 1A), whereas in Fig. 1B an octopamine peak is identified at 350 nm and there is a weak corresponding peak at 315 nm. Accordingly, it is suggested that the octopamine peak in Fig. 1B contains octopamine and other substance(s) which responded better at λ_{em} = 315 nm than at λ_{em} = 350 nm, and shows the same retention time as octopamine. To clarify this possibility, we can check this peak at different wavelengths. The HPLC–fluorescence detection system may be of use in a plot of octopamine fluorescence at different wavelengths.

Octopamine has been found by Martin *et al.* [5,6] and Bailey *et al.* [2], who also detected dopamine, 5-hydroxytryptamine and tyramine in the nerve cord of the American cockroach, *Periplaneta americana*, using the HPLC–ED procedure. Similarly, Robertson [7] has determined the octopamine, dopamine and noradrenaline content of the brain of the locust, *Schistocerca gregaria*, using a sensitive radiochem-

ical enzymic assay. Octopamine and dopamine were present in high concentration, but the noradrenaline content was only 1/25 that of octopamine. The octopamine content of SG from 6th-instar *Spodoptera littoralis* was 0.97 pg per tissue (measured by radioenzymic assay) [4]. The octopamine values are similar to those in the SG of *Mamestra* SG (0.497 pg) using HPLC with native fluorescence detection. Radioenzymic assay for octopamine has been criticized for lack of specificity [8], and the levels using HPLC are lower than those using radioenzymic techniques. Therefore, direct comparisons are difficult because of the variety of analytical methods.

In the present experiments, a high level of tyrosine was found in the SG (Fig. 1B). Vaughan and Neuhoff [9] reported the presence of tyrosine in the cerebral and thoracic ganglia of *Schistocerca gregaria*. Tyrosine is well known as a precusor of two pathways, tyramine–octopamine and L-dopa–dopamine metabolites, but the biological function in the ganglion is not clear. Octopamine is synthesized from tyrosine in the thoracic ganglia of *Manduca sexta* [10]. Octopamine in the brains of the bertha armyworm, *Mamestra configurata*, is also synthesized from L-tyrosine [11].

ACKNOWLEDGEMENTS

We thank Professor R. G. H. Downer, University of Waterloo, and Dr. R. P. Bodnaryk, Agriculture Canada, Research Station, for their criticism of the manuscript.

REFERENCES

1 R. E. Shoup, in E. E. Shoup (Editor), *Recent Reports on Liquid Chromatography/Electrochemistry*, BAS Press, West Lafayette, IN, 1982.
2 B. A. Bailey, R. J. Martin and R. G. H. Downer, in A. A. Boulton, G. B. Baker, W. G. Dewhurst and M. Sandler (Editors), *Neurobiology of the Trace Amines*, Humana Press, Clifton, NJ, 1984, p. 85.
3 B. A. Bailey, R. J. Martin and R. G. H. Downer, *J. Liq. Chromatogr.*, 5 (1982) 2435.
4 A. P. Davenport and D. J. Wright, *J. Insect Physiol.*, 32 (1986) 987.
5 R. J. Martin, B. A. Bailey and R. G. H. Downer, *J. Chromatogr.*, 278 (1983) 265.
6 R. J. Martin, B. A. Bailey and R. G. H. Downer, in A. A. Boulton, G. B. Backer, W. G. Dewhurst and M. Sandler (Editors), *Neurobiology of the Trace Amines*, Humana Press, Clifton, NJ, 1984, p. 91.
7 H. A. Robertson, *Experientia*, 32 (1976) 552.
8 D. F. H. Dougan and D. N. Wade, *Trends Pharmacol. Sci.*, (1981) 113.
9 P. F. T. Vaughan and V. Neuhoff, *Brain Res.*, 117 (1976) 175.
10 G. D. Maxwell, J. F. Tait and J. G. Hildebrand, *Comp. Biochem. Physiol.*, 61C (1978) 109.
11 A. N. Starratt and R. P. Bodnaryk, *Insect Biochem.*, 11 (1981) 645.

Journal of Chromatography, 549 (1991) 404–409
Elsevier Science Publishers B.V., Amsterdam

CHROM. 23 360

Short Communication

The effect of ^2H_2O and an ion-pairing agent on the liquid chromatographic separation of dansylated amino acids

GEORGE N. OKAFO and PATRICK CAMILLERI*
SmithKline Beecham Pharmaceuticals, The Frythe, Welwyn, Herts., AL6 9AR (UK)
(First received August 24th, 1990; revised manuscript received February 12th, 1991)

ABSTRACT

The chromatographic separation of dansylated amino acids using either H_2O- or ^2H_2O-based eluent is compared. The retention time of the majority of solutes studied is found to be shorter in heavy water and this is thought to be related to the higher pK_a values of dansylated amino acids in ^2H_2O compared to H_2O solutions.

INTRODUCTION

The analysis of amino acids is of importance in the study of the constitution of proteins and peptides and in the monitoring of the concentration of physiologically active molecules [1,2] such as L-glutamic acid, L-glycine and γ-aminobutyric acid (GABA) in biological fluids. It is difficult to analyse amino acids directly by high-performance liquid chromatography (HPLC) because most of these molecules lack the appropriate chromophore necessary for detection at low concentrations. Several derivatisation procedures have been successfully used in the literature to circumvent this problem [3–6]. Four of the most common derivatisation methods involve the use of the following reagents: 1-dimethylaminonaphthalene-5-sulphonyl chloride (dansyl chloride, Dns-Cl) [3], 9-fluorenyl-methylchloroformate (FMOC-Dl) [4], *o*-phthalaldehyde (OPA) [5] and phenyl isothiocyanate (PITC) [6]. An advantage of some of these techniques is that high sensitivity can be achieved by fluorescence detection. As dansylation appears to have advantages over the other techniques (the derivatisation procedure is straightforward and the resulting derivatives are stable) we report the analysis of a number of Dns-amino acids using fluorescence detection and the use of ^2H_2O and tetra-*n*-butylammonium hydroxide (an ion-pairing agent) to improve chromatographic separation.

0021-9673/91/$03.50

EXPERIMENTAL

Reagents and chemicals

Acetonitrile used in all mobile phases was far UV HPLC-grade and was purchased from BDH. Amino acids L-Glu, L-Ser, L-Gly, L-Ala, β-Ala, Val, δ-amino-*n*-valeric acid and ε-amino-*n*-caproic acid) were 99% pure (Sigma) and were used without further purification. Tetra-*n*-butylammonium hydroxide was purchased from Aldrich as a 40% (w/w) solution in water. Deuterium oxide (^2H_2O) and deuterated acetic acid ($C^2H_3CO_2{}^2H$) were obtained 99.9 atom% deuterium from Aldrich. Dns-Cl was used as purchased from Aldrich (99%). Analar ammonium acetate (99% pure) from BDH was dissolved in distilled-deionised water (Milli-Q). All pH and p^{2}H measurements were recorded on a Radiometer PHM82 standard pH meter calibrated with standard pH buffers.

HPLC apparatus

The chromatographic system (Perkin-Elmer) consisted of a series 4 liquid chromatograph controller and pumps. Sample detection was achieved using a Perkin-Elmer LS4 fluorescence spectrometer set at an excitation maximum of 330 nm (10 nm slit width) and an emission maximum of 550 nm (10 nm slit width) with a flow cell volume of 3 μl. Data were acquired using the Perkin-Elmer LIMS/CLAS system.

HPLC separation

HPLC separation was carried out using a stainless-steel (25 cm × 2.1 mm I.D.) Ultrasphere octyldecylsilyl 5-μm particle size analytical column (supplied by Beckman). Column back-pressure varied from 10 to 11 MPa. Samples were loaded by a Model 7520 Rheodyne microinjector fitted with a 0.5-μl sample rotor. Initially, the HPLC separation of five Dns-amino acids was carried out under isocratic conditions using a mobile phase that consisted of [130 m*M* ammonium acetate (pH 6.8)–acetonitrile in the ratio 67:33 (v/v). The flow-rate was 70 μl/min at ambient temperature. The inclusion of 15 μ*M* tetra-*n*-butylammonium hydroxide (TBAH) improved the chromatography considerably (Fig. 1).

Gradient elution was then used to separate a larger number of amino acids using the following conditions: solvent A consisted of [130 m*M* ammonium acetate (pH 6.8) containing 15 μ*M* TBAH]–acetonitrile in the ratio 893:17 (v/v); solvent B was acetonitrile. In solvents containing ^2H_2O, the p^{2}H (measured from the meter reading with the addition of 0.4 units [7]) was adjusted with $C^2H_3CO_2{}^2H$ to a meter reading of 6.4, giving a p^{2}H of 6.8.

The following gradient program was used in all subsequent experiments: segment 1: isocratic at 0% of B for 10 min; segment 2: a linear gradient from initial conditions to 8% B in 12 min; segment 3: isocratic at 8% B for 30 min; segment 4: a linear gradient from preceding segment condition to 30% B for 8 min; segment 5: isocratic at 30% B for 40 min; segment 6: a linear gradient from preceding segment condition to 0% B for 6 min. The column was re-equilibrated to initial conditions (segment 1) for 40 min between each run. For clarification, we have summarised the above gradient profile in Fig. 2. The flow-rate was 70 μl min at ambient temperature. The gradient program was started simultaneously with injection. For both isocratic and gradient elution HPLC separations, volumes of sample injection were typically 0.5 μl.

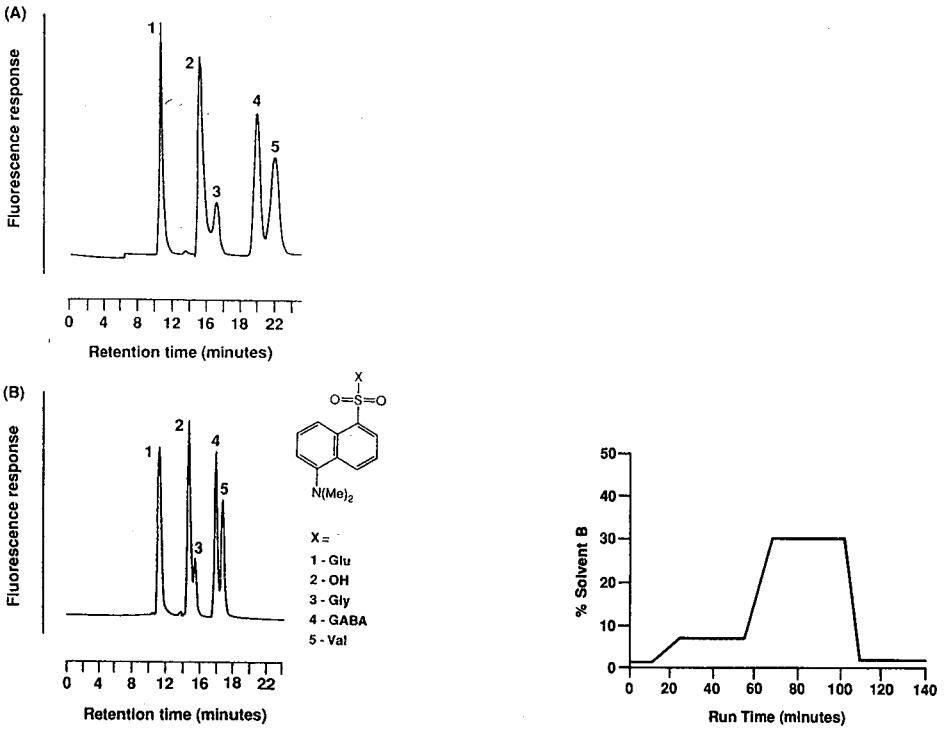

Fig. 1. A comparison of the chromatography obtained (A) without and (B) with the inclusion of 15 μM TBAH in the eluent. Conditions as in Fig. 1 except mobile phase: 130 mM ammonium acetate (pH 6.8)–acetonitrile (67:33).

Fig. 2. Gradient profile for the separation of Dns-amino acids. Gradient elution conditions: column: 25 cm × 2.1 mm I.D., 5-μm ODS (Beckman); fluorescence detector: excitation wavelength, 330 nm; emission wavelength, 550 nm; temperature: ambient; mobile phase: 140-min gradient elution; solvent A = [130 mM ammonium acetate (pH 6.8) containing 15 μM TBAH]–acetonitrile (83:17); solvent B = acetonitrile. Flow-rate: 70 μl/min.

Derivatisation procedure

Amino acids were derivatised using Dns-Cl according to the procedure by Tapuhi *et al.* [8]. The amino acid (0.001–0.1 mmol) dissolved in 40 mM sodium carbonate (pH 9.50, adjusted with hydrochloric acid), was treated with the Dns-Cl reagent (70 mM in acetonitrile) at room temperature. Some precipitation initially appeared upon reaction, but the precipitate dissolved immediately with agitation and the reaction was usually complete in 20–40 min. When not in use, solutions fo Dns-amino acids were stored at 5°C.

RESULTS AND DISCUSSION

It is well known that the use of an ion-pairing agent can improve the chromatography of a number of molecules [9,10]. In the present study, we initially investigated the use of ion-pairing agents such as tetra-*n*-butyl ammonium hydroxide (TBAH),

tetraethyl ammonium hydroxide (TEAH) and cetyltrimethyl ammonium bromide (CTAB) on the resolution of several Dns-amino acids under isocratic elution conditions. For all ion-pairing agents, the retention time of the dansyl amino acids was increased to a varying extent compared to the case where no ion-pairing agent was used. However, only the use of TBAH gave sharper peaks and an improvement in resolution (Fig. 3). The concentration of the ion-pairing agent used was to a large extent controlled by the amount of back pressure on the column. The concentration of 15 μM TBAH was the best compromise for these effects.

Using the chromatographic conditions detailed in the Experimental Section and in Fig. 2, the chromatograms shown in Fig. 3A and B are obtained for ten

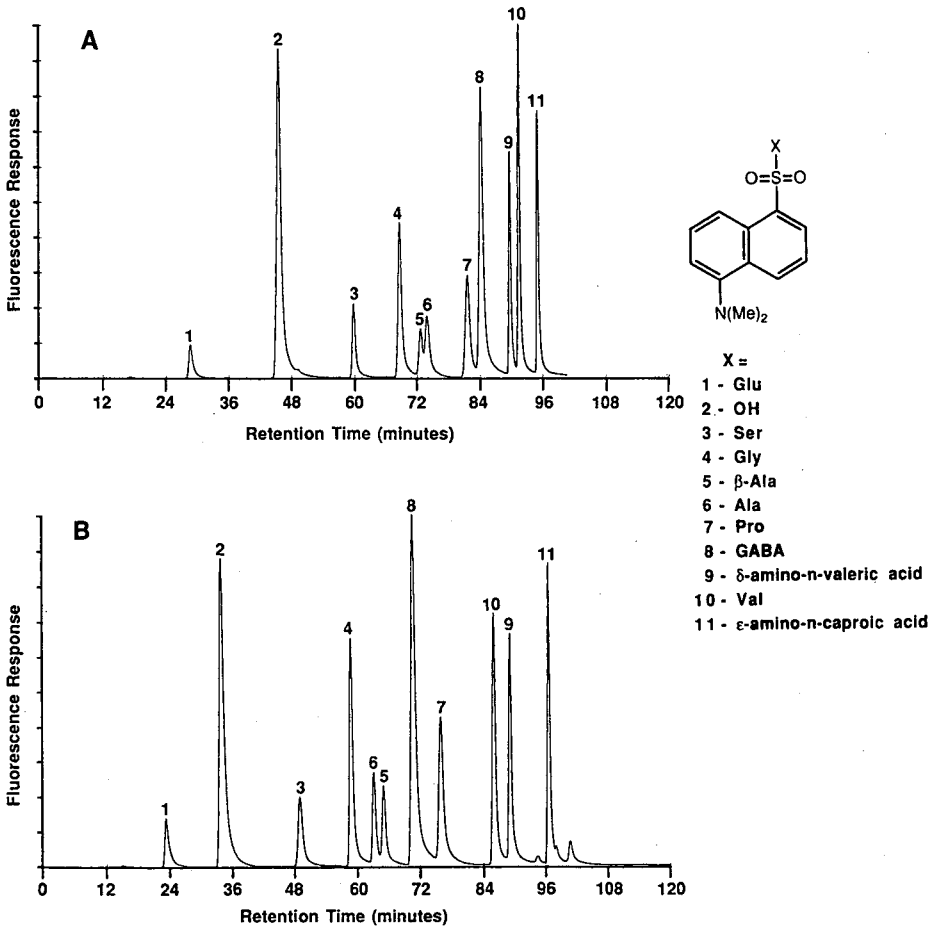

Fig. 3. A comparison of the elution order of dansylic acid and ten Dns-amino acids using either H_2O or ^2H_2O as the main component in the mobile phase. Chromatographic conditions are as detailed in the Experimental Section. (A) Chromatogram of derivatives eluted in H_2O mobile phase (pH 6.8). (B) Chromatogram of derivatives eluted in ^2H_2O-mobile phase (p^{2}H 6.8). The numbering system shown refers to (1 = Dns-Glu, 2 = dansylic acid, 3 = Dns-Ser, 4 = Dns-Gly, 5 = Dns-β-Ala, 6 = Dns-Ala, 7 = Dns-Pro, 8 = Dns-GABA, 9 = Dns-δ-amino-n-valeric acid, 10 = Dns-Val and 11 = Dns-ε-amino-n-caproic acid. 10–84 pmol of each compound was injected.

Dns-amino acids and dansylic acid (1-dimethylaminonaphthalene-5-sulphonic acid) using either water (H_2O) or deuterium oxide (^2H_2O) in the mobile phase. The retention times [t (H_2O) and t (^2H_2O)] for the compounds analysed in these two solvents are listed in Table I. It is clear from this table that t (^2H_2O) values are lower than the corresponding $t(H_2O)$ values. The shorter retention times in ^2H_2O compared to H_2O are probably due to a combination of two effects. The use of a counter-ion makes the ion pair more hydrophobic than the unpaired Dns-amino acid at pH values close to neutral. A second effect is related to the pK_a values of the Dns-amino acids in H_2O compared to ^2H_2O solutions. pK_a values are expected [11] to be higher in ^2H_2O than in H_2O so that slightly less dissociation is expected in the former mobile phase at pH 6.8 compared to pH 6.8 in H_2O. For instance, the pK_a value of N-acetylglycine is reported [12] as 3.7 (no pK_a values for the Dns-amino acid derivatives could be found in the literature). This will increase by about 0.4 units in ^2H_2O. The retention times of the Dns-amino acids studied decrease to a varying extent in ^2H_2O compared to H_2O (see Fig. 3A and B, and Table I). We have not studied the variation of retention times over a wide range of pH values. The order of elution is even changed in some cases in ^2H_2O *versus* H_2O solutions. We are aware that in some cases quoted in the literature [13,14] retention times of substrates measured using reversed-phase chromatography (RP-HPLC) and ^2H_2O or H_2O in the mobile phase gave longer retention times in the former solvent. In contrast, under our chromatographic conditions, shorter retention times of the Dns-amino acids are observed in ^2H_2O (Table I). This may be due to the more complex equilibria occurring when an ion pair reagent such as TBAH is used in the mobile phase in RP-HPLC. Two mechanisms can be involved [15,16]. The ion pair can be adsorbed onto the surface of the reversed-phase resulting in a situation close to ion-exchange chromatography or it can be closely associated with the negatively charged substrate in a neutral complex held together by electrostatic attraction. As the pK_a of the Dns-amino acids in ^2H_2O is higher than in H_2O due to the smaller extent of ionisation at equivalent pH and ^2H values (equal acidity) shorter retention times are expected in ^2H_2O when either mechanism is operative.

The procedure detailed was used in the determination of the concentration of

TABLE I

THE EFFECTS OF H_2O AND ^2H_2O ON THE RETENTION TIMES OF DANSYLIC ACID AND SOME Dns-AMINO ACIDS

Dns derivative	Peak No.	(H_2O) (min)	$t(^2H_2O)$ (min)	$t(H_2O)$-$t(^2H_2O)$ (min)
Glu	1	28.1	22.8	5.3
Dansylic acid	2	45.0	33.3	11.7
Ser	3	59.4	48.2	11.2
Gly	4	68.3	58.0	10.3
β-Ala	5	73.4	62.4	11.0
Ala	6	72.2	64.2	8.0
Pro	7	81.1	70.0	11.1
GABA	8	83.7	75.1	8.6
γ-Amino-*n*-valeric acid	9	89.3	88.5	0.8
Val	10	91.0	85.2	5.8
ε-Amino-*n*-caproic acid	11	94.6	96.4	− 1.8

Glu and GABA in plasma and brain tissue fluids from rats. In this analysis, the use of H_2O gave adequate resolution and sensitivity. No recourse to using ^2H_2O in place of H_2O in the buffer eluent was necessary, especially as this would be costly due to the large number of samples to be analysed.

REFERENCES

1 O. P. Ottersen and J. Storm-Mathisen, *J. Comp. Neurol.*, 229 (1984) 374.
2 D. R. Curtis and J. C. Watkins, *J. Neurochem.*, 6 (1960) 117.
3 K. T. Hsu and C. L. Currie, *J. Chromatogr.*, 166 (1978) 555.
4 S. Einarsson, *J. Chromatogr.*, 348 (1985) 213.
5 M. Roth, *Anal. Chem.*, 43 (1971) 880.
6 R. L. Heinrikson and S. C. Meredith, *Anal. Biochem.*, 136 (1984) 65.
7 P. K. Glasoe and F. A. Long, *J. Phys. Chem.*, 64 (1960) 188.
8 Y. Tapuhi, D. E. Schmidt, W. Lindier and B. L. Karger, *Anal. Biochem.*, 115 (1981) 123.
9 R. A. Wall, *J. Chromatogr.*, 194 (1980) 353.
10 W. S. Hancock, C. A. Bishop and M. T. W. Hearn, *Chem. N.Z.*, 43 (1979) 17.
11 W. P. Jencks, *Catalysis in Chemistry and Enzymology*, McGraw-Hill, New York, 1969, p. 251.
12 J. A. Dean (Editor), *Large's Handbook of Chemistry*, McGraw-Hill, New York, 12th ed., 1979, pp. 5–18.
13 K. Jinno and C. Fujimoto, *J. Liq. Chromatogr.*, 7 (1984) 2059.
14 N. Tanaka and E. R. Thornton, *J. Am. Chem. Soc.*, 99 (1977) 7300.
15 B. Fransson, K. G. Wahlund, I. M. Johannson and G. Schill, *J. Chromatogr.*, 125 (1976) 327.
16 J. C. Kraak, K. M. Jonker and J. F. K. Huber, *J. Chromatogr.*, 142 (1977) 671.

Journal of Chromatography, 549 (1991) 410–415
Elsevier Science Publishers B.V., Amsterdam

CHROM. 23 337

Short Communication

High-performance liquid chromatographic method for the determination of cloxacillin in commercial preparations and for stability studies

MEI-CHICH HSU* and MEI-CHAI CHENG

National Laboratories of Foods and Drugs, Department of Health, Executive Yuan, 161-2, Kuen-Yang St., Nankang, Taipei 11513 (Taiwan)

(First received December 20th, 1990; revised manuscript received March 26th, 1991)

ABSTRACT

A reversed-phase column liquid chromatographic method was developed for the assay of cloxacillin and its preparations. The linear calibration range was 0.2–3.0 mg/ml ($r = 0.9998$) and recoveries were generally greater than 99%. The relative standard deviation was 0.13% ($n = 10$). The high-performance liquid chromatographic assay results were compared with those obtained from a microbiological assay for bulk drug substance, capsule, injection and syrup formulations containing cloxacillin and degraded cloxacillin. At the 99% confidence level, no significant inter-method differences were noted for the paired results. Commercial formulations were also analysed and the results obtained by the proposed method closely agreed with those found by the microbiological method. The results indicated that the proposed method is a suitable substitute for the microbiological method for assays and stability studies of cloxacillin preparations.

INTRODUCTION

The US *Code of Federal Regulations* [1] described two official methods for potency assay of cloxacillin: a microbiological method and iodimetric titration. The regulations state that the results obtained from the microbiological method shall be conclusive. The present official assay method of *Minimum Requirements for Antibiotic Products of Japan* [2] for the analysis of potency of cloxacillin in bulk drug substance and its preparations is a microbiological method.

However, there has recently been a move to replace expensive microbiological assays by chemical assays, *e.g.*, high-performance liquid chromatography (HPLC). Several HPLC methods for the determination of cloxacillin in biological fluids have been reported [3–11]. Fewer methods have been reported for separating and identifying cloxacillin and the derivatives of penicillin [12–14] and for the determination of cloxacillin in pharmaceutical samples [15].

0021-9673/91/$03.50

In order to establish whether an HPLC method would be acceptable, it is important to determine whether it is robust enough for assaying samples kept under extreme conditions. Degradation in the sample should be equally reflected by microbiological and HPLC assays. This paper describes a comparison of a proposed HPLC method with a microbiological assay for the determination of cloxacillin in commercial formulations. Further, cloxacillin was kept at elevated temperatures as part of an accelerated degradation experiment and assayed by microbiological and HPLC methods.

EXPERIMENTAL

Instruments

A Waters Model 600E liquid chromatographic pump (Waters Chromatography Division, Millipore, Milford, MA, USA), a Waters Model 490E UV detector and a Waters Model 745 Data Module were employed during the study. The mobile phase was pumped through a reversed-phase column (μBondapak C_{18}, 30 cm × 3.9 mm I.D., 10 μm; Waters P/N 27324) with an isocratic flow-rate of 1.5 ml/min. The detector was set at 254 nm. Chromatography was performed at room temperature. Injections of 10 μl were made of all solutions to be analysed.

Mobile phase

The mobile phase was methanol–4% acetic acid (60:40, v/v). The mobile phase was filtered (0.45-μm Millipore filter) and degassed with an ultrasonic bath prior to use.

Standard solutions

Internal standard dimethyl phthalate (3 g) was dissolved in 100 ml of acetonitrile–water (1:1). To an accurately weighed amount of cloxacillin sodium standard (National Laboratories of Foods and Drugs, Taiwan), equivalent to 50 mg potency of cloxacillin, was added 0.5 ml of internal standard stock solution and the volume was made up to 50.0 ml with distilled water.

Sample preparations

To an accurately weighed amount of bulk drugs, homogeneous capsule contents, injection or syrup formulations, equivalent to 50 mg potency of cloxacillin was added 0.5 ml of internal standard stock solution, and the volume was made up to 50.0 ml with distilled water.

Solution for linearity response

Seven concentrations of cloxacillin sodium, which ranged from 0.2 to 3.0 mg/ml, were prepared. Each concentration was chromatographed six times.

Solution for recovery studies

To an accurately wieghed 50 mg potency of sample composites of commercial preparations were added different amounts of cloxacillin standard and 0.5 ml of internal standard stock solution. Each solution was made up to 50.0 ml with distilled water and was chromatographed in triplicate.

Microbiological assay procedure

Bacillus subtilis (Culture Collection and Research Center, Taiwan) was used in the microbiological assay. According to the cup plate method, standards and test drugs were diluted to 1.0 mg/ml (potency) concentrated solution with distilled water and then diluted to 16.0 and 4.0 μg/ml with 1% phosphate buffer solution (pH 6.0) on the day of analysis. Five Petri dishes of 9.0 cm I.D. were used for each sample. After incubation for 16–18 h, the zone diameter was measured by a zone analyser (Model ZA-F; Toyo, Tokyo, Japan).

RESULTS AND DISCUSSION

The linearity of the peak-area ration (cloxacillin *vs.* internal standard) was verified by injection of seven solutions containing cloxacillin in the concentration range 0.2–3.0 mg/ml. A straight line with a correlation coefficient of 0.9998 ($y = 0.0379 + 0.1483x$) was obtained.

The reproducibility (C.V.) of the proposed method, on the basis of peak-area ratios for ten replicate injections was 0.13%. The standard deviation was 0.19%.

The results of standard addition recovery studies of cloxacillin from sample composites of commercial preparations are shown in Table I. The average recovery was greater than 99%. These data indicate that the proposed HPCL method is relatively unaffected by the sample matrix.

Typical chromatograms of cloxacillin commercial dosage forms are shown in Fig. 1. The retention time was about 3.7 min for the internal standard and 5 min for cloxacillin. Excipients from commercial formulations did not interfere.

When samples of capsule, injection and syrup formulations were heat degraded, the resulting mixtures yielded chromatograms containing additional peaks, none of which interfered with the interpretation and measurement of the chromatographic peaks for cloxacillin and dimethyl phthalate, as shown in Fig. 1. In addition, a decrease in peak height (and/or peak area) with increase in temperature and time can be observed.

TABLE I

RECOVERY OF CLOXACILLIN FROM VARIOUS COMMERCIAL COMPOSITES

Formulation	Added (mg)	Found (mg)	Recovery (%)	Average recovery (%)
Capsule	11.1	11.18	100.7	99.83
	16.7	16.58	99.3	
	22.2	22.08	99.5	
Injection	11.8	11.73	99.4	99.57
	16.7	16.51	98.9	
	22.3	22.39	100.4	
Syrup	11.7	11.81	100.9	100.37
	16.9	17.20	101.8	
	22.2	21.04	98.4	

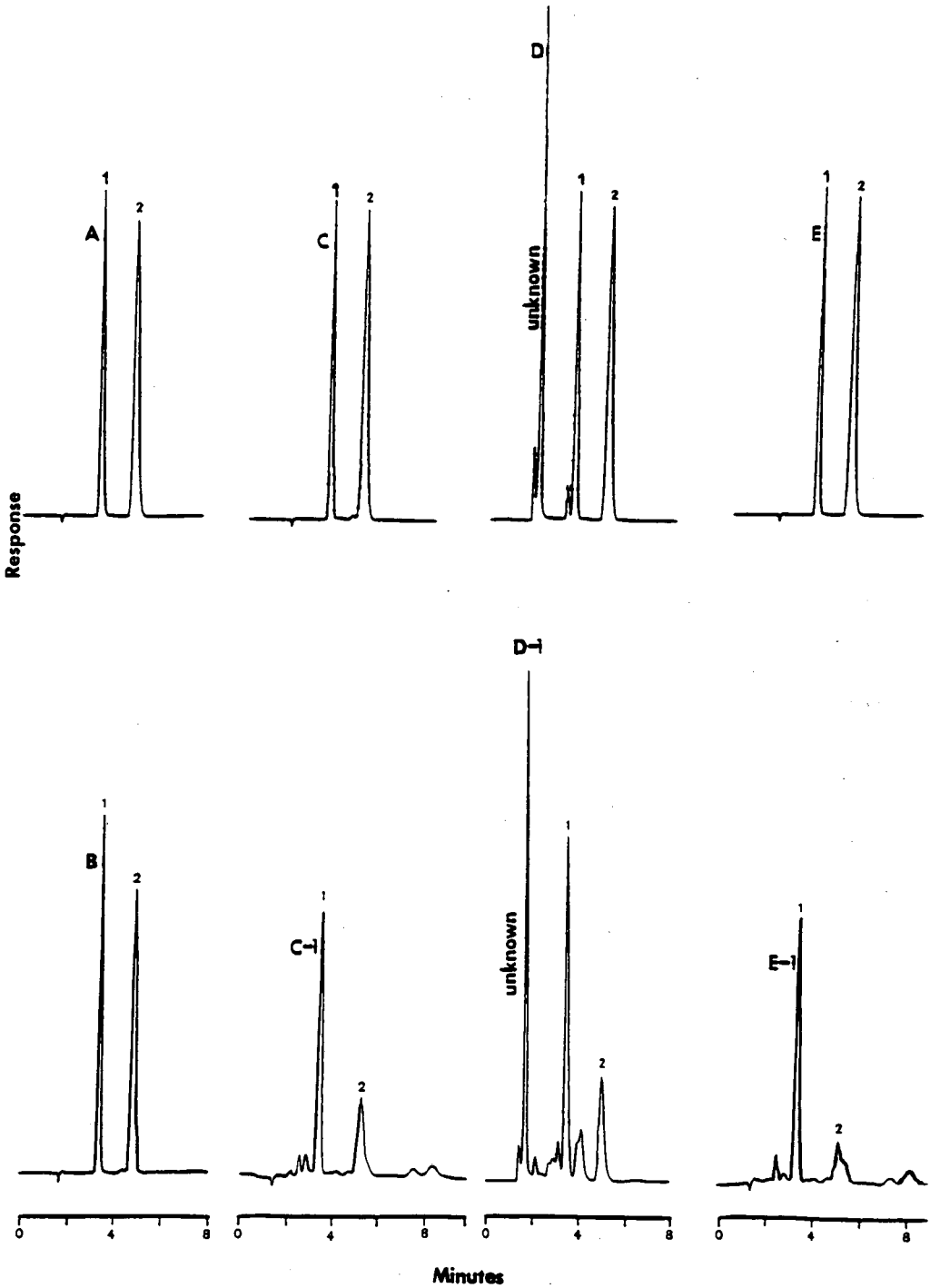

Fig. 1. Chromatograms of cloxacillin preparations: (A) house standard; (B) bulk drug substance; (C) 250-mg capsule; (C-1) degraded 250-mg capsule; (D) 125 ml per 5 ml syrup; (D-1) degraded 125 mg per 5 ml syrup; (E) 250 mg per vial injection; (E-1) degraded 250 mg per vial injection. Peaks: 1 = dimethyl phthalate; 2 = cloxacillin (10 μg).

TABLE II

COMPARISON OF MICROBIOLOGICAL AND HPLC ASSAYS FOR CLOXACILLIN

Sample	Potency[a]	
	Microbiological method[b]	HPLC[c]
Bulk drug		
House standard	899.7	899.7
USP standard	924.8	920.3
Brand A: 1	849.2	855.9
2	917.0	893.0
3	900.2	892.4
Brand B: 1	887.2	891.6
2	927.8	920.6
3	925.0	914.6
Dosage form, declared		
Brand A: 1 250 mg/cap.	104.1	103.2
2 250 mg/cap.	102.5	102.2
Brand C: 250 mg/cap.	101.1	102.2
Brand D: 1 250 mg/cap.	100.2	102.8
2 250 mg/vial	105.0	105.7

[a] The potency was determined as μg/mg for bulk drug and percentage of declared for dosage form.
[b] Average of five determinations.
[c] Average of three determinations.

TABLE III

COMPARISON OF PERCENT POTENCY OF CLOXACILLIN IN CAPSULE, INJECTION AND SYRUP FORMULATIONS AS DETERMINED BY MICROBIOLOGICAL AND HPLC METHODS

% of declared concentration

Capsule, 250 mg		Injection, 250-mg vial		Syrup, 125 mg per 5 ml	
Microbiological method	HPLC	Microbiological method	HPLC	Microbiological method	HPLC
107.4	107.3	109.9	105.0	117.2	116.4
107.1	101.3	106.1	105.9	113.7	114.7
105.9	106.3	105.8	106.3	112.8	107.4
105.7	101.5	105.5	103.3	102.2	101.8
103.5	104.4	92.7	90.9	99.4	96.7
103.2	102.1	90.1	89.2	91.5	87.9
102.8	100.8	88.5	85.2	89.7	84.0
101.8	104.1	73.6	72.3	75.2	72.0
101.3	101.0	51.6	54.2	74.3	71.5
101.1	102.3	44.0	43.9	62.1	58.5
100.8	100.1	18.0	21.1	45.9	47.4
99.9	102.4	15.7	18.2	42.0	43.5
90.1	88.2			25.9	27.6
84.8	86.1				
76.6	77.6				
38.2	43.7				
37.0	39.3				
31.4	26.6				

A number of samples of bulk drug substance and commercial preparations of three brands were analysed for cloxacillin content by HPLC. These samples were also assayed by the microbiological method. The results are shown in Table II. A *t*-test was applied to the data: analysis showed no significant difference at the 99% confidence level for any of the preparations when assayed by the microbiological or HPLC methods.

A study was initiated to ascertain the suitability of the proposed method for stability studies. Samples of capsule, injection and syrup formulations were stored in temperature-controlled cabinets (ambient or 55–150°C). Samples were taken from the cabinets periodically for microbiological and HPLC assays. The assay values, expressed as a percentage of the label claim, are given in Table III. The paired values in Table III have correlation coefficients of 0.994 for capsule, 0.999 for injection and 0.997 for syrup dosage forms, respectively. Hence no significant difference in the assay values obtained by the two analytical methods was found for degraded or non-degraded samples.

This study demonstrates the applicability of the proposed HPLC method for the potency determination of cloxacillin in bulk drug and capsule, injection and syrup formulations. The method can be successfully used for routine quality control and stability assays and offers advantages in speed, simplicity and reliability.

ACKNOWLEDGEMENTS

The authors thank Bristol Industries and China Biological and Chemical Laboratories for the supply of cloxacillin sodium bulk drugs.

REFERENCES

1 *Code of Federal Regulations, Title 21, Part 440,* US Government Printing Office, Washington, DC, 1988.
2 *Minimum Requirements for Antibiotic Products of Japan,* English Version, Japan Antibiotics Research Association, Tokyo, 1986.
3 H. H. W. Thijssen, *J. Chromatogr.*, 183 (1980) 339.
4 A. Brunetta, L. Mosconi, S. Pongiluppi, U. Scagnolari and G. Zambonin, *Boll. Chim. Farm.*, 120 (1981) 335.
5 F. W. Teare, R. H. Kwan, M. Spino and S. M. MacLeod, *J. Pharm. Sci.*, 71 (1982) 938.
6 W. A. Moats, *J. Chromatogr.*, 317 (1984) 311.
7 D. M. Paton, *J. Clin. Pharmacol. Res.*, 6 (1986) 347.
8 F. Jehl, P. Birckel and H. Monteil, *J. Chromatogr.*, 413 (1987) 109.
9 M. A. Abuirjeie and M. E. Abdel Hamid, *J. Clin. Pharmacol. Ther.*, 13 (1988) 101.
10 C. T. Hung, J. K. C. Lim, A. R. Ziest and F. C. Lam, *J. Chromatogr.*, 425 (1988) 331.
11 H. S. Lee, T. Y. Yi and Y. M. Khoo, *Ther. Drug Monit.*, 10 (1988) 340.
12 G. T. Briguglio and C. A. Lau-Cam, *Assoc. Off. Anal. Chem.*, 67 (1984) 228.
13 J. Martin, R. Mendez and A. Negro, *J. Liq. Chromatogr.*, 11 (1988) 1707.
14 M. A. S. Salem and H. N. Alkaysi, *Drug Dev. Ind. Pharm.*, 13 (1987) 2771.
15 G. Lauriault, M. J. Lebelle and A. Vilim, *J. Chromatogr.*, 246 (1982) 157.

Journal of Chromatography, 549 (1991) 416–422
Elsevier Science Publishers B.V., Amsterdam

CHROM. 23 311

Short Communication

Hydrogen–deuterium exchange in fused-silica capillary columns

MOHAMED E. MAHMOUD
Barnett Institute of Chemical Analysis and Department of Chemistry, Northeastern University, Boston, MA 02115 (USA)
ADEL M. MOUSSA
Barnett Institute of Chemical Analysis, Northeastern University, Boston, MA 02115 (USA)
DAVID A. FORSYTH
Department of Chemistry, Northeastern University, Boston, MA 02115 (USA)
and
PAUL VOUROS*
Barnett Institute of Chemical Analysis and Department of Chemistry, Northeastern University, Boston, MA 02115 (USA)
(First received January 9th, 1991; revised manuscript received March 13th, 1991)

ABSTRACT

Ketones deuteriated α to the carbonyl have been observed to undergo significant isotope exchange on fused-silica capillary columns during gas chromatography–mass spectrometry. The residence time of the compounds on the column was found to influence the extent of isotope exchange. The degree of exchange was examined using a variety of columns and the isotope exchange was found to occur even with brand new columns. Conversion of the keto compounds into the methyloxime derivatives resulted in retention of the "correct" isotope content during gas chromatography–mass spectrometry.

INTRODUCTION

Hydrogens α to a carbonyl are well known for their activity and this property is exploited to introduce deuterium atoms in that position via exchange under acidic or basic conditions [1]. The preparation of labeled compounds for use as internal standards in quantitative analysis by gas chromatography–mass spectrometry (GC–MS) often involves the use of appropriate keto intermediates to facilitate incorporation of the label(s) in the desired molecule.

In packed column GC–MS, chromatographic columns have been used to provide a source of isotopic label for the exchange of labile hydrogens (or entire function-

0021-9673/91/$03.50

al groups) on-line in order to assist in the interpretation of spectra. For example, hydroxylic or amino hydrogens can be readily replaced with deuterium by prior saturation of the column's active sites with CH_3O^2H [2,3]. Columns impregnated with $Ba(O^2H)_2$ have been used on-line to exchange hydrogen α to carbonyls in alicyclic systems [4]. Isotopic labeling using different sources of isotopes have been reported [5–8]. Moreover, the higher acidity of trimethylsilyl (TMS) esters of TMS-phosphates has been taken advantage of in order to effect selective exchange of the former groups in packed columns previously saturated with [$^2H_9$]bis-trimethylsilyl acetamide [9,10].

In recent experiments we observed that fused-silica capillary columns exhibit sufficient activity to cause exchange of hydrogens α to a carbonyl. We initially encountered this *a priori* unexpected tendency for ^1H–^2H exchange while working with capillary columns that had been previously used for general analytical purposes. In this paper we report a more detailed examination of the phenomenon using both "old" and "new" fused-silica capillary columns from different manufacturers. The results of these studies are presented below.

EXPERIMENTAL

Instrumentation

GC–MS studies were conducted with a Finnigan 4021B mass spectrometer interfaced to a Hewlett-Packard 5890 gas chromatograph (equipped with on-column injector) and Incos data system. The mass spectrometer was operated in the electron impact (EI) mode over a limited mass range so as to record the molecular ion region of each compound of interest. The ion source temperature was set at 250°C and the ionizing energy at 70 eV. The unlabeled counterparts of all compounds were examined in order to establish the potential contribution from (M − 1] and/or [M + 1] peaks to the spectra.

Compounds

The isotopically labeled compounds used in this study were prepared as follows: 4,4-Dimethyl-2-cyclohexen-1-one, 4-methylcyclohexanone, and 3-keto-androstane were prepared by dissolving 50 mg of the respective compound in 10 ml solution of 40% NaO^2H and ^2H_2O and stirring the reaction mixture for 3–4 hours at 80°C. The products were then extracted from diethyl ether and dried over Na_2SO_4.

The correct isotopic ratios for the various compounds were established by analyzing them via the direct insertion probe (DIP) in order to avoid extensive contact of the analytes with active surfaces. To compensate for the high volatility of most of the studied deuteriated compounds, mass spectra were obtained by using a cold probe tip and scanning the mass spectrometer immediately upon opening the valve leading to the high vacuum system and the ion source.

RESULTS AND DISCUSSION

The structures of the ketones used to ascertain the propensity of α hydrogens to undergo exchange, the position of deuterium incorporation and their molecular weights are presented below. Since the percentage of isotopic incorporation in the

I: 4,4-Dimethyl-2-cyclohexene-1-one

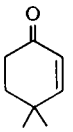

(124)

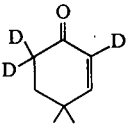

(127)

II: 4-Methylcyclohexanone

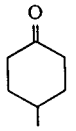

(112)

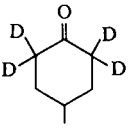

(116)

III: 3-Keto-androstane

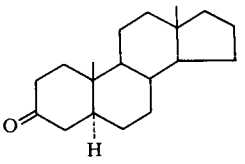

(274)

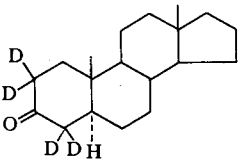

(278)

compounds was less than 100%, the ratio of several "molecular ion" peaks encompassing various degrees of isotopic content from $M^{+\cdot}$ to $M^{+\cdot} + n_i$ (where n_i = the number of deuterium atoms) had to be monitored.

TABLE I

RATIO OF MOLECULAR ION PEAKS OF $^2H_3$-LABELED 4,4-DIMETHYL-2-CYCLOHEXENE-1-ONE INTRODUCED AT DIFFERENT FLOW-RATES WITH NEW AND OLD COLUMNS

Ratio is expressed as a percentage relative to the most intense peak which is assigned a value of 100% in the multiplet of peaks relative to the molecular ion. A = Old 30-m DB1 column (J&W), oven-temperature = 150°C, split injector and variable flow-rates. B = Old 60-m DB1 column (J&W), oven-temperature = 200°C, split injector and variable flow-rates. C = New 30-m DB1 column (J&W), oven-temperature = 150°C, split injector and variable flow-rates. D = New 30-m DB1 column (HP), oven-temperature = 150°C, split injector and variable flow-rates.

m/z	Peak ratio at different flow-rates																Probe run
	6 ml/min				4 ml/min				2 ml/min				1 ml/min				
	A	B	C	D	A	B	C	D	A	B	C	D	A	B	C	D	
124 ($^2H_0$)	87	31	32	42	100	51	42	42	100	100	57	58	100	100	60	–	35
125 ($^2H_1$)	100	100	100	97	41	100	100	100	28	67	100	100	24	31	100	–	96
126 ($^2H_2$)	20	15	93	100	18	18	94	90	15	21	84	81	16	16	73	–	100
127 ($^2H_3$)	19	15	45	53	12	17	47	41	11	16	40	34	10	11	28	–	61
128 ($^2H_4$)	11	10	9	8	3	10	7	4	2	6	6	4	2	2	2	–	17

Effect of residence time

The contribution of the column to the exchange process was initially evaluated under isothemal conditions by varying the flow-rate in order to assess the influence of residence time. Two old, but otherwise well-performing columns as well as two new 30-m columns from different manufacturers (HP and J&W Scientific) were evaluated. For 4,4-dimethyl-2-cyclohexan-1-one, the results are summarized in Table I. Listed here are the ratios of the undeuteriated ($^2H_0$: *m/z* 124) and the corresponding labeled analogues ($^2H_1$: *m/z* 125; $^2H_2$: *m/z* 126; $^2H_3$ *m/z* 127) of the compound. The following general trends are observed:

(1) At lower flow-rates (higher residence time) there is an enhancement of the relative abundance of the *m/z* 124 ion. Note, for example, the variation in the peak intensity ratio from 87:100:20:19 (6 ml/min) to 100:24:16:10 (1 ml/min) for the $^2H_0$–$^2H_1$–$^2H_2$–$^2H_3$ species.

(2) Even at the highest flow-rate examined (6 ml/min), used columns exhibit sufficient activity to induce exchange.

(3) New columns, as expected, appear less reactive and the ion mass ratios are more comparable to direct insertion probe data especially at shorter residence times.

(4) At longer residence time, *i.e.*, lower flow-rates, the new columns are also sufficiently active to favor formation of an analog with lower deuterium content.

A plot of the variation in distribution of peak intensities "normalized; total = 100" from the 30-m DB1 old column (J&W) is shown in Fig. 1. The peak intensities from analysis of I via the direct insertion probe are included for comparison. An increase in the peak intensity of the unlabeled compound with lower flow-rate is apparent, indicating increased exchange with longer residence time.

Two other related carbonyl compounds labeled at the α position with deuterium were also examined in order to assess the generality of the phenomenon discussed above. The behavior of these compounds on the "new" columns is summarized in

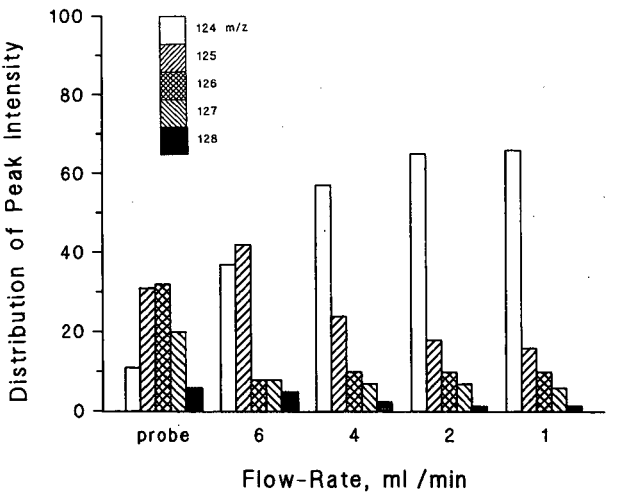

Fig. 1. Variation of the peak intensities "normalized; total = 100" for I from the 30-m DB1 old column (J&W) at different flow-rates.

TABLE II

RATIO OF MOLECULAR ION PEAKS OF $^2H_4$-LABELED 4-METHYLCYCLOHEXANONE INTRODUCED AT DIFFERENT FLOW-RATES WITH TWO DIFFERENT NEW COLUMNS

Ratio is expressed as a percentage relative to the most intense peak which is assigned a value of 100% in the multiplet of peaks relative to the molecular ion. A = New 30-m DB1 column (J&W). B = New 30-m DB1 column (HP).

m/z	Peak ratio at different flow-rates						Probe run
	6 ml/min		4 ml/min		1 ml/min		
	A	B	A	B	A	B	
112 ($^2H_0$)	29	18	33	26	35	25	24
113 ($^2H_1$)	78	68	100	100	100	80	68
114 ($^2H_2$	100	100	98	100	100	100	100
115 ($^2H_3$)	60	76	54	75	50	61	91
116 ($^2H_4$)	15	29	18	29	14	21	13

Tables II and III. Again a definite trend is observed that shows increased exchange with longer residence time on the columns. Moreover, a somewhat stronger activity is evident for the (J&W) column as compared to the HP column. Significantly, conversion of compounds II and III to their methyloxime derivatives suppressed any exchange of the α protons. In the latter case, the ratios of peak intensities corresponding to the different molecular ion masses were identical for both the direct insertion probe and GC–MS analyses.

Effect of temperature

In the preceding section we discussed the effect of flow-rate or residence time on the exchange process under isothermal conditions. Clearly temperature is another variable which needs to be considered since, from a practical point of view, GC–MS

TABLE III

RATIO OF MOLECULAR ION PEAKS OF $^2H_4$-LABELED 3-KETOANDROSTANE INTRODUCED AT DIFFERENT FLOW-RATES WITH TWO DIFFERENT NEW COLUMNS

Ratio is expressed as a percentage relative to the most intense peak which is assigned a value of 100% in the multiplet of peaks relative to the molecular ion. A = New 30-m DB1 column (J&W). B = New 30-m DB1 column (HP).

m/z	Peak ratio at different flow-rates						Probe run
	6 ml/min		4 ml/min		1 ml/min		
	A	B	A	B	A	B	
274 ($^2H_0$)	2	0	0	1	2	1	1
275 ($^2H_1$)	18	3	14	20	62	44	12
276 ($^2H_2$)	87	43	88	36	100	44	37
277 ($^2H_3$)	100	100	100	100	78	100	100
278 ($^2H_4$)	49	96	47	66	19	58	57

TABLE IV

RATIO OF MOLECULAR ION PEAKS OF $^2H_3$-LABELLED 4,4-DIMETHYL-2-CYCLOHEXENE-1-ONE AT DIFFERENT ISOTHERMAL ANALYSES AND CONSTANT FLOW-RATE WITH A 30-METER DB1 OLD COLUMN

Ratio is expressed as a percentage relative to the most intense peak which is assigned a value of 100% in the multiplet of peaks relative to the molecular ion.

m/z	Peak ratio at different isothermal analyses				Probe run
	200°C	150°C	120°C	100°C	
124 ($^2H_0$)	19	22	100	100	35
125 ($^2H_1$)	100	100	87	33	96
126 ($^2H_2$)	19	15	23	16	100
127 ($^2H_3$)	18	15	18	10	61
128 ($^2H_4$)	11	9	7	1	17

analyses are usually conducted by programming the column temperature. The trends for ^1H–^2H exchange in I as a function of column temperature were examined. Two sets of experiments were conducted. In the first, the flow-rate was maintained constant at different column temperatures. Table IV summarizes the obtained data which show that more exchange occurs at lower temperature. In the second, the column temperature was ramped at different heating rates. Fig. 2 shows that as the heating rate is decreased, the amount of hydrogen exchange increases significantly. Both of these observations are consistent with more exchange due to longer residence time on the column.

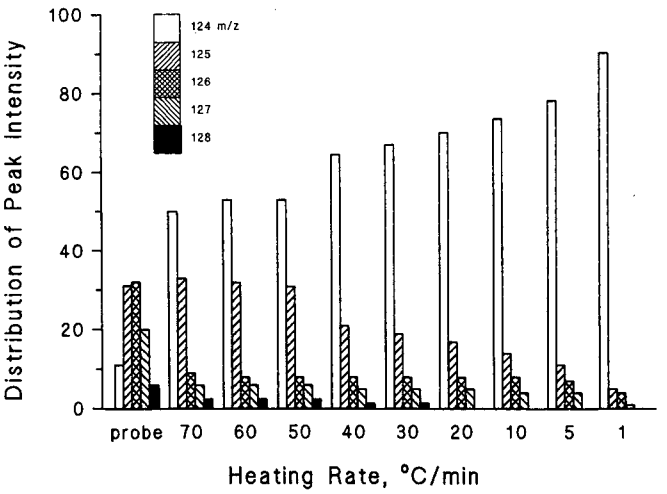

Fig. 2. Variation of the peak intensities "normalized; total = 100" for I from the 30-m DB1 old column (J&W) at different heating rates.

CONCLUSIONS

The data presented above demonstrate that fused-silica capillary columns exhibit sufficient activity to effect exchange of hydrogens α to carbonyls as well. After some use, columns appear to develop a stronger activity towards effecting such an exchange even though they still appear to function well for general analytical purposes. In fact, even the two brand new columns examined here were not inert. In synthesizing isotopically labeled compounds, it is common to test the isotopic purity of intermediates or the final products by capillary GC–MS. While it may be dangerous to generalize from the limited number of examples and columns examined here, it is reasonable to suggest that caution should be exercised in attaching significance to such analyses especially when dealing with deuterium at active positions.

ACKNOWLEDGEMENT

Financial support of this study by Biomedical Support Grant RR07143 is gratefully acknowledged. This is contribution No. 485 from the Barnett Institute of Chemical Analysis.

REFERENCES

1 H. Budzikiewicz, C. Djerassi and D. H. Williams, *Structure Elucidation of Natural Products by Mass Spectrometry, Vol. 1: Alkaloids*, Holden-Day, San Fancisco, CA, 1964, p. 17.
2 M. Senn, W. J. Richter and A. L. Burlingham, *J. Am. Chem. Soc.*, 87 (1965) 680.
3 P. Vouros, *J. Org. Chem.*, 38 (1973) 3555.
4 G. M. Anthony and G. J. W. Brooks, *J. Chem. Soc.*, D (1970) 200.
5 K. Mislow, M. A. W. Glass, H. B. Hopps, E. Simon, and G. H. Wahl, Jr., *J. Am. Chem. Soc.*, 86 (1964) 1710.
6 G. J. Kallos and L. B. Westover, *Tetrahedron Lett.*, 13 (1967) 1223.
7 W. J. Richter, M. Senn and A. L. Burlingam. *Tetrahedron Lett.* 17 (1965) 1235.
8 A. I. Mikaya, V. G. Zaikin, A. V. Antonova and N. S. Prostakoov, *Org. Mass Spectrom*, 19 (1984) 521.
9 D. J. Harvey, M. G. Horning and P. Vouros, *Tetrahedron*, 27 (1971) 4231.
10 D. J. Harvey, M. G. Horning and P. Vouros, *J. Chem. Soc., Perkin Trans.*, 1, (1972) 1074.

Journal of Chromatography, 549 (1991) 423–428
Elsevier Science Publishers B.V., Amsterdam

CHROM. 23 352

Short Communication

Application of substituted liquid crystals as stationary phases in gas–liquid chromatography for the separation of mono- and dimethyl naphthalenes

B. B. GHATGE[a] and NALINI V. BHALERAO*
National Chemical Laboratory, Pune 411 008 (India)
(First received December 12th, 1990; revised manuscript received April 5th, 1991)

ABSTRACT

Thirteen mono- and dilaterally substituted liquid crystalline compounds were investigated for their gas chromatographic behaviour as stationary phases for the separation of mono- and dimethylnaphthalenes. A normal packed column system was used. These compounds offered a good separation for some pairs of methylnaphthalenes.

INTRODUCTION

Liquid crystalline stationary phases are being increasingly used for the separation of close boiling positional isomers by gas–liquid chromatography (GLC) [1–14]. In general, liquid crystalline compounds with longer nematic ranges give the best separation of close boiling positional isomers [11]. However, investigations using laterally substituted liquid crystalline compounds as substrates have shown that higher relative retention values (α) are obtained for positional isomers of disubstituted benzenes than when laterally unsubstituted liquid crystalline compounds with longer nematic ranges are used as stationary phases [10].

In continuation of the work carried out in this laboratory [14] on the screening of laterally substituted liquid crystalline compounds for the separation of close boiling positional isomers and the effect of lateral substitution on selectivity, thirteen methyl-, chloro- and nitro-substituted aromatic liquid crystalline stationary phases have been studied. These compounds were synthesized in this laboratory some time ago [15]. A normal packed column system was used for this purpose. The analysis of

[a] Author deceased.

0021-9673/91/$03.50

methylnaphthalenes is very important as a result of their solubility in water and their toxicity towards aquatic life. Their analysis has always been difficult because of their close boiling points and other similar properties. Liquid crystalline stationary phases in GLC are known to separate such pairs on the basis of the shape of the solute molecules [1,12,13,16–34].

EXPERIMENTAL

The synthesis of these liquid crystals has been described elsewhere [15]. All the liquid crystalline compounds were purified by crystallization from a light petroleum (b.p. 60–80°C)–benzene mixture to give constant transition temperatures, which were determined by the open capillary melting point method. All the melting points are uncorrected. The substituents and transition temperatures are presented in Table I. The solid support used was 80–120 mesh Celite (BDH, Poole, UK). The Celite was coated with the liquid crystalline compound (5%, w/w, coating) using chloroform as the solvent. The chloroform was gradually evaporated on a water-bath. The coated Celite was dried and packed in aluminium columns (6 ft. × $\frac{1}{4}$ in. I.D.). An AIMIL gas–liquid chromatography with thermal conductivity detection and hydrogen as the carrier gas at a flow-rate of 30 ml/min was used to record the retention times.

All the columns were conditioned for 5 h at 10°C below the nematic to isotropic transition temperature of the liquid crystalline compound used as the stationary phase.

TABLE I

STRUCTURE, SUBSTITUENTS AND TRANSITION TEMPERATURES OF THE LIQUID CRYSTALLINE COMPOUNDS USED FOR THE COLUMNS STUDIED HERE

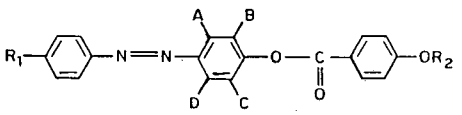

Column No.	R1	R2	A	B	C	D	Transition temperature[a] (°C)	
							C–N	N–I
1	CH_3	CH_3	CH_3	H	H	CH_3	125	170
2	CH_3	C_2H_5	CH_3	H	H	CH_3	123	180
3	OC_2H_5	CH_3	CH_3	H	H	CH_3	140	210
4	OC_2H_5	CH_3	H	CH_3	CH_3	H	182	205
5	OC_2H_5	CH_3	CH_3	CH_3	H	H	198	275
6	OCH_3	CH_3	CH_3	CH_3	H	H	200	270
7	CH_3	n-C_6H_{13}	CH_3	CH_3	H	H	120	200
8	CH_3	CH_3	CH_3	CH_3	H	H	168	236
9	OC_2H_5	n-C_4H_9	CH_3	CH_3	H	H	140	240
10	CH_3	CH_3	CH_3	H	H	H	140	207
11	CH_3	CH_3	Cl	H	H	H	180	230
12	CH_3	C_2H_5	Cl	H	H	H	128	185
13	CH_3	CH_3	H	NO_2	H	H	121	190

[a] C–N = Nematic; N–I = isotropic.

TABLE II

RELATIVE RETENTION TIMES OF MONO- (MN) AND DIMETHYL (DMN) NAPHTHALENES WITH RESPECT TO NAPHTHALENE

Compound	Boiling point at 760 mmHg (°C)	Conditions: (column No.) temperature (°C)											
		(1) 162	(2) 162	(3) 176	(4) 182	(5) 199	(6) 200	(7) 169	(8) 166	(9) 171	(10) 172	(11) 180	(12) 170	(13) 170
		Relative retention time												
Naphthalene	217.7	2.15	1.73	0.93	1.83	0.92	0.97	1.47	0.73	1.20	1.50	1.00	1.88	1.37
1-MN	240.4	2.02	1.94	1.53	1.85	1.66	1.57	1.87	1.92	2.23	2.35	1.88	1.79	1.79
2-MN	241.42	1.78	1.73	1.37	1.70	1.58	1.47	1.71	1.67	2.17	2.22	1.63	1.63	1.62
1,2-DMN	266	4.15	4.00	2.94	3.59	3.10	3.01	3.91	3.49	4.61	4.91	4.00	2.78	3.94
1,3-DMN	263	3.40	3.24	2.44	2.95	2.63	2.34	3.20	3.04	3.46	4.09	3.00	2.19	3.29
1,4-DMN	268	3.80	3.71	2.66	3.45	2.83	2.73	3.48	3.05	3.75	4.45	3.46	2.33	3.3
1,5-DMN	265	3.67	3.60	2.77	3.37	2.85	2.75	3.50	3.40	4.00	4.25	3.35	2.42	3.52
1,6-DMN	264	3.38	3.31	2.42	3.16	2.66	2.53	3.24	3.29	3.82	4.33	3.40	2.32	3.22
2,3-DMN	269	3.94	3.73	2.88	3.49	3.02	2.78	3.59	3.26	4.23	4.19	3.39	2.43	3.52
2,6-DMN	262	3.02	2.89	2.23	2.74	2.48	2.44	3.15	2.88	3.73	3.67	2.66	2.13	2.73

The injector temperature was maintained at 190°C and detector temperature at 240°C. The transition temperatures observed by GLC were 2–5°C lower than the actual transition temperatures, which might be due to the uneven heating of the columns at the injector and detector ends. The retention times were measured from the air peak maxima to the sample peak maxima. The flow-rate of the carrier gas was measured using a soap film flow meter.

RESULTS AND DISCUSSION

Most of these stationary phases gave good separations for a number of combinations of pairs. A literature survey [1,12,13,16–34] shows that the separation mechanism for mono- and dimethylnaphthalene isomers is complex.

The retention time data determined here (Table II) show that the elution order of all the methylnaphthalene isomers is more or less the same on all the liquid crystalline stationary phases under investigation. The separation mechanism for the liquid crystalline phases depends on the interaction of the solute and solvent molecules according to the shape parameter. For isomeric methylnaphthalenes the main factor determining their retention behaviour is the symmetry of substitution [22] (the mutual arrangement of the methyl groups relative to each other and to the aromatic skeleton).

In these observations, when the retention pattern of monomethyl naphthalenes is considered, it is seen that the lower boiling 1-methylnaphthalene is retained on the column and the higher boiling 2-methylnaphthalene isomer elutes first, thus following the shape parameter.

The elution order of dimethylnaphthalene (DMN) shows the predominance of

TABLE III

SEPARATION FACTORS (α) FOR MONO- AND DIMETHYL NAPHTHALENES

Name of pair[a]	Column number												
	1	2	3	4	5	6	7	8	9	10	11	12	13
1-MN/2-MN	1.14	1.16	1.12	1.08	1.05	1.06	1.09	1.14	1.03	1.06	1.15	1.1	1.1
1,2-DMN/2,3-DMN	1.05	1.07	1.07	1.03	1.06	1.08	1.09	1.07	1.08	1.17	1.22	1.05	1.11
1,2-DMN/2,6-DMN	1.37	1.38	1.31	1.3	1.29	1.23	1.24	1.21	1.24	1.34	1.5	1.3	1.45
1,2-DMN/1,3-DMN	1.22	1.24	1.2	1.22	1.29	1.22	1.22	1.15	1.33	1.2	1.33	1.27	1.19
1,2-DMN/1,4-DMN	1.09	1.08	1.11	1.04	1.13	1.1	1.12	1.14	1.23	1.1	1.16	1.19	1.19
1,2-DMN/1,5-DMN	1.13	1.11	1.06	1.06	1.13	1.09	1.12	1.03	1.15	1.16	1.19	1.15	1.12
1,2-DMN/1,6-DMN	1.23	1.21	1.21	1.14	1.12	1.2	1.21	1.06	1.21	1.13	1.18	1.19	1.22
2,3-DMN/2,6-DMN	1.30	1.29	1.29	1.22	1.22	1.14	1.14	1.13	1.14	1.14	1.23	1.24	1.3
2,3-DMN/1,4-DMN	1.04	1.01	1.08	1.01	1.06	1.01	1.03	1.07	1.13	1.06	1.05	1.13	1.06
1,3-DMN/2,6-DMN	1.13	1.12	1.1	1.07	1.06	1.04	1.01	1.06	1.07	1.06	1.13	1.03	1.21
1,4-DMN/2,6-DMN	1.26	1.28	1.19	1.26	1.14	1.12	1.11	1.06	1.01	1.21	1.30	1.1	1.21
1,5-DMN/2,6-DMN	1.22	1.25	1.25	1.23	1.15	1.13	1.11	1.18	1.07	1.16	1.26	1.14	1.3
1,6-DMN/2,6-DMN	1.12	1.15	1.09	1.15	1.07	1.03	1.03	1.14	1.02	1.18	1.28	1.09	1.19
1,6-DMN/1,3-DMN	1.01	1.02	1.00	1.07	1.01	1.07	1.01	1.08	1.1	1.06	1.13	1.06	1.02
1,5-DMN/1,6-DMN	1.09	1.08	1.15	1.06	1.07	1.08	1.08	1.03	1.05	1.01	1.01	1.04	1.09
1,4-DMN/1,5-DMN	1.03	1.03	1.04	1.02	1.00	1.09	1.0	1.1	1.06	1.04	1.03	1.04	1.06

[a] MN = Methylnaphthalene; DMN = dimethylnaphthalene.

the "*ortho* effect" present in 2,3- and 1,2-DMN, which are retained for longer times on all columns.

The change of position of the dimethyl substituents on the substrate does not have any distinct effect on the separation capacity (Table III, columns 3–5). In similar manner the change from methoxy to ethoxy at position R1, R2 has a negligible effect on (columns 5 and 6, 1 and 2).

An increase in the alkoxy chain length has very little effect on the selectivity, as seen when the results on columns 7 and 8 are compared.

All the columns under investigations have very good pair separations for (1,2- and 2,6-) and (2,3- and 2,6-)DMN. A comparison of the results obtained on columns 10 and 11 shows that the substitution of a chloro group in place of the methyl group on the liquid crystalline moiety influences the selectivity towards the resolution of DMN isomers (Table III, column 13). The behaviour of this column shows that the introduction of the nitro group onto the substrate molecule gives a longer nematic range and a good separation of these positional isomers.

Different pair combinations may be separated on a variety of columns. The choice of column depends on the pair of interest. Pairs which are usually difficult to separate, such as (1,2- and 2,6-), (2,6- and 2,3-)DMN and 1-methyl- and 2-methylnaphthalenes are well resolved on all the columns. Column 1, 2, 10, 12, 13 can separate ten out of the sixteen pair combinations under investigation.

ACKNOWLEDGEMENT

The author gratefully acknowledges help received from Dr. B. V. Bapat, Dr. D. G. Panse and S. M. Likhite during these investigations.

REFERENCES

1 S. Wasik and S. Chesler, *J. Chromatogr.*, 122 (1976) 451.
2 G. M. Janini, K. Johnsten and W. L. Zielinski, Jr., *Anal. Chem.*, 47 (1975) 670.
3 G. M. Janini, J. M. Muschik, J. A. Schroer and W. Zielinski, Jr., *Anal. Chem.*, 48 (1976) 1879.
4 G. M. Janini, J. M. Muschik and W. L. Zielinski, Jr., *Anal. Chem.*, 48 (1976) 809.
5 G. M. Janini, B. Shaikh and W. L. Zielinski, Jr., *J. Chromatogr.*, 132 (1977) 136.
6 L. E. Cook and R. C. Spangeld, *Anal. Chem.*, 46 (1974) 122.
7 Z. Witkiewicz and S. Popiel, *J. Chromatogr.*, 154 (1978) 60.
8 F. Vernon and A. N. Khakoo, *J. Chromatogr.*, 157 (1978) 412.
9 Z. Witkiewicz and A. Waclawczyk, *J. Chromatogr.*, 173 (1979) 42.
10 K. P. Naikwadi, D. G. Panse, B. V. Bapat and B. B. Ghatge, *J. Chromatogr.*, 195 (1980) 309.
11 J. P. Schroeder, in G. W. Gray and P. A. Winsor (Editors), *Liquid Crystals and Plastic Crystals*, Vol. I, Ellis Horwood, Chichester, 1974, p. 361.
12 Z. Witkiewiez, 251 (1982) 311; and references cited therein.
13 Z. Witkiewicz, *J. Chromatogr.*, 466 (1989) 37; and references cited therein.
14 D. G. Panse, A. Bhale, V. K. Gumaste, M. V. Mane, S. M. Likhite and B. V. Bapat, *J. Chromatogr.*, 411 (1987) 456; and references cited therein.
15 N. V. Bhalerao, D. G. Panse, B. V. Bapat and B. B. Ghatge, *Ind. J. Chem.*, 24B (1985) 327.
16 R. V. Vigalok, G. G. Maidatschennko, G. A. Setschasova, R. K. Nasnoullina, T. R. Bankovskaja, N. A. Palikov and M. S. Vigdergauz, *Usp. Gazov Khromatogr.*, 4 (1975) 115.
17 M. S. Vigdergauz and R. V. Vigalok, *Westn. Akad. Akad. Nauk, SSSR*, 10 (1977) 73.
18 K. Tesarik, J. Frycka and S. Ghyczy, *J. Chromatogr.*, 148 (1978) 223.
19 A. Waclawczyk and Z. Witkiewicz, *Binl. Wojsk, Akad. Tech.*, 28, No. 6 (1979) 87.
20 A. Radecki, H. Lamparczyk and R. Kaliszan, *Chromatographia*, 12 (1979) 595.

21 V. Hlozek and H. Gutwillinger, *Chromatographia*, 13 (1980) 234.
22 Z. Suprynowiez, W. M. Buda, M. Mardarowicz and A. Patrykiejew, *J. Chromatogr.*, 333 (1985) 11.
23 T. Kreczmer and A. Gutorska, *Chem. Anal. (Warsaw)*, 30 (1985) 419.
24 G. Chiavari, L. Pastorelli and G. Perrakis, *Talanta*, 33 (1986) 979.
25 D. E. Martire, *J. Chromatogr.*, 406 (1987) 27.
26 R. Fu, L. Tian, G. Z. Liu, *Huwei Sepu*, 5(4) (1987) 203.
27 J. Mazur, Z. Wietkiwicz and R. Dabrowski, *Biul. Wojsk. Akad. Techn.*, 37, No. 9 (1988) 33.
28 V. A. Gerasimenko and V. M. Nobivach, *Zh. Anal. Khim.*, 43 (1988) 109.
29 H. L. Davies, K. D. Bartle, P. T. Williams and A. E. Gorden, *Anal. Chem.*, 60 (1988) 204.
30 W. Püttmann, C. B. Eckhardt and R. G. Schaeffer, *Chromatographia*, 25 (1988) 279.
31 N. Hiroshi, S. Akirsj, K. Masatoshi, Y. Hiroshi and H. Ksoru, *Chem. Lett.*, 5 (1988) 831.
32 K. Sun, Y. He, M. Zhu, R. Tang and G. Li, *Fenxi Huaxue*, 16 (1988) 999.
33 J. F. Schneider, L. A. Repaelian, S. Amrit Boparai, M. C. Hansen, M. D. Erickson, *J. Chromatogr. Sci.*, 27 (1989) 5925.
34 X. Min and F. Bruner, *J. Chromatogr.*, 468 (1989) 365.

Journal of Chromatography, 549 (1991) 429–433
Elsevier Science Publishers B.V., Amsterdam

CHROM. 23 350

Short Communication

Cyclic aryleneazachalcogenenes

IV[a]. Gas chromatographic properties of polyfluorinated 2,1,3-benzoselenadiazoles

VYACHESLAV L. SALENKO, MIKHAIL L. TROSHKOV and ANDREY V. ZIBAREV*
Institute of Organic Chemistry, 630090 Novosibirsk (USSR)
(First received July 31st, 1990; revised manuscript received April 3rd, 1991)

ABSTRACT

Polysubstitution of hydrogen atoms in 2,1,3-benzoselenadiazoles (piaselenoles), used in the determination of selenium by gas chromatography with electron-capture detection (GC–ECD), by fluorine atoms raises the sensitivity of a ^{63}Ni electron-capture detector to substances by more than an order of magnitude, without reducing their high volatility. The corresponding polyfluorinated 1,2-diaminobenzenes react quantitatively with Se(IV) derivatives in aqueous acidic media and the selenadiazoles formed are effectively extracted with 1 ml of toluene from 500 ml of solution. Thus, polyfluorinated 1,2-diaminobenzenes potentially form a new group of analytical reagents for the GC–ECD determination of selenium.

INTRODUCTION

Important biological and medical functions of selenium [2] make the development of new method for its determination, and the improvement of known methods, highly desirable.

For the determination of selenium at the ultra-trace level by gas chromatography with electron-capture detection (GC–ECD) a convenient analyte form is the 2,1,3-benzoselenadiazoles (piaselenoles), obtained by the reaction of Se(IV) with 1,2-diaminobenzenes in acidic media (for a review see ref. 3). In this determination, derivatives with a fluorine atom or trifluoromethyl group have advantages over other compounds owing to the shorter relative retention times (t_R) and lower detection limits [4,5].

The next logical step in this direction is the use of polyfluorinated derivatives. As reported [6], the reaction of selenious acid with 1,2-diamino-3,4,5,6-tetrafluoro-

[a] For part III, see ref. 1.

0021-9673/91/$03.50

benzene leads to 4,5,6,7-tetrafluoro-2,1,3-benzoselenadiazole, which forms a synthetic background for the use of polyfluorinated 2,1,3-benzoselenadiazoles in the GC–ECD determination of selenium. However, neither the GC properties of these compounds nor the efficiency of their extraction from acidic media by organic solvents before injection into the chromatograph have been investigated. In addition, polyfluorinated 2,1,3-benzoselenadiazoles may have advantages over their hydrocarbon analogues owing to the high volatility [7], high electron affinity [8] and hydrophobicity (oleophilicity) [7] inherent in polyfluoroaromatic compounds.

In this work, we carried out comparative studies of the GC properties of 4,5,6,7-tetrafluoro-2,1,3-benzoselenadiazole (**1**) and 6-trifluoromethyl-4,5,7-trifluoro-2,1,3-benzoselenadiazole (**2**) *vs.* 5-trifluoromethyl-2,1,3-benzoselenadiazole (**3**), the most volatile compound among those investigated earlier and having one of the lowest detection limits [3–5]. We also performed a model experiment to detect 10^{-8} g-atom (0.79 μg) of selenium in 500 ml of water using 1,2-diamino-3,4,5,6-tetrafluorobenzene (**4**), a counterpart of compound **1**.

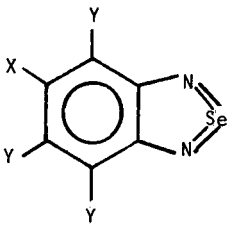

	X	Y
1	F	F
2	CF_3	F
3	CF_3	H

1-3

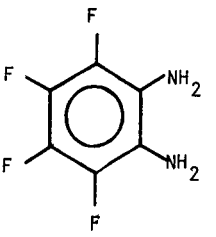

4

EXPERIMENTAL

Instrumentation

The GC measurements were carried out on a Model 3700 chromatograph (a complete copy of the Varian 3700 instrument produced in the USSR under Varian licence), using glass columns (2 m × 3.5 mm I.D.; Institute of Organic Chemistry, Novosibirsk, USSR) packed with SE-30 (5%) on Chromaton N AW DMCS or XE-60 (5%) on Chromaton N AW (LaChema, Czechoslovakia), a ^{63}Ni electron-capture detector and an Interchrom-1 electronic integrator. The injector and detector temperatures were 220°C and the column temperature was 130°C (isothermal). The working gas in the detector and the carrier gas were nitrogen. The carrier gas flow-rate was 50 ml/min. Toluene solutions of 10^{-5}–10^{-6} mol/l concentration were used, with an injection volume of 2 μl.

The ^1H, ^{19}F and ^{77}Se NMR spectra of compound **3** were measured on a Bruker AM-400 spectrometer at 400.134, 376.479 and 76.312 MHz, respectively, as C^2HCl_3 solutions (standards: internal, tetramethylsilane and perfluorobenzene; external, dimethyl selenide). Mass spectra were measured on a Finnigan MAT MS-8200 instrument (electron impact; 70 eV). UV–visible spectra were recorded on a Specord UV–VIS spectrophotometer as ethanol solutions.

Substances

Compounds **1**, **2** and **4** were synthesized and purified according to ref. 1. Compound **3** was obtained by a modified procedure [1] as follows. A solution of 2.21 g (0.01 mol) selenium tetrachloride in 20 ml of monoglyme was added dropwise in an argon atmosphere at 0°C to a stirred suspension of 2.49 g (0.01 mol) of 1,2-diamino-4-trifluoromethylbenzene dihydrochloride and 4.74 g (0.06 mol) of pyridine in 25 ml of monoglyme. Stirring was continued for 0.5 h, the solution was filtered, the solvent distilled off at reduced pressure and the residue recrystallized from hexane and sublimed in vacuum. Compound **3**, colourless crystals, yield 2.13 g (85%), m.p. 90–91°C (lit. [4] m.p., 91°C). Mass spectrum, M^+ (*m/z*, relative intensity), measured (calculated): 251.9422, 100% (251.9413). NMR spectra (δ, ppm): ^1H, 8.03 s, 7.78 d (^3J = 9.5 Hz), 7.46 d (^3J = 9.5 Hz); ^{19}F, 98.19 s; ^{77}Se, 1545 s. UV–VIS spectrum [λ_{max}, nm, (log ε)]: 334 (4.30),238 (3.89).

The purity of all compounds was monitored by GC using ECD and flame ionization detection.

Solutions for model experiment on the detection of selenium in water

A working solution of **4** was prepared by dissolving 0.45 g ($2.5 \cdot 10^{-3}$ mol) in 500 ml of hydrochloric acid.

A stock solution of selenium (IV) was prepared by dissolving 1.1096 g (0.01 mol) of selenium dioxide in 100 ml of distilled water. Working solutions were prepared by appropriate dilution.

Calibration solutions of **1** were obtained by dissolving 0.2550 g ($1 \cdot 10^{-3}$ mol) in 100 ml of toluene with subsequent appropriate dilution.

Model experiment procedure (modified procedure [9])

Aqueous selenium dioxide (500 ml), theoretically containing 0.79 μg ($1 \cdot 10^{-8}$ g-atom) of selenium, and 40 ml of concentrated hydrochloric acid were thoroughly mixed in a separating funnel. The solution was vigorously shaken with 25 ml of toluene until saturation. After phase separation, the aqueous phase was transferred to another separating funnel and 10 ml of the acidic solution of **4** were added. After 2 h, 1 ml of toluene was added and the mixture was vigorously shaken for 5 min. The toluene extract was separated and 2 μl were injected into the chromatograph (XE-60 column). The amount of selenium (IV) was determined by comparing the area of the peak of compound **1** in the chromatogram with that of the calibration solution of **1**. The results was avereged from a series of five repeated measurements.

RESULTS AND DISCUSSION

It has been established earlier that procedures based on piaselenoles and GC–ECD allow selenium determinations at the ultra-trace levels (1–10 ng/l). Selenadiazoles possessing the highest electron affinity (providing the lowest detection limits) contain bromine atoms or a nitro group, which reduce their volatility. On the other hand, more volatile selenadiazoles do not give such low detection limits because of the insufficient sensitivity of the electron-capture detector towards then [3–5].

We have found that the use of polyfluorinated 2,1,3-benzoselenadiazoles **1** and **2** makes it possible to combine high volatility with high electron-capture ability.

TABLE I

GAS CHROMATOGRAPHIC PROPERTIES OF POLYFLUORINATED 2,1,3-BENZOSELENADIAZOLES **1–3** AND POLYFLUORINATED 1,2-DIAMINOBENZENE **4**

Glass packed column, 2 m × 3.5 mm I.D., 130°C.

Compound	SE-30		XE-60	
	t_R	MS^a	t_R	MS^a
1	1.00	11.0	1.92	11.0
2	1.23	11.0	2.77	11.0
3	1.00	1.0	1.00	1.0
4	0.83	0.07	3.36	0.07

[a] Relative standard deviation 10%.

Table I lists t_R values and the molar sensitivity (MS) of the ^{63}Ni electron-capture detector to compounds **1** and **2** measured relative to those of compound **3**. Fig. 1 presents some typical chromatograms.

It follows from Table I that the ECD sensitivity to compounds **1** and **2** exceeds

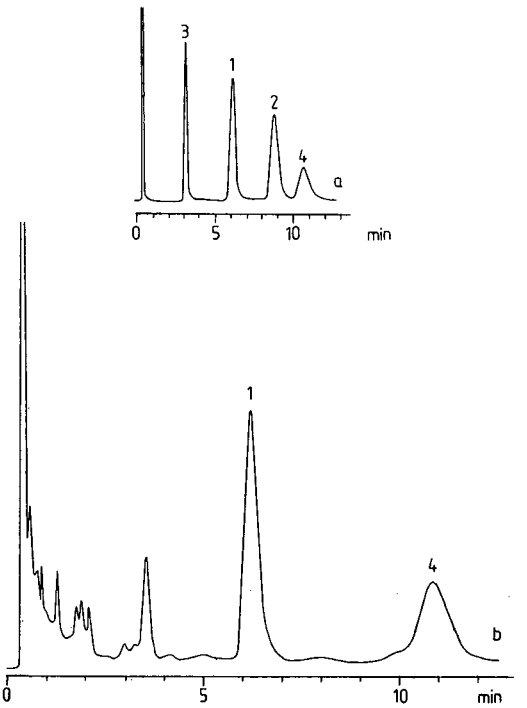

Fig. 1. Typical chromatograms. (a) Chromatogram of the toluene solution of a model mixture of compounds **1–4** (mole ratio 1:1:10:10, respectively); XE-60 column, 130°C. (b) Chromatogram of the toluene extract (1 ml) from aqueous acidic selenium dioxide solution (500 ml of water, 0.79 μg of selenium treated with a hydrochloric acid solution of compound **4**; XE-60 column, 130°C.

to **3** by more than an order of magnitude. On the non-polar SE-30, the t_R values of **1** and **3** are the same, whereas that of **2** slightly exceeds them. On passing to the polar XE-60, the t_R values of **1** and **2** markedly increase, but the overall time of chromatographic analysis at the same column temperature as for SE-30 remains satisfactory (see Fig. 1).

The t_R of **4** on SE-30 is shorter than that of **1**, but on passing to XE-60 this order is reversed (Table I). This creates an additional possibility. Although the *MS* towards **4** is low (Table I), the similarity of the t_R values of **4** and **1** and the use of a large molar excess of a diamine in standard procedures (10^2–10^4 [3–5,9]) hinder the recording of the peak of **1** aganist the background of the preceding peak of **4**. For that reason, the excess of diamine is generally removed from the sample before injecting it into the chromatograph by washing it with an acid [3–5,9]. On the XE-60 column, the excess of diamine **4** does not hinder identification and peak intensity measurement of **1** (Fig. 1), and the washing operation to remove the excess may be omitted from the analytical procedure.

The efficiency of detection of selenium (IV) in aqueous solutions using **4** is also fairly high. In the model experiment, the efficiency of detecting $1 \cdot 10^{-8}$ g-atom (0.79 μg) of selenium in 500 ml of water using **4** at a molar excess of the latter of $5 \cdot 10^3$ was 80% (relative standard derivation = 10%) of the theoretical value (the conditions were not optimized). It should be noted that the real content of selenium (IV) in the model solution was smaller than the theoretical value (thermogravimetric standardization of the stock solution was not carried out; a chromatographic analysis error made it superfluous).

The results obtained suggest that **4** and 1,2-diamino-5-trifluoromethyl-3,4,6-trifluorobenzene (corresponding to **2**) are potential analytical reagents for the GC–ECD determination of selenium. Compound **4** is slightly advantageous, which is associated not so much with its greater volatility as with its greater synthetic availability (see ref. 1 and references cited therein).

REFERENCES

1 A. V. Zibarev and A. O. Miller, *J. Fluorine Chem.*, 50 (1990) 359.
2 A. Wendel (Editor), *Selenium in Biology and Medicine*, Springer, Berlin, 1989.
3 S. Dilli and I. Sutikno, *J. Chromatogr.*, 300 (1984) 265.
4 S. Dilli and I. Sutikno, *J. Chromatogr.*, 298 (1984) 21.
5 A. F. Al-Attar and G. Nickless, *J. Chromatogr.*, 440 (1988) 333.
6 J. Fajer, B. H. J. Bielski and R. H. Felton, *J. Phys. Chem.*, 72 (1968) 1281.
7 N. Ishikawa, in N. Ishikawa (Editor), *Novoe v Tekhnologii Soedinenii Ftora*, Mir, Moscow, 1984, pp. 11–14. (Russian translation).
8 P. Kebarle and S. Chowdhuri, *Chem. Rev.*, 87 (1987) 513.
9 Y. Shimoishi and K. Toei, *Anal. Chim. Acta*, 100 (1987) 65.

Journal of Chromatography, 549 (1991) 434–439
Elsevier Science Publishers B.V., Amsterdam

CHROM. 23 329

Short Communication

Application of a metal capillary column in gas chromatographic determination of catechol-O-methyltransferase activity

SEISHU KOH, KOJI URAYAMA and SATOSHI KAWAI*
Gifu Pharmaceutical University, Mitahora, Gifu 502 (Japan)
and
YUZI TAKAYAMA
Department of Materials Science, Toyohashi University of Technology, Tempaku, Toyohashi 440 (Japan)
(First received October 22nd, 1990; revised manuscript received March 22nd, 1991)

ABSTRACT

The utility of a deactivated metal capillary column, Rascot, in the measurement of an enzymatic reaction, in this case measurement of rat catechol-O-methyltransferase activity, was examined. 3,4-Dihydroxybenzaldehyde, 3,4-dihydroxybenzylalcohol and 3,4-dihydroxybenzoic acid were used as substrates and the *m*- and *p*-O-methylated products were separated by using Rascot after derivatization. The peaks on the chromatograms were symmetrical. The data obtained were compared with those reported in previously published papers. Good agreement with previous results proved that Rascot is able to withstand practical use in biological materials.

INTRODUCTION

Capillary gas chromatography (GC) has a long history. The first metal capillary columns were very far from being of practical use, because of strong adsorption of solutes, especially polar ones.

Recently, we have published some papers on the use of a deactivated metal capillary column, Rascot, which has been shown to be of much practical use [1–5].

GC [6,7] and high-performance liquid chromatographic [8–12] techniques have been developed as reliable procedures for the measurement of catechol-O-methyltransferase (COMT) activity. The present paper describes the assay of COMT activity using the following three compounds as substrates: 3,4-dihydroxybenzaldehyde (DHBAd), 3,4-dihydroxybenzylalcohol (DHBAl) and 3,4-dihydroxybenzoic acid (DHBAc). The utility of Rascot was examined by separating the *m*- and *p*-O-methylated products.

0021-9673/91/$03.50

EXPERIMENTAL

Materials

S-Adenosyl-L-methionine (SAM) hydrogen sulphate was purchased from Boehringer (Mannheim, Germany). Vanillyl alcohol, vanillin, isovanillin, isovanillic acid, *p*-diiodobenzene and homovanillic acid were obtained from Tokyo Kasei Kogyo (Tokyo, Japan), vanillic acid from Sigma (St. Louis, MO, USA) and isovanillyl alcohol from Aldrich (Milwaukee, WI, USA). DHBAd and DHBAc were obtained from Wako Junyaku Kogyo (Osaka, Japan) and DHBAl was synthesized. All other reagents were of analytical grade and purchased from commercial sources.

Preparation of DHBAl

DHBAl was synthesized by the reduction of DHBAd. A 0.3-g sample of palladium–carbon was put in a flask, and 30 ml of methanol were slowly added to it. To the solution mixture were added 0.3 g of DHBAd, which was reduced on the palladium–carbon with hydrogen. The reaction mixture was filtered and the filtrate was evaporated to dryness. The residue was recrystallized from 2 ml of benzene containing three drops of ethyl acetate. m.p. 134–135°C (reported 136°C). Elemental analysis for $C_7H_3O_3$: calculated, C 59.77%, H 5.79%; found, C 59.64%, H 5.77%.

Enzyme preparation

Adult Wistar rats (150–200 g) of either sex were decapitated and their livers were homogenized in four volumes of 50 m*M* phosphate buffer (pH 7.5). The homogenate was centrifuged at 100 000 *g* for 30 min at 4°C. The supernatant solution was used as a crude source of COMT to study the ratio of *m*-/*p*-methylation. Protein determinations were made by the method of Lowry *et al.* [13] with bovine serum albumin as a standard.

Apparatus and GC conditions

A gas chromatograph (Type 103C, Okura Riken) was furnished with a flame ionization detector and an on-column processor (Nippon Chromato, Tokyo, Japan; an instrument having an injector and a precolumn which is capable of rapid heating independently from the GC column oven) [1,14]. A precolumn, RAS 80 (an uncoated deactivated metal tube, 100 cm × 0.8 mm I.D.), was connected to an analytical capillary column, Rascot OV-1 (a deactivated metal column coated with OV-1, 25 m × 0.25 mm I.D., film thickness 0.4 μm, Nippon Chromato), with a metal connector.

A 5-μl aliquot of the sample solution was taken in a microsyringe with a long needle (15 cm × 0.5 mm O.D.). After the sample solution was slowly introduced into the precolumn, which was kept at room temperature, the precolumn was rapidly heated to about 150°C by a flash heater [1,14]. Next, the column oven temperature was raised from 60°C to 150°C at a rate of 4°C/min.

Assay of COMT

Procedure 1 (substrate DHBAd). The standard incubation mixture consisted of following components in a total volume of 1.0 ml in 50 m*M* phosphate buffer (pH 7.2): 2 m*M* substrate, 1 m*M* SAM, 5 m*M* magnesium chloride and 2 mg of enzyme protein. The mixture was incubated for 1 h. Incubation was stopped by adding 0.1 ml

of 1 *M* hydrochloric acid. The incubation mixture was extracted with 4 ml of chloroform containing *p*-diiodobenzene (internal standard, I.S.) under saturated sodium chloride. The extract was evaporated using a rotary evaporator. Three drops of ethyl acetate and 0.2 ml of trifluoroacetic anhydride (TFAA) were added to the residue and the derivatization was performed in a water bath at 60° for 15 min. A 5-μl aliquot of the mixture was determined by GC. Blanks were prepared by omitting SAM or the substrate.

Procedure 2 (substrate DHBAl). The standard incubation mixture consisted of the same components except in phosphate buffer (pH 7.6) and 1 m*M* substrate, and incubation and derivatization were performed in the same manner as in procedure 1.

Procedure 3 (substrate DHBAc). The standard incubation mixture and incubation conditions were the same as in procedure 1. Incubation was stopped by adding 0.1 ml of 1 *M* hydrochloric acid. The incubation mixture was extracted with 4 ml of chloroform containing homovanillic acid (I.S.) under saturated sodium chloride. The extract was evaporated using a rotary evaporator. To the residue, 0.1 ml of ethyl acetate and 0.2 ml of diazomethane in diethyl ether were added and the solution was allowed to stand in iced water for 10 min. After evaporating again, 0.1 ml of ethyl acetate and 0.2 ml of TFAA were added to the residue and the solution was allowed to stand at room temperature for 30 min. A 5-μl aliquot of the solution was injected into the gas chromatograph.

RESULTS AND DISCUSSION

At present, fused-silica columns are exclusively used for capillary GC owing to their inert surface and flexibility. Metal capillary columns seem to have been abandoned mainly because of the strong adsorption of solutes on the first metal capillaries. However, the problem of the brittleness of fused-silica capillaries still awaits solution. Although they are flexible, we often find that breakage occurs during handling. After a long time of use, especially at high temperature, the material becomes brittle, because the outer protective polyimide coating is easily damaged and cannot withstand high temperature. Recently, an excellent technique of deactivating the inner surface of metal capillaries was developed by Takayama, and a deactivated metal capillary column named Rascot has been put on the market by Nippon Chromato. We previously reported an excellent separation of a polarity mixture containing 2,3-butanediol, *n*-butyric acid, 2,6-xylenol, 2,6-xylidine, 1-decanol and some alkanes using this Rascot [2] and confirmed its inertness. In the present study we wanted to demonstrate the usefulness of Rascot in the determination of compounds in biological samples as well as pure standard compounds, and the measurement of rat COMT activity was selected as a typical example. In order to decrease the polarity and increase the volatility of the O-methylated products obtained from incubation with the substrate and COMT according to the procedures described, the derivatizations were performed prior to injection into the gas chromatograph. Three typical separations of the derivatives are illustrated in Fig. 1. Rascot was chemically and physically inert. The peaks on the chromatograms were symmetrical, without tailing or leading, and there were no interfering components. In the blanks no O-methylated products were formed.

The metal capillary column was mechanically though and very easy to handle

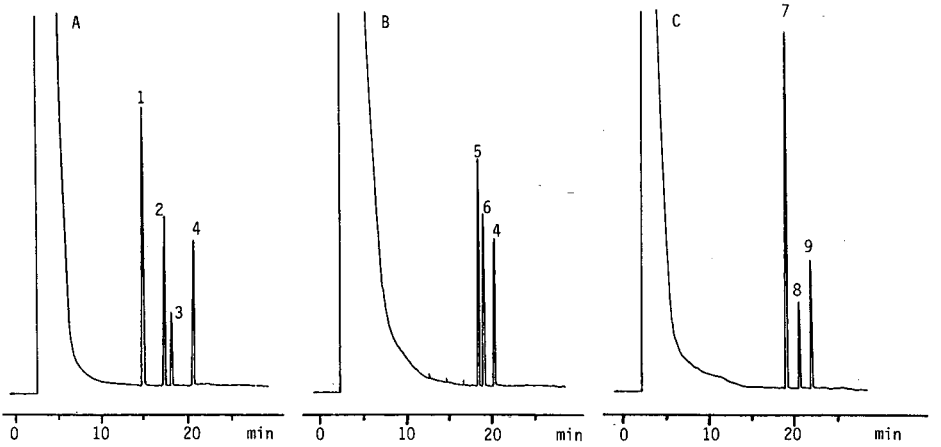

Fig. 1. Typical separation of O-methylated products obtained from incubation with three different substrates and COMT through their derivatives according to the procedures described. Substrates: A, DHBAd; B, DHBAl; C, DHBAc. Peaks: 1 = DHBAd; 2 = vanillin-TFA; 3 = isovanillin-TFA; 4 = *p*-diiodobenzene (I.S.); 5 = vanillyl alcohol-TFA; 6 = isovanillyl alcohol-TFA; 7 = vanillic acid-CH_3-TFA; 8 = isovanillic acid-CH_3-TFA; 9 = homovanillic acid-CH_3-TFA (I.S.): TFA = trifluoroacetate; CH_3-TFA = methyl ester-trifluoroacetate. For GC conditions, see Experimental section.

without breakage in small oven. In addition, the durability of its inertness was superior to that of fused-silica capillaries and it had the advantage of being usable for a very long time. Furthermore, a special sampling technique, "on-column processor", has also been developed by Takayama and Sumiya [14]. When a large sample volume is injected, this technique makes the injection easy and prevents degradation of the stationary phase. Use of the uncoated precolumn results in sharp peaks because of the solvent effect on the head of the analytical capillaries or the cold-trapping effect after the solvent has gone [15].

Chloroform was a suitable extraction solvent against substrates and for products. The recoveries from solutions containing of 100 nmol/ml of each compound were 93.2% for vanillin, 98.0% for isovanillin, 95.4% for vanillyl alcohol, 76.2% for isovanillyl alcohol, 100.0% for vanillic acid and 100.4% for isovanillic acid.

Methylation of vanillic acid and isovanillic acid was carried out in iced water for 10 min, where O-methylation of the phenolic hydroxyl group was not observed. Trifluoroacetylation of the products (vanillin, isovanillin, vanillyl alcohol and isovanillyl alcohol) was achieved by heating at 60°C for 15 min, while the derivatization of methyl esters of vanillic acid and isovanillic acid with TFAA proceeded completely at room temperature for 30 min.

The calibration graphs which were prepared from ratios of peak height of the I.S. were linear in the range from 10 to 150 nmol/ml vanillin (the correlation coefficient was 0.999), isovanillin (0.999), vanillyl alcohol (0.994), isovanillyl alcohol (0.992), vanillic acid (0.998) and isovanillic acid (0.998) in their reaction mixtures, and the detection limits at a signal-to-noise ratio of 2 were about 4 nmol/ml. The mean relative standard deviations for replicate assays (n = 5) using an identical parent solution spiked with 50 nmol/ml of each component were from 2.8% to 5.4%.

TABLE I

KINETIC PARAMETERS OBTAINED WITH THE THREE SUBSTRATES

Substrate	*Meta*/*para* ratio at pH 7.2	K_m (m*M*)	V_{max} (nmol/mg protein/min)
DHBAd	2.38	*Meta* 0.21	0.74
		Para 0.30	0.37
DHBAl	1.29	*Meta* 0.12	1.00
		Para 0.09	0.74
DHBAc	4.50	*Meta* 0.57	8.34
		Para 0.40	1.39

The kinetic parameters of rat liver COMT were measured by this GC method and the results are shown in Table I.

It is now clear that the *in vitro meta*/*para* ratio depends on a variety of factors, including pH in the incubation solution and the nature of substituent on the catechol ring [6,8].

In order to confirm the influence of the side-chain on the *meta*/*para* ratio, we used the three different substrates, DHBAd, DHBAl and DHBAc, which have characteristic properties on their side group and their *m*- and *p*-O-methylated products are easily be derivatized for GC.

The apparent Michaelis–Menten coefficients (K_M) were approximately $2.1 \cdot 10^{-4}$ *M* for vanilline, $3.0 \cdot 10^{-4}$ *M* for isovanillie, $1.2 \cdot 10^{-4}$ *M* for vanillyl alcohol, $8.6 \cdot 10^{-5}$ *M* for isovanillyl alcohol, $5.7 \cdot 10^{-4}$ *M* for vanillic acid and $4.0 \cdot 10^{-4}$ *M* for isovanillic acid.

The ratio of *meta* in *para* of the methylated products using the three different substrates was also calculated at pH 7.2, and the results are shown with the K_M values and V_{max} values in Table I. The K_M values for DHBAl were the lowest of the three, while those for DHBAc were higher and their V_{max} values were also higher.

Several studies dealing with the ratio of *m*/*p*O-methylation from rat liver COMT have been presented [6,8]. Creveling *et al.* [6] have reported that *p*-methylation is not favored by the presence of either a cationic or an anionic substituent, while neutral substituents favor a lower *meta*/*para* ratio. The *meta*/*para* ratio of O-methylatan of DHBAc was 4.5 at pH 7.2 and 6.0 at pH 8, which was in good agreement with the value (5.5) obtained at pH 8.0 by Creveling *et al.* [6] and was similar to that (4.6) obtained at pH 7.9 by Pennings and Van Kempen [8], and the ratios for DHBAd (2.38) and DHBAl (1.29) were lower and were also close to those (2.1 and 2.0, respectively) reported by Creveling *et al.* [6]. The good agreement between these results proves that Rascot is able to stand practical use in biological materials.

As far as we are aware, there have been only two papers [6,7] on GC for the assay of COMT activity. GC seems to be one of the most useful methods with regard to determination of *m* and *p* isomers. We have also proposed a simple and specific GC method for the measurement of rat COMT activity. A metal capillary column has been applied for the first time to the study of an enzymatic reaction.

REFERENCES

1 Y. Takayama, E. Sumiya and S. Kawai, *J. High Resolut. Chromatogr. Chromatogr. Commun.*, 10 (1987) 201.
2 Y. Takayama, T. Takeichi and S. Kawai, *J. High Resolut. Chromatogr. Chromatogr. Commun.*, 11 (1988) 732.
3 Y. Takayama, T. Takeichi and S. Kawai, *J. Chromatogr.*, 464 (1989) 172.
4 S. Kawai, R. Nishioka, M. Nakahigashi, K. Kondo and Y. Takayama, *Anal. Sci.*, 5 (1989) 301.
5 Y. Takayama, T. Takeichi, S. Kawai and M. Morikawa, *J. Chromatogr.*, 514 (1990) 259.
6 C. R. Creveling, N. Morris, H. Shimizu, H. H. Ong and J. W. Daly, *Mol. Pharmacol.*, 8 (1972) 398.
7 R.-L. Lin and N. Narasimhachari, *Anal. Biochem.*, 57 (1974) 46.
8 E. J. M. Pennings and G. M. J. Van Kempen, *Anal. Biochem.*, 98 (1979) 452.
9 S. Koh, M. Arai and S. Kawai, *J. Chromatogr.*, 226 (1981) 461.
10 T. Ishimitsu and S. Hirose, *Anal. Biochem.*, 150 (1985) 300.
11 E. Nissinen and P. Manisto, *Anal. Biochem.*, 137 (1984) 69.
12 H. Nohta, S. Noma and Y. Ohkura, *Chem. Pharm. Bull.*, 34 (1986) 4693.
13 O. H. Lowry, N. J. Rosebrough, A. L. Farr and R. J. Randal, *J. Biol. Chem.*, 193 (1951) 265.
14 Y. Takayama and E. Sumiya, *J. High Resolut. Chromatogr. Chromatogr. Commun.*, 9 (1986) 747.
15 Y. Takayama, T. Yamaguchi and S. Kawai, *Bunseki kagaku*, 36 (1987) 761.

Journal of Chromatography, 549 (1991) 440–445
Elsevier Science Publishers B.V., Amsterdam

CHROM. 23 309

Short Communication

Gas chromatography of some polymethoxylated flavones and their determination in orange peel oils

EMILE M. GAYDOU*, TAHAR BERAHIA, JEAN-CLAUDE WALLET and JEAN-PIERRE BIANCHINI

Laboratoire de Phytochimie de Marseille, Faculté des Sciences et Techniques de Saint Jérôme, Avenue Escadrille Normandie Niemen, 13397 Marseille Cédex 13 (France)

(First received January 7th, 1991; revised manuscript received March 13th, 1991)

ABSTRACT

Separation of 27 polymethoxylated flavones (PMFs) was achieved using gas chromatography with a capillary column coated with OV-1. The procedure was applied to the separation and determination of the most important PMFs contained in three samples of industrial orange peel oils. The relative contents of sinensetin, nobiletin and heptamethoxyflavone range from 19 to 30%, showing that these three PMFs are characteristic of orange peel oils. Tetra-O-methylscutellarein, tangeretin and 3,5,6,7,3′,4′-hexametoxyflavone are less abundant in all three samples.

INTRODUCTION

Polymethoxylated flavones (PMFs) constitute a special group of flavones (phenylbenzo-γ-pyrones) which are widely distributed in the vegetable kingdom. PMFs, sometimes found in certain *Citrus* species [1,2], have pharmacodynamic properties, *e.g.*, sinesetin and nobiletin, which are effective in decreasing erythocyte aggregation and sedimentation in human blood [3]. As PMF determination has also been used in chemotaxonomic studies [4,5], for the detection of *Citrus* juice adulterations [6], to ascertain the geographical origin of industrial peel oils [7] and for dietary control in clinical experiments [3], various chromatographic techniques have been investigated.

Thin-layer chromatography [8] has been rapidly supplanted by normal- [7–9] and reversed-phase high-performance liquid chromatography (HPLC) using a single-channel UV detector [6,10], a UV diode-array detector [11,12] or combined UV and fluorescence stop-flow scanning [13,14]. Few reports have been published on the gas chromatography (GC) of flavones [15–17] or trimethylsilyl ethers of flavonoids [18]. In the work cited, using packed columns of Chromosorb W coated with SE-30 [16–18] or OV-17 [17], only a partial separation of various PMFs was achieved.

0021-9673/91/$03.50

The purpose of this paper is to report the resolution of 27 PMFs by GC using a capillary column coated with an apolar phase such as OV-1. This method was applied to the quantitative analysis of three samples of industrial peel oil.

EXPERIMENTAL

Materials

Mono-, di-, tri- and tetramethoxyflavones were synthesized as described previously, using a modified Baker–Venkataraman procedure [19–20]. Products **23** (tangeretin), **24** (sinensetin), **25** (nobiletin), **26** (3,5,6,7,3′,4′-hexamethoxyflavone) and **27** (3,5,6,7,8,3′,4′-heptamethoxyflavone) were obtained from orange peel oil using preparative thin-layer chromatography according to the procedure reported by Tatum and co-workers [4,21].

All products were identified by comparison with published data (R_F, UV or m.p.) and by ^{1}H nuclear magnetic resonance spectrometry.

Chromatographic conditions

For the separation of PMFs, a Delsi 30 gas chromatograph (Delsi-Nermag) equipped with a glass injector and a fused-silica capillary column (50 m × 0.32 mm I.D.) coated with OV-1 (A.M.L.-Chromato) (0.15 μm phase thickness) was used at 280°C with a flame ionization detector. The detector and injector temperatures were set at 300°C. Hydrogen was used as the carrier gas (inlet pressure, 0.5 bar).

Peak identification of PMF

Mixtures of two to five PMFs, depending on their ease of separation, were prepared in ethyl acetate; each PMF was present in at least four mixtures. For simple identification, components were mixed in different proportions. Retention times were determined for each PMF and relative retention times (RRT) were expressed relative to flavone (**1**).

Application to quantitative analysis of industrial orange peel oils

Samples of various origin (Brazil, Israel, Morocco) were diluted in ethyl acetate. For the determination of PMFs in the oils, 5-methoxyflavone (**3**) was used as an internal standard. Mixed standard solutions of PMF and 5-methoxyflavone were chromatographed and response factors expressed relative to the standard. The results obtained for PMFs **22–27** were found to be the same.

RESULTS AND DISCUSSION

Gas chromatographic separation of synthetic flavone mixtures

The various flavones investigated are listed in Table I. They are composed of flavone, seven monomethoxyflavones, seven dimethoxyflavones, six trimethoxyflavones, one tetramethoxyflavone, two pentamethoxyflavones, two hexamethoxyflavones and one heptamethoxyflavone. Fig. 1 shows the chromatogram obtained using a silica capillary column coated with OV-1 for most of these compounds. Relative retention times for the 27 compounds investigated are given in Table I. On this apolar phase, the order of emergence of the PMFs varies not only with the number of the

TABLE I

GAS CHROMATOGRAPHIC SEPARATION OF POLYMETHOXYLATED FLAVONES

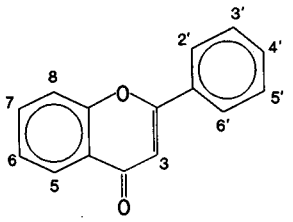

Flavone No.	Substituent									RRT[a]
	3	5	6	7	8	2'	3'	4'	5'	
1	H	H	H	H	H	H	H	H	H	1.00
2	OCH_3	H	H	H	H	H	H	H	H	1.09
3	H	OCH_3	H	H	H	H	H	H	H	4.43
4	H	H	OCH_3	H	H	H	H	H	H	1.77
5	H	H	H	OCH_3	H	H	H	H	H	2.03
6	H	H	H	H	H	OCH_3	H	H	H	1.54
7	H	H	H	H	H	H	OCH_3	H	H	1.77
8	H	H	H	H	H	H	H	OCH_3	H	2.08
9	H	H	H	OCH_3	H	OCH_3	H	H	H	3.01
10	H	H	H	H	H	OCH_3	OCH_3	H	H	2.08
11	H	H	H	H	H	OCH_3	H	OCH_3	H	3.01
12	H	OCH_3	H	H	H	H	H	OCH_3	H	3.65
13	H	H	H	OCH_3	H	H	H	OCH_3	H	4.11
14	H	H	H	H	H	H	OCH_3	OCH_3	H	3.13
15	H	OCH_3	H	OCH_3	H	H	H	H	H	3.39
16	OCH_3	OCH_3	H	OCH_3	H	H	H	H	H	3.54
17	H	OCH_3	H	H	H	H	OCH_3	OCH_3	H	5.51
18	H	H	OCH_3	H	H	OCH_3	OCH_3	H	H	3.70
19	H	H	H	OCH_3	OHC_3	H	H	OCH_3	H	5.36
20	H	H	H	H	H	OCH_3	OCH_3	OCH_3	H	3.17
21	H	H	H	H	H	H	OCH_3	OCH_3	OCH_3	4.06
22	H	OCH_3	OHC_3	OCH_3	H	H	H	OCH_3	H	7.91
23	H	OCH_3	OCH_3	OCH_3	OCH_3	H	H	OCH_3	H	8.25
24	H	OCH_3	OCH_3	OCH_3	H	H	OCH_3	OCH_3	H	8.07
25	H	OCH_3	OHC_3	OCH_3	OCH_3	H	OCH_3	OCH_3	H	12.2
26	OCH_3	OCH_3	OCH_3	OCH_3	H	H	OCH_3	OCH_3	H	11.7
27	OCH_3	OCH_3	OCH_3	OCH_3	OCH_3	H	OCH_3	OCH_3	H	11.9

[a] Determined using a fused-silica capillary column (50 m × 0.32 mm I.D.) coated with OV-1 (0.15 μm film thickness) at 280°C with hydrogen as carrier gas. Relative retention time (RRT) expressed relative to flavone (**1**).

methoxy groups but also with the substituent positions on the flavonic skeleton. For the monomethoxyflavones, substitution at positions 5, 7 and 4' greatly increased the RRT (4.43, 2.03 and 2.08, respectively). Substitution at position 2 and 2' affected the RRT only slightly. Some di- and trimethoxylated flavones have a smaller RRT than 5-methoxyflavone, particularly with 5,7-dimethoxy- and 3,5,7-trimethoxyflavones (3.39 and 3.54, respectively, *vs.* 4.43).

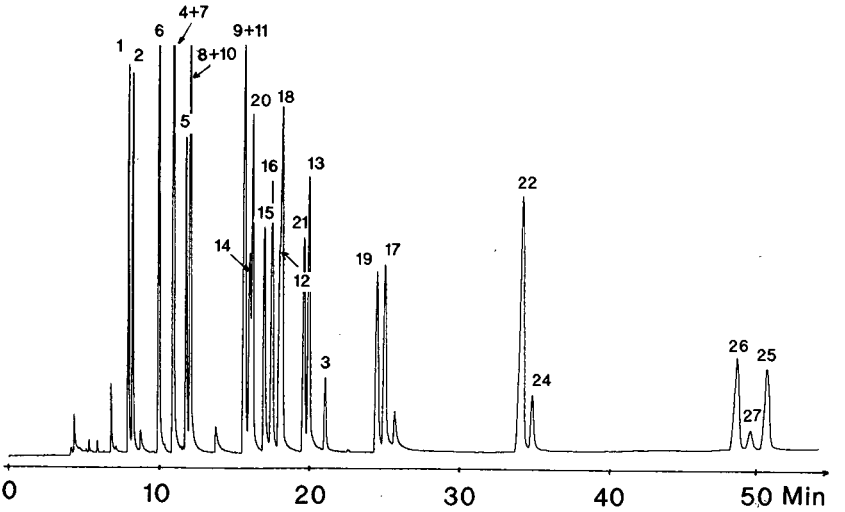

Fig. 1. Gas chromatogram of various PMFs (see Table I for peak identification) using a fused-silica capillary column (50 m × 0.32 mm I.D.) coated with OV-1 (0.15 μm film thickness) at 280°C with hydrogen as carrier gas.

The good separations obtained for such a complex mixture of compounds suggested that GC would be a usefull tool for the determination of PMFs in natural mixtures.

Determination of PMF in industrial orange peel oils

Relative percentages of PMFs were determined for three samples of industrial orange peel oils from Brazil, Israel and Morocco. As shown in Fig. 2, six PMFs were identified in the Israeli oil. These six PMFs were found in all the oils and the results obtained are given in Table II. It can be seen that **25** (nobiletin) is the major compo-

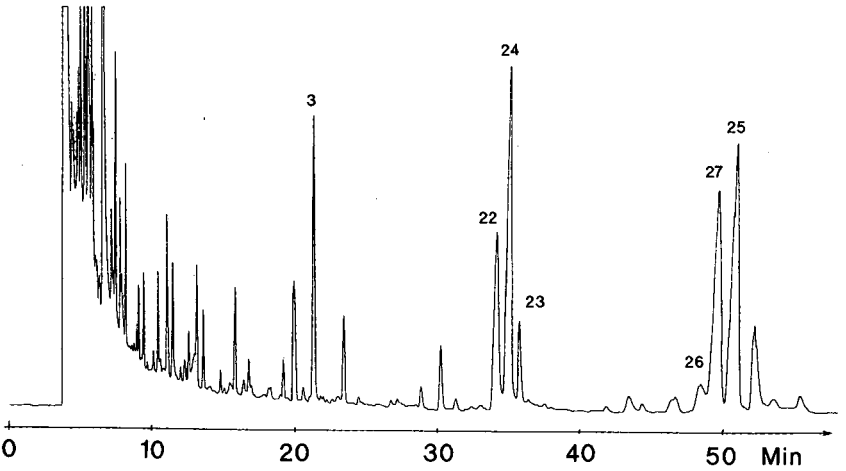

Fig. 2. Gas chromatogram of industrial orange peel oil from Israel. For peak identification of various PMFs see Table I. Experimental conditions as in Fig. 1.

TABLE II

DETERMINATION OF PMF IN INDUSTRIAL ORANGE PEEL OILS

Determined by GC with 5-methoxyflavone as internal standard.

Flavone No.	RRT[a]	Name	Industrial peel oil					
			Brazil		Israel		Morocco	
			PMF (%)[b]	C[c]	PMF (%)	C	PMF (%)	C
22	1.73	Tetra-O-methyl-scutellarein	10.6	0.62	13.2	0.46	12.0	0.35
24	1.77	Sinensetin	30.5	1.78	23.9	0.83	20.4	0.60
23	1.82	Tangeretin	10.0	0.58	4.5	0.16	7.0	0.22
26	2.55	3,5,6,7,3′,4′-Hexamethoxyflavone	3.3	0.19	3.8	0.13	2.9	0.09
27	2.61	Heptamethoxyflavone	19.3	1.13	25.4	0.88	27.4	0.80
25	2.70	Nobiletin	26.4	1.54	29.2	1.02	30.4	0.89

[a] Retention time relative to 5-methoxyflavone (**3**).
[b] Relative percentage of PMF.
[c] Amount found in industrial oils (g l^{-1}).

nent of the Israeli and Moroccan samples. For the Brazilian sample, the content of **24** (sinesetin) is slightly higher than that of nobiletin (30.5% *vs.* 26.4%. The contents of sinensetin, nobiletin and heptamethoxyflavone range from 19.3 to 30.5%, showing that these three PMFs are characteristic of orange peel oils. These results are in good agreement with previous determinations either in orange peel oils [4,7,14] or in orange juice [8,11], since it is well known that the PMF pattern is almost identical in the peel and in the juice [13]. PMFs **22** (tetra-O-methylscutellarein), **23** (tangeretin) and **26** (3,5,6,7,3′,4′-hexamethoxyflavone) are less abundant in all three samples.

By using compound **3** (5-methoxyflavone) as an internal standard, it was possible to determine the PMF concentrations and the results obtained are given in Table II.

The total flavone contents (2.95–5.84 g l^{-1}) differ considerably for these samples. The results are in the same range as those determined for similar samples using HPLC [5,9].

CONCLUSION

The GC separation of 27 PMFs using a capillary column coated with OV-1 was achieved, demonstrating the possibility of using this technique for the determination of PMFs in natural mixtures. This procedure, applied to the separation and determination of the most important PMFs in *Citrus* fruits, offers an alternative to the existing HPLC techniques and can be automated in pharmaceutical or clinical laboratories.

ACKNOWLEDGEMENT

We are grateful to J. C. Lesage, Orangina Vitrolles, for providing orange peel oil samples.

REFERENCES

1 L. J. Swift, *J. Agric. Food Chem.*, 15 (1967) 99.
2 J. F. Kefford and B. V. Chandler, *The Chemical Constituents of Citrus Fruits*, Academic Press., New York, 1970.
3 R. C. Robbins, *Int. J. Vitam. Nutr. Res.*, 46 (1976) 338.
4 J. H. Tatum, C. J. Hearn and R. E. Berry, *J. Am. Soc. Hort. Sci.*, 103 (1978) 492.
5 E. M. Gaydou, J. P. Bianchini and R. P. Randriamiharisoa, *J. Agric. Food Chem.*, 35 (1987) 525.
6 S. V. Ting, R. L. Rouseff, M. H. Dougherty and J. A. Attaway, *J. Food Sci.*, 44 (1979) 69.
7 J. P. Bianchini and E. M. Gaydou, *J. Chromatogr.*, 190 (1980) 233.
8 M. K. Veldhuis, L. J. Swift and W. C. Scott, *J. Agric. Food Chem.*, 18 (1970) 590.
9 J. P. Bianchini and E. M. Gaydou, *J. Chromatogr.*, 211 (1981) 61.
10 J. P. Bianchini, E. M. Gaydou, A. Siouffi, G. Mazerolles, D. Mathieu and R. Phan Tan Luu, *Chromatographia*, 23 (1987) 15.
11 J. M. Sendra, J. L. Navarro and L. Izquierdo, *J. Chromatogr. Sci.*, 26 (1988) 443.
12 B. Heimhuber, R. Galensa and K. Herrmann, *J. Chromatogr.*, 439 (1988) 481.
13 R. L. Rouseff and S. V. Ting, in G. Charalambous (Editor), *Liquid Chromatographic Analysis of Food and Beverages*, Vol. 2, Academic Press, New York, 1979, p. 537.
14 R. L. Rouseff and S. V. Ting, *J. Chromatogr.*, 176 (1979) 75.
15 T. Katagi, A. Horii, Y. Omura, H. Miyakawa, T. Kyu, Y. Ikeda, K. Isoi and M. Makita, *J. Chromatogr.*, 79 (1973) 45.
16 N. Narasimhachari and E. Rudloff, *Can. J. Chem.*, 40 (1962) 1123.
17 M. Munekazu, S. Matsuura, K. Kurogochi and T. Tanaka, *Chem. Pharm. Bull.*, 28 (1980) 717.
18 T. Furuya, *J. Chromatogr.*, 19 (1965) 607.
19 E. M. Gaydou and J. P. Bianchini, *Ann. Chim. (France)*, 2 (1977) 303.
20 E. M. Gaydou and J. P. Bianchini, *Bull. Soc. Chim. Fr.*, II (1978) 43.
21 J. H. Tatum and R. E. Berry, *Phytochemistry*, 11 (1972) 2283.

Journal of Chromatography, 549 (1991) 446–451
Elsevier Science Publishers B.V., Amsterdam

CHROM. 23 351

Short Communication

Capillary zone electrophoresis with a linear, non-cross-linked polyacrylamide gel: separation of proteins according to molecular mass

ALEXANDRA WIDHALM and CHRISTINE SCHWER
Institute for Analytical Chemistry, University of Vienna, Währingerstrasse 38, A-1090 Vienna (Austria)
DIETER BLAAS
Institute for Biochemistry, Faculty of Medicine, University of Vienna, Währingerstrasse 17, A-1090 Vienna (Austria)
and
ERNST KENNDLER*
Institute for Analytical Chemistry, University of Vienna, Währingerstrasse 38, A-1090 Vienna (Austria)
(First received January 25th, 1991; revised manuscript received April 4th, 1991)

ABSTRACT

The separation of proteins according to their molecular masses using capillary zone electrophoresis was demonstrated in a buffer containing a linear, non-cross-linked polyacrylamide gel as a sieving medium. The four test proteins, covering a molecular mass range of between 17 800 and 77 000, were applied as sodium dodecyl sulphate (SDS) complexes. The separation was carried out at pH 5.5 (phosphate buffer, 0.5% SDS, 10% liquid, linear polyacrylamide gel). The retention times of the proteins correlated with the logarithm of their molecular masses.

INTRODUCTION

The use of polyacrylamide gels in capillary zone electrophoresis (CZE) was first described by Hjertén [1]. Karger and co-workers [2,3] introduced this method mainly for the separation of oligonucleotides. Only a few results have been reported for the separation of proteins [2,4], and in all these instances an immobilized, cross-linked gel was used.

The use of linear, non-cross-linked polyacrylamide gels in CZE has been reported for the separation of polynucleotides [5]. These analytes (and also the subunits of serum albumin) have also been separated using other linear polymers such as methylcellulose or polyethylene glycol as additives to the buffer solutions [6]. In contrast, for

0021-9673/91/$03.50

the separation of proteins, liquid, linear polyacrylamide has been reported so far only for classical zone electrophoresis, which was carried out with agar-agar [7,8], cellulose acetate [9], or glass beads as stabilizers [10].

In contrast to the cross-linked gel, linear polyacrylamide offers a number of advantages. These include the following: the preparation of the capillary system, containing the linear gel, is very simple, which is not the case for the cross-linked gel; the capillary can easily be emptied and refilled; the gel–buffer system can be replaced after each run, which leads to a great flexibility with respect to the application of different gels or buffers; the column is insensitive to sample components contaminating the separation system; and all types of capillaries from commercial equipment can be used.

In this paper, the applicability of linear, non-cross-linked polyacrylamide gels for the separation of proteins according to their molecular mass is demonstrated.

EXPERIMENTAL

Chemicals

The chemicals and reagents used were of the following qualities: sodium hydroxide and phosphoric acid, analytical-reagent grade (E. Merck, Darmstadt, Germany); sodium dodecyl sulphate (SDS), *N,N,N',N'*-tetramethylethylenediamine (TEMED) and ammonium persulphate, analytical-reagent grade (Serva, Heidelberg, Germany); acrylamide, research grade (doubly crystallyzed, Serva); egg albumin, research grade (five times recrystallyzed, Serva); myoglobin and conalbumin, research grade (lyophilyzed, Serva); and bovine serum albumin, analytical-reagent grade (Serva).

The water used was doubly distilled from a quartz apparatus before use.

Apparatus

The measurements were carried out with an instrument (P/ACE System 2000, Beckman, Palo Alto, CA, USA) equipped with a fused-silica capillary (100 μm I.D.; total length 57 cm; length to the detector 50 cm). The capillary was thermostated at 25°C.

A constant voltage of 20 kV, resulting in a current of about 120–160 μA for the SDS buffers, was applied. Injection into the capillary was carried out hydrodynamically for 4 s.

UV absorption was measured at 254 nm.

Procedures

Gel preparation [7]. For the preparation of 25 ml of a linear, non-cross-linked liquid polymer acrylamide gel of medium chain length, 1.88 g of acrylamide were dissolved in 15 ml of water; 19 mg of TEMED were added and the solution was degassed with a water-jet pump for 10 min. Polymerization was initiated with 23 mg of ammonium persulphate (dissolved in 10 ml of water). No cross-linker was applied. The resulting polyacrylamide gel solution was degassed for 15–20 min using a water-jet pump.

Buffer solution. The buffer was prepared by adjusting a solution of phosphoric acid (0.05 mol/l) to the appropriate pH with sodium hydroxide solution.

SDS buffer. To the phosphate buffer (0.05 mol/l), solid SDS was added to give a final concentration of 0.5% (w/w).

Running buffer. A 2-g mass of gel (prepared as just described) was mixed with the SDS buffer and diluted to 20 ml, giving a running buffer solution with 10% (w/v) gel. This buffer solution was used to fill the capillary and the electrolyte vessels.

Protein samples for SDS electrophoresis. Masses of 1–1.5 mg of the proteins were dissolved in 1 ml of SDS buffer and heated to about 100°C for 5 min in a water-bath.

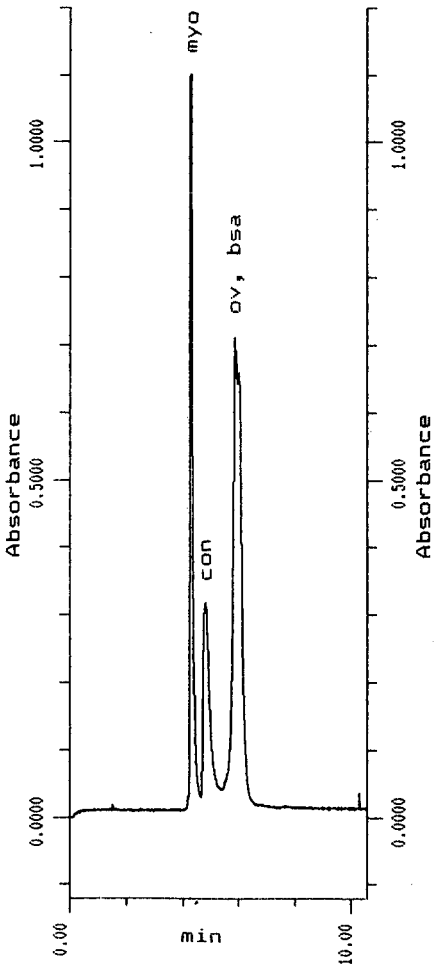

Fig. 1. Electropherogram of untreated proteins by free CZE (without polyacrylamide gel). The electropherogram was obtained at a pH of 7 (phosphate buffer, 0.05 mol/l). The proteins were moving towards the cathode. myo = Myoglobin, ov = ovalbumin, bsa = bovine serum albumin, con = conalbumin. The horizontal axis gives the migration time in minutes; UV absorbance at 254 nm.

TABLE I

REFERENCE PROTEINS USED FOR CZE

Protein	Molecular mass
Myoglobin	17 800
Ovalbumin	45 000
Bovine serum albumin	62 000
Conalbumin	77 000

RESULTS AND DISCUSSION

The zone electropherogram of a mixture of myoglobin, ovalbumin, bovine serum albumin and conalbumin, obtained at pH 7 without SDS and polyacrylamide gel is shown in Fig. 1. The molecular masses of the reference proteins are given in Table I. Owing to the electro-osmotic flow of the system, the proteins move towards the cathode. Under these conditions, the migration is a function of the effective mobilities of the proteins, but is not correlated with their molecular masses. It can be seen that myoglobin exhibits the lowest mobility (it has an isoelectric point, p*I*, of 6.8), having about the same velocity as a neutral compound (not shown in the electropherogram), followed by conalbumin. Ovalbumin and bovine serum albumin (with a p*I* of 4.8 and 5.0, respectively), migrating as anions with the highest mobility, are not separated under the given conditions.

After conversion of the proteins into their (anionic) SDS complexes, the elution order of myoglobin and the other proteins is reversed, as shown in Fig. 2. This electropherogram was obtained with a gel-free buffer, containing 0.5% SDS. It can be seen that the binding of SDS to the protein minimizes the difference in the mobilities, at least for ovalbumin, conalbumin and bovine serum albumin, which are eluted in a single, non-resolved peak. In contrast to Fig. 1, myoglobin is eluted (as a result of electroosmosis) with the largest migration time, because it has the highest mobility. However, as can be seen from Figs. 1 and 2, in both cases the migration sequence is not related to the molecular masses of the different proteins.

When liquid polymer acrylamide was added to the running buffer, the electropherogram shown in Fig. 3 was obtained. A reduction of the pH to 5.5 was necessary, because in the presence of the polyacrylamide gel the electroosmotic flow nearly opposes the electrophoretic velocity of the proteins, resulting in extremely long and irreproducible retention times. At pH 5.5 the electroosmotic flow is reduced so far that the anionic protein complexes can be detected within a reasonable time at the side of the anode. The migration sequence of the SDS–protein complexes is independent of the pH in this range.

Fig. 3 shows that all four proteins are well separated and that a correlation between the molecular mass and the migration time can be seen. The SDS complex of the smallest protein, myoglobin, has the shortest retention time, followed by ovalbumin, bovine serum albumin and conalbumin.

The broad peaks in Fig. 3 result partially from inhomogeneities in the proteins, especially the albumins, a fact which is well known from SDS-polyacrylamide gel

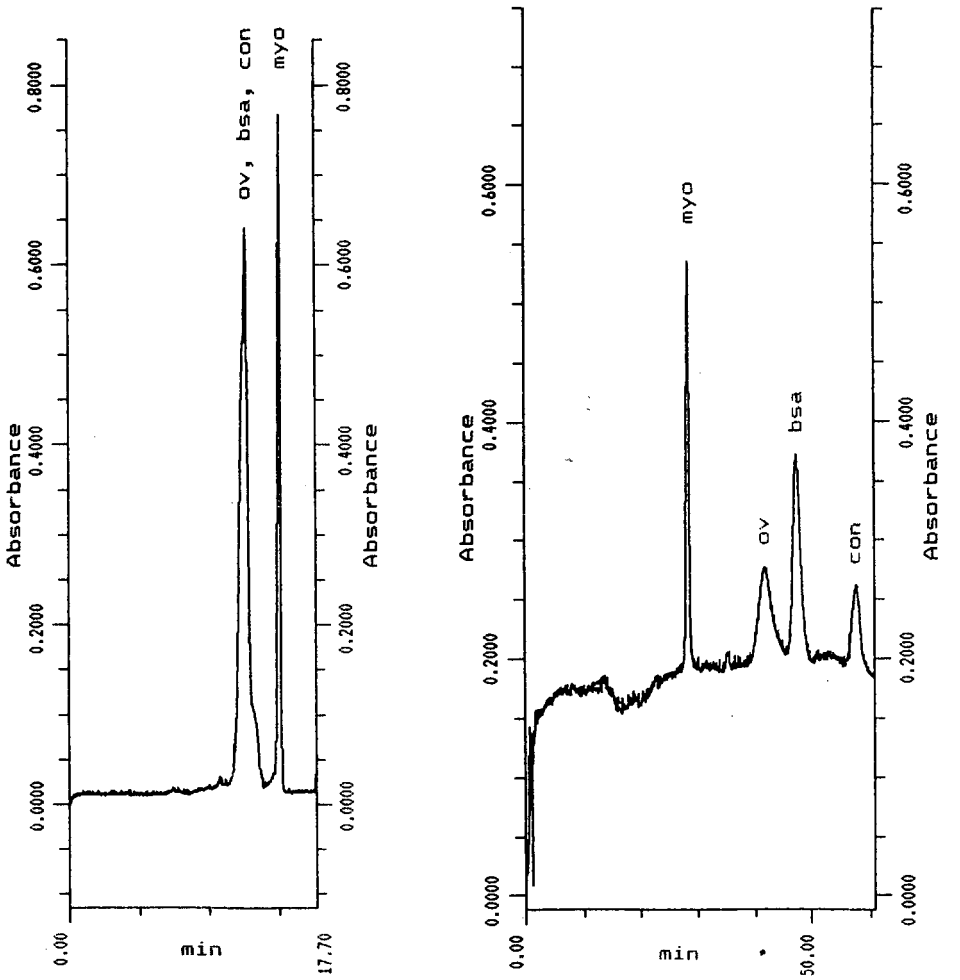

Fig. 2. Electropherogram of the protein–SDS complexes by free zone electrophoresis (without polyacrylamide gel). Buffer: phosphate, pH 7, 0.05 mol/l; 0.5% SDS. Proteins recorded at the side of the cathode. Symbols as in Fig. 1.

Fig. 3. Electropherogram of protein–SDS complexes obtained in a capillary filled with linear polyacrylamide. The capillary was filled with liquid, non-cross-linked polyacrylamide gel (10%) in a pH 5.5 running buffer (phosphate, 0.05 mol/l; 0.5% SDS). The proteins are separated according to their molecular mass. Symbols as in Fig. 1.

electrophoresis in slab gels. Furthermore, an excessive Joule's heat is produced by the high electric current, owing to the relatively high concentration of the SDS buffer. These effects explain to some extent the poor efficiency of the separation.

The relationship between the retention time and the molecular mass of the proteins is shown in Fig. 4. The shape of this curve indicates that the polyacrylamide acts as a sieving medium for the protein complexes, leading to a migration order

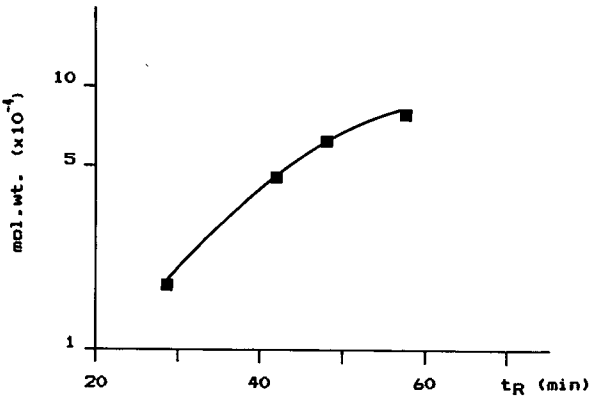

Fig. 4. Semi-logarithmic plot of the dependence of the molecular mass (mol/wt.) of the reference proteins on the retention times (t_R) in CZE with linear polyacrylamide. Data from Fig. 3.

according to their size. This is similar to the results obtained with the cross-linked gels commonly used in SDS-polyacrylamide gel electrophoresis.

These promising preliminary results on the use of linear, non-cross-linked polyacrylamide gels for the separation of proteins according to their molecular mass need further optimization. Studies in which parameters such as the pH of the buffer electrolyte and the percentage and chain length of the polyacrylamide gel are varied are being carried out.

REFERENCES

1 S. Hjertén, *J. Chromatogr.*, 270 (1983) 1.
2 A. S. Cohen and B. L. Karger, *J.Chromatogr.*, 397 (1987) 409.
3 A. Paulus, A. S. Cohen, A. Guttman and B. L. Karger, presented at the *6th International Symposium on Isotachophoresis and Capillary Zone Electrophoresis, Vienna, Austria, September 1988*, Abstr. No. 28.
4 S. Hjertén, K. Elenbring, F. Kilar and J.-L. Liao, *J. Chromatogr.*, 403 (1987) 47.
5 D. N. Heiger, A. S. Cohen and B. L. Karger, *J. Chromatogr.*, 516 (1990) 33.
6 M. Zhu, D. L. Hansen, S. Burd and F. Gannon, *J. Chromatogr.*, 480 (1989) 311.
7 H.-J. Bode, *Anal. Biochem.*, 83 (1977) 204.
8 H.-J. Bode, *Anal. Biochem.*, 83 (1977) 364.
9 H.-J. Bode, *Anal. Biochem.*, 92 (1979) 99.
10 H.-J. Bode, *Hoppe-Seylers Z. Physiol. Chem.*, 359 (1978) 1237.

Author Index

Ackermans, M. T., Everaerts, F. M. and Beckers, J. L.
Quantitative analysis in capillary zone electrophoresis with conductivity and indirect UV detection 549(1991)345
Ammon, H. U., see Karlaganis, G. 549(1991)229
Anderson, Jr., J. M., see Saari-Nordhaus, R. 549(1991)257
Araki, T., see Tanaka, N. 549(1991)29
Barros, A. M. V., see Gigante, B. 549(1991)217
Beckers, J. L., see Ackermans, M. T. 549(1991)345
Berahia, T., see Gaydou, E. M. 549(1991)440
Berthod, A.
Silica: backbone material of liquid chromatographic column packings (Review) 549(1991)1
Bhalerao, N. V., see Ghatge, B. B. 549(1991)423
Bianchini, J.-P., see Gaydou, E. M. 549(1991)440
Biswas, M., see Lookabaugh, M. 549(1991)357
Blaas, D., see Widhalm, A. 549(1991)446
Blackwell, J. A. and Carr, P. W.
Study of the fluoride adsorption characteristics of porous microparticulate zirconium oxide 549(1991)43
Blackwell, J. A. and Carr, P. W.
Fluoride-modified zirconium oxide as a biocompatible stationary phase for high-performance liquid chromatography 549(1991)59
Brice, K. A., see Williams, D. T. 549(1991)297
Burgi, D. S., see Salomon, K. 549(1991)375
Camenzind, R., see Karlaganis, G. 549(1991)229
Camilleri, P., see Okafo, G. N. 549(1991)404
Capangpangan, M. B., see Schnable, J. G. 549(1991)335
Cardinali, C., see Viscomi, G. C. 549(1991)175
Carr, P. W., see Blackwell, J. A. 549(1991)43
Carr, P. W., see Blackwell, J. A. 549(1991)59
Cheng, M.-C., see Hsu, M.-C. 549(1991)410
Chen, Jr., E. N. and Nero, V. P.
Separation and identification of sulfurized alkylphenols in oil by high-performance liquid chromatography with evaporative light scattering and mass spectrometric detection 549(1991)247
Cramer, S. M., see Kim, Y. J. 549(1991)89
Dimov, N. and Matisová, E.
Improved method for prediction of gas chromatographic retention indices of C_9–C_{12} alkylbenzenes 549(1991)325
Eiceman, G. A. and Lara, A. S.
Gas chromatographic properties of organoammonium exchanged montmorillonites. I. Tetraalkylammonium cations 549(1991)273
Eiceman, G. A., see Lara, A. S. 549(1991)283
El-Sayed Metwally, M.
Stability-indicating high-performance liquid chromatographic assay for α-methyldopa in sustained-release capsules 549(1991)221
Everaerts, F. M., see Ackermans, M. T. 549(1991)345
Fassina, G., see Zamai, M. 549(1991)195
Fellin, P., see Williams, D. T. 549(1991)297
Forsyth, D. A., see Mahmoud, M. E. 549(1991)416
Furusawa, M., see Kiba, N. 549(1991)127
Fuse, H., see Kiba, N. 549(1991)127
Gasa, S., see Kato, N. 549(1991)133
Gaur, R. K.
High-performance liquid chromatography of synthetic oligonucleotides. A new affinity protecting group 549(1991)207
Gawdzik, B.
Comparison of the selectivity of di-(methacryloyloxymethyl)-naphthalene–divinylbenzene copolymers in reversed-phase high-performance liquid chromatography 549(1991)77
Gaydou, E. M., Berahia, T., Wallet, J.-C. and Bianchini, J.-P.
Gas chromatography of some polymethoxylated flavones and their determination in orange peel oils 549(1991)440
Ghatge, B. B. and Bhalerao, N. V.
Application of substituted liquid crystals as stationary phases in gas–liquid chromatography for the separation of mono- and dimethyl naphthalenes 549(1991)423
Gigante, B., Barros, A. M. V., Teixeira, A. and Marcelo-Curto, M. J.
Separation and simultaneous high-performance liquid chromatographic determination of benzocaine and benzyl benzoate in a pharmaceutical preparation 549(1991)217
Groenland, W. P. T., see Verhaar, L. A. T. 549(1991)113

Grotjan, H. E., Schanbacher, B. D. and Keel, B. A.
Ovine luteinizing hormone. V. Significance of flow-through peaks observed during chromatofocusing as revealed by various methods of sample preparation and application 549(1991)141
Grotjan, H. E. and Zalesky, D. D.
Ovine luteinizing hormone. VI. Analysis of the misclassification errors in the separation of intrapituitary isohormones by chromatofocusing 549(1991)153
Helmer, J. C., see Salomon, K. 549(1991)375
Hendriks, H. E. J., see Verhaar, L. A. T. 549(1991)113
Herterich, R.
Gas chromatographic determination of nitrophenols in atmospheric liquid water and airborne particulates 549(1991)313
Hosoya, K., see Tanaka, N. 549(1991)29
Hsu, M.-C. and Cheng, M.-C.
High-performance liquid chromatographic method for the determination of cloxacillin in commercial preparations and for stability studies 549(1991)410
Incorvia Mattina, M. J.
Carrier effect in the analysis of phenylurea herbicides using high-performance liquid chromatography–particle beam-mass spectrometry 549(1991)237
Ito, K., Shoto, E. and Sunahara, H.
Ion chromatography of inorganic iodine species using C_{18} reversed-phase columns coated with cetyltrimethylammonium 549(1991)265
Kamahori, M., Watanabe, Y., Miyagi, H., Ohki, H. and Miyake, R.
Two-dimensional viscous flow analysis in a micro flow-cell of an ultraviolet absorption detector for high-performance liquid chromatography 549(1991)101
Karlaganis, G., Von Arx, R., Ammon, H. U. and Camenzind, R.
High-performance liquid chromatographic determination of atrazine, deisopropylatrazine and deethylatrazine in soils from corn fields 549(1991)229
Kato, N., Gasa, S., Makita, A. and Oguchi, H.
Improved separation of lysoglycolipids from solvolysates by reversed-phase high-performance liquid chromatography 549(1991)133
Kawai, S., see Koh, S. 549(1991)434
Keel, B. A., see Grotjan, H. E. 549(1991)141
Kenndler, E., see Widhalm, A. 549(1991)446
Kiba, N., Shitara, K., Fuse, H., Furusawa, M. and Takata, Y.
Column liquid chromatographic determination of saccharides with a single calibration graph using post-column enzyme reactors and coulometric detection 549(1991)127
Kim, Y. J. and Cramer, S. M.
Metal affinity displacement chromatography of proteins 549(1991)89
Kimata, K., see Tanaka, N. 549(1991)29
Koh, S., Urayama, K., Kawai, S. and Takayama, Y.
Application of a metal capillary column in gas chromatographic determination of catechol-O-methyltransferase activity 549(1991)434
Krull, I. S., see Lookabaugh, M. 549(1991)357
Kurantz, M. J., Maxwell, R. J., Kwoczak, R. and Taylor, F.
Rapid and sensitive method for the quantitation of non-polar lipids by high-performance thin-layer chromatography and fluorodensitometry 549(1991)387
Kuster, B. F. M., see Verhaar, L. A. T. 549(1991)113
Kwoczak, R., see Kurantz, M. J. 549(1991)387
Lanteri, P., see Vialle, J. 549(1991)159
Lara, A. S. and Eiceman, G. A.
Gas chromatographic retention properties of organoammonium exchanged montmorillonites. II. $CH_3N^+H_3$, $(CH_3)_4N^+$, $(CH_3)_3N^+CH_2C_6H_5$ and 1,4-diazabicyclo[2.2.2]octane · $2H^+$ 549(1991)283
Lara, A. S., see Eiceman, G. A. 549(1991)273
Longeray, R., see Vialle, J. 549(1991)159
Longobardi, M. G., see Viscomi, G. C. 549(1991)175
Lookabaugh, M., Biswas, M. and Krull, I. S.
Quantitation of insulin injection by high-performance liquid chromatography and high-performance capillary electrophoresis 549(1991)357
Mahmoud, M. E., Moussa, A. M., Forsyth, D. A. and Vouros, P.
Hydrogen–deuterium exchange in fused-silica capillary columns 549(1991)416
Makita, A., see Kato, N. 549(1991)133
Marcelo-Curto, M. J., see Gigante, B. 549(1991)217
Matisová, E., see Dimov, N. 549(1991)325
Mauri, P. L., see Pietta, P. G. 549(1991)367
Maxwell, R. J., see Kurantz, M. J. 549(1991)387
Miyagawa, F., Tsuchida, Y. and Shimizu, T.
Detection of octopamine in an insect ganglion by high-performance liquid chromatography–native fluorescence 549(1991)400

Miyagi, H., see Kamahori, M. 549(1991)101
Miyake, R., see Kamahori, M. 549(1991)101
Moussa, A. M., see Mahmoud, M. E. 549(1991)416
Navarro, P., see Vialle, J. 549(1991)159
Nero, V. P., see Chen, Jr., E. N. 549(1991)247
Nguyet, T. T., see Vialle, J. 549(1991)159
Oguchi, H., see Kato, N. 549(1991)133
Ohki, H., see Kamahori, M. 549(1991)101
Okafo, G. N. and Camilleri, P.
The effect of ^2H_2O and an ion-pairing agent on the liquid chromatographic separation of dansylated amino acids 549(1991)404
Pietta, P. G., Mauri, P. L., Rava, A. and Sabbatini, G.
Application of micellar electrokinetic capillary chromatography to the determination of flavonoid drugs 549(1991)367
Rava, A., see Pietta, P. G. 549(1991)367
Saari-Nordhaus, R. and Anderson, Jr., J. M.
Simultaneous analysis of anions and cations by single-column ion chromatography 549(1991)257
Sabbatini, G., see Pietta, P. G. 549(1991)367
Salenko, V. L., Troshkov, M. L. and Zibarev, A. V.
Cyclic aryleneazachalcogenenes. IV. Gas chromatographic properties of polyfluorinated 2,1,3-benzoselenadiazoles 549(1991)429
Salomon, K., Burgi, D. S. and Helmer, J. C.
Separation of seven tricyclic antidepressants using capillary electrophoresis 549(1991)375
Schanbacher, B. D., see Grotjan, H. E. 549(1991)141
Schnable, J. G., Capangpangan, M. B. and Suffet, I. H.
Continuous automatic monitoring of volatile organic compounds in aqueous streams by a modified purge-and-trap system 549(1991)335
Schwer, C., see Widhalm, A. 549(1991)446
Shimizu, T., see Miyagawa, F. 549(1991)400
Shitara, K., see Kiba, N. 549(1991)127
Shoto, E., see Ito, K. 549(1991)265
Stegehuis, D. S., Tjaden, U. R., Van den Beld, C. M. B. and Van der Greef, J.
Bioanalysis of the neuropeptide des-enkephalin-γ-endorphin by high-performance liquid chromatography with on-line sample pretreatment using gel permeation and solid-phase isolation 549(1991)185
Suffet, I. H., see Schnable, J. G. 549(1991)335
Sunahara, H., see Ito, K. 549(1991)265
Takata, Y., see Kiba, N. 549(1991)127
Takayama, Y., see Koh, S. 549(1991)434
Tanaka, N., Tanigawa, T., Kimata, K., Hosoya, K. and Araki, T.
Selectivity of carbon packing materials in comparison with octadecylsilyl- and pyrenylethylsilylsilica gels in reversed-phase liquid chromatography 549(1991)29
Tanigawa, T., see Tanaka, N. 549(1991)29
Taylor, F., see Kurantz, M. J. 549(1991)387
Teixeira, A., see Gigante, B. 549(1991)217
Tjaden, U. R., see Stegehuis, D. S. 549(1991)185
Tran, Q., see Williams, D. T. 549(1991)297
Troshkov, M. L., see Salenko, V. L. 549(1991)429
Tsuchida, Y., see Miyagawa, F. 549(1991)400
Urayama, K., see Koh, S. 549(1991)434
Van den Beld, C. M. B., see Stegehuis, D. S. 549(1991)185
Van der Greef, J., see Stegehuis, D. S. 549(1991)185
Verdini, A. S., see Viscomi, G. C. 549(1991)175
Verhaar, L. A. T., Hendriks, H. E. J., Groenland, W. P. T. and Kuster, B. F. M.
High-performance liquid chromatography of reaction mixtures from the oxidation and degradation of lactose 549(1991)113
Vialle, J., Navarro, P., Nguyet, T. T., Lanteri, P. and Longeray, R.
Experimental design for the optimization of the separation of aliphatic amines by ion chromatography 549(1991)159
Viscomi, G. C., Cardinali, C., Longobardi, M. G. and Verdini, A. S.
Large-scale purification of the synthetic peptide fragment 163–171 of human interleukin-β by multi-dimensional displacement chromatogaphy 549(1991)175
Von Arx, R., see Karlaganis, G. 549(1991)229
Vouros, P., see Mahmoud, M. E. 549(1991)416
Wallet, J.-C., see Gaydou, E. M. 549(1991)440
Watanabe, Y., see Kamahori, M. 549(1991)101
Widhalm, A., Schwer, C., Blaas, D. and Kenndler, E.
Capillary zone electrophoresis with a linear, non-cross-linked polyacrylamide gel: separation of proteins according to molecular mass 549(1991)446
Williams, D. T., Tran, Q., Fellin, P. and Brice, K. A.
Evaluation of gas chromatography–Fourier transform infrared spectroscopy–mass spectrometry for analysis of phenolic compounds 549(1991)297
Zalesky, D. D., see Grotjan, H. E. 549(1991)153
Zamai, M. and Fassina, G.
Mobile phase effects in the high-performance affinity purification of thermolysin 549(1991)195
Zibarev, A. V., see Salenko, V. L. 549(1991)429

Erratum

corrected 10 Jan. 92

J. Chromatogr., 538 (1991) 87–90

Page 87, the affiliation of John A. Beutler should read "PRI/DynCorp.". Dr. Beutler is currently affiliated with the Laboratory of Drug Discovery Research & Development at the address listed in the paper.

PUBLICATION SCHEDULE FOR 1991

Journal of Chromatography and Journal of Chromatography, Biomedical Applications

MONTH	D 1990–F 1991	M	A	M	J	J	A	S	O[a]
Journal of Chromatography	Vols. 535–539	540/1+2 541/1+2 542/1	542/2 543/1	543/2 544/1+2 545/1	545/2 546/1+2 547/1+2	548/1+2 549/1+2 550/1+2	552/1+2 553/1+2 554/1+2 555/1+2	556/1+2	
Cumulative Indexes, Vols. 501–550							551/1+2		
Bibliography Section		560/1			560/2			561/1	
Biomedical Applications	Vols. 562, 563	564/1	564/2 565/1+2	566/1 566/2	567/1	567/2 568/1	568/2	569/1+2	

[a] The publication schedule for further issues will be published later.

INFORMATION FOR AUTHORS

(Detailed *Instructions to Authors* were published in Vol. 522, pp. 351–354. A free reprint can be obtained by application to the publisher, Elsevier Science Publishers B.V., P.O. Box 330, 1000 AH Amsterdam, The Netherlands.)

Types of Contributions. The following types of papers are published in the *Journal of Chromatography* and the section on *Biomedical Applications:* Regular research papers (Full-length papers), Review articles and Short Communications. Short Communmications are usually descriptions of short investigations, or they can report minor technical improvements of previously published procedures; they reflect the same quality of research as Full-length papers, but should preferably not exceed six printed pages. For Review articles, see inside front cover under Submission of Papers.

Submission. Every paper must be accompanied by a letter from the senior author, stating that he/she is submitting the paper for publication in the *Journal of Chromatography*.

Manuscripts. Manuscripts should be typed in double spacing on consecutively numbered pages of uniform size. The manuscript should be preceded by a sheet of manuscript paper carrying the title of the paper and the name and full postal address of the person to whom the proofs are to be sent. As a rule, papers should be divided into sections, headed by a caption (*e.g.*, Abstract, Introduction, Experimental, Results, Discussion, etc.). All illustrations, photographs, tables, etc., should be on separate sheets.

Introduction. Every paper must have a concise introduction mentioning what has been done before on the topic described, and stating clearly what is new in the paper now submitted.

Abstract. All articles should have an abstract of 50–100 words which clearly and briefly indicates what is new, different and significant.

Illustrations. The figures should be submitted in a form suitable for reproduction, drawn in Indian ink on drawing or tracing paper. Each illustration should have a legend, all the *legends* being typed (with double spacing) together on a *separate sheet*. If structures are given in the text, the original drawings should be supplied. Coloured illustrations are reproduced at the author's expense, the cost being determined by the number of pages and by the number of colours needed. The written permission of the author and publisher must be obtained for the use of any figure already published. Its source must be indicated in the legend.

References. References should be numbered in the order in which they are cited in the text, and listed in numerical sequence on a separate sheet at the end of the article. Please check a recent issue for the layout of the reference list. Abbreviations for the titles of journals should follow the system used by *Chemical Abstracts*. Articles not yet published should be given as "in press" (journal should be specified), "submitted for publication" (journal should be specified), "in preparation" or "personal communication".

Dispatch. Before sending the manuscript to the Editor please check that the envelope contains four copies of the paper complete with references, legends and figures. One of the sets of figures must be the originals suitable for direct reproduction. Please also ensure that permission to publish has been obtained from your institute.

Proofs. One set of proofs will be sent to the author to be carefully checked for printer's errors. Corrections must be restricted to instances in which the proof is at variance with the manuscript. "Extra corrections" will be inserted at the author's expense.

Reprints. Fifty reprints of Full-length papers and Short Communications will be supplied free of charge. Additional reprints can be ordered by the authors. An order form containing price quotations will be sent to the authors together with the proofs of their article.

Advertisements. Advertisement rates are available from the publisher on request. The Editors of the journal accept no responsibility for the contents of the advertisements.